The Dissertation Committee for Luis Vicente Montiel Cendejas certifies that this is the approved version of the following dissertation:

Approximations, Simulation, and Accuracy of Multivariate Discrete Probability Distributions in Decision Analysis

Committee:

J. Eric Bickel, Supervisor

David P. Morton

John J. Hasenbein

James S. Dyer

Larry W. Lake

Approximations, Simulation, and Accuracy of Multivariate Discrete Probability Distributions in Decision Analysis

by

Luis Vicente Montiel Cendejas, B.E., M.S., M.S.

DISSERTATION

Presented to the Faculty of the Graduate School of

The University of Texas at Austin

in Partial Fulfillment

of the Requirements

for the Degree of

DOCTOR OF PHILOSOPHY

THE UNIVERSITY OF TEXAS AT AUSTIN

May 2012

A mis Padres por darme alas.

A las hormigas, por tí.

Acknowledgments

Anyone that has done a PhD can tell you how hard it can be, but only a few will tell you that anyone with at least an average IQ could do it. This last statement I believe to be true. A PhD surely requires a lot of effort also. Nonetheless, the main component of a PhD is not how smart you are, or how hard you work, but the people that nurture you intellectually, emotionally, and financially. To all of you: "THANK YOU" from the bottom of my heart.

In my case, I owe my intellectual support to J. Eric Bickel. He persevered with me as my advisor throughout the time it took me to complete this research and to write the dissertation. The inspiration for this work came from his curiosity to understand the relation between known models of uncertainty and the underlying uncertainty faced in real applications. I must say that I first met Eric at a moment in my life in which I was considering leaving the PhD program. With neither advisor nor money, my motivation was at its lowest. It was Eric's motivation and trust that put me back on track, and for that I have no words to let you know how grateful I am.

I would like to thank the members of my dissertation committee, David P. Morton, John J. Hasenbein, James S. Dyer, and Larry W. Lake, for their time and their insightful comments. I know that at times the discussions were tough, but the insights, ideas, and rigor greatly helped to strengthen this dissertation. I just want to let you know that you taught me well, and a portion of this work belongs to you.

Among all the people that I needed to acknowledge, the most important one is my mother, Maria Rosa Cendejas Huerta. As an immigrant, it is not easy to move to a new country; at times it is lonely and stressful. But I was lucky, because since the first day, I had with me two things: the sense that someone cares about me unconditionally, and the fact that no matter what, someone has my back. These two things might seem trivial, but you would be surprised at how few people can count them.

During this journey, I met who has become the most important person in my life, Sabrina Amador Vargas. As you can imagine, she has been the day-to-day moral and intellectual support of this work. As a scientist, Sabrina works with ants, and her arguments and perceptions about new ideas have always provided a different perspective that enriched my research. Without you, doing this dissertation would not have been this much fun.

As I said before, money is also an important component. I want to thank the institutions that provided the necessary financial support for this dissertation: ConsejoNacional de Ciencia y Tehnología (CONACYT), the Fulbright Foundation, the National Science Foundation under CAREER Grant No. SES-0954371, and the Center for Petroleum Asset Risk Management (CPARM). It surely was money well spent.

I must acknowledge as well the many friends, colleagues, students, and teachers who assisted, advised, and supported my research and writing efforts over the years. Unfortunately the page is running out of lines, but I can say to all of you: thank you for helping me keep perspective on what is important in life and helping me to release the pressure during hard times. For that, I will drink tonight.

Approximations, Simulation, and Accuracy of Multivariate Discrete Probability Distributions in Decision Analysis

Publication No. _____

Luis Vicente Montiel Cendejas, Ph.D.
The University of Texas at Austin, 2012

Supervisor: J. Eric Bickel

Many important decisions must be made without full information. For example, a woman may need to make a treatment decision regarding breast cancer without full knowledge of important uncertainties, such as how well she might respond to treatment. In the financial domain, in the wake of the housing crisis, the government may need to monitor the credit market and decide whether to intervene. A key input in this case would be a model to describe the chance that one person (or company) will default given that others have defaulted. However, such a model requires addressing the lack of knowledge regarding the correlation between groups or individuals.

How to model and make decisions in cases where only partial information is available is a significant challenge. In the past, researchers have made arbitrary assumptions regarding the missing information. In this research, we developed a modeling procedure that can be used to analyze many possible scenarios subject to strict conditions. Specifically, we developed a new Monte Carlo simulation procedure to create a collection of joint probability distributions, all of which match whatever information we have. Using this collection of distributions, we analyzed the accuracy of different approximations such as maximum entropy or copula-models. In addition, we proposed several new approximations that outperform previous methods.

The objective of this research is four-fold. First, provide a new framework for approximation models. In particular, we presented four new models to approxi-

mate joint probability distributions based on geometric attributes and compared their performance to existing methods.

Second, develop a new joint distribution simulation procedure (JDSIM) to sample joint distributions from the set of all possible distributions that match available information. This procedure can then be applied to different scenarios to analyze the sensitivity of a decision or to test the accuracy of an approximation method.

Third, test the accuracy of seven approximation methods under a variety of circumstances. Specifically, we addressed the following questions within the context of multivariate discrete distributions:

1. Are there new approximations that should be considered?
2. Which approximation is the most accurate, according to different measures?
3. How accurate are the approximations as the number of random variables increases?
4. How accurate are they as we change the underlying dependence structure?
5. How does accuracy improve as we add lower-order assessments?
6. What are the implications of these findings for decision analysis practice and research?

While the above questions are easy to pose, they are challenging to answer. For Decision Analysis, the answers open a new avenue to address partial information, which bing us to the last contribution.

Fourth, propose a new approach to decision making with partial information. The exploration of old and new approximations and the capability of creating large collections of joint distributions that match expert assessments provide new tools that extend the field of decision analysis. In particular, we presented two sample cases that illustrate the scope of this work and its impact on uncertain decision making.

Table of Contents

List of Tables

List of Figures

Chapter 1

Background And Motivation

Operations Research is an area of applied mathematics whose main concern is how to make optimal decisions. Sometimes the framework of a decision is deterministic but complex, often resulting in solutions that are counterintuitive. In other cases, the decision framework is fraught with uncertainty, which is the concern of Decision Analysis (DA).

Howard (1966) defined *decision* to mean an irrevocable allocation of resources. In some cases, the complexity of the decision is low or the outcome is trivial, in such cases the decision does not represent a real concern to the Decision Maker (DM). For example, when choosing a dessert in a new restaurant, one would try to select the dessert that would be most pleasing based on the description of the dish. But, the chosen dessert might not be what was expected, creating an unpleasant moment. This decision is a simple choice among alternatives, with an uncertainty factor.

Other decisions have the same complexity, but the outcomes are too important to be taken lightly. Examples include medical decisions, life-or-death scenarios, and decisions that require the allocation of vast resources (Figure 1.1). Moreover, industry and government often involve decisions with high complexity, requiring in-depth analysis such as sequential decision making.

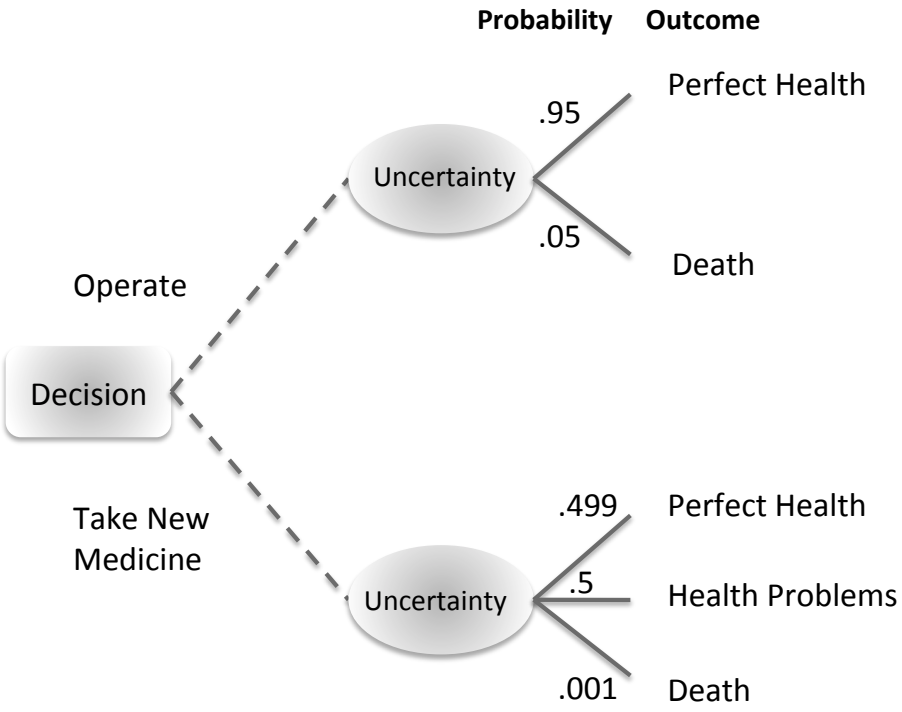

Figure 1.1: Tree diagram representing a medical decision.

Howard and Matheson (2004) defined DA as the discipline comprising the philosophy, theory, methodology, and professional practice necessary to formalize the analysis of important decisions. The methodology for DA is depicted in the DA Cycle (Fig. 1.2).

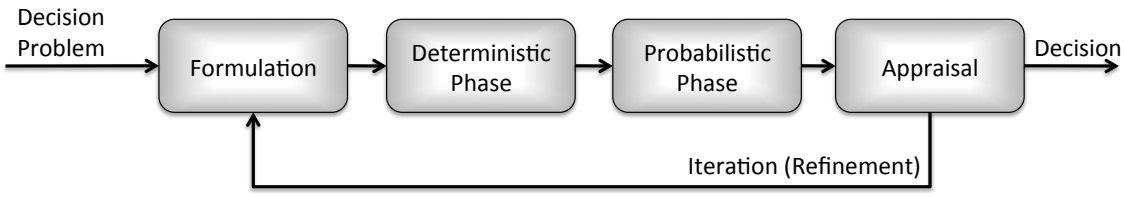

Figure 1.2: The Decision Analysis Cycle.

The cycle starts with a decision problem. From here:

- The Formulation phase: frame the decision problem, identify the alternatives, develop a value model, identify uncertainties, and derive the utility function.
- The Deterministic phase: identify key uncertainties of the model.
- The Probabilistic phase: encode the probabilities of the relevant variables including their pairwise dependence structure, and derive a probability distribution on the output measure (e.g., net present value).
- The Appraisal phase: Analyze sensitivity-to-probability to determine whether a change in our assessments changes the optimal action. Determine the value of gathering additional information to refine the decision. Consider whether further modeling of probabilistic dependence is warranted, an often neglected step that will be discussed in more detail.

Howard (1988) describes several steps were DA has found important challenges:

- Framing the problem.
- Creating alternatives.
- Measuring the decision quality.
- Selecting relevant uncertainties.
- Assessing probabilities and probabilistic dependence.
- Deriving risk attitude and risk tolerance for the DM.

All these steps have grown into sub-disciplines of decision analysis, each with its own extensive literature. However, this dissertation will address problems related to probability assessment and probabilistic dependence.

Modeling real-world decision situations often requires multivariate discrete probability distributions,[1] which model not only uncertainty but how uncertain events relate to each other. In finance, for example, the price of an asset over time is considered a random variable. However, when managing a portfolio, brokers are concerned also with the interactions among prices of various assets over time, since that can transform a bad portfolio into substantial revenue or vice versa. In gas/oil exploration, wells can be wet or dry, meaning they have or lack a considerable deposit of gas/oil, respectively. Geologists and other experts determine the probability of a well being wet or dry, but having a complete discrete joint probability distribution for all combinations of well outcomes provides important information about reservoir connections underground. Knowing this information could greatly affect the expected revenue of the project, and in most cases, could change the development plans. In medicine, drug development is considered a risky investment because it takes many years for a drug to be approved by the FDA, and a company can go bankrupt if a series of drugs fails the approval process. However, if there is a relation among the approval of *Drug A*, *Drug B*, and *Drug C*, then a joint probability distribution could provide information about which drug to develop first, thereby reducing the risk of bankruptcy.

In other words, the information about random events and their interactions is encoded in multivariate joint probability distributions, making them an important tool in mathematical modeling. The existence of a discrete joint probability distribution function has an impact on the strategy used in optimization. For example, procedures such as stochastic optimization and robust optimization are mainly concerned with optimization under uncertainty. However, they differ in that the former assumes knowledge of the underlying probability distribution and the latter disregards the underlying distribution. As a result, stochastic optimization provides

[1]We will use the terms multivariable distributions and joint distributions interchangeably.

results based on a higher degree of information, and robust optimization provides optimization over worst-case scenarios. Both solutions are useful when a decision is considered, but the knowledge of a probability distribution may provide information that changes the decision.

1.1 Contributions

This dissertation addresses decision situations for which partial information about the joint probability distribution is known. From here, our first contribution was to develop *four new approximations* to recreate a joint probability distribution. These approximations complement existing models such as maximum entropy, which is still the most popular approximation method.

A second contribution develops *a simulation procedure* we named *JDSIM*, to create a collection of joint distribution approximations. We consider JDSIM to be a powerful method for helping to characterize the uncertainty generated by the missing information about the joint distribution. This dissertation will focus on the philosophy behind and tools generated from this procedure.

A third contribution develops the concept of *accuracy of an approximation*. Up to now, there has been no clear procedure to test which approximation was best. Using JDSIM, we implement a procedure to determine the accuracy of several approximations under various scenarios.

Finally, our fourth contribution develops *a new approach to decision analysis*. We describe a new methodology for analyzing decisions in the face of partial information. We exemplify our methodology by revisiting two decisions in the literature and providing fresh insights. This contribution is the most applied of them all, but it perhaps has the greatest impact on society.

1.2 Motivation

In DA practice, it is common for the DM to work with people who deeply understand the behavior of the random variables. These experts provide the decision analysis team with estimates for the required assessments. Formally, assume the DM must choose an alternative a from a set $\mathbb{A}$.

If there are no uncertainties, the DM needs merely to order the set by preference and choose the most preferred option. Under uncertainty, however, it is common practice to use a utility function that encodes risk behavior into the decision. Then, if there is an uncertainty X, the utility of the pair $\{a, X\}$ is $u(a, X = x)$, which represents the utility as a function of the alternative chosen and the realization of the uncertainty.

The DM then solves the problem

$$\max_{a \in \mathbb{A}} \quad \mathbf{E}_X \Big[u(a, X) \Big], \tag{1.1}$$

which is the problem of finding the alternative that maximizes the DM's expected utility.

The DA cycle derives this decision step by step. In the Framing phase, the DA team helps the DM to define $\mathbb{A}$, X, and $u(\cdot)$. The Deterministic phase studies X to observe which uncertainties are relevant to the decision. During the Probabilistic phase, experts derive $f(X)$ and the problem is solved. Finally, during the Appraisal phase, a series of sensitivity analyses is performed to determine if more information could be relevant to the problem.

It has been shown that for simple assessments, experts can provide accurate values (Lichtenstein et al., 1982). However, experts face two important challenges. The first one appears when there are two or more uncertainties, e.g., $X = (X_1, X_2, \ldots, X_n)$. In this case, the assessment process becomes complex and often in-

tractable. To illustrate, assume each variable in the vector X is binary. Then, a simple joint probability distribution comprised of n binary random variables requires the assessments of marginal probabilities, pairwise probabilities, three-way probabilities, and so on. The total number of assessments is $2^n - 1$, which increases exponentially with n and represents a real challenge for DA practice.

This exponential increase in the number of assessments is due to probabilistic dependence. For example, if all variables were independent, only n assessments would be required, which is feasible (Bickel et al., 2008). Then, by ignoring probabilistic dependence, we can simplify the assessment process. However, this loss of information reduces the decision quality (Korsan, 1990).

The second challenge is presented when the assessments are heavily conditioned. To illustrate this, observe the joint distribution in Equation 1.2.

$$P(X) = P(X_1) \cdot P(X_2|X_1) \dots P(X_n|X_1, X_2, \dots, X_{n-1}). \tag{1.2}$$

To simplify the assessments, the joint distribution is usually factored into several conditional assessments such as $P(X_1)$ and $P(X_2|X_1)$. However, higher order conditional probabilities such as $P(X_3|X_1, X_2)$, $P(X_4|X_1, X_2, X_3)$, $P(X_5|X_1, X_2, X_3, X_4)$, $\dots$, $P(X_n|X_1, X_2, \dots, X_{n-1})$ are difficult to assess, producing inconsistencies or unreliable values. Ravinder et al. (1988) showed the degradation of quality in the assessments when experts work with highly conditional information.

These two challenges force experts and DMs into a tradeoff between complexity and information. On one hand, the more information they encode into the joint probability, the harder the assessments and the higher the chance to compromise their quality. On the other hand, using less information reduces the quantity of assessments, thus degrading the quality of the decision.

Despite its relevance, probabilistic dependence is often ignored because it greatly complicates probability assessment (Korsan, 1990; Lowell, 1994). In fact, Winkler (1982) identified the assessment and modeling of probabilistic dependence as one of the most important research topics facing decision analysts. Miller (1990) argued, "We need a way to assess and process dependent probabilities efficiently. If we can find generally applicable methods for doing so, we could make significant advances in our ability to analyze and model complex decision problems." These challenges have gone largely unanswered.

The Decision Analysis Cycle derives joint distributions using experts and available data. However, when based on partial information, such distributions are approximations of the "true" joint distribution. That is, if all possible conditional probabilities could be assessed, the resultant distribution would be unique and would match all the information at hand. The main goal is therefore to get as close as possible to the true joint distribution using partial information. Every approximation method generates a bias according to how it compensates for missing information, i.e., by disregarding parts of the dependence structure.

Given a portfolio with three assets and for simplicity, that the DM's only concern is with respect to the assets going up or down, the resulting joint probability distribution would have eight possibilities (Fig 1.3).

Figure 1.3(a) shows the initial tree structure. The question marks in the Figure are unknowns that an expert must assess. The expert starts by assessing P(asset 1 goes up), and then works toward more complex assessments (Fig 1.3(b)). The next step is to assess P(asset 2 goes up|asset 1 goes up) and P(asset 2 goes up|asset 1 goes down). These assessments capture the dependence between assets 1 and 2. Figure 1.3(c) shows that the outcome of asset 2 depends on the outcome of asset 1. Finally, we must assess P(asset 3 goes up|asset 1 and asset 2 go up), P(asset 3 goes up|asset 1 goes up and asset 2 goes down), P(asset 3 goes up|asset 1 goes down and asset 2 goes

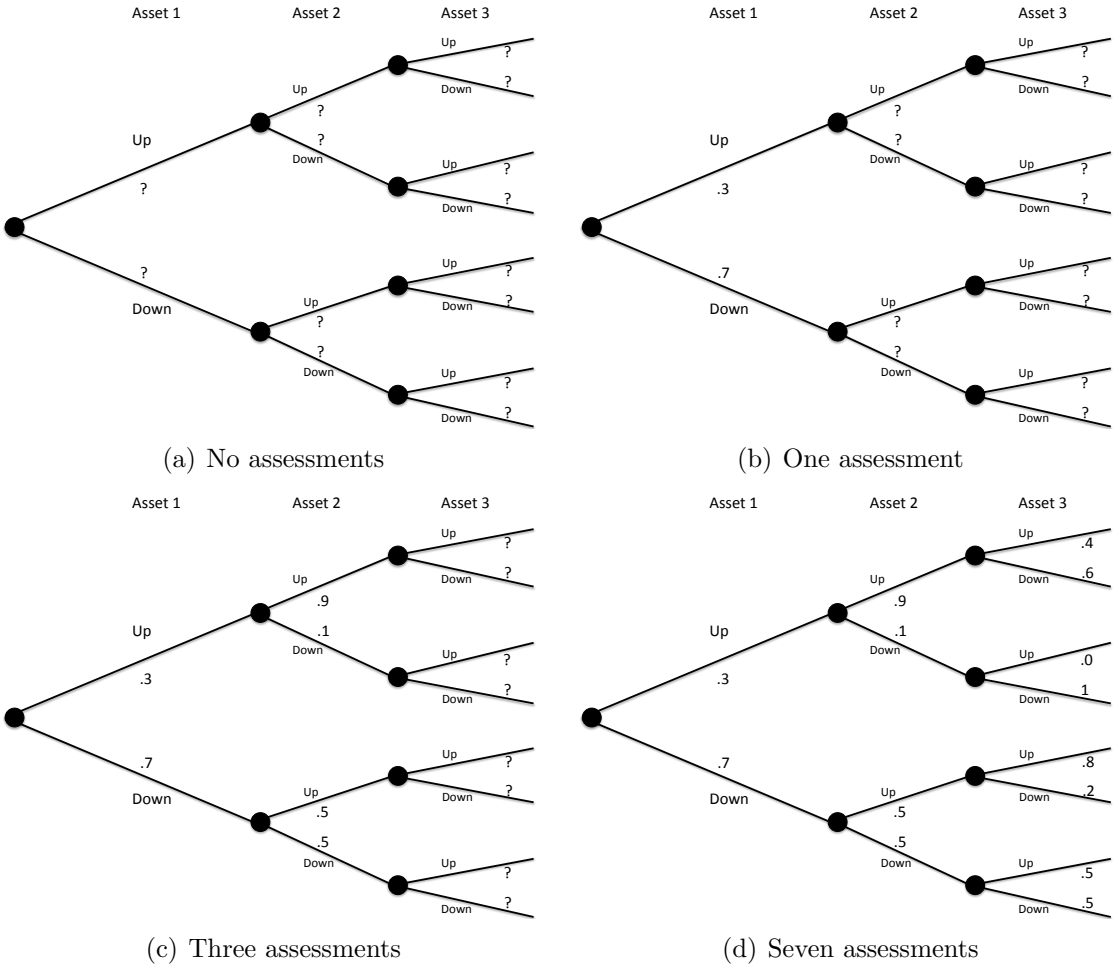

(a) No assessments

(b) One assessment

(c) Three assessments

(d) Seven assessments

Figure 1.3: Probabilistic dependence, tree representation.

up), and P(asset 3 goes up|asset 1 and asset 2 go down). This completely determines the discrete joint probability distribution using Equation 1.2 and the parameters in Figure 1.3(d).

For three assets, deriving a joint probability is a simple process that requires only seven assessments. However, the general case is considerably more complicated. For example, Bickel et al. (2008) considered a problem having six binary variables. This requires 63 assessments to fully characterize the joint distribution, and some of these assessments are very difficult. If only 21 of the 63 probabilities can be assessed,

the equivalent probability tree will have 42 degrees of freedom. As a result, we would need to work with a set of joint distributions or to select the joint distribution that best represents the set, that is, to generate an approximation to a joint distribution.

Lowell (1994) and Keefer (2004) described various methods to choose a joint probability approximation. Abbas (2006) and Bickel and Smith (2006) utilized an extension where the different joint distributions are compared to its maximum entropy counterpart. However, there remains this important unresolved question: how good are these approximations in relation to a true joint distribution? This is not easily answered, since the true joint distribution can never be observed. The main purpose of this dissertation is to develop a method to evaluate an approximate distribution $P(\mathbf{X}^A)$ with respect to the true joint distribution $P(\mathbf{X})$.

Although an approximate distribution's accuracy cannot be directly assessed, the approximation can still be compared to all the joint distributions that have the same partial information. Any approximation is just one of the elements of this set, in which any element could be the true joint distribution. Figure 1.4 illustrates this idea: the largest set is that for which the least information is provided, but as more information is available, the set shrinks until all information is known and the set become a singleton where the distribution is uniquely determined.

The partial information from the assessments defines the shape and size of the truth set, which in turn determines the accuracy and precision for any single approximation. We informally describe accuracy as a measure related to the location of $P(\mathbf{X^A})$ with respect to all other distributions in the set, and precision as a measure associated to the relative volume of the set. Accuracy and precision help to determine how good the approximation is. For example, with no information, the truth set is an n-dimensional simplex, since the only constraint is that the probabilities must sum to one. A possible approximation is the center $P(\mathbf{X^A}) = (\frac{1}{n}, \frac{1}{n} \ldots \frac{1}{n})$, which corresponds to the discrete uniform distribution and minimizes the maximum Euclidean distance

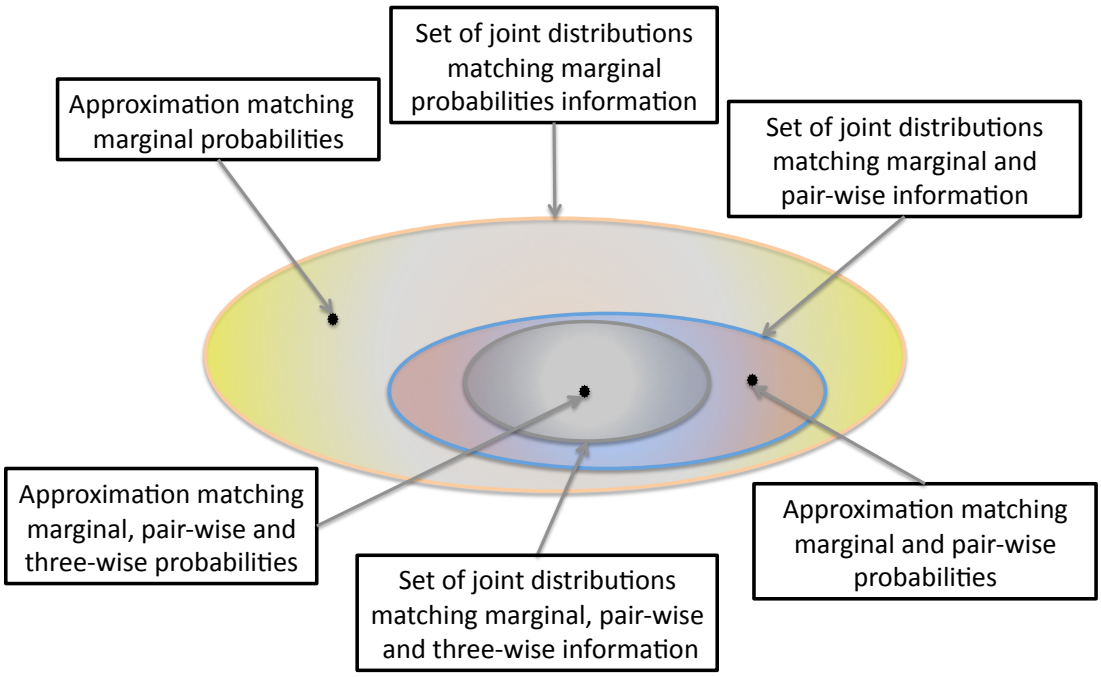

Figure 1.4: Information sets as we increase the available information.

from the approximation to any other joint distribution. $P(\mathbf{X^A})$ is the most accurate approximation possible for the information available. Even though the accuracy is the best possible, the set is too big, reducing the precision of the approximation. In a similar way, a set containing $P(\mathbf{X^A})$ could be very flat and elongated, in which case the size of the set is not a concern, but the location of $P(\mathbf{X^A})$ becomes extremely important.

To illustrate these concepts, take two binary random variables and assume no knowledge of the variables or their interactions (Figure 1.5). Since we have no information on the variables, we know that the truth set is a full symmetric simplex and that the best (most accurate) approximation is the uniform distribution. However, an infinite number of distributions could be the true distribution, some of which are far from $(\frac{1}{4}, \frac{1}{4}, \frac{1}{4}, \frac{1}{4})$ in at least four possible directions. Figure 1.6 gives an example of

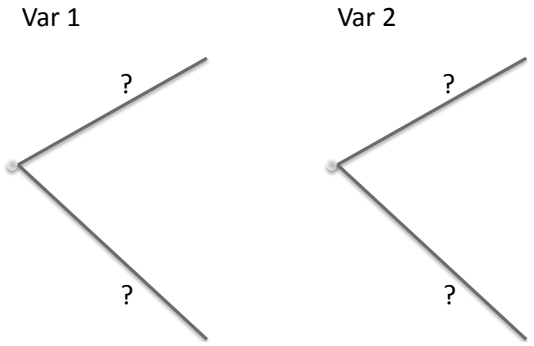

Figure 1.5: Two binary variables with unknown information.

an accurate approximation with low precision. The distributions defined as "Other possible approximations" are just a few from an infinite number of possibilities in three dimensions that match the available information (No Information).

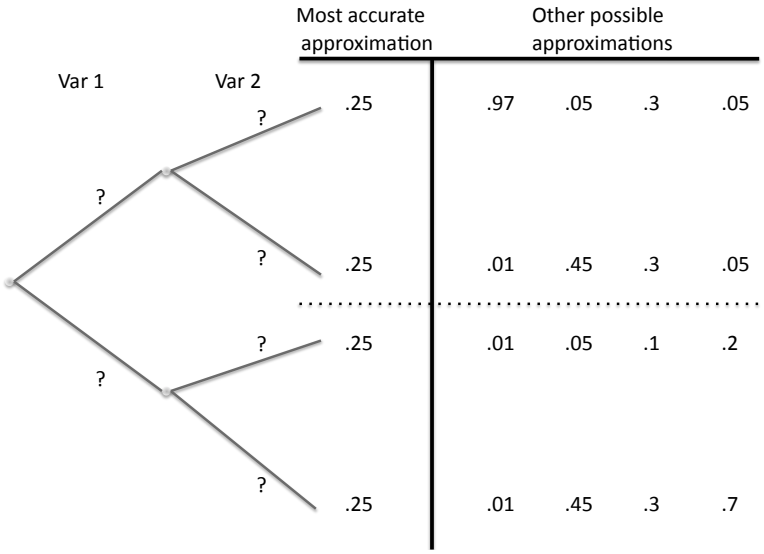

Figure 1.6: Accuracy vs. precision. Accurate approximation in a low-precision set.

Now assume that we have some knowledge of the marginal probabilities for both variables (Figure 1.7). Then the truth set is a line with extremes in {.9, 0, 0, .1} and {.8, .1, .1, 0}. The set has been reduced in size from the previous set, but we still need a point that better represents it.

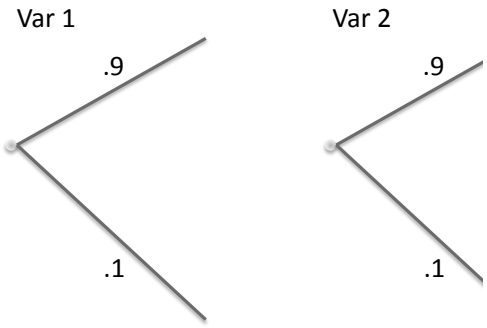

Figure 1.7: Two binary variables with information on their marginal probabilities.

Assuming independence between the two variables would yield {.81, .09, .09, .01}. This distribution is almost in the corner of the set, providing an approximation with low accuracy. Hence, we may want to consider a distribution in the center of the set, which is perhaps a better description of the possible joint distributions. Figure 1.8 shows some of the alternatives to approximate the set.

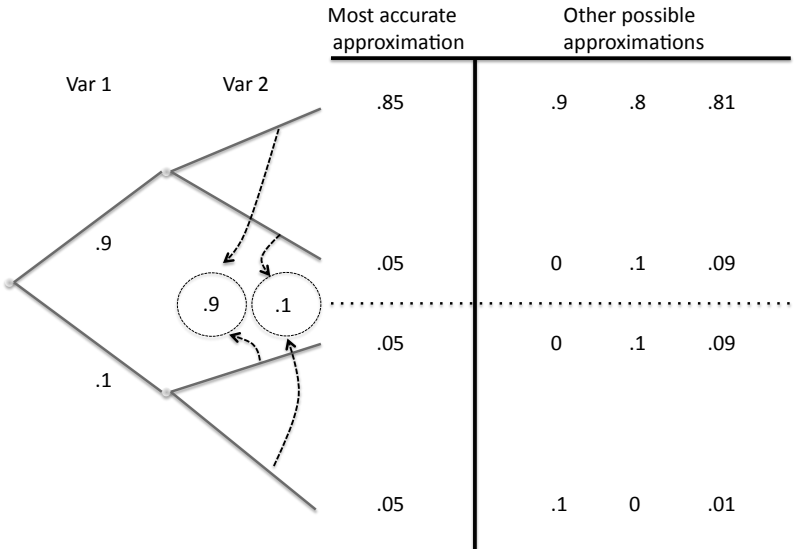

Figure 1.8: Accuracy vs. precision. An example of an accurate approximation in a set with higher precision.

Later chapters will provide a formal definition of accuracy in terms of the location within the truth set. The objective of this dissertation is to measure the accuracy of different distributions, while recognizing the importance of the precision of a set in terms of its size. However, the precision can be modified only by gathering more information, and since it is assumed that the information is given, the precision of a joint approximation is beyond the scope of this research. Nonetheless, some initial ideas for future research are given in the last chapter.

1.3 General Approach

Measuring the accuracy of an approximation is challenging because of the lack of a point of reference. Accuracy as a concept can exist only in relation to something else. However, the same information that is used in deriving an approximate joint distribution can be used to provide a framework that serves as a point of reference.

To measure accuracy requires comparing the approximate distribution to all other distributions that match the DM's beliefs. This entails generating a set $\mathbb{T}$ (truth set) of joint distributions that match the DM's beliefs. This set needs to contain *all* possible joint distributions that match the given information. Using this set, it is possible to develop an accuracy model as follows.

Figure 1.9: General accuracy approach to evaluate approximation joint distributions.

To be able to measure accuracy efficiently requires the truth set $\mathbb{T}$ to be convex. However, $\mathbb{T}$ is a function of the information gathered $\mathbb{I}$, and may not always be convex.

To demonstrate that, assume that the truth set was created using two variables x_1 and x_2 with possible outcomes $\{2, 4\}$ and $\{7, 8, 9\}$, respectively. If the only information known is the correlation $\rho = 0.5$, then $P_1(x_1, x_2)$ and $P_2(x_1, x_2)$ from Table 1.1 are elements of $\mathbb{T}$. However, the convex combination $P_3(x_1, x_2)$ is not, because as shown in Table 1.2, the correlation for $P_3(x_1, x_2)$ does not equal 0.5.

Table 1.1: Joint Distributions for a Series of Events.

Event		Joint Distributions		
x_1	x_2	$P_1(x_1, x_2)$	$P_2(x_1, x_2)$	$P_3(x_1, x_2)^a$
4	8	0.511	.163	.338
2	7	0.117	.096	.106
4	9	0.117	.096	.106
2	8	0.255	.645	.45

[a] $P_3(x_1, x_2) = \frac{1}{2}P_1(x_1, x_2) + \frac{1}{2}P_2(x_1, x_2)$.

Table 1.2: Correlations for Different Distributions.

Distribution	$\rho_{x_1 x_2}$
$P_1(x_1, x_2)$	0.5
$P_2(x_1, x_2)$	0.5
$P_3(x_1, x_2)$	0.46

Using correlations without the knowledge of the marginal distributions could result in sets that are hard to work with (non-convex). Fortunately, marginal assessments are easy to perform, and once known, $\mathbb{T}$ becomes a convex set. A later chapter will describe families of equations and their requirements such that $\mathbb{T}$ is assured to be a convex set. Equations outside the proposed families might generate a non-convex set and are left for future research.

Once $\mathbb{T}$ is defined, a method is required to sample the set $\mathbb{T}$ and provide random joint distributions. These distributions can be used to generate comparisons against the selected approximation. Finally, a set of measures of accuracy is needed for these comparisons.

The use of the samples and the measures of accuracy with the approximate distribution allows us to evaluate which approximation is most appropriate for a given situation. Figure 1.10 shows that by observing the behavior of a given approximation and its relation to the elements in the set $\mathbb{T}$, we can develop the tools required to

understand the accuracy of an approximation.

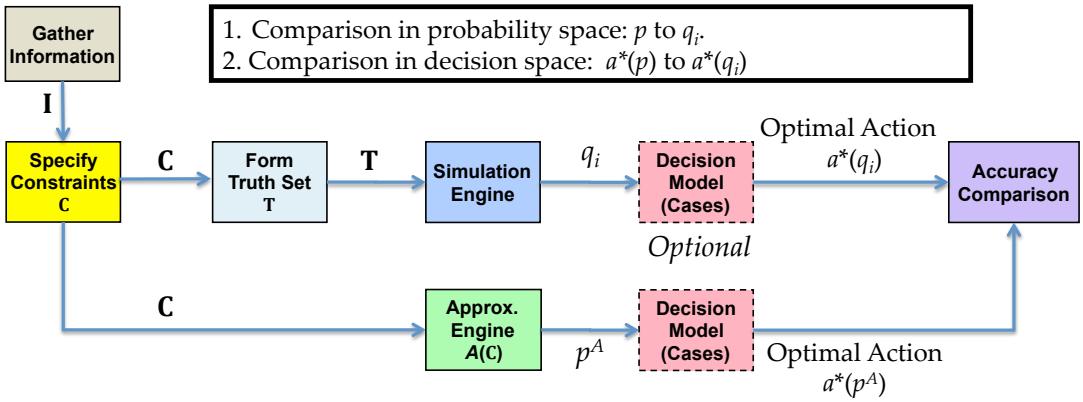

Figure 1.10: A procedure to test the accuracy of joint probability approximations.

The following sections formalize the problem and expand the general approach to characterize the accuracy of an approximation. Additionally, we present a literature review and an outline of the rest of the dissertation.

1.3.1 Problem Definition

Given a truth set $\mathbb{T}$ of joint distributions that match a specific set of information $\mathbb{I}$, and an approximation model A with solution p^*_A that represents a discrete joint probability distribution:

How does p^*_A relate to the elements in $\mathbb{T}$? *Specifically, for $p^*_A, q \in \mathbb{T}$,*

- *What is the relation between p^*_A and any arbitrary q?*
- *How great is the maximum absolute distance?*
- *How great is the total variation?*
- *How large is the distance between both distributions?*
- *How does the information encoded in the approximation compare to the distributions in the sample?*

To provide answers to these questions, it is necessary to characterize $\mathbb{T}$ as a function of $\mathbb{I}$ and to define a procedure to generate $q \in \mathbb{T}$ such that q is distributed in proportion to the volume of the relative interior of $\mathbb{T}$.

Although the main result of this dissertation is to generate a framework to measure the accuracy of an approximate distribution p_A^*, this approach leads to new formulations that generate different joint probability distribution approximations. Further chapters will analyze old and new models and provide general guidance.

1.3.2 Sampling Procedure

The "sampling procedure" assumes that the information is consistent and can be used to characterize a closed, bounded, and convex set $\mathbb{T}$. The information provided is assumed to be consistent in that the truth set is not empty. See Lichtenstein et al. (1982), Korsan (1990), and Chessa et al. (1999) for methods to enforce consistency.

The set is bounded by the definition of a probability distribution (all probabilities are positive and sum to one). Again, we consider only linear constraints; hence, $\mathbb{T}$ is convex. Convexity is required by the algorithms we use to sample the truth set $\mathbb{T}$ and to approximate the true joint distribution. Finally, we require that $\mathbb{T}$ is closed, which means that the boundary also belongs to $\mathbb{T}$.

Given that $\mathbb{T}$ is a continuous set, it contains an infinite number of distributions. Therefore, we must discretize $\mathbb{T}$ (i.e., sample from it) in order to test the accuracy of a given joint probability distribution. Figure 1.11 shows the basic idea: starting with the truth set, we sample joint distributions within the interior of $\mathbb{T}$ and use these distributions to make observations and inferences with respect to the approximation p_A^*.

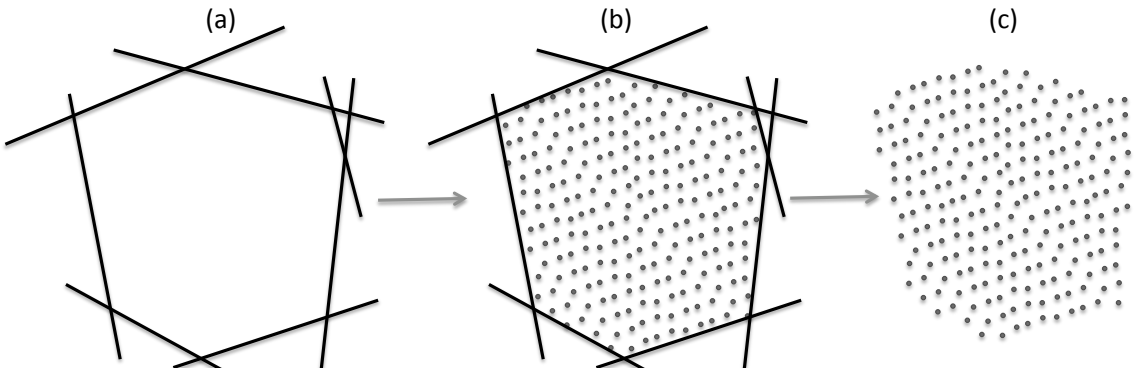

Figure 1.11: (a) Representation of $\mathbb{T}$, (b) Sampling from $\mathbb{T}$, (c) New set $\mathbb{T}'$.

To accurately represent $\mathbb{T}$ with a discrete sample, we need to sample sections of $\mathbb{T}$ in proportion to their volume (or d-content). That is, we need to create a uniform sample of the truth set. Smith (1984) presented a method called the Hit and Run sampler. This algorithm samples uniformly from $\mathbb{T}$ and has a mixing time of $\mathbf{O}(d^3)$, where d is the dimension of the set.

By sampling uniformly, we are implicitly assuming that every distribution in the interior of the set has the same chance of being the true joint distribution, although this conjecture cannot be proved or disproved. Thus, the method described here might best be thought of as a type of sensitivity analysis.

In higher dimensions, the truth set has an interesting behavior: the extreme corners of the set contain almost no volume. As a consequence, the samples in these neighborhoods are scarce or nonexistent. For this reason, we also present as a part of our future research, a method that increases the probability of sampling distributions close to the corners. We call this method the Ping-Pong sampler because of its bouncing characteristics. The Ping-Pong sampler does not create a uniform sample. However, preliminary results show that it has a fast convergence to a steady state distribution and that the samples replicate the symmetry embedded in $\mathbb{T}$.

1.3.3 Measures

Finally, we can observe relations between the joint probability approximation p^*_A and the sample (Figure 1.12). Some of the most important measures to be observed on the information space are "entropy," "differences of entropy" among distributions, and "relative entropy" (also known as KullbackLeibler divergence). From the geometric perspective, the main measures are "maximum absolute difference," "total variation," and "Euclidean distance." We also consider the χ^2 distance as an alternative measure. A full description of the measures is presented in Chapter 4.

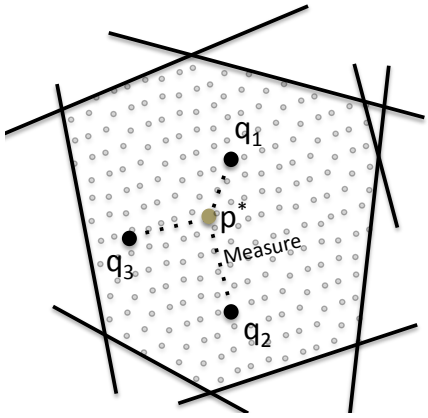

Figure 1.12: Using measures to compare p^* to $\mathbb{T}$.

1.4 Literature Review

In 1940, Deming and Stephan were the first to use partial information to approximate an unknown target. This problem was called "The matching of tabular data tables," where the census provided marginal information on the universal sample, and frequency information on a small sample. The problem was to extrapolate the sample to the complete universe while preserving consistency of the data tables. The approach to the matching of tabular data tables was concerned only with finding a solution; the quality of such a solution was not fully explored.

Later, Shannon (1948) developed the function $H(p_1, p_2, \ldots, p_n)$ to measure certainty in probability distributions, which is the basis for the the definition of entropy. After Shannon, Kullback and Leibler (1951) published a paper generalizing some of the fundamental concepts of entropy and developed the concept of cross-entropy also known as KL divergence.

Using Shannon's descriptive measure, Jaynes (1957, 1963) proposed a normative principle, the principle of maximum entropy, to guide the assignment of probability distributions. This principle states that when information about an uncertainty does not uniquely specify a distribution, one should assign the probability distribution with maximum entropy subject to the partial information. The principle of maximum entropy is a generalization of Laplace's principle of insufficient reason, which states that knowing the possibilities with no additional information, one should assign equal probabilities to all events. We will challenge some of these conclusions.

Jaynes (1968) presented an application of the maximum entropy principle and solved the problem of choosing the correct priors on Bayesian estimation of probabilities. That same year, Ireland and Kullback (1968) returned to the problem proposed by Deming and Stephan and applied the concept of entropy by minimizing the KL divergence among tables. Later, Thomas (1979) demonstrated how to apply the principle of maximum entropy to obtain a unique probability distribution from bounded probabilities and moments.

The work already mentioned was the foundation for information theory and the basis for several applications in relation to probability assessments. However, the main concern was still to develop solutions to approximate joint probability distributions, without regard to the quality of such solutions.

Jaynes (1982) considered the quality of the maximum entropy approximation and presented the Entropy Concentration Theorem (ECT), which states that for a set of distributions that match the same information, the distributions tend to

concentrate near the point of maximum entropy. In other words, an ϵ-Ball containing the maximum entropy distribution will be more heavily populated than any other ϵ-Ball. This argument supports the maximum entropy approximation as a good alternative. However, our work will show that the assumptions made by the ECT do not necessarily yield an approximation having good accuracy. Therefore, the problem of measuring the accuracy of an approximation is still unsolved.

In 1994, two authors published papers that advanced the understanding of accuracy in a probability distribution. First, Mackenzie (1994) explored a discrete version of the theory of copulas by Sklar (1959) and developed a method to recreate discrete maximum entropy copulas. This work developed a family of copulas that share the same dependence structure, and from that family, presented the copula with maximum entropy. Second, Lowell (1994) analyzed the sensitivity to dependence on random variables for a decision process. The correlation structure of the joint probabilities and their relation with entropy provide an important step in the development of the theory. Moreover, Lowell was also interested in the possibility of reducing the size of the family of distributions by detecting which information is most sensible. This was the first paper to deem accuracy as being related to $\mathbb{T}$.

Not all the distribution approximations follow the principle of maximum entropy, even though professionals frequently assume independence to model joint distributions. Keefer (2004) gave an interesting approximation that does not follow the principle of maximum entropy. This method consists of finding an external variable that explains the correlation structure. The problem with this method is its being limited to binary variables. To allow for this, the paper presented evaluation tables comparing this method to other methods.

A similar procedure to the one used in Keefer (2004) was used later in Abbas (2006) and Bickel and Smith (2006). Abbas presented a decision evaluation and quantified the changes generated by the entropy approximation and the number of

assessments. Bickel and Smith presented an entropy model for sequential exploration where the decision to drill an oil well is given by the interactions among all random variables. Both papers measure the goodness of the approximation by choosing appropriate measures and comparing maximum entropy to previous known approximations through a simulation process. The findings of these papers make clear that most of the time, the entropy model has higher accuracy than previous models. All the previous work presented the accuracy measures in terms of "relative accuracy," that is, the accuracy of an approximation with respect to other approximations. Hence, there is still work to be done in measuring the accuracy of a distribution in relation to $\mathbb{T}$, and not just in relation to other approximations.

1.5 Dissertation Outline

This introduction has briefly described the components of the joint probability distribution evaluation procedure. The remainder of this dissertation is organized as follows:

Chapter 2 discusses methods to approximate probability distributions based on the geometric properties of the set $\mathbb{T}$. We review three existing approximations and introduce four new approximations that have interesting properties. Chapter 3 presents a sampling procedure to create a collection of distributions in the interior of $\mathbb{T}$. Chapter 4 presents the measures of accuracy to be used to compare the approximations to the truth set $\mathbb{T}$. Chapter 5 presents our accuracy results for a number of truth sets. Chapter 6 develops a new approach to model decisions with partial information based on concepts described in previous chapters. Chapter 7 identifies future research directions.

Chapter 2

Approximation Methods

Three models for approximating joint probability distributions were found in the literature. This chapter presents these models and adds four new ones based on different centers of polyhedra.

2.1 Existing Approximation Models

The Independence Approximation (IA), the Underlying Event Model (UE), and the Maximum Entropy Model (ME) are three of the most discussed methods to recreate joint distributions in the literature. The IA assumes that there are no dependencies among random variables. The UE, proposed by Keefer (2004), assumes that all variables are conditionally independent given an external random variable Y. Finally, the ME, described by Lowell (1994), uses concepts first developed by Kullback (1968) and Jaynes (1957) to recreate higher-order assessments from simple conditional probabilities. The three approximations present different assumptions about the use and manipulation of available information.

Figure 2.1 presents the influence diagrams or Bayesian networks (Howard and Matheson, 2005) for these three approximation methods in the case of three random variables. Case (a) corresponds to a joint distribution based on full information, and cases (b-d) represent the IA, UE, and ME approximations, respectively.

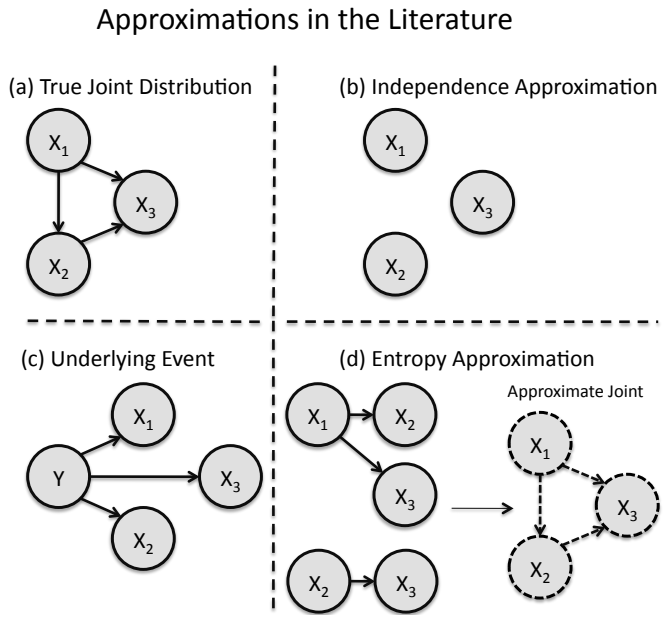

Figure 2.1: Influence diagrams for variables X_1, X_2, X_3 (absence of arrows denotes lack of influence between variables). (a) True Joint Distribution (unknown). (b) Approximation according to IA. (c) UE, in which all dependences are captured by means of an additional variable Y. (d) ME generates an approximation (dotted lines) by recovering information from partial assessments.

2.1.1 Independence Approximation Model

The Independence Approximation (IA) assumes there are no interactions among any of the random variables. Under this model, the probability decomposition in Equation (1.2) becomes Equation (2.1).

$$P(\mathbf{X}^{IA}) = P(X_1)P(X_2)\dots P(X_n). \tag{2.1}$$

By assuming independence among variables, the number of assessments required is low and the assessments become easy to perform. The main concern with the IA is the processing of information. If two variables are known to have a large correlation, the IA will treat them is if they were independent, which in turn deny the ability to

use of the information available. As will be seen later, the IA is just a special case of ME with limited information.

2.1.2 Underlying Event Model

The Underlying Event Model (UE), proposed by Keefer (2004), recovers some information on the probabilistic dependence among variables and uses a new variable Y to model such dependence while requiring few assessments. This model assumes that X_i for $i = 1, 2, \ldots, n$ are independent given Y, leaving the correlation structure depending entirely on the random variable Y. According to this model, Equation (1.2) becomes:

$$P(\mathbf{X}^{UE}) = P(Y) \cdot P(X_1|Y) \cdot P(X_2|Y) \ldots P(X_n|Y). \tag{2.2}$$

The UE works only with binary random variables and has no flexibility to incorporate more information into the model. However, it is easy and fast to implement. The model defines p_i as the probability of success of variable i, and $p_{j|k}$ as the probability of success of variable j given that variable k is a success. Then the following assessments are required:

- Assess the marginal probabilities, $p_i, \quad i = 1, 2, \ldots, n$.
- Choose j and k that correspond to the largest and second largest values of p_i, respectively.
- Assess $p_{j|k}$ and define $p_0 = \frac{p_j}{p_{j|k}}$.
- Define $p_{i|0} = \frac{p_i}{p_0}, \quad i = 1, 2, \ldots, n$.
- Define $p(i$ success, j success, k success $) = p_0 \cdot p_{i|0} \cdot p_{j|0} \cdot p_{k|0}$.

2.1.3 Maximum Entropy Model

Proposed initially by Jaynes (1957) and Kullback (1968), the Maximum Entropy model (ME) derives an approximate distribution using partial information. Various authors, such as Lowell (1994), Abbas (2006), and Bickel and Smith (2006), have expanded this model and found interesting applications in the DA framework.

Maximization of entropy can be achieved through the minimization of the Kullback-Leibler divergence (KL) between $\mathbf{p}$ and the IA noted as $\bar{\mathbf{p}}$, as described in Bickel and Smith (2006):

$$\min_{\mathbf{p}=\{p_1,\ldots,p_n\}} \sum_{i=1}^{n} \quad p_i \ln(\frac{p_i}{\bar{p}_i}), \tag{2.3}$$

$$s.t. \quad \mathbf{A}\cdot\mathbf{p} = \mathbf{b}, \tag{2.4}$$

$$\mathbf{p} \geq 0. \tag{2.5}$$

The optimization is relative to $\bar{\mathbf{p}} = \{\bar{p}_1, \ldots, \bar{p}_n\}$ and subject to the set of linear constraints $\mathbf{A}\cdot\mathbf{p} = \mathbf{b}$ that match the expert's beliefs. However, it is easier to solve the problem by transforming it into an unconstrained convex optimization model using the dual formulation as follows:

$$\max_{\lambda} \left(-\sum_{i=1}^{n} \bar{p}_i \cdot \exp^{-1+\sum_j a_{i,j}\lambda_j} + \sum_j \lambda_j b_j \right), \tag{2.6}$$

where $i = 1, \ldots, n$ indexes the n joint outcomes of $\mathbf{p}$, and j indexes the rows of matrix $\mathbf{A}$. The vector $\mathbf{b}$ encodes the DM's beliefs into the constraints $\mathbf{A}\cdot\mathbf{p} = \mathbf{b}$. And the scalar $a_{i,j}$ is the element of the i^{th} column and the j^{th} row of $\mathbf{A}$.

Solving Equation (2.6) and finding the optimal λ^* yields $p_i = \bar{p}_i \cdot \exp^{-1+\sum_j a_{i,j}\lambda_j^*}$.

Then the decomposition in Equation (1.2) becomes:

$$P(\mathbf{X}^{ME}) = P_{X_1} \cdots P_{X_n} \cdot \exp^{-1+\sum_j a_{i,j}\lambda_j^*} = P(\mathbf{X}^{IA}) \cdot \exp^{-1+\sum_j a_{i,j}\lambda_j^*} . \tag{2.7}$$

Equation (2.7) is a modification of the IA, where $\exp^{-1+\sum_j a_{i,j}\lambda_j^*}$ works as a discrete copula (Sklar, 1959; Nelsen, 2005) that corrects the IA to match the expert's beliefs.

The ME is easy to implement and fast to solve. Additionally, the model has the flexibility to manage any amount of information as long as it is consistent with a joint probability structure. As with the truth set, the feasible region of the optimization problem is defined exclusively by linear constraints. The ME provides a joint distribution with a rich information structure, that is, the encoding of the outcomes of the joint distribution requires a maximum expected number of bits to be described efficiently (Cover and Thomas, 2006).

2.1.4 First Example to Illustrate the Various Models

To illustrate these models, assume a discrete joint distribution (see Table 2.1), which in most circumstances will be unknown. Although the joint probability mass function (pmf) can not be observed, other information may be known, as shown in Table 2.2. As discussed before, the amount of available information and the assumptions made by each particular model define a uniquely approximated pmf. Table 2.3 shows the approximated pmfs for IA, UE, and ME.

In this example, more information results in a pmf closer to the original one. Unfortunately, this cannot be generalized because the true distribution would be unknown in real life. Therefore, direct comparisons are infeasible.

Table 2.1: True joint pmf.

Joint events			Real pmf
x_1	x_2	x_3	$P(x_1, x_2, x_3)$
1	1	1	0.300
1	1	0	0.050
1	0	1	0.050
1	0	0	0.100
0	1	1	0.125
0	1	0	0.125
0	0	1	0.125
0	0	0	0.125

Table 2.2: Marginal and pairwise information.

Marginal and conditional assessments	
$P(X_1 = 1)$	0.5
$P(X_2 = 1)$	0.6
$P(X_3 = 1)$	0.6
$P(X_2 = 1 \mid X_1 = 1)$	0.700
$P(X_3 = 1 \mid X_1 = 1)$	0.700
$P(X_3 = 1 \mid X_2 = 1)$	0.708

Table 2.3: Joint pmf approximations.

Joint events			IA pmf	UE pmf	ME pmf
1	1	1	0.1800	0.2509	0.2687
1	1	0	0.1200	0.1033	0.0815
1	0	1	0.1200	0.1033	0.0815
1	0	0	0.0800	0.0425	0.0685
0	1	1	0.1800	0.1741	0.1563
0	1	0	0.1200	0.0717	0.0936
0	0	1	0.1200	0.0717	0.0936
0	0	0	0.0800	0.1825	0.1563

2.2 Proposed Approximation Models

We explore four "new" approximations based on different centers of polyhedra. The idea of using centers of polyhedra as approximations is related to the center of mass (CM) of a convex body with uniform density, as shown in Equation (2.8).

$$CM(\mathbb{T}) = \frac{\int_{\mathbf{x}\in\mathbb{T}} \mathbf{x} d\mathbf{x}}{\int_{\mathbf{x}\in\mathbb{T}} d\mathbf{x}}. \tag{2.8}$$

We want to find a point inside $\mathbb{T}$ that shares similar properties with the CM, which has been well studied. However, the CM is a difficult point to compute. As

Ong et al. (2003) showed, there are methods to calculate $\int_{\mathbf{x}\in\mathbb{T}} d\mathbf{x}$ exactly, but the efficiency of the algorithms is exponential in the dimension of the set, making the CM unsuitable for practical applications.

Although it is not practical to calculate the CM for general polytopes, the concept itself provides us with desirable properties, such as having a pmf far from the boundary and equidistant to all the extreme points of $\mathbb{T}$. The following new approximation models satisfy some of these requirements under arbitrary polytopes.

2.2.1 Analytic Center

The analytic center (AC) has been mainly used to initialize interior point algorithms. The simplicity of this model makes it easy to implement and quick to solve. The main idea is to generate an optimization problem that pushes the solution as far as possible from boundaries. The model is defined in Bertsimas and Tsitsiklis (1997) as:

$$\begin{aligned} \max \quad & \sum_{i=1}^{n} \log p_i, \\ s.t. \quad & \mathbf{Ap} = \mathbf{b}, \end{aligned}$$

where $\mathbf{p} = \{p_1, \ldots, p_n\}$ represents the joint distribution approximation. The model can be expanded to use inequality constraints of the form $\mathbf{A}_j \cdot \mathbf{p} \geq b_j$, where $\mathbf{A}_j$ is the j^{th} row of $\mathbf{A}$, by adding the term $\log(\mathbf{A}_j \cdot \mathbf{p} - b_j)$ to the objective function. However, the rest of this dissertation considers only equality constraints.

One disadvantage of AC is the inconsistency of the polytope representation. As shown by Ye (1997), different representations of the same set have different AC solutions. For example, the addition of a redundant constraint pushed the AC far from this constraint. Hence, it is in principle a useful method so long as $\mathbb{T}$ its free of

redundant constraints.

In Figure 2.2 (taken from Boyd and Vandenberghe, 2004), we can observe the analytic center and the influence generated by the inequality constrains for a two dimensional polytope.

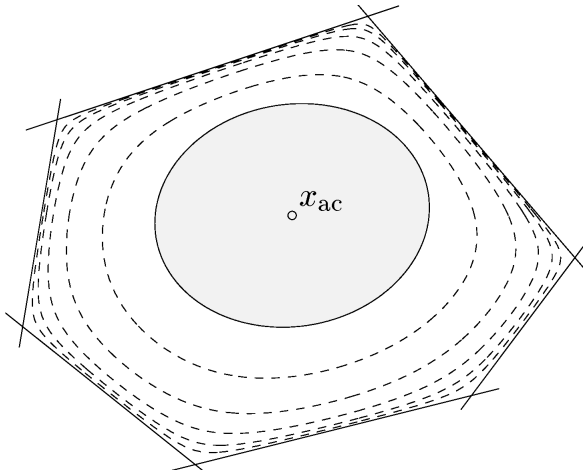

Figure 2.2: Analytic Center.

From the information perspective, if the ME yields the maximum "expected" number of bits to encode the outcome of a random variable, then the AC yields the minimum "total" number of bits to encode all the outcomes of a random variable. For example, Abbas (2006) provided an intuitive interpretation of ME as the maximum expected number of yes/no questions needing to be asked to determine which random event was realized. Using the same analogy, the AC corresponds to the minimum number of yes/no questions we need to ask to find which random event was realized in every possible outcome of the realization.

2.2.2 Chebyshev's Center

Chebyshev's center (ChSC) provides an alternative to the analytic center. The main idea of this method is to expand a ball in the interior of the set until the boundary of the ball reaches the boundary of the set and can not be further expanded.

Then the center of the ball is taken to be the approximation.

ChSC provides a point in $\mathbb{T}$ that is the farthest from the boundary of $\mathbb{T}$. Unlike the AC, this model is invariant to the representation of $\mathbb{T}$, which means that redundant constraints do not modify the optimal solution. Once the model is feasible for the optimal set of active constraints, it is also feasible for all redundant constraints. Figure 2.3 (taken from Boyd and Vandenberghe, 2004) depicts the main idea behind ChSC in a two-dimensional polytope. ChSC is the center of the largest volume hypersphere inscribed in $\mathbb{T}$.

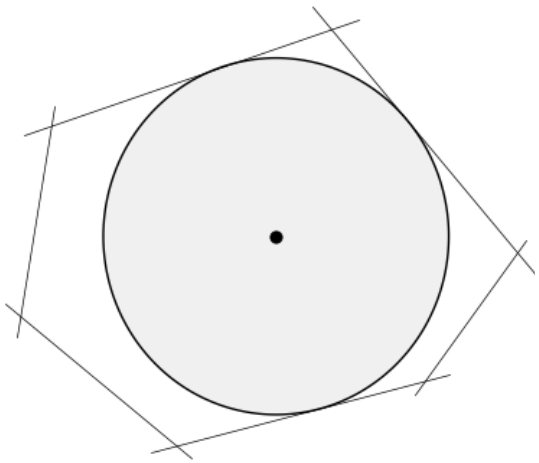

Figure 2.3: Chebyshev's center. Figure taken from Boyd and Vandenberghe (2004).

In Model 2.9 (referring to Equations 2.9a-2.9b), as described in Boyd and Vandenberghe (2004), r and $\mathbf{x_c}$ represent the radius and center of the hypersphere, m is the number of constraints, $\mathbf{a}_i^T \in \mathbb{R}^n$ represents the i^{th} constraint, and b_i represents the beliefs that define $\mathbb{T}$ for $i = 1, \ldots, m$.

$$\max \quad r, \tag{2.9a}$$

$$s.t. \quad \mathbf{a}_i^T \mathbf{x_c} + r||\mathbf{a}_i^T||_2 \leq b_i, \qquad i = 1, \ldots, m. \tag{2.9b}$$

This model does require $\mathbb{T}$ to be a full dimensional set, i.e., the use of equality constraints is not permitted. This is a problem since $\mathbb{T}$ is not a full dimensional

polytope. To address this problem, Model 2.9 is modified to become Model 2.10 by forcing $\mathbf{x_c}$ to be constrained by $\mathbf{Ax_c} = \mathbf{b}$ while leaving the hypersphere to expand in the interior of the set defined by the inequality and non-negativity constraints $\mathbf{g}_i^T\mathbf{x} \leq h_i$ for $i = 1, \ldots, k$. The new model becomes:

$$\begin{aligned} \max \quad & r, && && (2.10a) \\ s.t. \quad & \mathbf{g}_i^T\mathbf{x_c} + r||\mathbf{g}_i^T||_2 \leq h_i, && i = 1, \ldots, k, && (2.10b) \\ & \mathbf{Ax_c} = \mathbf{b}. && && (2.10c) \end{aligned}$$

This modification defines the largest ball in the interior of $\mathbf{Gx} \leq \mathbf{h}$ whose center is on the hyperplane $\mathbf{Ax_c} = \mathbf{b}$. One of the main advantages of ChSC is that it can be solved using linear programing, which is easy to implement and fast to solve. The model provides a joint distribution in the relative interior of $\mathbb{T}$, while trying to increase the distance from $\mathbf{x_c}$ to the boundary of the set defined by the inequality and non-negativity constraints. In particular, if the only inequality constraints are the non-negativity constraints (as assumed in this dissertation), ChSC provides an approximation for which the smallest-probability event is maximized.

2.2.3 Maximum Volume Inscribed Ellipsoid Center

The maximum volume inscribed ellipsoid center (MVIE), first studied by Fritz (1948), uses the relative interior of $\mathbb{T}$ to provide a center to the set of joint probability distributions. As with ChSC, the MVIE assumes the set $\mathbb{T}$ to be full dimensional. MVIE creates a ball in the interior of the set and expands its axes in an independent and symmetric way, generating an ellipse. When the ellipse reaches the maximum volume (i.e., reaches the boundary of $\mathbb{T}$), its center serves as a center for the truth set.

One particular problem in the MVIE is the dimensionality of $\mathbb{T}$. Each equality constraint reduces the dimension by one degree, making the set unsuitable for the model, given the full-dimensionality requirement. This problem can be solved by forcing the set $\mathbb{T}$ into a full dimensional polytope $\mathbb{T}_\epsilon^+$ by perturbing the space a distance $\epsilon > 0$ into the two directions given by each vector perpendicular to $\mathbb{T}$. For example, by assuming $\mathbb{T} = \{\mathbf{x}|\mathbf{A}\mathbf{x} = \mathbf{b},\ \mathbf{x} \geq 0\}$, perturbing $\mathbb{T}$ yields $\mathbb{T}_\epsilon^+ = \{\mathbf{x}|\mathbf{A}\mathbf{x} \leq \mathbf{b} + \epsilon,\ \mathbf{A}\mathbf{x} \geq \mathbf{b} - \epsilon,\ \mathbf{x} \geq 0\}$. See Figure (2.4).

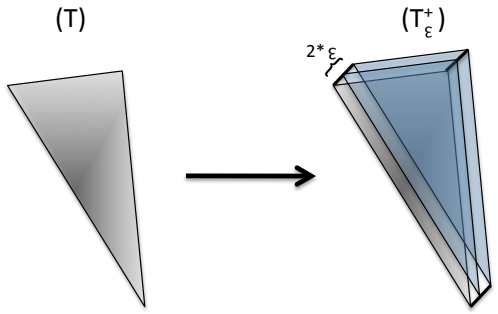

Figure 2.4: Polyhedron perturbation.

Using the perturbed set $\mathbb{T}_\epsilon^+$ permits solving for the ellipsoid $\mathcal{E}(\mathbf{x_c}, \mathbf{E})$, where $\mathbf{x_c}$ is the center of $\mathcal{E}$, and $\mathbf{E}$ is a symmetric positive definite matrix that define eigenvectors and eigenvalues that describe the direction and magnitude of the axes in the ellipse.

The maximum volume inscribed ellipsoid is part of the "maxdet" family of problems. This family can be solved using positive semi-definite programing, as described in Vandenberghe et al. (1998). We present the MVIE (Model 2.11) as described in Boyd and Vandenberghe (2004).

$$\max_{(\mathbf{x},\mathbf{E})} \quad \log\det \mathbf{E}, \tag{2.11a}$$

$$s.t. \quad \mathbf{A}\mathbf{x} + \mathbf{H}(\mathbf{E}) \leq \mathbf{b}, \tag{2.11b}$$

$$\mathbf{E} \succ 0, \tag{2.11c}$$

$$\mathbf{H}(\mathbf{E}) = (||\mathbf{E}\mathbf{a}_1||, \ldots, ||\mathbf{E}\mathbf{a}_m||)^T \in \mathbb{R}^m. \tag{2.11d}$$

Equation (2.11b) forces $\mathcal{E} \subseteq \mathbb{T}_\epsilon^+$. Equation (2.11d) defines $\mathbf{H}(\mathbf{E})$ as the vector whose elements are the norms of $\mathbf{E}\mathbf{a}_i$ $\forall i = 1, \ldots, m$ and $\mathbf{a}_i$ is the i^{th} row of $\mathbf{A}$. Finally, Equation (2.11c) provides necessary conditions for $\mathcal{E}$ to be an ellipse.

Figure 2.5 (taken from Boyd and Vandenberghe, 2004) illustrates the main idea behind the MVIE in a two-dimensional polytope. The MVIE is the center of the largest volume hyper-ellipsoid inscribed in $\mathbb{T}$.

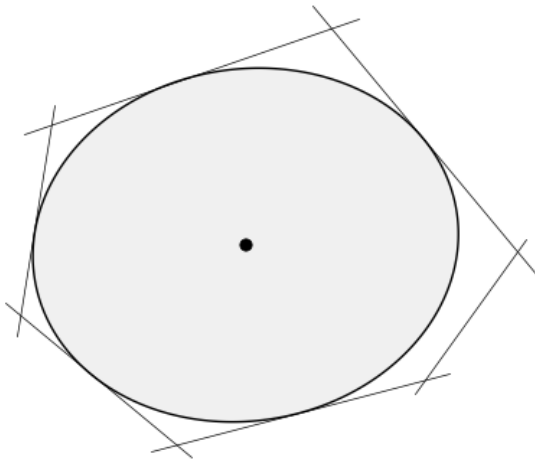

Figure 2.5: Maximum Volume Inscribed Ellipsoid Center.

This method provides the center of mass of an ellipsoid $\mathcal{E}$ that mimics the geometric shape of $\mathbb{T}_\epsilon^+$. In principle, this method should be a good alternative to the AC and ChSC, but it has flaws, such as longer running time than the approximations

previously discussed in this chapter. Zhang (1999) observed expected running times of about 97 seconds for random problems with 100 variables and 500 inequality constraints. These running times increase considerably with the number of variables and constraints.

2.2.4 Dynamic Average Sample Center

The last center of polyedra we consider is the dynamic average center (DAC). This center is generated by calculating the average (element-wise) of all the joint distributions in a sampled collection from $\mathbb{T}$:

$$\mathbf{x}_n = \sum_{i=1}^{n} \frac{\mathbf{x}_i}{n}. \tag{2.12}$$

Since $\mathbb{T}$ is closed and bounded, the limit of $\mathbf{x}_n$ converges to the first moment of the uniform sample with support on $\mathbb{T}$. The DAC is perhaps the best approximation, given a sufficient collection of samples. However, sufficient can mean billions of iterations for high dimensional polytopes.

It is expected that the DAC will achieve better accuracy than that of any other approximation, given that it is created with the same sample used to measure its accuracy. This bias needs to be considered when testing accuracy of results. This study will use the DAC as a frame of reference for accuracy comparisons among approximations.

Algorithm Implementations.

The algorithms for the main four centers proposed in Chapter 2 were implemented in CVX: Matlab Software for Disciplined Convex Programming (Grant and Boyd, 2011).

```
cvx_begin
variable x(64);
maximize(log(x(1))+log(x(2))+log(x(3))+log(x(4))+log(x(5))+
log(x(6))+log(x(7))+log(x(8))+log(x(9))+log(x(10))+log(x(11))+
log(x(12))+log(x(13))+log(x(14))+log(x(15))+log(x(16))+log(x(17))+
log(x(18))+log(x(19))+log(x(20))+log(x(21))+log(x(22))+log(x(23))+
log(x(24))+log(x(25))+log(x(26))+log(x(27))+log(x(28))+log(x(29))+
log(x(30))+log(x(31))+log(x(32))+log(x(33))+log(x(34))+log(x(35))+
log(x(36))+log(x(37))+log(x(38))+log(x(39))+log(x(40))+log(x(41))+
log(x(42))+log(x(43))+log(x(44))+log(x(45))+log(x(46))+log(x(47))+
log(x(48))+log(x(49))+log(x(50))+log(x(51))+log(x(52))+log(x(53))+
log(x(54))+log(x(55))+log(x(56))+log(x(57))+log(x(58))+log(x(59))+
log(x(60))+log(x(61))+log(x(62))+log(x(63))+log(x(64)))
subject to
A*x==B;
cvx_end
```

(a) Analytic Center.

```
cvx_begin
variable x(64);
Variable r;
maximize(r)
subject to
A*x==B;
-x+r<=0;
cvx_end
```

(b) Chebyshev's Center.

```
x=ones(64,1);
cvx_begin
variable L(22);
maximize(L'*B-exp(-1+L'*A(:,1))-exp(-1+L'*A(:,2))-exp(-1+L'*A(:,3))-
exp(-1+L'*A(:,4))-exp(-1+L'*A(:,5))-exp(-1+L'*A(:,6))-exp(-1+L'*A(:,7))-
exp(-1+L'*A(:,8))-exp(-1+L'*A(:,9))-exp(-1+L'*A(:,10))-exp(-1+L'*A(:,11))-
exp(-1+L'*A(:,12))-exp(-1+L'*A(:,13))-exp(-1+L'*A(:,14))-exp(-1+L'*A(:,15))-
exp(-1+L'*A(:,16))-exp(-1+L'*A(:,17))-exp(-1+L'*A(:,18))-exp(-1+L'*A(:,19))-
exp(-1+L'*A(:,20))-exp(-1+L'*A(:,21))-exp(-1+L'*A(:,22))-exp(-1+L'*A(:,23))-
exp(-1+L'*A(:,24))-exp(-1+L'*A(:,25))-exp(-1+L'*A(:,26))-exp(-1+L'*A(:,27))-
exp(-1+L'*A(:,28))-exp(-1+L'*A(:,29))-exp(-1+L'*A(:,30))-exp(-1+L'*A(:,31))-
exp(-1+L'*A(:,32))-exp(-1+L'*A(:,33))-exp(-1+L'*A(:,34))-exp(-1+L'*A(:,35))-
exp(-1+L'*A(:,36))-exp(-1+L'*A(:,37))-exp(-1+L'*A(:,38))-exp(-1+L'*A(:,39))-
exp(-1+L'*A(:,40))-exp(-1+L'*A(:,41))-exp(-1+L'*A(:,42))-exp(-1+L'*A(:,43))-
exp(-1+L'*A(:,44))-exp(-1+L'*A(:,45))-exp(-1+L'*A(:,46))-exp(-1+L'*A(:,47))-
exp(-1+L'*A(:,48))-exp(-1+L'*A(:,49))-exp(-1+L'*A(:,50))-exp(-1+L'*A(:,51))-
exp(-1+L'*A(:,52))-exp(-1+L'*A(:,53))-exp(-1+L'*A(:,54))-exp(-1+L'*A(:,55))-
exp(-1+L'*A(:,56))-exp(-1+L'*A(:,57))-exp(-1+L'*A(:,58))-exp(-1+L'*A(:,59))-
exp(-1+L'*A(:,60))-exp(-1+L'*A(:,61))-exp(-1+L'*A(:,62))-exp(-1+L'*A(:,63))-
exp(-1+L'*A(:,64)))
cvx_end
for i=1:64
  x(i)=exp(-1+L'*A(:,i));
end
```

(c) Entropy Center.

```
ep=.0001;
I=eye(64);
cvx_begin
variable E(64,64) symmetric;
variable x(64);
maximize(log_det(E))
subject to
for i=1:22
A(i,:)*x+norm(E*A(i,:)',2)<=B(i)+ep;
end
for i=1:22
-A(i,:)*x+norm(E*A(i,:)',2)<=-B(i)+ep;
end
for i=1:64
-I(i,:)*x+norm(E*I(i,:)',2)<=0;
end
cvx_end
```

(d) MVIE Center.

Figure 2.6: CVX code for AC, ChSC, ME, and MVIE approximations.

Chapter 3

Generating Collections of Joint Probability Distributions

Chapter 2 defined seven methods to use partial information to generate single joint distribution approximations. This chapter presents a simulation procedure to create not one, but a collection of joint distributions uniformly sampled from a finite dimensional set consistent with the given information. Specifically, our procedure generates a collection of finite-dimensional, discrete, joint probability distributions whose marginals have finite support.

This procedure provides the necessary tools to create a collection of distributions that serves as a discrete representation of $\mathbb{T}$. Although the intention of this collection is to measure the accuracy of the approximation methods presented in Chapter 2, it can be also used independently to approach problems where the joint probability distribution is unknown.

The main idea of this sampling procedure is as follows. Consider a random vector $\mathbf{X} = \{X_1, X_2, \ldots, X_n\}$ with specified marginal distributions $F_i(X_i)$ and correlation matrix $\mathbf{\Sigma_X}$. There are infinitely many joint distributions $G(\mathbf{X})$ that match these constraints. We refer to this set of distributions as the "truth set" ($\mathbb{T}$). By "truth" we mean that any distribution within this set is consistent with the stated constraints and therefore could be the true joint distribution. Our goal is to generate a collection of joint distributions $G_i(\mathbf{X})$, i = 1 to N, that are consistent with the given

information, where N is the number of samples in our collection. As detailed below, we use the Hit-and-Run (HR) sampler to produce a collection of samples uniformly distributed in $\mathbb{T}$ (Smith, 1984).

The method suggested here is fundamentally different from other methods of random variate generation such as NORTA (Ghosh and Henderson, 2003) and chessboard techniques (Mackenzie, 1994; Ghosh and Henderson, 2001). These methods produce instantiations $\mathbf{x}$ of $\mathbf{X}$ based on a *single* distribution $G(\mathbf{X})$ that is consistent with a set of specified marginal distributions, correlation matrix, and in the case of NORTA, the assumption that the underlying dependence structure can be modeled with a normal copula. Thus, NORTA and the chessboard techniques produce random variates based on a single distribution contained within $\mathbb{T}$.

As will be seen, in our discrete setting, we envision the sample space of $\mathbf{X}$ as being fixed and therefore seek to create a set of discrete *probabilities* that are consistent with the given information. This focus is on generating probabilities $G(\mathbf{X})$ rather than outcomes of $\mathbf{X}$. Within the decision analysis community, for example, the problem of specifying a probability distribution given partial information is well known (Jaynes, 1968) and of great practical importance (Abbas, 2006; Bickel and Smith, 2006). For example, suppose the average number rolled on a six-sided die is known to be 4.5. What probability should one assign to each of the six faces? As discussed previously, some possible approaches were described in Chapter 2. If we use ME (Jaynes, 1957, 1968), the approximation will specify the (unique) probability mass function (pmf) that is closest to uniform, while having a mean of 4.5. The procedure described in this chapter was developed to test the accuracy of these approximations. Hence, it explores a larger number of probability distributions uniformly sampled from $\mathbb{T}$.

3.1 State of Knowledge

The literature does not directly address the creation of a collection of joint probability distributions, but some papers have indirectly developed simple ideas in an attempt to generate data to test different models. Keefer (2004) and Bickel and Smith (2006) used Bayesian trees to create collections of joint probabilities with correlation matrices that on average approximate $\frac{1}{2}$. Abbas (2006) instead sampled distributions using an order statistics method developed by David (1981). These methods generate consistent arbitrary joint distributions. However, both produce collections that are inconsistent with respect to pre-specified partial information.

Because no existing methodology can sample a collection of discrete joint probability distributions consistent with pre-specified partial information, we turn to methods for sampling the interior of a polytope as a basis to develop a collection of joint distributions. Among different sampling procedures, HR showed to be effective and easy to implement. However, it is not the only possible sampling procedure. The following presents a brief review of alternative methods and discusses their shortcomings.

The first set of sampling procedures are acceptance-rejection methods (von Newmann, 1963). These methods embed the region of interest S within a region D for which a uniform sampling algorithm is known. For example, one might embed S within the union of non-overlapping hyperrectangles or hyperspheres (Rubin, 1984) and then uniformly sample from D, rejecting points that are not also in S. As noted by Smith (1984), this method suffers from two significant problems as far as our work is concerned. First, embedding the region of interest within a suitable superset may be very difficult (Rubin, 1984). Second, as the dimension of S increases, the number of rejections per accepted sample (i.e., the rejection rate) grows exponentially. For

example, Smith (1984) showed that when S is a 100-dimensional hypercube and D is a circumscribed hypersphere, 10^{30} samples are required on average for every sample that is accepted. The polytopes that we consider are at least this large and more complex.

The second alternative, described by Devroye (1986), consists of generating random points within the polytope by taking random convex combinations of the polytope's vertices. This method is clearly infeasible for most problems of practical interest, since it requires specifying all of the polytope's vertices in advance. For high-dimensional polytopes, this is very difficult if not infeasible. For example, consider a simple joint probability distribution comprised of eight binary random variables, whose marginal distributions are known. The polytope encoding these constraints could have up to 10^{13} vertices (McMullen, 1970). Although this is an upper bound, the number of vertices likely to be encountered in real problems is still enormous (Schmidt and Mattheiss, 1977).

The final alternative is based on decomposition, in which the area of interest is divided into non-overlapping segments for which uniform sampling is easy to perform. Again, this method requires full knowledge of all the extreme points of $\mathbb{T}$. Rubin (1984) provided a brief review of such methods and noted that they entail "significant computational overhead" and are practical only for low-dimensional polytopes.

HR is a random walk through the region of interest. As such, it avoids the above problems because every sampled point is feasible and knowledge of the polytope's vertices is not required. The drawback of this method is that the samples are only asymptotically uniformly distributed, implying that to bring the sample set acceptably close to uniform may entail numerous samples (Rubin, 1984; Smith, 1984). This issue is addressed below.

3.2 Sampling Example to Illustrate Proposed Technique

To illustrate and motivate the proposed technique, suppose we are deciding whether to market a new product. At present, we are uncertain about our production costs and whether a competitor will enter the market. Let V_1 represent that the competitor will enter the market ($V_1 = 1$) or will not ($V_1 = 0$), and let V_2 represent our production costs being high ($V_2 = 1$) or low ($V_2 = 0$). Graphically, these scenarios can be represented using the binary probability tree in Figure 3.1(a).

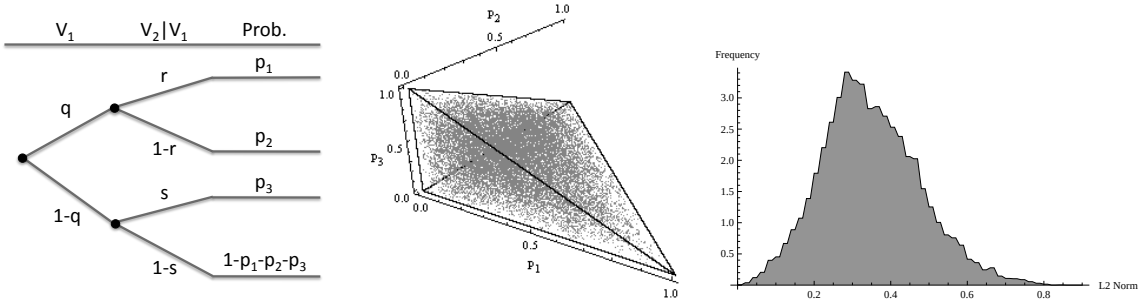

(a) Probability Tree. (b) Truth Set. (c) Euclidean Distance Distribution.

Figure 3.1: Sampling two binary variables with unknown information.

We start by assuming no knowledge of the marginal distributions of V_1 and V_2 or of their dependence structure. In this case, $\mathbb{T}$ consists of all joint distributions of (V_1, V_2) with four outcomes $n = 4$ and probabilities $\mathbf{p} = (p_1, p_2, p_3, p_4)$. The joint distributions can be simplified to use only three probabilities (p_1, p_2, p_3) because $p_4 = 1 - p_1 - p_2 - p_3$. The truth set, shown in Figure 3.1(b), is a polytope in three dimensions and its vertices represent extreme joint distributions. In this case, the center of $\mathbb{T}$ is the joint pmf $\mathbf{p} = (0.25, 0.25, 0.25, 0.25)$, which assumes the random variables are independent and with uniform marginals. The small dots in Figure 3.1(b) are samples (complete pmfs) generated by HR as described below. Measuring the Euclidean distance ($L2$-Norm) from the center of $\mathbb{T}$ to all other joint distributions

in $\mathbb{T}$ (Figure 3.1(c)) indicates that most of the samples are at 0.3 units from the center. The samples, which correspond to the distribution of volume in the truth set, are less concentrated close to the center and the corners.

Now, suppose we know that there is a 70% chance the competitor will enter the market and a 30% chance that production cost will be high (unconditioned on the entry of the competitor). The new information yields a modified probability tree (Figure 3.2(a)) and introduces two new constraints to restrict the joint distributions matching the marginal probabilities (Figure 3.2(b)).

Each constraint is a hyperplane that cuts $\mathbb{T}$, reducing its dimension by one. As shown in Figure 3.2(c), $\mathbb{T}$ is now a line with extremes at (0.3, 0.4, 0.0) and (0.0, 0.7, 0.3). As a reference, the distribution that assumes independence (i.e., the maximum entropy approximation in this case) is located at (0.21, 0.49, 0.09) and is marked with a large black dot.

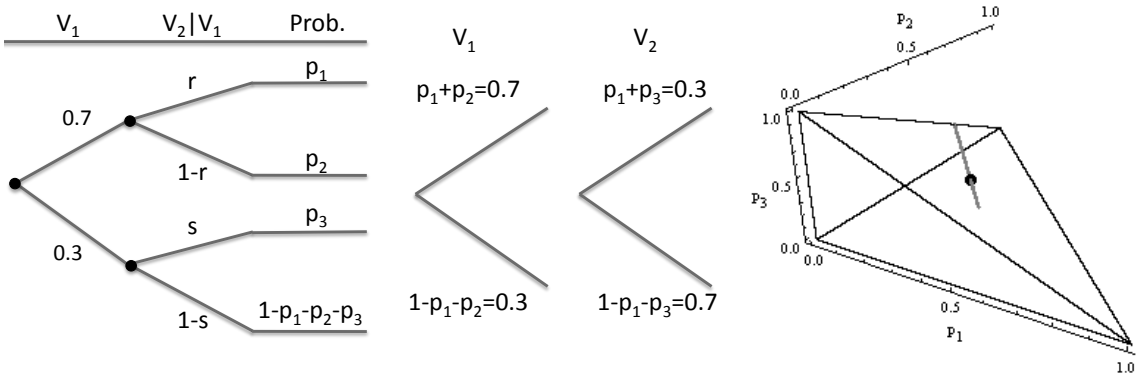

(a) Probability Tree. (b) Marginal Variables. (c) New Truth Set $\mathbb{T}$.

Figure 3.2: Sampling two binary variables with marginal probability information.

3.3 General Procedure

3.3.1 Problem Statement

The objective of this procedure is to create a collection of discrete joint probability distributions uniformly sampled from a finite-dimensional, continuous, convex, and compact set that contains all possible realizations of the joint distribution that are consistent with given information. We assume that the joint distributions are discrete with finite support, as are the marginal distributions. To ensure that our truth set is convex, we admit only information that can be encoded with linear equality constraints. Although this is certainty a limitation, it does not preclude our addressing a large class of problems that are of practical importance (Bickel and Smith, 2006).

3.3.2 Notation

In order to describe the sampling procedure, we first establish the notation through a simple example using a joint distribution with two variables: the first variable having "High," "Medium," and "Low" outcomes, and the second variable having "Up" and "Down" outcomes. This case requires one set that includes two random variables $\mathbb{V} = \{V_1, V_2\}$, plus two sets for the outcomes $\mathbb{O}^{V_1} = \{H, M, L\}$ and $\mathbb{O}^{V_2} = \{U, D\}$. Finally, we create a set including the cardinal product of all the outcomes:

$$\mathbb{U} = \{[H, U], [H, D], [M, U], [M, D], [L, U], [L, D]\}.$$

Additional sets are required to include more information, such as sets that include joint outcomes where V_1 is set to "High." A formal definition of the notation is presented next.

Notation:

Indices and sets:

$\mathbb{I}$	Set of available information.
$\mathbb{V}$	Set of random variables.
$V_i \in \mathbb{V}$	Random variable i in $\mathbb{V}$.
$\mathbb{O}^{V_i}$	Set of possible outcomes for random variable V_i.
$\omega_r^{V_i} \in \mathbb{O}^{V_i}$	Realizations for random variable V_i indexed by $r = 1, 2, \ldots, \lvert\mathbb{O}^{V_i}\rvert$.
$\mathbb{U}$	Set of all joint outcomes, $\mathbb{U} = \mathbb{O}^{V_1} \times \mathbb{O}^{V_2} \times \cdots \times \mathbb{O}^{V_{\lvert\mathbb{V}\rvert}}$.
$\omega_k \in \mathbb{U}$	Joint outcomes $\omega_k = \{\omega_r^{V_1}, \omega_s^{V_2}, \ldots, \omega_z^{V_{\lvert\mathbb{V}\rvert}}\}$ indexed by $k = 1, 2, \ldots \prod_{V_i} \lvert\mathbb{O}^{V_i}\rvert$.
$\mathbb{U}_{\omega_r^{V_i}}$	Set of joint outcomes for which random variable V_i obtains the value $\omega_r^{V_i}$.
$\mathbb{U}_{\omega_r^{V_i}\omega_s^{V_j}}$	Set of joint outcomes for which random variables V_i and V_j obtain values $\omega_r^{V_i}$ and $\omega_s^{V_j}$.

Data:

$q_{\omega_r^{V_i}}$	Probability that $V_i = \omega_r^{V_i}$.
$q_{\omega_r^{V_i}\omega_s^{V_j}}$	Probability that $V_i = \omega_r^{V_i}$ and $V_j = \omega_s^{V_j}$.
ρ_{V_i,V_j}	Moment correlation between V_i and V_j.
$\rho^r_{V_i,V_j}$	Rank correlation between V_i and V_j.
σ_{V_i,V_j}	Covariance between V_i and V_j.
$m^z_{V_i}$	The z^{th} moment of random variable V_i.

Decision variables:

$\mathbf{p}$	Vector of decision variables defining the joint probability mass function.
$p_{\omega_k} \in \mathbf{p}$	Decision variables describing the probability of the joint event ω_k.

Table 3.1 applies the set notation to the example. The variables are V_1 and V_2, and their respective marginal outcomes are $\mathbb{O}^{V_1} = \{H, M, L\}$ and $\mathbb{O}^{V_2} = \{U, D\}$. $\omega_1^{V_1} = H$ is the first possible realization of V_1. The joint outcomes $\omega_k \in \mathbb{U}$ are defined as $\omega_1 = [H, U]$, $\omega_2 = [H, D]$, $\omega_3 = [M, U], \ldots, \omega_6 = [L, D]$. The probabilities of these outcomes are $p_{\omega_1} = P(V_1 = H, V_2 = U)$, $p_{\omega_2} = P(V_1 = H, V_2 = D)$, $p_{\omega_3} = P(V_1 = M, V_2 = U), \ldots, p_{\omega_6} = P(V_1 = L, V_2 = D)$.

Dot-notation is used to marginalize the random variables. For example, $\mathbb{U}_{\omega_1^{V_1}} = \mathbb{U}_{H\cdot}$ and $\mathbb{U}_{\omega_2^{V_2}} = \mathbb{U}_{\cdot D}$, where "$\cdot$" implies marginalization over the random variable whose position it is occupying. Using the same index k for ω_k yields $\mathbb{U}_{\cdot D} = \{\omega_2, \omega_4, \omega_6\}$.

Table 3.1: Notation example.

$\mathbb{V} = \{V_1, V_2\}, \quad \mathbb{O}^{V_1} = \{H, M, L\}, \quad \mathbb{O}^{V_2} = \{U, D\},$
$\mathbb{U}_{\cdot\cdot} = \{[H, U], [H, D], [M, U], [M, D], [L, U], [L, D]\},$
$\mathbb{U}_{H\cdot} = \{[H, U], [H, D]\}, \quad \mathbb{U}_{\cdot U} = \{[H, U], [M, U], [L, U]\},$ $\mathbb{U}_{M\cdot} = \{[M, U], [M, D]\}, \quad \mathbb{U}_{\cdot D} = \{[H, D], [M, D], [L, D]\},$ $\mathbb{U}_{L\cdot} = \{[L, U], [L, D]\},$
$\mathbb{U}_{HU} = \{[H, U]\}, \quad \mathbb{U}_{HD} = \{[H, D]\}, \quad \mathbb{U}_{MU} = \{[M, U]\},$ $\mathbb{U}_{MD} = \{[M, D]\}, \quad \mathbb{U}_{LU} = \{[L, U]\}, \quad \mathbb{U}_{LD} = \{[L, D]\}.$

The set of available information, denoted as $\mathbb{I} \equiv \{q_{\omega_r^{V_i}}, q_{\omega_r^{V_i}\omega_s^{V_j}}, \rho_{V_i,V_j}, \sigma_{V_i,V_j}, m^z_{V_i}\}$, includes all the information to be included in the model. $q_{\omega_r^{V_i}} \equiv P(V_i = \omega_r^{V_i})$ is the marginal distribution for variable V_i, and $q_{\omega_r^{V_i}\omega_s^{V_j}} \equiv P(V_i = \omega_r^{V_i}, V_j = \omega_s^{V_j})$ is the pairwise joint distribution for variables $V_i,\ V_j$. When marginal information is available, it is possible to describe the moment correlation ρ_{V_i,V_j}, the rank correlation $\rho^r_{V_i,V_j}$, and the covariance σ_{V_i,V_j} for the variables V_i and V_j. Additionally, if the marginals are unknown, we can make use of known moments $m^z_{V_i}$ to constrain the truth set. Our notation can be extended to more than two variables and to match three-way or four-way probabilities.

3.3.3 Constraints

The truth set can now be constrained to match the information provided by $\mathbb{I}$. This section presents families of equations that can be used to constrain $\mathbb{T}$, creating a system of m linear equations $\mathbf{Ap} = \mathbf{b}$ and n non-negativity constraints $\mathbf{p} \geq 0$, where $\mathbf{p} = \{p_{\omega_1}, p_{\omega_2}, \ldots, p_{\omega_{|\mathbb{U}|}}\}$. $\mathbf{A} \in \mathbb{R}^{m \times n}$ defines the properties we want to constrain, and $\mathbf{b} \in \mathbb{R}^m$ represents the available information.

Matching Necessary Conditions

In all cases, the joint pmf must sum to one and each probability must be non-negative. We represent these constraints with Equations (3.1a) and (3.1b).

$$\sum_{\omega_k \in \mathbb{U}} \quad p_{\omega_k} = \ 1, \tag{3.1a}$$

$$p_{\omega_k} \geq \ 0, \qquad \forall \omega_k \in \mathbb{U}. \tag{3.1b}$$

Equations (3.1a) through (3.1b) give the necessary and sufficient conditions for $\mathbf{p}$ to be a pmf and are required in all cases. Equation (3.1a) reduces the dimension of the polytope $\mathbb{T}$ from n to $n-1$, and Equation (3.1b) limits $\mathbb{T}$ to positive quadrants. This constraint alone assures that $\mathbb{T}$ is a compact set.

Matching Marginal and Pairwise Probabilities

A second set of equations is used when information is available regarding the marginal and pairwise probabilities. Equation (3.2a) requires that the joint probabilities match the marginal assessments, while Equation (3.2b) requires that they match pairwise joint assessments.

$$\sum_{\omega_k \in \mathbb{U}_{\omega_r^{V_i}}} p_{\omega_k} = q_{\omega_r^{V_i}} \qquad \forall\, V_i \in \mathbb{V},\ \omega_r^{V_i} \in \mathbb{O}^{V_i}, \tag{3.2a}$$

$$\sum_{\omega_k \in \mathbb{U}_{\omega_r^{V_i}\omega_s^{V_j}}} p_{\omega_k} = q_{\omega_r^{V_i}\omega_s^{V_j}} \ \forall\ V_i, V_j \in \mathbb{V}, (\omega_r^{V_i}, \omega_s^{V_j}) \in \mathbb{O}^{V_i} \times \mathbb{O}^{V_j}. \tag{3.2b}$$

Equations (3.2a) and (3.2b) can be extended to cover three-way, four-way, or higher-order joint probability information.

Equations Matching Moments

If the outcomes can be represented as numerical values instead of categorical data, moment information can be matched using Equations (3.3a) through (3.3c). This family of equations is useful for well-known continuous distributions, or simply when the moments are available. These equations are always linear, making them easy to implement.

$$\sum_{\omega_l^{V_i} \in \mathbb{O}^{V_i}} \left[\omega_l^{V_i} \cdot \sum_{\omega_k \in \mathbb{U}_{\omega_l^{V_i}}} p_{\omega_k} \right] = m^1_{V_i} \quad \forall\, V_i \in \mathbb{V}, \tag{3.3a}$$

$$\sum_{\omega_l^{V_i} \in \mathbb{O}^{V_i}} \left[\left(\omega_l^{V_i}\right)^2 \cdot \sum_{\omega_k \in \mathbb{U}_{\omega_l^{V_i}}} p_{\omega_k} \right] = m^2_{V_i} \quad \forall\, V_i \in \mathbb{V}, \tag{3.3b}$$

$$\sum_{\omega_l^{V_i} \in \mathbb{O}^{V_i}} \left[\left(\omega_l^{V_i}\right)^z \cdot \sum_{\omega_k \in \mathbb{U}_{\omega_l^{V_i}}} p_{\omega_k} \right] = m^z_{V_i} \quad \forall\, V_i \in \mathbb{V}. \tag{3.3c}$$

Equation (3.3a) matches the joint distribution with the expected value for variable V_i. Equation (3.3b) matches the second moment and can be used to match variance if $m^1_{V_i}$ is known. Equation (3.3c) is a generalization for the z^{th} moment.

This equation can be illustrated by taking the example in Section 3.3.2 and providing numerical values for the current outcomes {High=10, Medium=6, Low=2} and {Wet=10, Dry=1} for V_1 and V_2, respectively. The first moments become:

$$10 \cdot \sum_{\omega_k \in \mathbb{U}_H} p_{\omega_k} + 6 \cdot \sum_{\omega_k \in \mathbb{U}_M} p_{\omega_k} + 2 \cdot \sum_{\omega_k \in \mathbb{U}_L} p_{\omega_k} = m^1_{V_1},$$
$$10 \cdot \sum_{\omega_k \in \mathbb{U}_W} p_{\omega_k} + 1 \cdot \sum_{\omega_k \in \mathbb{U}_D} p_{\omega_k} = m^1_{V_2},$$

where

$$P(V_1 = 10) = \sum_{\omega_k \in \mathbb{U}_H} p_{\omega_k} \qquad P(V_1 = 6) = \sum_{\omega_k \in \mathbb{U}_M} p_{\omega_k} \qquad P(V_1 = 2) = \sum_{\omega_k \in \mathbb{U}_L} p_{\omega_k},$$
$$P(V_2 = 10) = \sum_{\omega_k \in \mathbb{U}_W} p_{\omega_k} \qquad P(V_2 = 1) = \sum_{\omega_k \in \mathbb{U}_D} p_{\omega_k}.$$

If the marginal distributions are known, Equation 3.3 becomes redundant. However, in any other scenario, the moment-matching family will be a relevant constraint.

Matching Covariance and Correlation

If the first moments for variables V_i and V_j are known, the joint distribution can be restricted to match a given covariance σ_{V_i,V_j}. Moreover, the correlation can be matched if the variances for V_i and V_j are also known. Equations (3.4a) and (3.4b) match the covariance and moment correlation, respectively.

$$\sum_{\omega_r^{V_i} \in \mathbb{O}^{V_i}} \sum_{\omega_s^{V_j} \in \mathbb{O}^{V_j}} \left[\omega_r^{V_i} \cdot \omega_s^{V_j} \cdot \sum_{\omega_k \in \mathbb{U}_{\omega_r^{V_i} \omega_s^{V_j}}} p_{\omega_k} \right] = \sigma_{V_i,V_j} + m^1_{V_i} \cdot m^1_{V_j} \quad \forall\ V_i, V_j \in \mathbb{V}, \quad (3.4a)$$

$$\sum_{\omega_r^{V_i} \in \mathbb{O}^{V_i}} \sum_{\omega_s^{V_j} \in \mathbb{O}^{V_j}} \left[\omega_r^{V_i} \cdot \omega_s^{V_j} \cdot \sum_{\omega_k \in \mathbb{U}_{\omega_r^{V_i} \omega_s^{V_j}}} p_{\omega_k} \right] = \rho_{V_i,V_j} \cdot \sqrt{\sigma^2_{V_i} \cdot \sigma^2_{V_j}} \quad \forall\ V_i, V_j \in \mathbb{V}, \quad (3.4b)$$

where $\sigma^2_{V_i}$ is the variance of variable V_i, and ρ_{V_i,V_j} is the moment correlation of variables V_i and V_j.

Matching Spearman's Correlation Coefficient

Another measure of variation that requires less information than Equations 3.4a and 3.4b, and can be used with numerical as well as categorical information, is the Spearman's rank correlation. The rank correlation is defined as

$$\rho^r_{V_i,V_j} = \frac{Cov(P(V_i \leq \omega_r^{V_i}), P(V_j \leq \omega_s^{V_j}))}{\sqrt{Var(P(V_i \leq \omega_r^{V_i})) \cdot Var(P(V_j \leq \omega_s^{V_j}))}}. \quad (3.5)$$

Unlike the Pearson product-moment correlation, rank correlation is invariant with respect to the marginal outcomes. This and other characteristics make it a reliable measure of association. (For more on rank correlation and assessment methods see Clemen and Reilly (1999) and Clemen et al. (2000).) Rank correlation requires information only regarding the marginal probabilities for V_i and V_j and can be de-

scribed as a linear function. We start by introducing the *H-volume* (Nelsen, 2005) in Definition 3.3.1.

Definition 3.3.1. *Let S_1 and S_2 be nonempty subsets of $\overline{\mathbb{R}}$ and let H be a two-place real function, $H : \overline{\mathbb{R}}^2 \to \overline{\mathbb{R}}$, such that $DomH = S_1 \times S_2$. Let $\mathbf{B} = [x_1, x_2] \times [y_1, y_2]$ be a rectangle all of whose vertices are in $DomH$. Then, the H-volume of $\mathbf{B}$ is given by:*

$$\mathbf{V}_H(\mathbf{B}) = H(x_2, y_2) - H(x_2, y_1) - H(x_1, y_2) + H(x_1, y_1), \tag{3.6}$$

where the first-order difference of H on $\mathbf{B}$ is $\triangle_{x_1}^{x_2} H(x, y) = H(x_2, y) - H(x_1, y)$. Then, the H-volume, $\mathbf{V}_H(\mathbf{B})$, is the second-order difference of H on $\mathbf{B}$.

$$\mathbf{V}_H(\mathbf{B}) = \triangle_{y_1}^{y_2} \triangle_{x_1}^{x_2} H(x, y). \tag{3.7}$$

Additionally, we provide a definition of the interval $I_{\omega_k}(V_i)$, in Definition 3.3.2.

Definition 3.3.2. *Let $\omega_k^+(V_i)$ be the outcome $\omega_r^{V_i}$ of variable V_i at the joint outcome ω_k and let $\omega_k^-(V_i)$ be the outcome $\omega_{r-1}^{V_i}$ of V_i at the joint outcome ω_k. $\omega_{r-1}^{V_i}$ is the outcome that precedes $\omega_r^{V_i}$ in the marginal distribution of V_i. The cumulative probabilities that V_i and V_j are less than the outcomes $\omega_k^+(V_i)$ and $\omega_k^+(V_j)$ are $p_k^+(V_i) = P(V_i \leq \omega_k^+(V_i))$ and $p_k^-(V_i) = P(V_i \leq \omega_k^-(V_i))$, respectively. These cumulative probabilities define the interval $I_{\omega_k}(V_i)$ as follows:*

$$I_{\omega_k}(V_i) \equiv \left[p_k^+(V_i), p_k^-(V_i)\right]. \tag{3.8}$$

The intervals $I_{\omega_k}(V_i)$ and $I_{\omega_k}(V_j)$ can be used to define a rectangular area $I_{\omega_k}(V_i) \times I_{\omega_k}(V_j)$ equivalent to $\mathbf{B}$. Then, the *H-volume* can be used to define the rank correlation between V_i and V_j as

$$\sum_{\omega_k \in \mathbb{U}} \quad p_{\omega_k} \frac{\mathbf{V}_{x^2 * y^2}\left[I_{\omega_k}(V_i) \times I_{\omega_k}(V_j)\right]}{q_{\omega_k^+(V_i)} \cdot q_{\omega_k^+(V_j)}} = \frac{\rho_{V_i, V_j}^r + 3}{3}, \tag{3.9}$$

where $q_{\omega_k^+(V_i)} = P(V_i = \omega_k^+(V_i))$, which is the marginal probability of variable V_i having the outcome $\omega_r^{V_i}$ at the joint outcome ω_k. Additionally, the *H-volume* $\mathbf{V}_H$ is as defined for $H = x^2 \cdot y^2$, where $x \in I_{\omega_k}(V_i)$ and $y \in I_{\omega_k}(V_j)$.

The rank correlation ρ^r is bounded by a scalar such that $|a_{\hat{m}}| < 1$, where $\hat{m}$ is the maximum number of possible outcomes of variables V_i and V_j. The bounds were proven by Mackenzie (1994) for uniform discrete distributions. Mackenzie (1994) also proved that $\lim_{\hat{m}\to\infty} |a_{\hat{m}}| = 1$, meaning that using more outcomes in each marginal distribution provides a more refined rank correlation bounded by [-1, 1].

The derivation of Equation (3.9) starts from basic principles as follows:

$$\rho^r_{V_i,V_j} + 3 = \frac{Cov(F_{V_i}, F_{V_j})}{\sqrt{Var(F_{V_i}) * Var(F_{V_j})}} + 3 = \frac{E(F_{V_i}, F_{V_j}) - \frac{1}{4}}{\frac{1}{12}} + 3, \tag{3.10a}$$

$$12 \cdot E(F_{V_i}, F_{V_j}) = 12 \int_0^1 \int_0^1 V_i \cdot V_j \cdot c(V_i, V_j)\ dV_j\ dV_i, \tag{3.10b}$$

$$= 12 \sum_{\omega_k \in \mathbb{U}} c_{\omega_k}(V_i, V_j) \cdot \int_{p_k^-(V_i)}^{p_k^+(V_i)} \int_{p_k^-(V_j)}^{p_k^+(V_j)} V_i \cdot V_j\ dV_j\ dV_i, \tag{3.10c}$$

$$= 3 \sum_{\omega_k \in \mathbb{U}} c_{\omega_k}(V_i, V_j) \Big[\left[p_k^+(V_i) p_k^+(V_j)\right]^2 - \left[p_k^+(V_i) p_k^-(V_j)\right]^2 - \left[p_k^-(V_i) p_k^+(V_j)\right]^2 + \left[p_k^-(V_i) p_k^-(V_j)\right]^2 \Big], \tag{3.10d}$$

$$= 3 \sum_{\omega_k \in \mathbb{U}} c_{\omega_k}(V_i, V_j) \mathbf{V}_{x^2 * y^2} \left[I_{\omega_k}(V_i) \times I_{\omega_k}(V_j) \right], \tag{3.10e}$$

$$= 3 \sum_{\omega_k \in \mathbb{U}} p_{\omega_k} \frac{\mathbf{V}_{x^2 * y^2} \left[I_{\omega_k}(V_i) \times I_{\omega_k}(V_j) \right]}{q_{\omega_k^+(V_i)} \cdot q_{\omega_k^+(V_j)}}. \tag{3.10f}$$

Note to Equation (3.10a) : Given $F_{V_i} \sim U[0, 1]$, for which mean and variance are known.

Note to Equation (3.10b) : Expand the expectation.

Note to Equation (3.10c) : Create a partition of the integrals in rectangles. Set $c_{\omega_k}(V_i, V_j)$ as constant inside each rectangle (Mackenzie, 1994).

Note to Equation (3.10d) : Solve the integrals and evaluate each rectangle area.

Note to Equation (3.10e) : Substitute by the $H\text{-}Volume$.

Note to Equation (3.10f) : Set $c_{\omega_k}(V_i, V_j)$ as in Equation 3.11.

For each rectangle area in $\mathbf{B}$, the probability p_{ω_k} is the volume of a body with base area $q_{\omega_k^+(V_i)} \cdot q_{\omega_k^+(V_j)}$ and height $c_{\omega_k}(V_i, V_j)$. This yields:

$$c_{\omega_k}(V_i, V_j) = \frac{p_{\omega_k}}{q_{\omega_k^+(V_i)} \cdot q_{\omega_k^+(V_j)}}. \tag{3.11}$$

A similar derivation is possible for Kendall τ, but the resultant function is not linear and destroys the convexity of the set. The derivation is presented in Appendix B.1.

3.4 Sampling Procedure

With the truth set $\mathbb{T}$ having been characterized, the next step uses the Hit-and-Run (HR) sampler (Smith, 1984) to uniformly sample distributions from $\mathbb{T}$. HR is the fastest known algorithm to sample the interior of an arbitrary polytope. The algorithm has been proven to mix in $\mathbf{O}(h^3)$ time, where $h = (n - m)$ is the dimension of the polytope. Although the mixing time is polynomial, as discussed above, the number of samples required to guarantee convergence to the uniform distribution can be large (Lovasz, 1998). To overcome this problem, the following sections propose a practical definition for convergence that reduces the number of samples required to create a discrete representation of the truth set.

3.4.1 Hit-and-Run Sampler

The algorithm is described below and illustrated in two dimensions in Figure 3.3.

Step 1: Set $i = 0$ and select an arbitrary point $x_i \in \mathbb{T}$.

Step 2: Generate a set $D \subseteq \mathbb{R}^n$ of directions.

Step 3: Choose a random direction d_i uniformly distributed over D.

Step 4: Find the line set $L = \mathbb{T} \cap \{x | x = x_i + \lambda d_i, \lambda \text{ a real scalar}\}$.

Step 5: Generate a random point uniformly distributed over $x_{i+1} \in L$.

Step 6: If $i = N$, stop. Otherwise, set $i = i + 1$ and return to Step 2.

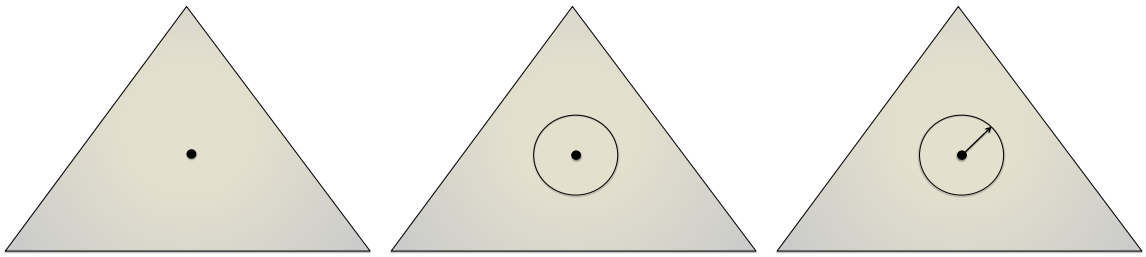

Step 1: $x_i \in \mathbb{T}$. Step 2: Generate set D. Step 3: Choose $d_i \in D$.

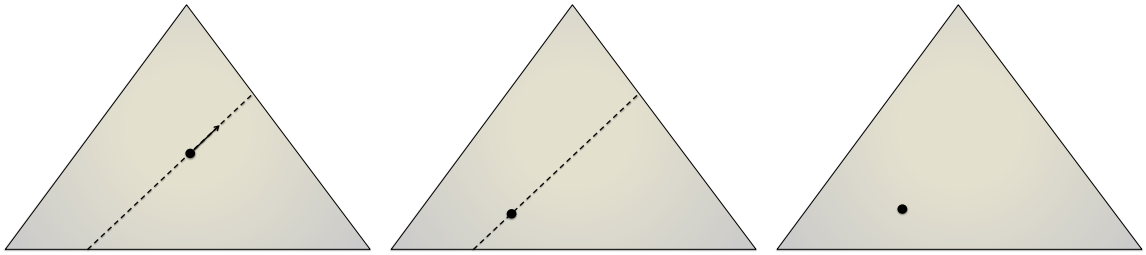

Step 4: Use d_i to set L. Step 5: Select $x_{i+1} \in L$. Step 6: Return to Step 2.

Figure 3.3: Hit-and-Run Sampler. Illustration of the algorithm in two dimensions.

HR was designed for full-dimensional polytopes. However, minor modifications allow it to sample efficiently from non-full-dimensional sets. These modifications are presented in the following section.

3.4.2 Sampling Non-Full-Dimensional Polytopes

As we noted in §3.3.3, the characterization of $\mathbb{T}$ describes the polytope as a system of m linear equations and n non-negative variables: $\mathbf{Ap} = \mathbf{b},\ \mathbf{p} \geq 0$. The HR sampler is designed to sample points in full-dimensional polytopes. However, the polytope $\mathbb{T}$ is not full-dimensional, since $h = n - m < n$. To overcome this problem, the projection of $\bar{\mathbf{p}} \in \mathbb{R}^n$ into the hyperplane $\mathbf{Ap} = \mathbf{b}$ is found using Equation (3.12), where $\mathbf{I}$ represents the identity matrix.

$$\mathbf{p} = (\mathbf{I} - \mathbf{A}^T(\mathbf{A}\mathbf{A}^T)^{-1}\mathbf{A})\bar{\mathbf{p}} + \mathbf{A}^T(\mathbf{A}\mathbf{A}^T)^{-1}\mathbf{b} \tag{3.12}$$

Then, a hypersphere $D \in \mathbb{R}^n$ in the full-dimensional space can be created by sampling independent vectors of size n from the multivariate standard normal and normalizing them so that each vector has equal magnitude. Using Equation 3.12, the direction set D can be projected into $\mathbb{T}$. With the proper scaling, the final result is a set of directions $D \in \mathbb{T}$ from which uniformly distributed directions can be selected. The line L is created by extending the directions $\pm\mathbf{d}_i \in D$ until $\mathbf{p} \geq 0$ is violated. The rest of the implementation is straightforward.

This step removes the non-full-dimensional problem by reducing the dimension from n to $n - m$ for all the steps that require this. $\mathbb{T}$ can now be treated as a full-dimensional polytope in $n - m$ dimensions.

3.4.3 Stopping Time

HR guarantees that the sampled collection eventually converges to the uniform distribution over $\mathbb{T}$ (Smith, 1984). However, as pointed by Rubin (1984), the theoretical number of required samples to reach this convergence can be large. Yet, as will be shown in this section, the number of samples required to achieve reasonable performance in practical applications in generally much smaller.

Measuring the rate of convergence to the uniform distribution, even in low-dimensional polytopes, is very difficult. Uniformity would imply that any possible partition of $\mathbb{T}$ contains a fraction of samples that is proportional to the ratio of that partition's volume to the volume of the polytope. Computing the volume of arbitrary polytopes is difficult (Bárány and Füredi, 1987). In fact, in many cases, the volume of the polytope can only be approximated by a random walk through the polytope (Dyer et al., 1995; Kannan et al., 1996), a procedure similar to HR. Therefore, we propose a measure of convergence that does not directly rely on global properties of the polytope and is easy to compute.

We begin by noting that for $\mathbf{p}_i$, a random vector sampled from $\mathbb{T}$ using HR, there exist unique vectors $\boldsymbol{\mu} = \{\mu_1, \ldots, \mu_n\}$ and $\boldsymbol{\sigma^2} = \{\sigma_1^2, \ldots, \sigma_n^2\}$ such that $\lim_{N\to\infty} \sum_{i=1}^{N} \frac{\mathbf{p}_i}{N} = \boldsymbol{\mu}$ and $\lim_{N\to\infty} \sum_{i=1}^{N} \frac{(\mathbf{p}_i - \boldsymbol{\mu})^2}{N-1} = \boldsymbol{\sigma^2}$, where all calculations over $\mathbf{p}_i$ are performed element-wise. Since $\mathbf{p}_i$ has bounded support and HR assures convergence in distribution, all the moments must converge (Casella and Berger, 2002, p. 65). As discussed below, we measure convergence of HR by measuring the convergence of the sample mean and variance. These moments are of particular interest due to their intuitive interpretation. The sample mean describes the closeness of the center of the collection to the center of $\mathbb{T}$. The variance describes how the dispersion of the samples matches the dispersion of $\mathbb{T}$'s volume. Hence, the following definitions are proposed for what we term "fair-convergence".

Definition 3.4.1.

A collection of joint distributions of size N is called "fair-in-mean" if the average vectors of the joint distributions in a collection for the first $\frac{N}{2}$ and N samples of the HR algorithm are within an ϵ-ball of diameter α.

Definition 3.4.2.

A collection of joint distributions of size N is called "fair-in-dispersion" if the standard-deviation vectors of the joint distributions in a collection for the first $\frac{N}{2}$ and N samples

of the HR algorithm are within an ϵ-ball of diameter β.

Definition 3.4.3.

A collection of joint distributions of size N is called "fair" if it is fair-in-mean and fair-in-dispersion for selected small parameters $\alpha, \beta > 0$.

These definitions have been expressed in Equations (3.13) and (3.14), where $\mathbf{p}_i$ is the i^{th} sampled discrete probability distribution with n joint elements. To make notation easier, we use $\mathbf{p}_i$ and assume all calculations are performed element-wise except for $||\cdot||_2$. Equation (3.13) computes the average of the collection sampled after N iterations ($\sum_{i=1}^{N} \frac{\mathbf{p}_i}{N}$) and compares it to the average after $\frac{N}{2}$ iterations. If after N iterations the vector of averages is within an *ϵ-ball* of diameter α of the previous vector (for some small $\alpha > 0$), the sample is assumed to be fair-in-mean.

Equation (3.14) is the equivalent version for the variance, where

$$(\textstyle\sum_{j=1}^{N} \mathbf{p}_i - \mathbf{p}_j)^2 = (N\mathbf{p}_i - \sum_{j=1}^{N} \mathbf{p}_j)^2 = N^2(\mathbf{p}_i - \frac{\sum_{j=1}^{N} \mathbf{p}_j}{N})^2 = N^2(\mathbf{p}_i - \boldsymbol{\mu})^2$$

and where $\boldsymbol{\mu}$ is the vector of averages for each joint element of the sample. Similarly, if after N iterations the new vector of variances is within a *ϵ-ball* of diameter β of the previous vector (for some small $\beta > 0$), the sample is assumed to be fair-in-dispersion.

$$\left|\left| \sum_{i=1}^{N} \frac{\mathbf{p}_i}{N} \; - \; \sum_{i=1}^{\frac{N}{2}} \frac{2 \cdot \mathbf{p}_i}{N} \right|\right|_2 \; \leq \; \alpha \tag{3.13}$$

$$\left|\left| \sum_{i=1}^{N} \frac{(\sum_{j=1}^{N} \mathbf{p}_i - \mathbf{p}_j)^2}{N-1} \; - \; \sum_{i=1}^{\frac{N}{2}} \frac{4 \cdot (\sum_{j=1}^{\frac{N}{2}} \mathbf{p}_i - \mathbf{p}_j)^2}{(\frac{N}{2}-1)} \right|\right|_2 \; \leq \; \beta \cdot N^2 \tag{3.14}$$

The implementation of this stopping time for the mean can be performed by keeping track of $\sum_{i=1}^{N} \mathbf{p}_i$ at each iteration and dividing it by the number of samples at each checkpoint. Additionally, using the recursion in Equation (3.15), we can keep

track of the variance of each joint element at each iteration.

$$
\begin{aligned}
(i-1)\sigma^2_{w,(i)} &= (i-2)\sigma^2_{w,(i-1)} + \left(\frac{f(i)}{i}\cdot\frac{f(i)}{i-1}\right), \\
f(i) &= \sum_{j=1}^{i-1} p^j_w - (i-1)p^i_w \quad \forall\ i = 2,3,\ldots,N.
\end{aligned}
\tag{3.15a}
$$

$$
\sigma^2_{w,(1)} = 0, \quad \forall\ w \in \{1,2,\ldots,n\}. \tag{3.15b}
$$

Our experience suggests that the number of samples required for fair convergence is on the order of $\approx 10^9$ of the theoretical lower bound of Lovasz (1998) (Appendix B.2). As an example, Figure 3.4 and Table B.1 (Appendix B.2) provides illustrative results for fair convergence in six unconstrained polytopes (Equation 3.1 only) of different dimensions.

If $\mathbb{T}$ is unconstrained ($h = n-1$), the truth set is symmetric and the center of mass of $\mathbb{T}$ is known to be the discrete uniform distribution. Therefore, the convergence of HR can be tested by starting the algorithm at a point close to a corner and monitoring the number of samples needed for the mean to arrive within an ϵ-ball of radius $\alpha > 0$ with center at the discrete uniform distribution. For these collections, the algorithm will stop once the sample is fair-in-mean, and Equation (3.14) will be used to check for fair-in-dispersion. This is a strong test because we are selecting the worst possible point to initialize the algorithm.

In particular, we initialize the algorithm by measuring the distance from the center to a corner of $\mathbb{T}$: $\sqrt{\frac{n-1}{n}}$. We then use $\delta = \frac{1-\tau}{n}$ and $\tau = .9$ to define the initial point $\mathbf{p}_0 = \{1-\delta\cdot(n-1), \delta, \ldots, \delta\}$, where $||\mathbf{p}_0 - \mathbf{p}_\infty||_2 = \tau\sqrt{\frac{n-1}{n}}$. After the initial point is set, we look for the smallest N such that $||\sum_{i=1}^{N}\frac{\mathbf{p}_i}{N} - \mathbf{p}_\infty||_2 < \alpha = \varphi\sqrt{\frac{n-1}{n}}$ for $\varphi = 0.05$. Finally, we check for convergence every $K = 100$ iterations. For the sample sizes proposed, the collections are also fair-in-dispersion.

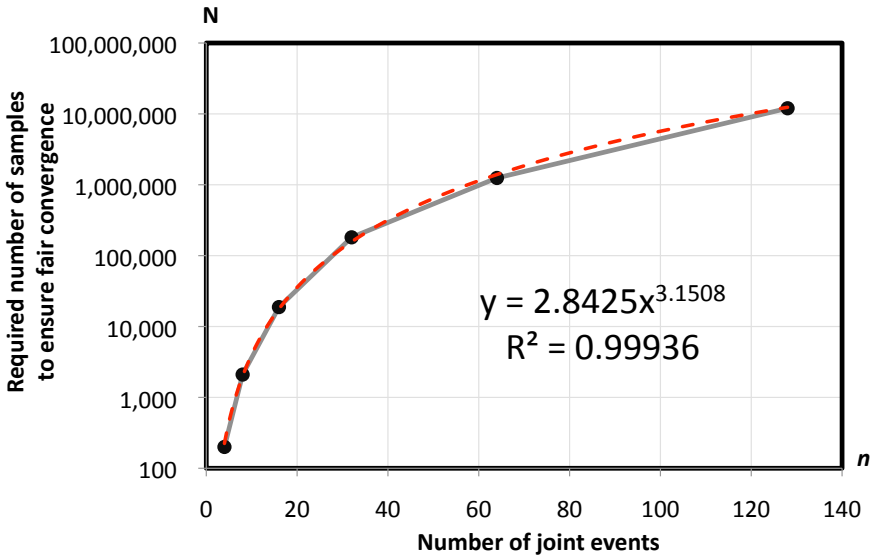

Figure 3.4: Minimum required number of samples (N) to generate a fair sample vs. the number of events (n) in the distribution for six unconstrained polytopes. A solid line connects the empirical data, and the dashed line presents the best fit.

3.5 Sampling in Practice

HR creates a discrete replica of $\mathbb{T}$ from which we can derive conclusions that otherwise would be hard to calculate. This section examines the relation between the discrete sampled collection and the continuous set $\mathbb{T}$.

To illustrate this relation, consider an unconstrained set $\mathbb{T}$ generated by a single random variable with three outcomes $\mathbf{p} = \{p_1, p_2, p_3\}$. The set is a two-dimensional simplex ($h = 2$) located in a three-dimensional coordinate system. The h-content of $\mathbb{T}$ is $\frac{\sqrt{3}}{2}$, and its projection into the hyper-plane generated by $\{\mathbf{p} \in \mathbb{T} | p_1, p_2 \geq 0, p_3 = 0\}$ has an h-content of $\frac{1}{2}$.

The integral of $f(p_1 p_2) = 1 - p_1 - p_2$, along the projection of $\mathbb{T}$ is the volume under $\mathbb{T}$, which is known to be $\frac{1}{3!}$, and is calculated as

$$Vol(\mathbb{T}_{<1}) = \int_0^1 \int_0^{1-p_1} 1 - p_1 - p_2 \; dp_2 \, dp_1 = \frac{1}{3!} = 0.166667.$$

Approximating the volume using $N = 10,000$ samples created with HR yields the following:

$$Vol(\widehat{\mathbb{T}}_{<1^N}) = \sum_{i=1}^{N} \frac{1 - p_1^i - p_2^i}{2 \cdot N} \; = \; 0.167602,$$

where $\mathbf{p}^i = \{p_1^i, p_2^i, p_3^i\}$ is the i^{th} distribution in the sample. For $N = 10,000$, the original volume is close to the approximate volume $Vol(\mathbb{T}_{<1}) \approx Vol(\widehat{\mathbb{T}}_{<1^N})$. Alternative values of $N = 1000$ ($N = 100,000$) yield $Vol(\widehat{\mathbb{T}}_{<1^N}) = 0.16573$ (0.166674). As $N \to \infty$, $Vol(\widehat{\mathbb{T}}_{<1^N}) \to Vol(\mathbb{T}_{<1})$, which is granted by the definition of an integral (Strichartz, 2000).

The discrete approximation will now be examined under two measures of accuracy: Kullback-Leibler divergence (KL), defined in Equation 3.16, and quadratic variation (QV), defined in Equation 3.17.

$$KL_n(\mathbf{p}||\bar{\mathbf{p}}) = \sum_{i=1}^{n-1} p_i \log\left(\frac{p_i}{\bar{p}_i}\right) + (1 - \sum_{i=1}^{n-1} p_i) \log\left(\frac{1 - \sum_{i=1}^{n-1} p_i}{1 - \sum_{i=1}^{n-1} \bar{p}_i}\right), \tag{3.16}$$

$$QV_n(\mathbf{p}, \bar{\mathbf{p}}) = \sum_{i=1}^{n-1} |p_i - \bar{p}_i|^2 + \Big| \sum_{i=1}^{n-1} p_i - \bar{p}_i \Big|^2. \tag{3.17}$$

Both measures can be integrated numerically for the continuous case, and approximated by sampling uniformly as follows:

$$\int_0^1 \int_0^{1-p_1} KL_n(\mathbf{p}||\bar{\mathbf{p}}) \; dp_2 \, dp_1 \approx \sum_{k=1}^{N} KL_n(\mathbf{p}^k||\bar{\mathbf{p}}) \cdot \frac{1}{N \cdot n!}, \tag{3.18}$$

$$\int_0^1 \int_0^{1-p_1} QV_n(\mathbf{p}, \bar{\mathbf{p}}) \; dp_2 \, dp_1 \approx \sum_{k=1}^{N} QV_n(\mathbf{p}^k, \bar{\mathbf{p}}) \cdot \frac{1}{N \cdot n!}. \tag{3.19}$$

Table 3.2 presents the results for both measures considering different values for N, where $\bar{\mathbf{p}} = \{\frac{1}{n}, \ldots, \frac{1}{n}\}$ is the discrete uniform distribution.

Table 3.2: Discrete approximations for different values of N and its continuous measures.

Discrete Set	$KL_3(\mathbf{p}\|\|\bar{\mathbf{p}})$	$QV_3(\mathbf{p},\bar{\mathbf{p}})$
N=10	0.158543	0.061775
N=100	0.162837	0.067702
N=1,000	0.182989	0.079307
N=10,000	0.186991	0.081201
N=100,000	0.183113	0.079546
N=1,000,000	0.183643	0.079775
Continuous Set	0.191358	0.083333

As N increases, the discrete approximation gets closer to the continuous measure from below. This behavior is explained by the convexity of the accuracy measures that reach their maxima in the neighborhood of the vertices of $\mathbb{T}$, where HR takes longer to sample (see Section 3.6). For large enough N, the collection sample converges to the uniform distribution over $\mathbb{T}$, and the gap between the discrete approximation and the continuous measure decreases. The reduction of the gap is not a monotonic function of N because the sample has a random component, which explains the decrease for $N = 100,000$ in Table 3.2.

3.6 The Sea Urchin Effect

The spread of the volume in $\mathbb{T}$ causes an interesting and non-intuitive behavior, which is reflected in HR's sampled collection. Observing the Euclidean distance from the center of $\mathbb{T}$ to all other joint distributions in the collection reveals that the collection becames more concentrated as the dimension of the polytope increases. For example, consider three unconstrained polytopes of dimensions 7, 31, and 127 generated using 3, 5, and 7 binary marginal random variables, respectively. Measuring 20,000 samples in each polytope shows that the range of measures of the Euclidean

distance from the discrete uniform distribution on the first set (Figure 3.5(a)) goes from 0.1 to 0.65. In contrast, for the second and third sets (Figures 3.5(b) and 3.5(c)), the range goes from 0.07 to 0.25 and 0.05 to 0.1, respectively.

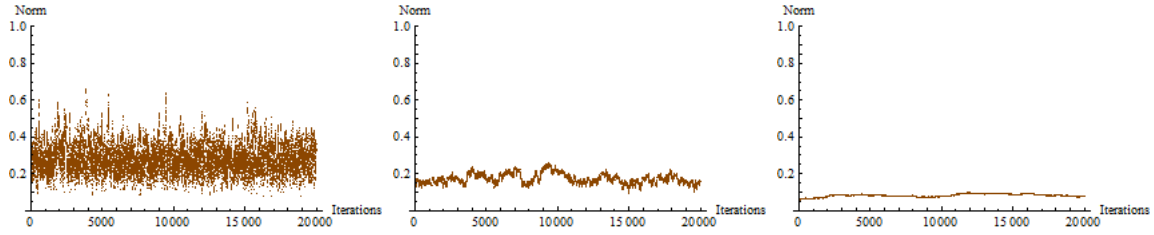

(a) Three Variables. (b) Five Variables. (c) Seven Variables.

Figure 3.5: HR: Norm distance from the center of $\mathbb{T}$. All variables are binary.

At first sight, the algorithm's sample appears to become deficient as dimensionality increases. However, this effect is rather explained by the spread of the volume in $\mathbb{T}$.

The distributions in Figure 3.5 yield the histograms shown in Figure 3.6. These figures have been replicated in Appendix A Figure A.1 for marginal variables with three outcomes.

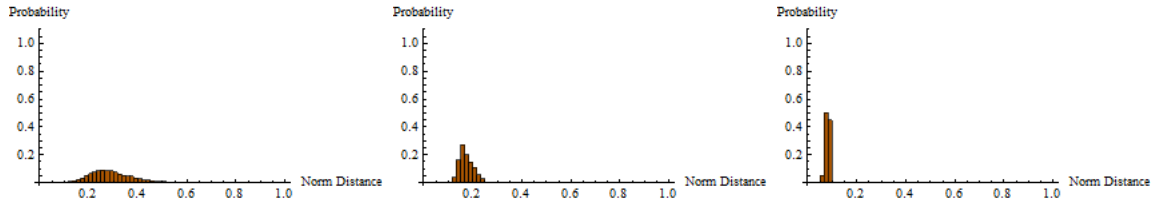

(a) Three Variables. (b) Five Variables. (c) Seven Variables.

Figure 3.6: HR histogram for the norm distance from the center of $\mathbb{T}$. All variables are binary.

The increase in dimension of different geometric bodies may have unexpected results. For example, in a hyper-cube, an increase in dimension pushes a large portion of the volume into the corners. In the case of a hyper-sphere or a hyper-ellipsoid, a similar increase pushes the volume into the outside shell of the geometric figure

(Jimenez and Landgrebe, 1998). In the case of an unconstrained polytope $\mathbb{T}$, most of the volume mass is pushed away from the center and the corners, becoming concentrated in the middle region.

To analyze the spread of the volume over $\mathbb{T}$, we create a partition of an unconstrained polytope (a unit simplex) from a corner to its base along the height (H), each cut's being done at equidistant steps as shown in Figure 3.7(a). Each part in the partition has volume $Vol(\mathbb{T}_i)$, and the summation over a portion of the partition $\sum_{k=1}^{i} Vol(\mathbb{T}_k)$ is the volume of the shadow area in Figure 3.7(b), generated by a single cut of $\mathbb{T}$ perpendicular to H at a distance $\frac{i}{S}H$, where S is the total number of parts in the partition.

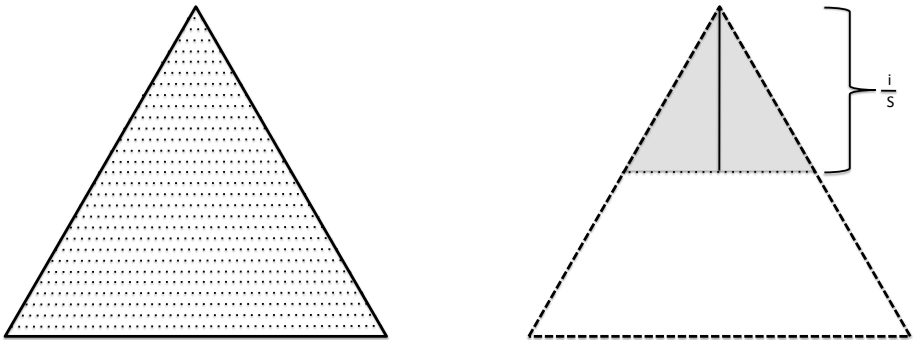

(a) Partition into S sections. (b) Partition at distance $\frac{i}{S}$.

Figure 3.7: Partition of a polytope.

Then, for an unconstrained polytope $\mathbb{T}$, the volume of different sections can be calculated as

$$\sum_{k=1}^{i} Vol(\mathbb{T}_k) = \left(\frac{i}{S}\right)^n \cdot \frac{\sqrt{n+1}}{n!}, \quad \forall \;\; i = 1, \ldots, S. \tag{3.20}$$

For example, for $S = 100$, we measure Vol($\mathbb{T}_i$) and take the ratio $Pr_i = \frac{Vol(\mathbb{T}_i)}{Vol(\mathbb{T})}$ for $i = 1, \ldots, 100$. If we sampled 20,000 distributions, the expected number of distributions on section i is $20,000 * Pr_i$. Figure 3.8 shows the expected concentration of samples for three polytopes generated with 3, 5, and 7 binary marginal random variables.

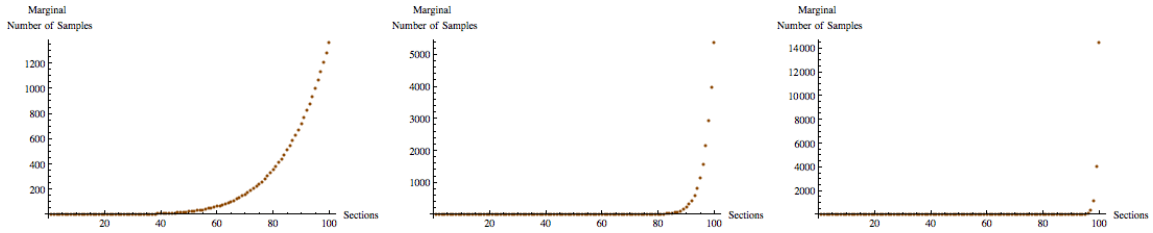

(a) Three Variables. (b) Five Variables. (c) Seven Variables.

Figure 3.8: Theoretical number of samples based on volume, for 20,000 samples.

As the dimension of the polytope increases, the corners lose volume at a faster rate closer to the vertices. Additionally, the maximum-volume-inscribed hyper-sphere is proportional to the radius $r^n = \left(\frac{1}{n*(n+1)}\right)^{\frac{n}{2}}$. Since $\lim_{n\to\infty} r = 0$, the volume of the inner sphere approaches zero as the number of dimensions increases, draining the volume at the center of $\mathbb{T}$. These geometric facts help to describe what we call "The Sea Urchin Effect," which consists of the apparent transformation of a unit simplex into an alternative figure with thin and long spikes, a dense body close to the center, and with a cavity in the nucleus. This effect is generated by the volume dispersion and does not change the basic properties of $\mathbb{T}$ such as convexity, compactness, and continuity.

The sea urchin effect challenges our intuition; adding more joint events into a distribution increases the set of distributions that match the available information. However, the volume of the set is more concentrated. This apparent paradox is resolved by observing that even though $\mathbb{T}$ is larger, the n-content (the relative-interior volume) decreases, and the proportional volume in the corners and the center decays faster, which results in a higher concentration of volume close to the outside shell of the maximum-volume inner sphere. For example, consider the volume of an unconstrained set $Vol(\mathbb{T}) = \frac{\sqrt{n+1}}{n!}$, and let $n \to \infty$. Then, even though we are considering the largest possible set of joint distributions, every possible joint distribution exists in a neighborhood with zero volume.

Chapter 4

Measures of Accuracy

The previous two chapters presented several joint probability distribution approximations and a sampling methodology to create a collection of joint distributions that serves as a discrete representation of the set $\mathbb{T}$. This chapter presents a framework to compare the distribution approximations to the sampled collection using a family of functions named "measures of accuracy."

The five measures of accuracy proposed here are strict quasi-convex Lyapunov functions. That is, the accuracy measures are monotonically increasing and positive everywhere, except for one inflection point $\mathbf{p}_A^* = \mathbf{q}_i$, which has zero value. Many functions with these characteristics can be used to define accuracy. However, those discussed here were chosen for their usefulness and intuitive appeal.

- Maximum Absolute Difference.
- Total Variation.
- Euclidean Distance.
- Kullback−Leibler Divergence.
- χ^2 Distance.

The first three measures of accuracy, maximum absolute difference, total variation, and Euclidean distance, are also metrics and can be interpreted as distances in the interior of the truth set. Kullback−Leibler divergence is not a metric because it does not follow the triangle inequality and is not symmetric. However, it measures the difference on the number of information units (bits) required to encode the outcome of a distribution $\mathbf{q}_i$ given the assumption that the actual distribution is $\mathbf{p}_A^*$. The χ^2

distance is also not a metric, because it is not symmetric, but it is commonly used in statistics and has an interpretation through the χ^2 distribution.

In addition to these measures, we include the difference of entropy between the approximation and the samples in the collection. This is not formally a measure of accuracy, but it provides a direct evaluation of the difference between the probabilistic dependence of two distributions.

Some of these measures of accuracy have been used in the literature. The maximum absolute difference, the total variation, and KL divergence have been used in Abbas (2006) and Bickel and Smith (2006) to measure differences among discrete probability distributions.

4.1 Proposed Measures of Accuracy

We begin by formalizing the meaning of measures of accuracy using definition 4.1.1.

Definition 4.1.1. *Let* $M : \mathbb{R}^n \rightarrow \mathbb{R}$ *be a scalar function.* M *is a "measure of accuracy" if for any two joint probability distributions,* $\mathbf{p} = \{p_1, p_2, \cdots, p_n\} \in \mathbb{T} \subset \mathbb{R}^n$*, an arbitrary distribution in the truth set, and* $\bar{\mathbf{p}} = \{\bar{p}_1, \bar{p}_2, \cdots, \bar{p}_n\}$*, a distribution approximation, the following hold:*

$$M(\mathbf{p},\ \bar{\mathbf{p}}) = 0 \ \ \forall\ \mathbf{p} \ = \ \bar{\mathbf{p}}. \tag{4.1}$$

$$M(\mathbf{p},\ \bar{\mathbf{p}}) < M(\mathbf{p} + \alpha\mathbf{d},\ \bar{\mathbf{p}}) \ \ \forall \ \ \mathbf{p} \ \neq \ \bar{\mathbf{p}},\ \mathbf{d} = (\mathbf{p} - \ \bar{\mathbf{p}}),\ \alpha > 0. \tag{4.2}$$

This definition will be used to propose the following measures of accuracy.

4.1.1 Maximum Absolute Difference

The maximum absolute difference is also known as the $\mathbf{L}^{\infty}$-Norm of $f(i) = (p_i - \bar{p}_i)$ for $i = 1, \ldots, n$ and can be expressed as:

$$\mathbf{L}_n^{\infty}(\mathbf{p}, \bar{\mathbf{p}}) = \max\{|p_1 - \bar{p}_1|, \cdots, |p_n - \bar{p}_n|\}, \tag{4.3}$$

where $\mathbf{p} = \{p_1, p_2, \cdots, p_n\} \in \mathbb{T}$ is any arbitrary distribution in the truth set, and $\bar{\mathbf{p}} = \{\bar{p}_1, \bar{p}_2, \cdots, \bar{p}_n\}$ is the approximation of interest.

$\mathbf{L}^{\infty}$ is directly related to the Kolmogorov-Smirnov distance and has an important interpretation under the two-sample Kolmogorov-Smirnov test, which measures the difference between two empirical distributions $\mathbf{p}$ and $\bar{\mathbf{p}}$ and shows statistical significance if $\sqrt{\frac{n}{2}} \cdot \mathbf{L}_n^{\infty} > K_{\alpha}$, where the K_{α} statistic comes from $Pr(k \leq K_{\alpha}) = 1 - \alpha$ and is distributed as:

$$Pr(k \leq K_{\alpha}) = \frac{\sqrt{2\pi}}{k} \sum_{i=1}^{\infty} e^{-\frac{(2i-1)^2 \pi^2}{8k^2}}. \tag{4.4}$$

The measure is bounded by $0 \leq \mathbf{L}_n^{\infty} \leq \min\{1, \frac{\mathbf{L}_n^1}{2}\}$, where $\mathbf{L}_n^1$ is the $\mathbf{L}^1$-Norm, also known as total variation.

4.1.2 Total Variation

Total Variation measures the sum of the absolute differences. It is also known as $\mathbf{L}^1$-Norm of $f(i)$ for $i = 1, \ldots, n$ and can be expressed as

$$\mathbf{L}_n^1(\mathbf{p}, \bar{\mathbf{p}}) = \sum_{i=1}^{n} |p_i - \bar{p}_i|. \tag{4.5}$$

The $\mathbf{L}^1$-Norm between two distributions is zero if and only if the two distributions are identical. This measure has a special relevance when consider the subspace where $\mathbb{T}$ is located, because it is a natural metric for an n-polytope. Moreover, it constitutes a useful mathematical tool to define bounds. For example, in Kullback (1967), a lower bound for $\mathbf{KL}_n(\mathbf{p}||\bar{\mathbf{p}})$ was defined in terms of the total variation as

$$\mathbf{KL}_n(\mathbf{p}||\bar{\mathbf{p}}) \geq \mathbf{L}_n^1(\mathbf{p}, \bar{\mathbf{p}}) - \log\left(1 + \mathbf{L}_n^1(\mathbf{p}, \bar{\mathbf{p}})\right). \tag{4.6}$$

Devroye and Lugosi (2000) presented an upper bound for $\mathbf{L}^\infty$ as a function of $\mathbf{L}^1$:

$$\mathbf{L}_n^\infty(\mathbf{p}, \bar{\mathbf{p}}) \leq \frac{\mathbf{L}_n^1(\mathbf{p}, \bar{\mathbf{p}})}{2}. \tag{4.7}$$

Finally, $\mathbf{L}^1$ is invariant to the dimension of the vector $\mathbf{p}$. Hence, it is more stable than the average absolute distance $\frac{\mathbf{L}_n^1}{n}$ yet provides equivalent information.

4.1.3 Euclidean Distance

Using $\mathbb{T}$ as a framework, we can think of the direct distance between two points inside a polyhedron. The Euclidean distance, also known as the $\mathbf{L}^2$-Norm (Bertsekas, 1999), measures the length of the straight line connecting any two points (joint distributions in our setting). $\mathbf{L}^2$ is defined as

$$\mathbf{L}_n^2(\mathbf{p}, \bar{\mathbf{p}}) = \left[\sum_{i=1}^{n} (p_i - \bar{p}_i)^2\right]^{\frac{1}{2}}. \tag{4.8}$$

$\mathbf{L}^2$-Norm describes how an approximate distribution is related to the set $\mathbb{T}$ in a spherical topology with center in $\bar{\mathbf{p}}$. The maximum and average distance from $\bar{\mathbf{p}}$ to any arbitrary distribution $\mathbf{p}$ in a sampled collection is defined as

$$\max_{\mathbf{p}\in\mathbb{T}} \quad \mathbf{L}_n^2(\mathbf{p},\bar{\mathbf{p}}) \qquad\qquad E_{\mathbf{p}\sim U(\mathbb{T})}\Big[\mathbf{L}_n^2(\mathbf{p},\bar{\mathbf{p}})\Big]. \tag{4.9}$$

The level sets of $\mathbf{L}^2$ are defined as

$$\mathbb{L}_\alpha^2(\bar{\mathbf{p}}) = \{\ \mathbf{p} \mid\ \ \mathbf{L}_n^2(\mathbf{p},\bar{\mathbf{p}})) \leq \alpha\} \tag{4.10}$$

for radius α. These sets help to calculate probabilities of different neighborhoods of $\bar{\mathbf{p}}$ using the frequencies generated by the sample of $\mathbb{T}$.

4.1.4 Kullback-Leibler Divergence

Proposed by Kullback and Leibler (1951), Kullback-Leibler Divergence (**KL**) measures the divergence or loss of information from the sampled distribution $\mathbf{p}$ to the approximation $\bar{\mathbf{p}}$. **KL** is bounded below by zero, and the bound is tight if and only if $\mathbf{p} = \bar{\mathbf{p}}$. **KL** Divergence is defined as:

$$\mathbf{KL}_n(\mathbf{p}||\bar{\mathbf{p}}) = \sum_{i=1}^{n} p_i \log\left(\frac{p_i}{\bar{p}_i}\right). \tag{4.11}$$

An intuitive expression for this measure is

$$\mathbf{KL}_n(\mathbf{p}||\bar{\mathbf{p}}) = \sum_{i=1}^{n} p_i \ln\left(\frac{1}{\bar{p}_i}\right) - \left(-\sum_{i=1}^{n} p_i \ln p_i\right) \tag{4.12}$$

$$= E_{\mathbf{p}}\left[\ln\left(\frac{1}{\bar{\mathbf{p}}}\right)\right] - H(\mathbf{p}) \geq 0. \tag{4.13}$$

Then, if entropy (H) is the expected value on the number of bits necessary to encode a distribution. $\mathbf{KL}_n(\mathbf{p}||\bar{\mathbf{p}})$ is the expected number of "penalty" bits as a result of confusing $\mathbf{p}$ with $\bar{\mathbf{p}}$. In other words, it is the increase in descriptive complexity due

to incorrect information.

Given that $\lim_{p_i \to 0} E_{\mathbf{p}}[\ln \frac{1}{\bar{\mathbf{p}}}] = \infty$, any approximation distribution needs to be in the interior of $\mathbb{T}$. That is, it can not contain elements equal to zero. As before, it is possible to observe values for

$$\max_{\mathbf{p} \in \mathbb{T}} \ \mathbf{KL}_n(\mathbf{p}||\bar{\mathbf{p}}) \qquad\qquad E_{\mathbf{p} \sim U(\mathbb{T})}\Big[\mathbf{KL}_n(\mathbf{p}||\bar{\mathbf{p}})\Big]. \tag{4.14}$$

These values describe the maximum and average behavior of the penalties generated by choosing $\bar{\mathbf{p}}$ instead of a possible true distribution $\mathbf{p}$. We can also observe the level sets:

$$\mathbb{KL}_\alpha(\bar{\mathbf{p}}) = \{\ \mathbf{p} \mid \ \mathbf{KL}_n(\mathbf{p}||\bar{\mathbf{p}}) \leq \alpha\}. \tag{4.15}$$

4.1.5 χ^2 Distance

Correspondence analysis shows where the joint outcomes of $\mathbf{p}$ work as factors where the probabilities describe attraction or rejection among outcomes. Then, the natural distance between distributions is the χ^2 distance. The name of this measure comes from the "Goodness-of-fit χ^2 Test." Here, the expected probabilities comprise the approximated distribution $\bar{\mathbf{p}}$. The χ^2 distance is defined as

$$\chi^2_n(\mathbf{p}, \bar{\mathbf{p}}) = \sum_{i=1}^{n} \frac{(p_i - \bar{p}_i)^2}{\bar{p}_i}. \tag{4.16}$$

The measure provided by this metric can be interpreted as a standardized quadratic variation $QV_n(\mathbf{p}, \bar{\mathbf{p}})$, where outcomes with low expected probability are more unstable. This metric has zero value if and only if $\mathbf{p} = \bar{\mathbf{p}}$, and as a statistic, the $\chi^2_n(\mathbf{p}, \bar{\mathbf{p}})$ distance is distributed as χ^2 with $n - m - 1$, where m is the number of constraints in $\mathbb{T}$.

4.1.6 Entropy Difference

As mentioned, entropy difference is not formally a measure of accuracy. However, it provides insight when we consider the description of the outcomes using two different distributions.

Proposed by Kullback and Leibler (1951) and later by Jaynes (1982), entropy difference measures the expected value of the number of bits necessary to encode the outcomes of a distribution. Entropy difference is defined as

$$H_n(\mathbf{p}) = -\sum_{i=1}^{n} p_i \log(p_i). \tag{4.17}$$

Entropy difference is bounded by $0 \leq H_n(\mathbf{p}) \leq \ln(n)$, where the lower bound is reached for $\mathbf{p} = \{1, 0, \cdots, 0\}$ and the upper bound is reached for $\mathbf{p} = \{\frac{1}{n}, \cdots, \frac{1}{n}\}$. Some values of interest for H are

$$\max_{\mathbf{p}\in\mathbb{T}} H(\mathbf{p}), \qquad \min_{\mathbf{p}\in\mathbb{T}} H(\mathbf{p}), \qquad E_{\mathbf{p}\sim U(\mathbb{T})}\Big[H(\mathbf{p})\Big]. \tag{4.18}$$

Based on H, the entropy difference for two distributions can be represented as

$$\Delta H(\mathbf{p}, \bar{\mathbf{p}}) = H_n(\bar{\mathbf{p}}) - H_n(\mathbf{p}). \tag{4.19}$$

This measure is bounded by $-H_{max} \leq \Delta H(\mathbf{p}, \bar{\mathbf{p}}) \leq H_{max}$, where $\Delta H(\mathbf{p}, \bar{\mathbf{p}})$ allows for negative values. Positive values of ΔH indicate that the information structure of $\bar{\mathbf{p}}$ is closer to uniform than $\mathbf{p}$, whereas negative values of ΔH imply that the information structure is farther from uniform. Some values of interest are

$$\max_{\mathbf{p}\in\mathbb{T}} \Delta H(\mathbf{p}, \bar{\mathbf{p}}), \qquad \min_{\mathbf{p}\in\mathbb{T}} \Delta H(\mathbf{p}, \bar{\mathbf{p}}), \qquad E_{\mathbf{p}\sim U(\mathbb{T})}\Big[\Delta H(\mathbf{p}, \bar{\mathbf{p}})\Big]. \tag{4.20}$$

4.2 Illustration

We now provide a small visualization of the measures of accuracy. For this purpose, we use a binary random variable with estimated distribution $\bar{\mathbf{p}} = \{q_1, 1-q_1\}$. The estimated distribution is compared then to all possible distributions $\mathbf{p} = \{p_1, 1-p_1\}$. We consider five different values of q_1: $\{0.1, 0.3, 0.5, 0.7, 0.9\}$, where p_1 may range in the interval [0, 1].

Figure 4.1 shows the behavior of the measures in a binary setup with no assessment constraints. The measures are symmetric, convex, and except for Figure 4.1(e), (ΔH) are always positive. An interesting characteristic of the first three measures is the linear shape, which can be interpreted as alternative measures of distance from $\bar{\mathbf{p}}$ to $\mathbf{p}$. In contrast, the last three measures show a non-linear behavior, which is related to the logarithmic nature of the information and the rescale by $\bar{\mathbf{p}}$ in the case of the χ^2.

As shown in Figures 4.1(d) and 4.1(f), KL and χ^2 distance are the most sensitive to extreme values of $\bar{\mathbf{p}}$. In fact, these measures are undefined (∞) for $\bar{\mathbf{p}}$ in the boundary of $\mathbb{T}$. χ^2 distance is the most unstable of them all. Whereas, maximum absolute difference is the most stable one.

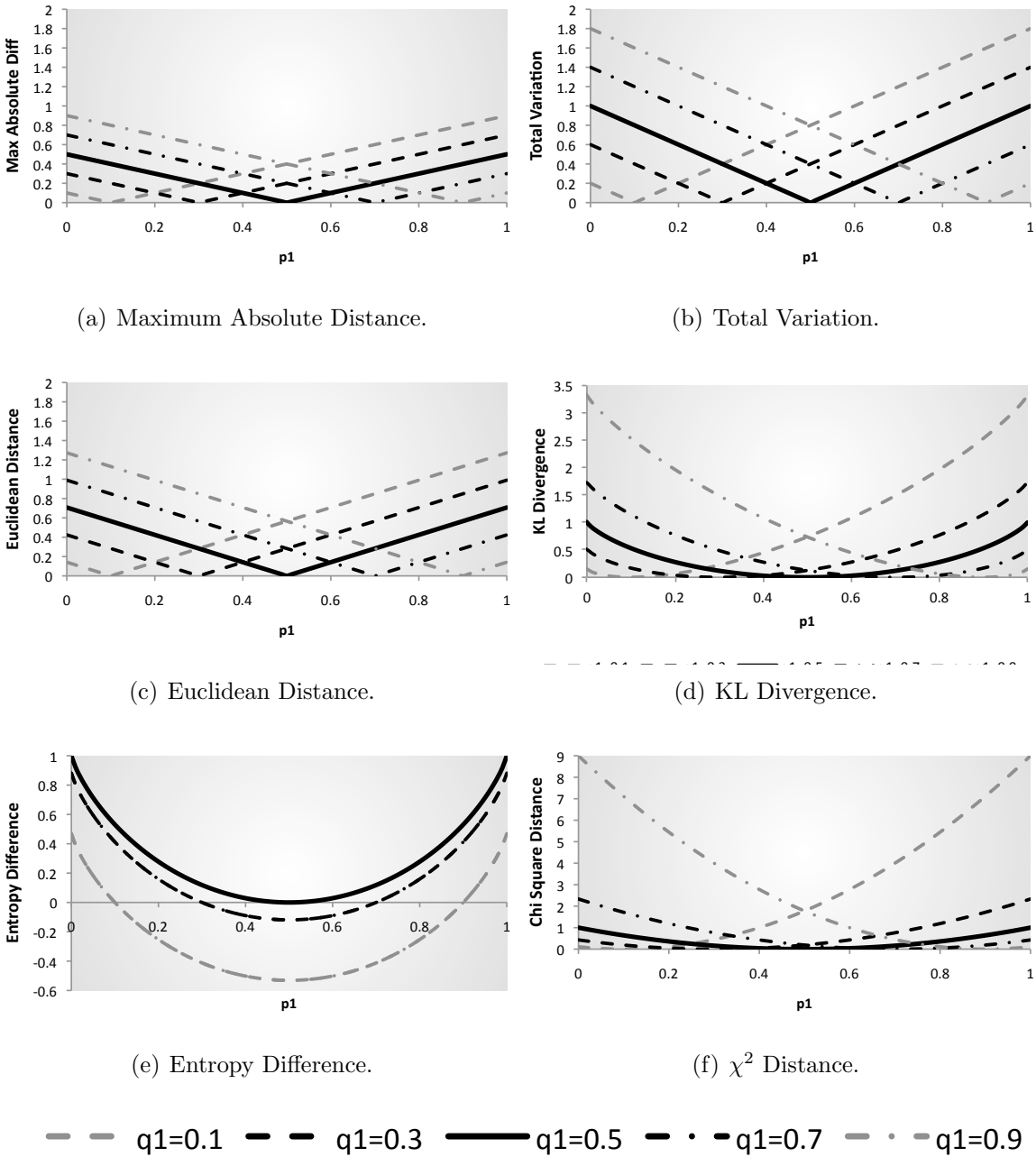

(a) Maximum Absolute Distance.

(b) Total Variation.

(c) Euclidean Distance.

(d) KL Divergence.

(e) Entropy Difference.

(f) χ^2 Distance.

Figure 4.1: Illustration of accuracy measures for $\bar{\mathbf{p}} = \{q_1, 1-q_1\}$ and $\mathbf{p} = \{p_1, 1-p_1\}$.

Chapter 5

Accuracy of Joint Probability Approximations

In this chapter, we test the accuracy of different approximations of joint distributions described in Chapter 2, starting with known distribution families and gradually increasing their complexity and generality. In §5.1, we test the Hypergeometric and Multinomial Families. In §5.2, we test unconstrained truth sets and analyze the effects of increasing the number of random variables and the number of outcomes. We also test the accuracy of sets having symmetric constraints (e.g., equal marginal probabilities, or equal pairwise correlations). In §5.3, we test for effects of adding constraints and of changing existing constraints. In §5.4, we test the accuracy of arbitrarily constrained polytopes, the most general case, using marginal and rank correlation constraints and generate random assessments.

The results presented in this chapter are based on the approximation methods, simulation procedure, and measures of accuracy defined in Chapters 2, 3, and 4 respectively.

5.1 Selected Families of Multivariate Distributions

We start by measuring the differences between well-known multivariate distributions and the approximations. Rather than use HR sampling, we create a sample from the respective family, extract the marginal assessments, derive the distribution

approximations, and measure the accuracy. A similar comparison was done by Abbas (2006) and Bickel and Smith (2006) for a random set of distributions based on binary variables.

We now extend the results from Abbas and from Bickel and Smith to observe how the proposed approximations behave with respect to a known family of discrete joint distributions. We have chosen two families of distributions with discrete and finite support: the hypergeometric and multinomial distributions. These multivariate families allow us to control the number of outcomes and permit some control over the probabilistic dependence in the distributions.

5.1.1 Approximating the Hypergeometric Joint Distribution

Generation of Hypergeometric Distributions: We consider the multivariate hypergeometric distribution, which can be intuitively understood using urns and balls, as follows. For an urn with a total of N balls, where the balls are of c different colors {Red, Green, Yellow,...}, there are m_i balls of color $i = 1,...,c$, where $i = 1$ represents Red, $i = 2$ represents Green, and so on. Then, if we take $n \leq N$ balls from the urn, the hypergeometric distribution describes the probability of having x_1 Red balls, x_2 Green balls, and so on. The different colors represent different variables, where variable x_i is bounded by $[0, \min(n, m_i)]$.

To create an arbitrary hypergeometric distribution, we need to choose the number of colors c and the number of balls taken n. We then randomly define m_i for $i = 1, 2, \ldots, c$ using non-negative integers, and set $N = \sum_i^c m_i$. The joint probability mass function is defined as:

$$P(X_1 = x_1, X_2 = x_2, \ldots, X_c = x_c) = \frac{\binom{m_1}{x_1} \cdot \binom{m_2}{x_2} \cdots \binom{m_c}{x_c}}{\binom{N}{n}}.$$

We now provide an example of a specific hypergeometric distribution and the approximations derived from it using only marginal assessment information. Then, we present the accuracy results for a large number of randomly generated hypergeometric distributions.

Procedure Example. An instance of a hypergeometric distribution for $c = 3$ and $n = 8$ is presented in Table 5.1, which includes four approximations generated using only marginal information taken from the original hypergeometric distribution. The first three columns in the table describe the joint events of the distribution. The first event consists of selecting 8 Red balls from the urn. The fourth column contains the probabilities of the joint events under the hypergeometric distribution. For example, the probability of drawing 8 Red balls is 0.0004. Columns 5 to 8 are approximations to the hypergeometric distribution. For each approximation, we calculate the probabilities of the marginal events and use this information with the algorithms in Chapter 2. Each of the approximations is distinct, even though they use the same information. These differences are generated by assumptions made by each model. One objective of this work is to find which assumptions provide better approximations.

In this instance, the maximum entropy (ME) approximation replicates exactly the original distribution using only marginal information. This result will later be confirmed for a larger number of samples. This shows that the hypergeometric family is the maximum entropy distribution. Nonetheless, because of the hypergeometric distribution's structure, it does not have independent marginal variables. The comparison among these approximation distributions shows the effects of the different assumptions in the model. For example, the analytic center (AC), Chebyshev's center, (ChSC) and maximum volume inscribed ellipsoid center (MVIE) create distributions that imply higher probabilistic dependence.

Table 5.1: Hypergeometric Distribution and Approximations.

Joint Events			Probability Distributions				
Red	Green	Yellow	Hypergeometric Distribution	AC	ChSC	MVIE	ME
8	0	0	0.00040	0.00040	0.00040	0.00040	0.00040
7	1	0	0.00290	0.00270	0.00270	0.00340	0.00290
7	0	1	0.00670	0.00680	0.00680	0.00610	0.00670
6	2	0	0.00500	0.00380	0.00380	0.00330	0.00500
6	1	1	0.03500	0.03290	0.03330	0.03590	0.03500
6	0	2	0.03500	0.03830	0.03790	0.03580	0.03500
5	3	0	0.00200	0.00330	0.00330	0.00310	0.00200
5	2	1	0.04200	0.04240	0.04220	0.03930	0.04200
5	1	2	0.12600	0.12900	0.12870	0.13430	0.12600
5	0	3	0.07000	0.06530	0.06580	0.06330	0.07000
4	3	1	0.01170	0.01320	0.01300	0.01410	0.01170
4	2	2	0.10500	0.10320	0.10360	0.10190	0.10500
4	1	3	0.17500	0.17670	0.17640	0.17080	0.17500
4	0	4	0.05830	0.05700	0.05710	0.06330	0.05830
3	3	2	0.02000	0.01560	0.01590	0.01410	0.02000
3	2	3	0.10000	0.10240	0.10230	0.10940	0.10000
3	1	4	0.10000	0.09930	0.09950	0.09470	0.10000
3	0	5	0.02000	0.02270	0.02250	0.02190	0.02000
2	3	3	0.01250	0.01320	0.01310	0.01410	0.01250
2	2	4	0.03750	0.03860	0.03850	0.03690	0.03750
2	1	5	0.02250	0.02070	0.02090	0.02190	0.02250
2	0	6	0.00250	0.00250	0.00250	0.00210	0.00250
1	3	4	0.00280	0.00370	0.00370	0.00370	0.00280
1	2	5	0.00500	0.00410	0.00420	0.00370	0.00500
1	1	6	0.00170	0.00170	0.00160	0.00210	0.00170
1	0	7	0.00010	0.00010	0.00010	0.00010	0.00010
0	3	5	0.00020	0.00020	0.00010	0.00020	0.00020
0	2	6	0.00020	0.00020	0.00020	0.00020	0.00020
0	1	7	0.00001	0.00001	0.00010	0.00010	0.00001

This example is consistent with more general scenarios. In particular, we analyze three sets with parameters c= 4, 5, and 6 (marginal variables), where each variable can have up to m=4, 3, and 8 different outcomes, respectively. For each of these sets we examine 100 hypergeometric distributions and observe the performance of the approximations with respect to the original distribution.

Accuracy Results. Figure 5.1 shows the results for four approximations, each evaluated under six measures (similar figures for five and six variables are shown in Appendix C, Figure C.1 and C.3). Each sub-figure shows the results for a measure.

As with the initial example, ME matches the original distribution 100% of the time under every measure used. The same behavior can be observed with five and six variables (see Appendix C). As mentioned before, the hypergeometric family is the ME distribution with respect to the sets generated with marginal information. In contrast, Figure 5.1 shows MVIE to have the worst performance of all, which suggests that the center defined by the maximum volume inscribed ellipsoid is far from the point of maximum entropy in the set defined by the marginal assessments.

Figure 5.2 shows the histograms for each approximation and each measure. The histograms show the frequency of the measures for each approximation. Again, for all measures, the ME approximation provides values close to zero (10^{-15}), while the MVIE shows measures distributed over a higher range of values. Finally, the AC and ChSC approximations show results close to each other. Table 5.2 presents the percentage of time each approximation is the best, second best, third best, and worst. Although the difference between ChSC and the AC is small in this particular case, the former is slightly better about 80% of the time.

When the same experiment is run for different values of parameters c and n (Appendix C, Figures C.2 and C.4, and Tables C.1 and C.2), the AC and the ChSC

approximations sometimes interchange, depending on the structure of the family studied. However, the ME approximation clearly dominates the other three, whereas the MVIE center is clearly the weakest approximation.

Although neither the ChSC nor the AC dominates the other, the ChSC, being a linear model, runs faster than the AC, which is a non-linear model that becomes unstable when variables take values close to zero. Also, the ChSC model is easier to implement because it requires fewer iteration adjustments.

Table 5.2: Percentage of hypergeometric distributions for which a given approximation obtained a given ranking for a given measure, with parameters $c = 4$, $n = 4$.

Approximation	Measure	% of distributions Best	% of distributions Second best	% of distributions Third best	% of distributions Worst
ME	L^∞	100	0	0	0
	L^1	100	0	0	0
	L^2	100	0	0	0
	$\|\Delta H\|$	100	0	0	0
	KL	100	0	0	0
	χ^2	100	0	0	0
AC	L^∞	0	13	87	0
	L^1	0	15	85	0
	L^2	0	15	85	0
	$\|\Delta H\|$	0	34	66	0
	KL	0	22	78	0
	χ^2	0	50	50	0
ChSC	L^∞	0	86	6	8
	L^1	0	85	7	8
	L^2	0	85	7	8
	$\|\Delta H\|$	0	66	23	11
	KL	0	78	12	10
	χ^2	0	50	28	22
MVIE	L^∞	0	1	7	92
	L^1	0	0	8	92
	L^2	0	0	8	92
	$\|\Delta H\|$	0	0	11	89
	KL	0	0	10	90
	χ^2	0	0	22	78

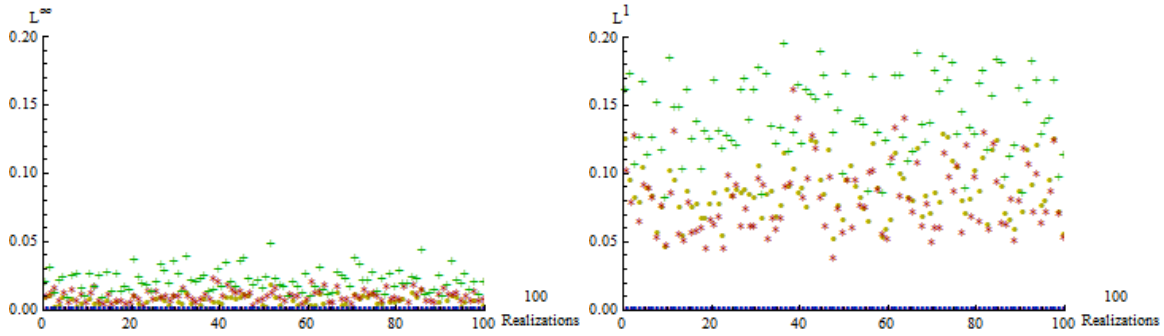

(a) Maximum Absolute Distance.

(b) Total Variation.

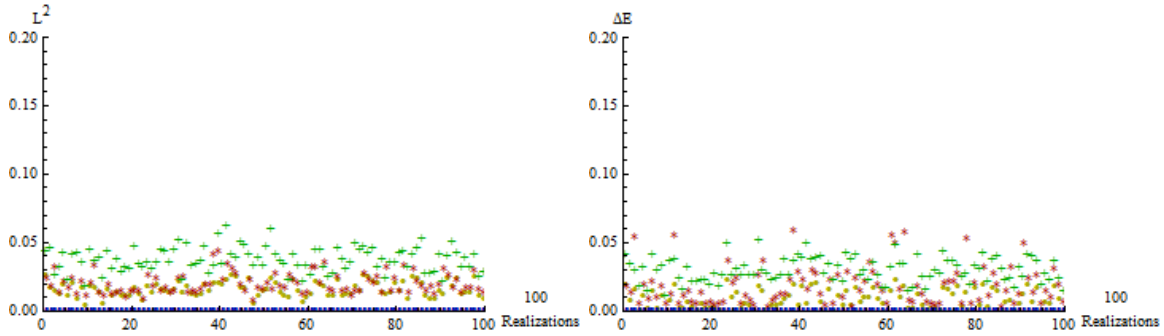

(c) Euclidean Distance.

(d) Absolute Entropy Difference.

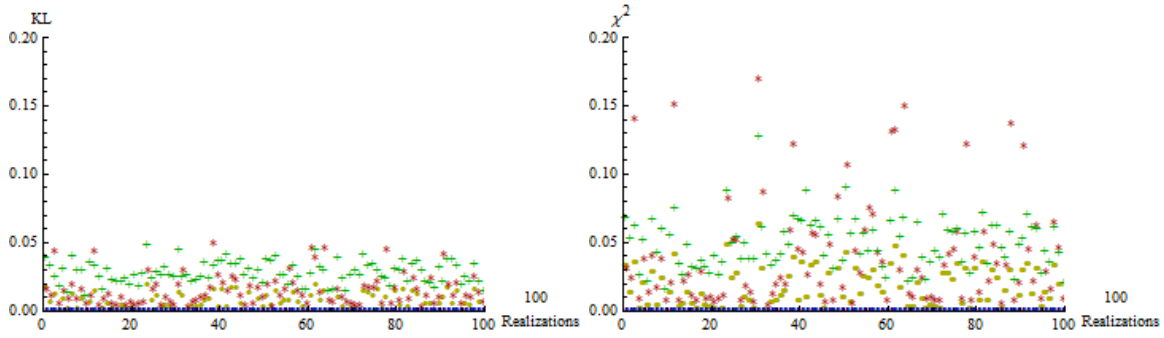

(e) KL Divergence.

(f) χ^2 Distance.

Figure 5.1: Hypergeometric family: Results for ME (Blue, "@"), ChSC (Red, " * "), MVIE (Green, " + "), and AC (Yellow, " • ") approximations. The hypergeometric distributions were created using parameters $c = 4, n = 4$, as described above.

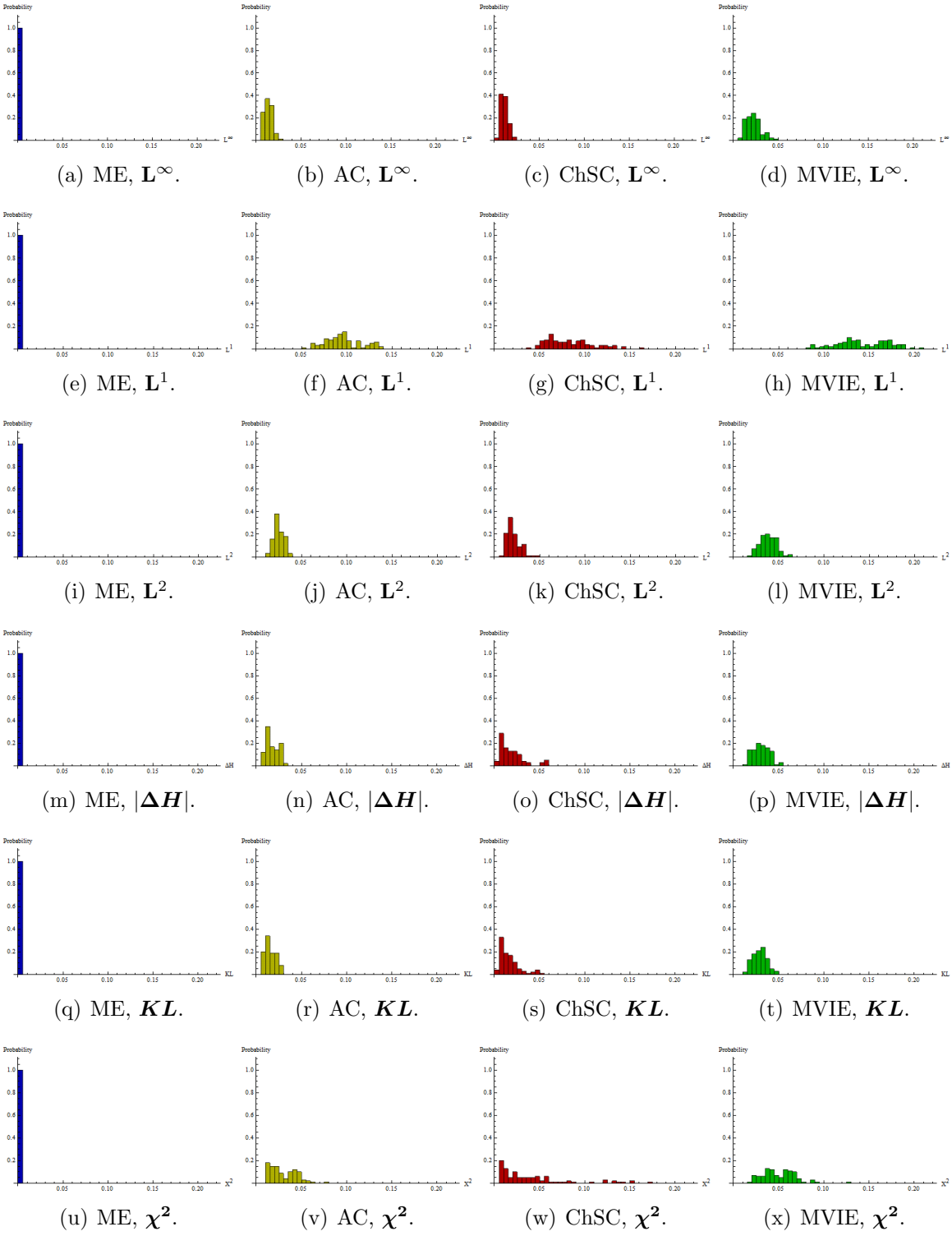

(a) ME, $\mathbf{L}^{\infty}$. (b) AC, $\mathbf{L}^{\infty}$. (c) ChSC, $\mathbf{L}^{\infty}$. (d) MVIE, $\mathbf{L}^{\infty}$.

(e) ME, $\mathbf{L}^{1}$. (f) AC, $\mathbf{L}^{1}$. (g) ChSC, $\mathbf{L}^{1}$. (h) MVIE, $\mathbf{L}^{1}$.

(i) ME, $\mathbf{L}^{2}$. (j) AC, $\mathbf{L}^{2}$. (k) ChSC, $\mathbf{L}^{2}$. (l) MVIE, $\mathbf{L}^{2}$.

(m) ME, $|\boldsymbol{\Delta H}|$. (n) AC, $|\boldsymbol{\Delta H}|$. (o) ChSC, $|\boldsymbol{\Delta H}|$. (p) MVIE, $|\boldsymbol{\Delta H}|$.

(q) ME, $\boldsymbol{KL}$. (r) AC, $\boldsymbol{KL}$. (s) ChSC, $\boldsymbol{KL}$. (t) MVIE, $\boldsymbol{KL}$.

(u) ME, $\boldsymbol{\chi^2}$. (v) AC, $\boldsymbol{\chi^2}$. (w) ChSC, $\boldsymbol{\chi^2}$. (x) MVIE, $\boldsymbol{\chi^2}$.

Figure 5.2: Hypergeometric family histograms. From left to right, ME, AC, ChSC, and MVIE. From top to bottom, $\mathbf{L}^{\infty}$, $\mathbf{L}^{1}$, $\mathbf{L}^{2}$, $\boldsymbol{\Delta H}$, $\boldsymbol{KL}$, and $\boldsymbol{\chi^2}$ distance measures.

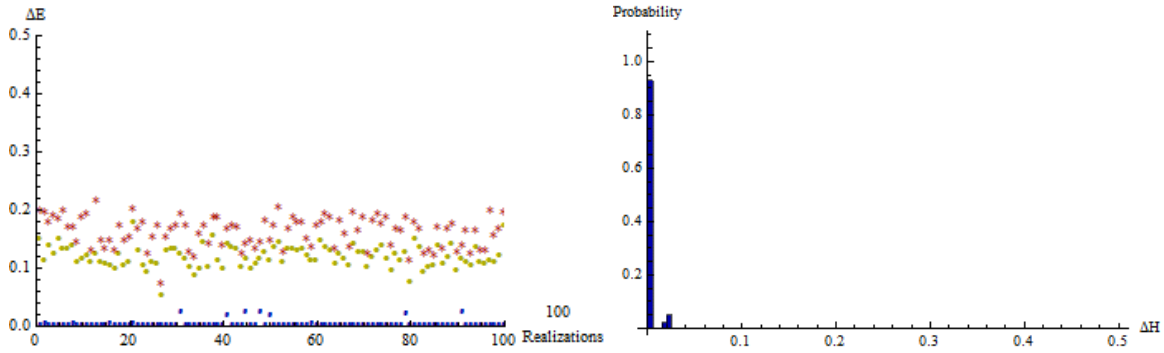

(a) Absolute Entropy Difference.

(b) Entropy, $|\boldsymbol{\Delta H}|$.

Figure 5.3: Hypergeometric family scatterplot and histogram using $|\boldsymbol{\Delta H}|$ for distributions created using parameters $c = 6, n = 8$. (a) Scatterplot results for ME (Blue, "@"), ChSC (Red, " * "), MVIE (unable to calculate), and AC (Yellow, " • ") approximations. (b) Histogram for the ME approximation.

Comparing Figure 5.3 to Figures 5.1(d) and 5.2(m) shows the degradation of the algorithms with respect to the number of joint events. First, the ME approximation fails to replicate exactly the hypergeometric distribution (Figure 5.3(b)), instead creating a distribution with less entropy than the original, showing that the precision of the algorithms falters for large problems. In particular, this last scenario has a total of 1,231 joint events and a variable for each event, which represents a large problem for a non-linear model. In addition, the MVIE (not shown) shows to be sensitive to increments in problem size, e.g., for $c = 6, n = 8$, obtaining a solution would have taken a large amount of time.

Summary of Accuracy Results. The data resulting from the above tests are now summarized by presenting the mean and standard deviations of the measures of accuracy.

Figure 5.4 shows the aggregate mean for three scenarios: $[c = 4,\ n = 4]$, $[c = 5,\ n = 3]$, and $[c = 6,\ n = 8]$. The results are shown using the mean and

standard deviation for all approximation distributions as proportions, i.e.,

$$p_{KL}^{(\cdot)} = 100 \cdot \frac{KL^{(\cdot)}}{KL^{E} + KL^{AC} + KL^{ChSV} + KL^{MVIE}}. \tag{5.1}$$

Figure 5.4 shows that ME replicates the original distribution 100% of the time, having proportion $p_{(\cdot)}^{E} = 0$ for any measure. The AC is shown to have similar characteristics to the ChSC. On average, the worst results come from the MVIE approximation. The MVIE in scenario 3 was not calculated due to long running times.

Table 5.2 and Figure 5.4 provide different conclusions about the accuracy of some of the approximations. The percentage of accuracy describes which distribution is closest to the original without regard of the magnitude of the error, whereas the mean proportion of accuracy describes the error in relation to the magnitude of all the approximations. This explains the behavior of $|\boldsymbol{\Delta H}|$ in scenario 1 and $\boldsymbol{\chi^2}$ in scenario 2 with respect to AC and ChSC approximations.

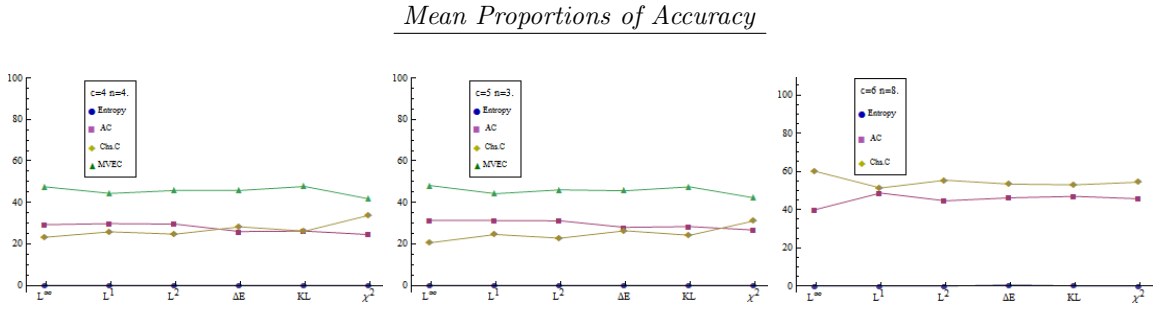

(a) Scenario 1. ($c = 4,\ n = 4$) (b) Scenario 2. ($c = 5,\ n = 3$) (c) Scenario 3. ($c = 6,\ n = 8$)

Figure 5.4: Hypergeometric family: Results for ME, AC, ChSC, and MVIE, in three scenarios observing the mean proportion $p_{KL}^{(\cdot)} = 100 \cdot \frac{KL^{(\cdot)}}{KL^{E}+KL^{AC}+KL^{ChSV}+KL^{MVIE}}$.

The standard deviation (SD) of the proposed measures is shown in Figure 5.5. As with the mean proportions, ME matches the original approximation almost all the

time. The dispersion of the measures of accuracy corresponds to Figure 5.1. The SDs of AC, ChSC, and MVIE are similar. However, the approximation with the worst accuracy (MVIE) is not always the one with the most variation.

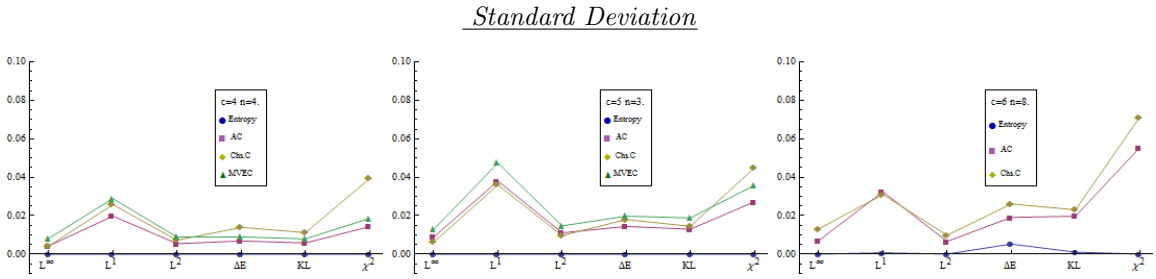

(a) Scenario 1. ($c = 4,\ n = 4$) (b) Scenario 2. ($c = 5,\ n = 3$) (c) Scenario 3. ($c = 6,\ n = 8$)

Figure 5.5: Hypergeometric family: Standard deviation for ME, AC, ChSC, and MVIE for each measure..

5.1.2 Approximating the Multinomial Joint Distribution

Generation of Multinomial Distributions. The multinomial distribution is an extension of the binomial distribution, where we count the number of successful trials from n attempts. We can think of it as taking n balls from an urn one at a time, and returning each ball before taking the next one. Then the probability of a ball's being red, for example, is constant for all trials. In the multinomial distribution, we extend the concept of success used in the binomial distribution: if the balls' colors are {Red, Green, Yellow,...}, then we count the number of Reds, Greens, and so on. As with the hypergeometric distribution, the different colors represent different random variables, where each variable is bounded by $[0, n]$.

An arbitrary multinomial distribution can be created by choosing the number of colors c and the number of balls taken n. p_i would be randomly defined for $i = 1, 2, \ldots, c$ using random numbers in the interval [0 , 1] such that $\sum_i^c p_i = 1$. The

joint probability is defined as:

$$P(X_1 = x_1, X_2 = x_2, \ldots, X_c = x_c) = \frac{n!}{x_1! \cdot x_2! \ldots x_c!} \cdot p^{x_1} \cdot p^{x_2} \ldots p^{x_c} \quad \forall \sum_{i}^{c} x_i = n.$$

We consider multinomial distributions from the following three sets of parameters $[c, n]$: $[4, 4]$, $[5, 3]$, and $[6, 8]$. We create 100 multinomial distributions for each set of parameters and compare the performance of the different approximations with respect to the original distribution. As in the previous subsection, we will first show an example of a specific instance of a multinomial distribution, and the approximations derived from it using only marginal assessment information. Then, we present the accuracy results for a large number of randomly generated multinomial distributions.

Procedure Example. Table 5.3 presents an instance of a multinomial distribution for $c = 3$ and $n = 8$ and includes the four approximations generated using only marginal information taken from the original distribution. Even though the same parameters are used as before, the events have a different probability structure. In the hypergeometric distribution, each ball taken is assumed to change the proportion of balls in the urn. But in the multinomial case, the proportion is constant, which makes each draw independent.

ME replicates exactly the original distribution using only marginal information. Then, the multinomial family, similarly to the hypergeometric, is the ME distribution for a specific set of marginal assessments, which as before does not mean independence among marginal variables. The following results support that the differences between these two families are given by the probability and the structure of the marginal events and not by the interactions of dependence among marginal variables.

Table 5.3: Multinomial Distribution and Approximations.

Joint Events			Probability Distributions				
Red	Green	Yellow	Multinomial Distribution	AC	ChSC	MVIE	ME
8	0	0	0.0063549	0.0063549	0.0063549	0.0063326	0.0063549
7	1	0	0.0123676	0.0098625	0.0103884	0.0097762	0.0123676
7	0	1	0.0324706	0.0349758	0.0344498	0.0350598	0.0324706
6	2	0	0.0105304	0.0098886	0.0101825	0.0093035	0.0105304
6	1	1	0.0552940	0.0532781	0.0543473	0.0482028	0.0552940
6	0	2	0.0725858	0.0752435	0.0738805	0.0809039	0.0725858
5	3	0	0.0051235	0.0072535	0.0066860	0.0077986	0.0051235
5	2	1	0.0403542	0.0412609	0.0409103	0.0461958	0.0403542
5	1	2	0.1059480	0.1086595	0.1081504	0.1089450	0.1059480
5	0	3	0.0927204	0.0869721	0.0883993	0.0812065	0.0927204
4	4	0	0.0015580	0.0025107	0.0022767	0.0026262	0.0015580
4	3	1	0.0163617	0.0160858	0.0160673	0.0162712	0.0163617
4	2	2	0.0644351	0.0630403	0.0637868	0.0581449	0.0644351
4	1	3	0.1127807	0.1162244	0.1149140	0.1192765	0.1127807
4	0	4	0.0740250	0.0712992	0.0721156	0.0728416	0.0740250
3	5	0	0.0003032	0.0003710	0.0003621	0.0003517	0.0003032
3	4	1	0.0039803	0.0030750	0.0031138	0.0029336	0.0039803
3	3	2	0.0209002	0.0177273	0.0186606	0.0168025	0.0209002
3	2	3	0.0548724	0.0559270	0.0556827	0.0581421	0.0548724
3	1	4	0.0720324	0.0727373	0.0723262	0.0724435	0.0720324
3	0	5	0.0378235	0.0400745	0.0397668	0.0392387	0.0378235
2	6	0	0.0000369	0.0000337	0.0000244	0.0000441	0.0000369
2	5	1	0.0005810	0.0003793	0.0001785	0.0003548	0.0005810
2	4	2	0.0038133	0.0030024	0.0031065	0.0028831	0.0038133
2	3	3	0.0133489	0.0138796	0.0138124	0.0142437	0.0133489
2	2	4	0.0262851	0.0272889	0.0270101	0.0262120	0.0262851
2	1	5	0.0276040	0.0261119	0.0266032	0.0275596	0.0276040
2	0	6	0.0120788	0.0130522	0.0130129	0.0124507	0.0120788
1	7	0	0.0000026	0.0000021	0.0000019	0.0000320	0.0000026
1	6	1	0.0000471	0.0000336	0.0000213	0.0000440	0.0000471
1	5	2	0.0003711	0.0003637	0.0004305	0.0003476	0.0003711
1	4	3	0.0016237	0.0022018	0.0022534	0.0023186	0.0016237
1	3	4	0.0042629	0.0050946	0.0049287	0.0049331	0.0042629
1	2	5	0.0067153	0.0060000	0.0059308	0.0054249	0.0067153
1	1	6	0.0058769	0.0051168	0.0052535	0.0057497	0.0058769
1	0	7	0.0022042	0.0022911	0.0022836	0.0022538	0.0022042
0	8	0	0.0000001	0.0000001	0.0000001	0.0000346	0.0000001
0	7	1	0.0000016	0.0000021	0.0000023	0.0000308	0.0000016
0	6	2	0.0000150	0.0000317	0.0000533	0.0000414	0.0000150
0	5	3	0.0000790	0.0002202	0.0003633	0.0002376	0.0000790
0	4	4	0.0002593	0.0004447	0.0004842	0.0004344	0.0002593
0	3	5	0.0005445	0.0005009	0.0003866	0.0004642	0.0005445
0	2	6	0.0007148	0.0005015	0.0004041	0.0004702	0.0007148
0	1	7	0.0005362	0.0004493	0.0004569	0.0004866	0.0005362
0	0	8	0.0001760	0.0001760	0.0001760	0.0001515	0.0001760

Accuracy Results. Figure 5.6 displays the results for four approximations evaluated under the six measures of accuracy. As with the previous example, ME matches the original distribution 100% of the time under any measure used. This result is similar to that in Figure 5.1, driving equivalent conclusions for the multinomial case. Other results that support this claim are shown in Appendix C Figures C.5 and C.7 for the other scenarios. Hence, ME is shown to be the most accurate approximation for both tested families.

Figure 5.7 shows the histograms for each approximation and each measure with parameters $c = 4, n = 4$. The histograms show in more detail the frequencies of the measures for each approximation. Again, for all measures, ME provides values of zero, while the measures for MVIE are more widely distributed. Finally, AC and ChSC show results similar to those described for the hypergeometric family. Equivalent figures are shown in Appendix C Figures C.6 and C.8 for $[c = 5n = 3]$ and $[c = 6, n = 8]$, respectively.

The histograms in Figure 5.7 provide insight into how the values of the measures of accuracy are distributed. In general, the values have a slightly bell-shaped distribution without being normal. These results and the percentages of accuracy in Table 5.4, have implications for the behavior of the approximations. After sampling 100 distributions, ME was the best alternative for 96% of the samples and second best for 4% of the samples by a slight margin of 10^{-7}. Scatterplots and histograms show ME as an exact approximation. Opposed to ME, MVIE approximation was the worst alternative, with about 97% to 100% of the samples in the last column of Table 5.4.

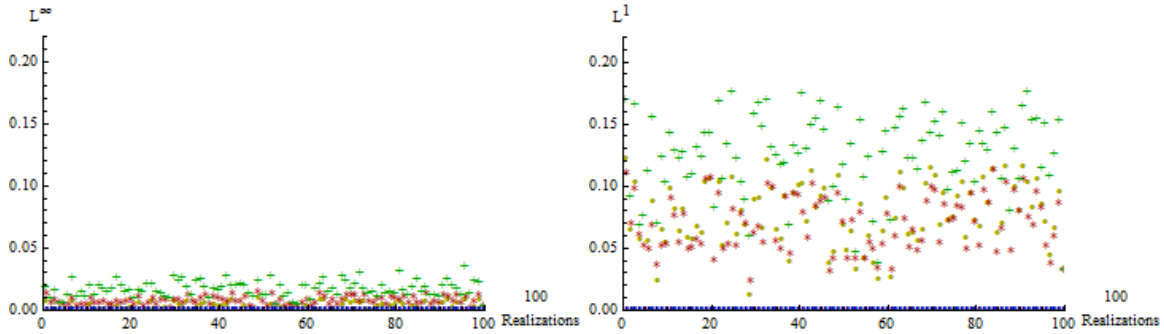

(a) Maximum Absolute Distance.

(b) Total Variation.

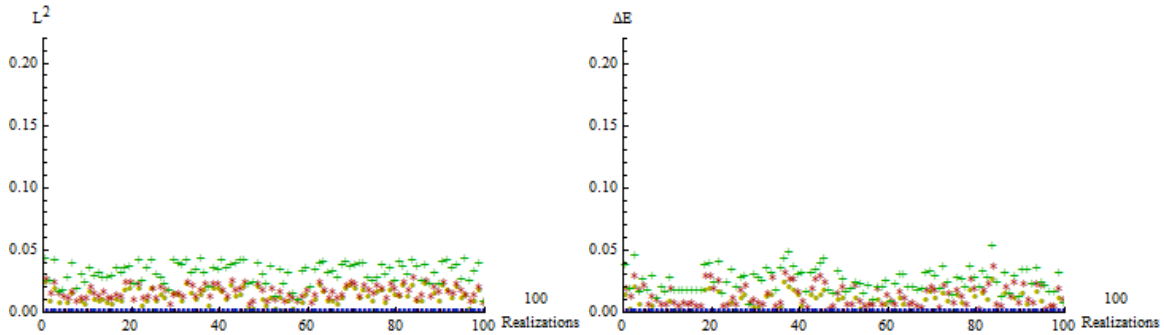

(c) Euclidean Distance.

(d) Absolute Entropy Difference.

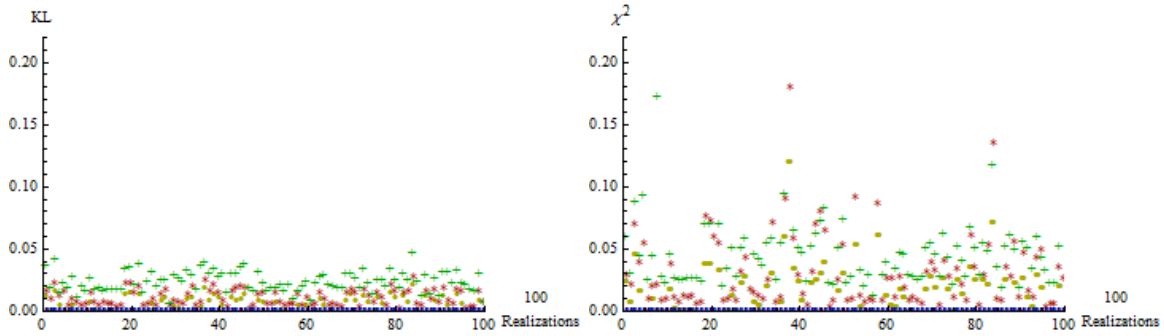

(e) KL Divergence.

(f) χ^2 Distance.

Figure 5.6: Multinomial family: Results for ME (Blue, "@"); ChSC (Red, " * "); MVIE (Green, " + "); and AC (Yellow, " • ") approximations. The multinomial distributions were created using parameters $c = 4, n = 4$ as described above.

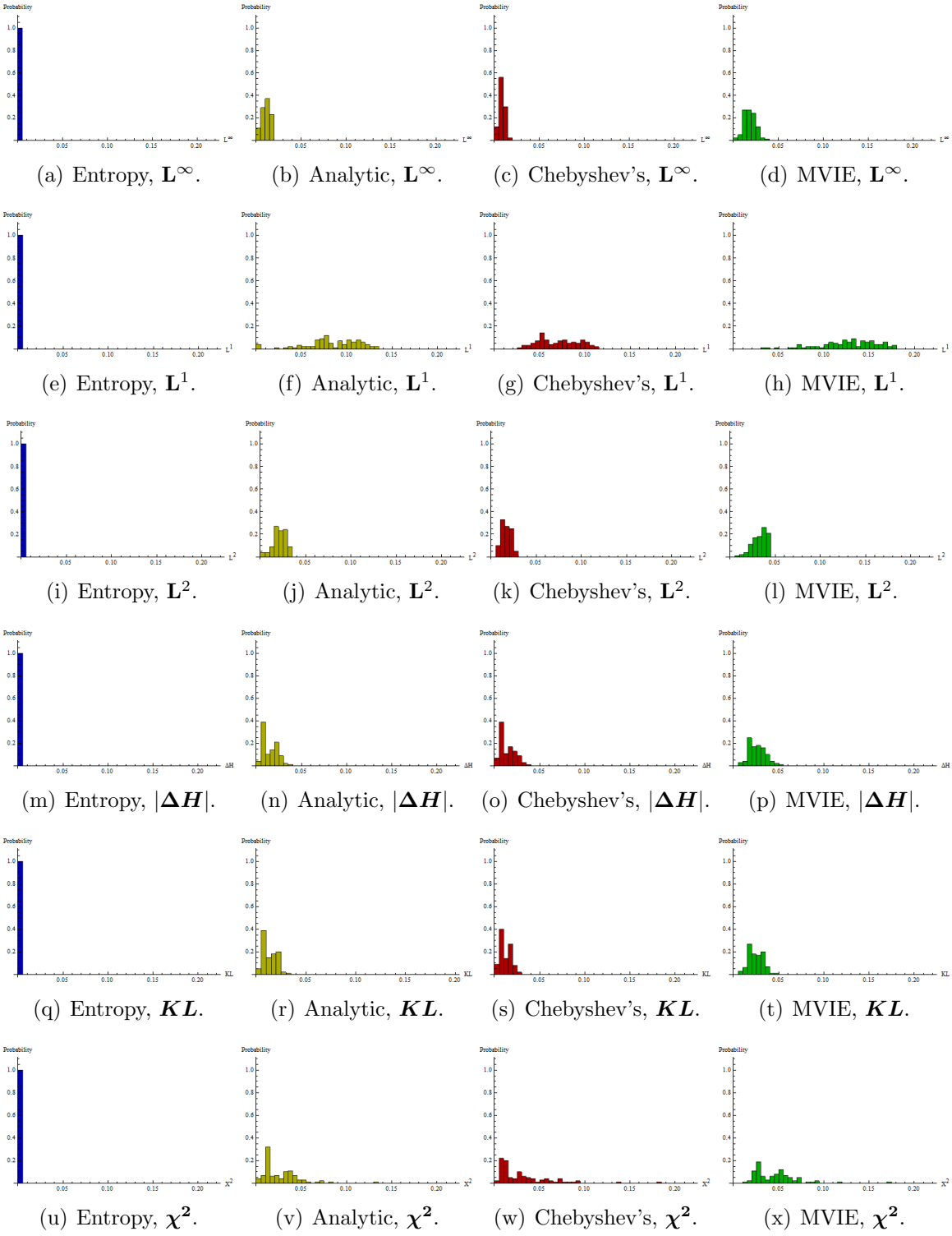

(a) Entropy, $\mathbf{L}^{\infty}$. (b) Analytic, $\mathbf{L}^{\infty}$. (c) Chebyshev's, $\mathbf{L}^{\infty}$. (d) MVIE, $\mathbf{L}^{\infty}$.

(e) Entropy, $\mathbf{L}^{1}$. (f) Analytic, $\mathbf{L}^{1}$. (g) Chebyshev's, $\mathbf{L}^{1}$. (h) MVIE, $\mathbf{L}^{1}$.

(i) Entropy, $\mathbf{L}^{2}$. (j) Analytic, $\mathbf{L}^{2}$. (k) Chebyshev's, $\mathbf{L}^{2}$. (l) MVIE, $\mathbf{L}^{2}$.

(m) Entropy, $|\boldsymbol{\Delta H}|$. (n) Analytic, $|\boldsymbol{\Delta H}|$. (o) Chebyshev's, $|\boldsymbol{\Delta H}|$. (p) MVIE, $|\boldsymbol{\Delta H}|$.

(q) Entropy, $\boldsymbol{KL}$. (r) Analytic, $\boldsymbol{KL}$. (s) Chebyshev's, $\boldsymbol{KL}$. (t) MVIE, $\boldsymbol{KL}$.

(u) Entropy, $\boldsymbol{\chi^2}$. (v) Analytic, $\boldsymbol{\chi^2}$. (w) Chebyshev's, $\boldsymbol{\chi^2}$. (x) MVIE, $\boldsymbol{\chi^2}$.

Figure 5.7: Multinomial family histogram results. From left to right, ME, AC, ChSC, and MVIE. From top to bottom, $\mathbf{L}^{\infty}$, $\mathbf{L}^{1}$, $\mathbf{L}^{2}$, $|\boldsymbol{\Delta H}|$, $\boldsymbol{KL}$, $\boldsymbol{\chi^2}$ distance measures.

Table 5.4: Percentage of monomial distribution for different approximations and measures with parameters $c = 4$, $n = 4$.

Approximation	Measure	% of distributions Best	% of distributions Second best	% of distributions Third best	% of distributions Worst
Entropy	L^∞	96	4	0	0
	L^1	96	4	0	0
	L^2	96	4	0	0
	$\|\Delta H\|$	96	4	0	0
	KL	96	4	0	0
	χ^2	96	4	0	0
Analytic C	L^∞	4	3	90	3
	L^1	4	5	91	0
	L^2	4	3	93	0
	$\|\Delta H\|$	4	22	74	0
	KL	4	10	86	0
	χ^2	4	35	61	0
ChSC	L^∞	0	93	7	0
	L^1	0	91	9	0
	L^2	0	93	7	0
	$\|\Delta H\|$	0	74	23	3
	KL	0	86	13	1
	χ^2	0	61	30	9
MVIEC	L^∞	0	0	3	97
	L^1	0	0	0	100
	L^2	0	0	0	100
	$\|\Delta H\|$	0	0	3	97
	KL	0	0	1	99
	χ^2	0	0	9	91

AC and ChSC approximations yield results that resemble the hypergeometric results. Neither approximation is superior in all cases. For parameters $c = 4, n = 4$, ChSC is better than AC. But for $c = 6, n = 8$ (Appendix C, Table C.4), AC shows higher accuracy.

Due to the large amount of data, a portion of the figures needed to be included in Appendix C. Below, all the data generated are summarized by presenting the mean and standard deviations of the measures of accuracy.

Summary of Accuracy Results. Figure 5.8 presents the mean aggregate results for three tested scenarios ([c = 4, n = 4], [c = 5, n = 3], and [c = 6, n = 8]). For each scenario, the six measures of accuracy were noted. The data were summarized using the mean and standard deviation for all approximation-distributions as proportions (Equation 5.1). This figure is equivalent to Figure 5.4 and describes the average accuracy for each measure in each of the three scenarios. Consistent with previous results, ME is the best approximation and MVIE is the worst.

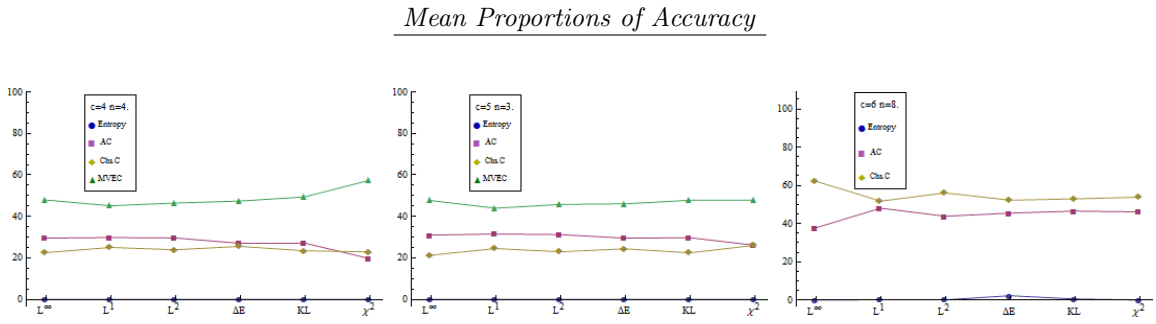

(a) Scenario 1. ($c = 4,\ n = 4$) (b) Scenario 2. ($c = 5,\ n = 3$) (c) Scenario 3. ($c = 6,\ n = 8$)

Figure 5.8: Multinomial family: Results for ME, AC, ChSC, and MVIE approximations, in three different scenarios observing the mean proportions $p_{KL}^{(\cdot)} = 100 \cdot \frac{KL^{(\cdot)}}{KL^{E}+KL^{AC}+KL^{ChSV}+KL^{MVIE}}$.

Figure 5.9 shows the standard deviation that corresponds to Figure 5.8. The results are similar to Figure 5.5, showing again ME as the best approximation. As seen in the hypergeometric results, some approximations manifest numerical problems. This is true of $|\boldsymbol{\Delta H}|$ in Figure 5.9(c), where ME is not a perfect match to the multinomial distribution. Moreover, as the number of joint events increases, the $\boldsymbol{\chi^2}$ distances becomes unstable (the probabilities of the multinomial distribution approach zero).

Standard Deviation

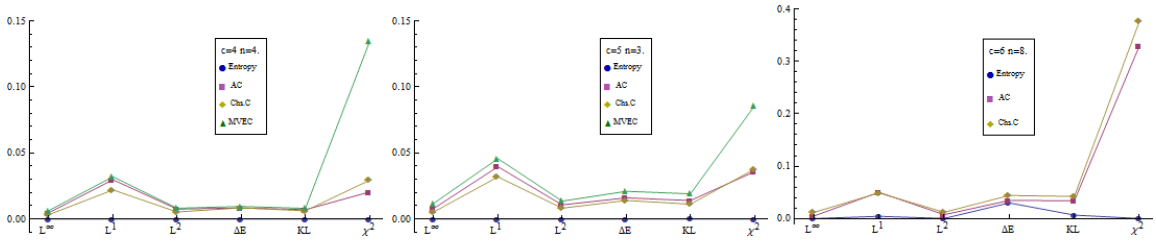

(a) Scenario 1. ($c = 4,\ n = 4$) (b) Scenario 2. ($c = 5,\ n = 3$) (c) Scenario 3. ($c = 6,\ n = 8$)

Figure 5.9: Multinomial family: Standard deviation for ME, AC, ChSC, and MVIE approximations for each measure of accuracy.

5.1.3 Accuracy Findings in Hypergeometric and Multinomial Families

1. The most accurate approximation to the hypergeometric and the multinomial families when marginal assessments are known is ME approximation. In fact, ME is an exact approximation for both families.

2. MVIE approximation is the least accurate approximation for both families of distributions when marginal assessments are known.

3. AC and ChSC are dominated by ME and dominate MVIE approximation. However, there is no dominance between the two.

4. ME is not aligned with the center of the largest volume ellipsoid inscribed in $\mathbb{T}$ (MVIE). This suggests that it is also not aligned with the center of mass of $\mathbb{T}$ when the truth set is defined with marginal assessments.

5. That ChSC approximation algorithm is linear makes it faster to compute than any of the other approximations.

6. For large instances (approx. 1,231 joint events), some of the approximation algorithms start degrading. Specifically, ME approximation fails to achieve optimality in some cases (approx. 8/100).

5.2 Unconstrained Multivariate Distributions

Section §5.1 determined the accuracy of different approximations when the true joint distribution was known to belong to a known family of distributions. This section considers a more general class of joint distributions. The *unconstrained truth set* is the set of joint distributions for which the support is known but there is no information about partial or conditional assessments (marginals, pairwise correlations, etc.). This case is of particular interest because all the approximations proposed result in the discrete uniform distribution, i.e., the center of $\mathbb{T}$. The study of unconstrained sets help us to observe how the changes in the truth set $\mathbb{T}$ affect the proposed accuracy measures for any given approximation. Of interest are two particular questions: How does changing the number of random variables affect the accuracy of the approximation? How does changing the number of outcomes for each random variable affect the accuracy of the approximation?

Sampling Details: To test the unconstrained set $\mathbb{T}$, 100,000 distributions are obtained using the HR sampler presented in Chapter 3. Then, we determine the "distance" (as defined by the measures in Chapter 4) from each of the samples to the discrete uniform distribution using the six measures proposed.

Six unconstrained sets are considered for this section. The first three correspond to joint distributions with 3, 5, and 7 marginal random variables with two outcomes each. The last three correspond to joint distributions with 3 marginal random variables with 2, 3, and 4 outcomes each.

Our results are presented in two parts. First, we consider the effects of increasing the number of marginal variables in a joint distribution. For this part we present a summary of the results and provide an in-depth analysis of the behavior of the sample and the measures of accuracy. Next, we consider the effects of increasing the number of outcomes of the marginal variables in a joint distribution. We present a summary of these results and link the observations to the analysis presented in the first part.

Results for Number of Variables. Figure 5.10 shows the proportion-histograms after taking 100,000 samples for three unconstrained sets. The first set contains all joint distributions that can be generated using three binary random variables. The second and third sets consider five and seven binary random variables, respectively. This series of histograms shows how the sample changes as the set increases in number of joint events and dimension.

As the number of variables increases, $\mathbf{L}^\infty$ and Euclidean distance decrease. This reduction is a direct effect of the concentration of volume in $\mathbb{T}$. As described in Chapter 3, the volume of $\mathbb{T}$ shrinks with dimensionality, and the shrinkage is exponentially higher as distance from the center increases. Therefore, the sample concentrates its mass closer to the center. This result is counterintuitive because the addition of a new dimension normally increases the existing space. However, the n-content (relative interior volume) decreases, which increases the concentration of the samples in $\mathbb{T}$.

Summary. Figure 5.11 presents the mean and standard deviation of the results presented in Figure 5.10. The mean of the measures is decreasing for $\mathbf{L}^\infty$ and $\mathbf{L}^2$, but it is increasing and then decreasing for $\mathbf{L}^1$, $\mathbf{KL}$, $\boldsymbol{\chi^2}$, and $\boldsymbol{\Delta H}$. However, all accuracy measures decrease in variance as dimensionality increases, making the samples closer to each other and improving the precision of the truth set.

Intuition and Theory. The behavior of the sampled distributions and the measures of accuracy shown in Figure 5.11 are intuitive, as follows. Take a binary distribution $P_a^* = \{\frac{1}{5}, \frac{1}{5}\}$, and perturb it to create $P_b^* = \{\frac{1}{5} + \epsilon, \frac{1}{5} - \epsilon\}$. Then, $\mathbf{L}^\infty(P_a^*, P_b^*) = \epsilon$, $\mathbf{L}^2(P_a^*, P_b^*) = \epsilon \cdot \sqrt{2}$, and $\mathbf{L}^1(P_a^*, P_b^*) = 2 \cdot \epsilon$. In general, for a joint distribution P_a at the center of $\mathbb{T}$ (the discrete uniform distribution) with n elements, where n is an even number, and a distribution P_b, which is a perturbation of P_a where every $+\epsilon$ has a corresponding $-\epsilon$ and every joint event is perturbed we have that $\mathbf{L}^\infty(P_a, P_b) = \epsilon$, $\mathbf{L}^2(P_a, P_b) = \epsilon \cdot \sqrt{n}$, and $\mathbf{L}^1(P_a, P_b) = n \cdot \epsilon$.

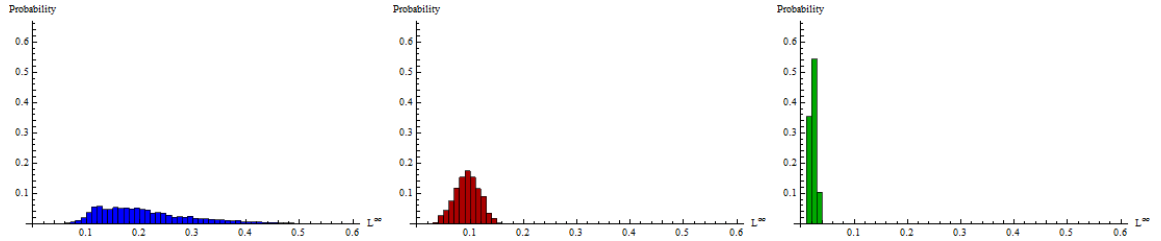

(a) 3 Var. $\mathbf{L}^{\infty}$. (b) 5 Var. $\mathbf{L}^{\infty}$. (c) 7 Var. $\mathbf{L}^{\infty}$.

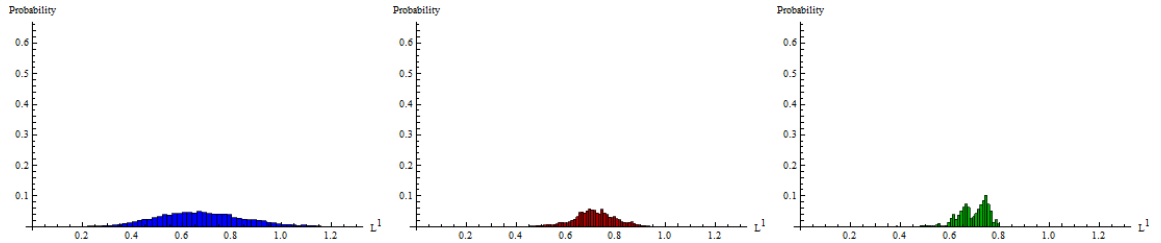

(d) 3 Var. $\mathbf{L}^{1}$. (e) 5 Var. $\mathbf{L}^{1}$. (f) 7 Var. $\mathbf{L}^{1}$.

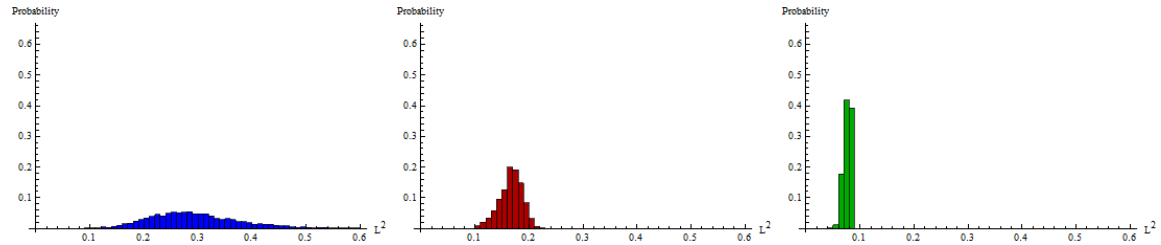

(g) 3 Var. $\mathbf{L}^{2}$. (h) 5 Var. $\mathbf{L}^{2}$. (i) 6 Var. $\mathbf{L}^{2}$.

Figure 5.10: Unconstrained sets (part one): Variations on accuracy measures as the number of binary variables increases.

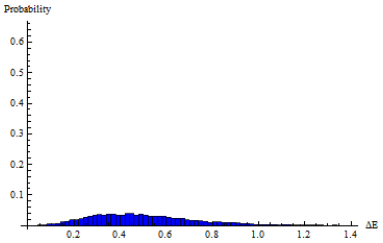

(j) 3 Var. $|\boldsymbol{\Delta H}|$.

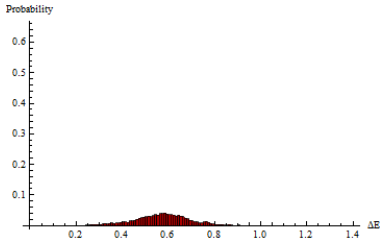

(k) 5 Var. $|\boldsymbol{\Delta H}|$.

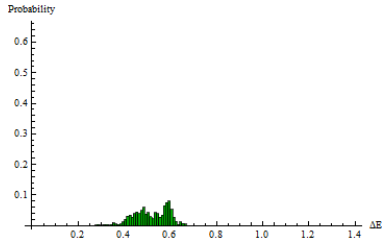

(l) 7 Var. $|\boldsymbol{\Delta H}|$.

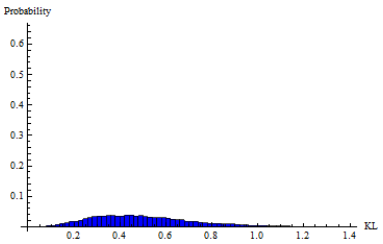

(m) 3 Var. $\boldsymbol{KL}$.

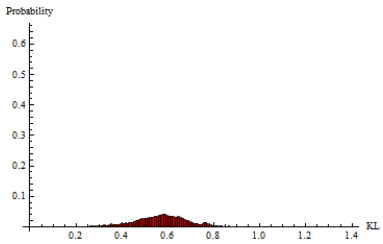

(n) 5 Var. $\boldsymbol{KL}$.

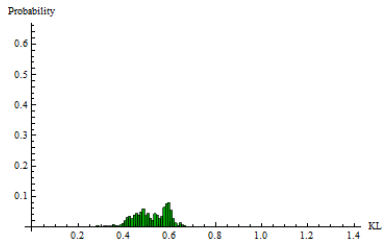

(o) 7 Var. $\boldsymbol{KL}$.

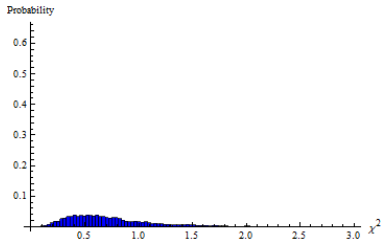

(p) 3 Var. $\boldsymbol{\chi^2}$.

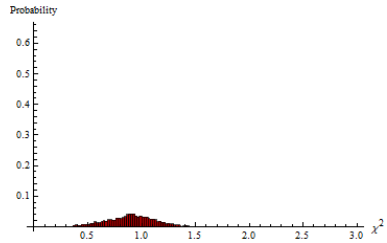

(q) 5 Var. $\boldsymbol{\chi^2}$.

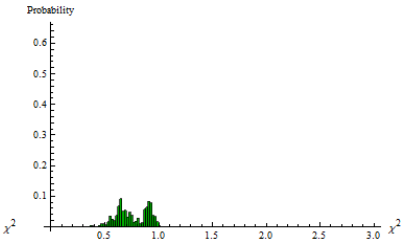

(r) 7 Var. $\boldsymbol{\chi^2}$.

Figure 5.10: Unconstrained sets (part two): Variations on accuracy measures as the number of binary variables increases.

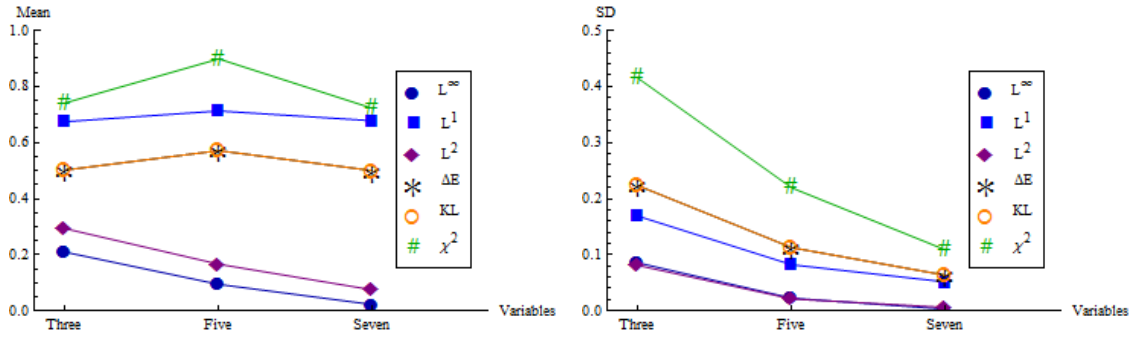

(a) Mean. (b) Standard Deviation.

Figure 5.11: Unconstrained sets: Mean and standard deviation as the number of binary variables increases.

As the dimension $d = n - 1$ of $\mathbb{T}$ increases, we can find the ϵ that matches the changes of the sampled joint distributions, where ϵ is a reference measure of the mean of the Euclidean distances from the center of $\mathbb{T}$ to the collection of sampled distributions. We start by sampling 100,000 joint distributions from eight polytopes of different dimensions and calculate the mean of the measures generated with $\mathbf{L}^2$ for each polytope. Then, we find the values of ϵ that match the same distance from P_a to P_b. In other words, we look for the perturbed joint distributions that have the same $\mathbf{L}^2$ as the mean of $\mathbf{L}^2$ on the sampled distributions.

Figure 5.12 shows the best fit for ϵ as a function of the dimension d. The figure depicts how the necessary perturbations decrease with d, explaining the changes in $\mathbf{L}^\infty$, $\mathbf{L}^1$, and $\mathbf{L}^2$ when the dimension of the set increases. In other words, the mean distance from the center to the sample decreases.

ϵ can be used to understand the behavior of the measures of accuracy in unconstrained sets. For example $\mathbf{L}^\infty(P_a, P_b) = \epsilon$ decreases as the number of variables increases. $\mathbf{L}^1(P_a, P_b) = n{\cdot}\epsilon$ increases and then decreases as part of a tradeoff between d and ϵ, and $\mathbf{L}^2(P_a, P_b) = \epsilon{\cdot}\sqrt{n}$ decreases since ϵ decays faster than $\sqrt{n}$. These tradeoffs explain the behavior shown in Figures 5.10 and 5.11. Additionally, a theoretical

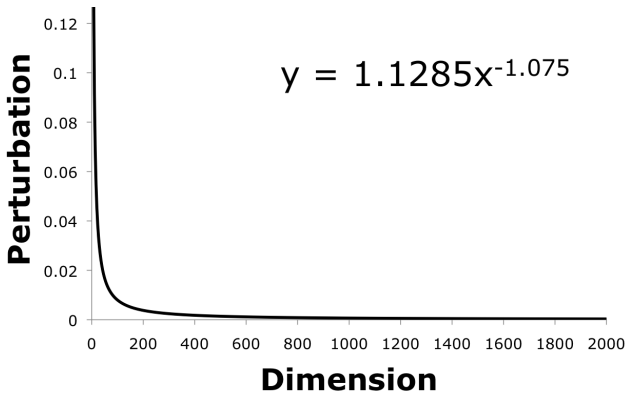

Figure 5.12: Symmetric perturbations vs. dimensionality.

extrapolation of these results for a larger range of dimensions is shown in Figure 5.13.

The symmetric perturbations for $\boldsymbol{KL}$, $\boldsymbol{\chi^2}$, and $\boldsymbol{\Delta H}$ can be derived using the procedure described earlier. For P_a and P_b as previously defined, $\boldsymbol{KL}(P_b, P_a) = \boldsymbol{\Delta H}(P_b, P_a)$. This fact does not hold in the more general case (assessment constraints) but provides an intuitive description of the $\boldsymbol{KL}$ divergence as the entropy difference between two joint distributions. For two arbitrary distributions $\mathbf{p}$ and $\bar{\mathbf{p}}$, $\boldsymbol{KL}_n(\mathbf{p}||\bar{\mathbf{p}}) = \boldsymbol{\Delta H}(\mathbf{p}, \bar{\mathbf{p}}) + \sum_i (\bar{p}_i - p_i) \log(\bar{p}_i)$. Then, $\boldsymbol{KL}$ approximates $\boldsymbol{\Delta H}$ with a bias generated by $\sum_i \epsilon_i \log(\bar{p}_i)$, where the perturbations $|\epsilon_i| = |\bar{p}_i - p_i| \leq \mathbf{L}^\infty$ tend to zero as the dimensionality increases.

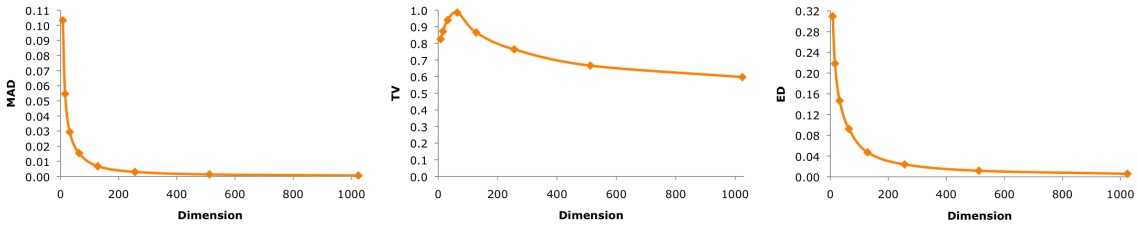

(a) $\mathbf{L}^\infty$. (b) $\mathbf{L}^1$. (c) $\mathbf{L}^2$.

Figure 5.13: Symmetric perturbations vs. dimensionality.

The accuracy measures based on information ($\boldsymbol{KL}, \boldsymbol{\Delta H}$) do not show a monotonic behavior with respect to the dimensionality of $\mathbb{T}$. However, for unconstrained

polytopes, we can show that $\boldsymbol{KL} = \log_2 \left[\frac{(1+\mathbf{L}^1)^{\frac{\mathbf{L}^1+1}{2}}}{(1-\mathbf{L}^1)^{\frac{\mathbf{L}^1-1}{2}}} \right] \approx \sum_i \frac{(\mathbf{L}^1)^{2i}}{2i(2i-1)\ln(2)}$ (Appendix B.3). This result shows that $\boldsymbol{\Delta H}, \boldsymbol{KL}$, and $\mathbf{L}^1$ share similar characteristics and behave similarly in unconstrained polytopes. These results cannot be expected to hold for constrained polytopes, but some similarities should remain after adding constraints to a truth set $\mathbb{T}$. Figure 5.14 shows a theoretical extrapolation for a larger range of dimensions. There are similarities among Figures 5.14(a), 5.14(b), and 5.13(b) given by the relation among $\boldsymbol{\Delta H}, \boldsymbol{KL}$, and $\mathbf{L}^1$. This same relation can be found in the $\boldsymbol{\chi^2}$ measure (Fig. 5.14(c)), which in the unconstrained case can be shown to be $\boldsymbol{\chi^2} = (\mathbf{L}^1)^2$ for symmetric perturbations.

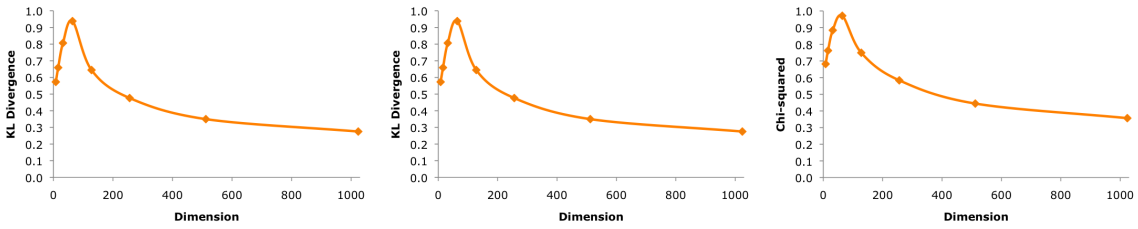

(a) $\boldsymbol{\Delta H}$. (b) **KL**. (c) $\boldsymbol{\chi^2}$.

Figure 5.14: Symmetric perturbations vs. dimensionality.

Figure 5.10 increases the dimension of the set $\mathbb{T}$ by increasing the number of marginal random variables in the joint distribution. A second alternative is to increase the number of possible outcomes of each variable. The following results are for joint distributions with three random variables and increasing number of outcomes.

Results for Number of Outcomes. The histograms in Figure 5.15 show similar behavior to those in Figure 5.10. This indicates that the effect of increasing the number of outcomes is similar to the effect of increasing the number of random variables. Moreover, the behavior of the samples is aligned with our theoretical results (Figures 5.14 and 5.13). In other words, what drives the behavior is the dimension of the set, and not how the dimension is increased.

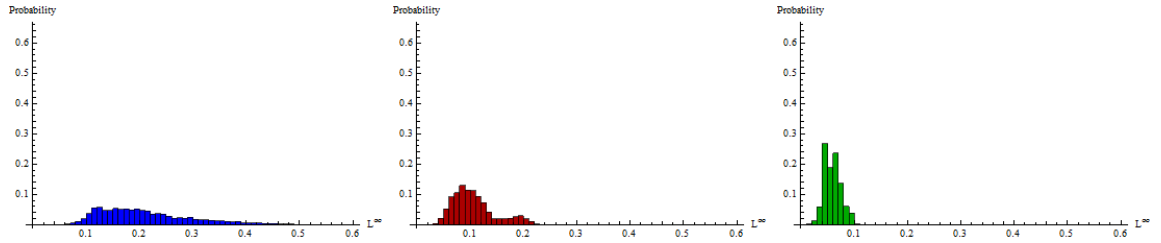

(a) 2 Outcomes, $\mathbf{L}^\infty$. (b) 3 Outcomes, $\mathbf{L}^\infty$. (c) 4 Outcomes, $\mathbf{L}^\infty$.

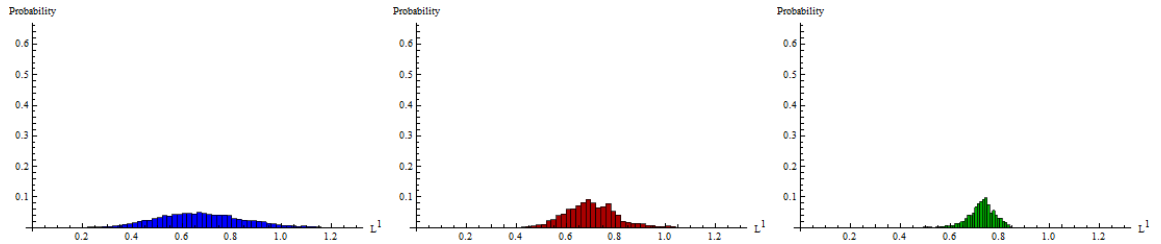

(d) 2 Outcomes, $\mathbf{L}^1$. (e) 3 Outcomes, $\mathbf{L}^1$. (f) 4 Outcomes, $\mathbf{L}^1$.

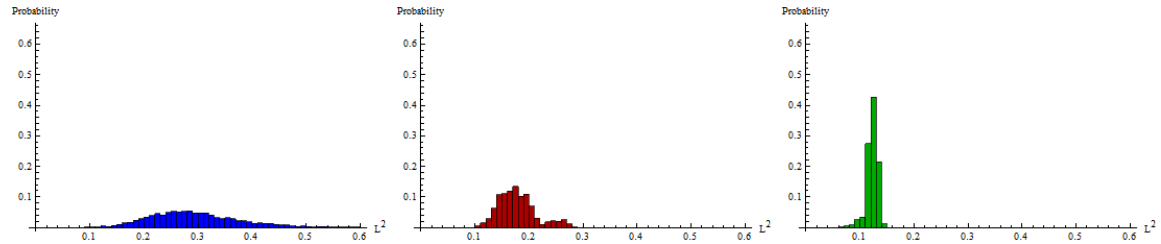

(g) 2 Outcomes, $\mathbf{L}^2$. (h) 3 Outcomes, $\mathbf{L}^2$. (i) 4 Outcomes, $\mathbf{L}^2$.

Figure 5.15: Unconstrained sets (part one): Variations in accuracy measures as the number of outcomes increases (for three random variables).

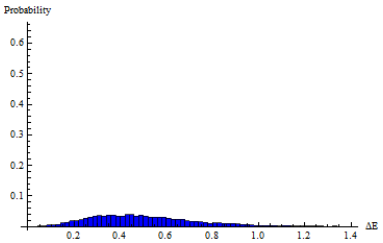

(j) 2 Outcomes, $|\boldsymbol{\Delta H}|$.

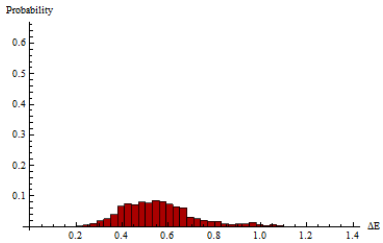

(k) 3 Outcomes, $|\boldsymbol{\Delta H}|$.

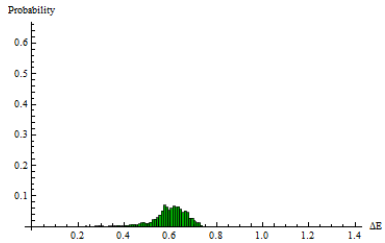

(l) 4 Outcomes, $|\boldsymbol{\Delta H}|$.

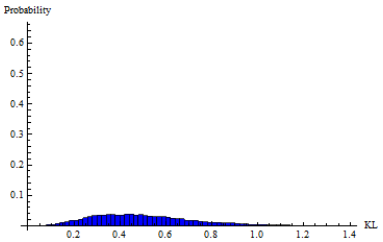

(m) 2 Outcomes, $\boldsymbol{KL}$.

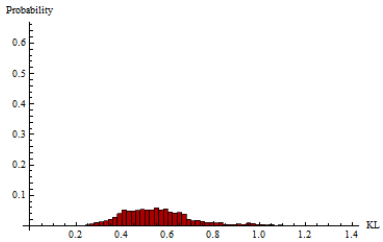

(n) 3 Outcomes, $\boldsymbol{KL}$.

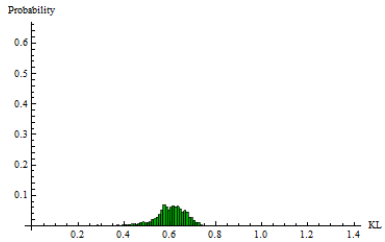

(o) 4 Outcomes, $\boldsymbol{KL}$.

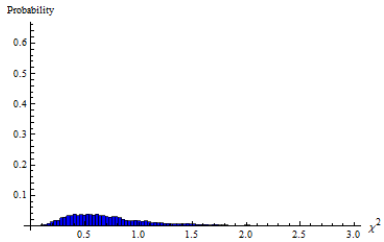

(p) 2 Outcomes, $\boldsymbol{\chi^2}$.

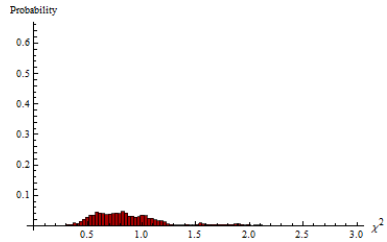

(q) 3 Outcomes, $\boldsymbol{\chi^2}$.

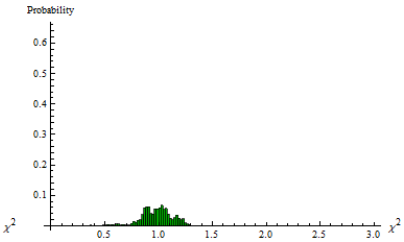

(r) 4 Outcomes, $\boldsymbol{\chi^2}$.

Figure 5.15: Unconstrained sets (part two): Variations in accuracy measures as the number of outcomes increases (for three random variables).

Results Summary. Figure 5.16 shows the mean and standard deviation of the results in Figure 5.15. The dimension of the three sets is 8, 27, and 64 for 2, 3, and 4 outcomes, respectively. Figures 5.13 and 5.14 showed that in the ranges from 2 to 64, the means for $\mathbf{L}^1$, $|\boldsymbol{\Delta H}|$, $\boldsymbol{KL}$, and $\boldsymbol{\chi^2}$ are increasing, whereas $\mathbf{L}^\infty$ and $\mathbf{L}^2$ are decreasing. In contrast, the standard deviation decreases for all six accuracy measures, indicating that the samples are more concentrated in specific areas of the polytope.

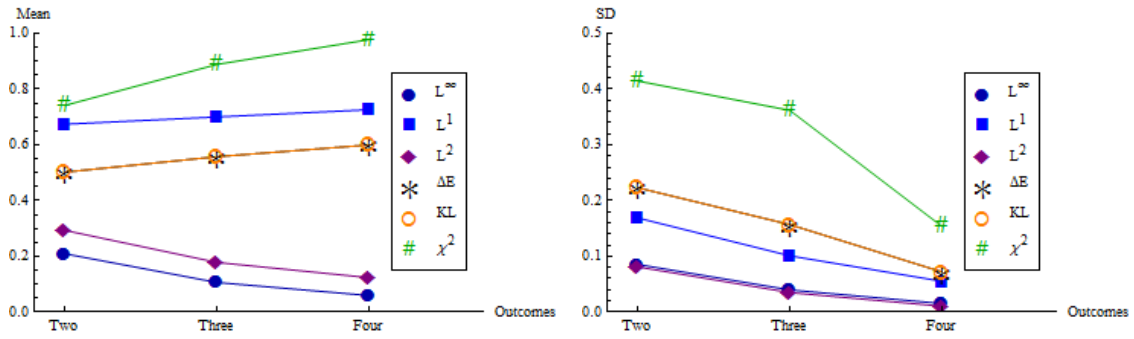

(a) Mean. (b) Standard Deviation.

Figure 5.16: Unconstrained sets: Mean and standard deviation as the number of outcomes increases (for three random variables).

5.2.1 Findings in Unconstrained Truth Sets

1. An increase in the number of joint events (dimensions) generates samples that show a higher level of concentration.

2. As the dimension of $\mathbb{T}$ increases, the measures of accuracy $\mathbf{L}^\infty$ and $\mathbf{L}^2$ decrease monotonically.

3. As the dimension of $\mathbb{T}$ increases, the measures of accuracy $\mathbf{L}^1$, $\boldsymbol{KL}$, and $\boldsymbol{\chi^2}$ exhibit an eventual decrease without being monotonic. These measures together with $\boldsymbol{\Delta H}$ are quasi convex functions of the dimension of $\mathbb{T}$.

4. The behavior of the samples and their relation to the approximation distributions are determined by the dimension of the set. How the dimension is increased (by increasing the number of constraints or the number of outcomes) does not make a difference.

5.3 Symmetrically Constrained Multivariate Distributions

In this section, we measure the effects of adding constraints to the truth set $\mathbb{T}$. We consider two questions: How does adding new constraints affect accuracy? How does changing the existing constraints affect the accuracy of the distribution approximations? Subsection 5.3.1 addresses the first question, while Subsections 5.3.2 and 5.3.3 address the second. For simplicity, this section uses only symmetric information, i.e., all marginal random variables are identically distributed and binary, and all rank correlations have the same correlation value. However, these results can easily be extended to random variables with any number of outcomes.

5.3.1 Effects of Increasing the Number of Constraints

Sampling Details. To observe the effects of new constraints on $\mathbb{T}$, the constraints are restricted to be consistent with the assessments of the discrete uniform distribution (Equation 3.2, marginals of $\frac{1}{2}$, pairwise of $\frac{1}{4}$, and three-wise of $\frac{1}{8}$). Then, all the constraints are consistent with the center of $\mathbb{T}$, and all the distribution approximations are equal to the uniform distribution. We start by using HR to create a collection of 100,000 sampled joint distributions from an unconstrained set with five binary random variables, and measure the distance to the discrete uniform distribution (Figures 5.17 and 5.18). Next, we add a new constraint (marginal assessments) and observe the changes in accuracy. This procedure is repeated for pairwise and three-wise constraints. (Results for 3 and 7 binary random variables can be observed in Appendix C, Figures C.9, C.10, and Figures C.11, C.12, respectively.)

Each column in Figure 5.17 and 5.18 describe the results for a measure of accuracy, while the rows describe the results for a truth set. For example, the superior row corresponds to the unconstrained set, and subsequent rows increase the number of constraints downward.

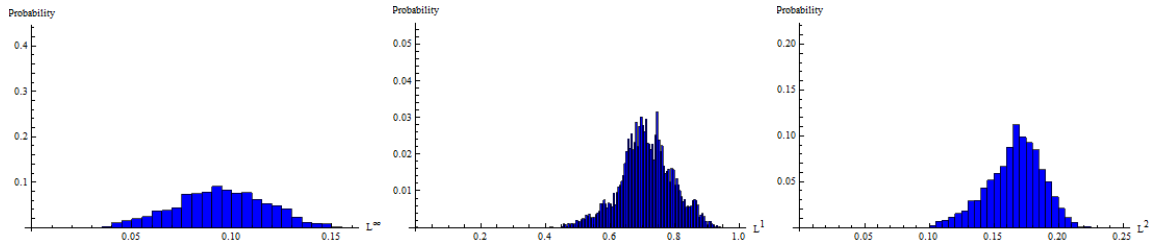

(a) Unconstrained, $\mathbf{L}^{\infty}$.

(b) Unconstrained, $\mathbf{L}^{1}$.

(c) Unconstrained, $\mathbf{L}^{2}$.

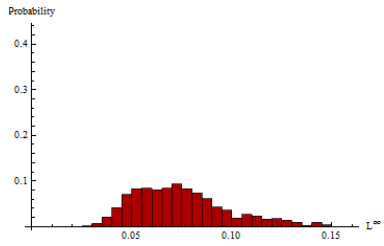

(d) Marginal, $\mathbf{L}^{\infty}$.

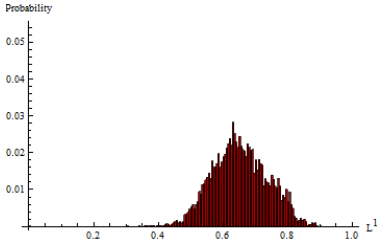

(e) Marginal, $\mathbf{L}^{1}$.

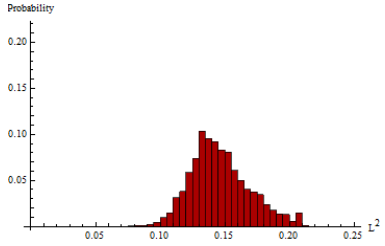

(f) Marginal, $\mathbf{L}^{2}$.

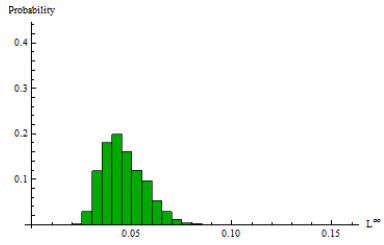

(g) Pairwise, $\mathbf{L}^{\infty}$.

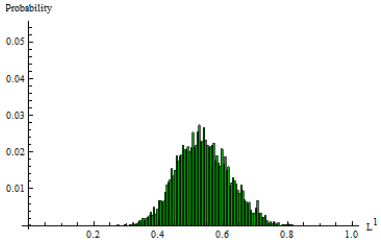

(h) Pairwise, $\mathbf{L}^{1}$.

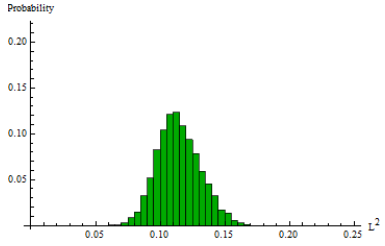

(i) Pairwise, $\mathbf{L}^{2}$.

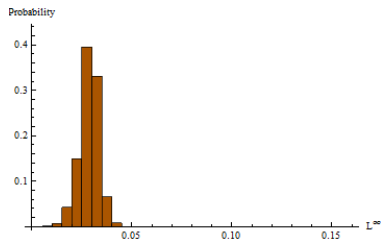

(j) Three-wise, $\mathbf{L}^{\infty}$.

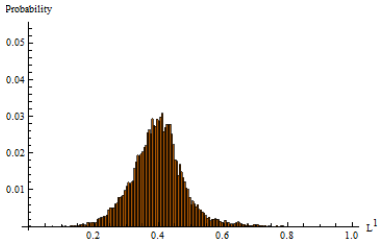

(k) Three-wise, $\mathbf{L}^{1}$.

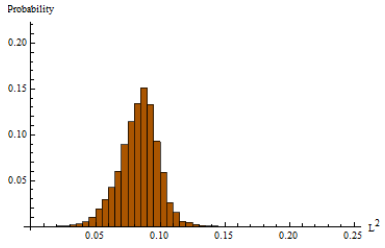

(l) Three-wise, $\mathbf{L}^{2}$.

Figure 5.17: Effects of including new constraints in truth set $\mathbb{T}$. The data are taken for a set that considers 5 binary variables. The unconstrained set uses 1 constraint. The marginal set uses 6 constraints. The pairwise set uses 16 constraints. The three-wise set uses 26 constraints.

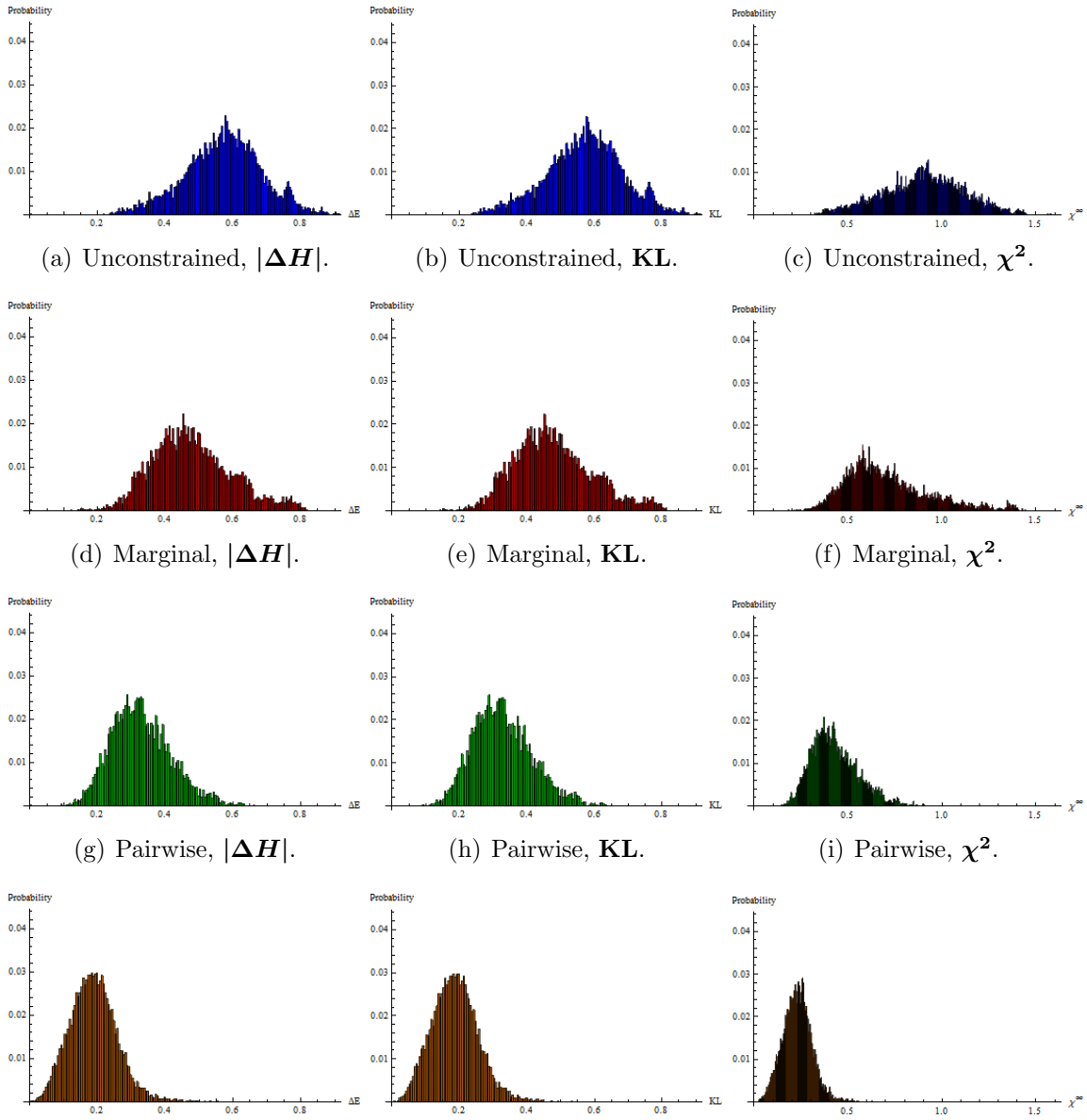

(a) Unconstrained, $|\boldsymbol{\Delta H}|$. (b) Unconstrained, **KL**. (c) Unconstrained, $\boldsymbol{\chi^2}$.

(d) Marginal, $|\boldsymbol{\Delta H}|$. (e) Marginal, **KL**. (f) Marginal, $\boldsymbol{\chi^2}$.

(g) Pairwise, $|\boldsymbol{\Delta H}|$. (h) Pairwise, **KL**. (i) Pairwise, $\boldsymbol{\chi^2}$.

(j) Three-wise, $|\boldsymbol{\Delta H}|$. (k) Three-wise, **KL**. (l) Three-wise, $\boldsymbol{\chi^2}$.

Figure 5.18: Effect of including new constraints in truth set $\mathbb{T}$. The data are taken for a set that considers 5 binary variables. The unconstrained set uses 1 constraint. The marginal set uses 6 constraints. The pairwise set uses 16 constraints. The three-wise set uses 26 constraints.

Results. As we add more constrains to $\mathbb{T}$ the histograms shift to the left, indicating that the samples get closer to the uniform distribution. The only exception happens when $\mathbb{T}$ becomes one dimensional (Figure C.9) in which case the samples become distributed uniformly over a line creating a non-bell-shaped pattern.

A different behavior is exhibited in the case of the dispersion of the samples. As the number of constraints increases, the collection does not necessarily become more concentrated. This effect is caused by a tradeoff between the dispersion of the n-content in the interior of $\mathbb{T}$ (§3.6), and the change of geometry of $\mathbb{T}$ generated by the new constraint. This accounts for why the variance may increase or decrease, according to the relation between the dispersion of the n-content and the geometric shape of $\mathbb{T}$.

Results Summary. Figure 5.19 shows the mean and Figure 5.20 shows the standard deviation of the results displayed in Figures C.9, C.10; Figures 5.17, 5.18; and Figures C.11, C.12; which pairs of figures correspond to sets with three, five, or seven binary random variables.

Since all the constraints are assessments aligned to the discrete uniform distribution, all the distribution approximations considered give as a result the discrete uniform distribution. In this case, the more constrained the truth set, the higher the accuracy of the approximations (the lower the mean). This result is not surprising because if enough constraints are added, the set $\mathbb{T}$ becomes a singleton in which any approximation in the interior of the truth set is exact. However, it is unexpected that when the truth set is close to dimension one, an additional constraint might decrease the accuracy for some of the measures of accuracy (e.g. $\boldsymbol{KL}, \mathbf{L}^2$). None the less, this last case is more an exception than a rule, since a large number of sets of interest are high dimensional polytopes.

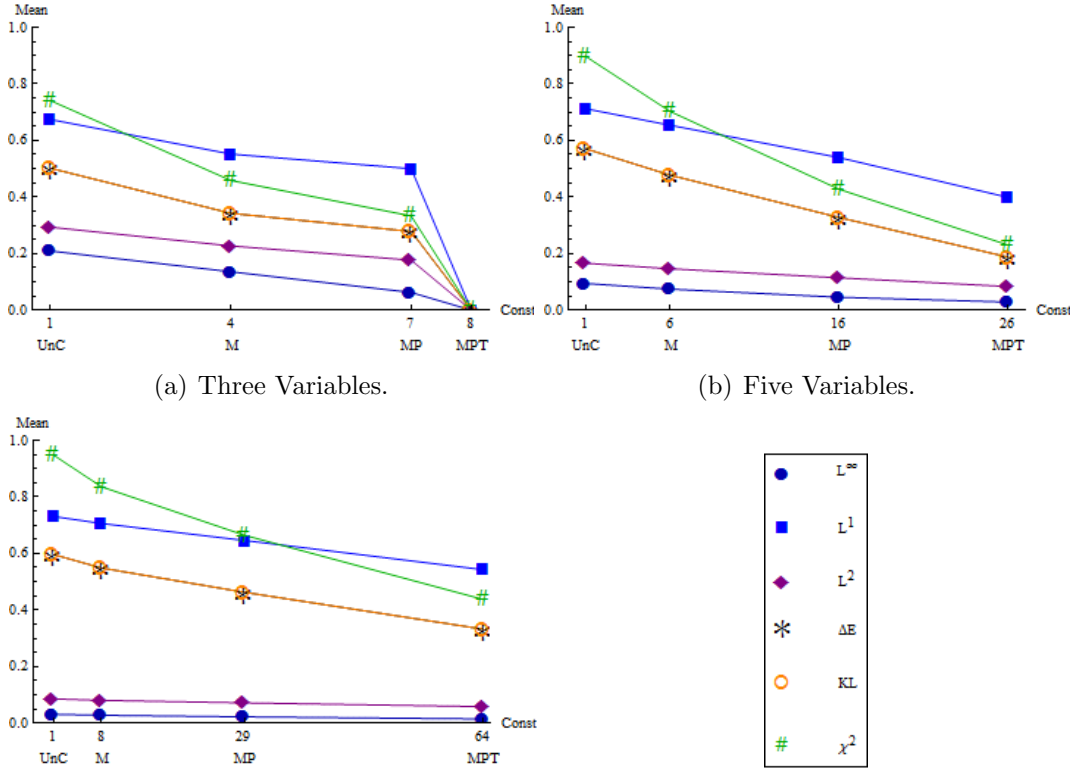

(a) Three Variables.

(b) Five Variables.

(c) Seven Variables.

Figure 5.19: Mean results for unconstrained sets (UnC), marginal constrained sets (M), marginal and pairwise constrained sets (MP), and marginal, pairwise, and three-wise constrained sets (MPT).

The standard deviation does not necessarily decrease as the number of constraints increases. For example, in Figure 5.20(a), the polytope goes from 7 dimensions ($d = n - 1$), to 4 dimensions after adding the marginal constraints, to 1 dimension after adding pairwise constraints, to a singleton after adding the three-wise constraints. Then the set with marginal and pairwise constraints (MP) becomes a line section. Adding the pairwise constraints has reduced the number of possible joint distributions and the n-content is now equivalent to the length of the line. The HR sampled this line uniformly, increasing the probability to sample joint distributions in the neighborhoods of the vertices of $\mathbb{T}$, which increase the standard deviation.

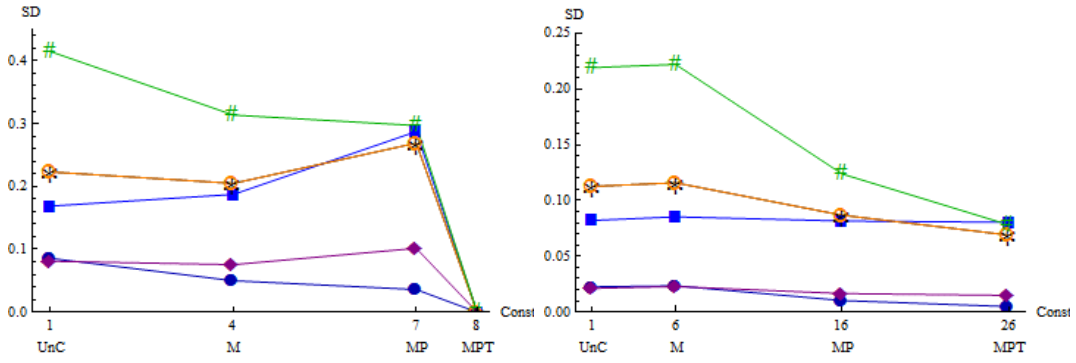

(a) Three Variables.

(b) Five Variables.

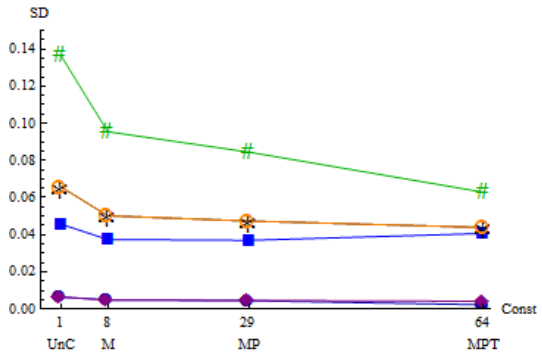

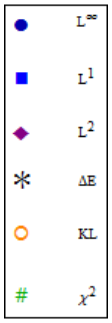

(c) Seven Variables.

Figure 5.20: Standard deviation results for unconstrained sets (UnC), marginal constrained sets (M), marginal and pairwise constrained sets (MP), and marginal, pairwise, and three-wise constrained sets (MPT).

5.3.2 Symmetric Marginal Constraints

Sampling Details. We now address the accuracy of the approximations under marginal symmetric constraints for different values of $\mathbf{b}$ ($\mathbf{Ap} = \mathbf{b}$). Specifically, we address how the accuracy of the approximations changes as the marginal assessments change. If X is a binary random variable, then, we consider marginal assessments with values of $P(X = 1)$ =0.5, 0.6, 0.7, 0.8, and 0.9 and consider joint distributions with 3, 4, 5, 6, and 7 marginal binary random variables. We start by generating the truth set $\mathbf{Ap} = \mathbf{b}, \quad \mathbf{p} \geq 0$, where $\mathbf{b} = \{b_1, b_2, \ldots, b_m\}$, $b_1 = b_2 = \cdots = b_m$ and running HR for 100,000 joint distributions in the case of 3 and 4 marginal random variables, and 200,000 in the case of 5, 6, and 7 marginal random variables. After the

collections are complete, we apply the measures of accuracy and calculate the mean and standard deviation of each approximation. Because the number of samples for 6 and 7 random variables does not meet the optimal requirements described in §3.4.3, we use these results under the caveat that some random noise is being introduced.

Results. Figures 5.21 and 5.22 show the mean and standard deviation for the maximum entropy (ME), the analytic center (AC), the Chebyshev's center (ChSC), the maximum volume inscribed ellipsoid center (MVIE), and the dynamic average sample center (DAC) under the six accuracy measures. Under all measures, for $b_1 = 0.5$, all approximations have the same accuracy. However, modifying b_1 causes the approximations to become differentiated. This is the first truth set for which the approximations provide different joint distributions.

ME Findings. In this results the accuracy of ME (blue circle) is consistently lower than most of the other approximations. This contrast the results in Section 5.1 and the beliefs from the decision analysis community that hold ME as a good approximations (Bickel and Smith, 2006).

One possible explanation is that for known families of joint distributions, the joint-probability mass functions (jpmf) are relatively simple. For these models to remain simple requires general assumptions that reduce the required number of parameters, such as the assumption of having higher-order relations as independent as possible (maximum entropy). A family of distributions with lower entropy will result in a jpmf having more parameters to account for all the unspecified assumptions. In our framework, those assumptions are not required. In fact, we are free to not assume anything with respect to higher-order assessments; we simply let the geometry of $\mathbb{T}$ describe what is possible, and in that space, maximum entropy is rare.

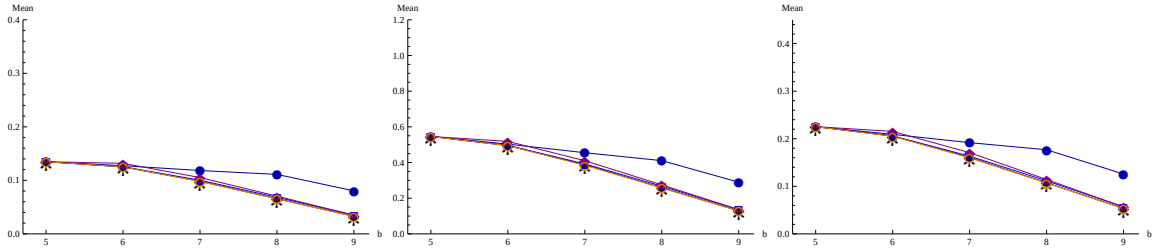

(i) 3 Variables, $\mathbf{L}^{\infty}$. (ii) 3 Variables, $\mathbf{L}^{1}$. (iii) 3 Variables, $\mathbf{L}^{2}$.

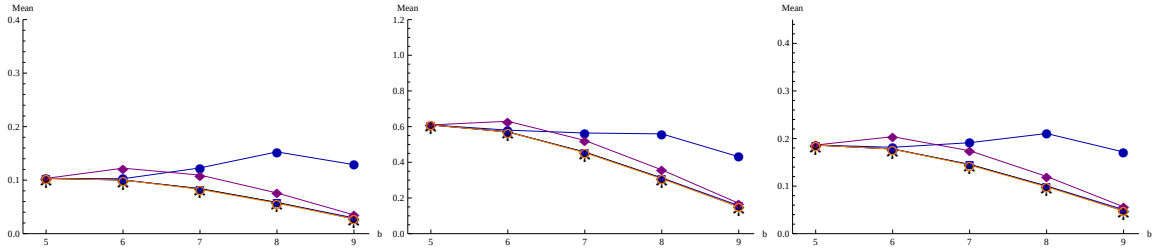

(iv) 4 Variables, $\mathbf{L}^{\infty}$. (v) 4 Variables, $\mathbf{L}^{1}$. (vi) 4 Variables, $\mathbf{L}^{2}$.

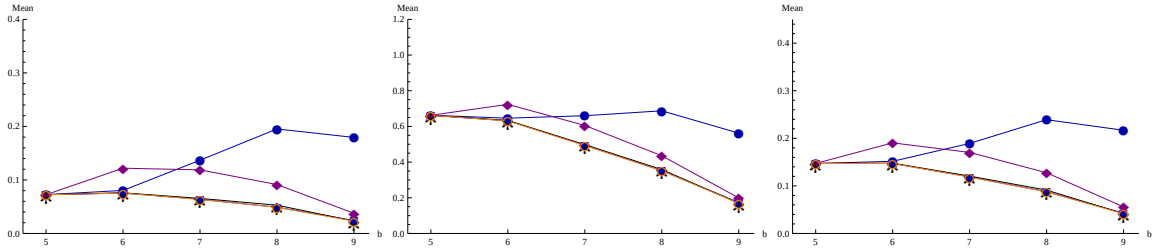

(vii) 5 Variables, $\mathbf{L}^{\infty}$. (viii) 5 Variables, $\mathbf{L}^{1}$. (ix) 5 Variables, $\mathbf{L}^{2}$.

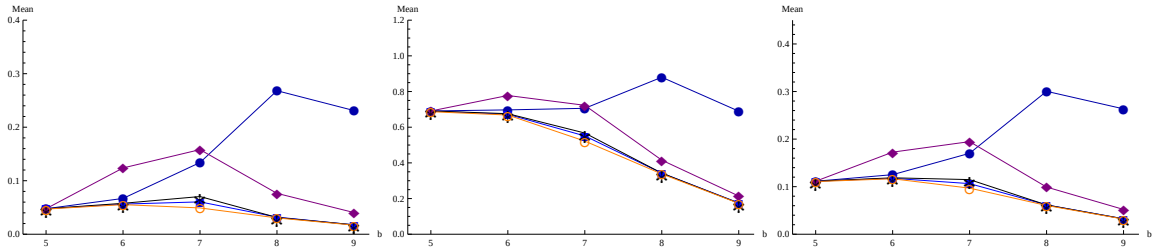

(x) 6 Variables, $\mathbf{L}^{\infty}$. (xi) 6 Variables, $\mathbf{L}^{1}$. (xii) 6 Variables, $\mathbf{L}^{2}$.

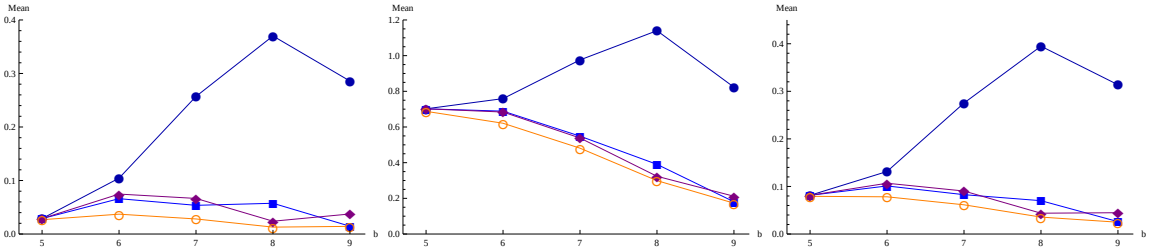

(xiii) 7 Variables, $\mathbf{L}^{\infty}$. (xiv) 7 Variables, $\mathbf{L}^{1}$. (xv) 7 Variables, $\mathbf{L}^{2}$.

Figure 5.21: Mean estimates for truth sets with variables 3 to 7 (part one).

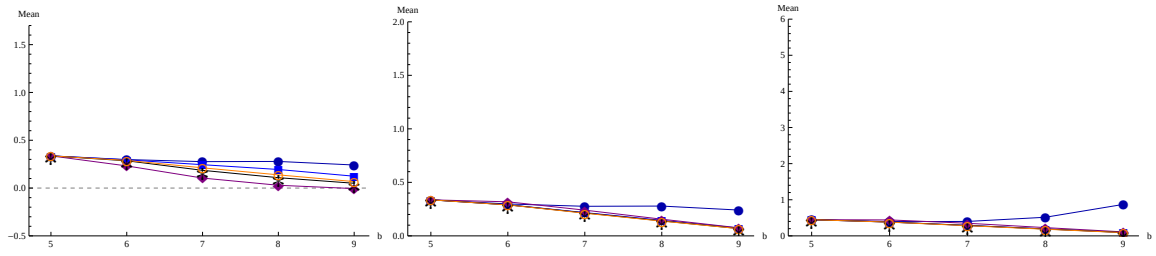

(xvi) 3 Variables, $\boldsymbol{\Delta H}$. (xvii) 3 Variables, **KL**. (xviii) 3 Variables, $\boldsymbol{\chi^2}$.

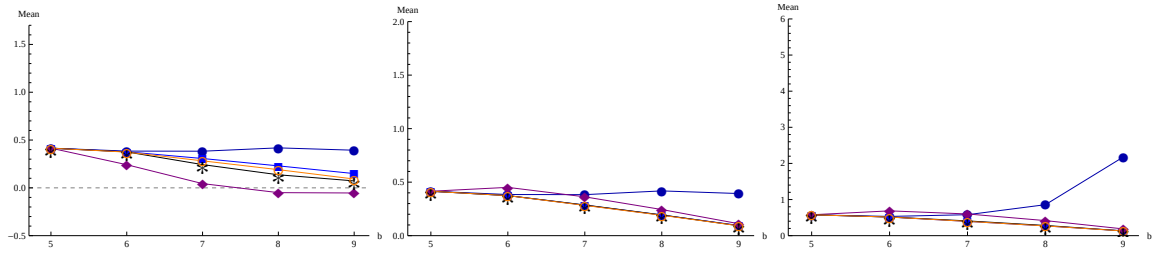

(xix) 4 Variables, $\boldsymbol{\Delta H}$. (xx) 4 Variables, **KL**. (xxi) 4 Variables, $\boldsymbol{\chi^2}$.

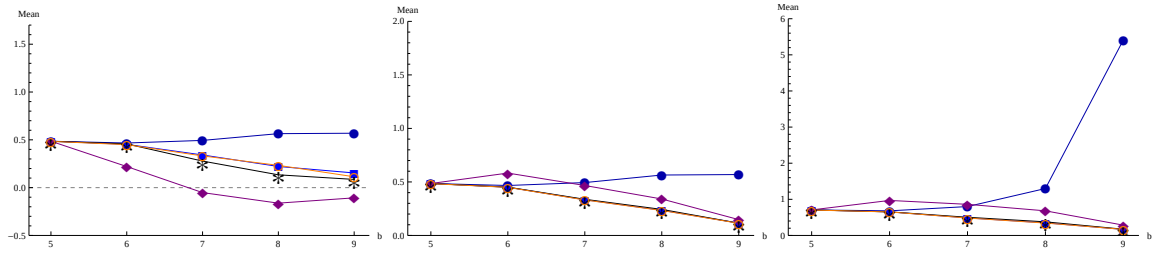

(xxii) 5 Variables, $\boldsymbol{\Delta H}$. (xxiii) 5 Variables, **KL**. (xxiv) 5 Variables, $\boldsymbol{\chi^2}$.

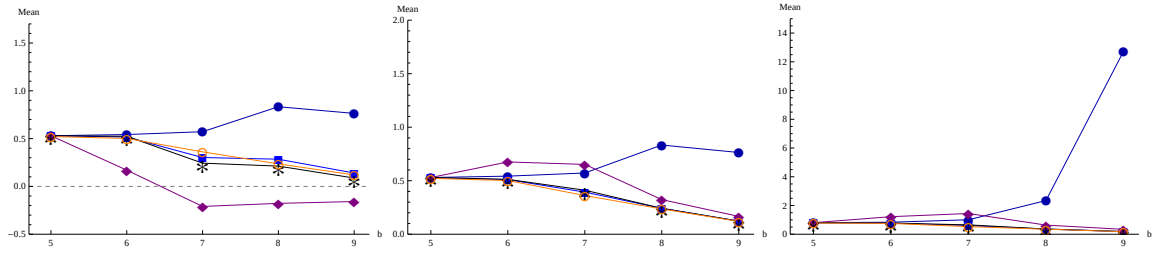

(xxv) 6 Variables, $\boldsymbol{\Delta H}$. (xxvi) 6 Variables, **KL**. (xxvii) 6 Variables, $\boldsymbol{\chi^2}$.

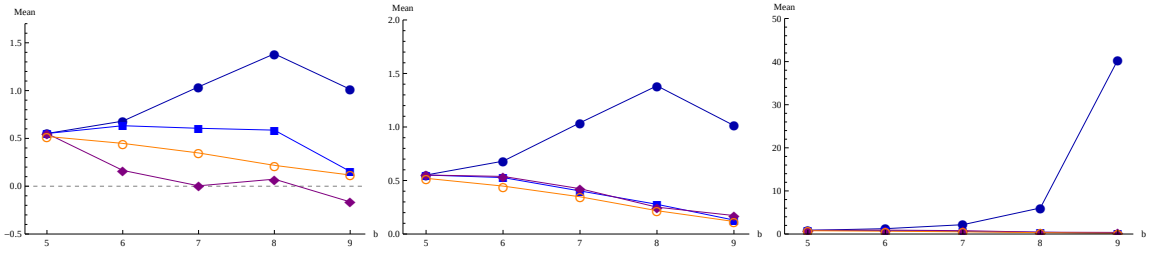

(xxviii) 7 Variables, $\boldsymbol{\Delta H}$. (xxix) 7 Variables, **KL**. (xxx) 7 Variables, $\boldsymbol{\chi^2}$.

Figure 5.21: Mean estimates for truth sets with variables 3 to 7 (rows). The figures indicate variation in accuracy due to change in the marginal constraints (part two).

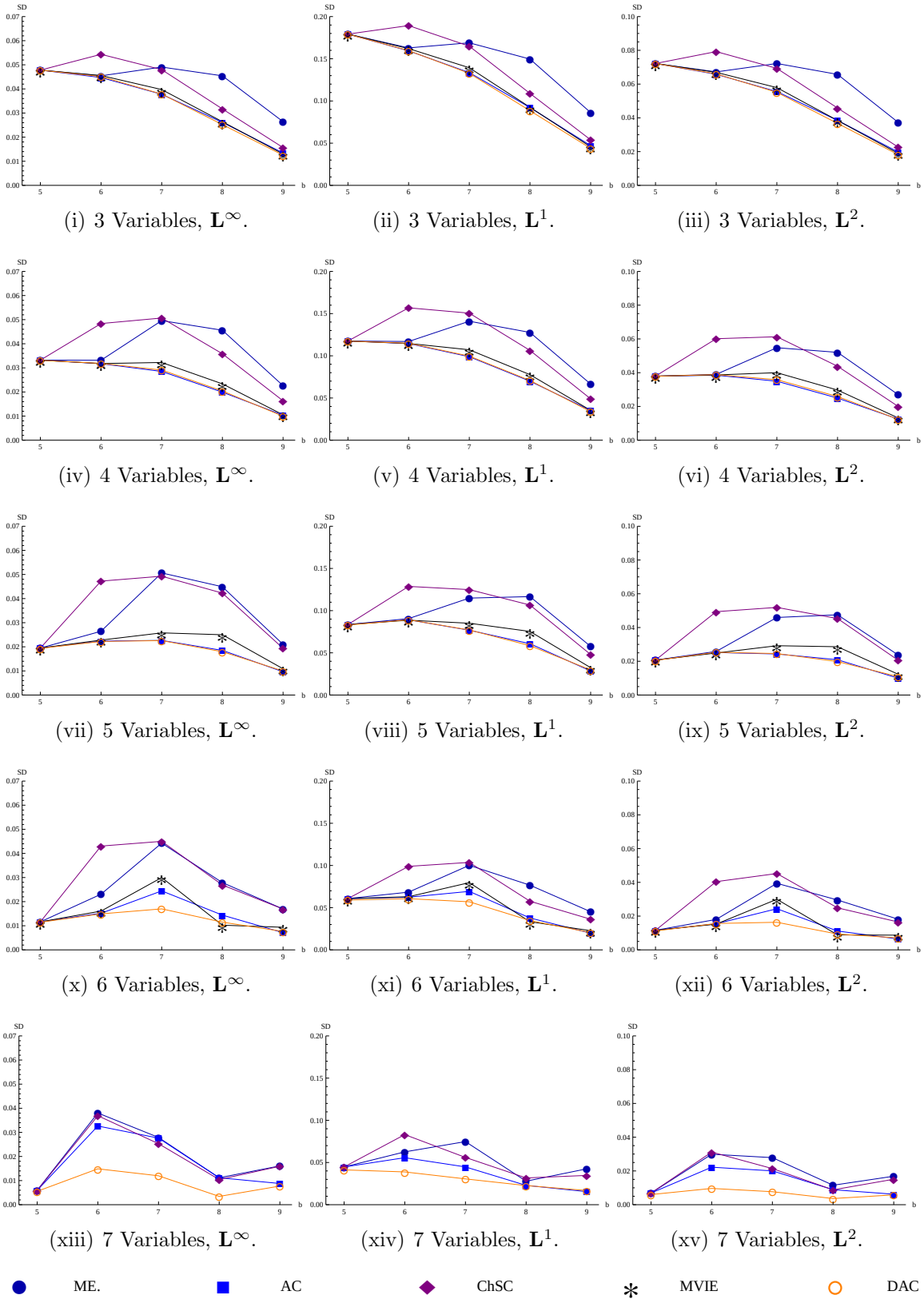

(i) 3 Variables, $\mathbf{L}^{\infty}$. (ii) 3 Variables, $\mathbf{L}^{1}$. (iii) 3 Variables, $\mathbf{L}^{2}$.

(iv) 4 Variables, $\mathbf{L}^{\infty}$. (v) 4 Variables, $\mathbf{L}^{1}$. (vi) 4 Variables, $\mathbf{L}^{2}$.

(vii) 5 Variables, $\mathbf{L}^{\infty}$. (viii) 5 Variables, $\mathbf{L}^{1}$. (ix) 5 Variables, $\mathbf{L}^{2}$.

(x) 6 Variables, $\mathbf{L}^{\infty}$. (xi) 6 Variables, $\mathbf{L}^{1}$. (xii) 6 Variables, $\mathbf{L}^{2}$.

(xiii) 7 Variables, $\mathbf{L}^{\infty}$. (xiv) 7 Variables, $\mathbf{L}^{1}$. (xv) 7 Variables, $\mathbf{L}^{2}$.

Figure 5.22: Standard deviation estimates for $\mathbb{T}$ with variables 3 to 7 (pat one).

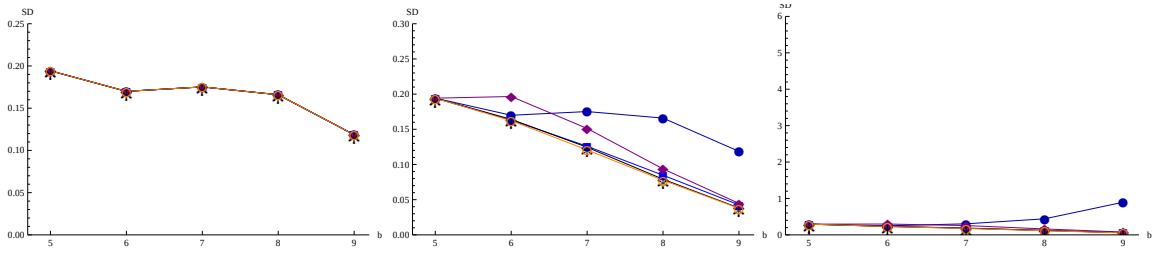

(xvi) 3 Variables, $\boldsymbol{\Delta H}$. (xvii) 3 Variables, **KL**. (xviii) 3 Variables, $\boldsymbol{\chi^2}$.

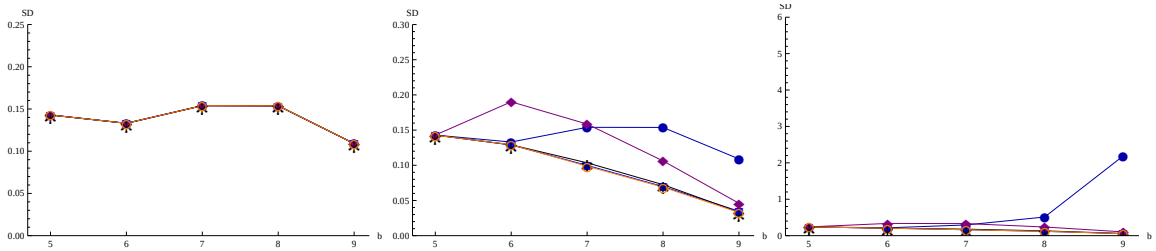

(xix) 4 Variables, $\boldsymbol{\Delta H}$. (xx) 4 Variables, **KL**. (xxi) 4 Variables, $\boldsymbol{\chi^2}$.

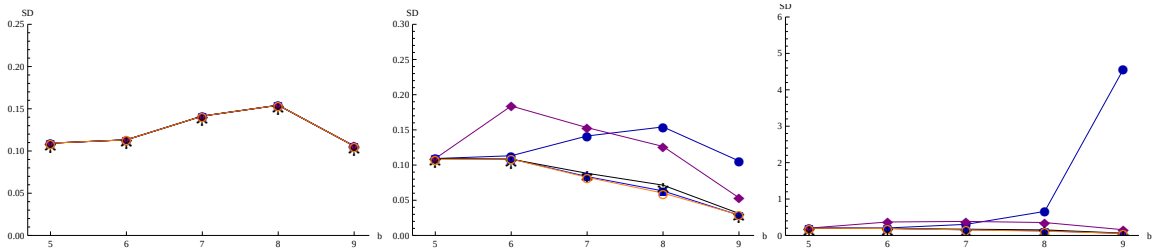

(xxii) 5 Variables, $\boldsymbol{\Delta H}$. (xxiii) 5 Variables, **KL**. (xxiv) 5 Variables, $\boldsymbol{\chi^2}$.

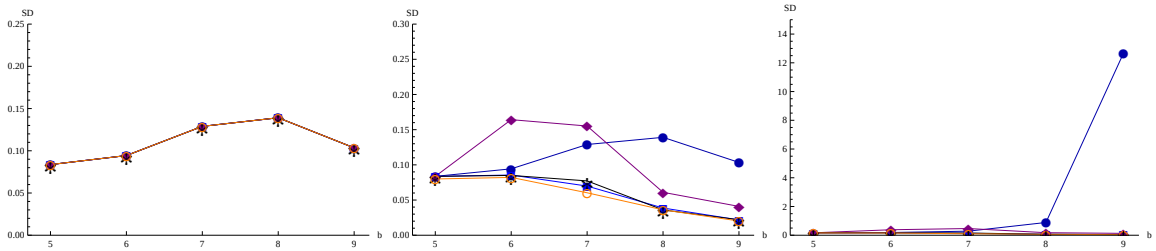

(xxv) 6 Variables, $\boldsymbol{\Delta H}$. (xxvi) 6 Variables, **KL**. (xxvii) 6 Variables, $\boldsymbol{\chi^2}$.

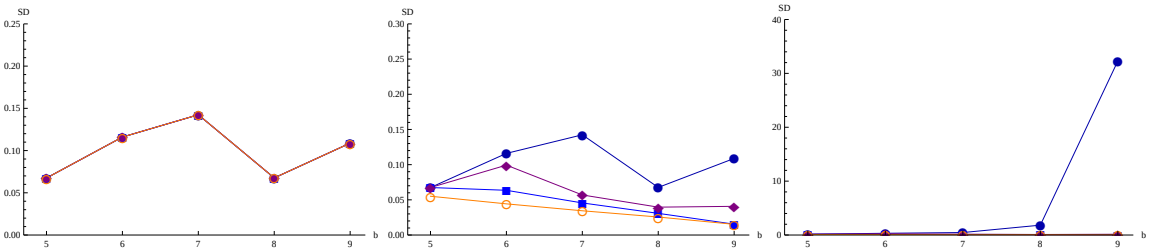

(xxviii) 7 Variables, $\boldsymbol{\Delta H}$. (xxix) 7 Variables, **KL**. (xxx) 7 Variables, $\boldsymbol{\chi^2}$.

Figure 5.22: Standard deviation estimates for $\mathbb{T}$ with variables 3 to 7 (rows). Variation in accuracy due to change in the marginal constraints (part two).

For example, construct a truth set $\mathbb{T}$ using two binary random variables Y_1 and Y_2 with marginal distributions $P(Y_1 = 1) = P(Y_2 = 1) = 0.9$. The jpmf $P(Y_1 = y_1, Y_2 = y_2) = p_{y_1,y_2}$ is unknown since we have no information regarding the correlation between the two variables. However, we know that any solution to the system of equations (5.2) is a joint distribution with the appropriate marginals, and therefore it could be the distribution that accurately models our problem.

The set of solutions of Equation (5.2) can be described as a convex combination of two extreme joint distributions, $\mathbf{p} + \lambda(\mathbf{q} - \mathbf{p}) \; \forall \; \lambda \in [0, 1]$, as shown in Figure 5.23. The λ that corresponds to the ME approximation is close to one of the extreme points of $\mathbb{T}$. This case shows that ME is not a good representation of $\mathbb{T}$, nor is an accurate approximation.

$$p_{1,1} + p_{1,0} + p_{0,1} + p_{0,0} = 1 \tag{5.2a}$$

$$p_{1,1} + p_{1,0} = 0.9 \tag{5.2b}$$

$$p_{1,1} + p_{0,1} = 0.9 \tag{5.2c}$$

$$p_{1,1}, \quad p_{1,0}, \quad p_{0,1}, \quad p_{0,0} \geq 0 \tag{5.2d}$$

Figure 5.21 and the example in Figure 5.23 explain the behavior of ME. As b_1 moves from 0.5 to 0.99, the ME approximation moves closer to the extremes of the truth set. However, at the same time, the size of the truth set decreases. For example, in the case of Equation 5.2, the line representing $\mathbb{T}$ shortens. This explains why for different values of b_1, the accuracy degrades and improves according to most accuracy measures. The only accuracy measure in disagreement is χ^2. However, this is attributable to the scaling generated by the distribution approximation. For example, the jump of the χ^2 measure in Figure 5.22(xxx) for $b_1 = 0.9$ indicates that ME has at least one element whose probability is close to zero.

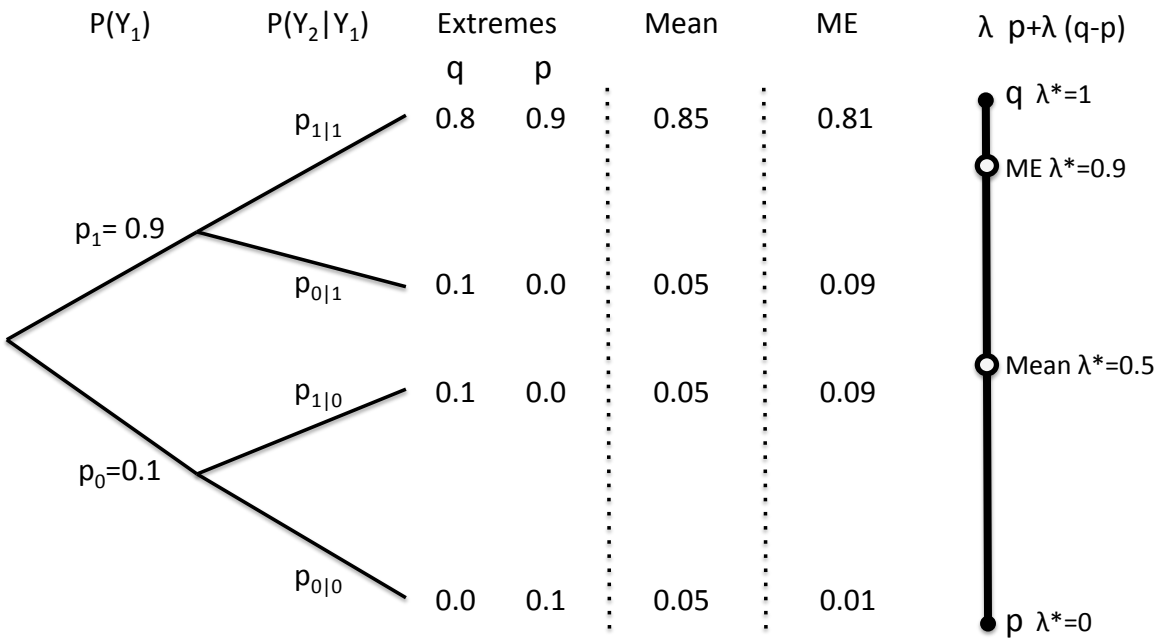

Figure 5.23: Illustration of ME behavior.

Figure 5.24 shows the progression of ME for changes in b_1. ME changes smoothly but not monotonically toward unit vector $\{1, 0, \ldots, 0\}$.

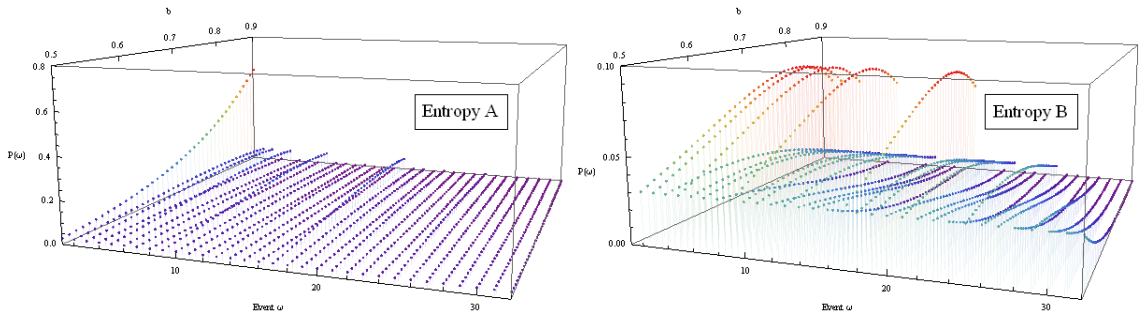

Figure 5.24: ME changes in $\mathbf{b}$ ($\mathbf{Ax} = \mathbf{b}$). Figure A presents the full distribution. Figure B presents the distributions without the first joint event (ω_1) and rescaled. These approximations were created with 5 binary random variables (32 joint events ω_1 to ω_{32}).

ChSC Findings. This approximation is superior to ME for large values of $b_1 > 0.7$, but has poor accuracy otherwise. The ChSC approximation is also sensitive to certain shapes of $\mathbb{T}$, e.g., when the polytope is closely parallel to positivity constraints (Figure 5.25).

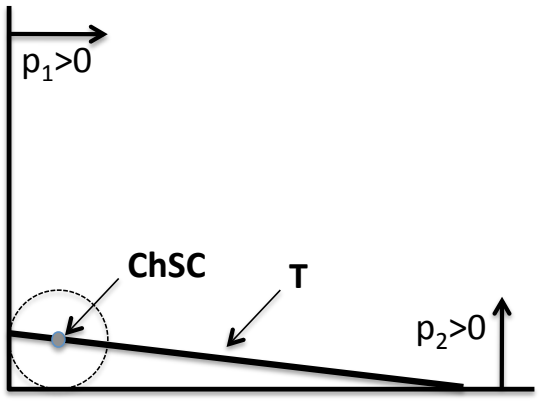

Figure 5.25: Illustration of ChSC behavior.

The ChSC approximation is not a minimum entropy approximation. However, it serves as a counterpart to ME by providing a distribution with lower entropy than all other approximations, and in some cases with less entropy than most of the distributions in the sampled collection as observed in Figures 5.21(xvi), 5.21(xix), 5.21(xxii), 5.21(xxv), and 5.21(xxviii).

The reduction of $\mathbb{T}$ as b_1 increases is more pronounced in ChSC than in ME. This effect is related to the structure of the ChSC approximation observed in Figure 5.26. That 31 of the 32 joint events have equal probabilities is explained by the attempt to evenly expand a hypersphere inside the positive hyper-octant with center in $\mathbb{T}$. Then, in the case of symmetric marginal constraints, a reduction of $\mathbb{T}$ as b_1 increases makes the set more perpendicular to the closest boundaries of the positive hyper-octant, providing more room for the hypersphere to expand and improving its accuracy.

This same behavior affects the variation of the accuracy measures in Figure 5.22, where ME and ChSC are the two approximations for which the accuracy measures show the largest variation.

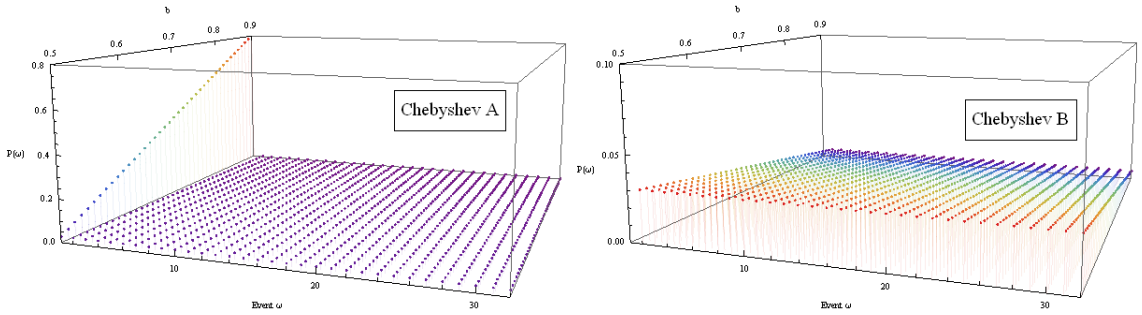

Figure 5.26: ChSC changes in $\mathbf{b}$ ($\mathbf{Ax} = \mathbf{b}$). Figure A presents the full distribution. Figure B presents the distributions without the first joint event (ω_1) and rescaled. These approximations were created with 5 binary random variables (32 joint events ω_1 to ω_{32}).

Findings on the Most Accurate Approximations. The three approximations that provide the best accuracy estimates are DAC, AC, and MVIE. Although they have similar accuracy on average, Figure 5.22 shows that MVIE has more variation in accuracy than the other two. However, when implemented, MVIE and DAC require a vast amount of memory and numerous iterations, leaving AC as the best overall alternative. AC provides a simpler and accurate description of the truth set when the marginal constraints are symmetric. Figure 5.27 shows how each approximation changes as the marginals (b_1) change from 0.5 (front of the cube) to 0.9 (back of the cube), where each point represents one of the 32 joint events at a specific value of b_1.

AC has a structure that mimics ME but has a range closer to MVIE (Figures 5.24 and 5.27). The curvature of ME and AC may be attributed to the logarithmic function's absence from all other approximations. AC and MVIE may seem strikingly similar, given that the ideas behind these approximations are so different. However, these similarities became less obvious as the available information increases.

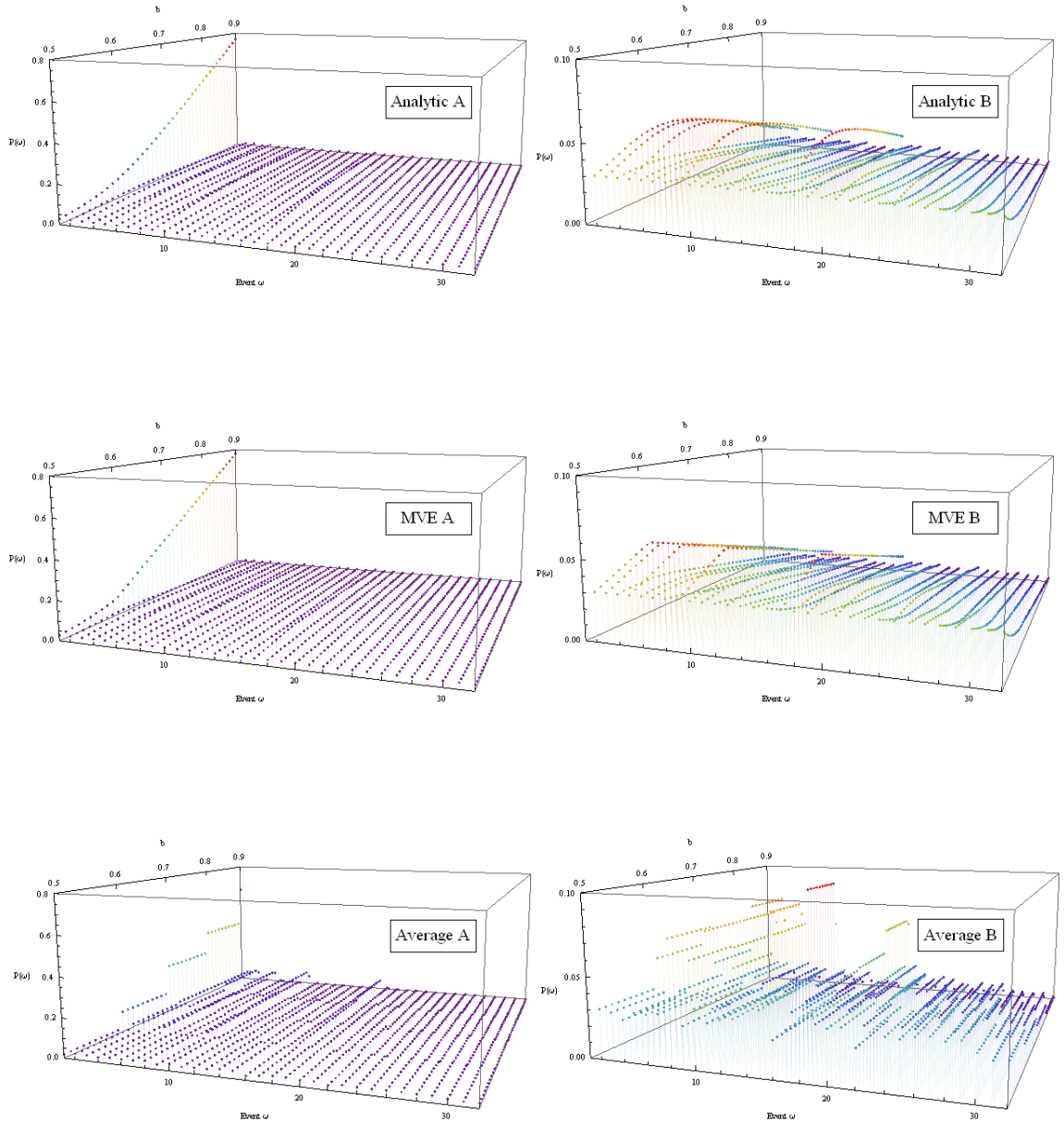

Figure 5.27: From top to bottom, AC, MVIE, and DAC as a function of $\mathbf{b}$ ($\mathbf{Ax} = \mathbf{b}$). Figures A present the full distribution. Figures B present the distributions without the first joint event (ω_1) and rescaled. These approximations were created with 5 binary random variables (32 joint events ω_1 to ω_{32}).

Finally, as expected, DAC is found to be the most accurate and the most work-intensive of all the approximations, mostly because it requires use of the JDSIM. Due to lack of computing resources, the last two sub-figures of Figure 5.27 were calculated running simulations only for b_1 =0.5, 0.6, 0.7, 0.8, and 0.9, giving the impression of a piecewise function. However, these figures do not represent the approximations' complete functions, even though they convey some aspects of those functions.

Percentage of Accuracy. Accuracy can also be expressed as the percentage of the time that one approximation is better that another. This measure can be observed in Tables 5.5 and 5.6. In these tables, the first column indicates the number of random variables and the second column indicates the value of b_1 (the values for $b_1 = 0.5$ are omitted since the results are trivial). The rest of the columns indicate the percentage of the time that a sampled distribution is more accurate than an alternative. Again the results favor DAC, AC, and MVIE.

For 3 and 4 marginal random variables, the MVIE outperforms the AC. However, increasing the dimension of the truth set to 5, 6, or 7 marginal random variables makes AC more accurate than the MVIE. The results show that DAC dominates all other approximations with respect to greater-accuracy percentage, and ME is dominated by all other approximations.

The values for the MVIE when the jpmf is constructed using 7 marginal random variables are omitted due to the complexity of the calculations. In particular, the problem requires exponential amounts of memory. Similar problems were found in the simulation procedure for sample distributions with many random variables. In particular, for 6 and 7 random variables, the sample size should be close to 1 and 10 million samples, respectively. The actual sample size of 200,000 added random noise to the results.

Table 5.5: Percentage of accuracy (i.e. fraction of times one approximation is better than other) for sets with marginal information (b_1 =M). For different approximations and number of variables (V= $3, 4, 5$).

		% of times	DAC	DAC	DAC	DAC	MVIE	MVIE	MVIE	AC	AC	ChSC
V	M	is better than	MVIE	AC	ChSC	ME	AC	ChSC	ME	ChSC	ME	ME
	6	$\mathbf{L}^\infty$	47%	43%	53%	47%	58%	55%	60%	52%	48%	50%
	6	$\mathbf{L}^1$	49%	53%	60%	57%	52%	61%	56%	57%	59%	46%
3	6	$\mathbf{L}^2$	47%	52%	59%	56%	53%	61%	56%	57%	59%	46%
	6	KL	47%	50%	59%	54%	53%	61%	55%	57%	57%	46%
	6	χ^2	46%	45%	63%	50%	50%	65%	52%	61%	53%	42%
	7	$\mathbf{L}^\infty$	45%	64%	55%	72%	59%	59%	68%	50%	76%	60%
	7	$\mathbf{L}^1$	52%	59%	60%	71%	55%	64%	68%	54%	76%	60%
3	7	$\mathbf{L}^2$	50%	59%	60%	72%	56%	64%	69%	53%	76%	61%
	7	KL	49%	59%	60%	71%	56%	65%	68%	54%	76%	59%
	7	χ^2	50%	56%	64%	71%	54%	69%	68%	58%	76%	57%
	8	$\mathbf{L}^\infty$	45%	65%	55%	82%	61%	59%	80%	48%	87%	74%
	8	$\mathbf{L}^1$	52%	61%	60%	84%	58%	65%	81%	51%	88%	76%
3	8	$\mathbf{L}^2$	50%	62%	60%	84%	59%	65%	82%	51%	88%	76%
	8	KL	49%	62%	60%	84%	58%	65%	81%	52%	88%	75%
	8	χ^2	51%	61%	65%	86%	57%	70%	84%	56%	90%	77%
	9	$\mathbf{L}^\infty$	44%	67%	54%	91%	64%	57%	90%	45%	94%	87%
	9	$\mathbf{L}^1$	51%	64%	59%	92%	61%	63%	91%	48%	95%	87%
3	9	$\mathbf{L}^2$	48%	64%	59%	92%	62%	63%	91%	47%	95%	88%
	9	KL	47%	64%	59%	93%	61%	63%	92%	48%	96%	88%
	9	χ^2	48%	63%	64%	96%	61%	68%	95%	52%	98%	92%
	6	$\mathbf{L}^\infty$	55%	54%	77%	44%	38%	76%	44%	76%	44%	29%
	6	$\mathbf{L}^1$	55%	53%	71%	58%	52%	70%	59%	69%	60%	37%
4	6	$\mathbf{L}^2$	54%	53%	72%	58%	53%	71%	59%	70%	59%	35%
	6	KL	54%	53%	72%	58%	53%	71%	58%	70%	59%	36%
	6	χ^2	54%	53%	77%	53%	49%	77%	53%	76%	54%	30%
	7	$\mathbf{L}^\infty$	52%	50%	77%	73%	57%	82%	69%	73%	75%	55%
	7	$\mathbf{L}^1$	53%	56%	71%	77%	51%	76%	73%	67%	80%	57%
4	7	$\mathbf{L}^2$	53%	57%	72%	77%	51%	77%	73%	68%	80%	57%
	7	KL	53%	57%	73%	78%	51%	78%	74%	69%	81%	55%
	7	χ^2	56%	54%	79%	77%	48%	84%	72%	76%	80%	50%
	8	$\mathbf{L}^\infty$	53%	53%	77%	93%	57%	83%	91%	72%	94%	82%
	8	$\mathbf{L}^1$	54%	58%	71%	92%	52%	78%	90%	66%	94%	82%
4	8	$\mathbf{L}^2$	54%	59%	72%	93%	52%	79%	91%	67%	95%	83%
	8	KL	54%	59%	74%	93%	52%	79%	91%	69%	95%	79%
	8	χ^2	58%	56%	80%	94%	48%	85%	92%	75%	96%	78%
	9	$\mathbf{L}^\infty$	50%	59%	76%	100%	63%	79%	100%	65%	100%	98%
	9	$\mathbf{L}^1$	51%	63%	69%	99%	60%	73%	99%	58%	100%	98%
4	9	$\mathbf{L}^2$	50%	63%	70%	100%	60%	74%	100%	59%	100%	99%
	9	KL	50%	63%	71%	100%	60%	75%	100%	62%	100%	97%
	9	χ^2	54%	59%	79%	100%	56%	82%	100%	69%	100%	99%
	6	$\mathbf{L}^\infty$	41%	50%	84%	43%	61%	82%	37%	84%	45%	24%
	6	$\mathbf{L}^1$	54%	54%	79%	61%	46%	77%	64%	78%	62%	30%
5	6	$\mathbf{L}^2$	53%	53%	82%	60%	46%	80%	63%	81%	61%	26%
	6	KL	53%	54%	82%	61%	46%	79%	64%	81%	62%	28%
	6	χ^2	51%	52%	88%	57%	52%	86%	59%	87%	57%	22%
	7	$\mathbf{L}^\infty$	66%	53%	85%	86%	35%	90%	83%	85%	87%	56%
	7	$\mathbf{L}^1$	58%	58%	82%	89%	44%	87%	84%	81%	89%	59%
5	7	$\mathbf{L}^2$	58%	58%	84%	89%	44%	89%	84%	83%	89%	57%
	7	KL	58%	57%	85%	91%	44%	89%	85%	84%	91%	54%
	7	χ^2	62%	54%	91%	90%	38%	94%	84%	90%	89%	46%
	8	$\mathbf{L}^\infty$	64%	54%	84%	100%	30%	92%	97%	86%	99%	85%
	8	$\mathbf{L}^1$	56%	52%	81%	99%	43%	89%	96%	82%	99%	85%
5	8	$\mathbf{L}^2$	57%	52%	83%	100%	42%	91%	97%	85%	100%	85%
	8	KL	58%	56%	85%	100%	43%	91%	96%	86%	99%	77%
	8	χ^2	66%	58%	91%	100%	34%	95%	97%	92%	99%	76%
	9	$\mathbf{L}^\infty$	51%	51%	82%	100%	43%	86%	100%	75%	100%	99%
	9	$\mathbf{L}^1$	50%	62%	77%	100%	58%	82%	100%	69%	100%	99%
5	9	$\mathbf{L}^2$	51%	62%	80%	100%	57%	85%	100%	73%	100%	99%
	9	KL	53%	63%	81%	100%	56%	85%	100%	76%	100%	99%
	9	χ^2	57%	56%	90%	100%	49%	92%	100%	86%	100%	100%

Table 5.6: Percentage of accuracy (i.e. fraction of times one approximation is better than other) for sets with marginal information (b_1 =M). For different approximations and number of variables (V= $6, 7$).

		% Of times	DAC	DAC	DAC	DAC	MVIE	MVIE	MVIE	AC	AC	ChSC
V	M	is better than	MVIE	AC	ChSC	ME	AC	ChSC	ME	ChSC	ME	ME
6	6	$\mathbf{L}^{\infty}$	61%	61%	93%	57%	60%	88%	68%	91%	47%	22%
	6	$\mathbf{L}^{1}$	63%	63%	86%	70%	43%	79%	73%	83%	69%	31%
	6	$\mathbf{L}^{2}$	60%	64%	93%	68%	43%	87%	71%	91%	67%	22%
	6	KL	69%	70%	92%	75%	43%	85%	73%	89%	69%	28%
	6	χ^2	69%	72%	98%	70%	51%	94%	67%	97%	63%	19%
6	7	$\mathbf{L}^{\infty}$	79%	75%	98%	92%	7%	100%	80%	100%	85%	39%
	7	$\mathbf{L}^{1}$	70%	65%	94%	97%	22%	100%	78%	99%	83%	46%
	7	$\mathbf{L}^{2}$	71%	66%	98%	94%	20%	100%	78%	100%	84%	39%
	7	KL	79%	77%	98%	99%	19%	100%	85%	100%	91%	38%
	7	χ^2	86%	79%	100%	99%	6%	100%	88%	100%	94%	27%
6	8	$\mathbf{L}^{\infty}$	66%	63%	86%	100%	35%	87%	100%	84%	100%	100%
	8	$\mathbf{L}^{1}$	64%	61%	84%	100%	45%	85%	100%	82%	100%	100%
	8	$\mathbf{L}^{2}$	68%	57%	86%	100%	45%	87%	100%	83%	100%	100%
	8	KL	67%	70%	88%	100%	46%	89%	100%	86%	100%	100%
	8	χ^2	71%	66%	96%	100%	36%	97%	100%	93%	100%	100%
6	9	$\mathbf{L}^{\infty}$	64%	59%	90%	100%	43%	95%	100%	88%	100%	100%
	9	$\mathbf{L}^{1}$	53%	66%	86%	100%	57%	92%	100%	82%	100%	100%
	9	$\mathbf{L}^{2}$	58%	65%	90%	100%	55%	95%	100%	87%	100%	100%
	9	KL	70%	65%	93%	100%	51%	95%	100%	90%	100%	100%
	9	χ^2	77%	63%	99%	100%	38%	100%	100%	97%	100%	100%
7	6	$\mathbf{L}^{\infty}$	-	75%	81%	89%	-	-	-	51%	99%	63%
	6	$\mathbf{L}^{1}$	-	81%	78%	93%	-	-	-	41%	100%	68%
	6	$\mathbf{L}^{2}$	-	76%	81%	89%	-	-	-	50%	100%	63%
	6	KL	-	89%	84%	99%	-	-	-	44%	100%	74%
	6	χ^2	-	89%	95%	99%	-	-	-	59%	100%	69%
7	7	$\mathbf{L}^{\infty}$	-	85%	87%	100%	-	-	-	65%	100%	100%
	7	$\mathbf{L}^{1}$	-	99%	85%	100%	-	-	-	57%	100%	100%
	7	$\mathbf{L}^{2}$	-	96%	87%	100%	-	-	-	65%	100%	100%
	7	KL	-	100%	90%	100%	-	-	-	65%	100%	100%
	7	χ^2	-	97%	97%	100%	-	-	-	82%	100%	100%
7	8	$\mathbf{L}^{\infty}$	-	100%	92%	100%	-	-	-	5%	100%	100%
	8	$\mathbf{L}^{1}$	-	100%	89%	100%	-	-	-	1%	100%	100%
	8	$\mathbf{L}^{2}$	-	100%	92%	100%	-	-	-	5%	100%	100%
	8	KL	-	100%	95%	100%	-	-	-	24%	100%	100%
	8	χ^2	-	96%	98%	100%	-	-	-	42%	100%	100%
7	9	$\mathbf{L}^{\infty}$	-	53%	85%	100%	-	-	-	84%	100%	100%
	9	$\mathbf{L}^{1}$	-	95%	83%	100%	-	-	-	80%	100%	100%
	9	$\mathbf{L}^{2}$	-	85%	84%	100%	-	-	-	83%	100%	100%
	9	KL	-	98%	85%	100%	-	-	-	85%	100%	100%
	9	χ^2	-	95%	93%	100%	-	-	-	87%	100%	100%

5.3.3 Symmetric Marginal and Rank Correlation Constraints

In this section, we add constraints to the polytopes described in §5.3.2. In particular, we add the rank correlation information for each pair of marginal variables (Equation 3.9). We explore the behavior of the joint distribution approximations using exclusively symmetric information, which means that all the random variables have the same marginal distributions and the same rank correlation.

Sampling Details. We measure the accuracy of the joint distribution approximations for all combinations of marginal distributions $\hat{p}$ =0.5, 0.6, 0.7, 0.8, 0.9 (as before), having rank correlation matrices with elements $\rho^r_{1,2} = \rho^r_{1,3} = \rho^r_{1,n} = \rho^r_{2,3} = \cdots = \rho^r_{n-1,n}$, where the correlation of $\rho^r_{1,2}$ can take values of 0.0, 0.1, 0.2, 0.3, 0.4, 0.5, 0.6, and 0.7.

Since all information is symmetric, even small negative values of $\rho^r_{1,2} \approx -0.1$ generate inconsistent rank correlation matrices. Therefore, we only sample polytopes for which the marginal random variables are non-negatively correlated. Additionally, we discard all polytopes for which the marginal probabilities and the rank correlation matrix result in an inconsistent system.

We test polytopes based in 3, 4, 5, 6, and 7 binary random variables. For the first two cases (3 and 4 random variables), 100,000 sampled distributions are collected. For the last three cases, 200,000 sampled distributions are collected. The sizes of these samples were constrained by the available computation power. In principle, JDSIM can create collections in the millions.

Results: The complete set of results is shown in Figures 5.28 to 5.32. The five figures show the mean of the six accuracy measures for all approximations except the independent approximation (IA), which is equivalent to ME without the rank correlation constraints and therefore has worse accuracy. Figures C.13 to C.17 in Appendix C show the standard deviation of those same measures.

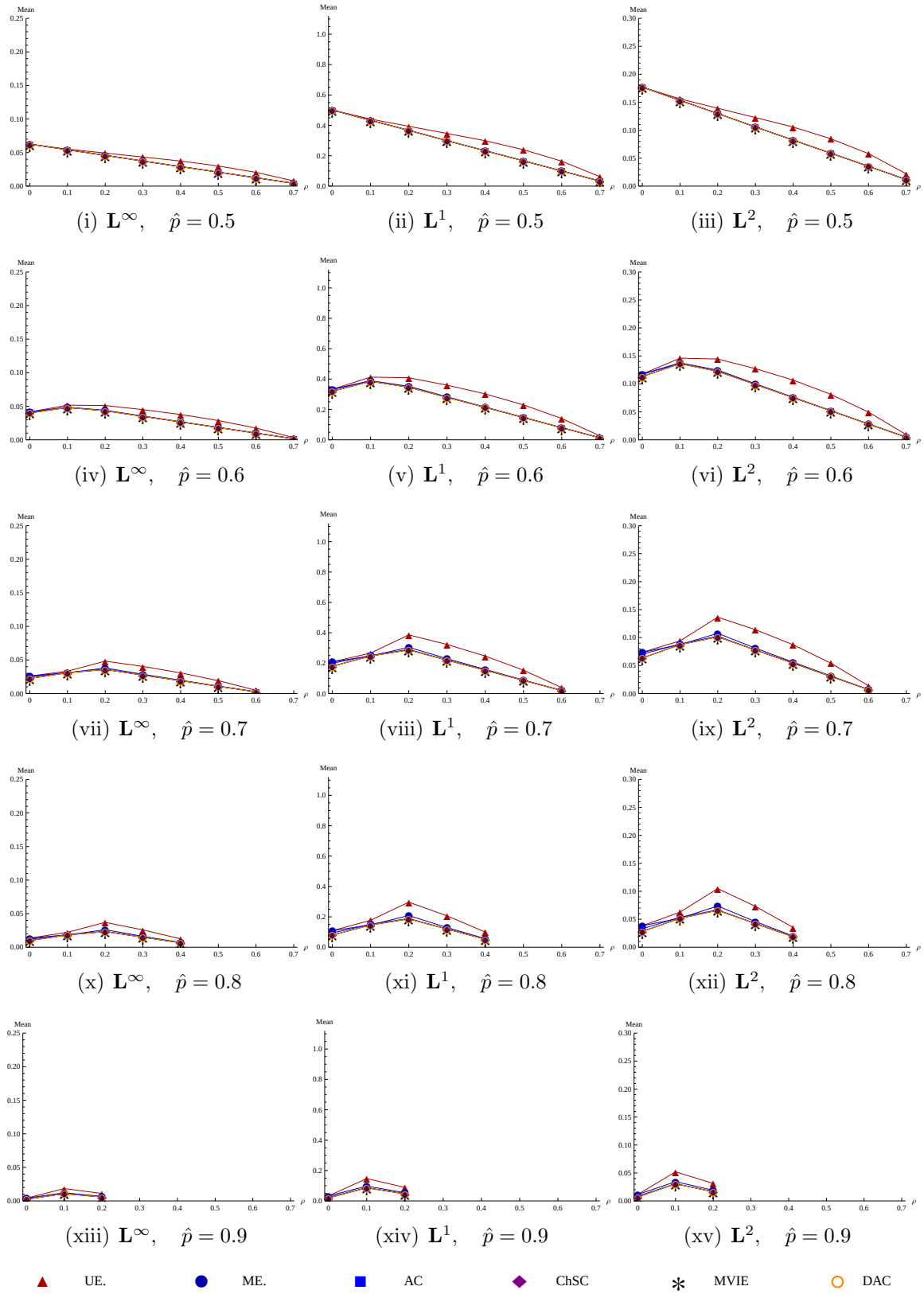

Figure 5.28: Mean estimates for $\mathbb{T}$ with 3 binary random variables (part one).

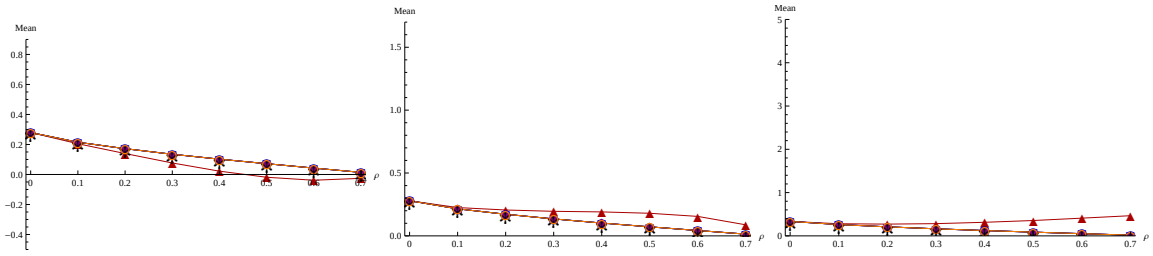

(xvi) ΔH, $\hat{p} = 0.5$ (xvii) KL, $\hat{p} = 0.5$ (xviii) χ^2, $\hat{p} = 0.5$

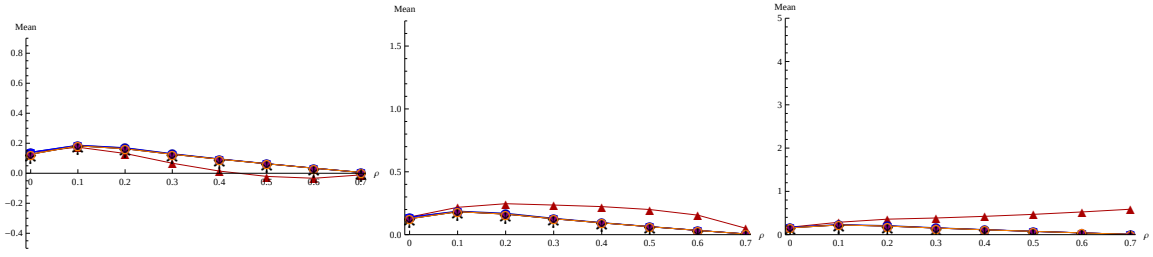

(xix) ΔH, $\hat{p} = 0.6$ (xx) KL, $\hat{p} = 0.6$ (xxi) χ^2, $\hat{p} = 0.6$

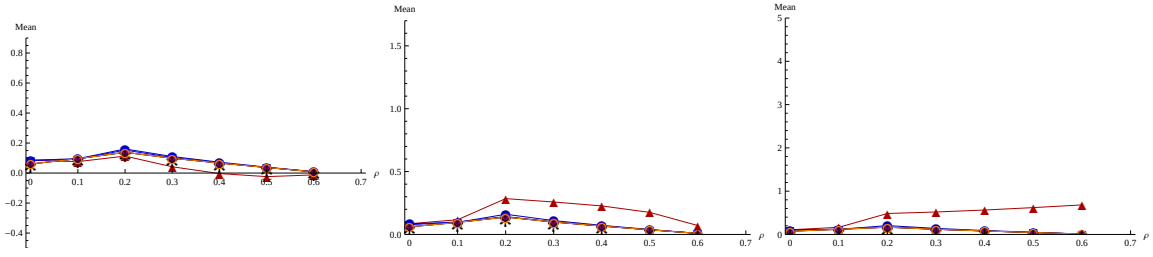

(xxii) ΔH, $\hat{p} = 0.7$ (xxiii) KL, $\hat{p} = 0.7$ (xxiv) χ^2, $\hat{p} = 0.7$

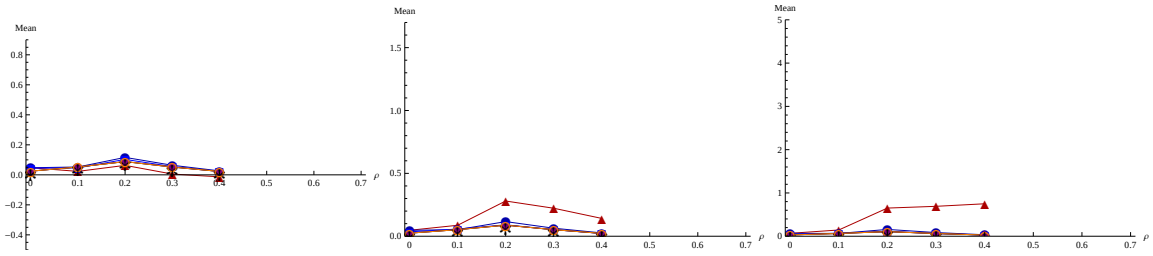

(xxv) ΔH, $\hat{p} = 0.8$ (xxvi) KL, $\hat{p} = 0.8$ (xxvii) χ^2, $\hat{p} = 0.8$

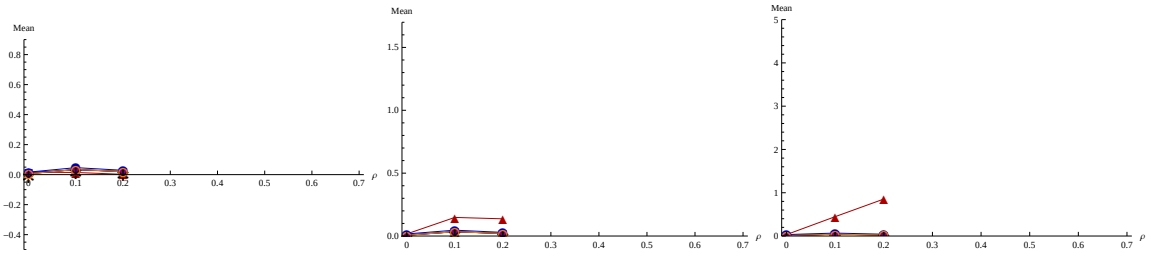

(xxviii) ΔH, $\hat{p} = 0.9$ (xxix) KL, $\hat{p} = 0.9$ (xxx) χ^2, $\hat{p} = 0.9$

Figure 5.28: Mean estimates for $\mathbb{T}$ with 3 binary random variables. The rank correlation is shown in the x-axes. Each row shows marginal assessments $\hat{p}$ and each column shows an accuracy measure (part two).

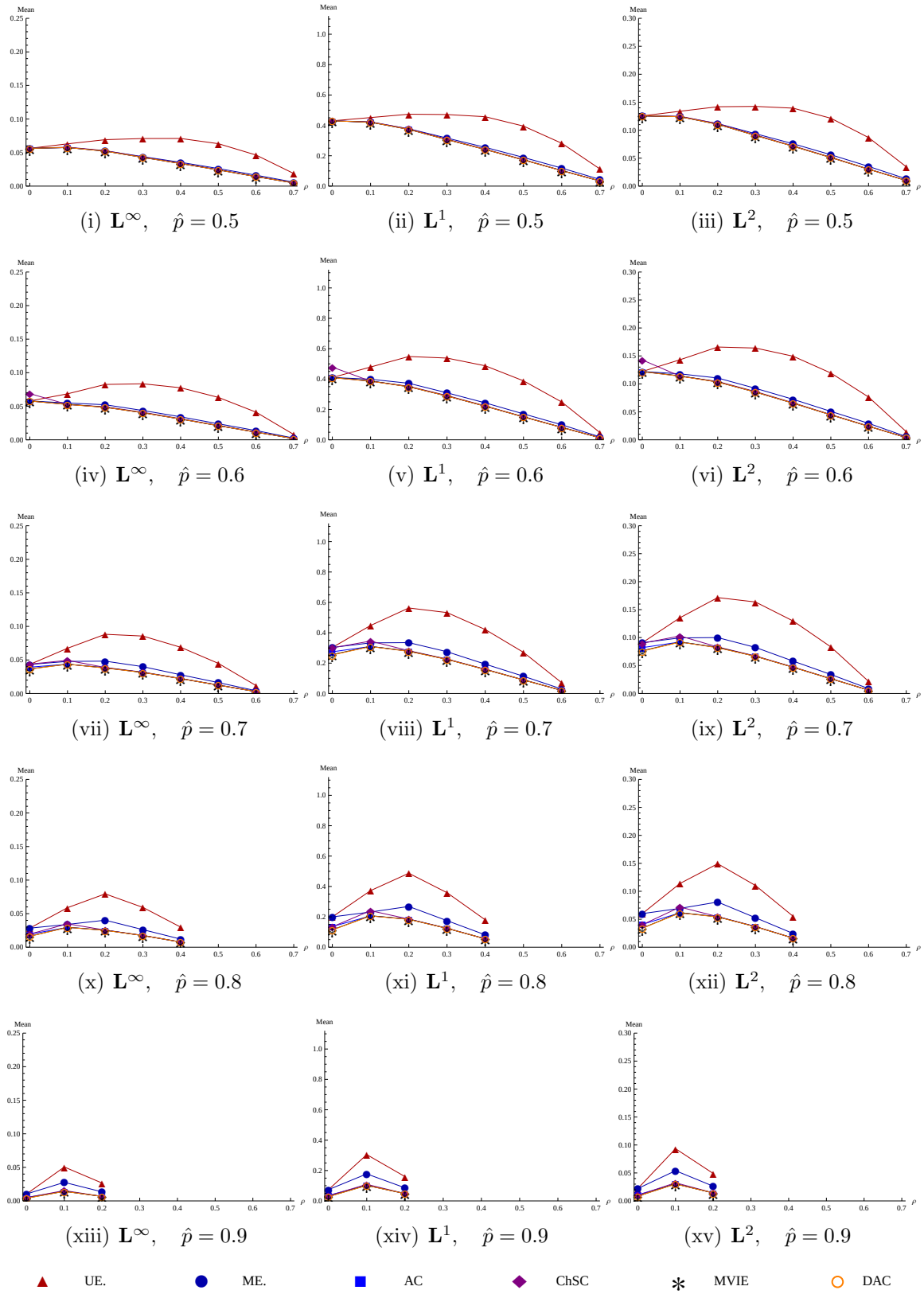

Figure 5.29: Mean estimates for $\mathbb{T}$ with 4 binary random variables (part one).

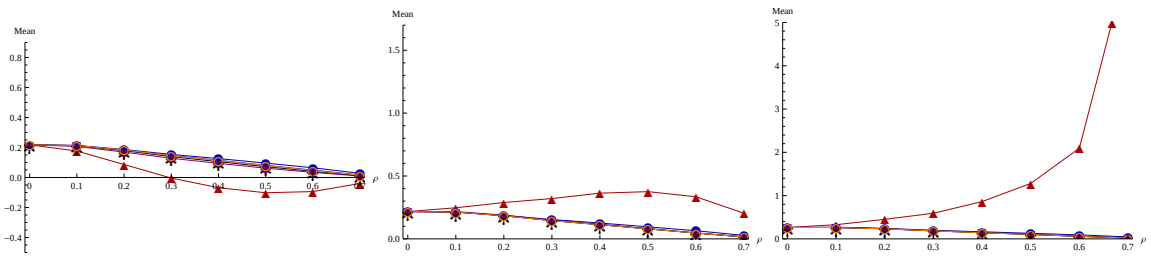

(xvi) ΔH, $\hat{p} = 0.5$ (xvii) KL, $\hat{p} = 0.5$ (xviii) χ^2, $\hat{p} = 0.5$

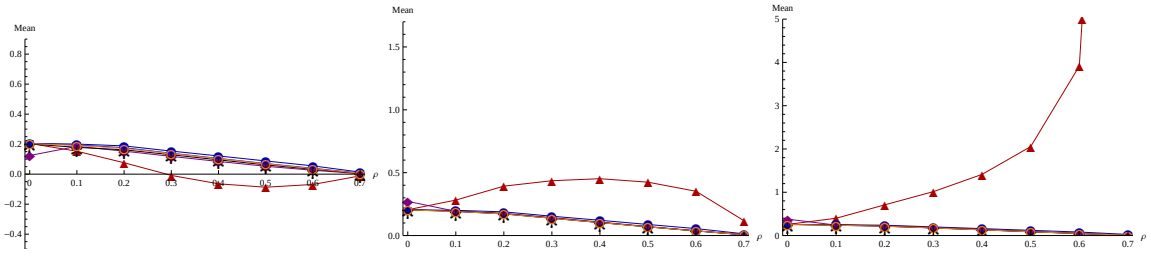

(xix) ΔH, $\hat{p} = 0.6$ (xx) KL, $\hat{p} = 0.6$ (xxi) χ^2, $\hat{p} = 0.6$

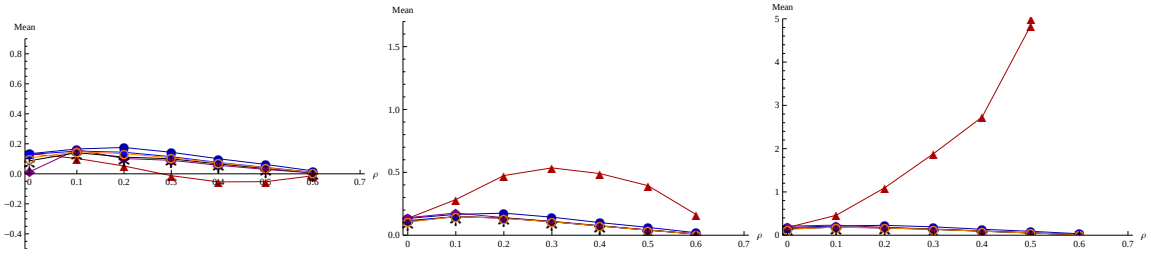

(xxii) ΔH, $\hat{p} = 0.7$ (xxiii) KL, $\hat{p} = 0.7$ (xxiv) χ^2, $\hat{p} = 0.7$

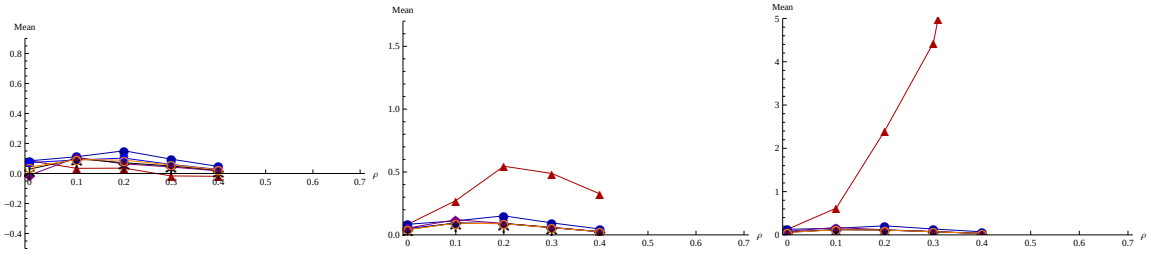

(xxv) ΔH, $\hat{p} = 0.8$ (xxvi) KL, $\hat{p} = 0.8$ (xxvii) χ^2, $\hat{p} = 0.8$

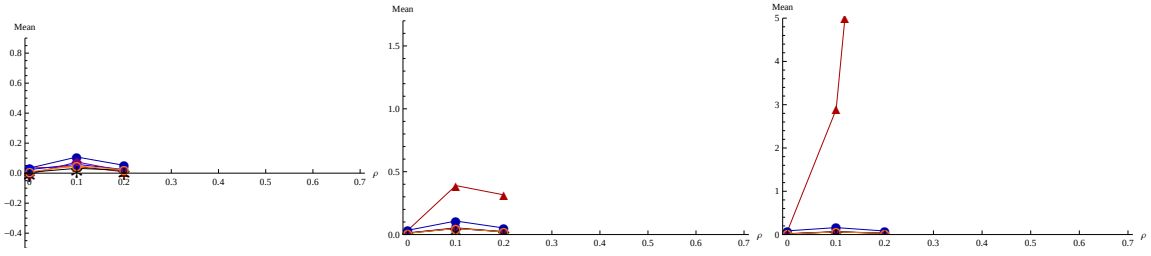

(xxviii) ΔH, $\hat{p} = 0.9$ (xxix) KL, $\hat{p} = 0.9$ (xxx) χ^2, $\hat{p} = 0.9$

Figure 5.29: Mean estimates for $\mathbb{T}$ with 4 binary random variables. The rank correlation is shown in the x-axes. Each row shows marginal assessments $\hat{p}$ and each column shows an accuracy measure (part two).

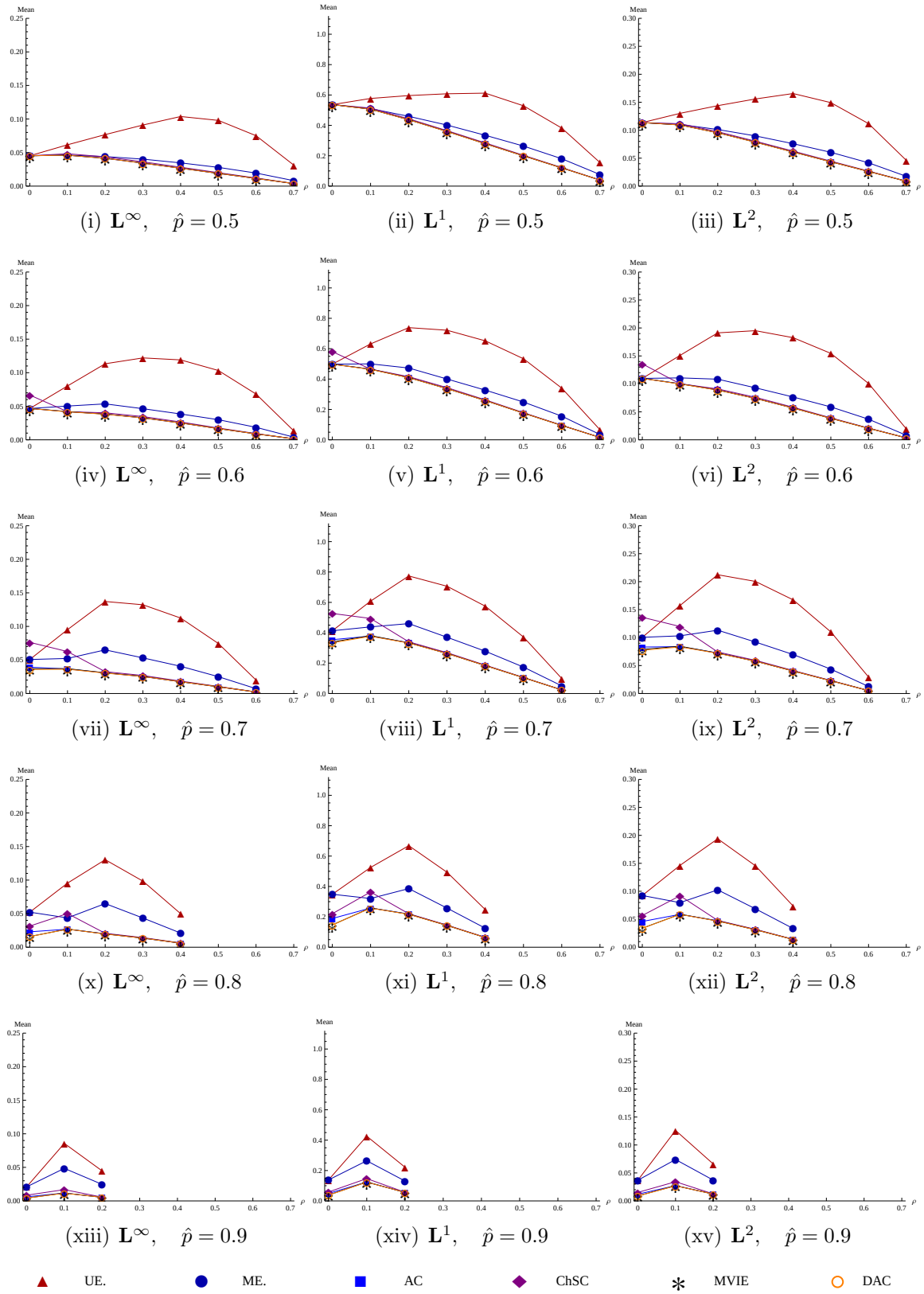

Figure 5.30: Mean estimates for $\mathbb{T}$ with 5 binary random variables (part one).

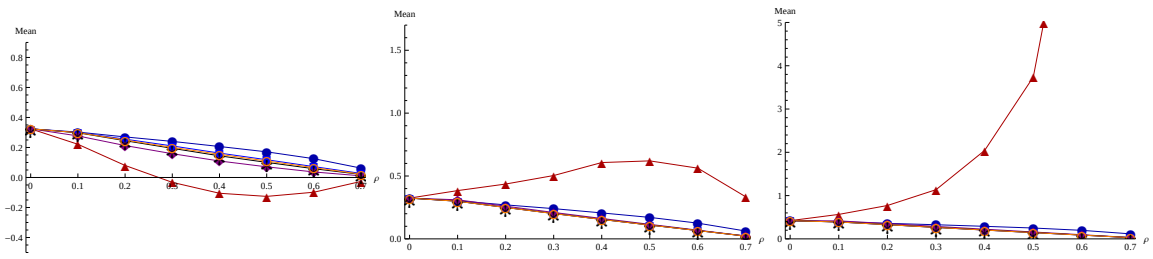

(xvi) ΔH, $\hat{p} = 0.5$ (xvii) KL, $\hat{p} = 0.5$ (xviii) χ^2, $\hat{p} = 0.5$

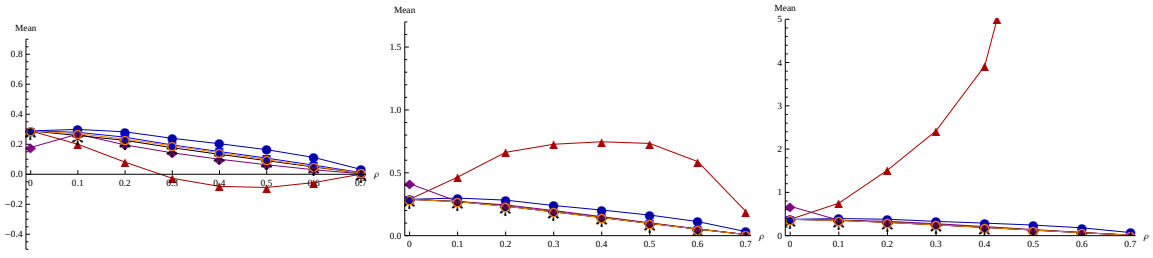

(xix) ΔH, $\hat{p} = 0.6$ (xx) KL, $\hat{p} = 0.6$ (xxi) χ^2, $\hat{p} = 0.6$

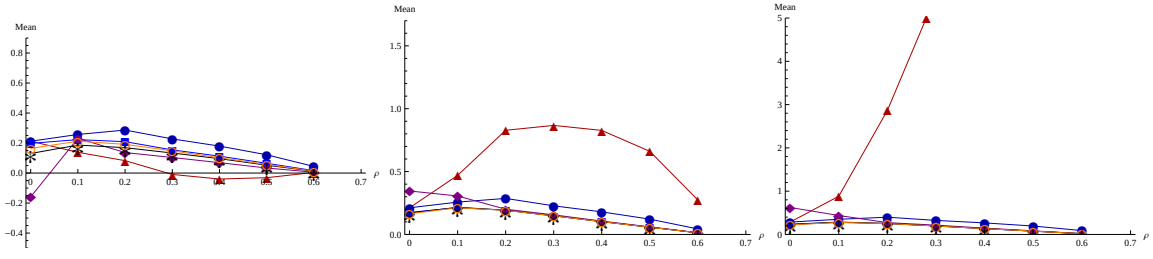

(xxii) ΔH, $\hat{p} = 0.7$ (xxiii) KL, $\hat{p} = 0.7$ (xxiv) χ^2, $\hat{p} = 0.7$

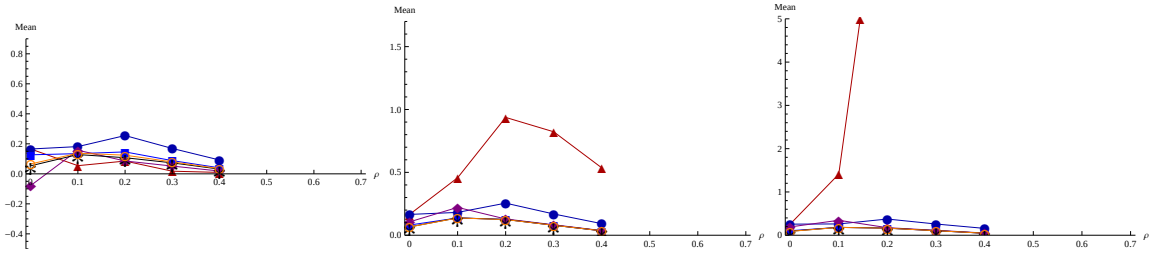

(xxv) ΔH, $\hat{p} = 0.8$ (xxvi) KL, $\hat{p} = 0.8$ (xxvii) χ^2, $\hat{p} = 0.8$

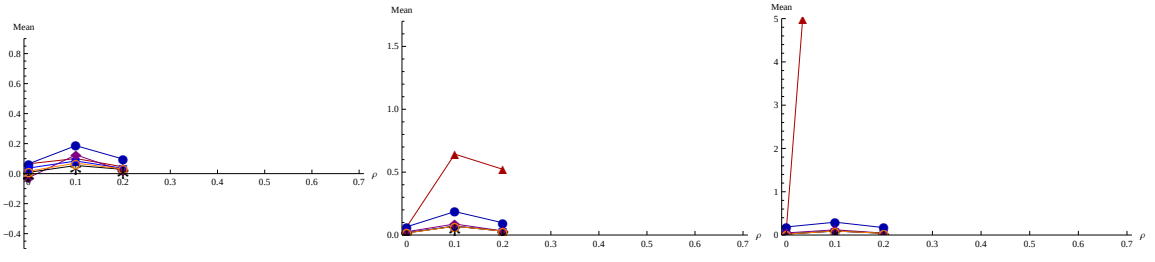

(xxviii) ΔH, $\hat{p} = 0.9$ (xxix) KL, $\hat{p} = 0.9$ (xxx) χ^2, $\hat{p} = 0.9$

Figure 5.30: Mean estimates for $\mathbb{T}$ with 5 binary random variables. The rank correlation is shown in the x-axes. Each row shows marginal assessments $\hat{p}$ and each column shows an accuracy measure (part two).

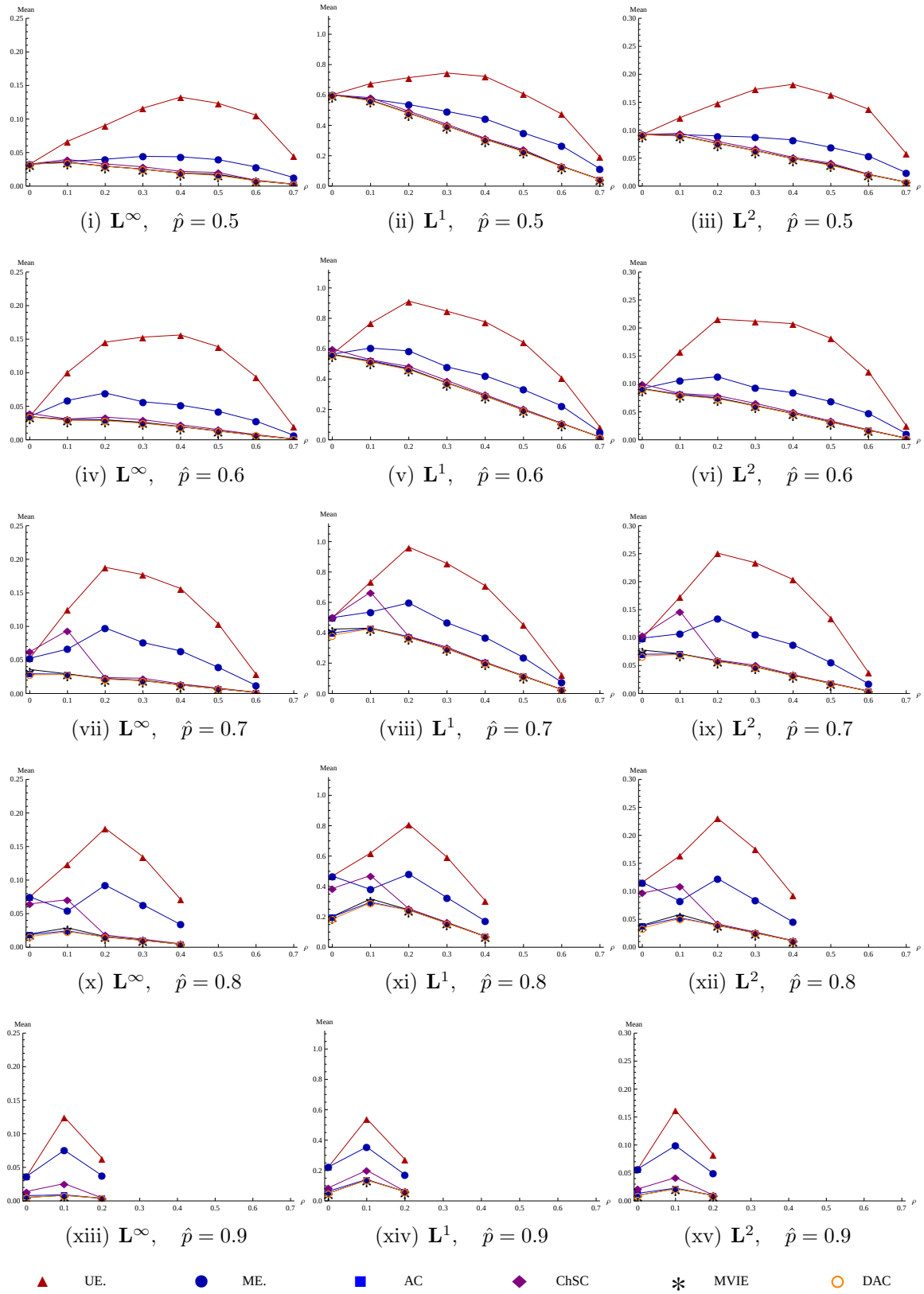

Figure 5.31: Mean estimates for $\mathbb{T}$ with 6 binary random variables (part one).

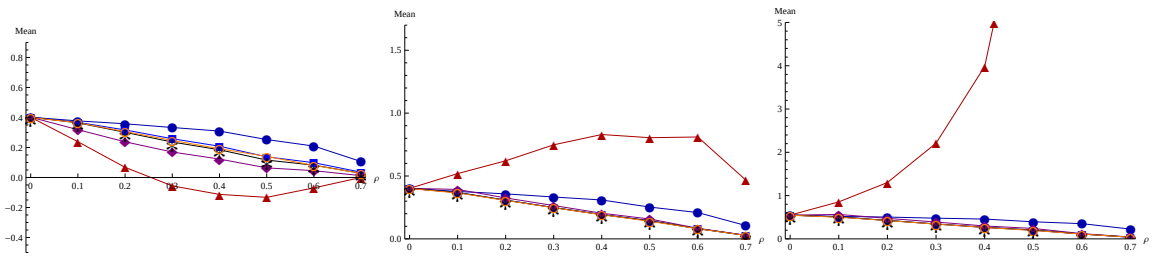

(xvi) ΔH, $\hat{p} = 0.5$ (xvii) KL, $\hat{p} = 0.5$ (xviii) χ^2, $\hat{p} = 0.5$

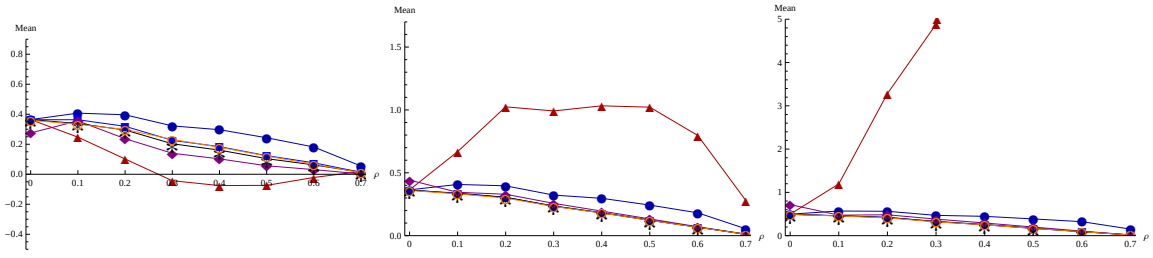

(xix) ΔH, $\hat{p} = 0.6$ (xx) KL, $\hat{p} = 0.6$ (xxi) χ^2, $\hat{p} = 0.6$

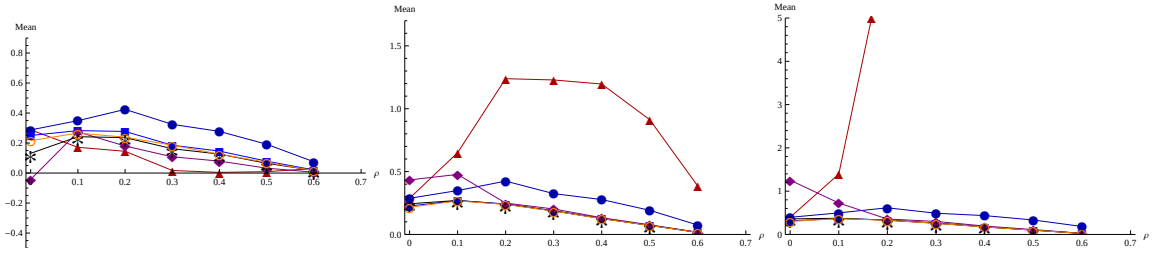

(xxii) ΔH, $\hat{p} = 0.7$ (xxiii) KL, $\hat{p} = 0.7$ (xxiv) χ^2, $\hat{p} = 0.7$

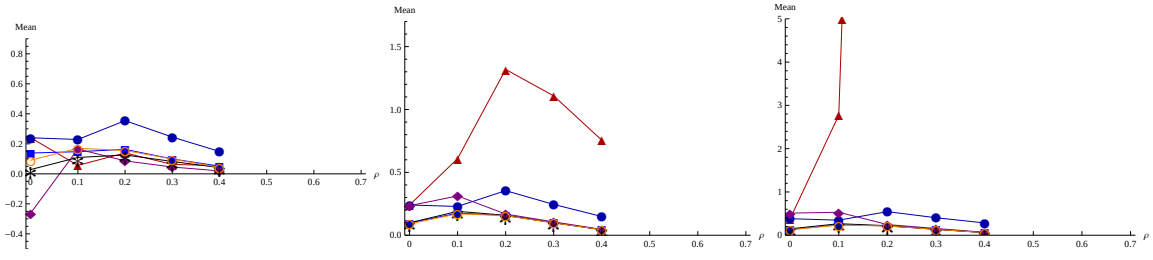

(xxv) ΔH, $\hat{p} = 0.8$ (xxvi) KL, $\hat{p} = 0.8$ (xxvii) χ^2, $\hat{p} = 0.8$

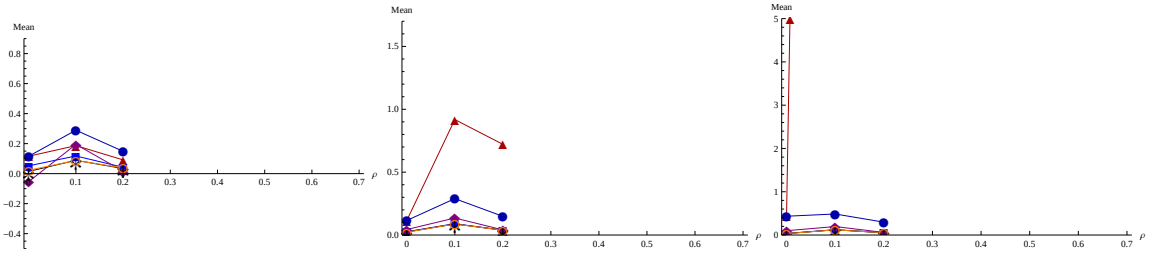

(xxviii) ΔH, $\hat{p} = 0.9$ (xxix) KL, $\hat{p} = 0.9$ (xxx) χ^2, $\hat{p} = 0.9$

Figure 5.31: Mean estimates for $\mathbb{T}$ with 6 binary random variables. The rank correlation is shown in the x-axes. Each row shows marginal assessments $\hat{p}$ and each column shows an accuracy measure (part two).

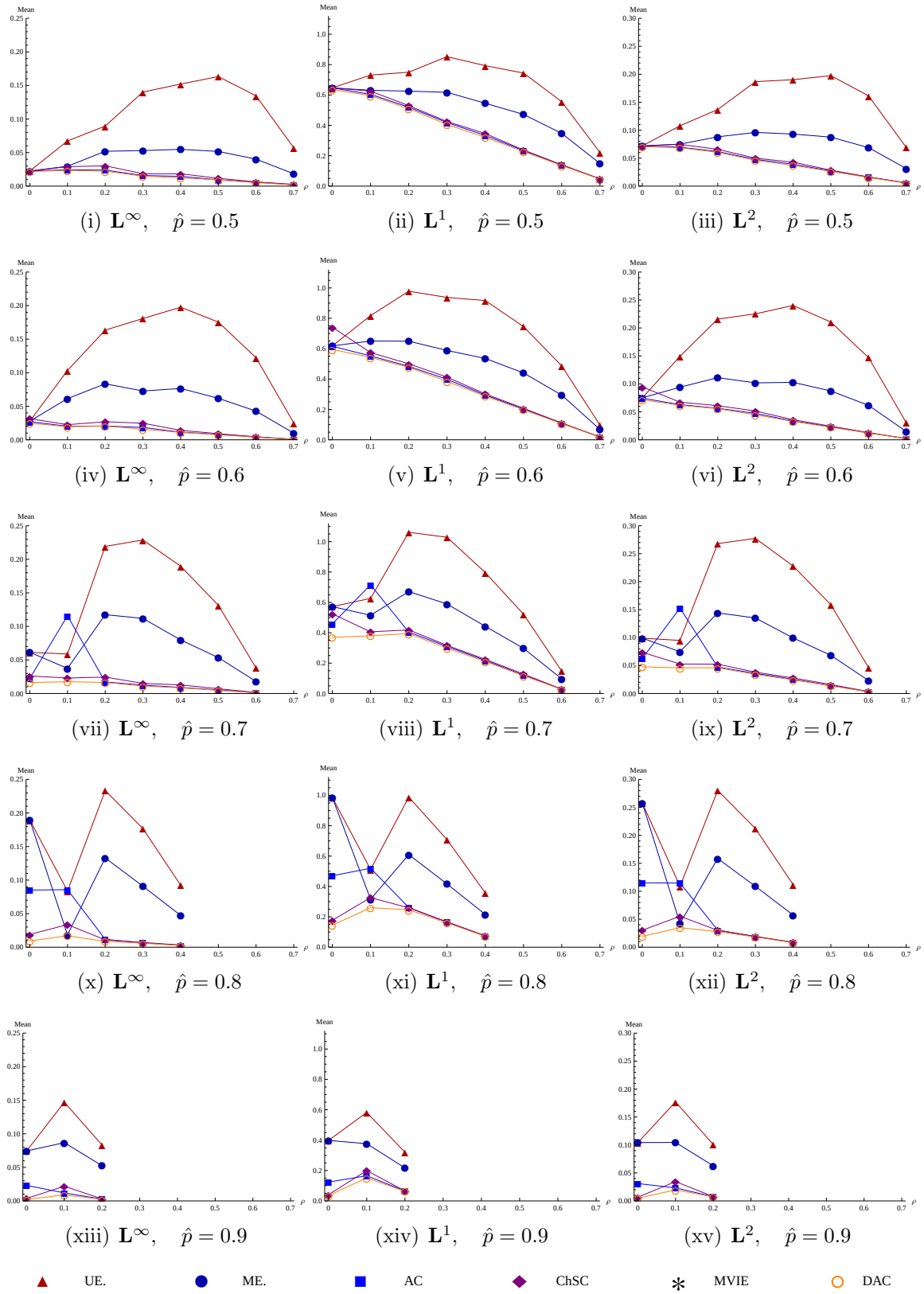

Figure 5.32: Mean estimates for $\mathbb{T}$ with 7 binary random variables (part one).

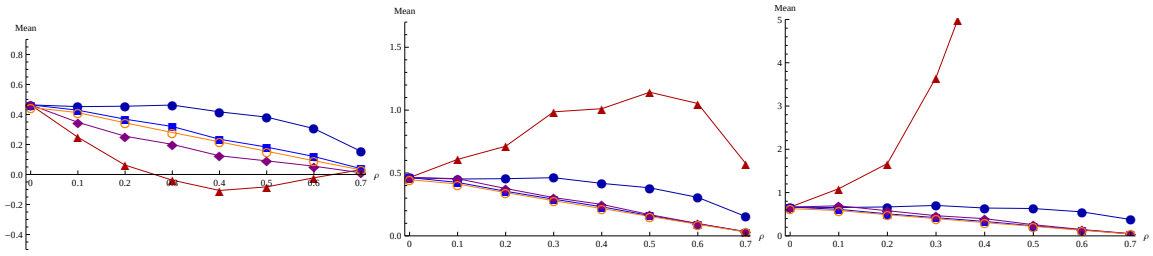

(xvi) ΔH, $\hat{p} = 0.5$ (xvii) KL, $\hat{p} = 0.5$ (xviii) χ^2, $\hat{p} = 0.5$

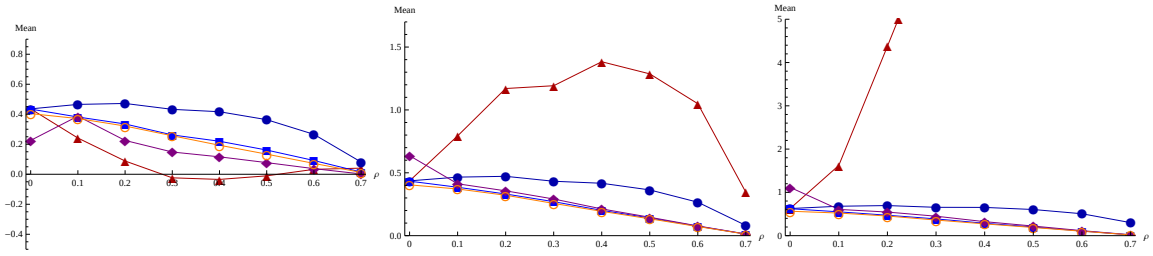

(xix) ΔH, $\hat{p} = 0.6$ (xx) KL, $\hat{p} = 0.6$ (xxi) χ^2, $\hat{p} = 0.6$

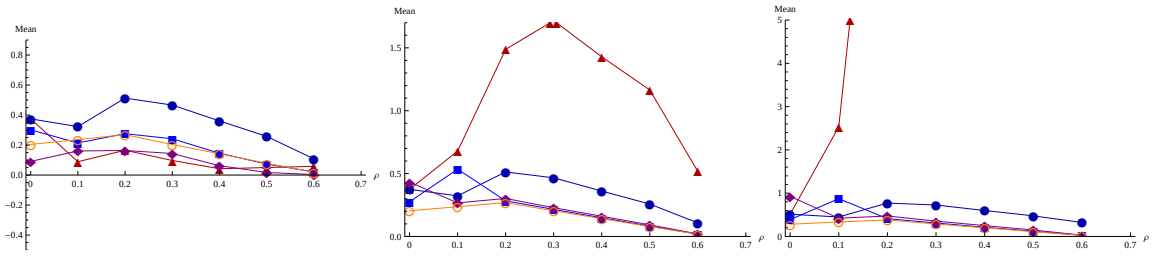

(xxii) ΔH, $\hat{p} = 0.7$ (xxiii) KL, $\hat{p} = 0.7$ (xxiv) χ^2, $\hat{p} = 0.7$

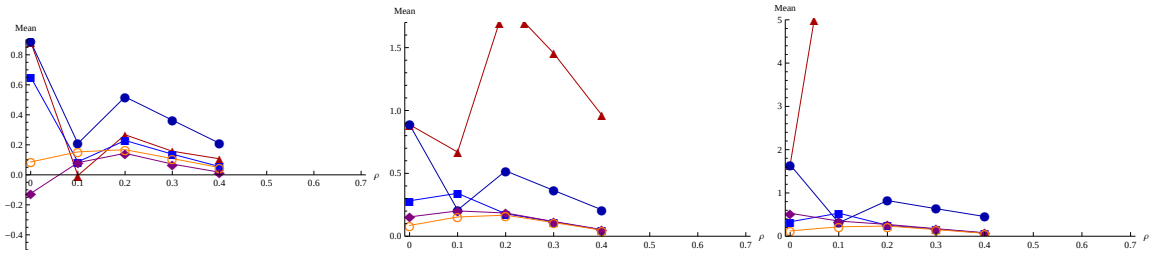

(xxv) ΔH, $\hat{p} = 0.8$ (xxvi) KL, $\hat{p} = 0.8$ (xxvii) χ^2, $\hat{p} = 0.8$

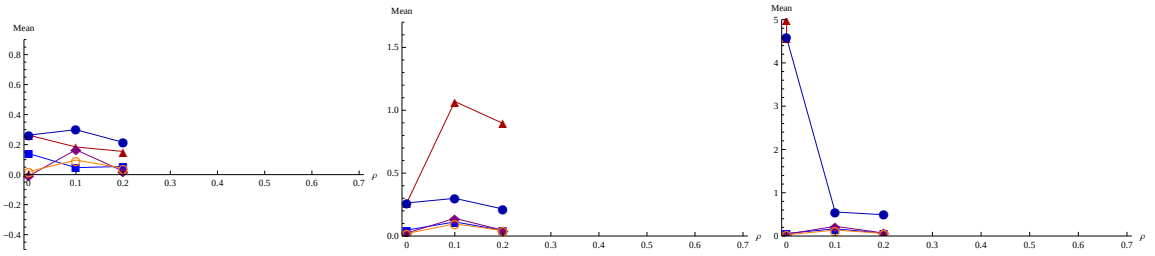

(xxviii) ΔH, $\hat{p} = 0.9$ (xxix) KL, $\hat{p} = 0.9$ (xxx) χ^2, $\hat{p} = 0.9$

Figure 5.32: Mean estimates for $\mathbb{T}$ with 7 binary random variables. The rank correlation is shown in the x-axes. Each row shows marginal assessments $\hat{p}$ and each column shows an accuracy measure (part two).

The figures should be read as follows: The joint approximations are shown in different markers; the respective rank correlation among variables ($\rho^r_{1,2}$) is shown in the horizontal-axes; the marginal probabilities are arranged by rows and the accuracy measures are arranged by columns. Then each subfigure show the changes generated by the correlation matrix, and each row show the changes generated by the marginal distributions.

UE Findings. The overall worst approximation among the models considered was UE. This approximation shows its worst behavior for $\hat{p} \approx 0.8$. The increment in the number of variables diminishes the accuracy of the approximation for almost all positive values of $\rho^r_{1,2}$. The accuracy improves for values of $\rho^r_{1,2}$ close to the extremes and is worst when $\rho^r_{1,2} \approx 0.3$. The observed behavior would be more intuitive if we scale down the dimension of the polytope. For example, in Figure 5.28(ix), the polytope has dimension $d = n - m = 1$ and can be described by a line. Then, we can analytically describe a series of polytopes (one for each correlation value) and the position of the UE in each one, as in Figure 5.33.

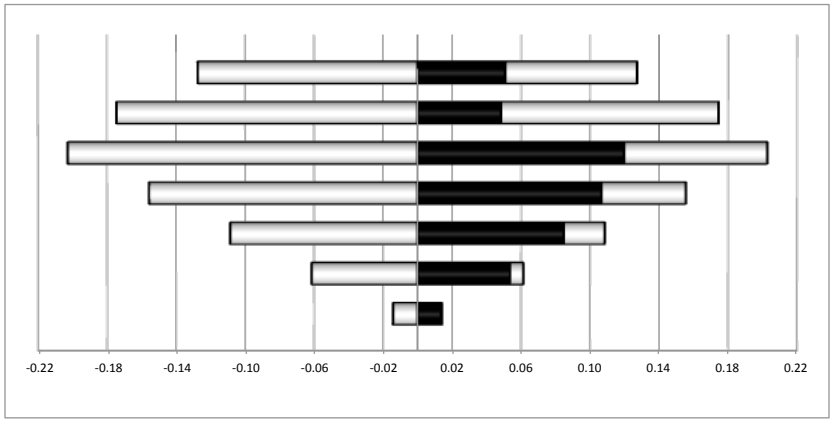

Figure 5.33: UE position in seven truth sets constructed with three random variables, $\hat{p} = 0.7$, and different correlation parameters. From top to bottom $\rho^r_{1,2}$ with values $0.0, 0.1, 0.2, 0.3, 0.4, 0.5$, and 0.6.

Each horizontal bar in Figure 5.33 represents a polytope with different rank correlation. The 0.0 represents the center of the polytope and the extremes of the bar mark the distance in $\mathbf{L}_2$-norm from the center to the vertices of $\mathbb{T}$. This figure shows that the set $\mathbb{T}$ expands and contracts as the correlation parameter is increased. Because we are considering only symmetric polytopes, the UE approximation is in the interior of $\mathbb{T}$, which is usually false in the general case. The black bars indicate the distance ($\mathbf{L}_2$-norm) from the center of $\mathbb{T}$ to the UE approximation.

As the truth set expands and contracts, the center of $\mathbb{T}$ and the UE approximation becomes more biased as the length of the polytope increases and decreases. For $\hat{p} = 0.5$, UE and ME are equivalent. This is because the UE model is strongly based on the IA, where the marginal random variables are independent given one random variable that explains all the dependencies. Therefore, the UE approximation is defined by the information structure and not by the shape of the truth set. As correlation increases, the information misguides the UE approximation, pushing it closer to the bound of the set. This approximation is easy to implement but is not recommended because of its low accuracy and high bias.

ME Findings. The second worst approximation was ME. This approximation is more accurate than UE for $\hat{p} \leq 0.7$. But as $\hat{p}$ increases, the UE becomes more accurate. This result is in direct conflict with Bickel and Smith (2006), which is explain by the difference on the sampling procedures used. We sampled up to two hundred thousand distributions for each polytope in a number of polytopes, whereas Bickel and Smith generate 5,000 polytopes and for each one they only observe three approximations.

Figure 5.34 depicts the equivalent of Figure 5.33 for the ME approximation. The figure shows similar behavior to the one described in Figure 5.23 and locates the ME on the extremes of the truth set. However, as the correlation parameter increases, the truth set rotates, leaving the ME approximation closer to the opposite

vertex of the set. The contraction of the set for high values of $\rho^r_{1,2}$ slightly increases the accuracy of the approximation.

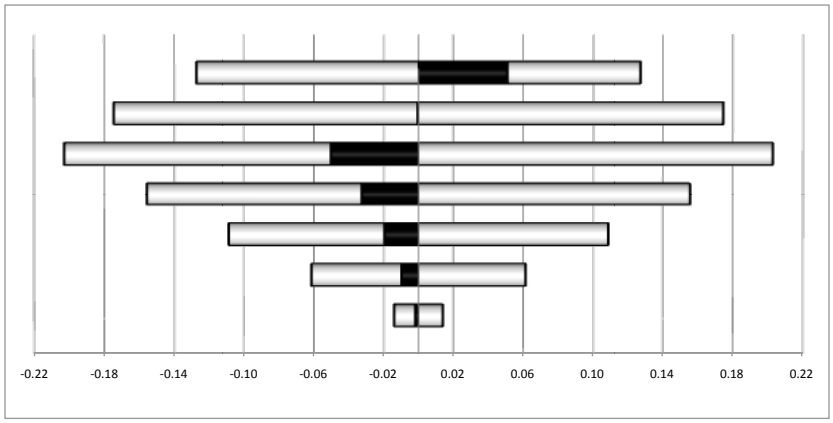

Figure 5.34: ME position in seven truth sets constructed with three random variables, $\hat{p} = 0.7$, and different correlation parameters. From top to bottom, $\rho^r_{1,2}$ with values $0.0, 0.1, 0.2, 0.3, 0.4, 0.5$, and 0.6.

ChSC Findings. The ChSC approximation shows a considerable improvement in accuracy for every $\hat{p}$ when the correlation parameters are $\rho^r_{1,2} > 0.2$. The intuition behind it relies on the fact that when $\rho^r_{1,2} \leq 0.2$, the distribution samples in the truth set have joint elements for which the joint probabilities are dispersed, i.e., many of the joint elements have probabilities far from zero and cover a large range of values. As $\rho^r_{1,2}$ increases, the probabilities of most of the joint elements in the sampled distributions became more concentrated closer to zero. Figure 5.26 showed that the ChSC approximation has a tendency to assign the same value to as many joint probabilities as possible. Therefore, when the samples have dispersed elements, the ChSC approximation behaves erratically. But as the joint probabilities in the sampled distributions became more concentrated, the approximation's accuracy dramatically increases.

Findings for the Most Accurate Approximations. The approximations with the best accuracy in symmetric polytopes were DAC, AC, and MVIE. As before, each of these approximations has advantages and disadvantages. For DAC the biggest flaw is the running time of the algorithm, which constrained us to sample only 200,000 distributions for polytopes constructed using 6 and 7 variables, rather than the more desirable orders of 1,000,000 and 10,000,000, respectively (see §3.4.3). Large sample sizes can be generated in less than 24 hours, but this is not always sufficient. The MVIE requires fewer iterations, but each iteration is computationally intensive. Finally, AC is easy to calculate but behaves erratically for a small number of polytopes (Figure 5.32 third and fourth rows). The reasons for these behavior are still unknown.

The standard deviation of the accuracy measures for marginal and rank correlation constraints can be observed in Appendix C, Figures C.13, C.14, C.15, C.16, and C.17. In general, the standard deviation corresponds to the principle of contraction and expansion of the truth set, which explains the general trend of increasing and decreasing standard deviation for changes in the rank correlation. Also, for most of the cases, DAC, AC, and the MVIE provide the lowest standard deviation.

Percentage of Accuracy. In addition to the mean and standard deviation of the accuracy measures, the percentage of accuracy was calculated. This statistic measures the percentage of time that a given approximation outperforms another. Tables 5.7, 5.8, 5.9, and 5.10 present the results for polytopes constructed using 5 binary random variables. The tables show changes in marginal and rank correlations for all distribution approximations and all measures considered. Values above 50% indicate that the approximation in row one is more accurate than the approximation in row two, and values below 50% indicate the opposite.

Appendix C presents the complete set of results for 3, 4, 6, and 7 binary random variables in Tables C.10, C.11, C.12, C.13, C.14, C.15, C.16, C.17, C.18, C.19, C.20, C.21, C.22, C.23, C.24, and C.25.

The overall results show that the approximations in descending order by percentage of accuracy are DAC, MVIE, AC, ChSC, ME, UE, and IA. This ordering will present a correct description of the accuracy of the joint approximations, although there are some scenarios for which the general results do not hold.

Interestingly, AC and ChSC show that in low-dimensional environments (polytopes generated with 3 binary random variables), ChSC outperforms AC, but as the dimension increases, AC considerably outperforms ChSC. This suggests that the dimensionality does affect the accuracy of the ChSC approximations. Because ChSC is a linear function, all of its elements are far from zero. As the dimension increases, the probability mass needs to be distributed among a larger number of joint events, creating a joint approximation that is less dispersed and has a larger number of elements close to zero, which reduces its accuracy.

Table 5.7: Percentage of accuracy (i.e. fraction of times one approximation is better than other) for sets with symmetric marginal and rank correlation information using 5 binary random variables and changing the values of $\hat{p} = 0.5$ and $\rho^r_{1,2} = 0, 0.1, 0.2, 0.3, 0.4, 0.5, 0.6$, and 0.7.

% Of times		DAC	DAC	DAC	DAC	DAC	DAC	MVIE	MVIE	MVIE	MVIE	MVIE	AC	AC	AC	AC	ChSC	ChSC	ChSC	ME	ME	UE
is better than		MVIE	AC	ChSC	ME	UE	IN	AC	ChSC	ME	UE	IA	ChSC	ME	UE	IA	ME	UE	IA	UE	IA	IA
$\hat{p}$	$\mathbf{L}^\infty$	62%	62%	62%	62%	62%	62%	66%	66%	66%	66%	66%	51%	51%	51%	51%	61%	61%	61%	50%	50%	50%
0.5	$\mathbf{L}^1$	52%	52%	52%	52%	52%	52%	49%	50%	50%	50%	50%	47%	47%	47%	47%	46%	46%	46%	50%	50%	50%
ρ	$\mathbf{L}^2$	52%	52%	52%	52%	52%	52%	47%	49%	49%	49%	49%	46%	46%	46%	46%	49%	49%	49%	50%	50%	50%
0	KL	52%	52%	52%	52%	52%	52%	47%	49%	49%	49%	49%	46%	46%	46%	46%	100%	100%	100%	50%	50%	50%
	χ^2	53%	53%	53%	53%	53%	53%	46%	49%	49%	49%	49%	43%	43%	43%	43%	64%	64%	64%	50%	50%	50%
$\hat{p}$	$\mathbf{L}^\infty$	51%	50%	56%	61%	74%	97%	56%	56%	61%	75%	97%	56%	62%	75%	97%	49%	74%	90%	74%	98%	74%
0.5	$\mathbf{L}^1$	51%	53%	60%	59%	76%	100%	50%	61%	56%	77%	100%	60%	57%	77%	100%	46%	75%	97%	75%	99%	55%
ρ	$\mathbf{L}^2$	50%	52%	62%	60%	76%	100%	51%	63%	58%	78%	100%	62%	59%	77%	100%	46%	76%	94%	75%	100%	56%
0.1	KL	51%	52%	62%	60%	77%	100%	51%	64%	58%	79%	100%	62%	59%	78%	100%	45%	77%	97%	75%	100%	60%
	χ^2	50%	51%	65%	60%	80%	100%	50%	66%	58%	81%	100%	64%	60%	81%	100%	43%	79%	95%	79%	100%	56%
$\hat{p}$	$\mathbf{L}^\infty$	44%	55%	57%	71%	87%	100%	57%	58%	69%	87%	100%	55%	74%	87%	100%	59%	85%	100%	85%	100%	99%
0.5	$\mathbf{L}^1$	49%	56%	59%	69%	86%	100%	52%	62%	67%	86%	100%	57%	71%	86%	100%	58%	85%	100%	83%	100%	75%
ρ	$\mathbf{L}^2$	48%	58%	62%	72%	88%	100%	53%	64%	70%	87%	100%	59%	74%	87%	100%	59%	86%	100%	85%	100%	90%
0.2	KL	49%	56%	62%	71%	90%	100%	53%	64%	69%	89%	100%	59%	74%	89%	100%	58%	88%	100%	85%	100%	88%
	χ^2	52%	54%	66%	71%	92%	100%	51%	68%	69%	92%	100%	63%	74%	92%	100%	56%	90%	100%	88%	100%	87%
$\hat{p}$	$\mathbf{L}^\infty$	46%	60%	57%	80%	95%	100%	56%	59%	77%	94%	100%	55%	82%	94%	100%	68%	92%	100%	92%	100%	100%
0.5	$\mathbf{L}^1$	49%	58%	59%	76%	94%	100%	52%	62%	74%	93%	100%	57%	78%	93%	100%	66%	92%	100%	91%	100%	96%
ρ	$\mathbf{L}^2$	49%	59%	60%	80%	95%	100%	53%	64%	78%	94%	100%	58%	82%	94%	100%	69%	93%	100%	93%	100%	100%
0.3	KL	49%	59%	62%	79%	96%	100%	53%	64%	77%	96%	100%	58%	82%	96%	100%	67%	95%	100%	93%	100%	99%
	χ^2	49%	59%	65%	80%	99%	100%	51%	68%	77%	98%	100%	62%	83%	98%	100%	65%	97%	100%	97%	100%	94%
$\hat{p}$	$\mathbf{L}^\infty$	46%	57%	58%	86%	98%	100%	56%	60%	83%	98%	100%	55%	87%	98%	100%	76%	98%	100%	98%	100%	100%
0.5	$\mathbf{L}^1$	52%	56%	61%	83%	98%	100%	51%	65%	81%	98%	100%	58%	84%	98%	100%	74%	98%	100%	98%	100%	100%
ρ	$\mathbf{L}^2$	51%	58%	63%	86%	98%	100%	52%	67%	84%	98%	100%	60%	88%	98%	100%	77%	98%	100%	98%	100%	100%
0.4	KL	52%	57%	64%	86%	99%	100%	52%	67%	83%	99%	100%	60%	87%	99%	100%	75%	99%	100%	99%	100%	100%
	χ^2	54%	56%	67%	87%	100%	100%	50%	71%	84%	100%	100%	64%	89%	100%	100%	75%	100%	100%	100%	100%	94%
$\hat{p}$	$\mathbf{L}^\infty$	48%	57%	58%	91%	100%	100%	56%	60%	90%	100%	100%	55%	93%	100%	100%	84%	100%	100%	100%	100%	100%
0.5	$\mathbf{L}^1$	52%	55%	62%	89%	100%	100%	51%	65%	88%	100%	100%	58%	90%	100%	100%	82%	100%	100%	100%	100%	100%
ρ	$\mathbf{L}^2$	52%	57%	63%	92%	100%	100%	52%	67%	91%	100%	100%	59%	93%	100%	100%	86%	100%	100%	100%	100%	100%
0.5	KL	52%	56%	63%	91%	100%	100%	52%	67%	90%	100%	100%	60%	93%	100%	100%	83%	100%	100%	100%	100%	100%
	χ^2	54%	54%	67%	93%	100%	100%	50%	71%	91%	100%	100%	63%	94%	100%	100%	83%	100%	100%	100%	100%	89%
$\hat{p}$	$\mathbf{L}^\infty$	48%	58%	58%	96%	100%	100%	56%	60%	95%	100%	100%	55%	96%	100%	100%	91%	100%	100%	100%	100%	100%
0.5	$\mathbf{L}^1$	51%	56%	61%	94%	100%	100%	51%	65%	92%	100%	100%	58%	94%	100%	100%	89%	100%	100%	100%	100%	100%
ρ	$\mathbf{L}^2$	50%	58%	62%	96%	100%	100%	52%	67%	95%	100%	100%	59%	96%	100%	100%	92%	100%	100%	100%	100%	100%
0.6	KL	52%	57%	63%	95%	100%	100%	52%	67%	94%	100%	100%	59%	96%	100%	100%	90%	100%	100%	100%	100%	100%
	χ^2	54%	55%	67%	96%	100%	100%	51%	71%	95%	100%	100%	63%	97%	100%	100%	91%	100%	100%	100%	100%	60%
$\hat{p}$	$\mathbf{L}^\infty$	53%	62%	55%	99%	100%	100%	60%	56%	99%	100%	100%	51%	100%	100%	100%	99%	100%	100%	100%	100%	100%
0.5	$\mathbf{L}^1$	51%	58%	59%	99%	100%	100%	56%	61%	99%	100%	100%	54%	99%	100%	100%	98%	100%	100%	100%	100%	100%
ρ	$\mathbf{L}^2$	50%	59%	61%	99%	100%	100%	57%	63%	99%	100%	100%	54%	100%	100%	100%	99%	100%	100%	100%	100%	100%
0.7	KL	52%	59%	62%	99%	100%	100%	57%	63%	99%	100%	100%	55%	100%	100%	100%	98%	100%	100%	100%	100%	100%
	χ^2	55%	57%	66%	100%	100%	100%	55%	67%	100%	100%	100%	59%	100%	100%	100%	99%	100%	100%	100%	100%	2%

Table 5.8: Percentage of accuracy (i.e. fraction of times one approximation is better than other) for sets with symmetric marginal and rank correlation information using 5 binary random variables and changing the values of $\hat{p} = 0.6$ and $\rho^r_{1,2} = 0, 0.1, 0.2, 0.3, 0.4, 0.5, 0.6$, and 0.7.

% Of times		DAC	DAC	DAC	DAC	DAC	DAC	MVIE	MVIE	MVIE	MVIE	MVIE	AC	AC	AC	AC	ChSC	ChSC	ChSC	ME	ME	UE
is better than		MVIE	AC	ChSC	ME	UE	IA	AC	ChSC	ME	UE	IA	ChSC	ME	UE	IA	ME	UE	IA	UE	IA	IA
$\hat{p}$	$\mathbf{L}^\infty$	48%	54%	80%	49%	49%	49%	61%	78%	60%	60%	60%	81%	37%	37%	37%	20%	20%	20%	50%	50%	50%
0.6	$\mathbf{L}^1$	54%	52%	76%	53%	53%	53%	48%	74%	46%	46%	46%	76%	50%	50%	50%	25%	25%	25%	50%	50%	50%
ρ	$\mathbf{L}^2$	53%	52%	78%	52%	52%	52%	49%	76%	47%	47%	47%	78%	50%	50%	50%	23%	23%	23%	50%	50%	50%
0	KL	53%	53%	80%	53%	53%	53%	48%	78%	47%	47%	47%	80%	50%	50%	50%	21%	21%	21%	50%	44%	36%
	χ^2	53%	54%	83%	52%	52%	52%	49%	81%	48%	48%	48%	83%	49%	49%	49%	18%	18%	18%	50%	50%	50%
$\hat{p}$	$\mathbf{L}^\infty$	43%	57%	49%	77%	90%	94%	61%	47%	74%	89%	93%	52%	81%	92%	95%	70%	90%	94%	96%	98%	95%
0.6	$\mathbf{L}^1$	51%	57%	54%	71%	90%	94%	53%	52%	68%	88%	92%	48%	74%	91%	96%	71%	90%	94%	96%	100%	25%
ρ	$\mathbf{L}^2$	50%	58%	56%	73%	91%	94%	54%	53%	70%	89%	92%	46%	76%	92%	95%	73%	91%	94%	97%	100%	53%
0.1	KL	51%	57%	55%	72%	93%	99%	54%	54%	69%	92%	97%	50%	75%	95%	100%	71%	92%	99%	97%	100%	24%
	χ^2	52%	56%	56%	73%	96%	100%	53%	55%	70%	94%	98%	51%	77%	96%	100%	71%	95%	100%	98%	100%	20%
$\hat{p}$	$\mathbf{L}^\infty$	48%	63%	57%	80%	96%	100%	68%	58%	79%	96%	100%	54%	83%	97%	100%	75%	95%	100%	99%	100%	100%
0.6	$\mathbf{L}^1$	48%	59%	60%	78%	96%	100%	56%	63%	77%	95%	100%	53%	81%	97%	100%	73%	95%	99%	99%	100%	48%
ρ	$\mathbf{L}^2$	48%	59%	62%	80%	96%	100%	57%	66%	78%	96%	100%	53%	82%	97%	100%	75%	95%	100%	99%	100%	98%
0.2	KL	49%	59%	63%	80%	97%	100%	57%	65%	78%	97%	100%	58%	83%	98%	100%	71%	97%	100%	99%	100%	53%
	χ^2	51%	60%	66%	82%	99%	100%	57%	69%	80%	99%	100%	61%	85%	99%	100%	70%	98%	100%	100%	100%	42%
$\hat{p}$	$\mathbf{L}^\infty$	51%	55%	58%	81%	98%	100%	54%	61%	80%	98%	100%	57%	82%	98%	100%	74%	98%	100%	99%	100%	100%
0.6	$\mathbf{L}^1$	53%	55%	62%	82%	98%	100%	51%	66%	80%	98%	100%	60%	83%	98%	100%	76%	98%	100%	99%	100%	99%
ρ	$\mathbf{L}^2$	52%	57%	63%	83%	98%	100%	53%	68%	82%	98%	100%	61%	84%	98%	100%	78%	98%	100%	99%	100%	100%
0.3	KL	52%	57%	64%	84%	99%	100%	51%	68%	81%	99%	100%	62%	86%	99%	100%	72%	98%	100%	100%	100%	90%
	χ^2	55%	56%	67%	86%	100%	100%	49%	72%	82%	100%	100%	65%	88%	100%	100%	71%	99%	100%	100%	100%	64%
$\hat{p}$	$\mathbf{L}^\infty$	49%	54%	58%	86%	99%	100%	56%	60%	85%	99%	100%	55%	87%	99%	100%	80%	99%	100%	100%	100%	100%
0.6	$\mathbf{L}^1$	50%	56%	61%	86%	99%	100%	51%	64%	84%	99%	100%	58%	86%	99%	100%	81%	99%	100%	100%	100%	100%
ρ	$\mathbf{L}^2$	48%	57%	62%	88%	99%	100%	53%	66%	86%	99%	100%	59%	88%	99%	100%	83%	99%	100%	100%	100%	100%
0.4	KL	51%	56%	63%	89%	100%	100%	52%	66%	86%	100%	100%	59%	90%	100%	100%	79%	100%	100%	100%	100%	100%
	χ^2	53%	55%	66%	89%	100%	100%	50%	70%	87%	100%	100%	63%	91%	100%	100%	78%	100%	100%	100%	100%	74%
$\hat{p}$	$\mathbf{L}^\infty$	51%	61%	57%	92%	100%	100%	58%	59%	92%	100%	100%	54%	94%	100%	100%	89%	100%	100%	100%	100%	100%
0.6	$\mathbf{L}^1$	51%	57%	61%	92%	100%	100%	53%	64%	92%	100%	100%	57%	93%	100%	100%	89%	100%	100%	100%	100%	100%
ρ	$\mathbf{L}^2$	49%	59%	62%	94%	100%	100%	55%	66%	94%	100%	100%	57%	95%	100%	100%	91%	100%	100%	100%	100%	100%
0.5	KL	51%	58%	63%	94%	100%	100%	54%	66%	93%	100%	100%	58%	95%	100%	100%	88%	100%	100%	100%	100%	100%
	χ^2	53%	57%	66%	95%	100%	100%	52%	70%	94%	100%	100%	62%	96%	100%	100%	88%	100%	100%	100%	100%	61%
$\hat{p}$	$\mathbf{L}^\infty$	50%	58%	56%	96%	100%	100%	59%	58%	96%	100%	100%	52%	97%	100%	100%	94%	100%	100%	100%	100%	100%
0.6	$\mathbf{L}^1$	50%	57%	60%	96%	100%	100%	54%	62%	96%	100%	100%	55%	97%	100%	100%	94%	100%	100%	100%	100%	100%
ρ	$\mathbf{L}^2$	49%	59%	61%	97%	100%	100%	56%	64%	97%	100%	100%	55%	98%	100%	100%	96%	100%	100%	100%	100%	100%
0.6	KL	52%	58%	62%	97%	100%	100%	56%	64%	97%	100%	100%	56%	98%	100%	100%	94%	100%	100%	100%	100%	100%
	χ^2	54%	57%	66%	98%	100%	100%	54%	68%	98%	100%	100%	60%	99%	100%	100%	95%	100%	100%	100%	100%	23%
$\hat{p}$	$\mathbf{L}^\infty$	52%	63%	55%	99%	100%	100%	61%	56%	99%	100%	100%	50%	99%	100%	100%	98%	100%	100%	100%	100%	100%
0.6	$\mathbf{L}^1$	50%	58%	59%	99%	100%	100%	56%	61%	99%	100%	100%	54%	99%	100%	100%	99%	100%	100%	100%	100%	100%
ρ	$\mathbf{L}^2$	48%	59%	61%	99%	100%	100%	58%	63%	99%	100%	100%	54%	99%	100%	100%	99%	100%	100%	100%	100%	100%
0.7	KL	50%	59%	61%	100%	100%	100%	57%	63%	100%	100%	100%	55%	100%	100%	100%	99%	100%	100%	100%	100%	100%
	χ^2	52%	57%	65%	100%	100%	100%	55%	67%	100%	100%	100%	58%	100%	100%	100%	100%	100%	100%	100%	100%	0%

Table 5.9: Percentage of accuracy (i.e. fraction of times one approximation is better than other) for sets with symmetric marginal and rank correlation information using 5 binary random variables and changing the values of $\hat{p} = 0.7$ and $\rho^r_{1,2} = 0, 0.1, 0.2, 0.3, 0.4, 0.5$, and 0.6.

% Of times		DAC	DAC	DAC	DAC	DAC	DAC	MVIE	MVIE	MVIE	MVIE	MVIE	AC	AC	AC	AC	ChSC	ChSC	ChSC	ME	ME	UE
is better than		MVIE	AC	ChSC	ME	UE	IA	AC	ChSC	ME	UE	IA	ChSC	ME	UE	IA	ME	UE	IA	UE	IA	IA
$\hat{p}$	$\mathbf{L}^\infty$	58%	60%	90%	72%	72%	72%	53%	93%	66%	66%	66%	82%	80%	80%	80%	30%	30%	30%	50%	50%	50%
0.7	$\mathbf{L}^1$	55%	63%	88%	76%	76%	76%	57%	92%	69%	69%	69%	79%	84%	84%	84%	33%	33%	33%	50%	50%	50%
ρ	$\mathbf{L}^2$	56%	63%	89%	75%	75%	75%	56%	93%	68%	68%	68%	81%	84%	84%	84%	32%	32%	32%	50%	50%	50%
0	KL	56%	63%	90%	75%	75%	75%	56%	93%	68%	68%	68%	83%	84%	84%	84%	28%	28%	28%	50%	50%	50%
	χ^2	61%	60%	94%	72%	72%	72%	51%	96%	65%	65%	65%	89%	81%	81%	81%	20%	20%	20%	50%	50%	50%
$\hat{p}$	$\mathbf{L}^\infty$	43%	63%	86%	80%	94%	98%	59%	82%	75%	92%	97%	88%	82%	95%	98%	6%	99%	100%	99%	100%	100%
0.7	$\mathbf{L}^1$	54%	56%	84%	77%	94%	96%	49%	79%	71%	92%	94%	85%	79%	95%	97%	8%	99%	99%	99%	100%	30%
ρ	$\mathbf{L}^2$	53%	58%	85%	79%	94%	97%	51%	81%	73%	92%	96%	87%	81%	95%	97%	6%	100%	100%	99%	100%	100%
0.1	KL	54%	57%	85%	79%	98%	99%	50%	80%	72%	97%	97%	87%	81%	99%	100%	11%	98%	99%	100%	100%	9%
	χ^2	54%	59%	88%	81%	99%	100%	51%	83%	74%	99%	100%	90%	84%	99%	100%	9%	99%	98%	100%	100%	8%
$\hat{p}$	$\mathbf{L}^\infty$	43%	64%	54%	90%	99%	100%	66%	56%	88%	99%	100%	50%	92%	99%	100%	85%	98%	100%	100%	100%	100%
0.7	$\mathbf{L}^1$	51%	59%	59%	88%	99%	100%	53%	64%	86%	99%	100%	54%	90%	99%	100%	83%	99%	100%	100%	100%	97%
ρ	$\mathbf{L}^2$	51%	60%	59%	90%	99%	100%	54%	65%	88%	99%	100%	53%	91%	99%	100%	85%	99%	100%	100%	100%	100%
0.2	KL	52%	59%	60%	89%	100%	100%	54%	65%	86%	100%	100%	55%	91%	100%	100%	81%	99%	100%	100%	100%	29%
	χ^2	53%	59%	62%	90%	100%	100%	53%	67%	87%	100%	100%	57%	92%	100%	100%	82%	100%	100%	100%	100%	17%
$\hat{p}$	$\mathbf{L}^\infty$	46%	56%	57%	90%	99%	100%	58%	60%	89%	99%	100%	56%	90%	99%	100%	87%	99%	100%	100%	100%	100%
0.7	$\mathbf{L}^1$	51%	55%	61%	89%	99%	100%	51%	64%	88%	99%	100%	58%	89%	99%	100%	86%	99%	100%	100%	100%	100%
ρ	$\mathbf{L}^2$	49%	56%	61%	90%	99%	100%	53%	66%	89%	99%	100%	59%	91%	99%	100%	87%	99%	100%	100%	100%	100%
0.3	KL	51%	55%	63%	91%	100%	100%	52%	66%	88%	100%	100%	60%	91%	100%	100%	84%	100%	100%	100%	100%	90%
	χ^2	52%	53%	66%	92%	100%	100%	50%	70%	90%	100%	100%	63%	93%	100%	100%	84%	100%	100%	100%	100%	48%
$\hat{p}$	$\mathbf{L}^\infty$	50%	58%	57%	93%	100%	100%	57%	59%	92%	100%	100%	54%	93%	100%	100%	91%	100%	100%	100%	100%	100%
0.7	$\mathbf{L}^1$	51%	57%	61%	93%	100%	100%	54%	64%	92%	100%	100%	57%	94%	100%	100%	91%	100%	100%	100%	100%	100%
ρ	$\mathbf{L}^2$	52%	59%	63%	94%	100%	100%	55%	66%	93%	100%	100%	58%	94%	100%	100%	92%	100%	100%	100%	100%	100%
0.4	KL	52%	57%	63%	94%	100%	100%	53%	66%	93%	100%	100%	59%	95%	100%	100%	90%	100%	100%	100%	100%	100%
	χ^2	55%	55%	67%	96%	100%	100%	51%	69%	95%	100%	100%	62%	97%	100%	100%	90%	100%	100%	100%	100%	56%
$\hat{p}$	$\mathbf{L}^\infty$	47%	58%	57%	94%	100%	100%	57%	59%	94%	100%	100%	54%	95%	100%	100%	93%	100%	100%	100%	100%	100%
0.7	$\mathbf{L}^1$	51%	57%	60%	96%	100%	100%	53%	63%	96%	100%	100%	56%	97%	100%	100%	95%	100%	100%	100%	100%	100%
ρ	$\mathbf{L}^2$	51%	58%	61%	97%	100%	100%	54%	65%	96%	100%	100%	57%	97%	100%	100%	95%	100%	100%	100%	100%	100%
0.5	KL	52%	58%	62%	97%	100%	100%	54%	65%	96%	100%	100%	57%	98%	100%	100%	94%	100%	100%	100%	100%	100%
	χ^2	54%	56%	66%	98%	100%	100%	52%	69%	97%	100%	100%	61%	98%	100%	100%	94%	100%	100%	100%	100%	35%
$\hat{p}$	$\mathbf{L}^\infty$	50%	62%	56%	98%	100%	100%	59%	58%	98%	100%	100%	52%	98%	100%	100%	97%	100%	100%	100%	100%	100%
0.7	$\mathbf{L}^1$	50%	58%	61%	99%	100%	100%	54%	63%	99%	100%	100%	56%	99%	100%	100%	99%	100%	100%	100%	100%	100%
ρ	$\mathbf{L}^2$	49%	60%	62%	99%	100%	100%	55%	65%	99%	100%	100%	56%	99%	100%	100%	99%	100%	100%	100%	100%	100%
0.6	KL	50%	59%	63%	100%	100%	100%	55%	65%	100%	100%	100%	57%	100%	100%	100%	99%	100%	100%	100%	100%	100%
	χ^2	51%	57%	67%	100%	100%	100%	53%	69%	100%	100%	100%	61%	100%	100%	100%	99%	100%	100%	100%	100%	0%

Table 5.10: Percentage of accuracy (i.e. fraction of times one approximation is better than other) for sets with symmetric marginal and rank correlation information using 5 binary random variables and changing the values of $\hat{p} = 0.8, 0.9$ and $\rho^r_{1,2} = 0, 0.1, 0.2, 0.3, 0.4$, $\rho^r_{1,2} = 0, 0.1, 0.2$ respectively.

% Of times		DAC	DAC	DAC	DAC	DAC	DAC	MVIE	MVIE	MVIE	MVIE	MVIE	AC	AC	AC	AC	ChSC	ChSC	ChSC	ME	ME	UE
is better than		MVIE	AC	ChSC	ME	UE	IA	AC	ChSC	ME	UE	IA	ChSC	ME	UE	IA	ME	UE	IA	UE	IA	IA
$\hat{p}$	$\mathbf{L}^\infty$	54%	75%	88%	96%	96%	96%	72%	90%	95%	95%	95%	67%	99%	99%	99%	79%	79%	79%	99%	98%	49%
0.8	$\mathbf{L}^1$	51%	79%	86%	97%	97%	97%	76%	89%	96%	96%	96%	61%	100%	100%	100%	82%	82%	82%	50%	50%	50%
ρ	$\mathbf{L}^2$	53%	79%	88%	97%	97%	97%	76%	90%	96%	96%	96%	63%	100%	100%	100%	82%	82%	82%	53%	50%	50%
0	KL	52%	79%	89%	96%	96%	96%	75%	91%	95%	95%	95%	66%	100%	100%	100%	77%	77%	77%	60%	0%	0%
	χ^2	61%	74%	94%	96%	96%	96%	69%	95%	95%	95%	95%	80%	99%	99%	99%	68%	68%	68%	55%	50%	7%
$\hat{p}$	$\mathbf{L}^\infty$	49%	50%	86%	81%	98%	100%	46%	84%	79%	97%	100%	85%	80%	98%	100%	4%	100%	100%	100%	100%	100%
0.8	$\mathbf{L}^1$	54%	54%	83%	77%	98%	100%	45%	81%	75%	97%	100%	82%	76%	98%	100%	7%	100%	100%	100%	100%	99%
ρ	$\mathbf{L}^2$	53%	52%	85%	79%	98%	100%	47%	83%	77%	97%	100%	84%	78%	98%	100%	5%	100%	100%	100%	100%	100%
0.1	KL	54%	54%	84%	80%	100%	100%	45%	83%	78%	100%	100%	83%	79%	100%	100%	14%	100%	100%	100%	100%	7%
	χ^2	52%	53%	89%	85%	100%	100%	46%	87%	83%	100%	100%	88%	84%	100%	100%	11%	100%	100%	100%	100%	7%
$\hat{p}$	$\mathbf{L}^\infty$	50%	68%	54%	98%	100%	100%	53%	55%	97%	100%	100%	47%	98%	100%	100%	96%	100%	100%	100%	100%	100%
0.8	$\mathbf{L}^1$	52%	61%	58%	97%	100%	100%	55%	61%	96%	100%	100%	50%	98%	100%	100%	95%	100%	100%	100%	100%	100%
ρ	$\mathbf{L}^2$	52%	61%	58%	97%	100%	100%	56%	62%	97%	100%	100%	50%	98%	100%	100%	96%	100%	100%	100%	100%	100%
0.2	KL	53%	61%	61%	96%	100%	100%	55%	61%	95%	100%	100%	53%	98%	100%	100%	93%	100%	100%	100%	100%	39%
	χ^2	54%	61%	64%	97%	100%	100%	55%	64%	96%	100%	100%	56%	99%	100%	100%	94%	100%	100%	100%	100%	17%
$\hat{p}$	$\mathbf{L}^\infty$	51%	55%	57%	97%	100%	100%	57%	59%	97%	100%	100%	54%	97%	100%	100%	96%	100%	100%	100%	100%	100%
0.8	$\mathbf{L}^1$	51%	57%	61%	96%	100%	100%	54%	63%	96%	100%	100%	56%	97%	100%	100%	95%	100%	100%	100%	100%	100%
ρ	$\mathbf{L}^2$	50%	59%	62%	97%	100%	100%	56%	65%	97%	100%	100%	57%	97%	100%	100%	96%	100%	100%	100%	100%	100%
0.3	KL	52%	58%	63%	97%	100%	100%	55%	65%	96%	100%	100%	58%	97%	100%	100%	94%	100%	100%	100%	100%	100%
	χ^2	55%	56%	67%	98%	100%	100%	53%	69%	97%	100%	100%	62%	98%	100%	100%	95%	100%	100%	100%	100%	54%
$\hat{p}$	$\mathbf{L}^\infty$	51%	59%	57%	98%	100%	100%	58%	59%	98%	100%	100%	53%	98%	100%	100%	97%	100%	100%	100%	100%	100%
0.8	$\mathbf{L}^1$	52%	56%	61%	98%	100%	100%	53%	64%	98%	100%	100%	57%	98%	100%	100%	98%	100%	100%	100%	100%	100%
ρ	$\mathbf{L}^2$	51%	58%	62%	98%	100%	100%	54%	65%	98%	100%	100%	57%	98%	100%	100%	98%	100%	100%	100%	100%	100%
0.4	KL	53%	58%	62%	99%	100%	100%	54%	65%	99%	100%	100%	58%	99%	100%	100%	97%	100%	100%	100%	100%	100%
	χ^2	55%	56%	66%	99%	100%	100%	52%	69%	99%	100%	100%	61%	100%	100%	100%	98%	100%	100%	100%	100%	31%
$\hat{p}$	$\mathbf{L}^\infty$	58%	74%	88%	100%	100%	100%	68%	91%	100%	100%	100%	66%	100%	100%	100%	95%	95%	95%	0%	0%	0%
0.9	$\mathbf{L}^1$	55%	76%	85%	100%	100%	100%	70%	89%	100%	100%	100%	61%	100%	100%	100%	97%	97%	97%	0%	0%	0%
ρ	$\mathbf{L}^2$	56%	76%	87%	100%	100%	100%	70%	90%	100%	100%	100%	63%	100%	100%	100%	97%	97%	97%	0%	0%	0%
0	KL	56%	77%	87%	100%	100%	100%	69%	91%	100%	100%	100%	67%	100%	100%	100%	93%	93%	93%	5%	0%	82%
	χ^2	65%	71%	94%	100%	100%	100%	61%	96%	100%	100%	100%	81%	100%	100%	100%	94%	94%	94%	13%	100%	94%
$\hat{p}$	$\mathbf{L}^\infty$	41%	68%	82%	99%	100%	100%	62%	78%	99%	100%	100%	85%	99%	100%	100%	100%	100%	100%	100%	100%	100%
0.9	$\mathbf{L}^1$	53%	59%	78%	99%	100%	100%	53%	74%	98%	100%	100%	81%	99%	100%	100%	100%	100%	100%	100%	100%	100%
ρ	$\mathbf{L}^2$	52%	60%	80%	99%	100%	100%	54%	76%	99%	100%	100%	83%	99%	100%	100%	100%	100%	100%	100%	100%	100%
0.1	KL	52%	60%	80%	98%	100%	100%	54%	76%	97%	100%	100%	83%	99%	100%	100%	100%	100%	100%	100%	100%	11%
	χ^2	53%	61%	83%	99%	100%	100%	55%	78%	98%	100%	100%	86%	100%	100%	100%	100%	100%	100%	100%	100%	11%
$\hat{p}$	$\mathbf{L}^\infty$	49%	61%	57%	99%	100%	100%	57%	59%	99%	100%	100%	54%	99%	100%	100%	99%	100%	100%	100%	100%	100%
0.9	$\mathbf{L}^1$	52%	57%	61%	99%	100%	100%	54%	64%	99%	100%	100%	56%	99%	100%	100%	99%	100%	100%	100%	100%	100%
ρ	$\mathbf{L}^2$	51%	60%	62%	99%	100%	100%	56%	66%	99%	100%	100%	57%	99%	100%	100%	99%	100%	100%	100%	100%	100%
0.2	KL	52%	58%	63%	99%	100%	100%	54%	66%	99%	100%	100%	58%	99%	100%	100%	98%	100%	100%	100%	100%	100%
	χ^2	54%	57%	67%	99%	100%	100%	52%	70%	99%	100%	100%	62%	100%	100%	100%	99%	100%	100%	100%	100%	70%

5.3.4 Findings in Symmetrically Constrained Truth Sets

Increasing the Number of Constraints:

1. Increasing the number of constraints increases the mean accuracy of the approximations. However, the same incase can not be used to predict the behavior of the standard deviation accuracy of the approximations (e.g. dispersion of the accuracy measures).

Symmetric Marginal Constrained Truth Sets:

1. The most accurate approximation was DAC, followed by AC.
2. The third-most accurate approximation was MVIE. This approximation has nearly the accuracy of DAC and AC but shows higher variance.
3. The approximation with the lowest entropy was ChSC. The accuracy of this approximation was the second worst.
4. The worst approximation was ME, showing its worst performance where the marginals assessments are close to 0.7.

Symmetric Marginal and Rank Correlation Constrained Truth Sets:

1. The most accurate approximation was DAC, followed by AC and MVIE.
2. The worst approximation was UE, followed by ME.
3. The ChSC is an accurate approximation for rank correlation assessments above 0.2 but otherwise has low accuracy in relation to AC, DAC, and MVIE.

5.4 Arbitrarily Constrained Multivariate Distributions

In this section, arbitrary polytopes are created using 3, 4, 5, and 6 binary random variables. Marginal assessments and rank correlation information are used to generate 20 polytopes for each of the four sets of binary random variables. For each of the 80 polytopes, we sample a collection of joint distributions and analyze the accuracy of the approximation distributions. The following two sections are dedicated to polytopes using arbitrarily selected marginal assessments and arbitrarily selected marginal and rank correlation assessments.

5.4.1 Arbitrary Marginal Constraints

Sampling Details. We observe the accuracy of the proposed approximations for non-symmetric polytopes with marginal constraints. The polytopes were generated using a uniform random generator to define the marginal probabilities of the binary random variables used to constraint $\mathbb{T}$. We generated sample collections of 50,000, 100,000, 200,000, and 400,000 distributions for polytopes based on 3, 4, 5, and 6 binary random variables, respectively.

Results. The mean accuracy for each polytope, each measure, and each distribution approximation based on 3 binary random variables, is described in Figure 5.35. Each subfigure describes the results for one measure, and the different joint approximations are described with different markers (and colors) for each of the 20 polytopes accommodated along the horizontal-axes. Similar results for 4, 5, and 6 binary random variables are shown in Figures 5.36, 5.37, and 5.38.

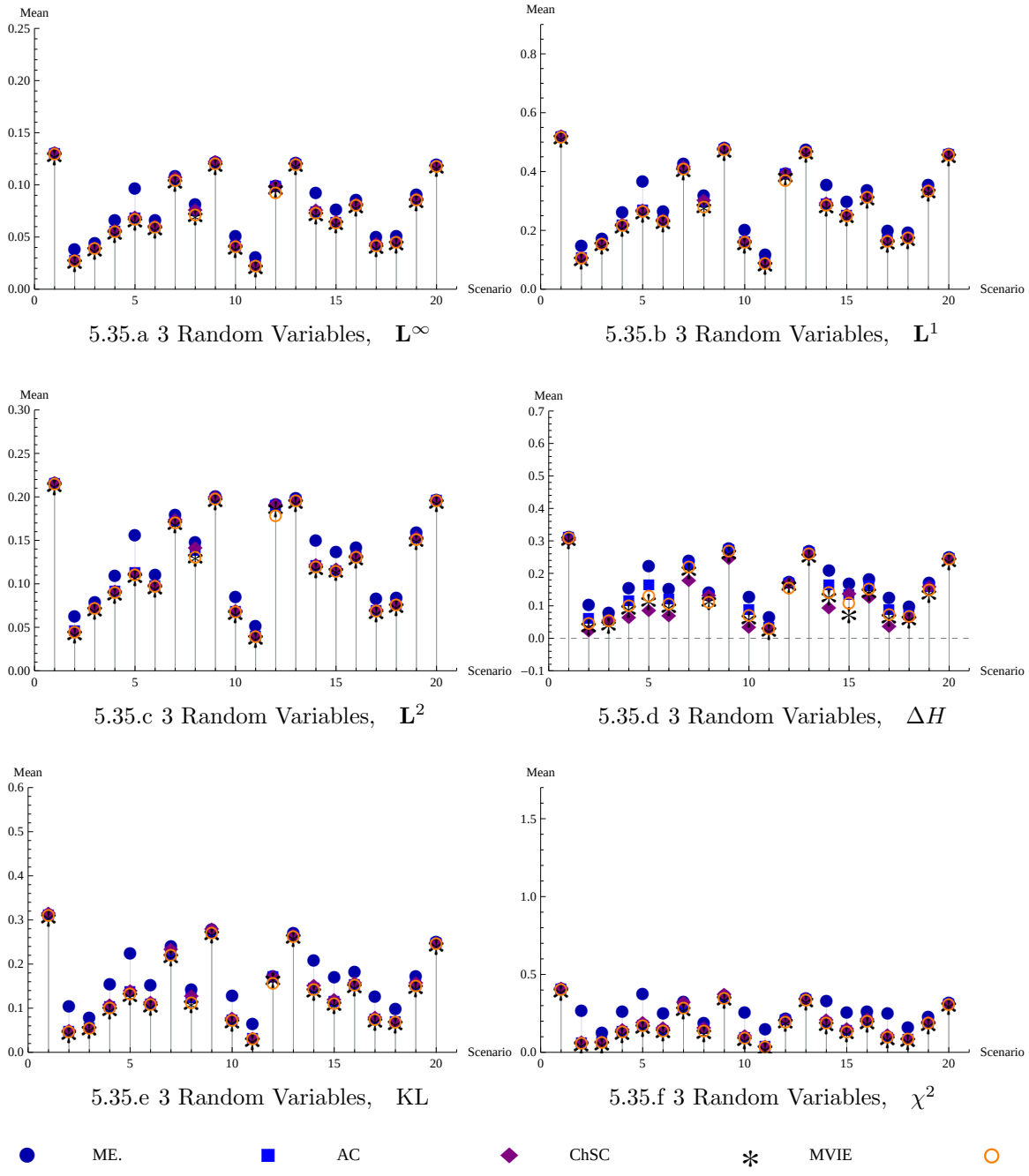

5.35.a 3 Random Variables, $\mathbf{L}^{\infty}$

5.35.b 3 Random Variables, $\mathbf{L}^{1}$

5.35.c 3 Random Variables, $\mathbf{L}^{2}$

5.35.d 3 Random Variables, ΔH

5.35.e 3 Random Variables, KL

5.35.f 3 Random Variables, χ^2

Figure 5.35: Mean estimates for accuracy measures for 20 realizations (scenarios along the x-axes) of truth sets with 3 binary random variables and marginal constraints.

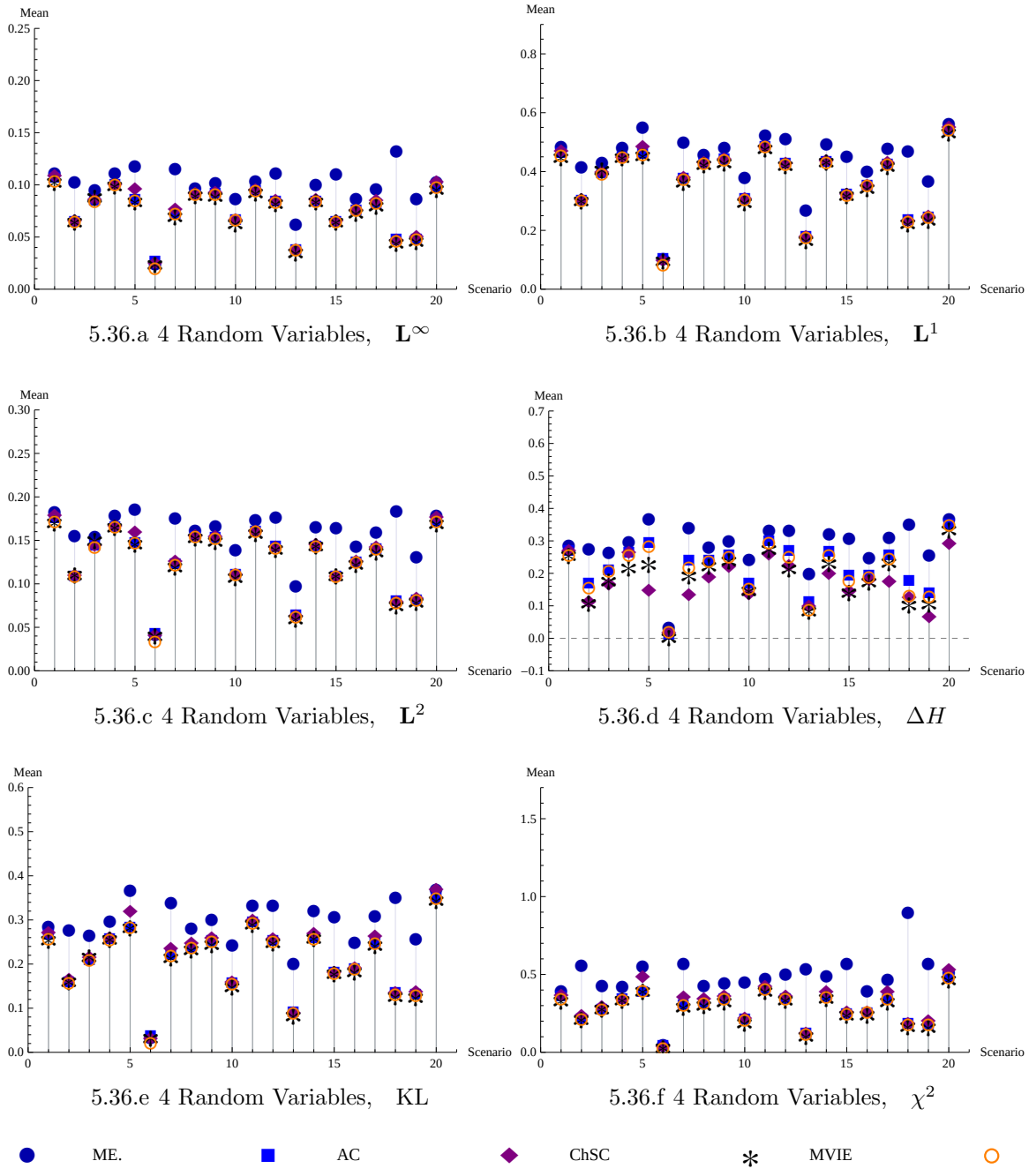

5.36.a 4 Random Variables, $\mathbf{L}^{\infty}$

5.36.b 4 Random Variables, $\mathbf{L}^{1}$

5.36.c 4 Random Variables, $\mathbf{L}^{2}$

5.36.d 4 Random Variables, ΔH

5.36.e 4 Random Variables, KL

5.36.f 4 Random Variables, χ^2

Figure 5.36: Mean estimates for accuracy measures for 20 realizations (scenarios along the x-axes) of truth sets with 4 binary random variables and marginal constraints.

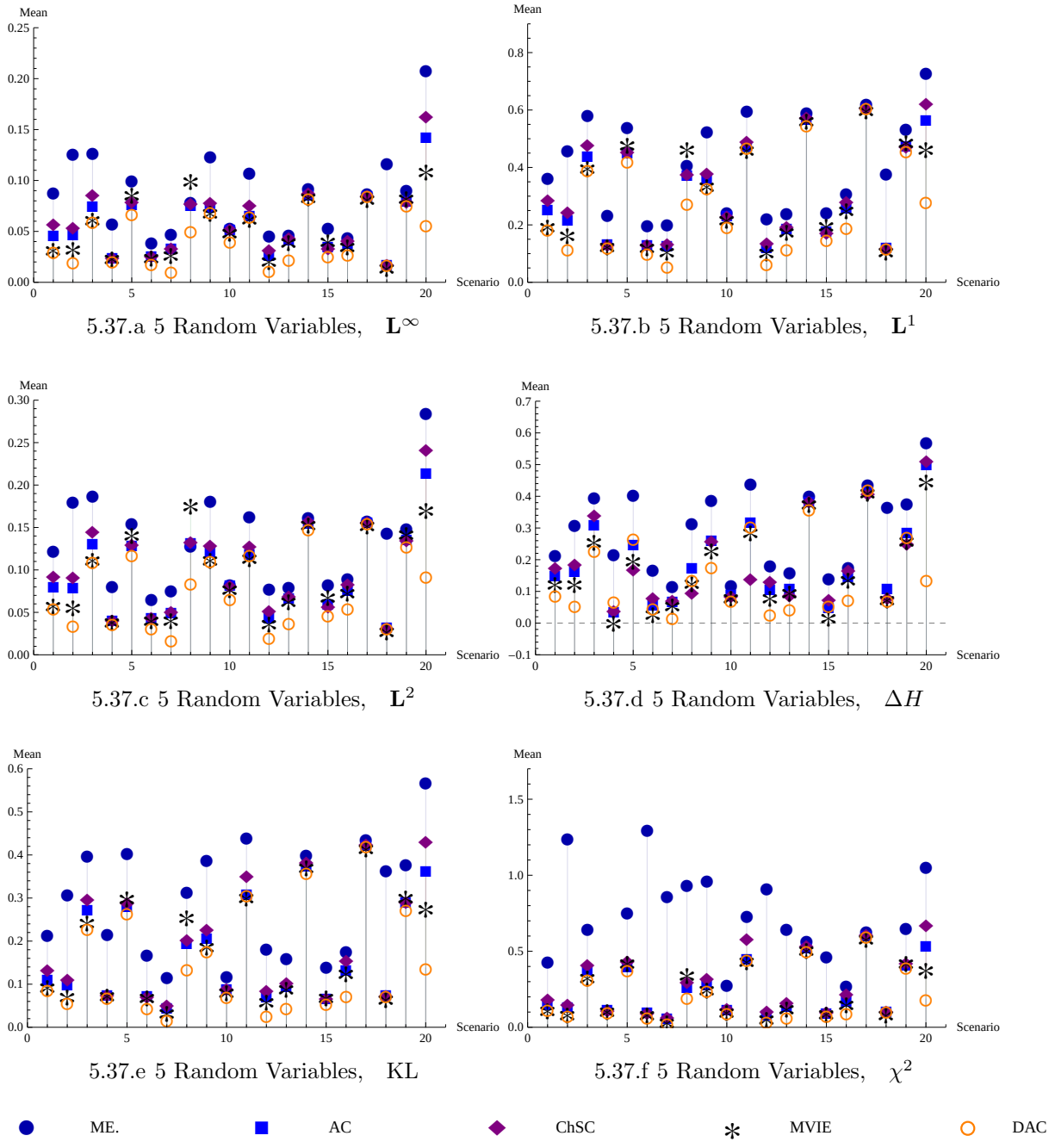

5.37.a 5 Random Variables, $\mathbf{L}^{\infty}$

5.37.b 5 Random Variables, $\mathbf{L}^{1}$

5.37.c 5 Random Variables, $\mathbf{L}^{2}$

5.37.d 5 Random Variables, ΔH

5.37.e 5 Random Variables, KL

5.37.f 5 Random Variables, χ^2

Figure 5.37: Mean estimates for accuracy measures for 20 realizations (scenarios along the x-axes) of truth sets with 5 binary random variables and marginal constraints.

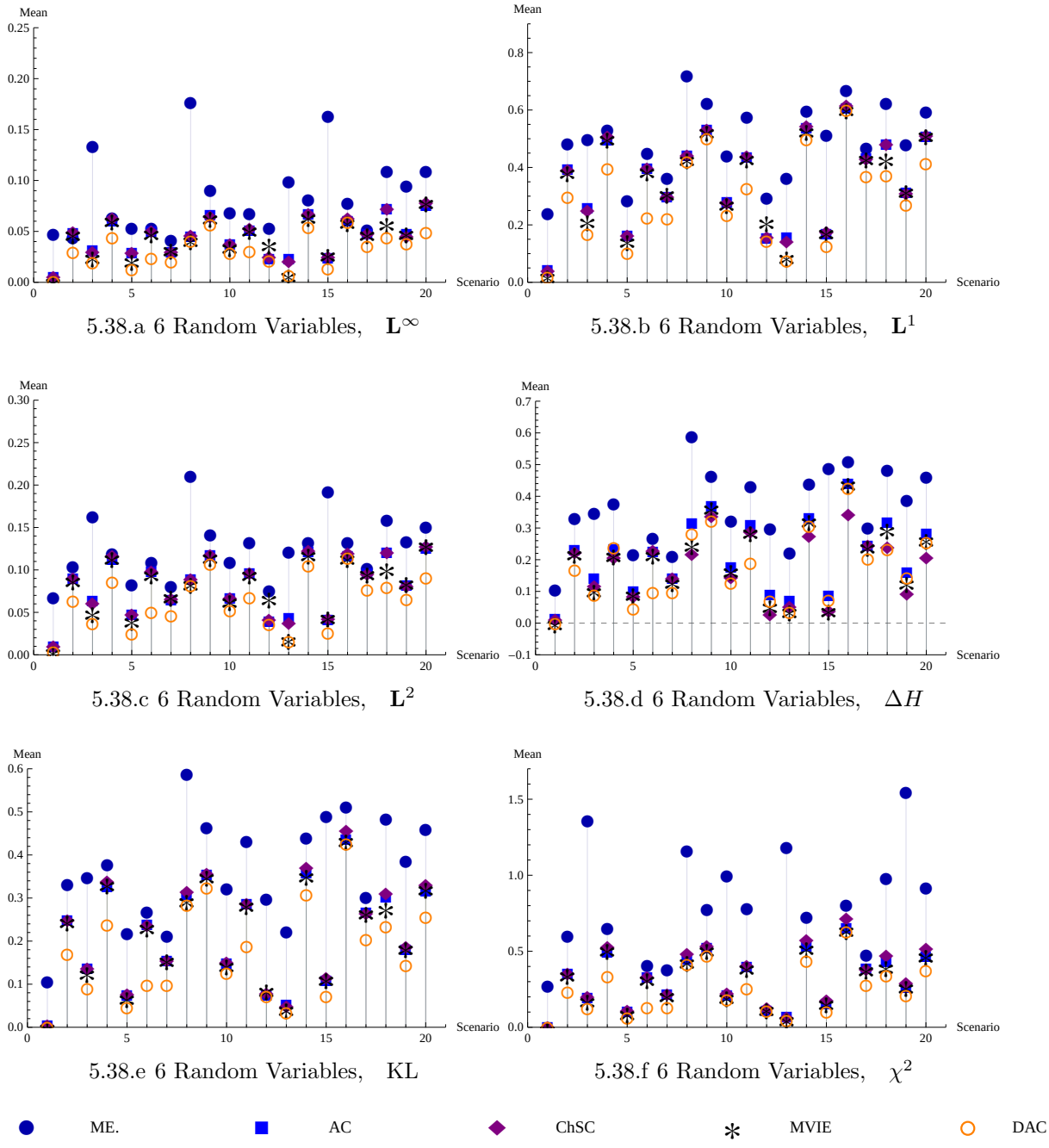

5.38.a 6 Random Variables, $\mathbf{L}^{\infty}$

5.38.b 6 Random Variables, $\mathbf{L}^{1}$

5.38.c 6 Random Variables, $\mathbf{L}^{2}$

5.38.d 6 Random Variables, ΔH

5.38.e 6 Random Variables, KL

5.38.f 6 Random Variables, χ^2

Figure 5.38: Mean estimates for accuracy measures for 20 realizations (scenarios along the x-axes) of truth sets with 6 binary random variables and marginal constraints.

Figures 5.35 through 5.38 are consistent with the results taken using symmetric constraints. As before, ME shows the worst accuracy under all measures considered, and DAC shows the greatest accuracy. This validates the explanation provided in Figure 5.23. However, it is surprising that as the dimension of $\mathbb{T}$ increases, the accuracy of ME worsens considerably. The explanation of this effect is given by the sea urchin effect described in Chapter 3: as the volume of $\mathbb{T}$ gets more concentrated, the approximations closer to the extreme points of $\mathbb{T}$ suffer a reduction in accuracy.

The results of the simulation show that AC and ChSC have accuracies close to each other, with slightly better accuracy for AC. However, there is no well-defined rule for the general case. A similar behavior can be observed for MVIE, which is more accurate than AC or ChSC for low-dimensions (3 binary random variables) but worsens as the dimension increases. A clear example of this can be observed in Figure 5.37 polytope 8, which shows that approximations that are typically accurate can occasionally be inaccurate.

In arbitrary polytopes, it is hard to draw inferences about the "why" of a particular behavior without considering a large number of instances (1000 polytopes). Therefore, we seek only to corroborate the findings from sets having symmetric constraints.

Percentage of Accuracy. In addition to the mean accuracy, the percentage of accuracy indicates which approximation provide the most accurate results a larger fraction of the times.

The accuracy comparisons between approximations are shown in Table 5.11, which shows the aggregated results for all polytopes of equal dimension. For low-dimensional polytopes, the most accurate approximation is DAC followed by MVIE. However as the dimension increases, MVIE decreases in accuracy. The accuracy of AC and ChSC increases with respect to MVIE as dimension increases. The accuracy of AC is somewhat better than that of ChSC, which can be observed in both the

table and figures of this section.

The most significant result can be observed in relation to ME, which has long been considered a good approximation. However, accuracy comparisons revealed ME to be the least accurate approximation for all measures in all dimensions. This reflects different philosophies toward treating unknown information. ME assumes the maximum possible independence wherever the actual dependence is unknown, whereas DAC allows for the unknown to remain hidden, providing an approximation that minimizes the Euclidean distance to all other possible approximations in the collection.

Table 5.11: Percentage accuracy comparisons for asymmetric sets with marginal information for random variables $V = 3, 4, 5$, and 6.

V	% Of times is better than	DAC MVIE	DAC AC	DAC ChSC	DAC ME	MVIE AC	MVIE ChSC	MVIE ME	AC ChSC	AC ME	ChSC ME
3	$\mathbf{L}^\infty$	51%	53%	56%	61%	52%	56%	62%	55%	64%	60%
	$\mathbf{L}^1$	51%	53%	56%	62%	52%	56%	62%	54%	65%	61%
	$\mathbf{L}^2$	51%	53%	56%	63%	52%	56%	63%	53%	66%	61%
	ΔH	30%	100%	30%	100%	95%	25%	100%	20%	100%	100%
	KL	51%	53%	56%	66%	52%	56%	66%	54%	69%	64%
	χ^2	51%	52%	57%	67%	51%	57%	66%	57%	70%	64%
4	$\mathbf{L}^\infty$	57%	56%	62%	71%	45%	57%	66%	60%	71%	68%
	$\mathbf{L}^1$	56%	57%	58%	76%	47%	51%	69%	52%	76%	73%
	$\mathbf{L}^2$	56%	56%	59%	75%	46%	52%	69%	55%	76%	72%
	ΔH	10%	90%	15%	100%	100%	30%	100%	15%	100%	100%
	KL	57%	57%	63%	81%	50%	57%	76%	60%	82%	76%
	χ^2	58%	56%	67%	82%	49%	61%	77%	65%	82%	74%
5	$\mathbf{L}^\infty$	77%	74%	75%	89%	45%	49%	76%	59%	81%	85%
	$\mathbf{L}^1$	76%	75%	76%	92%	41%	46%	82%	58%	87%	88%
	$\mathbf{L}^2$	76%	75%	77%	90%	42%	49%	79%	64%	83%	86%
	ΔH	60%	85%	65%	100%	90%	55%	100%	55%	100%	100%
	KL	77%	77%	81%	96%	43%	56%	89%	63%	91%	91%
	χ^2	77%	75%	82%	96%	44%	57%	91%	64%	91%	91%
6	$\mathbf{L}^\infty$	83%	81%	81%	94%	33%	33%	85%	52%	89%	87%
	$\mathbf{L}^1$	87%	84%	85%	97%	32%	30%	95%	51%	98%	97%
	$\mathbf{L}^2$	86%	83%	84%	96%	33%	30%	88%	54%	96%	95%
	ΔH	80%	85%	55%	100%	90%	25%	100%	5%	100%	100%
	KL	88%	87%	88%	99%	35%	44%	99%	65%	99%	98%
	χ^2	87%	85%	89%	99%	37%	58%	98%	74%	98%	97%

5.4.2 Arbitrarily Marginal Correlation Constraints

The previous arbitrarily marginal constrained polytopes are extended by adding arbitrary correlation constraints for 20 polytopes using 3, 4, 5, and 6 binary random variables, for a total of 80 polytopes. To the previous approximations, we add the UE and the IA.

Sampling Details. The constraints for these polytopes were selected by randomly choosing the marginal probabilities, which creates a polytope by itself, and selecting and arbitrary interior point. Then, by creating a random direction, an LP was solved to find the farthest extreme point in such direction, and a distribution was selected at random from the convex hull of the initial interior point and the extreme distribution. The correlation of these joint distributions varies from independence to heavily correlated. As before, we generate sample collections of 50,000, 100,000, 200,000, and 400,000 distributions for polytopes based on 3, 4, 5, and 6 binary random variables, respectively.

Results. For clearer presentation, the results are divided into two groups. The first group consists of UE, IA, ME, and DAC because their scale of accuracy is considerably larger. These results can be observed in Figure 5.39. The second group includes MVIE, AC, and ChSC and for reference also includes DAC and ME. These results can be observed in Figures 5.40, 5.41, 5.42, and 5.43.

The results of the first group indicates that the more information an approximation can process, the more accurate it will be. Then, the most accurate approximation is DAC, followed by ME, UE, and IA. However, there are scenarios for which the extra information can be misleading (as in Figure 5.39(x), polytope 20). This results of the first group and those in previous sections suggest that overall, DAC and ME are the most and second-most accurate distributions, respectively.

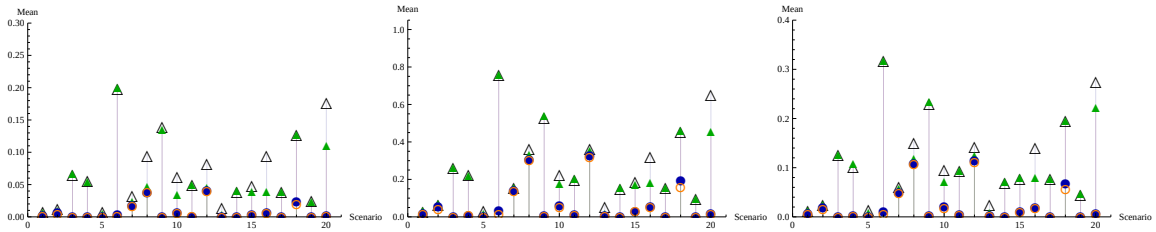

(i) $\mathbf{L}^{\infty}$, 3 Random Variables. (ii) $\mathbf{L}^{1}$, 3 Random Variables. (iii) $\mathbf{L}^{2}$, 3 Random Variables.

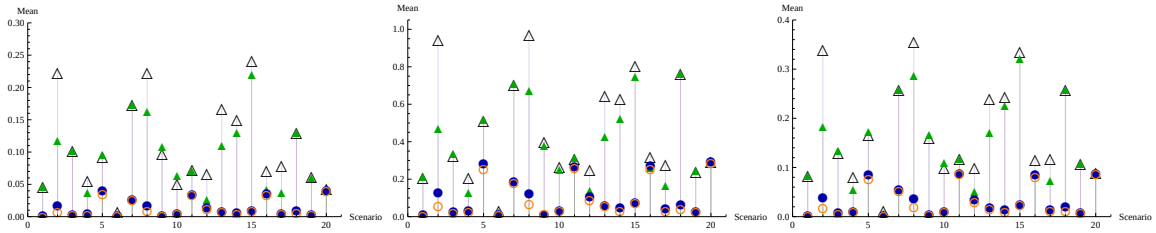

(iv) $\mathbf{L}^{\infty}$, 4 Random Variables. (v) $\mathbf{L}^{1}$, 4 Random Variables. (vi) $\mathbf{L}^{2}$, 4 Random Variables.

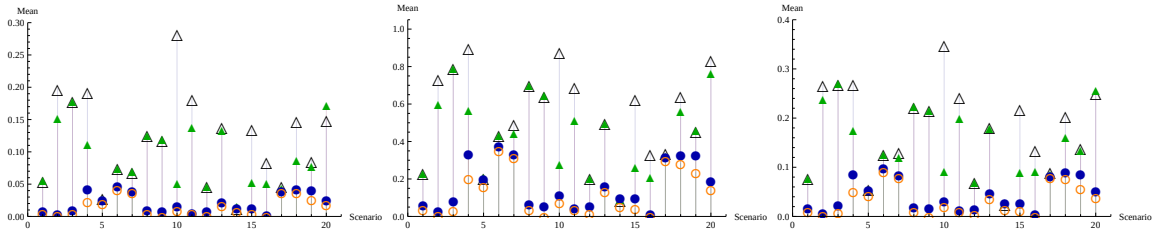

(vii) $\mathbf{L}^{\infty}$, 5 Random Variables. (viii) $\mathbf{L}^{1}$, 5 Random Variables. (ix) $\mathbf{L}^{2}$, 5 Random Variables.

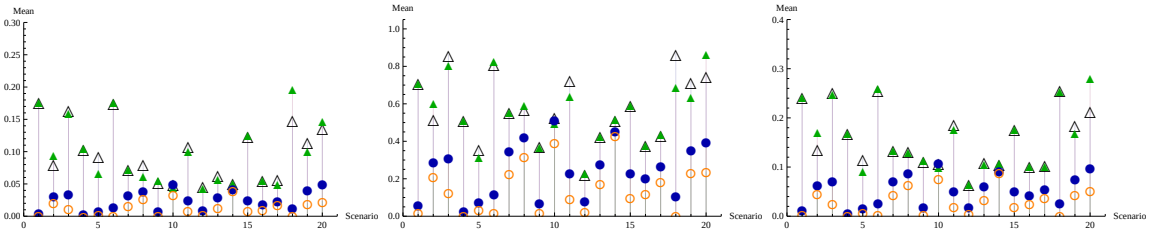

(x) $\mathbf{L}^{\infty}$, 6 Random Variables. (xi) $\mathbf{L}^{1}$, 6 Random Variables. (xii) $\mathbf{L}^{2}$, 6 Random Variables.

Figure 5.39: Mean estimates for accuracy measures for 20 realizations (scenarios along horizontal axes) of truth sets with 3, 4, 5, and 6 binary random variables (part one). Each polytope was created by choosing arbitrary marginal and rank correlation constraints.

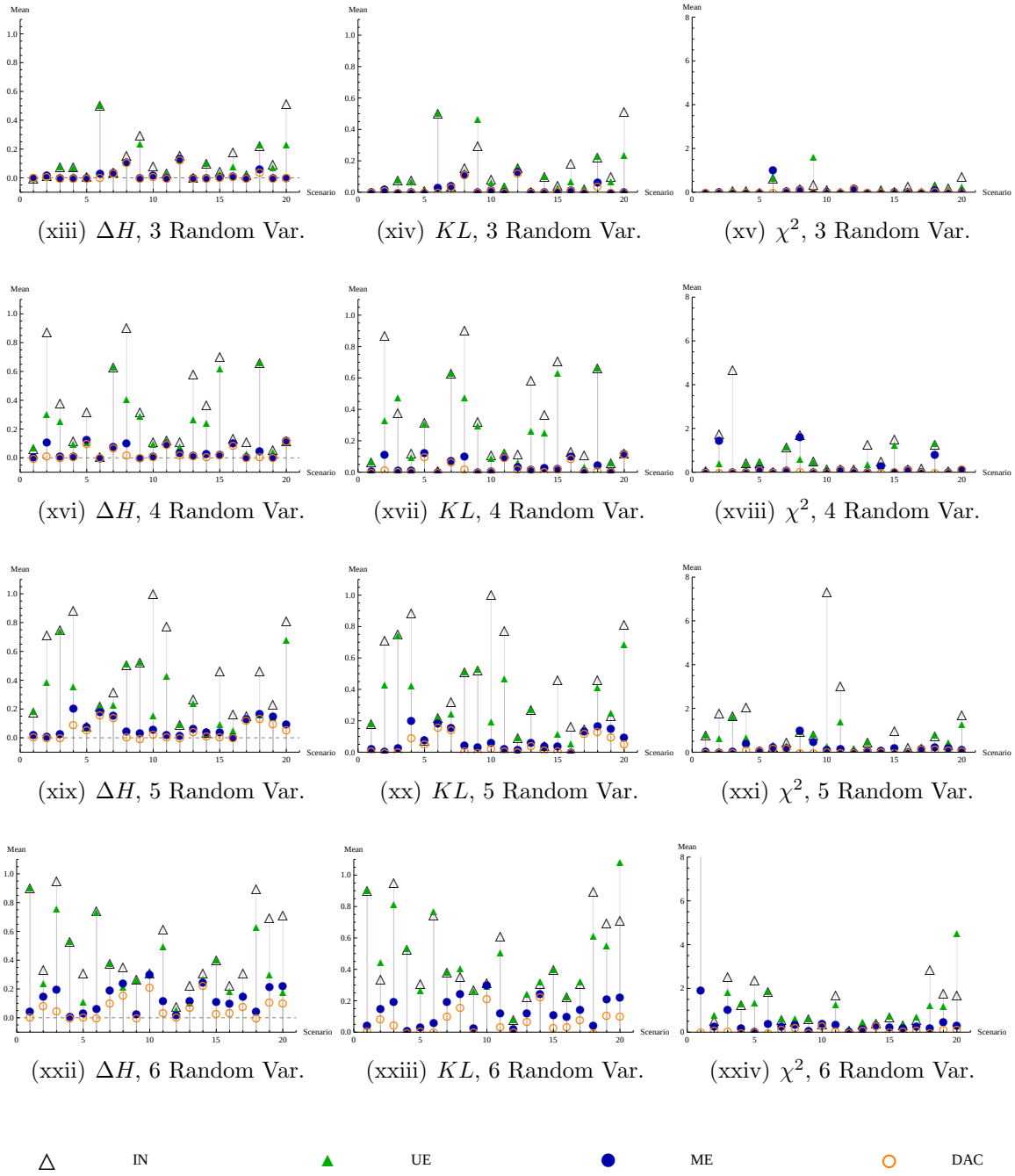

(xiii) ΔH, 3 Random Var. (xiv) KL, 3 Random Var. (xv) χ^2, 3 Random Var.

(xvi) ΔH, 4 Random Var. (xvii) KL, 4 Random Var. (xviii) χ^2, 4 Random Var.

(xix) ΔH, 5 Random Var. (xx) KL, 5 Random Var. (xxi) χ^2, 5 Random Var.

(xxii) ΔH, 6 Random Var. (xxiii) KL, 6 Random Var. (xxiv) χ^2, 6 Random Var.

Figure 5.39: Mean estimates for accuracy measures for 20 realizations (scenarios along horizontal axes) of truth sets with 3, 4, 5, and 6 binary random variables (part two). Each polytope was created by choosing arbitrary marginal and rank correlation constraints.

The results of the second group indicates that ME is the worst approximation, even though it is significantly improved by the addition of the rank correlation constraints. The random polytopes sampled in this section show that ME is close to all others for low-dimensional polytopes (3 random variables), but worsens faster than other approximations as the dimension increases.

MVIE, AC, and ChSC show similar behavior to the one described in the arbitrarily marginally constrained polytopes sub-section. MVIE shows the best accuracy after DAC but degrades as the dimension of the polytopes increases. AC and ChSC are less accurate but gain accuracy as the dimension increases. This behavior could be attributed to the geometric shape of $\mathbb{T}$, for as the dimension increases, the corners of the truth set lose volume exponentially. However such spaces still affect the shape of MVIE in $\mathbb{T}$, deforming the ellipsoid toward spaces that are hard to sample due to lack of volume. The results might also be related to the constraints and the sample size of the collection. Since the values for $\mathbf{b}$ ($\mathbf{Ap} = \mathbf{b}$) were chosen arbitrarily, some extreme values might be expected, which might subject the approximations to difficult and uncommon geometries. In addition, the sample size was set as standard for all polytopes, which might add noise to the results.

An important observation is the reduction of the measures of accuracy with respect to polytopes constrained only with marginal information. These polytopes have reduced dimensionality and altered shape of their n-content (relative volume) after the addition of the rank correlations for all pairs of variables. Additional information increase the accuracy, but the added benefit per constraint reduces dramatically.

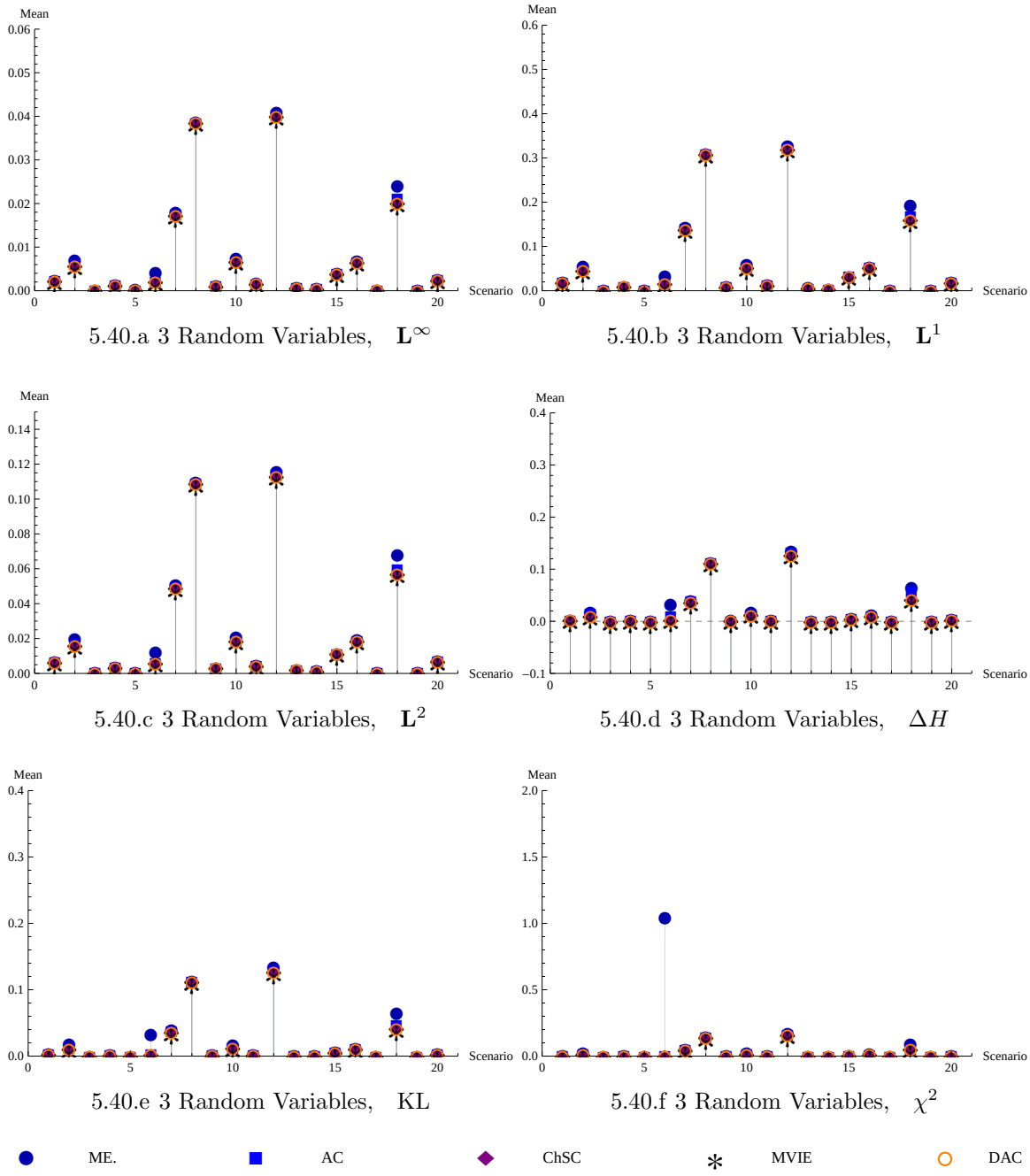

5.40.a 3 Random Variables, $\mathbf{L}^{\infty}$

5.40.b 3 Random Variables, $\mathbf{L}^{1}$

5.40.c 3 Random Variables, $\mathbf{L}^{2}$

5.40.d 3 Random Variables, ΔH

5.40.e 3 Random Variables, KL

5.40.f 3 Random Variables, χ^2

Figure 5.40: Mean estimates for accuracy measures for 20 realizations (scenarios along the x-axes) of truth sets with 3 binary random variables and marginal and correlation constraints.

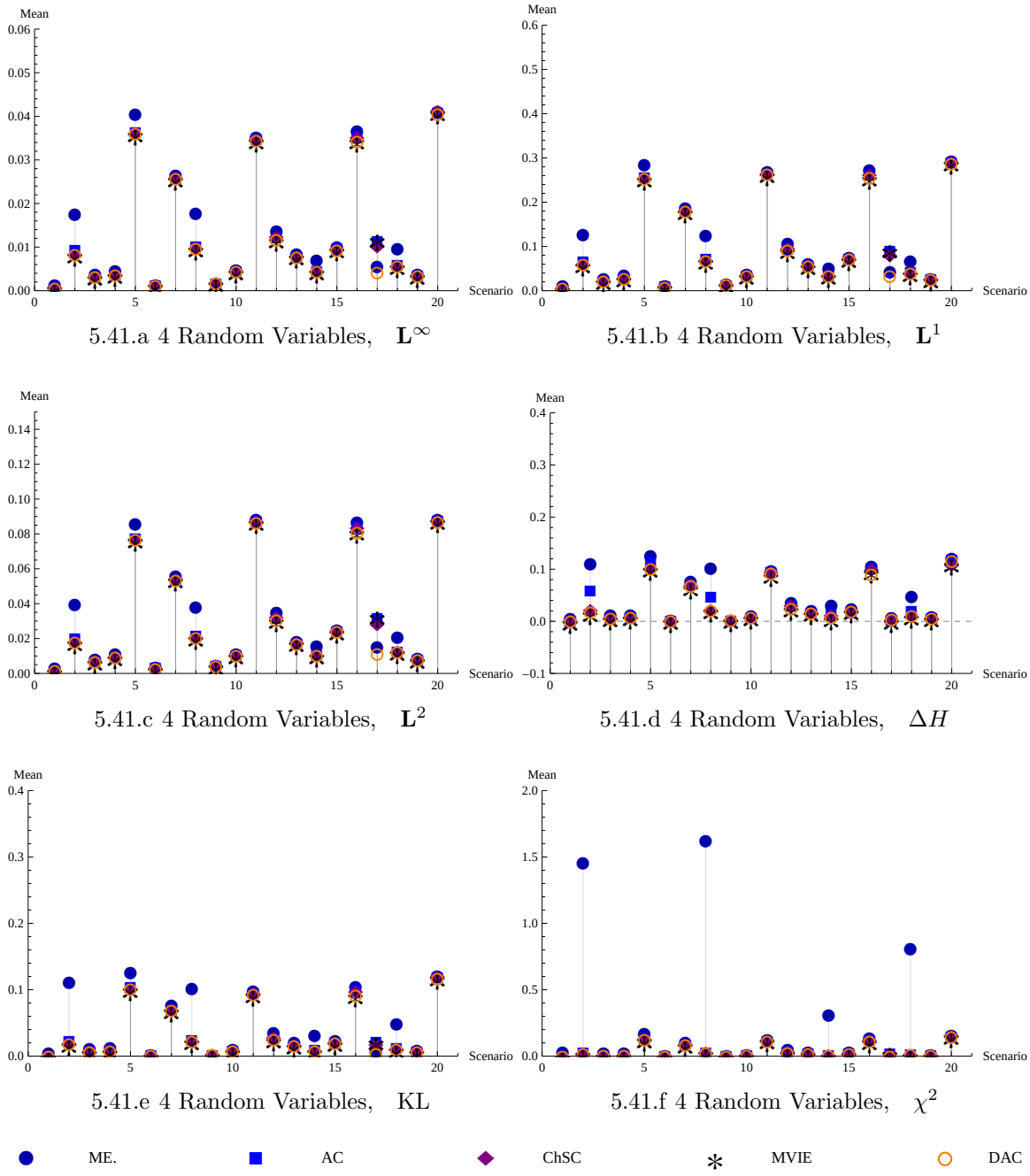

5.41.a 4 Random Variables, $\mathbf{L}^{\infty}$

5.41.b 4 Random Variables, $\mathbf{L}^{1}$

5.41.c 4 Random Variables, $\mathbf{L}^{2}$

5.41.d 4 Random Variables, ΔH

5.41.e 4 Random Variables, KL

5.41.f 4 Random Variables, χ^2

Figure 5.41: Mean estimates for accuracy measures for 20 realizations (scenarios along the x-axes) of truth sets with 4 binary random variables and marginal and correlation constraints.

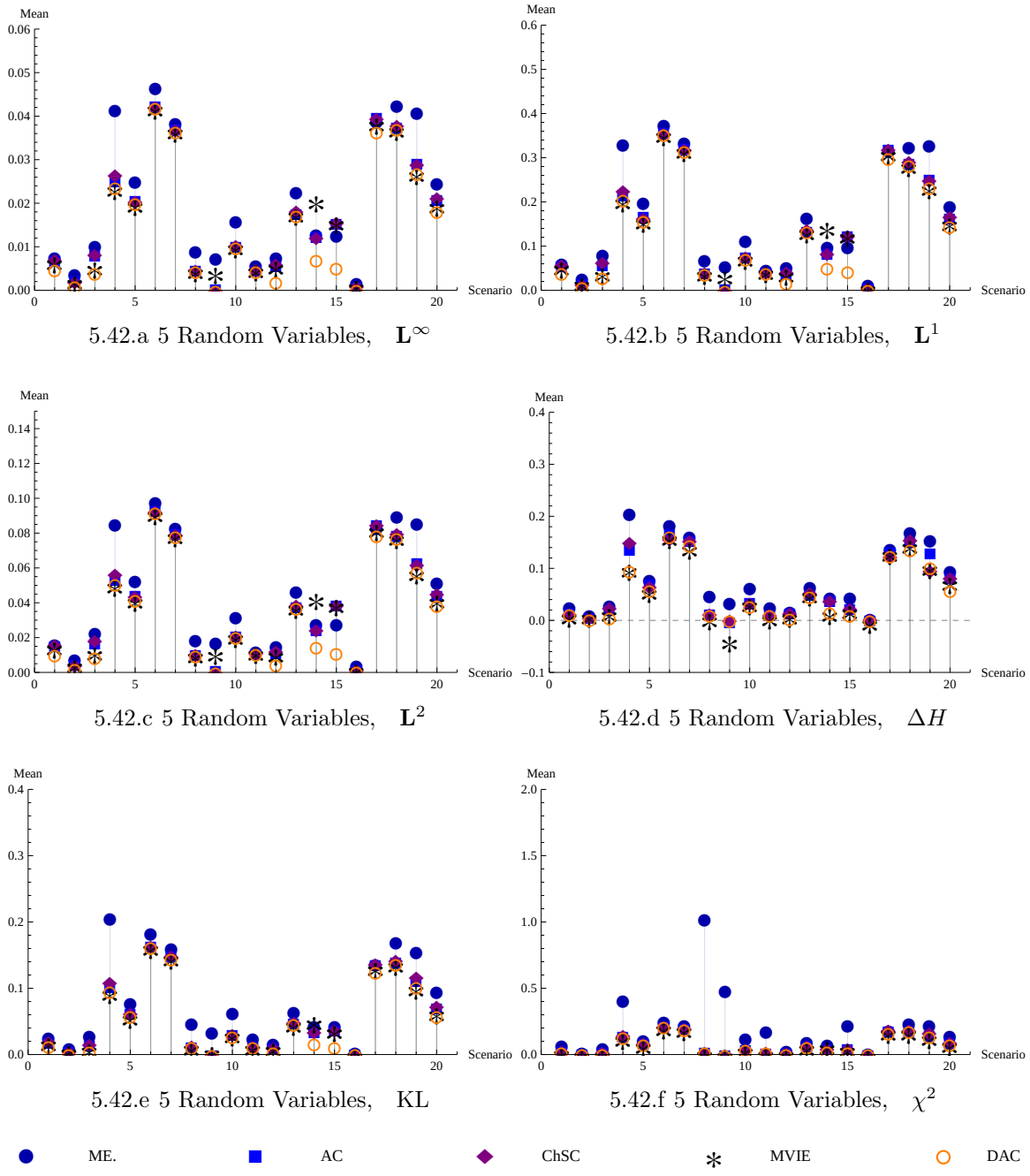

5.42.a 5 Random Variables, $\mathbf{L}^{\infty}$

5.42.b 5 Random Variables, $\mathbf{L}^{1}$

5.42.c 5 Random Variables, $\mathbf{L}^{2}$

5.42.d 5 Random Variables, ΔH

5.42.e 5 Random Variables, KL

5.42.f 5 Random Variables, χ^2

Figure 5.42: Mean estimates for accuracy measures for 20 realizations (scenarios along the x-axes) of truth sets with 5 binary random variables and marginal and correlation constraints.

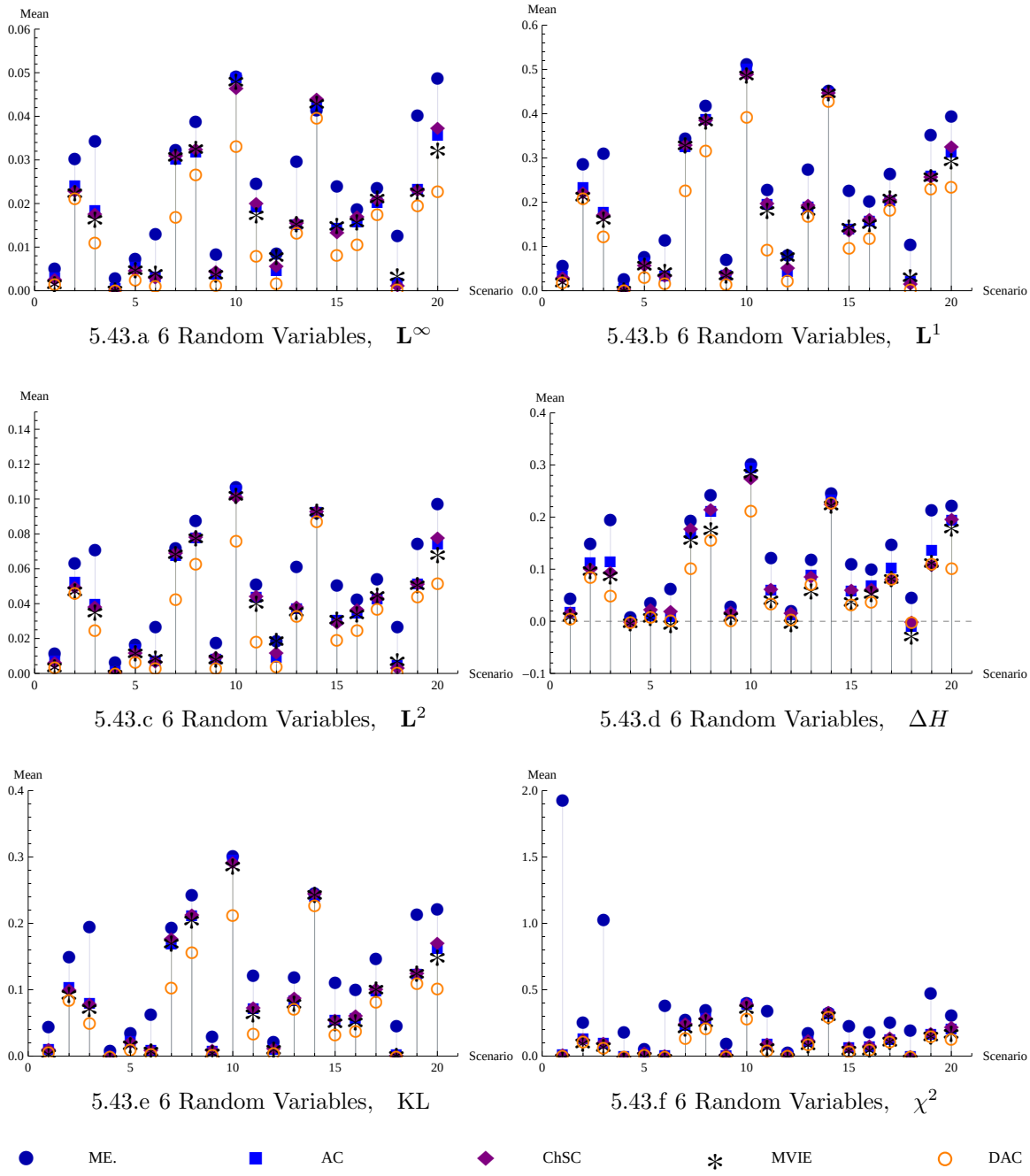

5.43.a 6 Random Variables, $\mathbf{L}^{\infty}$

5.43.b 6 Random Variables, $\mathbf{L}^{1}$

5.43.c 6 Random Variables, $\mathbf{L}^{2}$

5.43.d 6 Random Variables, ΔH

5.43.e 6 Random Variables, KL

5.43.f 6 Random Variables, χ^2

Figure 5.43: Mean estimates for accuracy measures for 20 realizations (scenarios along the x-axes) of truth sets with 6 binary random variables and marginal and correlation constraints.

Percentage of Accuracy. Tables 5.12 and 5.13 show the aggregated percentage of accuracy comparison per number of variables (3, 4, 5, 6) for all approximations considered. These results are strongly consistent with previous results confirming the effects of dimensionality on the approximations. DAC is clearly the best distribution approximation. MVIE, AC, and ChSC seem equivalent overall because the dimensionality can strongly affect their accuracy. The ME, UE, and IA are definitively less accurate than the above alternatives.

Table 5.12: Percentage of accuracy for asymmetric sets with marginal and correlation constraints for $V = 3, 4, 5$, and 6 random variables (part one).

V	% Times better than	DAC MVIE	DAC AC	DAC ChSC	DAC ME	DAC UE	DAC IN	MVIE AC	MVIE ChSC	MVIE ME	MVIE UE	MVIE IN
3	$\mathbf{L}^\infty$	50%	52%	50%	55%	90%	99%	52%	48%	55%	90%	99%
	$\mathbf{L}^1$	50%	52%	50%	55%	85%	93%	52%	50%	55%	85%	93%
	$\mathbf{L}^2$	50%	52%	50%	55%	86%	95%	52%	50%	55%	86%	94%
	ΔH	50%	70%	50%	100%	80%	100%	70%	15%	100%	80%	100%
	KL	50%	52%	50%	56%	85%	95%	52%	48%	56%	85%	95%
	χ^2	50%	52%	50%	56%	85%	95%	52%	49%	56%	85%	95%
4	$\mathbf{L}^\infty$	54%	56%	56%	65%	98%	99%	50%	50%	62%	98%	98%
	$\mathbf{L}^1$	54%	56%	55%	65%	94%	96%	51%	50%	61%	94%	95%
	$\mathbf{L}^2$	54%	56%	55%	65%	96%	97%	51%	50%	61%	96%	96%
	ΔH	35%	65%	60%	100%	100%	100%	60%	65%	95%	100%	100%
	KL	53%	57%	56%	72%	95%	97%	52%	51%	69%	96%	96%
	χ^2	54%	57%	57%	76%	96%	97%	52%	52%	72%	96%	96%
5	$\mathbf{L}^\infty$	73%	74%	75%	83%	97%	98%	41%	46%	70%	92%	93%
	$\mathbf{L}^1$	73%	74%	75%	83%	97%	97%	42%	46%	71%	91%	92%
	$\mathbf{L}^2$	73%	74%	76%	82%	97%	98%	43%	46%	70%	91%	92%
	ΔH	70%	90%	85%	100%	95%	100%	90%	75%	95%	95%	100%
	KL	74%	75%	77%	88%	98%	98%	41%	45%	81%	95%	95%
	χ^2	73%	74%	77%	90%	98%	98%	41%	48%	88%	98%	98%
6	$\mathbf{L}^\infty$	87%	85%	86%	94%	98%	99%	41%	38%	81%	96%	96%
	$\mathbf{L}^1$	87%	87%	87%	96%	99%	99%	38%	37%	87%	98%	99%
	$\mathbf{L}^2$	86%	86%	86%	95%	99%	99%	38%	36%	84%	97%	97%
	ΔH	80%	90%	85%	100%	95%	100%	90%	65%	100%	95%	100%
	KL	89%	90%	90%	96%	99%	99%	42%	45%	93%	99%	99%
	χ^2	88%	88%	90%	97%	99%	99%	39%	50%	93%	99%	99%

Table 5.13: Percentage of accuracy for asymmetric sets with marginal and correlation constraints for $V = 3, 4, 5$, and 6 random variables (part two).

V	% Times better than	AC ChSC	AC ME	AC UE	AC IN	ChSC ME	ChSC UE	ChSC IN	ME UE	ME IN	UE IN
3	$\mathbf{L}^\infty$	48%	55%	92%	100%	55%	90%	99%	89%	100%	87%
	$\mathbf{L}^1$	48%	55%	86%	94%	55%	85%	93%	83%	95%	65%
	$\mathbf{L}^2$	48%	55%	87%	96%	55%	86%	94%	83%	98%	57%
	ΔH	30%	100%	80%	100%	100%	80%	100%	75%	100%	90%
	KL	48%	55%	88%	97%	56%	85%	95%	82%	100%	79%
	χ^2	48%	55%	88%	98%	56%	85%	95%	82%	97%	80%
4	$\mathbf{L}^\infty$	45%	63%	96%	98%	61%	97%	98%	96%	98%	64%
	$\mathbf{L}^1$	44%	62%	94%	96%	62%	94%	96%	94%	97%	78%
	$\mathbf{L}^2$	44%	62%	95%	98%	61%	95%	98%	95%	98%	60%
	ΔH	35%	100%	100%	100%	100%	100%	100%	100%	100%	85%
	KL	44%	69%	96%	99%	68%	95%	98%	94%	100%	72%
	χ^2	46%	73%	97%	99%	72%	95%	98%	87%	95%	66%
5	$\mathbf{L}^\infty$	53%	76%	96%	96%	76%	96%	96%	95%	97%	55%
	$\mathbf{L}^1$	55%	78%	95%	95%	78%	95%	95%	91%	93%	64%
	$\mathbf{L}^2$	54%	76%	96%	96%	76%	95%	96%	93%	94%	60%
	ΔH	60%	100%	95%	100%	100%	95%	100%	95%	100%	80%
	KL	57%	88%	99%	99%	86%	99%	99%	99%	100%	72%
	χ^2	60%	92%	99%	99%	90%	98%	98%	96%	98%	70%
6	$\mathbf{L}^\infty$	50%	88%	96%	96%	87%	96%	96%	96%	96%	46%
	$\mathbf{L}^1$	46%	94%	99%	99%	94%	99%	99%	99%	100%	52%
	$\mathbf{L}^2$	47%	91%	97%	98%	91%	98%	99%	98%	98%	28%
	ΔH	55%	100%	95%	100%	100%	95%	100%	85%	100%	95%
	KL	54%	95%	99%	100%	94%	99%	99%	100%	100%	30%
	χ^2	64%	95%	99%	100%	94%	98%	99%	99%	100%	29%

5.4.3 Findings in Arbitrarily Constrained Truth Sets

Arbitrarily Marginal Constrained Truth Sets:

1. The most accurate approximation was DAC, followed by AC.
2. The third-most accurate approximation was MVIE. For low-dimensional sets, MVIE is nearly as accurate as DAC and AC. But as the dimension increases, the difference in accuracy becomes pronounced.
3. The worst approximation was ME.

Arbitrarily Marginal and Rank Correlation Constrained Truth Sets:

1. Approximations that can process larger amounts of information show better accuracy. Approximations such as UE and IA that can process only small amounts of information result in low accuracy approximations.
2. The most accurate approximation was DAC.
3. As dimension increases, MVIE and ME lose accuracy and AC and ChSC gain accuracy.
4. The least accurate approximations were IA, UE, and ME. Among these three, ME showed the best accuracy.

Chapter 6

A New Approach to Decision Analysis

Until now, we have being exploring the accuracy of a joint distribution approximation from the probability space. In this chapter we observe the accuracy of a joint distribution approximation from the decision space and its implications in DA. We present two decisions that needs to deal with probabilistic dependence and provide partial information about the uncertainties.

The first decision is an extension of Bickel et al. (2008). The paper presents a series of dynamic decisions in the oil industry to optimize the exploration of well-alternatives. The second decision is taken from Clemen (1996). This is a typical decision model and has being study in Clemen and Reilly (1999) and Reilly (2000) using different techniques.

6.1 Optimal Sequential Exploration

In this paper we are concern with decisions in which we lack complete information regarding the underlying joint probability distribution. In particular we analyze the optimal exploration strategy in a deep-water oil and gas exploration program when there is a limited amount of information. The problem was originally described in Bickel and Smith (2006), and was solved assuming the joint probability distribution match the maximum entropy distribution. We extend the analysis by considering

different joint approximation models and apply a new sensitivity analysis procedure as a significant extension to the original paper. This problem is of particular interest due to the complexity of the decision and the limited amount of information.

Although the lack of information could stem from an under specification of marginal distributions, we are primarily motivated by underspecification of the probabilistic dependence structure. Probabilistic dependencies are inherent to many decision environments, including medicine (Chessa et al., 1999), nuclear power (Cooke and Waij, 1986), environmental policy (Helton, 1993), financial engineering (Cherubini et al., 2004), critical infrastructure management (Min et al., 2007) and oil exploration (Bickel and Smith, 2006; Bickel et al., 2008). Failure to capture these relationships can have important and sometimes tragic consequences (Apostolakis and Kaplan, 1981; Smith et al., 1992). For example, the Space Shuttle Challenger accident was apparently caused, in part, by engineers' failure to understand the dependency between ambient temperature and o-ring resiliency (Presidential Commission on the Space Shuttle Challenger Accident, 1986). In finance, the multi-billion-dollar failure of Long-Term Capital Management stemmed from a failure to properly model complex dependencies between financial markets (Lowenstein, 2000).

Probabilistic dependence is often ignored because it complicates probability assessments (Lowell, 1994; Korsan, 1990). Winkler (1982) identified the assessment and modeling of probabilistic dependence as one of the most important research topics facing decision analysts. He suggested the development of sensitivity analyses that would identify key dependencies and decision-making methods that use less than full probabilistic information. Miller (1990) argued, "We need a way to assess and process dependent probabilities efficiently. If we can find generally applicable methods for doing so, we could make significant advances in our ability to analyze and model

complex decision problems." These critical challenges have gone largely unanswered.

In Bickel and Smith (2006) the author make use of the maximum entropy (maxent) method to generate a single joint distribution with the highest amount of uncertainty (highest entropy) selected from the set of all possible distributions that are consistent with the given information. Maxent was pioneered by Jaynes (1957, 1968), and further developed by Ireland and Kullback (1968), who were the first to approximate a discrete joint distribution given information on the lower-order component distributions. Lowell (1994) also used maxent to specify a joint distribution given lower order assessments (e.g., pairwise conditional assessments). More recently, Abbas (2006) and Bickel and Smith (2006) explored the use of maxent to facilitate the modeling of dependence.

In this paper, we go one step further and perform a new sensitivity analysis procedure that aloud us to describe the effects of unknown dependence structures in joint probability distributions. In particular, we create the set of all possible discrete distributions that are consistent with the available information. We then use a new simulation model described in Chapter 3 to uniformly sample from this set. Finally, we can evaluate our decision over a collection of joint distributions that represents a discrete version of the set of all possible joint distributions.

The literature presents other sensitivity procedures that have been developed to explore portions of the set of possible joint distributions. For example, Lowell (1994) developed a sensitivity analysis procedure to identify important pairwise conditional probability assessments. Clemen and Reilly (1999) proposed the use of a normal copula, characterized by pairwise correlation coefficients. They then perturbed the correlation matrix to explore a set of possible joint distributions. This set is restricted to joint distributions that can be modeled with a normal copula. Reilly

(2000) developed a sensitivity approach that uses synthetic variables based on a pairwise correlation coefficient matrix. However, our proposed approach is more robust in that it uniformly explores the complete space of possible joint distribution and can be subject to strict rules or constraints.

The new sensitivity analysis procedure can also be compared to robust procedures such as maximin or robust optimization (Ben-Tal et al., 2009) to evaluate decisions based on their worst possible outcomes. We do not directly address these methods. We note, however, that identifying the worst possible joint distribution is often difficult. Our procedure could be used in a robust setting to "stress test" decisions.

This paper is organized as follows: §6.1.1 we briefly describe the simulation procedure that serves as a basis for the rest of the analysis; §6.1.2 lay out the information available to the DM; §6.1.3 describe how the available information can be coded into a polytope; §6.1.4 test the sampled collection and present the accuracy measures to be used; §6.1.5 present the decision formulation of the sequential exploration problem; §6.1.6 show and analyze the results of the optimal sequential exploration problem. Finally, §6.1.7 conclude and discuss future research.

6.1.1 Joint Distributions Simulation Model

The joint distribution simulation approach (JDSIM) proposed in Chapter 3 samples from the set of all possible joint distributions that are consistent with the given information. In this way, it provides not one, but a collection of joint distributions under which the decision can be evaluated. The procedure begins with the specification of linear constraints on the joint distribution (e.g., specification of marginal probabilities or pairwise correlations) and the creation of a convex polytope

$\mathbb{T}$, the "truth set," that matches the given information. By "truth" we mean that any distribution within this set is consistent with the assessments and therefore could be the "true" joint distribution.

We generate a truth set using the notation described in Chapter 3 to define the following linear system:

$$\sum_{\omega_k \in \mathbb{U}} p_{\omega_k} = 1, \tag{6.1a}$$

$$\sum_{\omega_k \in \mathbb{U}_{\omega_r^{V_i}}} p_{\omega_k} = q_{\omega_r^{V_i}} \qquad \forall\ V_i \in \mathbb{V},\ \omega_r^{V_i} \in \mathbb{O}^{V_i}, \tag{6.1b}$$

$$\sum_{\omega_k \in \mathbb{U}_{\omega_s^{V_j} \omega_r^{V_i}}} p_{\omega_k} = q_{\omega_s^{V_j} \omega_r^{V_i}} \quad \forall\ V_i, V_j \in \mathbb{V},\ \omega_r^{V_i} \in \mathbb{O}^{V_i},\ \omega_s^{V_j} \in \mathbb{O}^{V_j}, \tag{6.1c}$$

$$p_{\omega_k} \geq 0, \qquad \forall \omega_k \in \mathbb{U}. \tag{6.1d}$$

This truth set is flexible and can integrate more or less information as needed. In this case of study we limit the information to marginal and pairwise assessments for which equations have being previously described (Chapter 3).

6.1.2 Optimal Sequential Exploration Information

In Bickel et al. (2008), the Author presents a practical and flexible framework for evaluating sequential exploration strategies where the exploration prospects are dependent. The paper was motivated by an oil exploration problem and presents a case where a field with six possible well locations needs to be developed. Each well location can be wet or dry, meaning there is an oil deposit or not. The probability of a well being wet is p_i. If a well is wet, the expected value of the success is s_i. However, if the well is dry, the expected value of failure is f_i.

We present a summary of the data in Table 6.1 from Bickel et al. (2008). This Table present expected values in millions of dollars and represent net present values (NPVs) in the period in which the well is drilled. The expected value given failure is the expected drilling cost. The expected value given success is the expected net present value of the hydrocarbon production stream less the drilling costs, costs of completion, production platforms, etc. These expectations take into account uncertainty in gas and/or oil prices, reserves, production, drilling costs, and all other uncertainties.

The intrinsic values shown in Table 6.1 are the unconditional expected values: $p_i s_i + (1 - p_i) f_i$. In this example, the intrinsic values are all negative, meaning the wells are "out of the money," and the company would not choose to drill them if they were considered in isolation. Additional to the marginal probabilities known for each well. Experts suspect that some of these wells could be connected through fractures. Therefore, the correlation of success among wells may be different from zero. Then, after assessing the marginal probabilities for each well, the expert assess the pairwise probabilities of success of well i given success of well j. The data is presented in Table 6.2 from Bickel et al. (2008).

Table 6.1: Example Well Data.

		Expected values		
Well	Probability of success	Given success (s_i)	Given failure (f_i)	Intrinsic value
1	0.35	60	-35	-1.75
2	0.49	15	-20	-2.85
3	0.53	30	-35	-0.55
4	0.83	5	-40	-2.65
5	0.33	40	-20	-0.20
6	0.18	80	-20	-2.00

Bickel et al. used the information in Table 6.2 to derive a joint probability approximation based on maxent to approximate the missing assessments. The maxent approximation seems to perform better than assuming independence or using the Underlying Event approximation. However, there was no conclusive evidence of the general performance of the approximation.

Table 6.2: Pairwise Information Data.

Direct conditional assessments $p(j \text{ wet } \vert i \text{ wet})$							Marginal p_i	Implied moment correlation matrix (ρ_{ij})					
$i \setminus j$	1	2	3	4	5	6		1	2	3	4	5	6
1		0.59	0.63	0.83	0.39	0.31	0.35		0.147	0.147	0	0.094	0.248
2			0.65	0.83	0.55	0.24	0.49			0.236	0	0.459	0.153
3				0.83	0.42	0.31	0.53				0	0.203	0.359
4					0.33	0.18	0.83					0	0
5						0.26	0.33						0.146
6							0.18						

6.1.3 Encoding The Information Constraints

After the information gathering, we needed to transform the partial information into a set of constraints that define the truth set. To do this, we first need to transform the conditional probabilities into pairwise joint probabilities, $p(j \text{ wet and } i \text{ wet}) = p(j \text{ wet } \vert i \text{ wet})p(i \text{ wet})$. Then, from Table 6.2 we generate Table 6.3.

Now we are ready to define the constrains of the truth set. Using the system of Equations 6.1 we can create a polytope $\mathbf{Ap} = \mathbf{b}$. Were $\mathbf{A}$ is a 22 by 64 matrix of zeros and ones that represent the 22 constraints of the 64 elements of the joint distribution. The vector $\mathbf{b} \in \mathbb{R}^{22}$ is the vector that encode the partial information (marginal and pairwise assessments). In this case, the first element forces the probabilities to

Table 6.3: Pairwise Information.

$p(j$ wet and i wet)						
$i \setminus j$	1	2	3	4	5	6
1		0.2065	0.2205	0.2905	0.1365	0.1085
2			0.3185	0.4067	0.2695	0.1176
3				0.4399	0.2226	0.1643
4					0.2739	0.1494
5						0.0858
6						

sum to one, the next six elements force the joint distribution to match the marginal information and the last 15 elements match the elements in Table 6.3.

We define the truth set $\mathbb{T} \equiv \{\mathbf{p} \mid \mathbf{Ap} = \mathbf{b},\ \mathbf{p} \geq 0\}$. Where the Matrix $\mathbf{A}$ and the vector $\mathbf{b}$ are described as follows:

$$\mathbf{A} = \left|\begin{array}{ccccccc

6.1.4 Sampling From $\mathbb{T}$

We generate a collection of 4 million samples. The collection meet the fair convergence requirements presented in Chapter 3. That is to say, the dynamic average center (DAC) converges to a stationary point in the interior of $\mathbb{T}$. The collection took 4 hours of processing time in an Intel(R) Core(TM)2 Quad CPU Q6700 @ 2.66GHz with 4GB of RAM. The process was run in Mathematica 8.0.

The collection of joint distributions generated by the HR consist of vectors in $\mathbb{R}^{64}$ located in a 42 dimensional subspace, making it difficult to observe. Hence, we use different mappings $\mathbb{R}^{64} \to \mathbb{R}$ (Equations 6.2) to understand how the sample path is behaving. In this paper we observe four of such mappings: The maximum absolute differences (L^∞ norm), the Euclidean distance (L^2 norm), the Kullback-Leibler divergence (KL) and entropy (H). The first three mappings are measured with respect to DAC which denotes the center of the collection sampled and converges to the center of $\mathbb{T}$, while the last mapping is relative to the uncertainty described by each distribution.

$$\mathbf{L}_n^\infty(\mathbf{p}, \mathbf{p}^{DAC}) = \max\{|p_1 - p_1^{DAC}|, \cdots, |p_n - p_n^{DAC}|\}, \tag{6.2a}$$

$$\mathbf{L}_n^2(\mathbf{p}, \mathbf{p}^{DAC}) = \left[\sum_{i=1}^{n}(p_i - p_i^{DAC})^2\right]^{\frac{1}{2}}, \tag{6.2b}$$

$$\mathbf{KL}_n(\mathbf{p}||\mathbf{p}^{DAC}) = \sum_{i=1}^{n} p_i \log\left(\frac{p_i}{p_i^{DAC}}\right), \tag{6.2c}$$

$$\mathbf{H}_n(\mathbf{p}) = \sum_{i=1}^{n} p_i \log p_i. \tag{6.2d}$$

The four different mappings provide one dimensional descriptions of a multidimensional topography as follows. L^∞ norm (6.2a) describes an upper bound for how far two corresponding elements of two different distributions can be. In specific, it

describes how far an element of a joint distribution can be from the corresponding element at the center of $\mathbb{T}$ (DAC). L^2 norm (6.2b) describes the direct distance between the DAC and the sampled distributions. KL (6.2c) measures the relative entropy between DAC and the distributions in the sample, the measure is always positive and is zero if and only if both distributions are identical. KL is not a distance measure but rather a measure of directed divergence between two distributions, since it does not follow the triangle inequality. KL divergence can be interpreted as the increase in the amount of information introduced by assuming DAC as the truth distribution when it is not (i.e. when DAC is used to determine the outcome of a random variable generated by a sampled distribution other than DAC). Finally, H (6.2d) describes the level of uncertainty encoded in the dependence structure of each joint.

Figures 5.1 and 5.6 show the results for the sampled collection. The dotted lines present the minimum and maximum sampled values, i.e the maximum and minimum values taken from a sampled distribution to DAC. In Figures 6.1(a), 6.1(b) and 6.2(a) a thick line shows the value of ME with respect to DAC, while in Figure 6.2(b) a dashed and a thick-dashed line shows the entropy value of ME and DAC respectively.

Figures 6.1(a) and 6.1(b) show the geometric position of the sampled distributions with respect to the center. The mean Euclidean distance from DAC to any sampled approximation is 0.069 while the mean of the maximum absolute difference is 0.029. Notice that for $\mathbf{L}^\infty$ and $\mathbf{L}^2$, ME has a value approximately equal or less than the respective mean values. In other words, ME is closer to the center of $\mathbb{T}$ than 50% of the sampled joint distributions. However, it is not the closest joint distribution to the center of the truth set.

Figure 6.2(a) shows that DAC and ME have a closer dependence structure than the average sample, but still we were able to sample distributions with smaller KL values than ME, and therefore, with closer probability dependence structure to DAC.

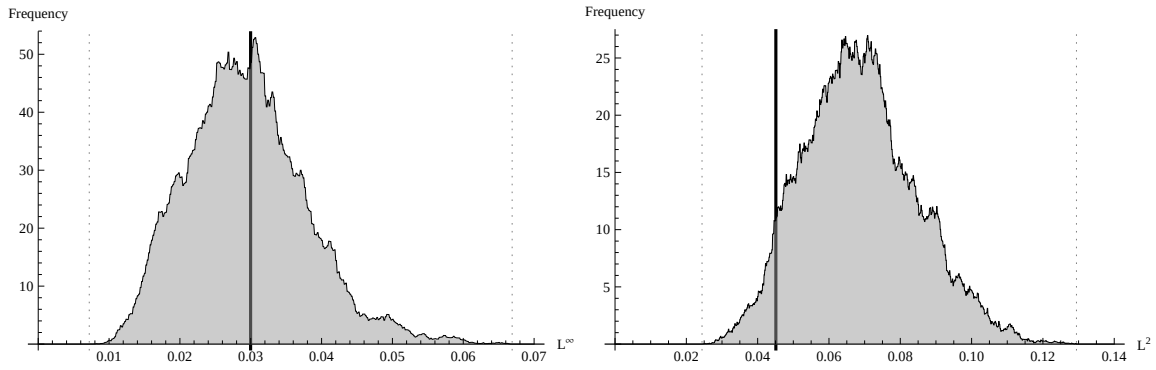

(a) Maximum absolute distance. (b) Euclidean distance.

Figure 6.1: Visualization of the truth set using geometric measures.

This is reflected in Figure 6.2(b), where the maximum entropy is 4.8, the entropy of DAC is 4.75 and the maximum entropy sampled is 4.73.

The collection of distributions generated shows that although ME is a good alternative for a true joint distribution, there might be other alternatives that better represents the space of possible distributions.

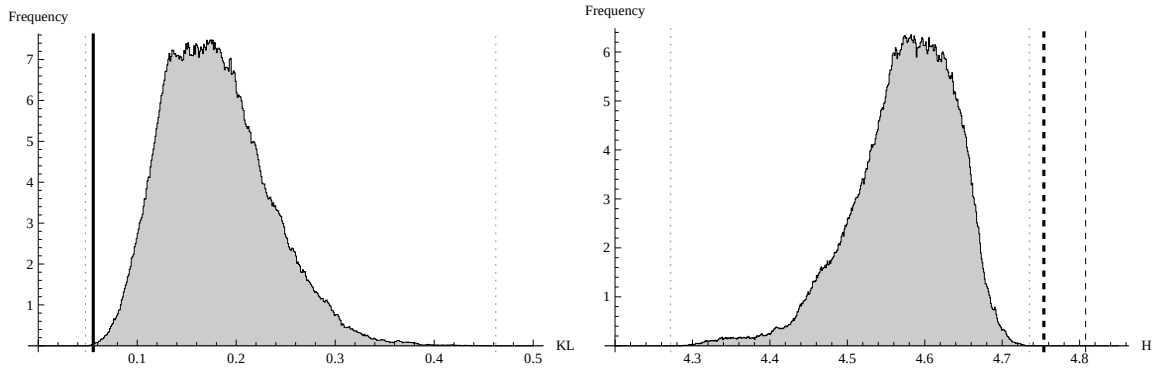

(a) Kullback-Leibler divergence. (b) Entropy.

Figure 6.2: Visualization of the truth set using information measures.

6.1.5 Decision Formulation

The structure of the decision is as follows: We need to decide which well, if any, to drill first; if that well is wet (or dry), which well do we drill next, and so on, through the n stages. A partial decision tree for this problem is shown in Figure 6.3. Although the tree is easy to interpret, it becomes quite complex even with a moderate number of wells. In our case of study, six wells leads to a total of 46,080 possible realizations. Such a tree is large but could be handled through programming. (Mathematica 8.0).

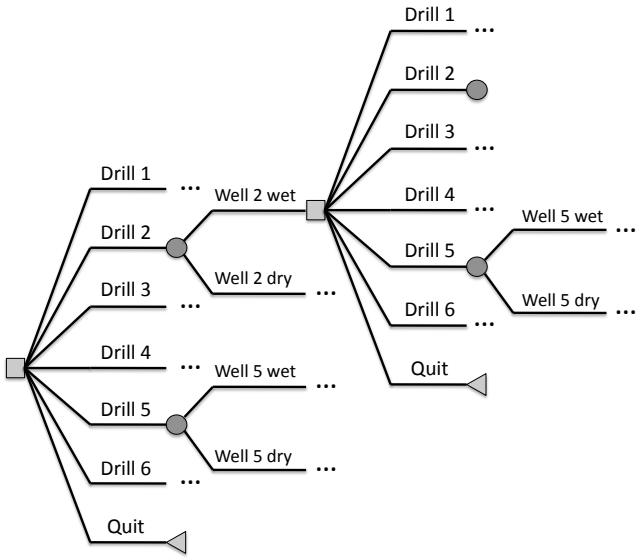

Figure 6.3: A Partial Decision Tree for the Sequential Drilling Problem

We solve the tree using typical methods in dynamic programing. Starting with the last decision, we evaluate whether you should drill the "last" well conditional on the outcomes of the first $n-1$ wells. We then decide which well to drill if we had two wells remaining. And so on to the initial decision. We describe the solution procedure following the notation used in Bickel et al. (2008). Then, let $\mathbf{w} = (\omega_1,\ \omega_2,\ \omega_3,\ \omega_4,\ \omega_5,\ \omega_6)$ denote the state where ω_i =0 or 1 if the well is dry or wet and equal to ω_i ="$*$" if the well has not been drilled. At the initial state

we have $\mathbf{w} = (*,\ *,\ *,\ *,\ *,\ *)$, which means no well has being drilled. The vector $\mathbf{w} = (0,\ *,\ 1,\ *,\ *,\ *)$ represents the state in which well 1 was dry and well 3 was wet and the other wells have not yet been drilled.

Given the joint probability distribution π over well outcomes, it is straight forward to calculate the transition probabilities required for the dynamic programming model. First, let $\mu(\mathbf{w})$ be the total probability associated with the vector $\mathbf{w}$, constructed by summing $\pi(\mathbf{w})$ over the possible scenarios for these unknown events. Then for $\mathbf{w} = (0,\ *,\ 1,\ *,\ *,\ *)$ we have:

$$\mu(\mathbf{w}) = \sum_{\omega_2,\ \omega_4,\ \omega_5,\ \omega_6} \pi(0,\ *,\ 1,\ *,\ *,\ *). \tag{6.3}$$

We can use the total probability function to calculate the transition probabilities required for the dynamic programming model. Suppose that you start in a state $\mathbf{w}$, where well i has not been drilled (thus $\omega_i = *$). If you drill well i, the probability that it is wet is $\mu(\mathbf{w}_i^1)/\mu(\mathbf{w})$, where $\mathbf{w}_i^1$ is identical to $\mathbf{w}$ except $\omega_i = 1$ and the probability that it is dry is $\mu(\mathbf{w}_i^0)/\mu(\mathbf{w})$ where $\mathbf{w}_i^0$ is identical to $\mathbf{w}$ except $\omega_i = 0$.

The dynamic programming model can now be formalized as follows. Let $v(\mathbf{w})$ denote the continuation value for state $\mathbf{w}$, that is, the expected NPV of future cash flows given that you start in state $\mathbf{w}$. In this value calculation, we include the expected future value for a successful well (s_i) or a failed well (f_i) in the period the well is drilled and discount cash flows using a discount factor δ that corresponds to the time required to drill the well. Recall, that s_i is the discounted expected net present value of production, in the period the well is drilled, from a successful well i (including drilling costs), and (f_i) is the expected cost of drilling an unsuccessful well i. If all the wells have been drilled (i.e., $\mathbf{w}$ is a vector of zeros and ones), then $v(\mathbf{w}) = 0$. For

earlier states $\mathbf{w}$, the expected NPV associated with drilling well i is:

$$v_i(\mathbf{w}) = \frac{\mu(\mathbf{w}_i^1)}{\mu(\mathbf{w})}(s_i + \delta v(\mathbf{w}_i^1)) + \frac{\mu(\mathbf{w}_i^0)}{\mu(\mathbf{w})}(f_i + \delta v(\mathbf{w}_i^0)), \tag{6.4}$$

The optimal action in state $\mathbf{w}$ is to drill the well with the largest $v(\mathbf{w})$ or, if no well has a positive value, to not drill at all. The optimal continuation value $v(\mathbf{w})$ is $\max[v_i(\mathbf{w}), 0]$, where the maximum is taken over all available wells and not drilling (0). There is no circularity in this definition of the value function because one never visits the same state twice; each time you drill a well, its state changes to either wet or dry.

6.1.6 Optimal Strategies

The optimal strategy describes a drilling policy that indicates wether to drill or not depending on the state of the previously drilled wells. In our case we can define an optimal strategy for each joint distribution approximation. In this paper we consider the independence approximation (IA) which is of common use in practice, the underling event (UE) approximation (Keefer, 2004) and the maximum entropy approximation as done in Bickel and Smith (2006). Additionally, we consider the AC, the CHSC, the MVIEC and the DAC approximations and compare the results to previous approximations.

Figure 6.4 present the optimal strategies for all the joint distribution approximations considered. These strategies are described as decision trees and must be read sequentially from left to right. For example, in Figure 6.4(a) the strategy indicates to start drilling well 3, and if the well is wet (Up), then we should drill well 6, otherwise we stop drilling more wells. In the same lines, if well 6 is wet, then we drill well 1, otherwise if well 6 is dry, we drill well 2. Additionally, the strategies in Figure 6.4 describe the net present values at each stage of the decision. i.e. the expected value

of each decision at the moment of choosing to drill or not.

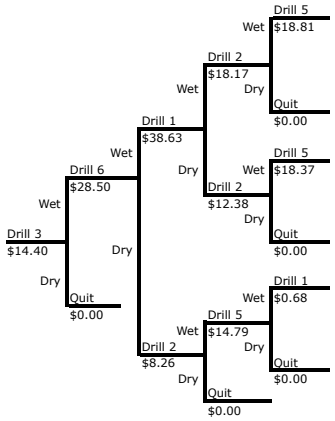

(a) ME strategy.

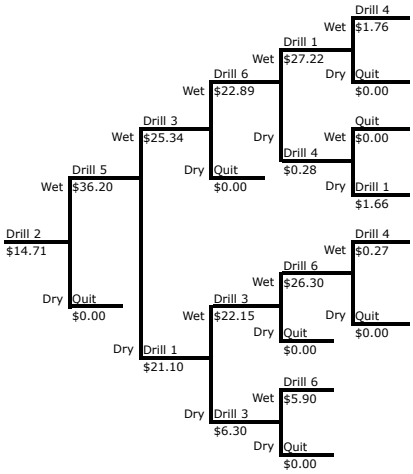

(b) DAC strategy.

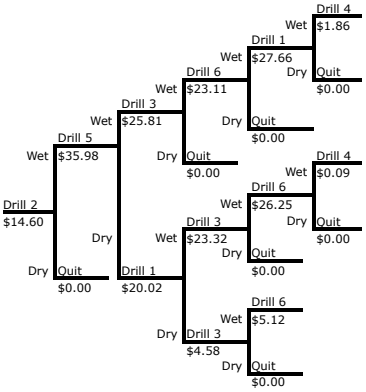

(c) AC strategy.

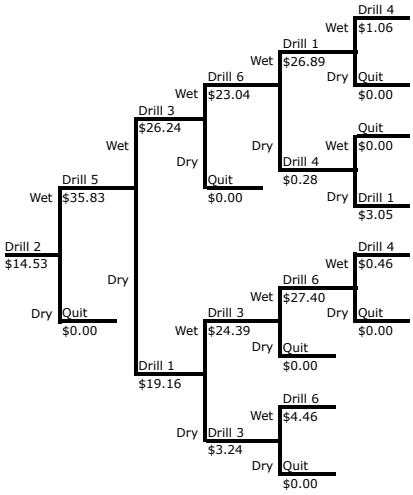

(d) ChSC strategy.

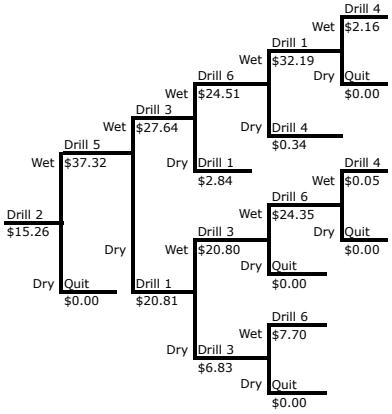

(e) MVIE strategy.

Figure 6.4: Strategies derived from approximation joint distributions.

The IA and the UE strategies have been omitted from Figure 6.4, since both

strategies are the same and present a trivial policy (never drill). As recall from Table 6.1, the expected value of each well independently is negative. Therefore, without any probabilistic dependence, the complete strategy is the same than the strategy for each particular well. The complete joint probability distribution approximations are presented in Table 6.4 including the IA/UE approximation.

The ME strategy (Figure 6.4(a)) was previously explore by Bickel and Smith. This strategy exploit the fact that the ME approximation assumes that all higher order assessments (three wise, four wise,...) are as close to independent as is aloud by the consistency of the joint distribution. For example, the pairwise assessments including well 4 show that this well is pairwise independent with respect to all others. Moreover, the ME approximation assumes that all higher order assessments are as close to independent as possible. Then, under ME, well 4 is independent and has negative expected value. The assumptions made by the ME approximation excludes well 4 as a viable drilling alternative.

The strategy presented by DAC (Figure 6.4(b)) search for a distribution that is the most conservative representation of the truth set. The DAC approximation does not care about independence among wells, but cares about to find the closest approximation to the center of mass of $\mathbb{T}$. One of the main differences is that the higher order assessments are not as close as independence as ME assumes. For example, the DAC strategy still considers well 4 to be pairwise independent, however, the well is not independent of all others. This strategy considers that under some scenarios well 4 can bring extra revenue.

The AC and the ChSC approximations attempt to find a joint distribution where each element is as far as possible from zero. In the case of AC, a log-barrier function is used to move the approximation far from the boundary, in the case of ChSC this same idea is done by means of expanding a hypersphere with center in $\mathbb{T}$. As with the DAC approximation, the AC and the ChSC attempt to find a point

Table 6.4: Joint Probability Distribution Approximations.

	IA/UE	ME	DAC	AC	ChSC	MVIE
1	0.00448	0.03825	0.03957	0.03799	0.03740	0.04059
2	0.02041	0.03720	0.02523	0.03198	0.03371	0.02606
3	0.00910	0.02089	0.02507	0.02587	0.02650	0.02455
4	0.04145	0.02713	0.02947	0.02727	0.02698	0.02868
5	0.00092	0.00783	0.00280	0.00285	0.00359	0.00273
6	0.00418	0.00762	0.00510	0.00511	0.00560	0.00469
7	0.00186	0.00428	0.00298	0.00317	0.00298	0.00303
8	0.00849	0.00556	0.00610	0.00654	0.00601	0.00597
9	0.00397	0.00192	0.00113	0.00116	0.00098	0.00115
10	0.01810	0.02053	0.02647	0.02358	0.02252	0.02619
11	0.00807	0.00167	0.00115	0.00116	0.00098	0.00115
12	0.03676	0.02379	0.02785	0.02645	0.02653	0.02887
13	0.00081	0.00039	0.00086	0.00085	0.00098	0.00086
14	0.00371	0.00421	0.00527	0.00496	0.00481	0.00487
15	0.00165	0.00034	0.00089	0.00088	0.00098	0.00089
16	0.00753	0.00487	0.00655	0.00671	0.00594	0.00624
17	0.00466	0.00441	0.00645	0.00571	0.00498	0.00637
18	0.02125	0.00515	0.00674	0.00615	0.00551	0.00612
19	0.00947	0.01952	0.01864	0.01988	0.01970	0.01789
20	0.04314	0.03045	0.03614	0.03239	0.03246	0.03718
21	0.00096	0.00090	0.00212	0.00204	0.00252	0.00216
22	0.00435	0.00105	0.00330	0.00315	0.00304	0.00334
23	0.00194	0.00400	0.00305	0.00315	0.00298	0.00330
24	0.00884	0.00624	0.00774	0.00728	0.00655	0.00785
25	0.00414	0.00042	0.00099	0.00100	0.00098	0.00100
26	0.01884	0.00540	0.00622	0.00605	0.00563	0.00614
27	0.00840	0.00297	0.00112	0.00116	0.00098	0.00115
28	0.03826	0.05078	0.03825	0.04271	0.04465	0.03743
29	0.00085	0.00009	0.00079	0.00076	0.00098	0.00079
30	0.00386	0.00111	0.00345	0.00318	0.00328	0.00345
31	0.00172	0.00061	0.00089	0.00089	0.00098	0.00091
32	0.00784	0.01040	0.00761	0.00801	0.00829	0.00843
33	0.00832	0.02075	0.01677	0.01908	0.01968	0.01626
34	0.03791	0.06186	0.08568	0.07744	0.07665	0.08498
35	0.01690	0.01170	0.01572	0.01387	0.01407	0.01590
36	0.07698	0.04657	0.03679	0.03892	0.03624	0.03634
37	0.00170	0.00425	0.00306	0.00319	0.00295	0.00306
38	0.00777	0.01267	0.00763	0.00885	0.00838	0.00814
39	0.00346	0.00240	0.00355	0.00351	0.00258	0.00343
40	0.01577	0.00954	0.01299	0.01288	0.01519	0.01410
41	0.00738	0.00128	0.00111	0.00113	0.00098	0.00111
42	0.03362	0.04189	0.03895	0.04205	0.04299	0.03945
43	0.01498	0.00115	0.00111	0.00112	0.00098	0.00111
44	0.06826	0.05011	0.03463	0.03764	0.03951	0.03433
45	0.00151	0.00026	0.00091	0.00088	0.00098	0.00089
46	0.00689	0.00858	0.00897	0.00842	0.00731	0.00849
47	0.00307	0.00023	0.00092	0.00091	0.00098	0.00092
48	0.01398	0.01026	0.01473	0.01362	0.01404	0.01500
49	0.00866	0.00374	0.00511	0.00515	0.00455	0.00480
50	0.03946	0.01340	0.00640	0.00729	0.00777	0.00637
51	0.01759	0.01710	0.01340	0.01303	0.01467	0.01435
52	0.08012	0.08177	0.07273	0.07789	0.07904	0.07348
53	0.00177	0.00077	0.00234	0.00225	0.00228	0.00229
54	0.00808	0.00274	0.00431	0.00439	0.00401	0.00466
55	0.00360	0.00350	0.00368	0.00358	0.00287	0.00361
56	0.01641	0.01675	0.01935	0.01818	0.01858	0.01774
57	0.00768	0.00044	0.00097	0.00098	0.00098	0.00096
58	0.03499	0.01725	0.00611	0.00717	0.00860	0.00637
59	0.01560	0.00319	0.00110	0.00112	0.00098	0.00109
60	0.07105	0.16731	0.20293	0.19562	0.19182	0.20262
61	0.00157	0.00009	0.00082	0.00079	0.00098	0.00081
62	0.00717	0.00353	0.00438	0.00445	0.00443	0.00488
63	0.00319	0.00065	0.00094	0.00092	0.00098	0.00093
64	0.01455	0.03427	0.02193	0.02370	0.02396	0.02155

in the center of the truth set that provide a robust (conservative) approximation, however, AC and ChSC have the advantage that are invariant with respect to the collection sampled from $\mathbb{T}$. That is to say, both approximations can be calculated without running a JDSIM procedure.

Finally, the MVIEC approximate the center of $\mathbb{T}$ by assuming it is close to the center of the ellipsoid with the largest volume inscribed in the truth set. This approximation is also invariant to the collection sampled, but it is computing intensive do to the number of variables required to calculate the shape of the hyper ellipse. Empirical observations suggest that the MVIEC and the DAC are close to each other, which explains why both strategies have a similar policy. However, this is just a conjecture for which no analytic results are known.

6.1.6.1 Accuracy of the Joint Distribution Approximations

Each of the strategies consider so far is directly link to an approximation. The question now is: How accurate are the approximations with respect to the possible distributions in $\mathbb{T}$? We answer this question using the JDSIM method described in Chapter 3.

In Bickel and Smith (2006) the authors propose a method to evaluate the accuracy of the approximations using a simulation procedure proposed by Keefer (2004). However, such simulation procedure is hard to control and can not be applied to constrained sets. As a result, the accuracy results provided by Bickel and Smith (2006) are taken over 5,000 arbitrary polytopes (truth sets), and in each set they test each approximation against one point in the set (the sampled distribution). Our approach differs in that we only sample distributions from one set defined by the assessed beliefs ($\mathbb{T}$). However, we sample 4 million distributions to fully explore the truth set and make a clear statement about the joint distribution approximations and its accuracy. Recall that in the JDSIM each sampled joint distribution could be the true distri-

bution, and therefore, any approximation proposed need to be compared to all the sampled distributions in order to measure its accuracy. Additionally, we randomly choose 160,000 samples from the 4 million and solve them for the corresponding optimal strategies. This process took an average of 20 seconds per distribution, which make it difficult to solve for the complete sample. However, 160,000 samples from the full collection can be use as an estimate for the hole sample.

We use four measures of accuracy to evaluate the four approximations: (i) the mean absolute difference between the approximate and sampled joint probabilities, (ii) the maximum absolute difference in these joint probabilities, (iii) the Euclidean distance, i.e. the length of the straight line between the approximation and the sampled distributions, and (iv) the KL divergence from the sampled distribution to the approximation. These error measures are all such that a value of zero indicates no error and larger values indicate larger errors. Measures (i) and (ii) were used in Keefer's analysis; Bickel and Smith, and Abbas considers (i),(ii), and (iv).

Using the sub collection of 160,000 samples for which we solve to optimality, we add two economic measures in the sequential exploration setting used by Bickel and Smith: (v) the absolute value of the difference between the optimal expected value given by the sampled probabilities and the optimal expected value given by the approximate probabilities and (vi) the difference between the expected value given by following the optimal strategy and the expected value given by following the approximation strategy, with both expected values calculated using the sampled joint probabilities. We refer to this as the expected value lost.

The error in the value estimate (measure v) is an appropriate error measure if the analysis is intended to estimate the value of the exploration opportunity, for example, if contemplating selling or acquiring the exploration opportunity. The expected value lost (measure vi) indicates how close you come to identifying the optimal exploration strategy.

Table 6.5 shows that for the accuracy measures based in probabilities (i, ii, iii, iv), the best approximation is DAC, followed by AC, ChSC, MVIEC, ME, UE, IA. The intuition behind these results can be observed when we consider the information used to create each approximation. It should not surprise us that the approximation with the least amount of information (IA) provide the worst results. Notice that in this case both approximations, IA and UE, do not even belong to the interior of $\mathbb{T}$. Alternatively, the ME distribution does belong to the interior of the truth set and uses all the information available, which increase its accuracy. However, it fill the missing information by assuming all other assessments should as independent as possible. Approximations such as AC, ChSC and MVIEC use the same amount of information

Table 6.5: Accuracy Results.

	Independent Approx. Underlying Event (IA / UE)	Maximum Entropy (ME)	Analytic Center (AC)	Chebyshev's Center (ChSC)	Max. Vol. Ins. Ellip. (MVIEC)	Dynamic Average (DAC)
i. Mean absolute difference						
Mean	0.0113	0.0063	0.0054	0.0054	0.0055	0.0054
Std dev	0.0008	0.0012	0.0011	0.0011	0.0012	0.0011
ii. Max absolute difference (L^∞ Norm)						
Mean	0.1262	0.0378	0.0294	0.0296	0.0300	0.0294
Std dev	0.0189	0.0119	0.0083	0.0083	0.0094	0.0084
iii. Euclidean distance (L^2 Norm)						
Mean	0.1734	0.0815	0.0687	0.0693	0.0701	0.0686
Std dev	0.0166	0.0188	0.0159	0.0159	0.0177	0.0159
iv. KL divergence						
Mean	0.6095	0.2334	0.1802	0.1830	0.1847	0.1795
Std dev	0.0649	0.0649	0.0536	0.0533	0.0580	0.0528
v. Absolute error in value estimate ($ million)						
Mean	17.62	3.22	3.02	3.09	2.36	2.91
Std dev	1.18	1.18	1.18	1.18	1.18	1.18
vi. Lost value from approximate policy ($ million)						
Mean	17.62	4.29	2.95	2.91	3.03	2.91
Std dev	1.18	2.16	1.51	1.54	1.72	1.54

as ME, but the assumptions taken in each case varies for each model, which make some approximations better that others in a case basis. Finally, in addition to the available information, DAC improves its accuracy by using the information of 4 million sampled joint distributions to fill higher assessment information.

The accuracy measures based on the strategies (v, vi) suggests that the DAC/ChSC and the MVIE are the best strategies. DAC and ChSC share the lowest lost value from approximate policy and the MVIE strategy has the lowest absolute error in value estimate followed by DAC.

6.1.6.2 Alternative Strategies

In the previous section we measure the accuracy of four approximations that derive in four different strategies. However, there are a number of strategies that are not the result of an approximation distribution, but generated by solving to optimality the sequential exploration problem using the sampled distributions. In other words, by taking the sub-collection of $160,000$ samples, we can create a collection of $160,000$ strategies (one for each sample). After accounting for redundancies, we are left with a collection of $82,205$ different strategies, some of which appear more frequent than others. Figure 6.5 shows the frequencies for each strategy in descending order, where each dot represents a single strategy.

We observe that a large portion of the strategies have frequency less than ten, and only ten strategies have frequency above 50, This last group includes the strategies that are optimal for the largest number of joint distributions sampled in the sub-collection. Then, we can test the performance of a small group of strategies (the ones with highest frequency) and compare them to the strategies generated from the approximation distributions. Figure 6.7 shows the nine strategies for which the frequency is the highest among the sub-collection.

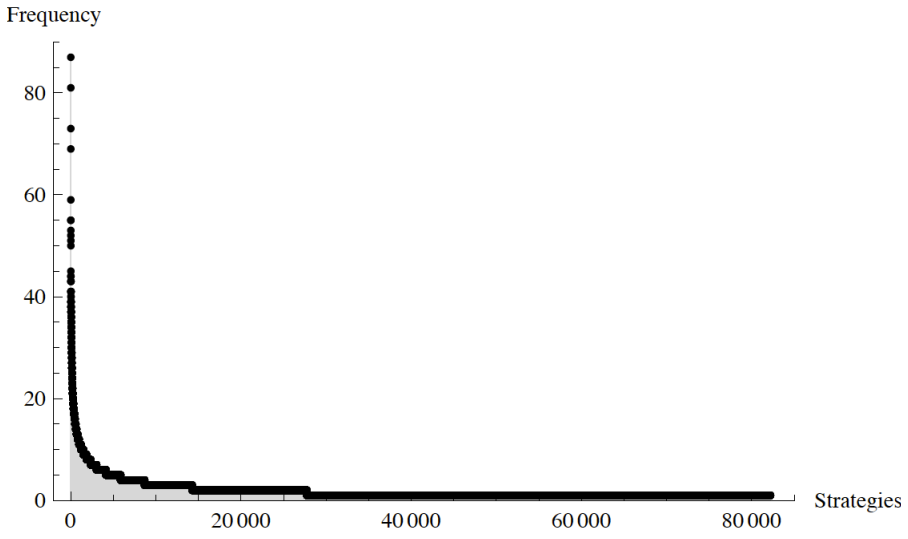

Figure 6.5: Most Common Optimal Strategies.

For each of these strategies we evaluate the profit under all 4 million joint distributions in the original collection sampled from $\mathbb{T}$. The result is a group of 15 strategies (six strategies from the approximation distributions and nine from the frequencies) that we can evaluate. Tables 6.6 and 6.7 show the mean, standard deviation, minimum and maximum values for the profits generated by all 15 strategies.

Table 6.6: Profit Statistics For Full Strategies Based on Approximation Distributions. (in millions)

	PMF Approximations				
	ME	AC	ChSC	MVIE	DAC
Mean	\$ 13.34	\$ 14.68	\$ 14.71	\$ 14.60	\$ 14.71
Std. Dev.	\$ 1.55	\$ 1.33	\$ 1.39	\$ 1.63	\$ 1.39
Min	\$ 9.26	\$ 10.33	\$ 9.73	\$ 8.86	\$ 9.73
Max	\$ 18.22	\$ 18.46	\$ 18.69	\$ 19.03	\$ 18.69

It result is surprising to find that there are strategies that closely match the some of the approximation joint distributions. This is the case of the fourth strategy (S4) with mean of \$14.42, which outperforms the mean of \$13.34 of ME and is close to the mean of \$14.71 of DAC. Even more, by observing the range $[9.9, 20.04]$, the

S4 shows a higher range than the rest of the strategies consider. Nonetheless, the results from both Tables 6.6 and 6.7 still conclude that the most profitable strategy in expectation is DAC.

Table 6.7: Profit Statistics For Full Strategies Based on Selected Strategies. (in millions)

	High Frequency Full Strategies								
	1^{st}	2^{nd}	3^{th}	4^{th}	5^{th}	6^{th}	7^{th}	8^{th}	9^{th}
Mean	\$12.84	\$13.27	\$13.05	\$14.42	\$13.46	\$12.99	\$13.39	\$13.04	\$13.26
St. Dev.	\$2.14	\$1.90	\$1.56	\$1.69	\$1.55	\$1.53	\$1.61	\$1.83	\$1.63
Min	\$7.16	\$7.03	\$8.80	\$9.90	\$8.17	\$7.65	\$7.43	\$7.26	\$7.12
Max	\$18.96	\$18.87	\$18.68	\$20.04	\$18.46	\$17.82	\$18.09	\$18.99	\$18.32

In Figure 6.6 we can see that some strategies tend to perform better than others a larger percentage of the time. An advantage of the alternative strategies comes from observing the robustness of the strategy. In other words, we can observe the fraction of time a strategy outperform all others for a collection of random joint

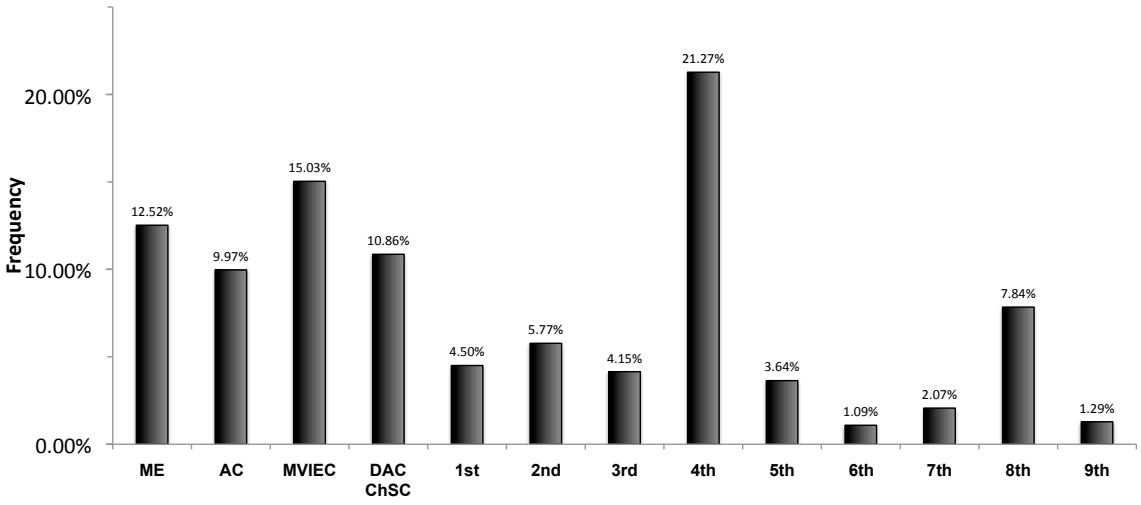

Figure 6.6: Fraction of Time Each Strategy is the Best Option In a Sample of 4 Million PMF.

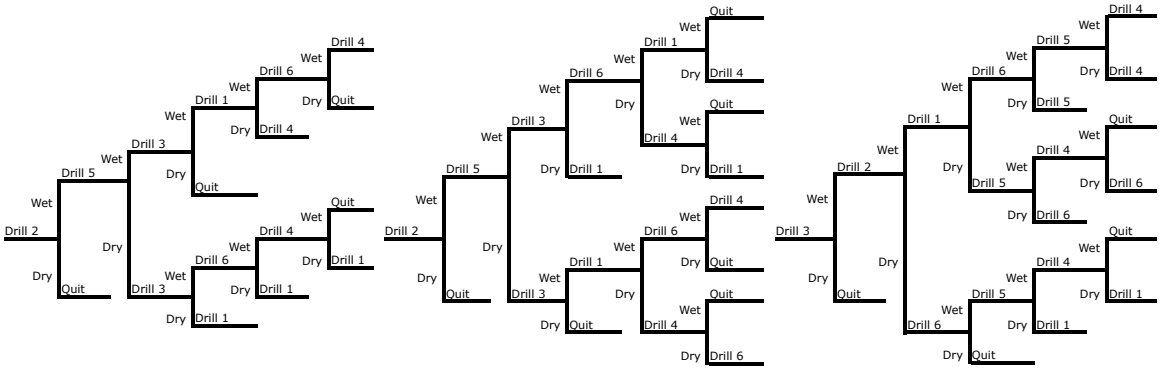

(a) Highest freq. (S1) (b) Second highest freq. (S2) (c) Third highest freq. (S3)

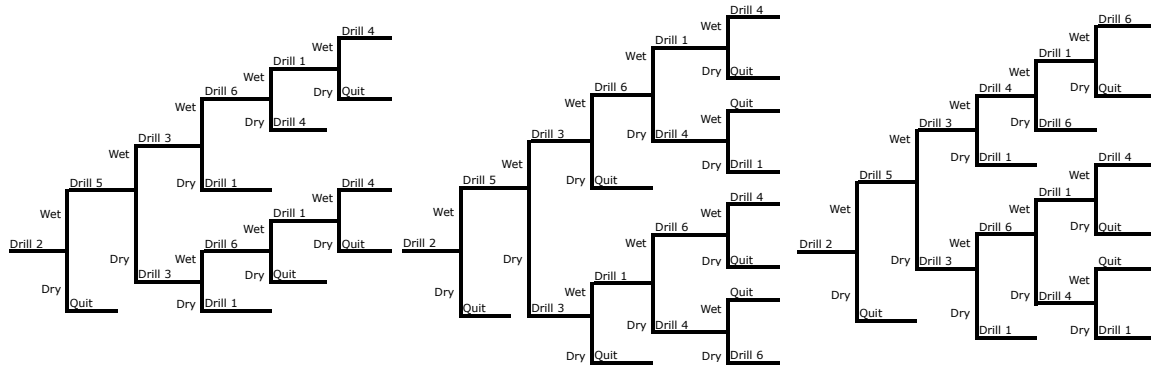

(d) Fourth highest freq. (S4) (e) Fifth highest freq. (S5) (f) Sixth highest freq. (S6)

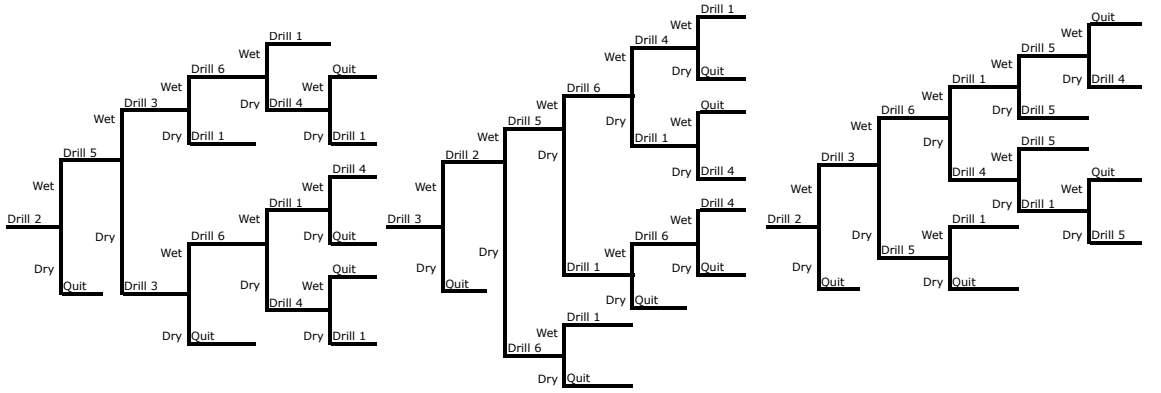

(g) Seventh highest freq. (S7) (h) Eighth highest freq. (S8) (i) Ninth highest freq. (S9)

Figure 6.7: Strategies With Highest Frequencies.

distributions. In particular, two strategies show to be the most robust, MVIE and S4. However, under this particular measure of robustness, S4 outperform MVIE by nearly 6% points. This means that by selecting S4 we will be better off approximately 21.27% of the time, while if we select MVIE or ME can expect to be better off approximately 15.03% and 12.52% of the time respectively.

6.1.6.3 One Step Strategies

Complete strategies are useful in scenarios where an entire policy needs to be defined at the beginning of an operation or when a contingency plan is required. For example, a complete strategy can be given to the operators in the field, and depending on their findings, the strategy will tell them which well they should drill (if any) without the need of more analysis.

An alternative to establish a complete strategy is to use the myopic approach, in which we only determine the next best well to drill. This is a useful approach when there is a possibility that the observations after drilling might change our assessed beliefs. In this case, after each well has being explored, we need to redo the analysis to determine the next well. In Bickel and Smith (2006), the myopic approach consist on creating a complete strategy using the ME approximation, and consider the first well of the strategy. However, the JDSIM procedure allow us to implement a more robust myopic approach.

As before, we have randomly selected 160,000 sampled joint probability distributions from a collection of 4 million samples and generate their respective optimal strategies. Figure 6.8 present the number of times we found each well to be the optimal alternative to drill next. According to ME, the optimal myopic strategy is to drill well 3 first. However, that strategy is only optimal for 33.4% of the sampled joint distributions. A more robust myopic strategy is to drill well 2 first. This strategy is optimal for 65.7% of the sampled joint distributions. In other words, by choosing to

drill well 2 first, we increase the probability of using an optimal strategy for any joint distribution uniformly sampled from $\mathbb{T}$.

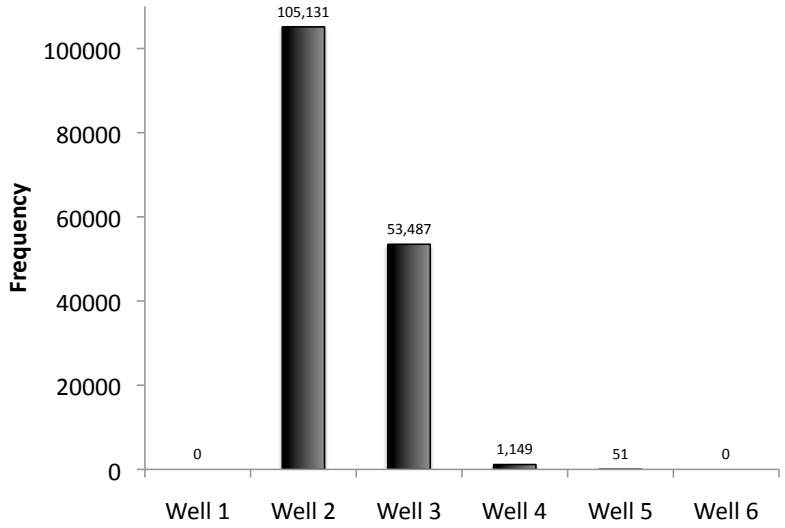

Figure 6.8: Frequency of Optimal Myopic Strategies.

In addition to the robustness of the decision, we can also observe the distribution of the expected profits for each well. In Table 6.8 we observe that by choosing well 2 first we will have an expected profit of \$17.47 million, whereas, if we use the myopic strategy proposed by ME (well 3), the expected revenue will drop by \$380,000 dollars. Moreover, well 2 offers a strategy for which the expected profit shows smaller standard deviation, and with the highest minimum and maximum observed values.

Table 6.8: Expected Profit Statistics For Six Myopic Strategies. (\$ million)

	Well 1	Well 2	Well 3	Well 4	Well 5	Well 6
Mean	\$13.97	\$17.47	\$17.09	\$16.37	\$14.69	\$14.07
Std. Dev.	\$1.39	\$1.24	\$1.32	\$1.33	\$1.22	\$1.32
Minimum	\$10.53	\$13.88	\$13.78	\$12.63	\$11.52	\$10.81
Maximum	\$20.21	\$22.84	\$22.57	\$21.97	\$20.46	\$19.31

Finally, in Figure 6.9 we observe cumulative distribution functions for the ex-

pected profits for all six wells. Notice that the "well 2" strategy, provides a probability distribution that is stochastic dominant with respect to all other pdf's. In fact, it is interesting that each strategy is completely dominant or completely dominated by the other 5, which simplifies our analysis.

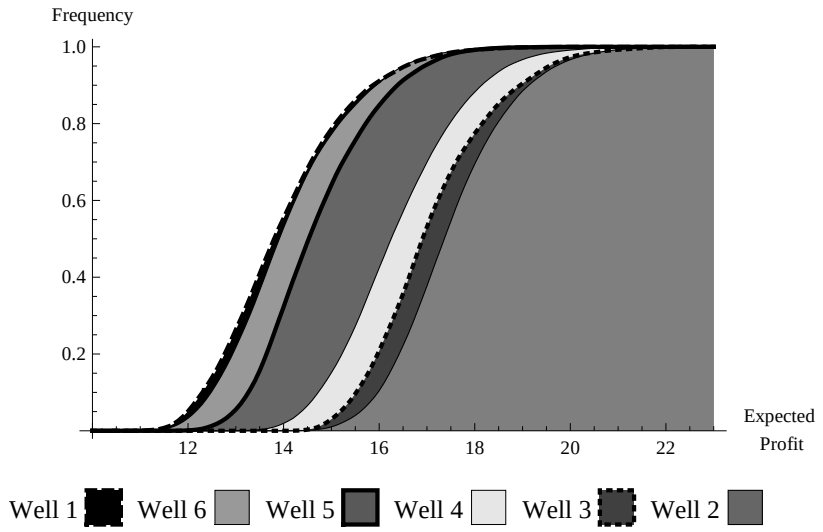

Figure 6.9: Stochastic Dominance Among Myopic Strategies.

6.1.7 Final Comments

We start this care of study with the idea to analyze the performance of ME in a decision framework where partial information drives the probabilistic dependence of the possible joint distributions. To achieve that, we needed to sample the space of possible joint distributions and compare them to the ME approximation. The Joint Distribution Simulation (JDSIM) applied to the gas and oil sequential exploration model provided a framework for this analysis with unexpected results.

The JDSIM provided a flexible tool to analyze stochastic decision models when the joint distribution is incompletely specified. The methodology is easy to implement, develops a collection of joint distributions, and represents a significant extension

to previous approximation models. The extensions to the original paper provide an important framework for analysis and represent a new recourse to generate alternative strategies in the face of uncertainty.

On average, the profit joint distributions produced by JDSIM resulted in expected values and standard deviations that outperforms the ME approximation. In fact, we were able to show that ME is not as good of a distribution as we were expecting it to be. However, we show alternatives that provide more accurate results to approximate a distribution with partial information.

The information provided by this new simulation procedure provides insight regarding the shape of the truth set. We can clearly state that assuming independence in scenarios with incomplete or unknown information provides approximations that are extreme relative to the other distributions in the truth set.

6.2 Eagle Airlines

6.2.1 Introduction

In this paper, we present a new methodology for modeling decisions given partial probabilistic information. In particular, we create the set of all possible discrete distributions that are consistent with the information that we do have. We then (uniformly) sample from this set using the Hit-and-Run Sampler (Smith, 1984). Our procedure is perhaps best thought of as a sensitivity analysis, since we do not claim that all distributions in our set are equally likely. Indeed, specifying the probability distribution over the set of all probability distributions presents its own difficulties.

Other approaches to the problem discussed here fall into three primary categories: (i) approximation methods that specify a single joint probability distribution given partial information, (ii) sensitivity analysis procedures that partially explore the space of feasible joint distributions, and (iii) "robust" decision-making methods

that attempt to ensure some minimum level of performance.

The most prominent example in the first category is the maximum entropy method (maxent) pioneered by Jaynes (1957, 1968), in which a single distribution (the one that is most uncertain, or has the highest entropy) is selected from the set of all possible distributions that are consistent with the given information. A closely related approach is the specification of a copula (Sklar, 1959), which encodes the dependence between marginal distributions. For example, Jouini and Clemen (1996), Frees et al. (1996), and Clemen and Reilly (1999), all used copulas to construct joint distributions based on lower-order assessments. In the copula-based approach, the continuous joint distribution is often discretized to facilitate modeling within a discrete decision-tree framework. In this paper, we compare our proposed methodology to the normal-copula approach, illustrated by Clemen and Reilly (1999), hereafter (CR).

In the second category, sensitivity procedures have been developed to explore portions of the set of possible joint distributions. For example, Lowell (1994) developed a sensitivity analysis procedure to identify important pairwise conditional probability assessments. As discussed above, CR proposed the use of a normal copula, characterized by pairwise correlation coefficients. They then perturbed the correlation matrix to explore a set of possible joint distributions. This set is restricted to joint distributions that can be modeled with a normal copula. Reilly (2000) developed a sensitivity approach that uses synthetic variables based on a pairwise correlation coefficient matrix.

Finally, in the third category, robust procedures such as maximin or robust optimization (Ben-Tal et al., 2009) evaluate decisions based on their worst possible outcomes. We do not directly address these methods. We note, however, that identifying the worst possible joint distribution is often difficult. Our procedure could be used in a robust setting to "stress test" decisions.

This case of study is organized as follows. §6.2.2 describes a new procedure

to generate joint probability distributions when only partial information is available. §6.2.3 introduces an illustrative example that we use to demonstrate our approach. §6.2.4 applies our new procedure to this example. Finally, §6.2.5 concludes and discusses future research directions.

6.2.2 Proposed Approach

The joint distribution simulation approach (JDSIM) samples from the set of all possible joint distributions that are consistent with the given information. In this way, it provides not one, but a collection of joint distributions under which the decision can be evaluated.

The procedure described in Chapter 3, begins with the specification of linear constraints on the joint distribution (e.g., specification of marginal probabilities or pairwise correlations) and the creation of a convex polytope $\mathbb{T}$, the "truth set," that matches the given information. By "truth" we mean that any distribution within this set is consistent with the assessments and therefore could be the "true" joint distribution.

We illustrate the characterization of $\mathbb{T}$ using a simple example with two binary random variables V_1 and V_2. This polytope has four joint events (Figure 6.10(a)), whose probabilities must be positive and sum to one (Figure 6.10(b)). The truth set can be expressed as a hyperplane in four dimensions or as a full-dimensional polytope in three dimensions (Figure 6.10(c)). We can constrain $\mathbb{T}$ to match marginal assessments such as $P(V_2) = P_1 + P_3 = \frac{3}{5}$, as shown in Figure 6.10(d). Each new constraint reduces the dimensionality of $\mathbb{T}$ by one. For example, adding a second marginal constraint reduces $\mathbb{T}$ to a one-dimensional line, and adding a correlation constraint reduces $\mathbb{T}$ to a single point.

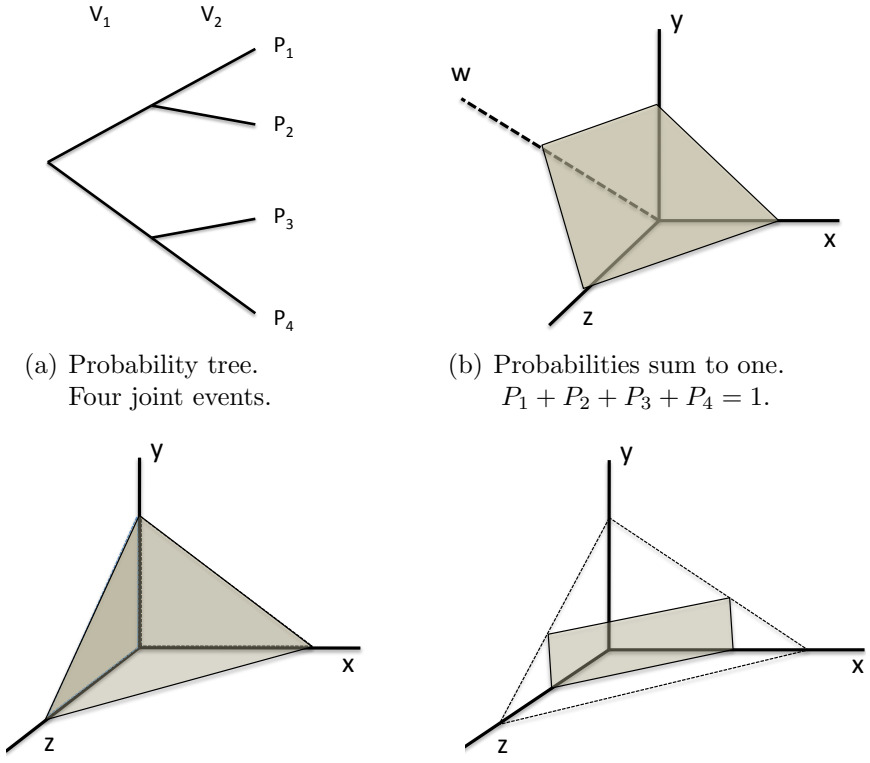

(a) Probability tree. Four joint events.

(b) Probabilities sum to one. $P_1 + P_2 + P_3 + P_4 = 1$.

(c) Projection to 3D. $P_1 + P_2 + P_3 \leq 1$.

(d) Add marginal info. $P_1 + P_3 = \frac{3}{5}$.

Figure 6.10: Example characterization of the truth set $\mathbb{T}$.

6.2.3 Illustrative Example

We now describe the illustrative example that we use to demonstrate our procedure. The Eagle Airlines example was introduced by Clemen (1996) and later extended by Clemen and Reilly (1999) and Reilly (2000). We describe the example from an excerpt (p. 559) in Reilly (2000):

"Dick Carothers, the owner of Eagle Airlines, is deciding whether to invest ... \$52,500 in a money market or to expand his fleet with the purchase of [an airplane; we will refer to this as the "Expand" alternative]. His decision criterion is whether the new plane will generate more profit than a money market alternative. The influence

diagram in [Figure 6.11] illustrates the relevant variables...

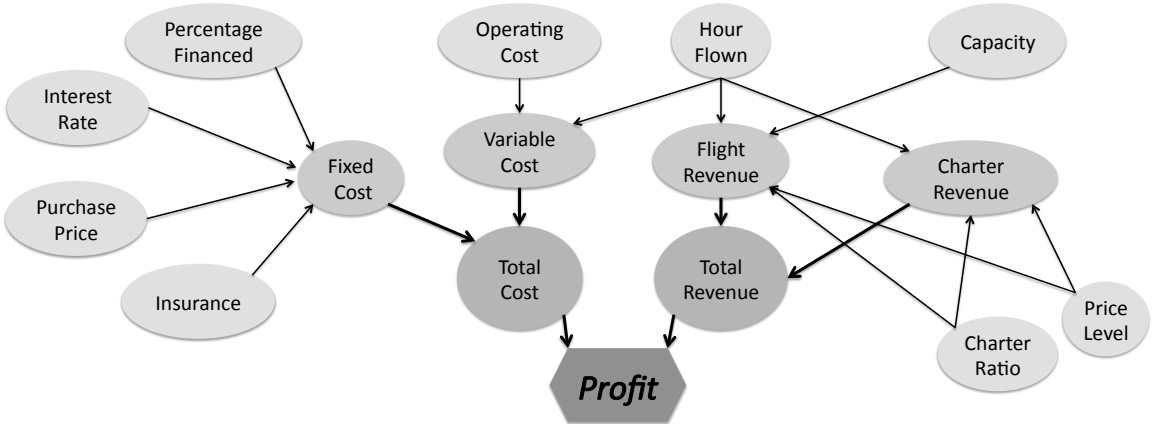

Figure 6.11: Influence Diagram For Eagle Airline's Decision

The profit function is given by: $Profit = Total\ Revenue - Total\ Cost$, where

$$Total\ Revenue = Charter\ Ratio * Hours\ Flown * Charter\ Price$$
$$+ (1 - Charter\ Ratio) * Hours\ Flown * Capacity * Number\ of\ Seats * Price\ Level,$$
$$Total\ Cost = Hours\ Flown * Operating\ Cost + Insurance$$
$$+ Purchase\ Price * Percentage\ Financed * Interest\ Rate,$$

where $Charter\ Price$ is $3.25 * Price\ Level$, and the $Number\ of\ Seats$ is five. Computing the profit using the [base-case values, described below], Carothers's annual profit is \$9,975, which is \$5,775 more than the minimum of \$4,200 (based on the opportunity cost of capital). The deterministic model indicates that Carothers should expand his fleet now. Some of the inputs, however, are highly variable, and these could possibly lower the profit below the \$4,200 benchmark."

Based on sensitivity analysis, Reilly (2000) showed that four variables most affect the decision: $Price\ Level\ (PL)$, $Hours\ Flown\ (H)$, $Capacity\ (C)$, and $Operating\ Cost\ per\ Hour$

(O). CR provided the 0.10 (Low), 0.50 (Base), and 0.90 (High) fractiles for each uncertainty and the Spearman rank correlations between each pair of uncertainties, which we repeat in Table 6.9.

Table 6.9: Ranges and Spearman Correlations for Critical Input Variables.

	Fractile			Spearman Correlations			
	Low	Base	High				
Uncertainty	0.10	0.50	0.90	PL	H	C	O
PL	\$95	\$100	\$108	1			
H	500	800	1000	-0.50	1		
C	40%	50%	60%	-0.25	0.5	1	
O	\$230	\$245	\$260	0	0	0.25	1

The non-critical uncertainties are fixed at their base values, which are $Charter\ Ratio = 50\%$, $Percentage\ \ Financed = 40\%$, $Interest\ Rate = 11.5\%$, $Insurance = \$20,000$, $Purchase\ Price = \$87,500$, $Number\ of\ \ Seats = 5$, and $Charter\ Price = 3.25 * Price\ Level$.

In order to apply their normal-copula (NC) procedure, CR assumed that the marginal distributions shown in Table 6.9 are from known families. In particular, they assumed that PL and H are scaled-beta distributions, C is beta, and O is normally distributed. CR's parameter assumptions for each uncertainty are presented in Table 6.10.

Table 6.10: Marginal Distributions For Eagle Airlines.

Uncertainty	Distribution	Parameters	Range
PL	Scaled beta	$\alpha = 9$, $\beta = 15$	[\$81.94, \$133.96]
H	Scaled beta	$\alpha = 4$, $\beta = 2$	[66.91, 1135.26]
C	Beta	$\alpha = 20$, $\beta = 20$	[0, 1]
O	Normal	$\mu = 245$, $\sigma = 11.72$	$(-\infty, +\infty)$

With this information, CR proposed a single continuous joint probability density function (pdf), based on an NC, and discretized it using the Extended Pearson-Tukey (EPT) technique (Keefer and Bodily, 1983; Pearson and Tukey, 1965). EPT

weights the 0.05, 0.50, and 0.95 fractiles with probabilities of 0.185, 0.630, and 0.185, respectively. CR's discrete cumulative distribution function (cdf) for the Expand alternative is shown in Figure 6.12 as a solid black line. This Figure should be compared to CR's "discrete approximation" in their Figure 5.

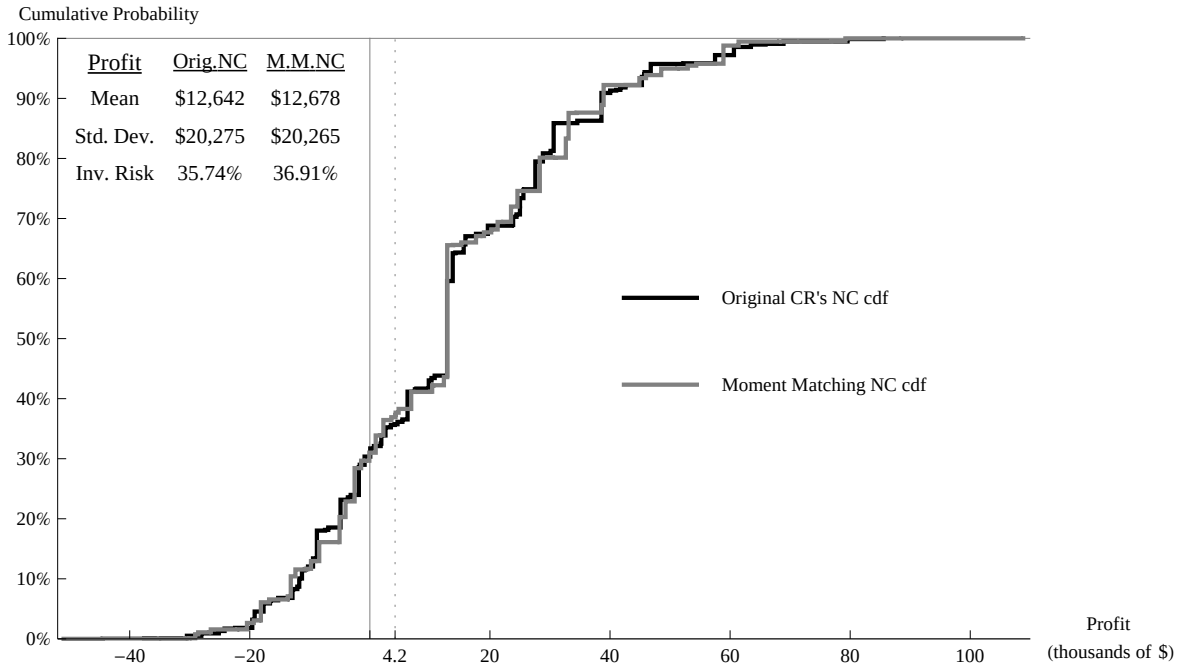

Figure 6.12: Eagle Airlines cdf, under original discretization (black) and new discretization (gray).

Because CR used EPT, they fixed the probabilities for marginal and conditional distributions, as described above, and solved for the 0.05, 0.50, and 0.95 fractiles. In our simulation procedure, we fix the values and solve for the probabilities. This approach is helpful for comparing our procedure to an approximation such as maxent, which is not a function of values and instead solves for probabilities. Therefore, to better compare our procedure to that of CR, we have discretized their joint pdf by fixing the marginal values at the 0.05, 0.50, and 0.95 fractiles (using their pdf assumptions in Table 6.10) and then solving for probabilities using moment matching (see Appendix D.1). This discrete cdf is shown in Figure 6.12 as the solid gray line.

While the two approaches are not identical, the discretizations are very close. We use the moment matching cdf in the remainder of the paper.

One potential difficulty with CR's procedure is that it does not preserve the original pairwise correlation assessments. This occurs because the discretization with three points reduces the possible correlation range, producing a new correlation matrix bounded by [-0.74, 0.74]. Please see Appendix D.2 for more detail. Table 6.11 presents the correlation matrix implied by CR's discrete cdf (the gray line in Figure 6.12). The non-zero correlations have all decreased. Our approach, in contrast, pre-

Table 6.11: NC Implied Spearman Correlation Matrix.

	PL	H	C	O
PL	0.74			
H	-0.38	0.74		
C	-0.19	0.38	0.74	
O	0	0	0.19	0.74

serves the assessed correlations. Of course, the expert would need to understand that the correlation range is not [-1,1] when they were assessing the correlation between discrete random variables with only three possible outcomes.

6.2.4 Application to Eagle Airlines Decision

In this section, we apply our JDSIM procedure to the Eagle Airlines case. We consider three information cases. The first case assumes we have information regarding only the marginal probabilities. The second case includes the previous marginal probabilities and adds information regarding the rank correlation between PL and H. The final case is equivalent to the original problem as presented by CR, and includes all the marginal assessments and pairwise correlations. To facilitate comparison of our results to CR, our JDSIM procedure use the correlations presented in Table 6.11.

6.2.4.1 Case 1: Given Information Regarding Marginals Alone

We begin by assuming that we have information regarding only the marginal assessments. To compare our procedure to CR, we also use EPT. In addition to the 0.50 fractile, EPT requires the 0.05 and 0.95 fractiles, which were not provided by CR. We estimate these fractiles using CR's distributional assumptions in Tables 6.9 and 6.10 and present the results in Table 6.12. We now assume that both the NC and JDSIM methods begin with Table 6.12.

Table 6.12: Fractiles Used in Eagle Airlines Example.

	Fractile		
	Low (l)	Base (b)	High (h)
Uncertainty	0.05	0.5	0.95
PL	\$93.47	\$100	\$110.05
H	432.92	800	1053.60
C	37.14%	50%	62.86%
O	\$225.72	\$245	\$264.28

Under the NC procedure, we must next assume a particular pdf family for each marginal distribution and specify a correlation matrix. We use the marginal assessments provided by CR in Table 6.10. Since we are assuming that dependence information is unavailable, it is unclear how to specify the correlation matrix. For the benefit of the comparison, and following common practice, we assume that all correlations are zero. The JDSIM method, in contrast, does not require the specification of marginal pdf families or a correlation matrix. Rather, we form a polytope that contains all possible joint distributions matching the marginal assessments given in Table 6.12. The polytope describing these marginal assessments has 72 dimensions, resulting from 81 joint probabilities (four random variables with three outcomes each), one constraint that requires the probabilities to sum to one, and eight constraints to match the marginal assessments (81-1-8=72).

The polytope $\mathbb{T}$ is defined using Equations (3.1a), (3.1b), and (3.2a). Equa-

tions (3.1a) and (3.1b) constrain the joint probabilities $p_{\omega_k} \in \mathbf{p}$ to sum to one and to be non-negative. Equation (3.2a) selects subsets of the joint probabilities and constrains their sum to be equal to the marginal assessments. For example, if we order the random variables as $\{PL, H, C, O\}$, each having values $\{l, b, h\}$, there are 81 joint events. Using dot notation, $\{h, \cdot, \cdot, \cdot\}$ refers to the 27 joint events with PL equal to 110.05 (the 95th percentile). From the marginal assessments, we know that $p_{h,\cdot,\cdot,\cdot} = 0.185$, which defines Equation (6.5). Similar equations can be defined for the remaining 11 marginal assessments (12 in total). However, four of these constraints are redundant given Equation (3.1a), reducing the total number of linear constraints to nine.

$$p_{h,\cdot,\cdot,\cdot} = \sum_{i \in F} \sum_{j \in F} \sum_{k \in F} p_{h,i,j,k} = 0.185, \ \forall \ F \equiv \{l, b, h\}. \tag{6.5}$$

We apply the JDSIM procedure to the polytope to create a discrete representation of $\mathbb{T}$ by sampling 10 million discrete joint distributions,[1] all of which are consistent with the information provided by CR. We calculate the mean and standard deviation of profit for each sampled joint distribution. Additionally, we calculate the frequency with which the Expand alternative yields less than the Money Market (MM) threshold of \$4,200. We refer to this frequency as the "investment risk." Based on our 10 million distributions, we calculate frequency distributions for the mean profit, the standard deviation of profit (Std. Dev.), and the investment risk (Inv. Risk). Table 6.13 shows these percentiles along with their theoretical lower bound (LB) and upper bound (UB), which we describe shortly. This table should be compared to CR's Table 5.

The observed mean profit ranges from \$10,160 to \$14,340, with an average (μ) and standard deviation (σ) of \$12,303 and \$496, respectively. The expected profit

[1]Run time: Five hours using Mathematica 8 on an Intel CPU Q6700@2.67GHz with 8GB of RAM.

Table 6.13: Percentiles for mean profit, standard deviation of profit, and investment risks for JDSIM joint distributions given only marginal information.

	Percentiles						
	0%	10%	25%	50%	75%	90%	100%
Mean	\$10,160	\$11,667	\$11,968	\$12,304	\$12,637	\$12,940	\$14,340
Std. Dev.	\$17,300	\$21,750	\$22,613	\$23,576	\$24,552	\$25,456	\$29,580
Inv. Risk	19.50%	26.25%	27.65%	29.30%	31.12%	32.79%	40.95%

	Statistics			
	LB	μ	σ	UB
Mean	\$4,332	\$12,303	\$496	\$21,750
Std. Dev.	NA	\$23,591	\$1,444	NA
Inv. Risk	0.00%	29.42%	2.54%	74%

under the NC is \$12,326. Our observed profit range and the percentiles closely match the results of CR's sensitivity results (see their Table 5).

We refer to the 0th and 100th percentiles as "probability bounds" because there could exist cdfs in $\mathbb{T}$ that result in profits outside of this range. However, we did not observe them in 10 million samples. Since the minimum expected profit that we sampled was \$10,160, every simulated joint distribution had a mean profit greater than the value of the MM alternative. Thus, in this case, the assessment of probabilistic dependence or differing marginal distributions, which still match the assessments in Table 6.12, is very unlikely to change the recommendation that Eagle Airlines should expand (assuming they are risk neutral).

The standard deviations of our sampled cdfs ranged from \$17,300 to \$29,580, with an average of \$23,641. The standard deviation of profit under the NC is \$23,605. On the high end, our results closely match CR. However, the smallest standard deviations in our sample were larger than CR's. We conjecture that this result is related to differences in our discretization procedure and CR's marginal/copula assumptions. Referring back to Figure 6.12, we see that our discretization procedure (fixed values) results in a slightly wider cdf (longer tails) than CR's approach (fixed probabilities). Furthermore, their marginal distributions (see Table 6.10) are either normal or close to normal, implying that they have very thin tails. Likewise, CR modeled dependence

with a normal copula, which also enforces thinner tails. JDSIM is not constrained by these assumptions and is therefore sampling from distributions that are most likely more spread and contain non-zero higher moments (e.g., skewness and kurtosis).

Table 6.13 indicates that investment risk, which averaged 29.42%, ranges from 19.50% to 40.95%. While the Expand alternative's expected profit always exceeds the MM, there may be a large probability of underperforming this benchmark. This surprisingly large range is driven by the underlying dependence structure, which highlights the importance of modeling and assessing dependence. The NC investment risk is 38.05%. The most significant difference between the DAC and NC cdfs is at the level of individual fractiles–their first two moments are relatively close.

The LB and UB in Table 6.13 were derived from a linear program (LP) described in Appendix D.3. We provide these hard bounds for the mean profit and investment risk only. Determining the minimum and maximum possible standard deviation requires solving an NP-hard problem, and this was not attempted. The expected-profit LB is \$4,332, which is greater than the MM. Thus, it is impossible to generate a joint distribution matching the assessments in Table 6.12 that would underperform the MM investment.

The LB and UB are quite distant from the minimum (\$10,160) and maximum (\$14,340) expected profits. The joint distributions associated with these hard bounds contain many events with zero probability. For example, the joint distributions for the expected profit LB and UP are, respectively:

$$\{p_{l,h,l,h} = 0.185, p_{b,b,b,b} = 0.63, p_{h,l,h,l} = 0.185, \text{ otherwise } p_{\cdot,\cdot,\cdot,\cdot} = 0\} \text{ and}$$

$$\{p_{l,l,l,h} = 0.185, p_{b,b,b,b} = 0.63, p_{h,h,h,l} = 0.185, \text{ otherwise } p_{\cdot,\cdot,\cdot,\cdot} = 0\}.$$

These distributions, consisting mostly of zeros, are located at the vertices of the polytope. As such, they are geometrically extreme and unlikely to be sampled. They are also extreme from a dependence perspective, since they assume perfect dependence

between the random variables. For example, under the minimum expected profit distribution, if PL is at its base value then H, C, and O are certain to be at their base values as well.

This difference between the minimum and maximum sampled values (i.e., the probability bounds) and the theoretical bounds is explained by what we call the "Sea Urchin" effect (§3.4). In high-dimension polytopes, the vertices become "thin" and comprise a very small portion of the total volume. Hence, the HR sampler is unlikely to sample them. We do not believe this is a limitation of the sampling method. To the contrary, these distributions are extreme. If the underlying dependence was as strong as the distributions above require (e.g., perfect), we believe the expert would know this and could, therefore, express it as a constraint. Under these conditions, the JDSIM methodology would only sample distributions that included the expressed level of dependence.

The cdfs for this case are presented in Figure 6.13. The DAC cdf is the solid black line, and the independence cdf (based on an NC) is the solid gray line. The dotted lines are the minimum and maximum probability bounds that were sampled during our 10 million trials. These bounds are not individual cdfs, but represent the minimum (lower line) and maximum (upper line) cumulative probabilities that were sampled at each profit level. Likewise, the solid lines represent the theoretical minimum and maximum. These bounds were calculated using the LP described in Appendix D.3. All cdfs must fall within these latter bounds. The vertical dashed line denotes the MM value, and a vertical solid line denotes zero profit. The chance of underperforming MM matches the investment risk in Table 6.13.

We pause here to emphasize the scope and importance of our results. We have sampled 10 million joint distributions from the set of *all* joint distributions matching the marginal constraints. In other words, we have sampled from the set of all possible marginal distributions and dependence structures, rather than a set limited

to marginals from particular families (e.g., beta) and whose dependence structure can be defined with a particular copula (e.g., normal). These 10 million joint distributions fall within the bounds denoted by the dotted lines. The (NC-based) independence cdf falls within these bounds, but is rather extreme (relative to the probability bounds) for profits between -$3,000 and $25,000. The DAC cdf might be thought of as being more representative of the set of possible joint distributions than is the independence cdf. The DAC and the independence cdfs differ rather dramatically at a profit level of $4,200, which is the MM benchmark.

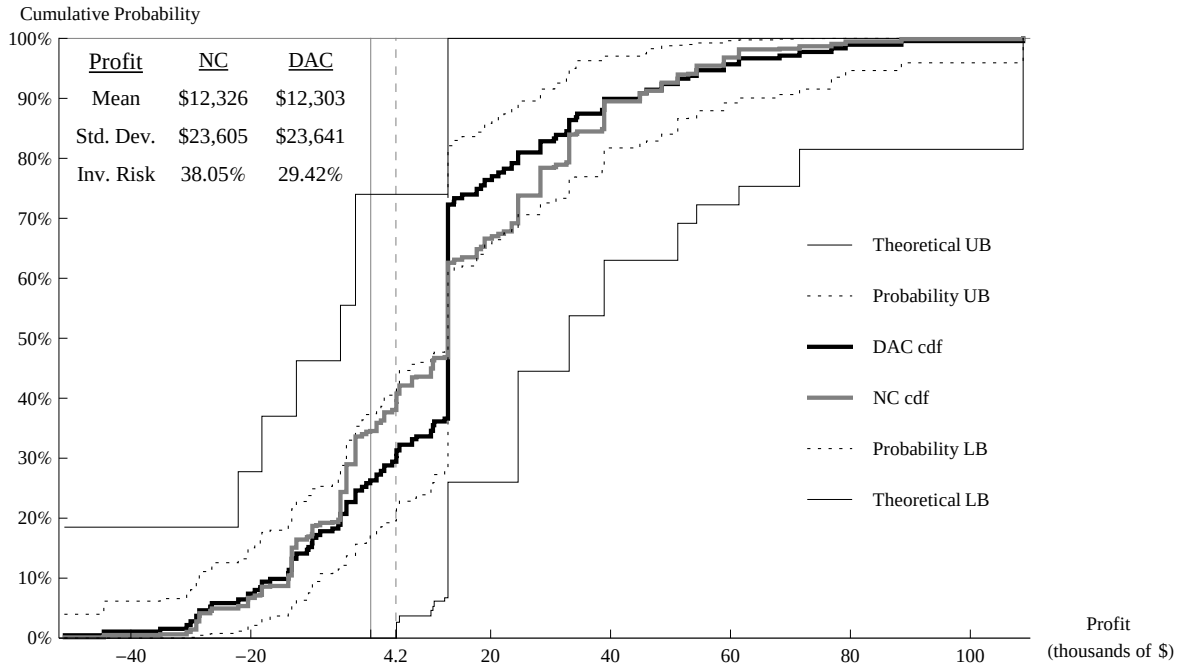

Figure 6.13: Risk profile range given only marginal information, minimum and maximum probability bounds (dashed), theoretical bounds (solid), DAC (black), and NC (gray).

Additionally to DAC, we can also observe in Figure 6.14 the risk profiles for the ME, AC, ChSC, and MVIE approximations. Notice that ME tend to be closer to the NC, this is given by the fact that both distributions share high entropy. The NC obtain the high entropy from the discretization of a normal distribution, which

has maximum entropy in continuous space, and ME is maximum entropy in discrete space. In the other extreme, the ChSC is closet to the probabilistic lower bounds in the lower portion of the graph and higher in the second one, which produce the lower investment risk among the approximations. Finally, AC and MVIE are closer to DAC, which suggest that could be used as approximations that are closer to the center of $\mathbb{T}$.

With respect to the profits, we see that in this case the results are close to each other. This is common in sets where the information is scarce. For example, as we have seeing before, with no information, all approximations converge to the uniform distribution providing the exact same results.

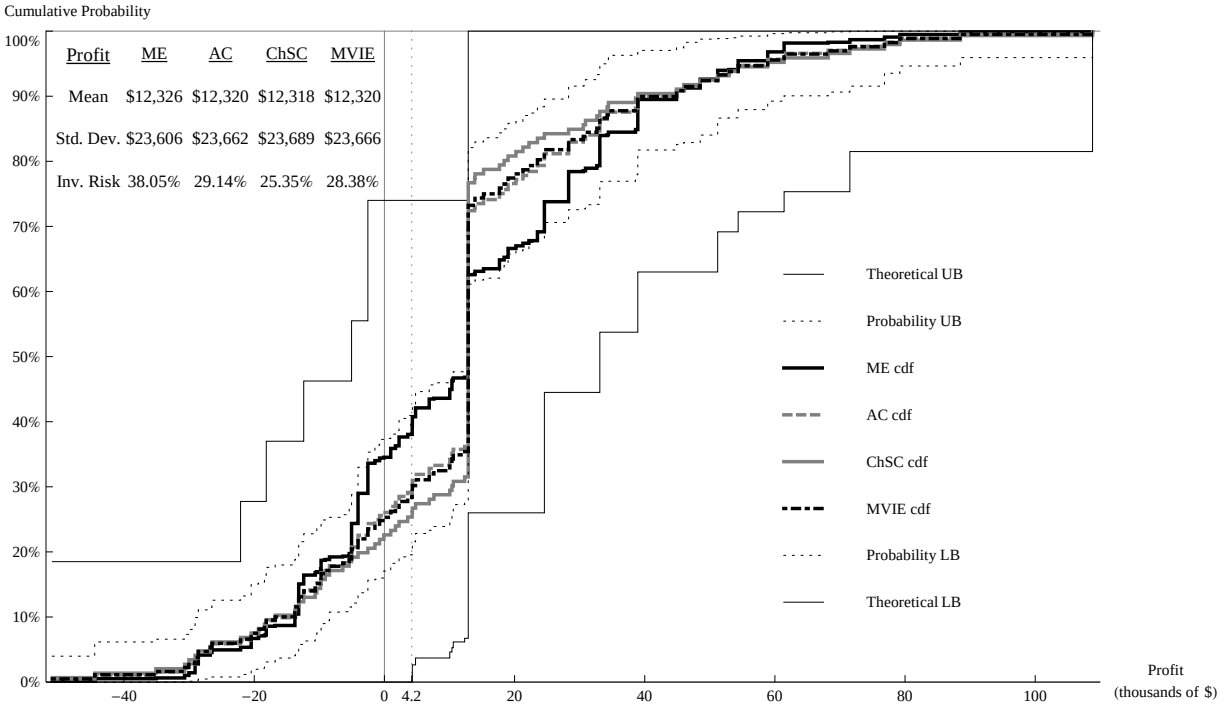

Figure 6.14: Risk profile range given only marginal information, minimum and maximum probability bounds (dashed), theoretical bounds (solid), ME (black), AC (gray-dashed), ChSC (gray), and MVIE (black-dotdashed).

6.2.4.2 Case 2: Given Information Regarding Marginals and Only One Rank Correlation

This section analyzes the case where the dependence structure is constrained by a single pairwise correlation. Specifically, we consider CR's implied correlation between PL and H, which is equal to -0.38 (see Table 6.11). We make no assumptions regarding the other five pairwise correlations. The truth set is generated using Equations (3.1a), (3.1b), (3.2a), and (3.9). As mentioned in §6.2.4.1, Equations (3.1a), (3.1b), and (3.2a) ensure the sampled points are pmfs that match the marginal assessments. We add one more constraint (Equation 3.9) to fix the rank correlation between PL and H.

To illustrate Equation 3.9, we describe the construction of one of the 81 coefficients for the joint events. Using the notation from §3.3, the 50th joint event corresponds to $\{b, h, b, b\}$ and is described as $\omega_{50} = \{PL = \$100, H = 1053.6, C = 50\%, O = \$245\}$. Equation 3.9 then yields:

$$\mathbf{B}_{\omega_{50}} = \left[I_{\omega_{50}}(PL) \times I_{\omega_{50}}(H)\right] = \left[p^{+}_{50}(PL), p^{-}_{50}(PL)\right] \times \left[p^{+}_{50}(H), p^{-}_{50}(H)\right],$$
$$\mathbf{B}_{\omega_{50}} = \left[0.815, 0.185\right] \times \left[1.0, 0.815\right].$$

Then,

$$\frac{\mathbf{V}_{(xy)^2}\left[\mathbf{B}_{\omega_{50}}\right]}{q_{\omega^{+}_{50}(PL)} q_{\omega^{+}_{50}(H)}} =$$

$$= \frac{(p^{+}_{50}(PL)p^{+}_{50}(H))^2 - (p^{+}_{50}(PL)p^{-}_{50}(H))^2 - (p^{-}_{50}(PL)p^{+}_{50}(H))^2 + (p^{-}_{50}(PL)p^{-}_{50}(H))^2}{P(PL = 100)P(H = 1053.6)},$$

$$= \frac{(0.815 \cdot 1.0)^2 - (0.815 \cdot 0.815)^2 - (0.185 \cdot 1.0)^2 + (0.185 \cdot 0.815)^2}{0.63 \cdot 0.185} = 1.815.$$

Calculating similar coefficients for all 81 joint events defines Equation (3.9) and yields

$$0.0342p_{_{l,l,\cdot,\cdot}} + 0.185p_{_{l,b,\cdot,\cdot}} + 0.3358p_{_{l,h,\cdot,\cdot}} + 0.185p_{_{b,l,\cdot,\cdot}} + p_{_{b,b,\cdot,\cdot}} +$$
$$1.815p_{_{b,h,\cdot,\cdot}} + 0.3358p_{_{h,l,\cdot,\cdot}} + 1.815p_{_{h,b,\cdot,\cdot}} + 3.2942p_{_{h,h,\cdot,\cdot}} = \frac{\rho_{_{PL,H}} + 3}{3}.$$

The maximum correlation occurs when the probabilities are $p_{_{l,b,\cdot,\cdot}} = p_{_{l,h,\cdot,\cdot}} = p_{_{b,l,\cdot,\cdot}} = p_{_{b,h,\cdot,\cdot}} = p_{_{h,l,\cdot,\cdot}} = p_{_{h,b,\cdot,\cdot}} = 0$, and $p_{_{l,l,\cdot,\cdot}} = 0.185$, $p_{_{b,b,\cdot,\cdot}} = 0.63$, $p_{_{h,h,\cdot,\cdot}} = 0.185$ with a value equal to 0.74, as was shown in Table 6.11.

We apply the JDSIM procedure to the new polytope and create a discrete representation of the new truth set by sampling 10 million possible joint distributions using the HR sampler. Each sampled distribution has marginals equal to 0.185, 0.63, 0.185, of the $\{l, b, h\}$, respectively, and rank correlation $\rho_{_{PL,H}} = -0.38$. Table 6.14 summarizes our results.

Table 6.14: Percentiles for mean profit, standard deviation of profit, and investment risks for JDSIM joint distributions given marginal information and one pairwise correlation coefficient.

	Percentiles						
	0%	10%	25%	50%	75%	90%	100%
Mean	\$9,215	\$10,376	\$10,641	\$10,919	\$11,198	\$11,441	\$12,570
Std. Dev.	\$16,500	\$19,820	\$20,499	\$21,269	\$22,062	\$22,833	\$26,180
Inv. Risk	20.50%	25.87%	27.40%	29.25%	31.17%	32.99%	42.20%

	Statistics			
	LB	μ	σ	UB
Mean	\$4,877	\$10,916	\$414	\$16,691
Std. Dev.	NA	\$21,296	\$1,174	NA
Inv. Risk	0.57%	29.36%	2.78%	73.43%

The sampled mean profit ranges from \$9,215 to \$12,570, with an average value of \$10,916 and a standard deviation of \$414. The NC expected profit is also \$10,916. The distribution of the mean profit shows that under the new information, the Expand alternative is less attractive than before. This occurs because the correlation between PL and H is negative; higher prices result in fewer hours being flown. However,

purchasing the plane is still more attractive than MM, even at the theoretical bounds (LB and UB). The standard deviations are slightly lower than in Case One because we have introduced negative dependence between PL and H. The investment risk now ranges from 20.50% to 42.20%, with an average of 29.36%.

The cdfs for this case are presented in Figure 6.15. The DAC cdf assumes that $\rho_{PL,H} = -0.38$ and all other correlations are unspecified. The NC cdf assumes that $\rho_{PL,H} = -0.38$ and all other correlations are zero. As in Case One, the NC cdf is near the probability bounds for profits of -$3,000 to $25,000. Again, the DAC seems to be more representative than the NC of the set of possible distributions.

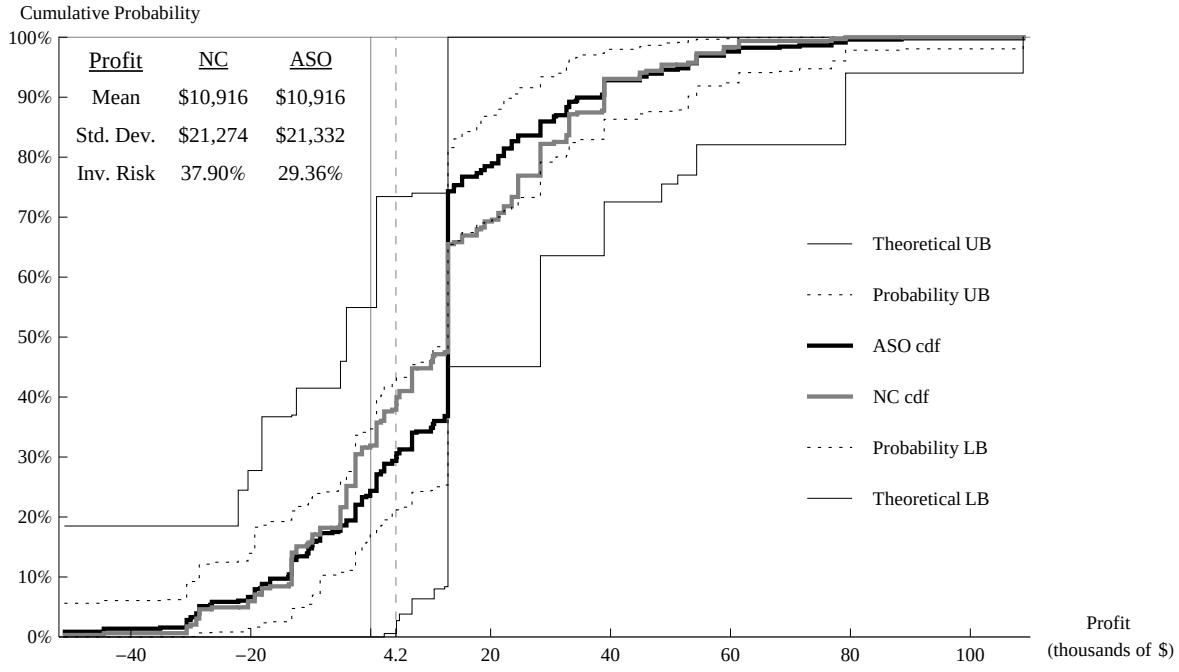

Figure 6.15: Risk profile range given marginal information and one pairwise correlation coefficient, minimum and maximum probability bounds (dashed), theoretical bounds (solid), DAC (black), and NC (gray).

Figure 6.16 shows the results for the rest of the approximations. We see that the information provided pushed the ChSC closer to AC and MVIEC. These approximations show expected profits lower than the previous ones. However, are

still better positioned with respect to the center of the truth set. We also observe that that ME and NC share similar shape and statistics values.

The distribution with the lowest investment risk is now MVIEC by a narrow margin, but it provides close to 10 percent points with respect to ME and NC. This suggest that the probability of loosing money is lower than what we would expect assuming the high entropy distributions.

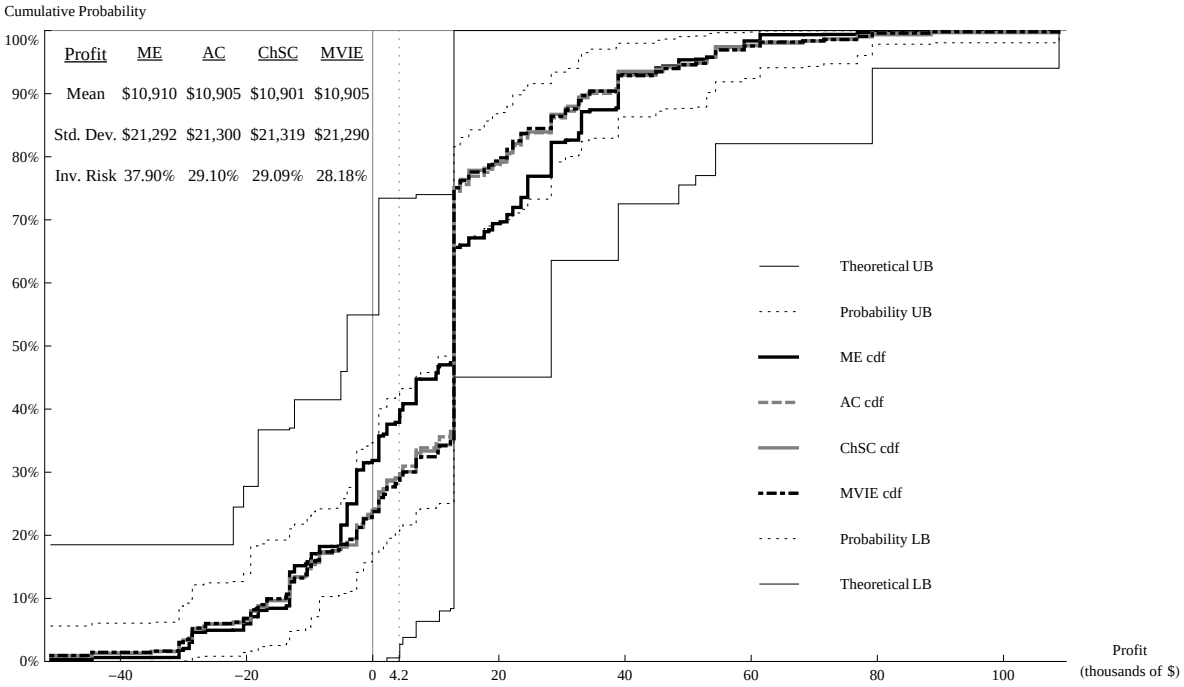

Figure 6.16: Risk profile range given only marginal information and one pairwise correlation coefficient, minimum and maximum probability bounds (dashed), theoretical bounds (solid), ME (black), AC (gray-dashed), ChSC (gray), and MVIE (black-dotdashed).

6.2.4.3 Case 3: Given Information Regarding Marginals and All Rank Correlations Coeficients

In this section, we adopt all of the information provided by CR and used in their NC approach. Specifically, we use the marginal assessments from the EPT

discretization, given in Table 6.12, and the implied correlations from Table 6.11. The implied correlations are used to make the comparison to CR as fair as possible. The new polytope is defined using Equations (3.1a), (3.1b), (3.2a), and (3.9), as illustrated in §6.2.4.1 and §6.2.4.2. To the previous ten constraints (and the non-negativity constraints), we add five new constraints to fix the values of all the pairwise correlations, defining a 66-dimensional polytope.

Table 6.15 displays a summary of our 10 million samples of the new polytope using the HR sampler. The additional constraints have significantly affected the mean profit distribution. The minimum and maximum sampled mean profits are now \$12,448 and \$12,910, respectively, with an average of \$12,662 and a standard deviation of \$62. The NC expected profit is \$12,678. Additionally, the difference between the theoretical mean profit UB and LB is only \$1,222, which is considerably less than in our previous cases. What little difference there is between mean profits is due to dependence in the joint distribution that cannot be described by pairwise correlations and a normal copula.

Table 6.15: Percentiles for mean profit, standard deviation of profit, and investment risks for JDSIM joint distributions given marginal information and all pairwise correlation coefficients.

	Percentiles						
	0%	10%	25%	50%	75%	90%	100%
Mean	\$12,448	\$12,583	\$12,620	\$12,662	\$12,704	\$12,741	\$12,910
Std. Dev.	\$18,530	\$19,767	\$20,063	\$20,400	\$20,750	\$21,051	\$22,280
Inv. Risk	18.45%	24.63%	25.98%	27.54%	29.18%	30.76%	36.50%

	Statistics			
	LB	μ	σ	UB
Mean	\$12,049	\$12,662	\$62	\$13.271
Std. Dev.	NA	\$20,404	\$499	NA
Inv. Risk	9.55%	27.64%	2.36%	63.72%

The new distribution of the standard deviation of profit ranges from \$18,530 to \$22,280, with an average \$20,404. The distribution of the investment risk has been shifted towards lower values (although the LB has increased), with a new range from

18.45% to 36.50%. The average investment risk is now 27.64%.

The bounds for the cdfs when all pairwise correlations are known are shown in Figures 6.17 and 6.18. Both the probability and the absolute boundaries are narrower than before. CR's NC-cdf falls slightly outside of the probability bounds for profit values of -$2,000 to $25,000. This suggests that the NC approach, which specifies a single joint distribution, may not generate an approximation that is representative of the set of all distributions matching the assessed information.

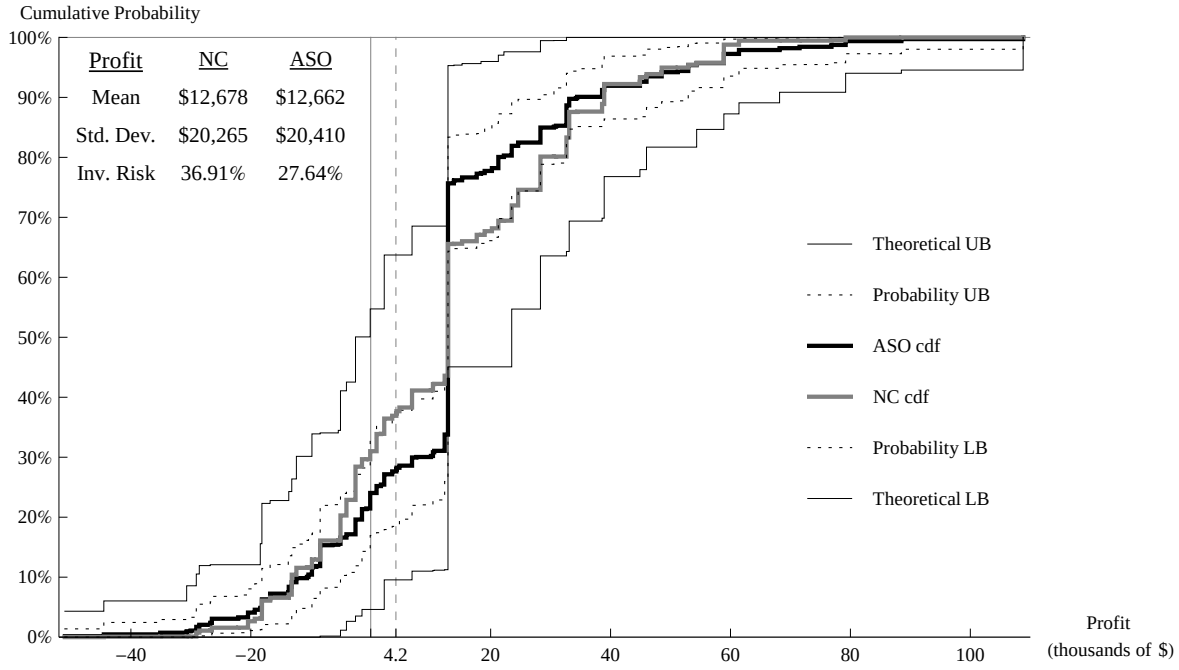

Figure 6.17: Risk profile range given marginal information and all pairwise correlation coefficients, minimum and maximum probability bounds (dashed), theoretical bounds (solid), DAC (black) and NC (gray).

We conjecture that the extreme behavior of the NC with respect to the probability bounds is related to the structure provided by the normal copula. The normal pdf has maximum entropy for a given mean and standard deviation. We suspect that joint distributions formed with a normal copula are also high in entropy. Indeed, in our case, CR's NC-cdf and the (Figure 6.18) maximum-entropy cdf (given

marginal and all pairwise correlations) are very close to each other, with a maximum absolute difference among the probabilities of the joint events of 0.0037, whereas the corresponding difference between NC and DAC is 0.1992. A maxent joint distribution based on marginals and pairwise correlations will enforce higher-order dependencies that are as close to independence as possible. This cdf will then tend to be an extreme point within our truth set. As a simple illustration, assume two identical binary random variables with marginals of $\{0.9, 0.1\}$ and unknown correlation. With this information, all the possible distributions are a convex combination of $\{0.9, 0, 0, 0.1\}$ and $\{0.8, 0.1, 0.1, 0\}$. Hence, $\mathbb{T}$ forms a line section with center at $\{0.85, 0.05, 0.05, 0.05\}$, whereas maxent is located at $\{0.81, 0.09, 0.09, 0.01\}$, close to the second extreme point.

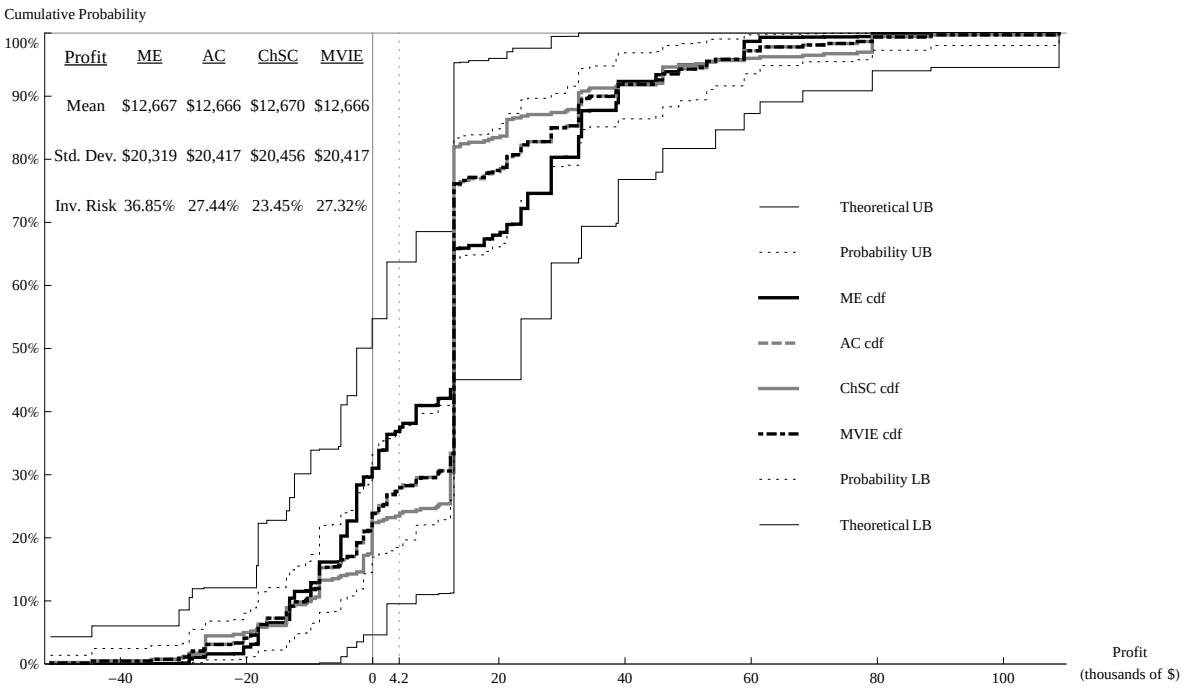

Figure 6.18: Risk profile range given only marginal information and all pairwise correlation coefficients, minimum and maximum probability bounds (dashed), theoretical bounds (solid), ME (black), AC (gray-dashed), ChSC (gray), and MVIE (black-dotdashed).

The new information has reduce the profits range and reshaped the approximations to the joint distribution. We are able to observe that, as before, ChSC and ME get closer (or violate) the probability bounds in opposite sides of the range. Whereas, AC and MVIEC get closer to each other and to DAC. In this case the approximation with smallest investment risk is ChSC. However, the approximation with largest expected profit is still the NC.

6.2.4.4 Comparing the Three Information Cases

Figures 6.19(a), 6.19(b), and 6.19(c) compare the pdfs (frequencies) of our sampled expected profits, standard deviations, and investment risk, respectively. The distribution for Case One, using only marginal information, is presented as the dotted line filled in white. Case Two, using marginal information and one pairwise correlation coefficient, is presented as the dashed line filled in gray. Finally, Case Three, with all marginal information and pairwise correlation assessments, is presented in a solid line filled in black. The vertical lines correspond to the probability bounds for each case mark in dotted (Case One), dashed (Case Two), and solid lines (Case Three).

The range of outcomes for Case One (only marginals) stems from our having not constrained marginal families or the dependence structure. The addition of a negative correlation between PL and H, in Case Two, shifted the set of possible profits to the left and narrowed it somewhat. The specification of all pairwise correlations, in Case Three, constrained the set considerably. The variability that does exist is related to our marginals' not having been based on known families and that higher-order dependencies (beyond pairwise) were not fixed. This indicates that assessing these higher-order distributions (e.g., all three-way assessments) will not improve the decision.

The investment-risk distributions show less sensitivity to the dependence structure. Although additional constraints had a significant impact on the distribution of

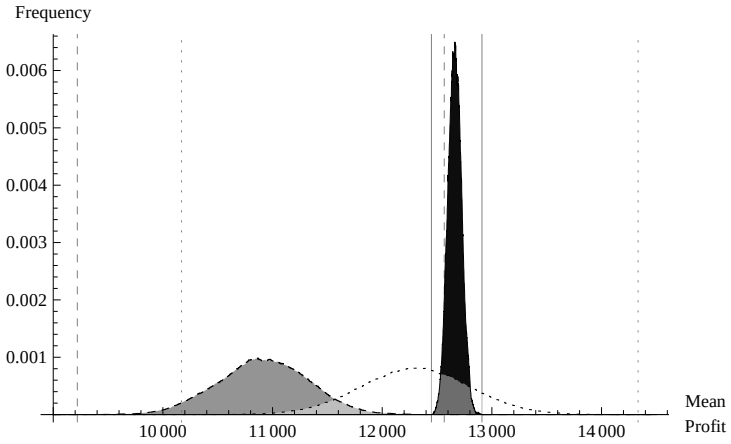

(a) Mean Profit.

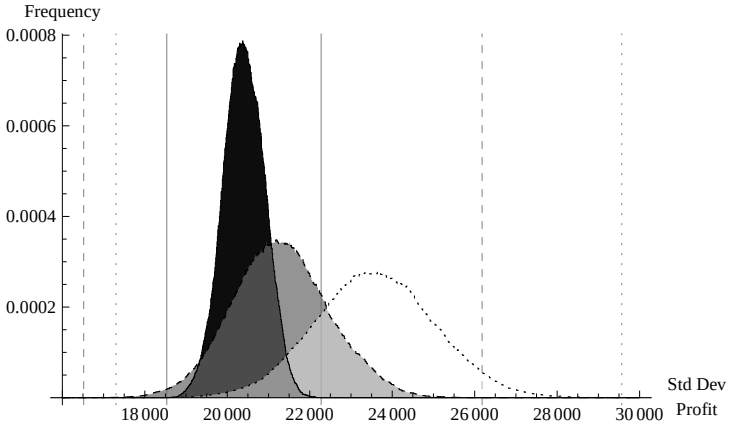

(b) Standard Deviation

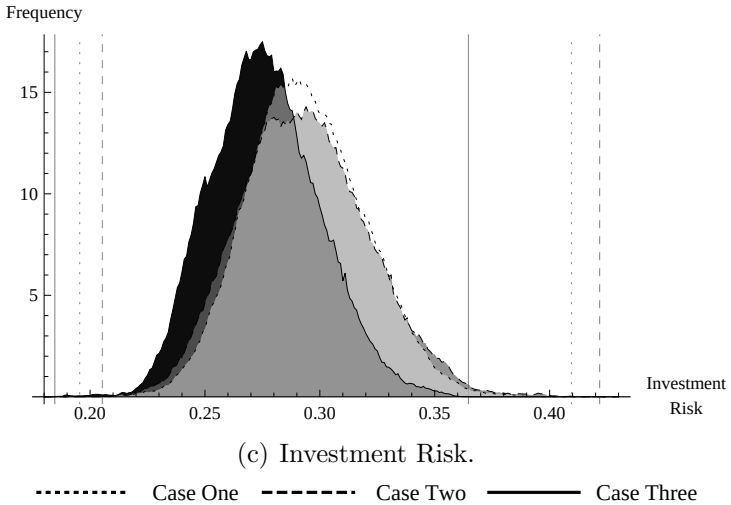

(c) Investment Risk.

Case One Case Two Case Three

Figure 6.19: Sampled distributions for mean profit, standard deviation of profit, and inv. risk given marginals only (white), marginals and one pairwise correlation (gray), and marginals and all pairwise correlations (black).

expected profit and the standard deviation of profit, the probability of being less than $4,200 has not changed significantly.

6.2.4.5 Decision Robustness

Since we are evaluating the decision (Expand versus MM, in this case) under each simulated joint distribution, we can test the robustness of each alternative. Specifically, we can determine in which fraction of our simulated joint distributions each alternative was preferred. As discussed above, none of our observed distributions results in the MM being the preferred alternative, even based solely on marginal information. Therefore, to demonstrate the idea of robustness, assume that Dick Carothers is considering an additional alternative that delivers $11,000 for certain.

Table 6.16 shows the fraction of times that the Expand alternative was optimal for our three cases (these frequencies can also be estimated directly from Figure 6.19(a)). Given only marginal assessments, Expand was optimal under 99.56% of simulated pmfs. This dropped to 42.27% given marginals and that the correlation between PL and H is -0.38. Finally, given marginals and all pairwise correlations, Expand was optimal (an expected value greater than $11,000) in all 10 million of our simulations (100%). We believe this degree of insight will address a primary concern held by most decision makers, "Am I making a mistake by choosing this alternative?" and will thereby increase decision quality and commitment to action. Approaches that posit a single joint distribution (e.g., copula-based methods) cannot provide this type of feedback.

Table 6.16: Percentage of Times the Alternative is Optimal

Information	Expand	11K	MM
Marginal assessments	99.56%	0.44%	0%
Marginal and one correlation assessment	42.27%	57.73%	0%
Marginal and correlation assessments	100.00%	0%	0%

6.2.5 Final Comments

Both the Joint Distribution Simulation (JDSIM) and the Normal Copula (NC) approaches propose a method to model probabilities and decisions when only partial probabilistic information is available. The NC approach assumes a copula in order to specify a single joint probability distribution. JDSIM, in contrast, explores the set of all joint distributions that match the available information.

JDSIM provides a flexible and powerful tool to analyze stochastic decision models when the joint distribution is incompletely specified. The methodology is easy to implement, develops a collection of joint distributions, and represents a significant extension to previous approximation models such as the copula-based approach illustrated by CR. We demonstrated the JDSIM procedure with a canonical example based on marginal and pairwise rank correlation coefficients. The methodology can be extended to more than four random variables, to random variables with more than three possible outcomes, and to higher-order conditioning such as three-way assessments.

On average, the profit joint distributions produced by JDSIM resulted in expected values and standard deviations similar to those of NC. The primary difference, in the case examined here, seems to be differing estimates for particular cumulative probabilities. For example, the NC cdf produced cumulative probabilities for mid-range profits that were extreme relative to our sample. This is potentially important in the Eagle Airlines case because this profit range included the value of the competing alternative. Thus, the two methods might produce very different estimates of investment risk (the probability of under performing the competing alternative). This being said, more research needs to be done to better understand if it is possible to faithfully represent the JDSIM sample with a single joint distribution across a range of applications.

JDSIM's strength is also a potential weakness, as the decision is not valued or made under a single distribution, but rather under thousands (possibly millions) of feasible distributions. NC provides a single, approximate distribution, but, as discussed above, our results suggest that this approximation may not be representative of the set of possible joint distributions. The accuracy of the normal copula approach is an open question, but one that could be addressed by comparing it to the JDSIM results.

The information provided by this new simulation procedure provides insight regarding the shape of the truth set. At this point, we do not claim to know the likelihood of the distributions in the collection sampled. However, we can clearly state that assuming independence in scenarios with incomplete or unknown information provides approximations that are extreme relative to the other distributions in the truth set. This provides yet another example of the importance of not ignoring dependence.

Chapter 7

Future Research

This chapter presents several ideas for future research that build upon the work presented in this dissertation. These consist of a new sampling procedure named the Randomized Ping-Pong Sampler, alternative procedures to measure the volume of the relative interior of $\mathbb{T}$ (measures of precision), and different bounds of polyhedra that work as worst cases for the approximation distributions.

7.1 The Randomized Ping-Pong Sampler

Modifying the HR algorithm can increase the probability of sampling low-probability neighborhoods of $\mathbb{T}$, specifically the areas close to the vertices. The proposed modification could be called the Randomized Ping-Pong Sampler algorithm. It is designed to force the Markov Chain to select a new point along the direction of one of the vertices of $\mathbb{T}$ with probability p, or a jump along the direction of the center of $\mathbb{T}$ with probability $1-p$. When $p = 0.5$, the algorithm would be expected to oscillate like a ping-pong ball.

The Randomized Ping-Pong behavior is created by means of two subproblems. The first one takes a random direction (as with the Hit-and-Run sampler), solves a Linear Program (LP) to find a vertex, and uses the vertex to create a new point. This problem needs to be solved at each iteration with probability p, but LPs run

efficiently in practice. The second subproblem is to find a center of $\mathbb{T}$, which would need to be run only once in the initialization. Hence, even if the problem is difficult, it does not affect the efficiency of the sampling process. The center of $\mathbb{T}$ is mainly used to ensure that as the dimension increases, the sample includes areas of the set that otherwise might be ignored.

Randomized Ping-Pong Sampler Algorithm

1. Select a starting point x_0 at the center of $\mathbb{T}$, define $\alpha \in [0, 0.5]$, set $i = 1$ and choose K as the number of iterations.

2. Generate a random point r in the interval $[0, 1]$.

3. If $r < \alpha$, go to Step 4. Else, go to Step 5.

4. Perform the following:

   (a) Generate the direction $d_i = (x_0 - x_i)/||x_0 - x_i||$.

   Find the line set $L = \mathbb{T} \cap \{x | x = x_i + \lambda d_i, \lambda \text{ a real scalar}\}$.

   (b) Generate a random point x_{i+1} uniformly distributed over L.

5. Perform the following:

   (a) Generate n independent normally distributed random deviates $N = \{N_1, N_2, \cdots, N_n\}$ and set $c_{i+1} = N/||N||$.

   (b) Solve the subproblem:

$$\begin{aligned} \max \quad & c_i \cdot v_i, \\ s.t. \quad & v_i \in \mathbb{T}. \end{aligned}$$

(c) Generate the direction $d_i = (v_i - x_i)/||v_i - x_i||$.

Find the line set $L = \mathbb{T} \cap \{x | x = x_i + \lambda d_i, \lambda \text{ a real scalar}\}$.

(d) Generate a random point x_{i+1} uniformly distributed over L.

6. If $i = K$ iterations, stop. Otherwise, set $i = i + 1$ and return to Step 2.

Initializing the algorithm requires defining a center, for which one simple procedure is to choose the center of the maximum volume ellipsoid inscribed in $\mathbb{T}$. Additionally, other centers of polyhedra can be used, such as the analytic center (used in interior point algorithms) or the Chebyshev's center, which is the farthest point from the boundary of $\mathbb{T}$.

Figures 7.1, 7.2, and 7.3 graphically describe the algorithm in two dimensions. After defining the center of $\mathbb{T}$ and the parameter α, we start with a random point in the interior of the set (Fig. 7.1(a)). Then, r is randomly chosen and brings about Step 4 if $r < \alpha$ or Step 5 if $r \geq \alpha$ (Fig. 7.1(b)).

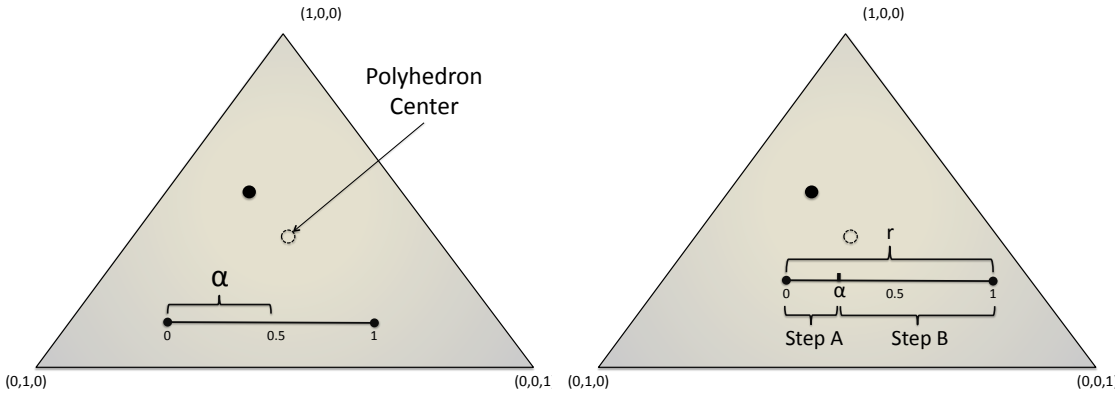

(a) Ping-Pong Sampler initialization

(b) Choose r uniformly from (0,1).

Figure 7.1: Randomized Ping-Pong Sampler. Initialization steps.

After choosing r, the algorithm selects between Step 4 and Step 5. If Step 4 is chosen, create the line L and select a random point uniformly from it (Fig. 7.2(a)-7.2(c)).

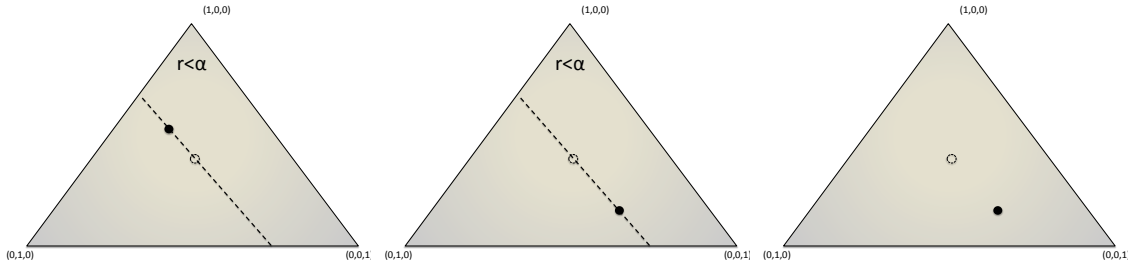

(a) Define L using center. (b) Select a uniform point in L. (c) Go to Figure 7.1(b).

Figure 7.2: Randomized Ping-Pong Sampler, Step 4. Illustration of the algorithm in two dimensions.

If Step 5 is chosen, define a direction (Fig. 7.3(a)-7.3(b)). Use the direction to solve the LP subproblem (Fig. 7.3(c)). Create the line L and select a random point uniformly from it (Fig. 7.3(d)-7.3(e)). Repeat the procedure from the new random point (Fig. 7.3(f) and 7.2(c)).

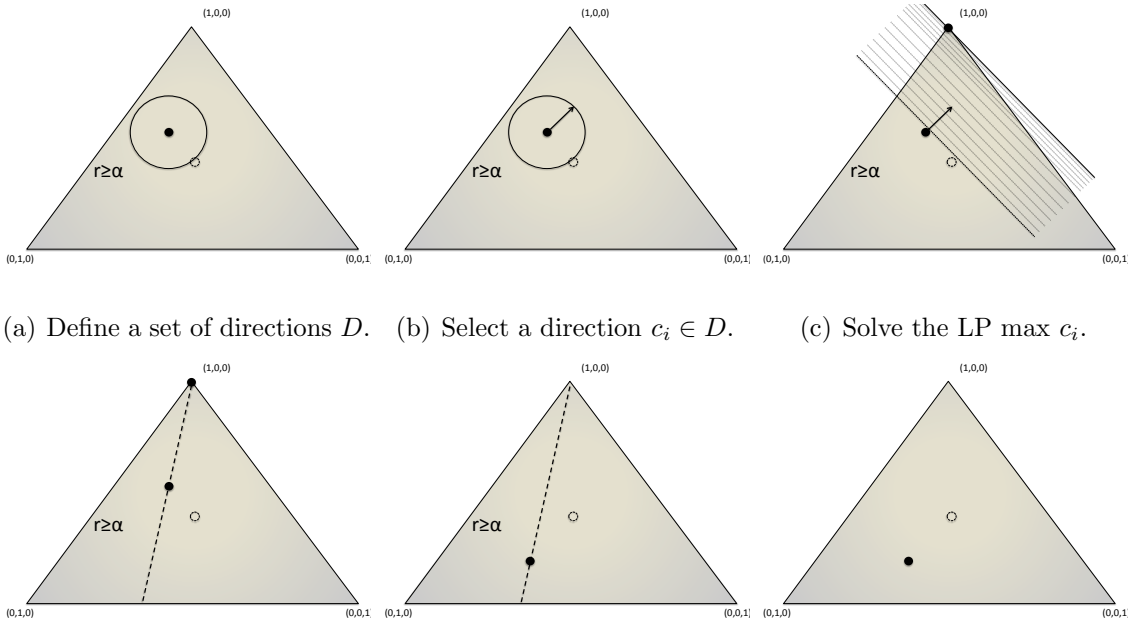

(a) Define a set of directions D. (b) Select a direction $c_i \in D$. (c) Solve the LP max c_i.

(d) Define L using v_i. (e) Select a uniform point over L. (f) Go to Figure 7.1.

Figure 7.3: Randomized Ping-Pong Sampler, Step 5. Illustration of the algorithm in two dimensions.

The samples produced by the Randomized Ping-Pong algorithm explore $\mathbb{T}$ using a different paradigm from the one used in HR. The sample finds joint distributions along the corners where the volume is scarce, thereby recovering distributions that are hard to sample using HR. Figure 7.4 describes the Euclidean distance from the center of an unconstrained set to a collection of joint distributions sampled with the Randomized Ping-Pong algorithm, for three, five, and seven binary r.v.. The Randomized Ping-Pong algorithm covers a broader range of distributions than those shown in Figure 3.5, most of which have low probability of being sampled under a uniform sampling.

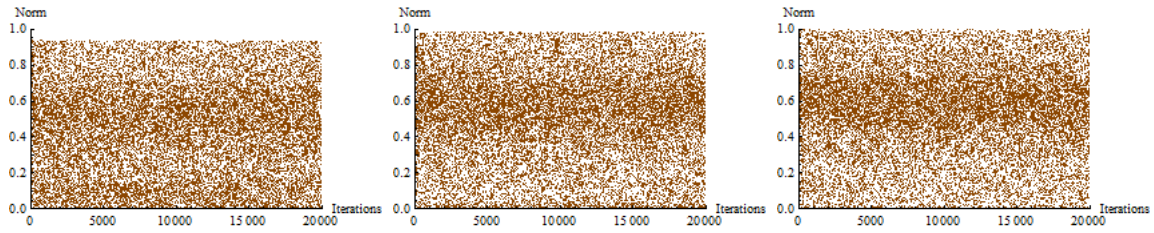

(a) Three Variables. (b) Five Variables. (c) Seven Variables.

Figure 7.4: Normalized Ping-Pong sampler: Norm distance from the center of $\mathbb{T}$, for various numbers of binary random variables.

Figure 7.5 shows the histogram of the Euclidean distance corresponding to Figure 7.4. The histogram clearly show that the distance from the center has a uniform pattern, which oppose the results from the samples taken using HR. The Randomized Ping-Pong sampler raises the probability of sample distributions that otherwise are rare or unlikely to occur in nature or through uniform sampling. The same behavior observed in Figures 7.4 and 7.5 can be observed for variables with three outcomes. (See Appendix A, Figure A.2.)

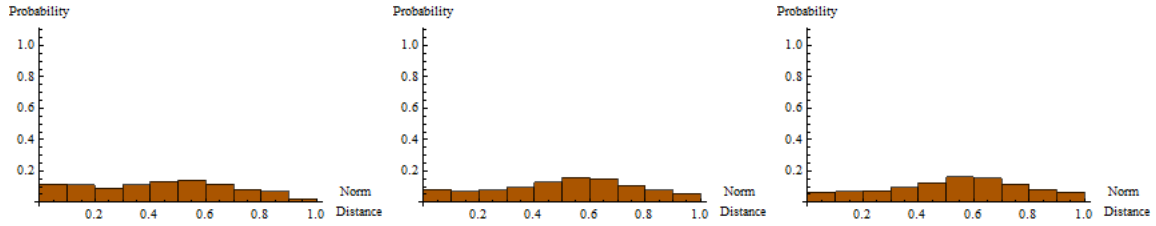

(a) Three Variables. (b) Five Variables. (c) Seven Variables.

Figure 7.5: Randomized Ping-Pong sampler: Norm distance from the center of $\mathbb{T}$, for various numbers of binary random variables.

7.2 Measures of Precision

New methods to measure the precision of a truth set $\mathbb{T}$ should be developed. The precision of a set can be characterized by its size. For example, in a small set $\mathbb{T}$, a sampled collection of distributions taken with the HR sampler will have joint elements close to each other. Then, any approximation inside $\mathbb{T}$ will be close to any element from the sample, and the difference in accuracy for two approximations will be minimal. However, if $\mathbb{T}$ is large, the accuracy of the approximations will vary significantly.

Because there are many definitions for size of $\mathbb{T}$. We informally define "measure of precision" as a function $f(\mathbb{T})$ that describes the n-content of a set $\mathbb{T}$.

7.2.1 Volume Ratio

The most intuitive concept to measure the size of a polytope is its relative volume (n-content). Bertsimas and Tsitsiklis (1997) defined the volume as

$$Vol(\mathbb{T}) = \int_{\mathbf{x}\in\mathbb{T}} d\mathbf{x}. \tag{7.1}$$

Equation (7.1) is zero for every $\mathbb{T}$ since the polytope is not full dimensional.

However, we can apply a transformation $\mathbf{A}$ such that $\mathbf{A}\mathbb{T}$ is full dimensional in a new cardinal system with fewer dimensions. For example, a random variable with three outcomes has a probability distribution that generates a set $\mathbb{T}$ shaped as a triangle with corners in the unit vectors. Then, the 2-content of $\mathbb{T}$, or $cont_2(\mathbb{T})$, is the area of a two-dimensional equilateral triangle $\left(\frac{\sqrt{3}}{2!}\right)$.

In general, for an unconstrained joint distribution with n outcomes, $cont_{n-1}(\mathbb{T}) = \frac{\sqrt{n}}{(n-1)!}$, which is equivalent to the surface of a hyper-plane that intersects the positive hyper-octant. Kannan et al. (1996) presented a method to calculate $cont_{n-1}$ in general convex bodies. However, the procedure can be slow for large n.

Unfortunately, this measure of precision is weak at comparing the size of polytopes with different dimensions. For example, for unconstrained polytopes of dimensions 3, 4, 5, and 6, the respective $cont_n(\cdot)$ are $\frac{\sqrt{3}}{2!}$, $\frac{\sqrt{4}}{3!}$, $\frac{\sqrt{5}}{4!}$, and $\frac{\sqrt{6}}{5!}$. As the dimension increases, $cont_n$ decreases, which is counterintuitive. Moreover, making its values meaningful would require a frame of reference. One solution is to standardize the relative volume as a percentage of the maximum volume (without constraints). Then, the volume ratio (VR) can be defined as follows:

$$VR(\mathbb{T}) = \frac{(n-1)!\ \ cont_n}{\sqrt{n}}, \tag{7.2}$$

where $VR(\mathbb{T}) = 1$ means $\mathbb{T}$ is at its maximum, and $VR(\mathbb{T}) = 0$ defines a singleton.

The method described by Kannan et al. is based on a series of concentric hyper-spheres $\mathbb{B}_0 \subset \mathbb{B}_1 \subset \cdots \subset \mathbb{B}_r$ where $\mathbb{B}_0 \subset \mathbb{T} \subset \mathbb{B}_r$. The ratio $\mathbb{S}_1 = \frac{Vol(\mathbb{T} \cap \mathbb{B}_1)}{Vol(\mathbb{T} \cap \mathbb{B}_0)}$ describes a differential in volume on the outer shell of $\mathbb{T} \cap \mathbb{B}_1$, Then,

$$Vol(\mathbb{T}) = Vol(\mathbb{T} \cap \mathbb{B}_r) = \frac{Vol(\mathbb{T} \cap \mathbb{B}_r)}{Vol(\mathbb{T} \cap \mathbb{B}_{r-1})} \cdot \frac{Vol(\mathbb{T} \cap \mathbb{B}_{r-1})}{Vol(\mathbb{T} \cap \mathbb{B}_{r-2})} \cdots \frac{Vol(\mathbb{T} \cap \mathbb{B}_1)}{Vol(\mathbb{T} \cap \mathbb{B}_0)} \cdot Vol(\mathbb{T} \cap \mathbb{B}_0)$$

$$Vol(\mathbb{T}) = cont_n(\mathbb{T}) = Vol(\mathbb{T} \cap \mathbb{B}_0) \cdot \mathbb{S}_r \cdot \mathbb{S}_{r-1} \ldots \mathbb{S}_1.$$

Then the ratio $\mathbb{S}_i \ \forall i$ can be calculated by uniformly sampling the set $\mathbb{T} \cap \mathbb{B}_i$ and observing the ratio of the samples that belong to the set $\mathbb{T} \cap \mathbb{B}_{i-1}$. This method requires extensive sampling for high-dimensional sets.

7.2.2 Long and Short Diameters

Diameter is determined by the longest chord embedded in $\mathbb{T}$. Determining this "long chord" (Ch_L) precisely is difficult, but it can be approximated by a simple heuristic. This measure is bounded by $\sqrt{2}$ in the case of unconstrained sets, and by zero in the case of a singleton. The long chord is a standardized measure of precision for a polytopes with different dimensions, since the bounds are invariant with $\mathbb{T}$.

As seen before, when sampling uniformly from $\mathbb{T}$, the probability of sampling in an area near a vertex is close to zero. Therefore, the long chord in $\mathbb{T}$ is larger than the longest chord of the convex hull of a uniform sample taken from $\mathbb{T}$ using the HR sampler. The latter is defined as the "short chord" (Ch_S) and describes the largest cord inside a subset of $\mathbb{T}$ that encloses most of the volume.

Then $Ch_S(\mathbb{T}) < Ch_L(\mathbb{T})$, where the left-hand term disregards the parts of the set where the volume is negligible, and the right-hand term utilizes all of the set. These values can be estimated by sampling $\mathbb{T}$ using the HR and Randomized Ping-Pong samplers as discussed in the next section. Once the sample is obtained, we need to find $\mathbf{p^1}$ and $\mathbf{p^2}$ such that $\mathbf{L}_n^2(\mathbf{p^1}, \mathbf{p^2}) \geq \mathbf{L}_n^2(\mathbf{p^i}, \mathbf{p^j}) \ \ \forall \ i, j$.

To find the diameters of the long and short chords is also computer intensive, since we need to observe the relations among a large series of data points. In future research, we will look for more efficient ways to achieve this goal. The measures of precision for any truth set could be used to infer the size of set $\mathbb{T}$.

7.3 Bounds of Polyhedra

After a uniform sample of $\mathbb{T}$ has been created, it could be of interest to explore differences among the sample and the original set to look for extreme or worst cases. This can be done by exploring the bounds of the polyhedra. Two particular cases of interest are the minimum entropy distribution and the farthest distribution from an approximation $\mathbf{p}_A^*$. Exact values for these bounds are difficult to calculate, but they can be approximated.

We propose two alternative procedures to find bounds: a sampling method that looks for extreme points, and one that looks algorithmically for distributions that are not necessarily the bounds but provide adequate solutions in the ρ-optimality range (Vazirani, 2003). Figure 7.6 shows the general idea: starting with $\mathbb{T}$, create a sample from $\mathbb{T}$ and complement it by looking for possible bounds for the set.

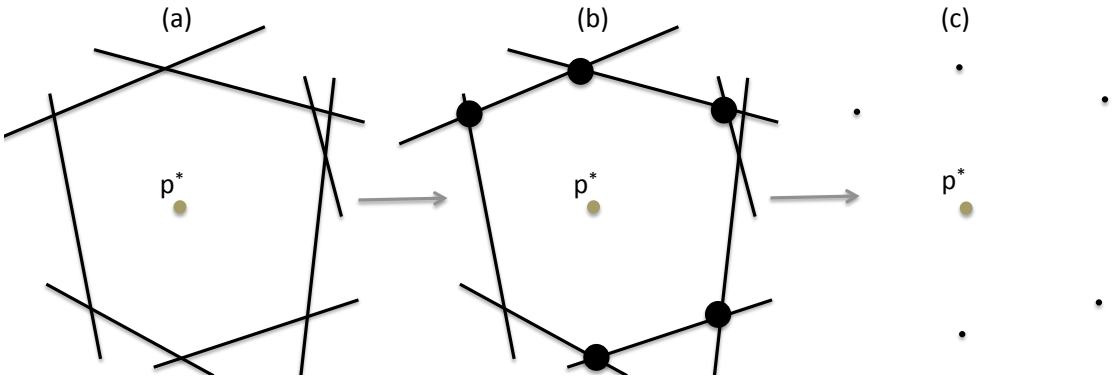

Figure 7.6: (a) Set $\mathbb{T}$, (b) Sample from $\mathbb{T}$, (c) Bounds for $\mathbb{T}$.

Previously, we mentioned that $\mathbb{T}$ can be evaluated in the geometric space or the information space. In the geometric space, the objective is to minimize the maximum Euclidean distance from the center to the boundary of the polyhedron, considering that the choice of center depends on the model used. In this context, the probability that a distribution is in the neighborhood of $\{\frac{1}{3}, \frac{1}{3}, \frac{1}{3}\}$ is the same as that of its being

in the neighborhood of $\{0, 0, 1\}$, that is, the vectors inside $\mathbb{T}$ are distributed uniformly.

In contrast, the information space establishes a distribution over $\mathbb{T}$ based on the multiplicity of each joint distribution. When dealing with uncertainty, distributions like $\{\frac{1}{3}, \frac{1}{3}, \frac{1}{3}\}$ seem more natural than distributions like $\{0.05, 0.05, 0.9\}$, in agreement with the principle of insufficient reason and the principle of maximum entropy. In this context, the most likely distributions are in the neighborhood of maximum entropy, which means that the vectors inside $\mathbb{T}$ are not distributed uniformly.

This section will provide bounds for $\mathbb{T}$ in both spaces, for the purpose of deriving worst-case scenarios for analysis.

7.3.1 Geometric Space Bounds

In the geometric space, we want to find the joint distribution in $\mathbb{T}$ for which our approximation distribution would be as inaccurate as possible (worst case). The problem can be represented as $\max ||x - x_c||$ s.t. $x \in \mathbb{T}$ for a given approximation x_c, and belongs to the NP-complete class. This objective function specifies a maximization of a convex function over a convex set, that is, that the global optimum is at a vertex of $\mathbb{T}$. This problem has many local optimum points, and the only way to find the worst possible case is to test them all.

To avoid an exhaustive search, two alternatives provide a reasonable approximate solution to the worst case.

7.3.1.1 Approximation Model

The first model consists of replacing $\mathbb{T}$ with a different set that imitates the shape of the original polyhedron. One option is to use the largest volume ellipsoid inscribed in $\mathbb{T}$, described in Chapter 2. The ellipse defined by problem 2.11 is represented by the matrix E, the eigenvectors of the matrix represent the axes of the

ellipsoid, and the eigenvalues represent the magnitude of the axes. The problem is to find the maximum geometric distance $\prod_{i=1}^{n} \lambda_i$ of the eigenvectors. The result yields an ellipse whose major axis (that with the largest eigenvalue) points in a direction that approximates the location of the vertices that are farthest from the ellipsoid center.

Then the axes of the ellipse can be used to define two directions c and $-c$, to solve:

$$\begin{array}{lll} \max & c \cdot x, & \max \quad -c \cdot x, \\ s.t. & x \in \mathbb{T}, & s.t. \quad x \in \mathbb{T}. \end{array}$$

The LP formulation uses the major axis to find a vertex far from the neighbor of x_c. This vertex can be used as an approximation for a worst-case scenario.

If we use all axes of the ellipsoid, and for each axis solve two LPs, the procedure is equivalent to creating a box around the ellipsoid and expanding that box to find the farthest vertices in each direction. In this case, our approximation could be off by at most $\sqrt{\sum_{i=1}^{n} \lambda_i^2)} - \lambda_{max}$. This bound is largest when all lambdas are equal, which makes the bound $(\sqrt{n} - 1) \cdot \lambda$.

The procedure generates an approximation of a worst-case joint distribution with an approximation factor of $(\sqrt{n} - 1)$. The approximation factor becomes weaker as the dimensionality of the set increases, making it less desirable for joint probability distributions with many elements. However, it is simpler than the heuristic alternative.

7.3.1.2 Heuristic Model

The second alternative consists of a boundary sampling procedure. We use the fact that the Randomized Ping-Pong algorithm creates at least one extreme point of

$\mathbb{T}$ at each iteration. Then we can sample a large number of vertices and observe the one that is the farthest one.

Creating a collection of samples using the Randomized Ping-Pong also defines a set of randomly selected extreme points. Thus, the problem can be simplified to an evaluation procedure of the distance to x_c for a randomly selected set of extreme points. The use of this heuristic boundary comes for free when running the Randomized Ping-Pong sampler, and as the number of iterations increases, the algorithm converges to a global optimum.

The farthest a joint distribution is from the center of $\mathbb{T}$, the easiest is to find it. For a distribution to be far from the neighborhood of x_c some of the active constraints must be as parallel as possible. When solving the sub-problem in Step 3 of the Randomized Ping-Pong sampler, the range of the vector c_i that returns this particular vertex also increases. And since c_i is uniformly distributed on a unit ball, the probability of choosing a given c_i increases as the distance of the resulting vertex from x_c increases.

This heuristic reduces to selecting points uniformly from a finite surface divided into sections of different size. If the points are selected uniformly, in the limit, there will be at least one point in each section, providing the optimal solution. Moreover, largest sections have largest probability of being selected, where the largest sections correspond to vertices that are further than most extreme points. Hence, the heuristic relies in that the worst cases are easier to find than all other extreme points.

The probability of finding the optimal solution in n iterations is $1 - (1 - p)^n$, from the binomial distribution with parameters n and p, where p is the probability of selecting the area that reaches the optimal solution. The rate to which the probability of finding a solution converges to one is $(1 - p)$, showing that the rate improves as the optimal vertex gets farther from the center.

7.3.2 Information Space Bounds

In contrast to the geometric space, the information space describes the structure of the joint events in a jpmf according to the number of bytes required to describe the outcome of the uncertainties. Entropy can be understood as the expected number of "yes/no" questions that need to be asked in order to find the outcome of an experiment for some joint distribution. Then, maximum entropy looks for the distribution in $\mathbb{T}$ for which the expected number of questions required to describe the outcome is as large as possible. In a similar way, minimum entropy looks for a distribution for which the expected number of questions is the lowest.

Minimum entropy reduces to maximizing a convex function over a convex set, and the only method to find a global optimizer is true exhaustive search of the vertices in $\mathbb{T}$. However, for an unconstrained joint distribution, the minimum entropy is given by a distribution of the form $\{1, 0, 0, \ldots, 0, 0\}$, showing that entropy is bounded below by zero. Then, a global worst case scenario can be approximated by finding distributions that share similar characteristics, specifically those with the largest quantity of zeros.

Unlike maximum entropy, minimum entropy does not necessarily have a unique optimal solution, e.g., an unconstrained binary distribution has two possible distributions with minimum entropy $\{1, 0\}$ and $\{0, 1\}$. And the problem became harder as the complexity of $\mathbb{T}$ increases. Moreover, the number of optimal solutions increases with the dimension of the set. We propose two alternatives to provide an approximate solution for the worst case in the information space.

7.3.2.1 Approximation Model

This approximation model looks for distributions with joint probabilities that have a mass as concentrated as possible. Such distributions are on the extreme

points of $\mathbb{T}$ and contain the most zeroes of any distribution. Additionally, of those distributions having the same number of zeroes, those with the least homogeneous arrangement will have the lowest entropy. These two characteristics provide distributions with entropy close to the minimum entropy, but under no circumstances represent necessary or sufficient conditions. We can provide a lower bound for the minimum entropy. This lower bound can be used to assess the approximation factor of the worst-case scenario. Then for a distribution $P = \{p_1, p_2, \cdots, p_n\}$, the entropy function $H(P) = -\sum_{i=1}^{n} p_i \cdot \log p_i$, and the largest element of P, p_{max}, we have:

$$H(P) \geq H_{LB} = H(p_{max}, 1 - p_{max}) + k \cdot p_{max} \cdot \log k, \quad \frac{1}{k+1} \leq p_{max} \leq \frac{1}{k}. \tag{7.3}$$

To find the tightest bound requires only to solve for the largest possible p_{max} that can exist in $\mathbb{T}$. This problem is simple and is defined as follows:

$$\begin{aligned} \max \quad & p_i, && \forall i = \{1, 2, \ldots, n\}, \\ s.t. \quad & p \in \mathbb{T}. \end{aligned}$$

Then the minimum entropy approximation problem is described as follows:

$$H_{\mathbb{T}} \min \quad \sum_{i=1}^{n} y_i - p_i^2, \tag{7.4}$$

$$s.t. \quad A \cdot p = b, \tag{7.5}$$

$$y_i - p_i \geq 0, \qquad \forall i = 1, \ldots, n, \tag{7.6}$$

$$p_i \geq 0, \qquad \forall i = 1, \ldots, n, \tag{7.7}$$

$$p = \{p_1, \ldots, p_n\} \in \mathbb{R}, \qquad y = \{y_1, \ldots, y_n\} \in \{0, 1\}. \tag{7.8}$$

Model 7.4 is a non-linear integer programing (NLIP) formulation. Its objective

function minimizes the number of nonzero elements, while the squared term helps to find the most uneven distribution from those with few nonzeros. Constraints 7.5 and 7.7 define the set $\mathbb{T}$, while constraints 7.6 and 7.8 push the elements of the distribution to zero. The solution of this model is a local optimum, where $H_{\mathbb{T}} \geq H_{min} \geq H_{LB}$.

7.3.2.2 Heuristic Model

The heuristic model is similar to the one described for the geometric space. Each iteration of the Randomized Ping-Pong sampler finds a vertex whose entropy then needs to be tested, in order to ultimately select the distribution with the least entropy.

The convergence rate for the minimum entropy heuristic is worse than that for the maximum distance heuristic. However, the convergence rate is bounded by $(1 - p_{max}) \leq (1 - p) \leq (1 - p_{min})$. In the limit, the heuristic finds the minimum entropy distribution.

The bounds, however, present a different challenge. Lowell (1994) presented the maximum entropy distribution as a maximization problem of a concave function over a convex set. Hence, the minimum entropy distribution needs to result from a minimization problem over a concave function, which means that the solution lies in an extremity of $\mathbb{T}$. Therefore, the minimum entropy problem is NP-hard and thus requires approximation algorithms. Lin Yuan Kesavan (1998) and Waterloo (1994) included special cases for which minimum entropy can be efficiently calculated, and Watanabe (1981) presented a method using pattern recognition to approximate minimum entropy in special cases. But the general case nonetheless remains a hard problem.

Appendix

Appendix A

Hit and Run Sampler and Ping-Pong Sampler Plots

The plots replicate the behavior of binary joint distributions seen in Chapter 2 and 7, using distributions with three outcomes.

- Hit and Run: Norm Distance And Histograms For 3, 5, and 7 Variables With 3 Outcomes.

- Ping-Pong: Norm Distance And Histograms For 3, 5, and 7 Variables With 3 Outcomes.

Hit and Run: Norm Distance And Histograms For 20000 Samples For 3, 5, and 7 Variables With 3 Outcomes.

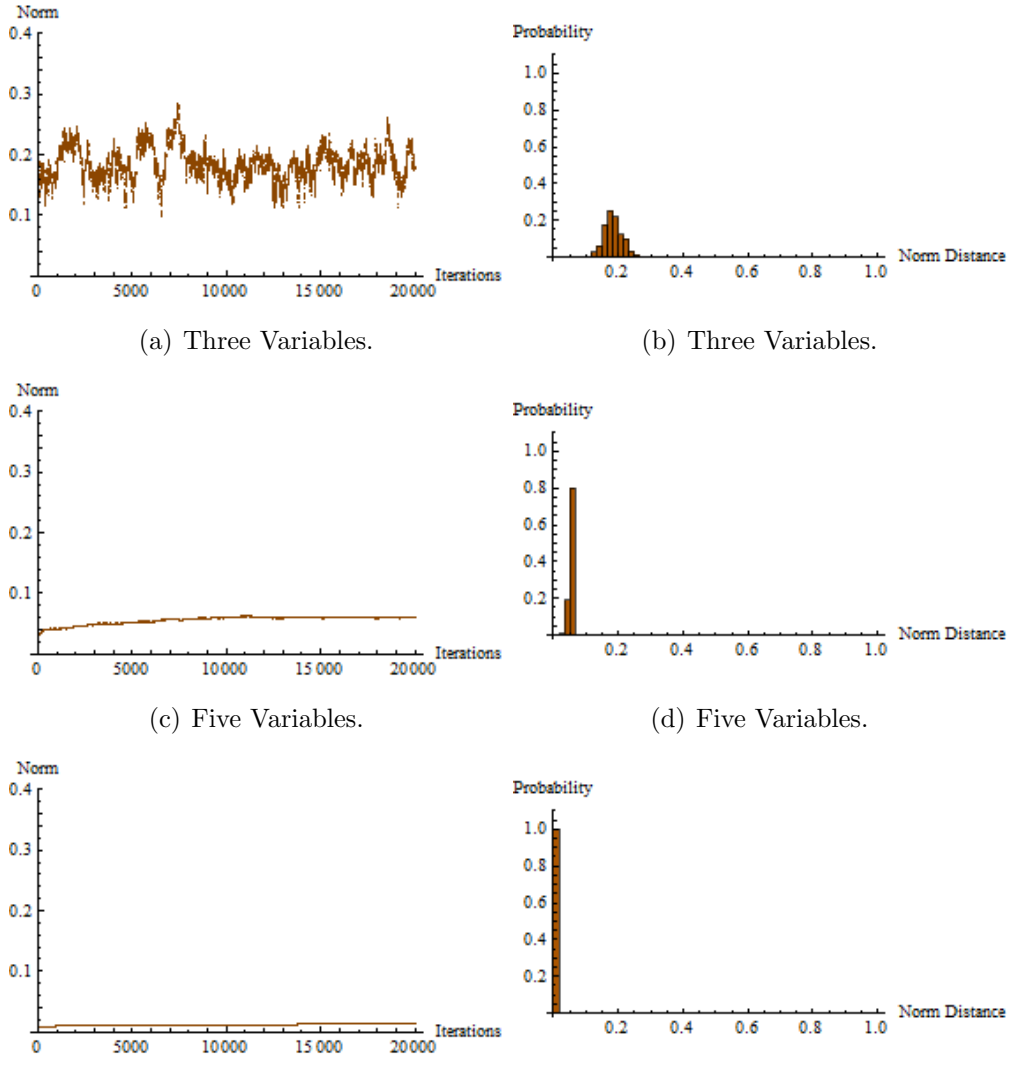

(a) Three Variables.

(b) Three Variables.

(c) Five Variables.

(d) Five Variables.

(e) Seven Variables.

(f) Seven Variables.

Figure A.1: Hit and Run: Euclidean norm distance from the center of $\mathbb{T}$ to 20,000 sampled distributions and histograms. All random variables have three outcomes.

Ping-Pong: Norm Distance And Histograms For 20000 Samples For 3, 5, and 7 Variables With 3 Outcomes.

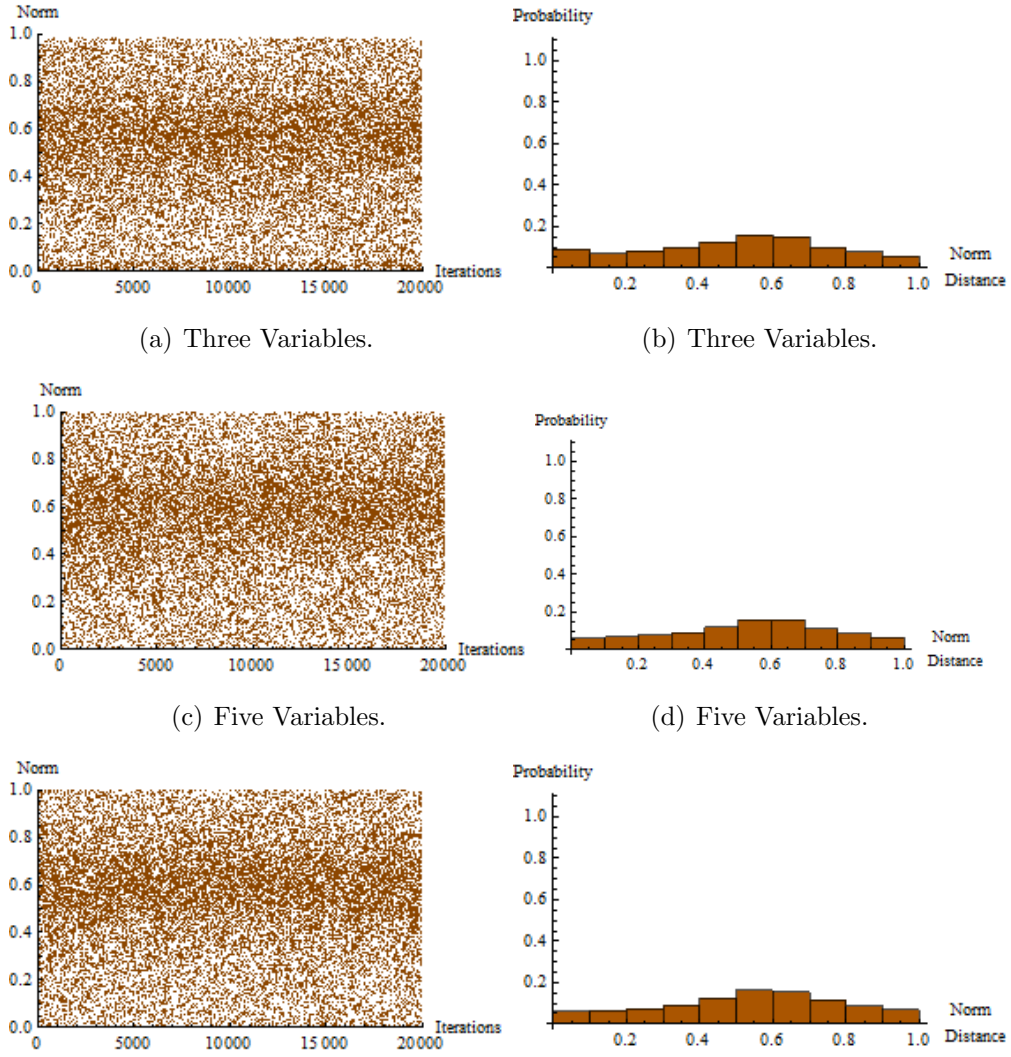

(a) Three Variables.

(b) Three Variables.

(c) Five Variables.

(d) Five Variables.

(e) Seven Variables.

(f) Seven Variables.

Figure A.2: Ping-Pong: Euclidean norm distance from the center of $\mathbb{T}$ to 20,000 sampled distributions and histograms. All random variables have three outcomes.

Appendix B

Additional Derivations

B.1 Kendall τ

We present the counterpart of the Spearman's ρ correlation constraint using the Kendall τ correlation coefficient. As we show, the constraint result in a non linear equation and is therefore not suitable to be implemented in the HR sample procedure. However, for a sample taken from $\mathbb{T}$, equation B.5 can be used to measure the dependence structure based on the Kendall τ correlation. Staring with the copula definition for Kendall τ from Nelsen (2005), we proceed as follows:

$$4\int_0^1\int_0^1 C_{U,V}(u,v)dC_{U,V}(u,v) - 1. \tag{B.1}$$

If variable U has marginal outcomes ω_i^U index by $i = 1, 2, \ldots, n$, and variable V has marginal outcomes ω_j^V indexed by $j = 1, 2, \ldots, m$. We can define a piecewise uniform continues copula using the intervals $I_i^U = [P(U \leq \omega_{i-1}^U), P(U \leq \omega_i^U)]$ and $I_j^V = [P(V \leq \omega_{j-1}^V), P(V \leq \omega_j^V)]$. To make the notation more compact we define $p_{i-1}^U = P(U \leq \omega_{i-1}^U)$ and $p_i^U = P(U \leq \omega_i^U)$ and do the same for $p_{i_1}^V$ and p_i^V. We also define $\Delta p_i^U = (p_i^U - p_{i-1}^U)$ and $\Delta p_j^V = (p_j^V - p_{j-1}^V)$. Then assuming $(u,v) \in I_{i,j} \equiv I_i^U \times I_j^V$, we can define $C_{U,V}(u,v) \equiv F_{U,V}(u,v)$ as:

$$C_{U,V}(u,v) = \frac{(u-p_{i-1}^U)(v-p_{j-1}^V)}{\Delta p_i^U \Delta p_j^V} p_{i,j} + \sum_{k=1}^{i-1} \frac{(v-p_{j-1}^V)}{\Delta p_j^V} p_{k,j} \tag{B.2}$$

$$+ \sum_{l=1}^{j-1} \frac{(u-p_{i-1}^U)}{\Delta p_i^U} p_{i,l} + \sum_{k=1}^{i-1}\sum_{l=1}^{j-1} p_{k,l},$$

$$dC_{U,V}(u,v) = \frac{p_{i,j}}{\Delta p_i^U \Delta p_j^V} dv\ du, \quad \forall (u,v) \in I_{i,j}. \tag{B.3}$$

By substituting in equation B.1 and create a partition for all $I_{i,j}$ we have:

$$\begin{aligned}
\frac{\tau_{V,U}+1}{4} =& \sum_{i=1}^{n}\sum_{j=1}^{m} \int_{p_{i-1}^U}^{p_i^U}\int_{p_{j-1}^V}^{p_j^V} \frac{p_{i,j}}{\Delta p_i^U \Delta p_j^V} \left[\frac{(u-p_{i-1}^U)(v-p_{i-1}^V)}{\Delta p_i^U \Delta p_j^V} p_{i,j} \right. \\
&\left. + \sum_{k=1}^{i-1} \frac{(v-p_{j-1}^V)}{\Delta p_j^V} p_{k,j} + \sum_{l=1}^{j-1} \frac{(u-p_{i-1}^U)}{\Delta p_i^U} p_{i,l} + \sum_{k=1}^{i-1}\sum_{l=1}^{j-1} p_{k,l} \right] dv\ du \\
=& \sum_{i=1}^{n}\sum_{j=1}^{m} \frac{p_{i,j}}{\Delta p_i^U \Delta p_j^V} \left[\frac{p_{i,j}}{\Delta p_i^U \Delta p_j^V} \int_{p_{i-1}^U}^{p_i^U}\int_{p_{j-1}^V}^{p_j^V} (u-p_{i-1}^U)(v-p_{i-1}^V)\ dv\ du \right. \\
&+ \sum_{k=1}^{i-1} \frac{p_{k,j}}{\Delta p_j^V} \int_{p_{i-1}^U}^{p_i^U}\int_{p_{j-1}^V}^{p_j^V} (v-p_{j-1}^V)\ dv\ du + \sum_{l=1}^{j-1} \frac{p_{i,l}}{\Delta p_i^U} \int_{p_{i-1}^U}^{p_i^U}\int_{p_{j-1}^V}^{p_j^V} (u-p_{i-1}^U)\ dv\ du \\
&\left. + \sum_{k=1}^{i-1}\sum_{l=1}^{j-1} p_{k,l} \int_{p_{i-1}^U}^{p_i^U}\int_{p_{j-1}^V}^{p_j^V} dv\ du \right] \\
=& \sum_{i=1}^{n}\sum_{j=1}^{m} \frac{p_{i,j}}{\Delta p_i^U \Delta p_j^V} \left[\frac{p_{i,j}(\Delta p_i^U)^2(\Delta p_j^V)^2}{4\Delta p_i^U \Delta p_j^V} + \sum_{k=1}^{i-1} \frac{p_{k,j}}{\Delta p_j^V} \frac{(\Delta p_j^V)^2 \Delta p_j^V}{2} \right. \\
&\left. + \sum_{l=1}^{j-1} \frac{p_{i,l}}{\Delta p_i^U} \frac{\Delta p_j^V (\Delta p_i^U)^2}{2} + \sum_{k=1}^{i-1}\sum_{l=1}^{j-1} p_{k,l} \Delta p_j^V \Delta p_i^U \right] \\
=& \sum_{i=1}^{n}\sum_{j=1}^{m} p_{i,j} \left[\frac{p_{i,j}}{4} + \sum_{k=1}^{i-1} \frac{p_{k,j}}{2} + \sum_{l=1}^{j-1} \frac{p_{i,l}}{2} + \sum_{k=1}^{i-1}\sum_{l=1}^{j-1} p_{k,l} \right].
\end{aligned}$$

The step is done by substituting B.2 in B.1 and create a partition based on the $I_{i,j}$ intervals. The exchange of integrals an summations in the second step is permitted since summations and integrals are finite and all its elements are positive. The next two steps solve the integrals and cancel the redundant terms. The final equation is as follows:

$$\tau_{V,U} = \sum_{i=1}^{n}\sum_{j=1}^{m}\left[p_{i,j}^2 + 2p_{i,j}\sum_{k=1}^{i-1}p_{k,j} + 2p_{i,j}\sum_{l=1}^{j-1}p_{i,l} + 4p_{i,j}\sum_{k=1}^{i-1}\sum_{l=1}^{j-1}p_{k,l}\right] - 1. \tag{B.5}$$

Equation B.5 is in therms of $p_{i,j}$ to translated in terms of p_{ω_k} we need to consider that:

$$p_{i,j} = \sum_{\omega_k \in \mathbb{U}^{U,V}_{\omega_i^U \omega_j^V}} p_{\omega_k}. \tag{B.6}$$

Then, we just need to substitute B.6 in B.5 and calculate $\tau_{V,U}$ for a given joint distribution.

B.2 Lovasz Lower Bound

In theory, we would like to sample N joint distributions $\mathbf{p}_i$, $\forall\, i = 1, 2, \ldots, N$, such that the probability of finding a joint distribution in a subset $\mathbb{S} \subset \mathbb{T}$ is the same as the ratio of the volume of $\mathbb{S}$ to the volume of $\mathbb{T}$. Call this ratio $\pi(\mathbb{S})$. The problem is that if we want a convergence $|P(\mathbf{p}_N \in \mathbb{S}) - \pi(\mathbb{S})| \leq \epsilon \;\; \forall \;\; \mathbb{S}$, we know from Lovasz (1998) that a lower bound for the number of samples required (N) is given by Equation (B.7), where $\hat{D}$ is the diameter of $\mathbb{T}$ and it is bounded by $\hat{D} \leq \sqrt{2}$, and $h = n - m$ is the dimension of the h-content of $\mathbb{T}$.

$$N = \left\lceil \frac{8 \cdot 10^8 \cdot h^2}{\epsilon^2} \ln\left(\frac{2}{\epsilon}\right) \right\rceil \geq \left\lceil \frac{4 \cdot 10^8 \cdot h^2 \cdot \hat{D}^2}{\epsilon^2} \ln\left(\frac{2}{\epsilon}\right) \right\rceil. \tag{B.7}$$

This bound defines values for N that are too large for most practical applications. For example, if the dimension of $\mathbb{T}$ is $h = 1$ and we have parameters $\epsilon = 0.1$ and $\hat{D} = 1$, then $N \approx 119,829,290,943$. This large sample size occurs because the bound is looking for the convergence for all possible sets $\mathbb{S}$ (even the tinniest ones).

If we where interested in having a sample such that $P(\mathbf{p}_N \in \mathbb{S}) \to \pi(\mathbb{S})$ for every subset $\mathbb{S}$, the sample requirements force $N = \infty$.

Table B.1: Comparison of fair-convergence vs. Lovasz lower-bound.

n	N fair-convergence	N Lovasz Lower-bound $\epsilon = \frac{5}{100}$
4	2.0×10^2	1.1×10^{13}
8	2.1×10^3	5.8×10^{13}
16	1.8×10^4	2.7×10^{14}
32	1.8×10^5	1.1×10^{15}
64	1.2×10^6	4.7×10^{15}
128	1.2×10^7	1.9×10^{16}

B.3 Symmetric Perturbations

For 2 distributions A and B where A is a uniform distribution with even number of events, and B is a symmetric perturbation of A. We have:

$$\begin{aligned}
KL_n(B,A) =& \sum_{i=1}^{n}(p_i^B)\log\left(\frac{p_i^B}{p_i^A}\right)\\
=& \sum_{i=1}^{n}(p_i^B)\log\left(p_i^B\right) - \sum_{i=1}^{n}(p_i^B)\log\left(p_i^A\right)\\
=& - H(B) - \sum_{i=1}^{\frac{n}{2}}(p_i^A+\epsilon)\log\left(p_i^A\right) - \sum_{i=1}^{\frac{n}{2}}(p_i^A-\epsilon)\log\left(p_i^A\right)\\
=& H(A) - H(B) - \sum_{i=1}^{\frac{n}{2}}\epsilon\ln\left(p_i^A\right) + \sum_{i=1}^{\frac{n}{2}}\epsilon\log\left(p_i^A\right)\\
=& \Delta H(B,A).
\end{aligned}$$

Given that A is the uniform distribution ($p_i^A = \frac{1}{n}$), and recalling that $\mathbf{L}^1 = \epsilon \cdot n$.

$$\begin{aligned}
KL_n(B,A) =& \sum_{i=1}^{n}(p_i^B)\log\left(\frac{p_i^B}{p_i^A}\right)\\
=& \sum_{i=1}^{\frac{n}{2}}(p_i^A+\epsilon)\log\left(\frac{p_i^A+\epsilon}{p_i^A}\right) + \sum_{i=1}^{\frac{n}{2}}(p_i^A-\epsilon)\log\left(\frac{p_i^A-\epsilon}{p_i^A}\right)\\
=& \frac{n}{2}\left[(p_i^A+\epsilon)\log\left(\frac{p_i^A+\epsilon}{p_i^A}\right) + (p_i^A-\epsilon)\log\left(\frac{p_i^A-\epsilon}{p_i^A}\right)\right]\\
=& \frac{n}{2}\log\left[\left(\frac{p_i^A+\epsilon}{p_i^A}\right)^{(p_i^A+\epsilon)}\left(\frac{p_i^A-\epsilon}{p_i^A}\right)^{(p_i^A-\epsilon)}\right]\\
=& \frac{n}{2}\log\left[\left(1+\frac{\epsilon}{p_i^A}\right)^{(p_i^A+\epsilon)}\left(1-\frac{\epsilon}{p_i^A}\right)^{(p_i^A-\epsilon)}\right]\\
=& \log\left[\left(1+n\cdot\epsilon\right)^{(\frac{1}{n}+\epsilon)\frac{n}{2}}\left(1-n\cdot\epsilon\right)^{(\frac{1}{n}-\epsilon)\frac{n}{2}}\right]
\end{aligned}$$

$$
\begin{aligned}
KL_n(B,A) &= \log\left[\left(1+n\cdot\epsilon\right)^{\frac{1+n\cdot\epsilon}{2}}\left(1-n\cdot\epsilon\right)^{\frac{1-n\cdot\epsilon}{2}}\right] \\
&= \log\left[\frac{\left(1+n\cdot\epsilon\right)^{\frac{n\cdot\epsilon+1}{2}}}{\left(1-n\cdot\epsilon\right)^{\frac{n\cdot\epsilon-1}{2}}}\right] \\
&= \log\left[\frac{\left(1+\mathbf{L}^1\right)^{\frac{\mathbf{L}^1+1}{2}}}{\left(1-\mathbf{L}^1\right)^{\frac{\mathbf{L}^1-1}{2}}}\right].
\end{aligned}
$$

Using the logarithmic series expansion of $\log(1+\mathbf{L}^1)$ and $\log(1-\mathbf{L}^1)$, we can approximate $KL_n(B,A)$.

$$
KL_n(B,A) = \log\left[\frac{\left(1+\mathbf{L}^1\right)^{\frac{\mathbf{L}^1+1}{2}}}{\left(1-\mathbf{L}^1\right)^{\frac{\mathbf{L}^1-1}{2}}}\right] = \sum_i^{\infty}\frac{(\mathbf{L}^1)^{2i}}{2i(2i-1)\ln(2)}.
$$

If B is not a symmetric perturbation, we still can make some observations:

$$
\begin{aligned}
KL_n(B,A) =& \sum_{i=1}^{n}(p_i^B)\log\left(\frac{p_i^B}{p_i^A}\right) \\
=& \sum_{i=1}^{n}(p_i^B)\log\left(p_i^B\right) - \sum_{i=1}^{n}(p_i^B+p_i^A-p_i^A)\log\left(p_i^A\right) \\
=& H(A) - H(B) - \sum_{i=1}^{n}(p_i^B-p_i^A)\log\left(p_i^A\right) \\
=& \Delta H(B,A) + \sum_{i=1}^{n}(p_i^A-p_i^B)\log\left(p_i^A\right).
\end{aligned}
$$

Appendix C

Additional Results

- Hypergeometric Family
  - Scatterplots for $c = 5, n = 3$.
  - Histograms for $c = 5, n = 3$.
  - Scatterplots for $c = 6, n = 8$.
  - Histograms for $c = 6, n = 8$.
  - Frequency Tables
- Multinomial Family
  - Scatterplots for $c = 5, n = 3$.
  - Histograms for $c = 5, n = 3$.
  - Scatterplots for $c = 6, n = 8$.
  - Histograms for $c = 6, n = 8$.
  - Frequency Tables
- Effects Of Increasing The Number Of Constraints
  - Histograms for 3 random variables.
  - Histograms for 7 random variables.
- Symmetric Sets With Marginal Constraints.
  - Tables for 3 random variables (r.v.).
  - Tables for 4 random variables.
  - Tables for 5 random variables.
  - Tables for 6 random variables.
  - Tables for 7 random variables.
- Symmetric Sets With Marginal and Rank Correlation Constraints.
  - Figures of the standard deviation for 3 r.v.
  - Figures of the standard deviation for 4 r.v.
  - Figures of the standard deviation for 5 r.v.
  - Figures of the standard deviation for 6 r.v.
  - Figures of the standard deviation for 7 r.v.
  - Tables for 3 random variables. Parts 1, 2, 3, and 4.
  - Tables for 4 random variables. Parts 1, 2, 3, and 4.
  - Tables for 5 random variables. Parts 1, 2, 3, and 4.
  - Tables for 6 random variables. Parts 1, 2, 3, and 4.
  - Tables for 7 random variables. Parts 1, 2, 3, and 4.

C.1 Hypergeometric Families Accuracy And Histograms.

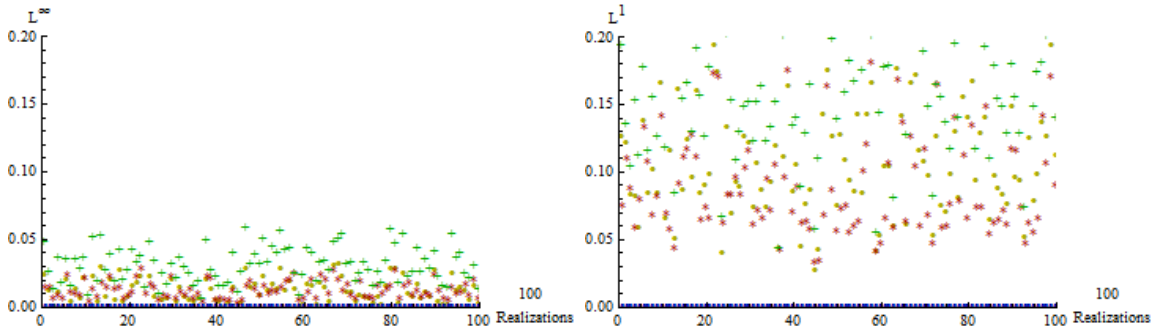

(a) Maximum Absolute Distance.

(b) Total Variation.

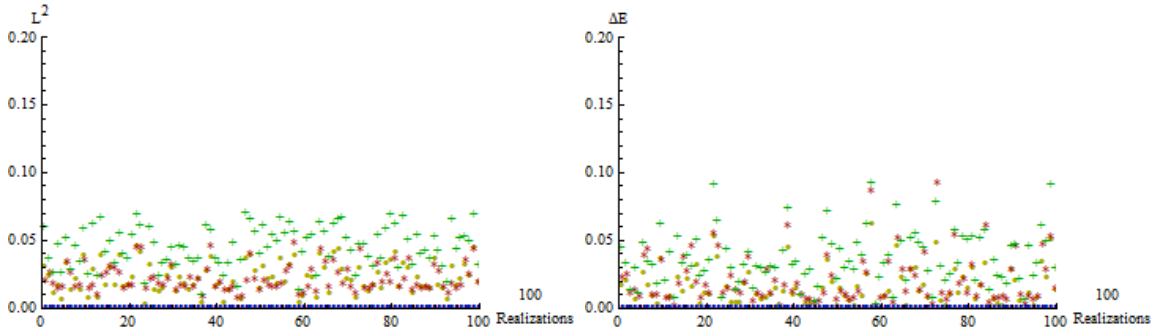

(c) Euclidean Distance.

(d) Absolute Entropy Difference.

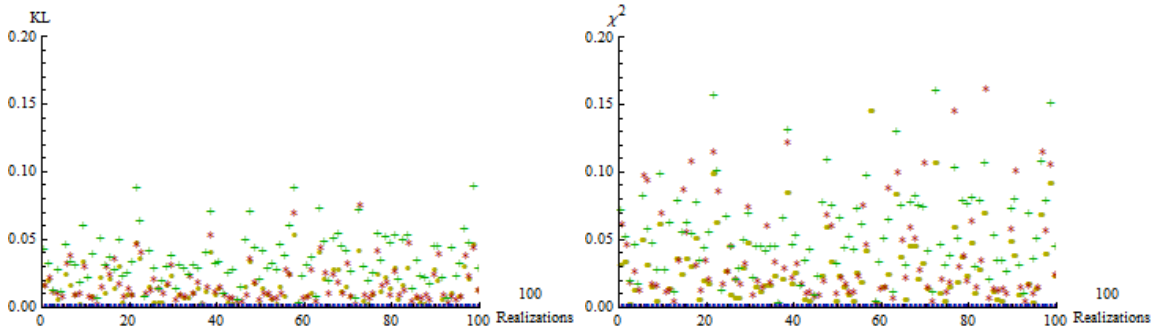

(e) KL Divergence.

(f) χ^2 Distance.

Figure C.1: Hypergeometric Family: Results for ME (Blue, "◎"); ChSC (Red, " * "); MVIE (Green, " + "); and AC (Yellow, " • "). For $c = 5$ and $n = 3$ (100 Samples).

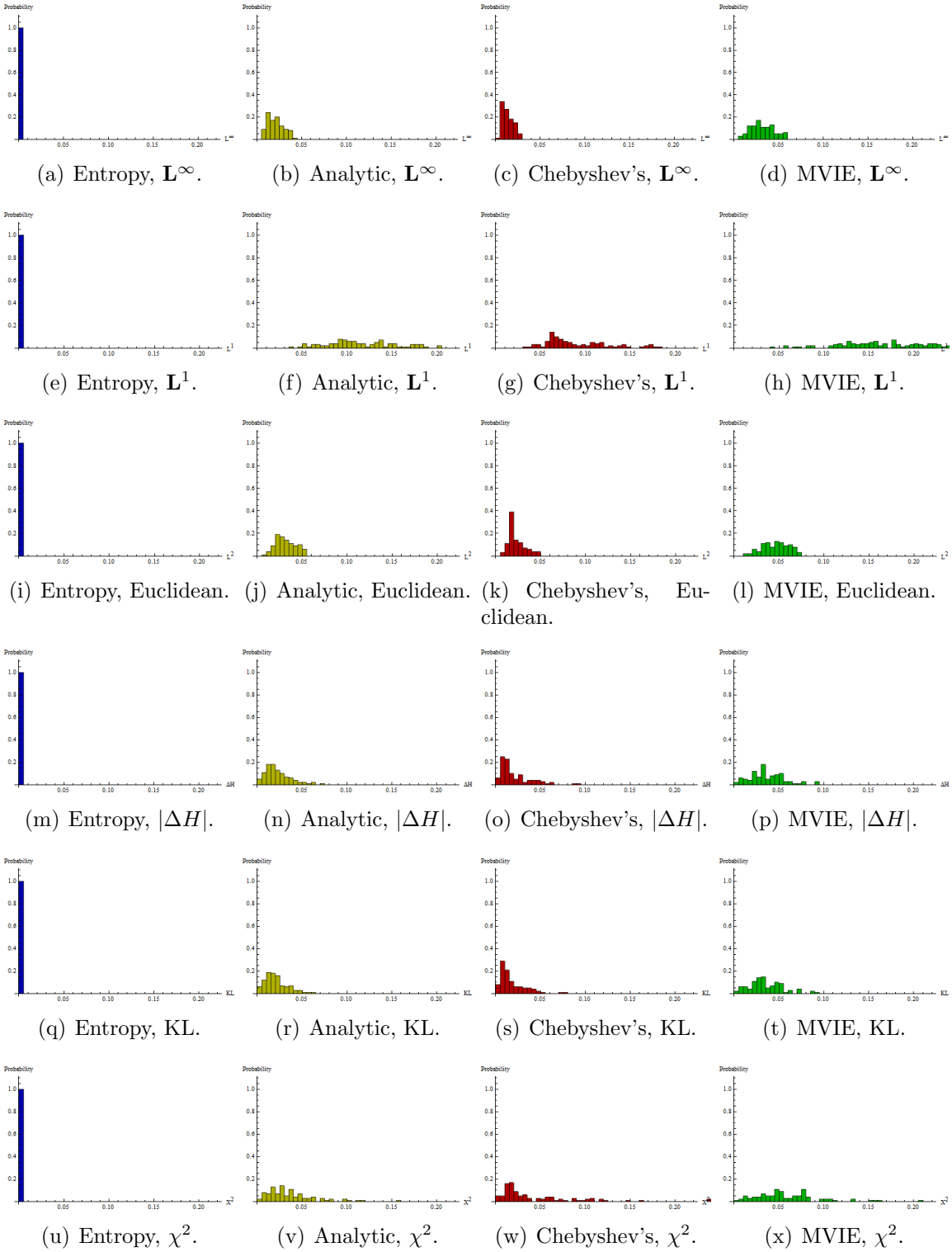

(a) Entropy, $\mathbf{L}^{\infty}$. (b) Analytic, $\mathbf{L}^{\infty}$. (c) Chebyshev's, $\mathbf{L}^{\infty}$. (d) MVIE, $\mathbf{L}^{\infty}$.

(e) Entropy, $\mathbf{L}^{1}$. (f) Analytic, $\mathbf{L}^{1}$. (g) Chebyshev's, $\mathbf{L}^{1}$. (h) MVIE, $\mathbf{L}^{1}$.

(i) Entropy, Euclidean. (j) Analytic, Euclidean. (k) Chebyshev's, Euclidean. (l) MVIE, Euclidean.

(m) Entropy, $|\Delta H|$. (n) Analytic, $|\Delta H|$. (o) Chebyshev's, $|\Delta H|$. (p) MVIE, $|\Delta H|$.

(q) Entropy, KL. (r) Analytic, KL. (s) Chebyshev's, KL. (t) MVIE, KL.

(u) Entropy, χ^2. (v) Analytic, χ^2. (w) Chebyshev's, χ^2. (x) MVIE, χ^2.

Figure C.2: Hypergeometric Family Histogram Results. From left to right distribution approximations. From Top to bottom measures of accuracy. For $c = 5$ and $n = 3$.

Hypergeometric Families Accuracy And Histograms (100 Samples).

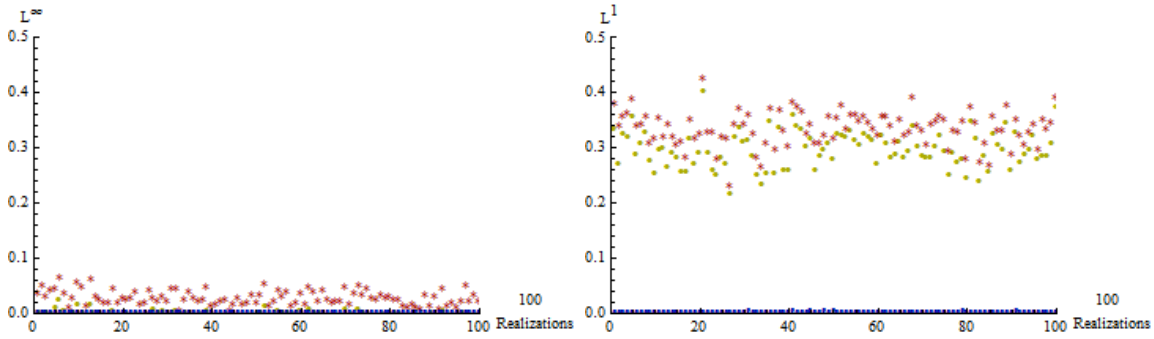

(a) Maximum Absolute Distance.

(b) Total Variation.

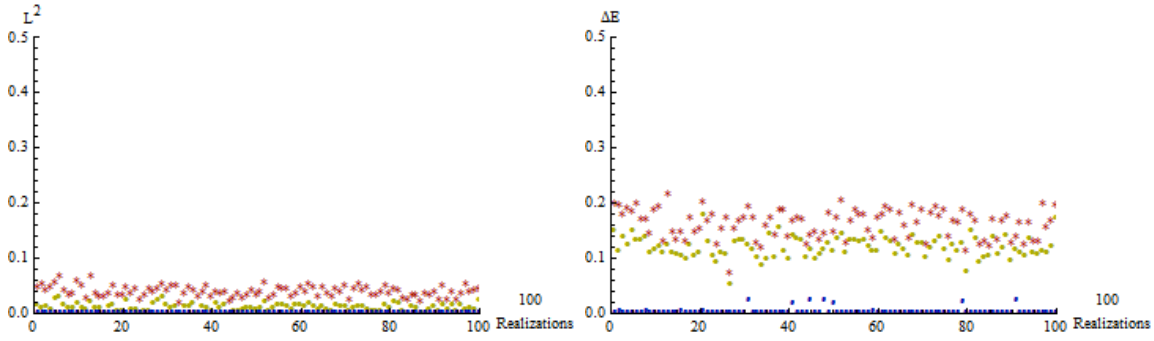

(c) Euclidean Distance.

(d) Absolute Entropy Difference.

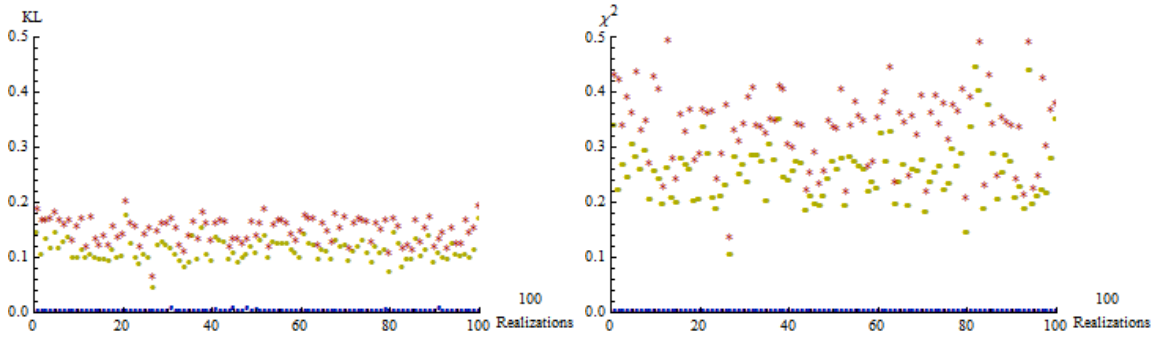

(e) KL Divergence.

(f) χ^2 Distance.

Figure C.3: Hypergeometric Family: Results for ME (Blue, "◎"); ChSC (Red, " * "); and AC (Yellow, " • ") approximations. For $c = 6$ and $n = 8$.

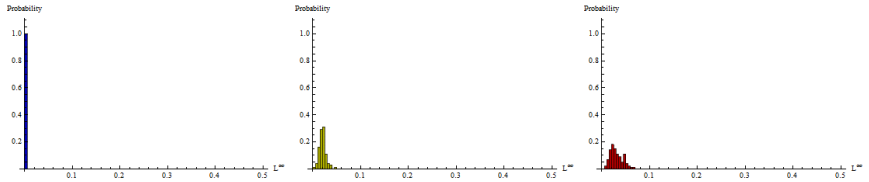

(a) Entropy, $\mathbf{L}^\infty$. (b) Analytic, $\mathbf{L}^\infty$. (c) Chebyshev's, $\mathbf{L}^\infty$.

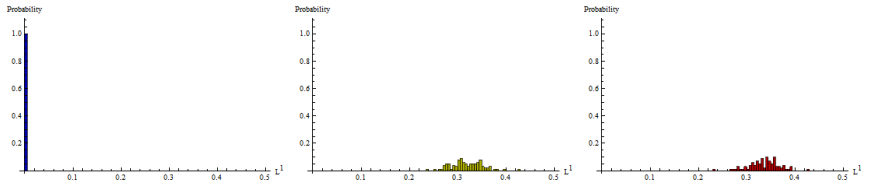

(d) Entropy, $\mathbf{L}^1$. (e) Analytic, $\mathbf{L}^1$. (f) Chebyshev's, $\mathbf{L}^1$.

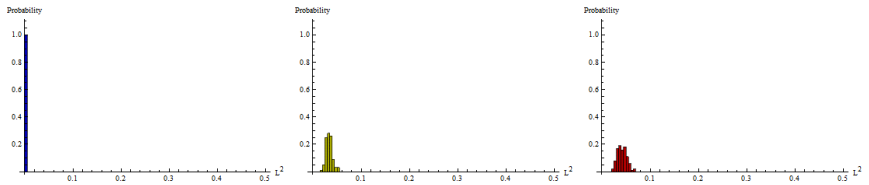

(g) Entropy, Euclidean. (h) Analytic, Euclidean. (i) Chebyshev's, Euclidean.

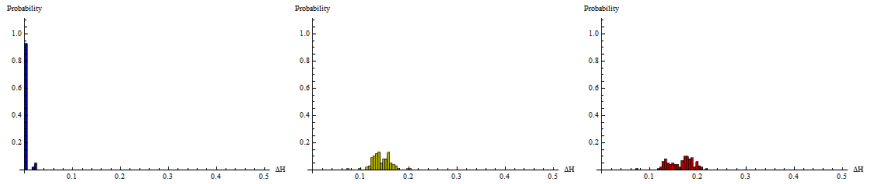

(j) Entropy, $|\Delta H|$. (k) Analytic, $|\Delta H|$. (l) Chebyshev's, $|\Delta H|$.

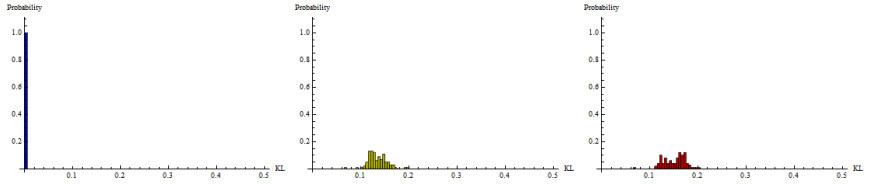

(m) Entropy, KL. (n) Analytic, KL. (o) Chebyshev's, KL.

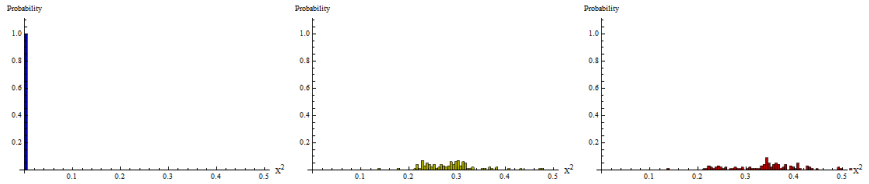

(p) Entropy, χ^2. (q) Analytic, χ^2. (r) Chebyshev's, χ^2.

Figure C.4: Hypergeometric Family Histogram Results. From left to right distribution approximations. From Top to bottom measures of accuracy. For $c = 6$ and $n = 8$.

Percentage Of Accuracy For The Hypergeometric Distribution.

Table C.1: Approximations And Measures With Parameters $c = 5$, $n = 3$.

Approximation	Measure	% Time Is The Best	% Time Is The Second Best	% Time Is The Third Best	% Time Is The Worst
Entropy	L^∞	100	0	0	0
	L^1	100	0	0	0
	L^2	100	0	0	0
	Δ H	100	0	0	0
	KL	100	0	0	0
	χ^2	100	0	0	0
Analytic C	L^∞	0	7	92	1
	L^1	0	16	83	1
	L^2	0	11	88	1
	Δ H	0	24	75	1
	KL	0	22	77	1
	χ^2	0	41	58	1
ChSC	L^∞	0	93	6	1
	L^1	0	84	16	0
	L^2	0	89	11	0
	Δ H	0	76	17	7
	KL	0	78	18	4
	χ^2	0	59	22	19
MVIEC	L^∞	0	0	2	98
	L^1	0	0	1	99
	L^2	0	0	1	99
	Δ H	0	0	8	92
	KL	0	0	5	95
	χ^2	0	0	20	80

Table C.2: Approximations And Measures With Parameters $c = 6$, $n = 8$.

Approximation	Measure	% Time Is The Best	% Time Is The Second Best	% Time Is The Third Best
Entropy	L^∞	100	0	0
	L^1	100	0	0
	L^2	100	0	0
	Δ H	100	0	0
	KL	100	0	0
	χ^2	100	0	0
Analytic C	L^∞	0	97	3
	L^1	0	91	9
	L^2	0	96	4
	Δ H	0	97	3
	KL	0	96	4
	χ^2	0	98	2
ChSC	L^∞	0	3	97
	L^1	0	9	91
	L^2	0	4	96
	Δ H	0	3	97
	KL	0	4	96
	χ^2	0	2	98

C.2 Multinomial Families Accuracy And Histograms.

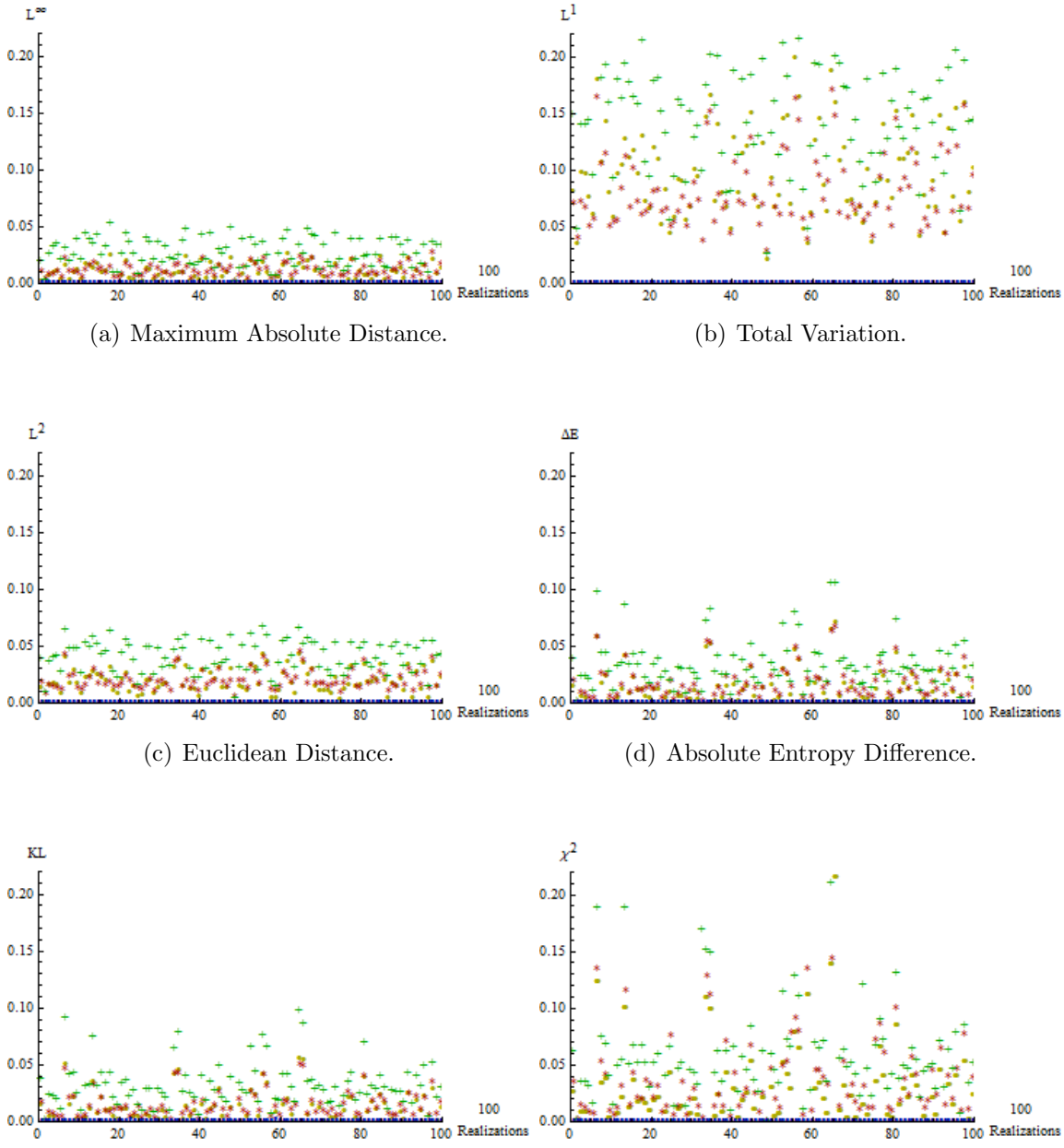

(a) Maximum Absolute Distance.

(b) Total Variation.

(c) Euclidean Distance.

(d) Absolute Entropy Difference.

(e) KL Divergence.

(f) χ^2 Distance.

Figure C.5: Multinomial Family: Results for ME (Blue, "@"); ChSC (Red, " * "); MVIE (Green, " + "); and AC (Yellow, " • ") approximations. For $c = 5$ and $n = 3$.

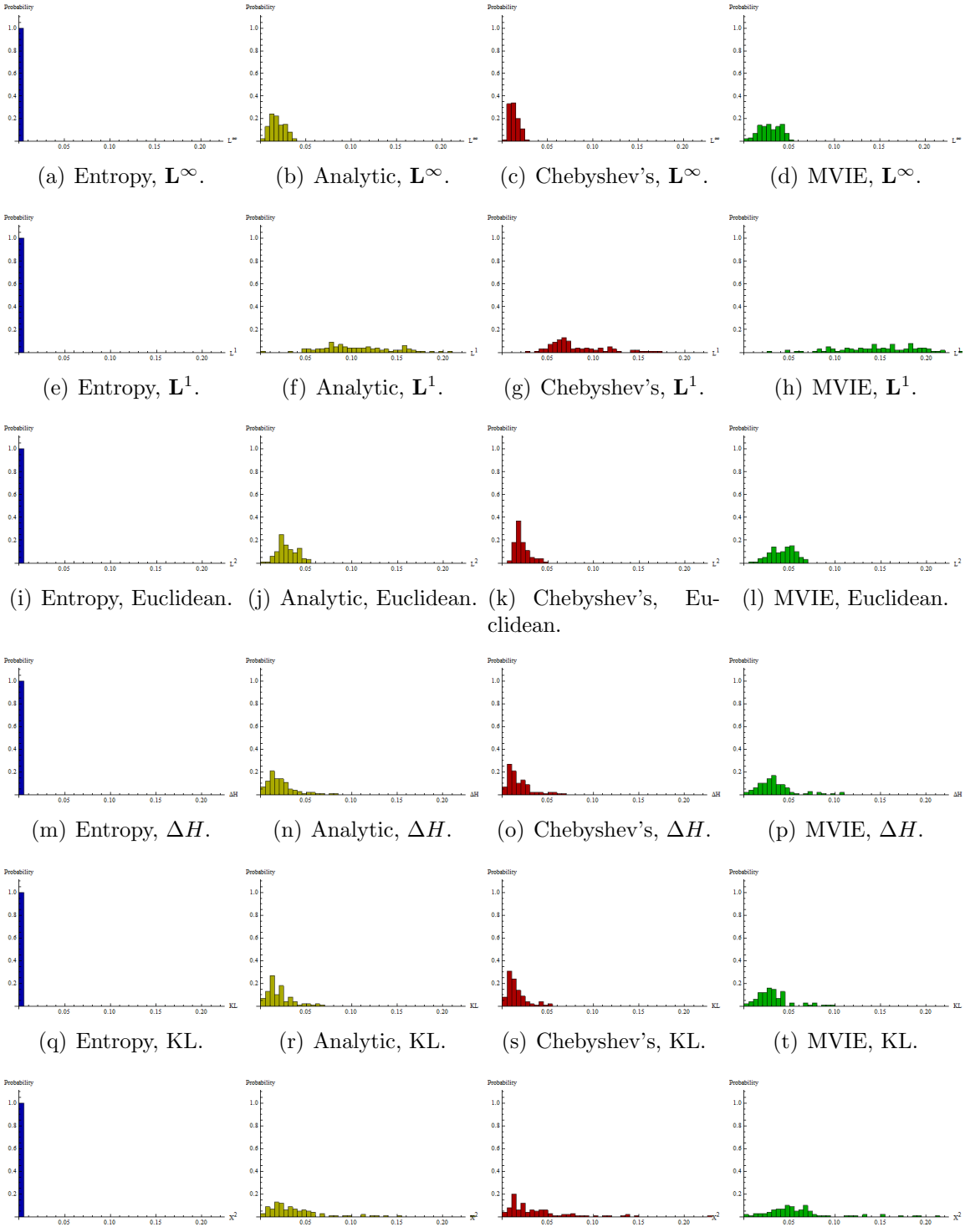

(a) Entropy, $\mathbf{L}^{\infty}$. (b) Analytic, $\mathbf{L}^{\infty}$. (c) Chebyshev's, $\mathbf{L}^{\infty}$. (d) MVIE, $\mathbf{L}^{\infty}$.

(e) Entropy, $\mathbf{L}^{1}$. (f) Analytic, $\mathbf{L}^{1}$. (g) Chebyshev's, $\mathbf{L}^{1}$. (h) MVIE, $\mathbf{L}^{1}$.

(i) Entropy, Euclidean. (j) Analytic, Euclidean. (k) Chebyshev's, Euclidean. (l) MVIE, Euclidean.

(m) Entropy, ΔH. (n) Analytic, ΔH. (o) Chebyshev's, ΔH. (p) MVIE, ΔH.

(q) Entropy, KL. (r) Analytic, KL. (s) Chebyshev's, KL. (t) MVIE, KL.

(u) Entropy, χ^2. (v) Analytic, χ^2. (w) Chebyshev's, χ^2. (x) MVIE, χ^2.

Figure C.6: Multinomial Family Histogram Results. From left to right distribution approximations. From Top to bottom measures of accuracy. For $c = 5$ and $n = 3$ (100 Samples).

Multinomial Families Accuracy And Histograms (100 Samples).

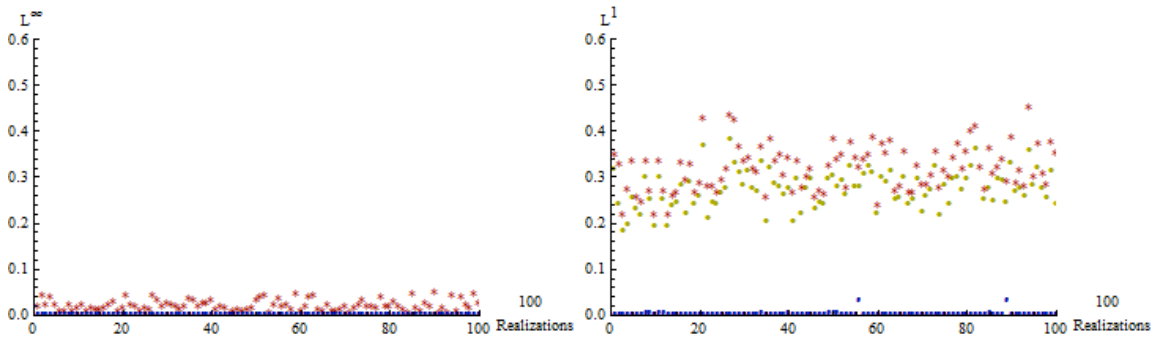

(a) Maximum Absolute Distance.

(b) Total Variation.

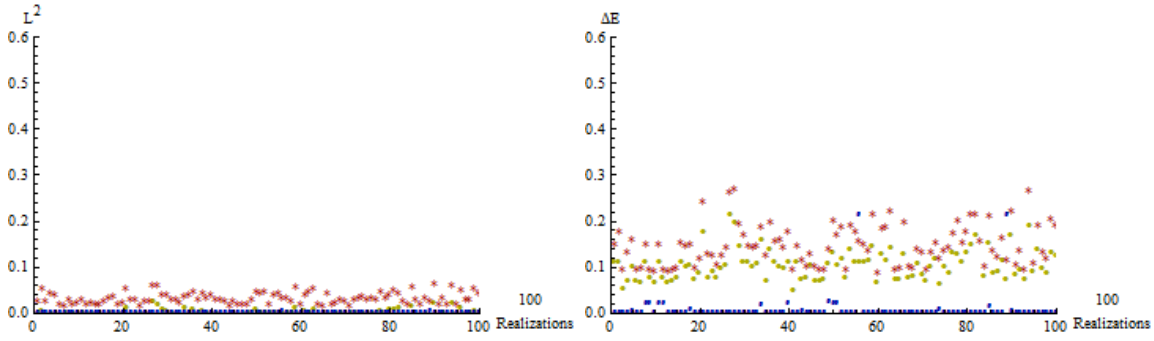

(c) Euclidean Distance.

(d) Absolute Entropy Difference.

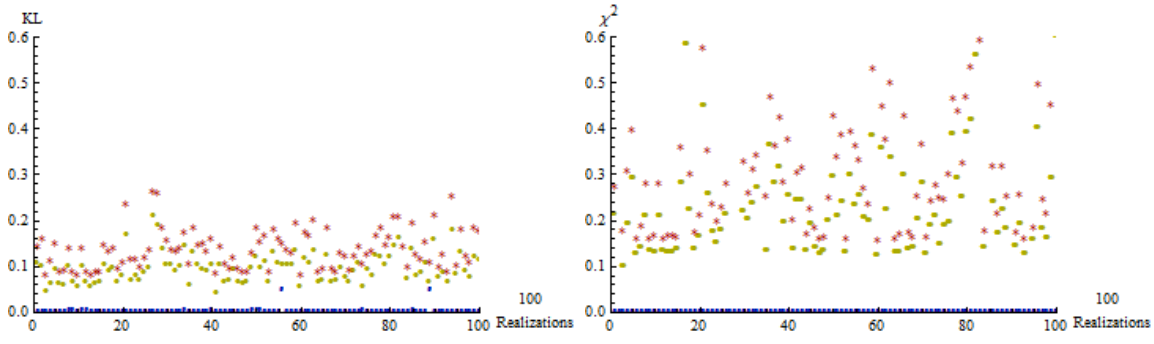

(e) KL Divergence.

(f) χ^2 Distance.

Figure C.7: Multinomial Family: Results for ME (Blue, "@"); ChSC (Red, " * "); and AC (Yellow, " • ") approximations. For $c = 6$ and $n = 8$.

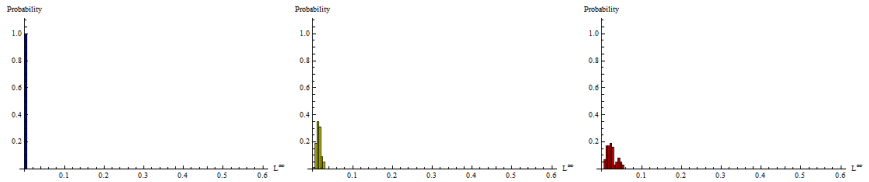

(a) Entropy, $\mathbf{L}^{\infty}$. (b) Analytic, $\mathbf{L}^{\infty}$. (c) Chebyshev's, $\mathbf{L}^{\infty}$.

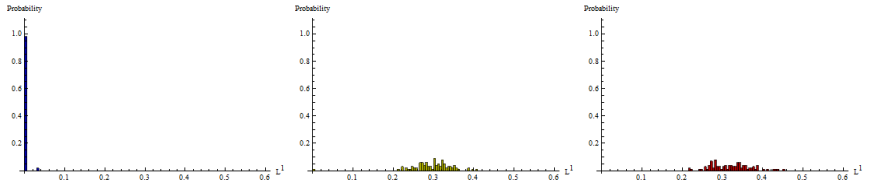

(d) Entropy, $\mathbf{L}^{1}$. (e) Analytic, $\mathbf{L}^{1}$. (f) Chebyshev's, $\mathbf{L}^{1}$.

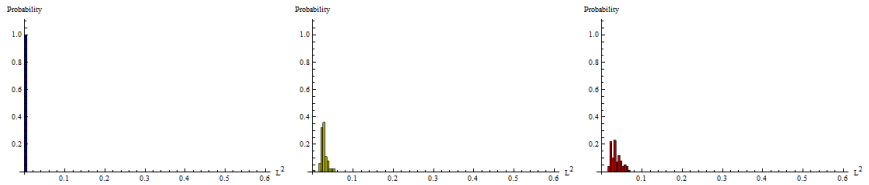

(g) Entropy, Euclidean. (h) Analytic, Euclidean. (i) Chebyshev's, Euclidean.

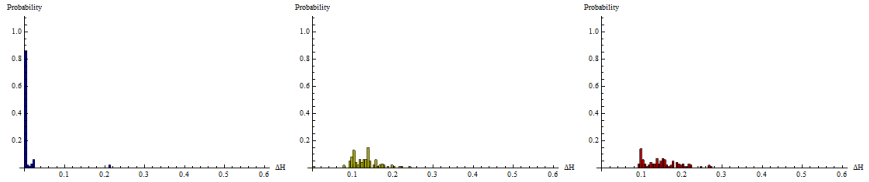

(j) Entropy, ΔH. (k) Analytic, ΔH. (l) Chebyshev's, ΔH.

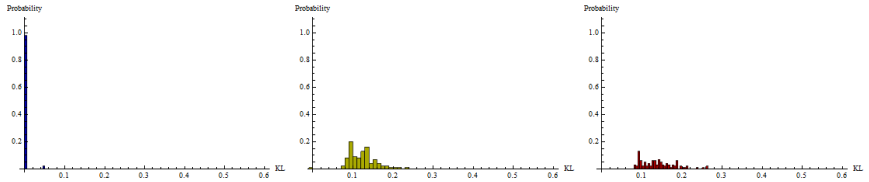

(m) Entropy, KL. (n) Analytic, KL. (o) Chebyshev's, KL.

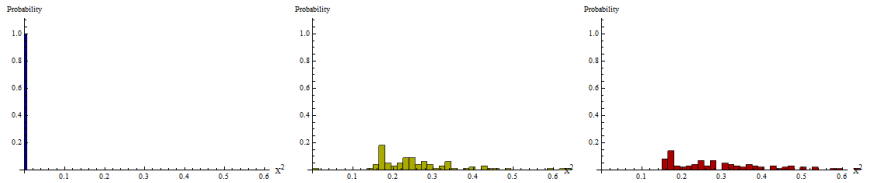

(p) Entropy, χ^2. (q) Analytic, χ^2. (r) Chebyshev's, χ^2.

Figure C.8: Multinomial Family Histogram Results. From left to right distribution approximations. From Top to bottom measures of accuracy. For $c = 6$ and $n = 8$.

Percentage Of Accuracy For The Monomial Distribution.

Table C.3: Approximations And Measures With Parameters $c = 5$, $n = 3$.

Approximation	Measure	% Time Is The Best	% Time Is The Second Best	% Time Is The Third Best	% Time Is The Worst
Entropy	L^∞	99	1	0	0
	L^1	99	1	0	0
	L^2	99	1	0	0
	Δ H	100	0	0	0
	KL	99	1	0	0
	χ^2	99	1	0	0
Analytic C	L^∞	1	2	95	2
	L^1	1	3	95	1
	L^2	1	3	94	2
	Δ H	0	15	84	1
	KL	1	6	92	1
	χ^2	1	39	59	1
ChSC	L^∞	0	95	5	0
	L^1	0	95	4	1
	L^2	0	95	5	0
	Δ H	0	83	15	2
	KL	0	91	8	1
	χ^2	0	58	36	6
MVIEC	L^∞	0	2	0	98
	L^1	0	1	1	98
	L^2	0	1	1	98
	Δ H	0	2	1	97
	KL	0	2	0	98
	χ^2	0	2	5	93

Table C.4: Approximations And Measures With Parameters $c = 6$, $n = 8$.

Approximation	Measure	% Time Is The Best	% Time Is The Second Best	% Time Is The Third Best
Entropy	L^∞	99	1	0
	L^1	99	1	0
	L^2	99	1	0
	Δ H	97	1	2
	KL	99	1	0
	χ^2	99	1	0
Analytic C	L^∞	1	82	17
	L^1	1	76	23
	L^2	1	77	22
	Δ H	3	79	18
	KL	1	83	16
	χ^2	1	80	19
ChSC	L^∞	0	17	83
	L^1	0	23	77
	L^2	0	22	78
	Δ H	0	20	80
	KL	0	16	84
	χ^2	0	19	81

C.3 Effects Of Increasing The Number Of Constraints.

Effects Of Increasing The Number Of Constraints Part One

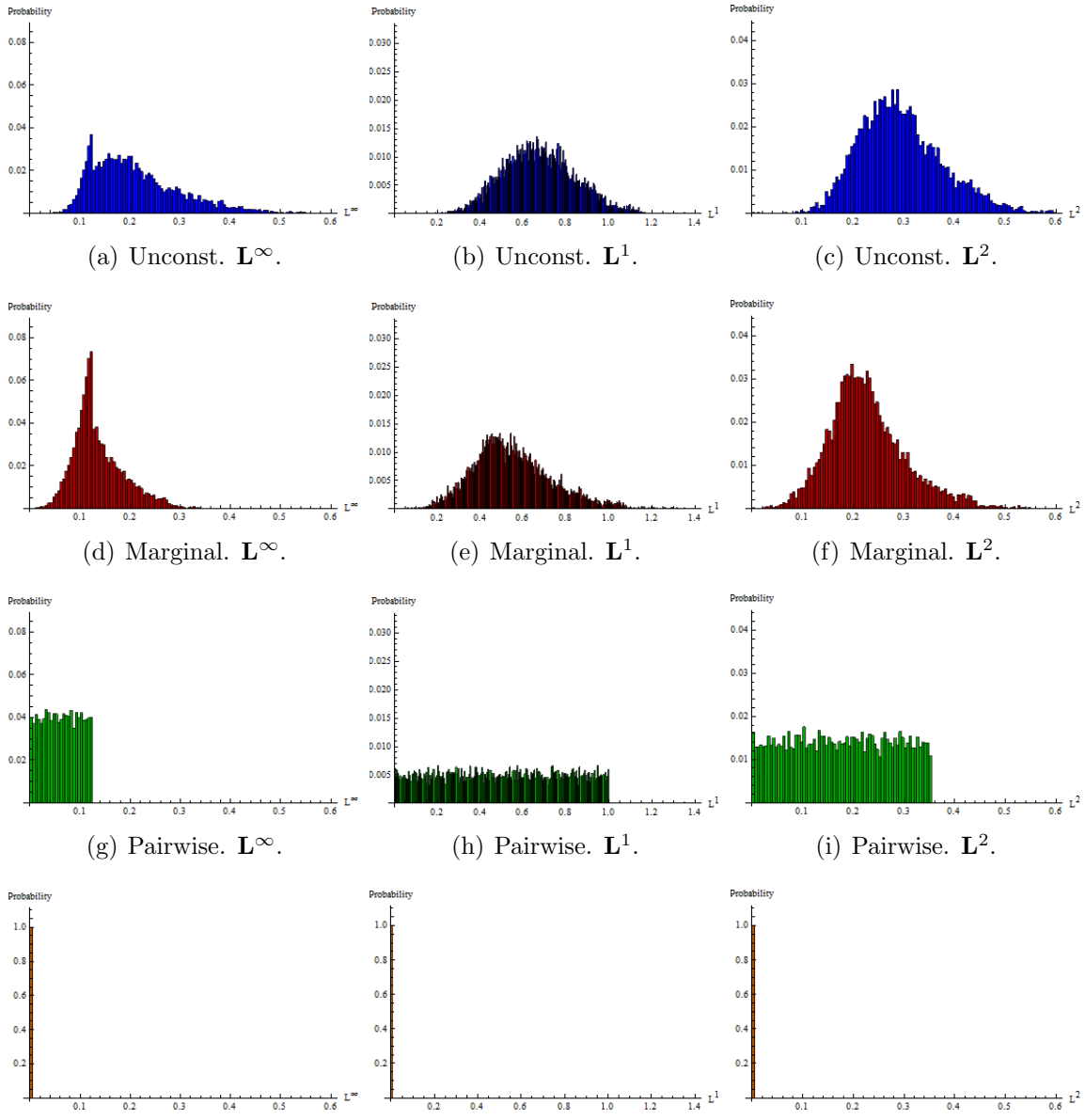

(a) Unconst. $\mathbf{L}^{\infty}$. (b) Unconst. $\mathbf{L}^{1}$. (c) Unconst. $\mathbf{L}^{2}$.

(d) Marginal. $\mathbf{L}^{\infty}$. (e) Marginal. $\mathbf{L}^{1}$. (f) Marginal. $\mathbf{L}^{2}$.

(g) Pairwise. $\mathbf{L}^{\infty}$. (h) Pairwise. $\mathbf{L}^{1}$. (i) Pairwise. $\mathbf{L}^{2}$.

(j) Threewise. $\mathbf{L}^{\infty}$. (k) Threewise. $\mathbf{L}^{1}$. (l) Threewise. $\mathbf{L}^{2}$.

Figure C.9: Effects of including new constraints in a truth set $\mathbb{T}$. The data is taken for a set that considers 3 binary variables. The unconstraint set uses 1 constraint. The Marginal set uses 4 constraints. The pairwise set uses 7 constraints. The three-wise set uses 8 constraints.

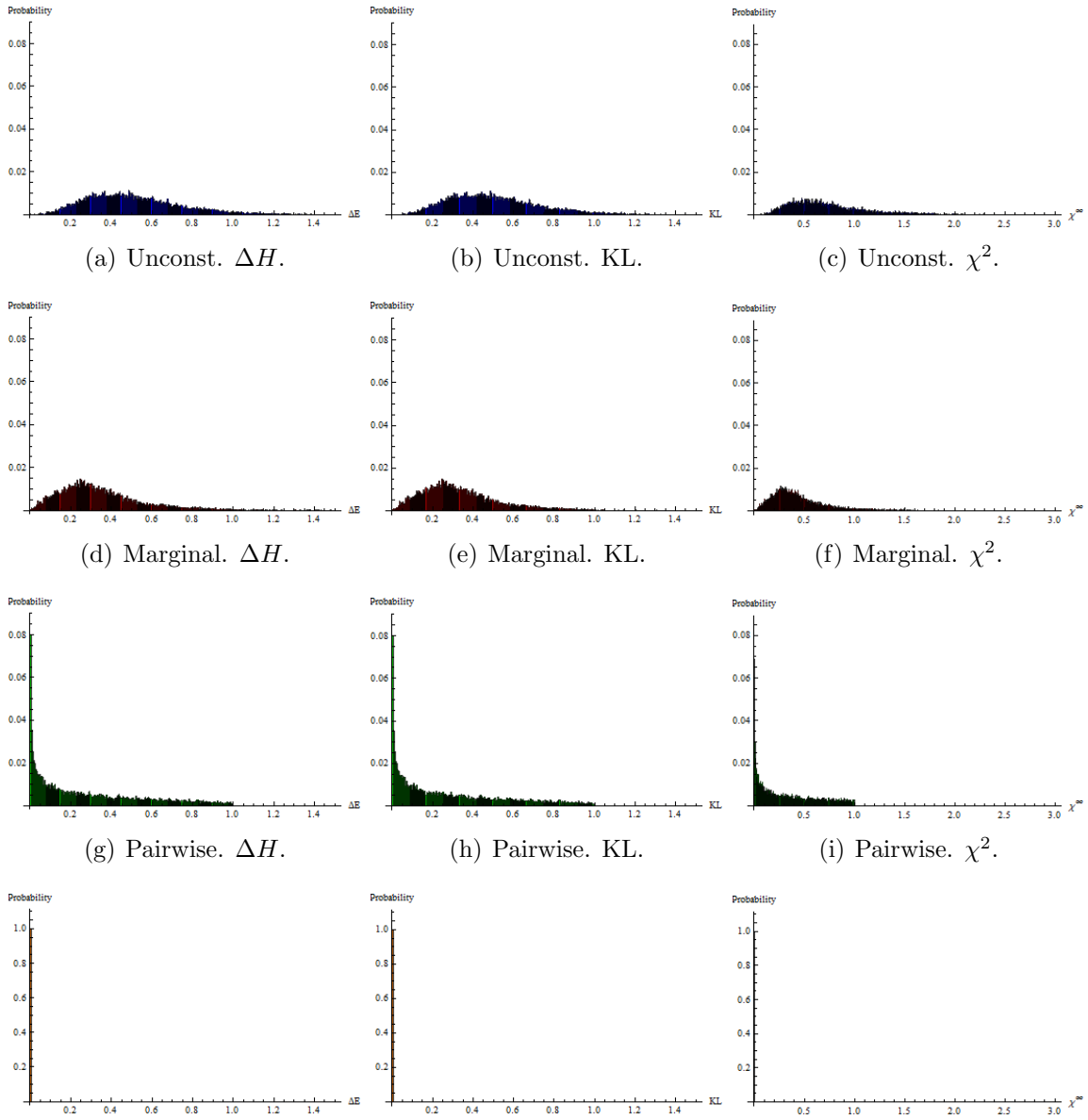

(a) Unconst. ΔH. (b) Unconst. KL. (c) Unconst. χ^2.

(d) Marginal. ΔH. (e) Marginal. KL. (f) Marginal. χ^2.

(g) Pairwise. ΔH. (h) Pairwise. KL. (i) Pairwise. χ^2.

(j) Threewise. ΔH. (k) Threewise. KL. (l) Threewise. χ^2.

Figure C.10: Effects of including new constraints in a truth set $\mathbb{T}$. The data is taken for a set that considers 3 binary variables. The unconstraint set uses 1 constraint. The Marginal set uses 4 constraints. The pairwise set uses 7 constraints. The three-wise set uses 8 constraints.

Effects Of Increasing The Number Of Constraints Part Two

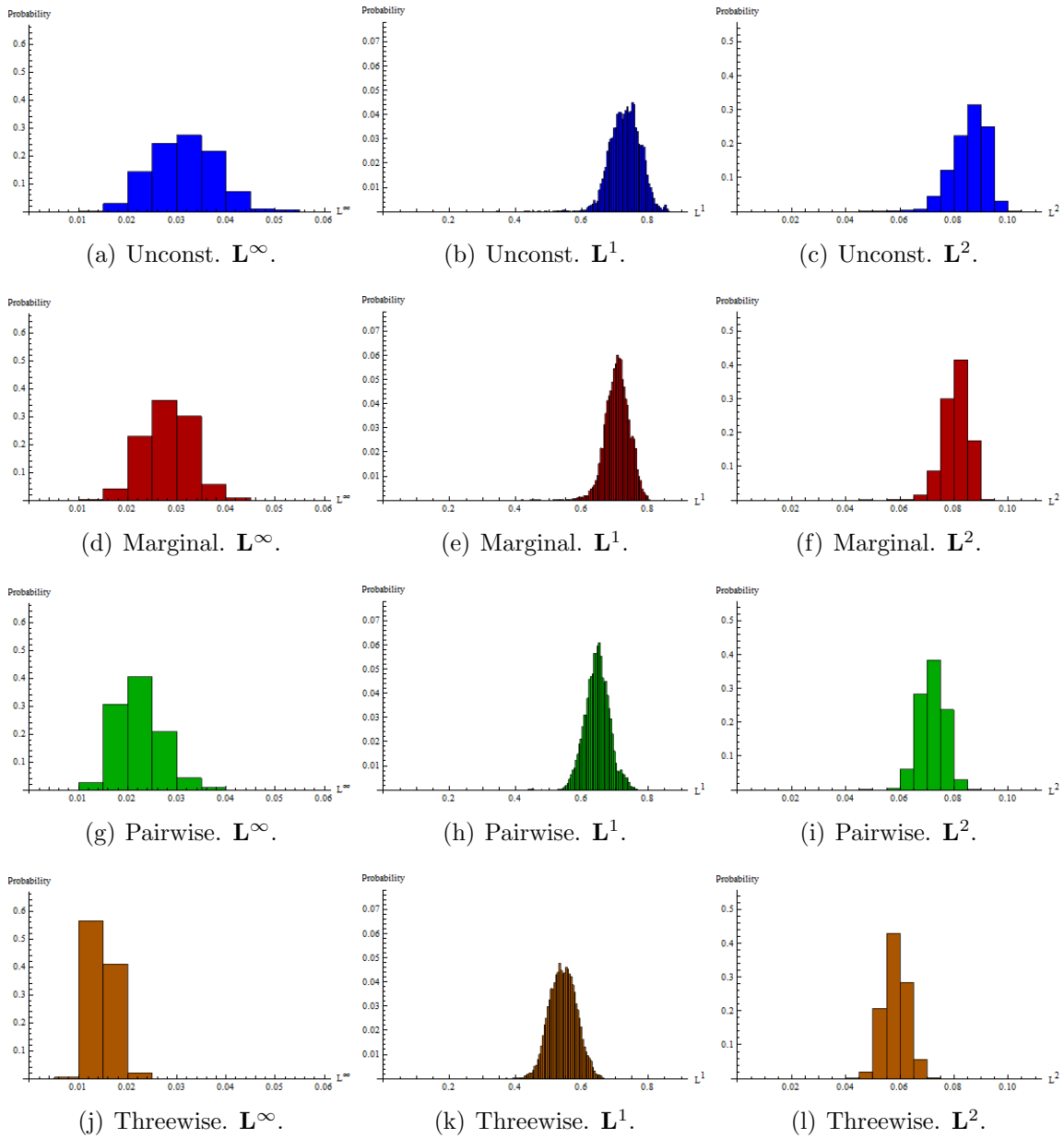

(a) Unconst. $\mathbf{L}^{\infty}$. (b) Unconst. $\mathbf{L}^{1}$. (c) Unconst. $\mathbf{L}^{2}$.

(d) Marginal. $\mathbf{L}^{\infty}$. (e) Marginal. $\mathbf{L}^{1}$. (f) Marginal. $\mathbf{L}^{2}$.

(g) Pairwise. $\mathbf{L}^{\infty}$. (h) Pairwise. $\mathbf{L}^{1}$. (i) Pairwise. $\mathbf{L}^{2}$.

(j) Threewise. $\mathbf{L}^{\infty}$. (k) Threewise. $\mathbf{L}^{1}$. (l) Threewise. $\mathbf{L}^{2}$.

Figure C.11: Effects of including new constraints in a truth set $\mathbb{T}$. The data is taken for a set that considers 7 binary variables. The unconstraint set uses 1 constraint. The Marginal set uses 8 constraints. The pairwise set uses 29 constraints. The three-wise set uses 64 constraints.

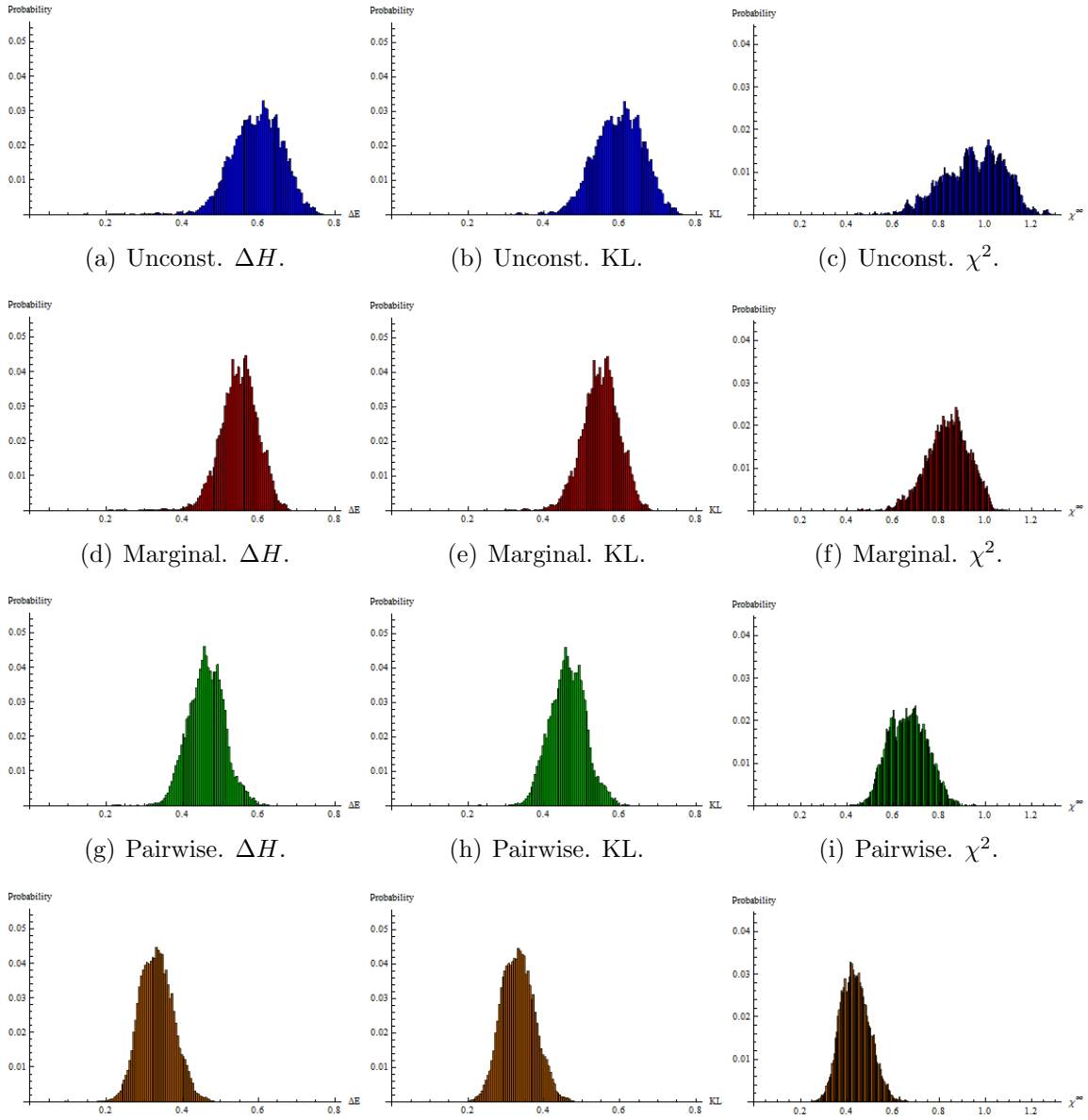

(a) Unconst. ΔH. (b) Unconst. KL. (c) Unconst. χ^2.

(d) Marginal. ΔH. (e) Marginal. KL. (f) Marginal. χ^2.

(g) Pairwise. ΔH. (h) Pairwise. KL. (i) Pairwise. χ^2.

(j) Threewise. ΔH. (k) Threewise. KL. (l) Threewise. χ^2.

Figure C.12: Effects of including new constraints in a truth set $\mathbb{T}$. The data is taken for a set that considers 7 binary variables. The unconstraint set uses 1 constraint. The Marginal set uses 8 constraints. The pairwise set uses 29 constraints. The three-wise set uses 64 constraints.

C.4 Raw Statistics in Symm. Marginal Constrained Sets.

Symmetric Sets With Marginal Constraints Part One

Table C.5: Accuracy measure statistics for 3 binary variables marginally constrained

Three Variables With Marginals of $p = 0.5$.						
ME	$\mathbf{L}^\infty$	$\mathbf{L}^1$	$\mathbf{L}^2$	ΔH	KL	χ^2
Mean	0.13483	0.54622	0.22541	0.33667	0.33667	0.44817
S.D.	0.04779	0.17924	0.07220	0.19426	0.19426	0.29461
Min	0.00734	0.02525	0.01077	0.00067	0.00067	0.00093
Max	0.34945	1.39468	0.56951	1.63090	1.63090	2.59473
AC						
Mean	0.13483	0.54622	0.22541	0.33667	0.33667	0.44817
S.D.	0.04779	0.17924	0.07220	0.19426	0.19426	0.29461
Min	0.00734	0.02525	0.01077	0.00067	0.00067	0.00093
Max	0.34945	1.39468	0.56951	1.63090	1.63090	2.59473
ChSC						
Mean	0.13483	0.54622	0.22541	0.33667	0.33667	0.44817
S.D.	0.04779	0.17924	0.07220	0.19426	0.19426	0.29461
Min	0.00734	0.02525	0.01077	0.00067	0.00067	0.00093
Max	0.34945	1.39468	0.56951	1.63090	1.63090	2.59473
MVIE						
Mean	0.13483	0.54622	0.22541	0.33667	0.33667	0.44817
S.D.	0.04779	0.17924	0.07220	0.19426	0.19426	0.29461
Min	0.00734	0.02525	0.01077	0.00067	0.00067	0.00093
Max	0.34945	1.39468	0.56951	1.63090	1.63090	2.59473
DAC						
Mean	0.13480	0.54613	0.22537	0.33657	0.33657	0.44799
S.D.	0.04777	0.17918	0.07218	0.19426	0.19419	0.29445
Min	0.00805	0.02849	0.01258	0.00057	0.00090	0.00126
Max	0.34912	1.39332	0.56891	1.63080	1.62687	2.58491

Three Variables With Marginals of $p = 0.6$.						
$\mathbf{L}^\infty$	$\mathbf{L}^1$	$\mathbf{L}^2$	ΔH	KL	χ^2	
0.12738	0.50316	0.20922	0.29811	0.29811	0.39538	
0.04543	0.16290	0.06721	0.16995	0.16995	0.24961	
0.00725	0.03087	0.01248	0.00094	0.00094	0.00130	
0.35072	1.31034	0.53902	1.50194	1.50194	2.61487	
0.12559	0.49615	0.20616	0.29499	0.29071	0.38225	
0.04472	0.15940	0.06581	0.16995	0.16310	0.23167	
0.00725	0.03439	0.01335	-0.00218	0.00098	0.00135	
0.33314	1.25589	0.51567	1.49882	1.36666	2.22531	
0.13183	0.51845	0.21546	0.23169	0.31829	0.44194	
0.05435	0.18934	0.07926	0.16995	0.19661	0.29790	
0.00787	0.02922	0.01237	-0.06547	0.00101	0.00141	
0.29999	1.17996	0.48191	1.43553	1.32450	2.01231	
0.12510	0.49491	0.20550	0.28541	0.29012	0.38280	
0.04556	0.16206	0.06697	0.16995	0.16417	0.23263	
0.00898	0.03303	0.01430	-0.01175	0.00139	0.00195	
0.31410	1.20511	0.49342	1.48924	1.26180	1.97555	
0.12524	0.49442	0.20540	0.28927	0.28927	0.38056	
0.04511	0.15969	0.06605	0.16995	0.16226	0.22914	
0.00943	0.03375	0.01429	-0.00789	0.00154	0.00210	
0.32135	1.21755	0.49948	1.49310	1.27818	1.99151	

Three Variables With Marginals of $p = 0.7$.						
ME	$\mathbf{L}^\infty$	$\mathbf{L}^1$	$\mathbf{L}^2$	ΔH	KL	χ^2
Mean	0.11841	0.45497	0.19176	0.27638	0.27638	0.39948
S.D.	0.04906	0.16893	0.07221	0.17522	0.17522	0.30382
Min	0.00412	0.01899	0.00822	0.00064	0.00064	0.00089
Max	0.33851	1.19043	0.49967	1.50838	1.50838	3.33831
AC						
Mean	0.10019	0.39209	0.16339	0.24444	0.21748	0.28755
S.D.	0.03777	0.13361	0.05555	0.17522	0.12592	0.18069
Min	0.00423	0.02414	0.00879	-0.03130	0.00063	0.00087
Max	0.28170	1.03479	0.42755	1.47644	1.12765	1.84165
ChSC						
Mean	0.10528	0.41035	0.17075	0.10456	0.24041	0.34964
S.D.	0.04799	0.16491	0.06930	0.17522	0.15122	0.25595
Min	0.00625	0.02766	0.01118	-0.17118	0.00088	0.00123
Max	0.34283	1.22946	0.51185	1.33657	1.25716	2.17363
MVIE						
Mean	0.09826	0.38654	0.16058	0.18547	0.21464	0.29003
S.D.	0.03973	0.13938	0.05791	0.17522	0.12447	0.18762
Min	0.00542	0.02134	0.00974	-0.09027	0.00065	0.00090
Max	0.30729	1.11731	0.46295	1.41748	1.00457	1.55146
DAC						
Mean	0.09795	0.38437	0.15984	0.21180	0.21180	0.28152
S.D.	0.03785	0.13276	0.05513	0.17522	0.12072	0.17556
Min	0.00676	0.02589	0.01090	-0.06394	0.00064	0.00089
Max	0.29181	1.06080	0.43958	1.44380	1.00053	1.50361

Three Variables With Marginals of $p = 0.8$.						
$\mathbf{L}^\infty$	$\mathbf{L}^1$	$\mathbf{L}^2$	ΔH	KL	χ^2	
0.11112	0.41058	0.17683	0.27846	0.27846	0.51535	
0.04543	0.14965	0.06575	0.16593	0.16593	0.44133	
0.00304	0.01187	0.00497	0.00027	0.00027	0.00037	
0.26780	0.88085	0.38391	1.16598	1.16598	4.28048	
0.06838	0.26737	0.11154	0.19430	0.14538	0.19284	
0.02612	0.09221	0.03850	0.16593	0.08475	0.12253	
0.00403	0.01412	0.00602	-0.08389	0.00046	0.00065	
0.18764	0.67637	0.28114	1.08183	0.66254	1.11941	
0.07051	0.27477	0.11435	0.02931	0.15598	0.22869	
0.03170	0.10894	0.04582	0.16593	0.09374	0.16270	
0.00461	0.01712	0.00715	-0.24888	0.00066	0.00092	
0.22176	0.79568	0.33189	0.91684	0.72048	1.29518	
0.06566	0.25864	0.10740	0.10852	0.13995	0.18991	
0.02641	0.09254	0.03847	0.16593	0.07906	0.12078	
0.00109	0.00626	0.00228	-0.16967	0.00007	0.00009	
0.19806	0.72090	0.29937	0.99604	0.58323	0.90601	
0.06538	0.25712	0.10685	0.13819	0.13819	0.18417	
0.02521	0.08847	0.03671	0.16593	0.07754	0.11387	
0.00215	0.00871	0.00366	-0.14000	0.00017	0.00024	
0.18753	0.68297	0.28368	1.02572	0.58507	0.85818	

Three Variables With Marginals of $p = 0.9$.						
ME	$\mathbf{L}^\infty$	$\mathbf{L}^1$	$\mathbf{L}^2$	ΔH	KL	χ^2
Mean	0.08041	0.28984	0.12572	0.24121	0.24121	0.87143
S.D.	0.02641	0.08625	0.03730	0.11861	0.11861	0.89689
Min	0.00132	0.00485	0.00206	0.00017	0.00017	0.00023
Max	0.16178	0.50381	0.22901	0.79239	0.79239	8.63525
AC						
Mean	0.03504	0.13635	0.05698	0.12395	0.07314	0.09699
S.D.	0.01344	0.04709	0.01975	0.11861	0.04263	0.06161
Min	0.00187	0.00723	0.00332	-0.11710	0.00030	0.00041
Max	0.09671	0.34655	0.14364	0.67513	0.33245	0.58519
ChSC						
Mean	0.03479	0.13588	0.05650	-0.00548	0.07530	0.11001
S.D.	0.01567	0.05395	0.02265	0.11861	0.04472	0.07805
Min	0.00102	0.00403	0.00168	-0.24652	0.00006	0.00008
Max	0.12062	0.43518	0.18078	0.54571	0.39968	0.74299
MVIE						
Mean	0.03269	0.12876	0.05347	0.05024	0.06838	0.09239
S.D.	0.01300	0.04561	0.01893	0.11861	0.03823	0.05826
Min	0.00104	0.00587	0.00214	-0.19080	0.00009	0.00013
Max	0.10877	0.39779	0.16453	0.60142	0.32094	0.52403
DAC						
Mean	0.03266	0.12833	0.05333	0.06778	0.06778	0.09018
S.D.	0.01252	0.04383	0.01818	0.11861	0.03771	0.05550
Min	0.00169	0.00823	0.00311	-0.17326	0.00022	0.00031
Max	0.10460	0.38203	0.15807	0.61897	0.29222	0.45628

Raw Statistics For Symmetric Sets With Marginal Constraints Part Two

Table C.6: Accuracy measure statistics for 4 binary variables marginally constrained

Four Variables With Marginals of $p = 0.5$.						
ME	$\mathbf{L}^\infty$	$\mathbf{L}^1$	$\mathbf{L}^2$	ΔH	KL	χ^2
Mean	0.10326	0.60959	0.18628	0.41504	0.41504	0.57825
S.D.	0.03320	0.11748	0.03796	0.14290	0.14290	0.24024
Min	0.02564	0.18192	0.05369	0.03251	0.03251	0.04613
Max	0.27133	1.13834	0.36311	1.11297	1.11297	2.10960
AC						
Mean	0.10326	0.60959	0.18628	0.41504	0.41504	0.57825
S.D.	0.03320	0.11748	0.03796	0.14290	0.14290	0.24024
Min	0.02564	0.18192	0.05369	0.03251	0.03251	0.04613
Max	0.27133	1.13834	0.36311	1.11297	1.11297	2.10960
ChSC						
Mean	0.10326	0.60959	0.18628	0.41504	0.41504	0.57825
S.D.	0.03320	0.11748	0.03796	0.14290	0.14290	0.24024
Min	0.02564	0.18192	0.05369	0.03251	0.03251	0.04613
Max	0.27133	1.13834	0.36311	1.11297	1.11297	2.10960
MVIE						
Mean	0.10326	0.60959	0.18628	0.41504	0.41504	0.57825
S.D.	0.03320	0.11748	0.03795	0.14290	0.14290	0.24023
Min	0.02563	0.18192	0.05369	0.03251	0.03250	0.04612
Max	0.27133	1.13834	0.36311	1.11297	1.11300	2.10951
DAC						
Mean	0.10321	0.60946	0.18624	0.41484	0.41484	0.57780
S.D.	0.03314	0.11740	0.03792	0.14290	0.14267	0.23945
Min	0.02634	0.18733	0.05549	0.03231	0.03476	0.04958
Max	0.26849	1.14126	0.36053	1.11277	1.11528	2.07109

Four Variables With Marginals of $p = 0.6$.						
$\mathbf{L}^\infty$	$\mathbf{L}^1$	$\mathbf{L}^2$	ΔH	KL	χ^2	
0.10264	0.58030	0.18156	0.38441	0.38441	0.53261	
0.03316	0.11695	0.03900	0.13305	0.13305	0.21531	
0.02275	0.15870	0.04871	0.03082	0.03082	0.04150	
0.27012	1.02570	0.33817	1.01482	1.01482	1.93592	
0.10030	0.57066	0.17806	0.37726	0.37448	0.51588	
0.03173	0.11448	0.03850	0.13305	0.12888	0.20506	
0.01912	0.14367	0.04460	0.02367	0.03166	0.04094	
0.24591	1.04104	0.32618	1.00767	0.97732	1.86197	
0.12235	0.63007	0.20385	0.24205	0.45119	0.68666	
0.04838	0.15687	0.06012	0.13305	0.19018	0.33597	
0.02335	0.17406	0.05367	-0.11154	0.03801	0.05346	
0.27519	1.18928	0.39988	0.87247	1.31573	2.31231	
0.10024	0.57028	0.17793	0.37590	0.37425	0.51583	
0.03179	0.11467	0.03866	0.13305	0.12909	0.20557	
0.01943	0.14634	0.04487	0.02231	0.03181	0.04105	
0.24592	1.04496	0.32582	1.00631	0.97572	1.86197	
0.10021	0.56976	0.17778	0.37390	0.37390	0.51559	
0.03185	0.11492	0.03885	0.13305	0.12930	0.20578	
0.01977	0.14350	0.04355	0.02032	0.02990	0.03840	
0.24747	1.04305	0.32895	1.00432	0.96946	1.81231	

Four Variables With Marginals of $p = 0.7$.						
ME	$\mathbf{L}^\infty$	$\mathbf{L}^1$	$\mathbf{L}^2$	ΔH	KL	χ^2
Mean	0.12285	0.56422	0.19120	0.38323	0.38323	0.58030
S.D.	0.04959	0.14099	0.05479	0.15392	0.15392	0.29392
Min	0.02042	0.13858	0.04234	0.02595	0.02595	0.03673
Max	0.31862	1.03304	0.39418	1.12777	1.12777	3.13612
AC						
Mean	0.08373	0.45758	0.14555	0.30688	0.28485	0.39501
S.D.	0.02852	0.09891	0.03494	0.15392	0.09985	0.16213
Min	0.01890	0.13020	0.04114	-0.05040	0.02200	0.03041
Max	0.22538	0.87573	0.31235	1.05142	0.76385	1.33524
ChSC						
Mean	0.10944	0.52264	0.17431	0.04439	0.36269	0.60063
S.D.	0.05067	0.15055	0.06130	0.15392	0.15858	0.33156
Min	0.01252	0.07112	0.02206	-0.31288	0.00905	0.01257
Max	0.31323	1.10271	0.41105	0.78893	1.21351	2.62028
MVIE						
Mean	0.08416	0.45638	0.14527	0.24313	0.28669	0.40842
S.D.	0.03223	0.10714	0.04000	0.15392	0.10352	0.17874
Min	0.01565	0.11441	0.03354	-0.11414	0.01988	0.02617
Max	0.24349	0.95023	0.34354	0.98768	0.87986	1.56655
DAC						
Mean	0.08283	0.45380	0.14408	0.28254	0.28254	0.39452
S.D.	0.02909	0.09964	0.03585	0.15392	0.09862	0.16287
Min	0.01699	0.11625	0.03354	-0.07473	0.01896	0.02500
Max	0.22342	0.90599	0.32557	1.02708	0.81423	1.41610

Four Variables With Marginals of $p = 0.8$.						
$\mathbf{L}^\infty$	$\mathbf{L}^1$	$\mathbf{L}^2$	ΔH	KL	χ^2	
0.15280	0.55942	0.21054	0.41817	0.41817	0.85751	
0.04560	0.12770	0.05204	0.15377	0.15377	0.51238	
0.01402	0.09787	0.03042	0.02746	0.02746	0.03936	
0.28293	0.91134	0.35281	1.02725	1.02725	6.75968	
0.05818	0.31256	0.10020	0.22998	0.19251	0.27006	
0.01992	0.06996	0.02496	0.15377	0.06980	0.11781	
0.01147	0.07936	0.02456	-0.16073	0.01242	0.01680	
0.14473	0.58690	0.21005	0.83906	0.50069	1.11569	
0.07607	0.35761	0.12032	-0.05002	0.24409	0.41692	
0.03585	0.10641	0.04382	0.15377	0.10624	0.23807	
0.01328	0.07723	0.02511	-0.44073	0.01903	0.02436	
0.22040	0.75574	0.29146	0.55906	0.73509	1.70095	
0.05823	0.31065	0.09966	0.13670	0.19394	0.28200	
0.02336	0.07767	0.02970	0.15377	0.07249	0.13189	
0.00424	0.02858	0.00895	-0.25400	0.00223	0.00307	
0.17390	0.64902	0.24212	0.74579	0.53727	1.11615	
0.05691	0.30794	0.09840	0.19022	0.19022	0.26938	
0.02041	0.07073	0.02587	0.15377	0.06887	0.11896	
0.01377	0.06485	0.02339	-0.20049	0.00564	0.00774	
0.15706	0.61936	0.22435	0.79930	0.49018	1.03395	

Four Variables With Marginals of $p = 0.9$.						
ME	$\mathbf{L}^\infty$	$\mathbf{L}^1$	$\mathbf{L}^2$	ΔH	KL	χ^2
Mean	0.12894	0.43116	0.17169	0.39360	0.39360	2.17852
S.D.	0.02261	0.06652	0.02696	0.10901	0.10901	2.18992
Min	0.04537	0.16572	0.06414	0.05390	0.05390	0.09628
Max	0.19940	0.60674	0.24897	0.81392	0.81392	33.95045
AC						
Mean	0.02950	0.15764	0.05058	0.14921	0.09580	0.13215
S.D.	0.01036	0.03526	0.01250	0.10901	0.03472	0.05607
Min	0.00484	0.03681	0.01062	-0.19050	0.00615	0.00806
Max	0.08339	0.31611	0.10863	0.56953	0.31329	0.55574
ChSC						
Mean	0.03503	0.17016	0.05640	-0.05363	0.11173	0.18677
S.D.	0.01633	0.04899	0.01998	0.10901	0.04603	0.10397
Min	0.00641	0.03889	0.01246	-0.39333	0.00951	0.01239
Max	0.11103	0.38005	0.14342	0.36669	0.40457	1.01582
MVIE						
Mean	0.02769	0.15132	0.04802	0.07259	0.09292	0.13252
S.D.	0.01053	0.03535	0.01319	0.10901	0.03347	0.05956
Min	0.00489	0.03073	0.01034	-0.26712	0.00508	0.00686
Max	0.08778	0.34125	0.12033	0.49291	0.32413	0.66874
DAC						
Mean	0.02752	0.15119	0.04792	0.09241	0.09241	0.12994
S.D.	0.00993	0.03393	0.01237	0.10901	0.03295	0.05671
Min	0.00429	0.02788	0.00892	-0.24729	0.00452	0.00616
Max	0.08358	0.33270	0.11647	0.51273	0.30616	0.60998

Raw Stat. For Symmetric Sets With Marginal Constraints Part Three

Table C.7: Accuracy measure statistics for 5 binary variables marginally constrained

Five Variables With Marginals of $p = 0.5$.						
ME	$\mathbf{L}^\infty$	$\mathbf{L}^1$	$\mathbf{L}^2$	ΔH	KL	χ^2
Mean	0.07249	0.66240	0.14713	0.48525	0.48525	0.70644
S.D.	0.01947	0.08348	0.02070	0.10928	0.10928	0.20087
Min	0.02516	0.25184	0.05570	0.09122	0.09122	0.09929
Max	0.16416	0.96684	0.23241	0.91726	0.91726	1.72842
AC						
Mean	0.07249	0.66240	0.14713	0.48525	0.48525	0.70644
S.D.	0.01947	0.08348	0.02070	0.10928	0.10928	0.20087
Min	0.02516	0.25184	0.05570	0.09122	0.09122	0.09929
Max	0.16416	0.96684	0.23241	0.91726	0.91726	1.72842
ChSC						
Mean	0.07249	0.66240	0.14713	0.48525	0.48525	0.70644
S.D.	0.01947	0.08348	0.02070	0.10928	0.10928	0.20087
Min	0.02516	0.25184	0.05570	0.09122	0.09122	0.09929
Max	0.16416	0.96684	0.23241	0.91726	0.91726	1.72842
MVIE						
Mean	0.07249	0.66240	0.14713	0.48525	0.48525	0.70644
S.D.	0.01947	0.08348	0.02070	0.10928	0.10928	0.20086
Min	0.02518	0.25184	0.05570	0.09122	0.09121	0.09928
Max	0.16418	0.96683	0.23242	0.91726	0.91731	1.72923
DAC						
Mean	0.07228	0.66179	0.14696	0.48391	0.48391	0.70309
S.D.	0.01935	0.08295	0.02055	0.10928	0.10823	0.19814
Min	0.02517	0.25499	0.05574	0.08987	0.09137	0.09989
Max	0.16704	0.97397	0.23449	0.91591	0.92660	1.84935

Five Variables With Marginals of $p = 0.6$.						
$\mathbf{L}^\infty$	$\mathbf{L}^1$	$\mathbf{L}^2$	ΔH	KL	χ^2
0.08041	0.64619	0.15163	0.46674	0.46674	0.68139
0.02645	0.09058	0.02583	0.11322	0.11322	0.20532
0.01706	0.12344	0.02926	0.01940	0.01940	0.02792
0.20866	0.94929	0.25827	0.90145	0.90145	1.69515
0.07552	0.63180	0.14720	0.45264	0.45049	0.65250
0.02237	0.08913	0.02518	0.11322	0.10877	0.19156
0.00984	0.10135	0.02216	0.00530	0.01075	0.01513
0.17833	0.96252	0.24888	0.88735	0.92705	1.60752
0.12193	0.72370	0.19043	0.22068	0.58280	0.96947
0.04725	0.12872	0.04940	0.11322	0.18391	0.36972
0.02130	0.31008	0.06622	-0.22666	0.13105	0.17368
0.22499	1.13007	0.33192	0.65539	1.33549	2.64987
0.07593	0.63345	0.14763	0.45703	0.45152	0.65299
0.02279	0.08866	0.02488	0.11322	0.10834	0.19035
0.00792	0.08748	0.01899	0.00970	0.00954	0.01349
0.18541	0.95624	0.24515	0.89175	0.90895	1.58001
0.07535	0.63096	0.14704	0.44957	0.44957	0.65069
0.02223	0.08917	0.02531	0.11322	0.10863	0.19080
0.01252	0.10928	0.02441	0.00223	0.01218	0.01720
0.17565	0.97235	0.25037	0.88428	0.95195	1.63698

Five Variables With Marginals of $p = 0.7$.						
ME	$\mathbf{L}^\infty$	$\mathbf{L}^1$	$\mathbf{L}^2$	ΔH	KL	χ^2
Mean	0.13679	0.66002	0.18925	0.49407	0.49407	0.79982
S.D.	0.05064	0.11488	0.04595	0.14134	0.14134	0.30512
Min	0.02558	0.26735	0.06421	0.11989	0.11989	0.17261
Max	0.28651	1.04497	0.33080	1.06028	1.06028	4.25448
AC						
Mean	0.06389	0.49480	0.11895	0.34166	0.33348	0.48548
S.D.	0.02265	0.07682	0.02433	0.14134	0.08364	0.15562
Min	0.01792	0.15705	0.04110	-0.03251	0.02704	0.03667
Max	0.16643	0.83775	0.22026	0.90787	0.71798	1.35700
ChSC						
Mean	0.11883	0.60551	0.17037	-0.05189	0.46677	0.86156
S.D.	0.04928	0.12492	0.05191	0.14134	0.15319	0.38549
Min	0.01845	0.21014	0.04501	-0.42607	0.07799	0.10688
Max	0.28625	1.01156	0.34235	0.51432	1.13269	2.70873
MVIE						
Mean	0.06547	0.49801	0.12062	0.27779	0.33786	0.50370
S.D.	0.02578	0.08507	0.02922	0.14134	0.08832	0.17196
Min	0.00782	0.09959	0.02167	-0.09639	0.01785	0.02396
Max	0.19326	0.87609	0.24433	0.84400	0.78185	1.40224
DAC						
Mean	0.06350	0.49314	0.11848	0.33157	0.33157	0.48229
S.D.	0.02258	0.07707	0.02457	0.14134	0.08254	0.15229
Min	0.01803	0.15028	0.03886	-0.04261	0.02597	0.03461
Max	0.17051	0.83547	0.22191	0.89778	0.71126	1.24376

Five Variables With Marginals of $p = 0.8$.						
$\mathbf{L}^\infty$	$\mathbf{L}^1$	$\mathbf{L}^2$	ΔH	KL	χ^2
0.19528	0.68752	0.23914	0.56455	0.56455	1.29941
0.04490	0.11661	0.04754	0.15420	0.15420	0.65939
0.08365	0.36192	0.12207	0.16648	0.16648	0.26760
0.31119	1.01488	0.36051	1.07385	1.07385	7.99695
0.04903	0.35220	0.08769	0.22136	0.23525	0.34888
0.01851	0.06080	0.02090	0.15420	0.06324	0.12595
0.01256	0.14568	0.03729	-0.17671	0.04528	0.06389
0.11549	0.58902	0.17506	0.73065	0.54580	1.06904
0.09136	0.43556	0.12764	-0.16217	0.34056	0.68140
0.04227	0.10665	0.04532	0.15420	0.12646	0.35450
0.01173	0.15145	0.03450	-0.56024	0.06644	0.08562
0.20117	0.74322	0.25038	0.34712	0.82576	2.24795
0.05282	0.35809	0.09110	0.13399	0.24344	0.37703
0.02500	0.07535	0.02861	0.15420	0.07146	0.15229
0.01058	0.13100	0.02703	-0.26407	0.03981	0.05541
0.13917	0.62503	0.19416	0.64329	0.59408	1.22019
0.04896	0.35167	0.08749	0.23318	0.23318	0.34267
0.01797	0.05852	0.01984	0.15420	0.06019	0.11566
0.01283	0.15320	0.03659	-0.16489	0.05116	0.07297
0.11591	0.56933	0.16871	0.74248	0.50387	0.92948

Five Variables With Marginals of $p = 0.9$.						
ME	$\mathbf{L}^\infty$	$\mathbf{L}^1$	$\mathbf{L}^2$	ΔH	KL	χ^2
Mean	0.17942	0.56225	0.21692	0.56907	0.56907	5.41303
S.D.	0.02100	0.05761	0.02370	0.10586	0.10586	4.55807
Min	0.09323	0.32094	0.11946	0.20882	0.20882	0.56803
Max	0.23446	0.69635	0.27593	0.87649	0.87649	49.73910
AC						
Mean	0.02409	0.17333	0.04267	0.15359	0.11518	0.16675
S.D.	0.00964	0.02851	0.00996	0.10586	0.02890	0.05326
Min	0.00685	0.03806	0.01515	-0.20665	0.00336	0.00439
Max	0.07848	0.31661	0.10406	0.46102	0.22713	0.40875
ChSC						
Mean	0.03772	0.19919	0.05572	-0.10679	0.14802	0.28483
S.D.	0.01936	0.04799	0.02059	0.10586	0.05358	0.15725
Min	0.00568	0.07737	0.01737	-0.46703	0.02454	0.04115
Max	0.12253	0.40756	0.14995	0.20064	0.43390	1.22346
MVIE						
Mean	0.02318	0.16966	0.04163	0.08607	0.11489	0.17293
S.D.	0.01089	0.03242	0.01229	0.10586	0.03126	0.06443
Min	0.00010	0.00095	0.00021	-0.27418	0.00000	0.00001
Max	0.09152	0.34344	0.11788	0.39349	0.26993	0.53751
DAC						
Mean	0.02295	0.16961	0.04144	0.11365	0.11365	0.16747
S.D.	0.00996	0.02974	0.01087	0.10586	0.02919	0.05642
Min	0.00430	0.01982	0.00694	-0.24660	0.00118	0.00157
Max	0.08618	0.33218	0.11164	0.42107	0.24141	0.44604

Raw Stat. For Symmetric Sets With Marginal Constraints Part Four

Table C.8: Accuracy measure statistics for 6 binary variables marginally constrained

Six Variables With Marginals of $p = 0.5$.						
ME	$\mathbf{L}^\infty$	$\mathbf{L}^1$	$\mathbf{L}^2$	ΔH	KL	χ^2
Mean	0.04767	0.69098	0.11142	0.52996	0.52996	0.80305
S.D.	0.01161	0.06077	0.01158	0.08365	0.08365	0.16834
Min	0.01106	0.24529	0.03835	0.06961	0.06961	0.09415
Max	0.09678	0.90657	0.15131	0.83298	0.83298	1.46521
AC						
Mean	0.04767	0.69098	0.11142	0.52996	0.52996	0.80305
S.D.	0.01161	0.06077	0.01158	0.08365	0.08365	0.16834
Min	0.01106	0.24529	0.03835	0.06961	0.06961	0.09415
Max	0.09678	0.90657	0.15131	0.83298	0.83298	1.46521
ChSC						
Mean	0.04767	0.69098	0.11142	0.52996	0.52996	0.80305
S.D.	0.01161	0.06077	0.01158	0.08365	0.08365	0.16834
Min	0.01106	0.24529	0.03835	0.06961	0.06961	0.09415
Max	0.09678	0.90657	0.15131	0.83298	0.83298	1.46521
MVIE						
Mean	0.04767	0.69098	0.11141	0.52996	0.52996	0.80303
S.D.	0.01161	0.06077	0.01158	0.08365	0.08365	0.16834
Min	0.01105	0.24540	0.03837	0.06961	0.06966	0.09421
Max	0.09678	0.90664	0.15131	0.83298	0.83287	1.46530
DAC						
Mean	0.04700	0.68696	0.11066	0.52187	0.52187	0.78255
S.D.	0.01146	0.05903	0.01123	0.08365	0.07992	0.15716
Min	0.01330	0.25260	0.04094	0.06152	0.07942	0.10810
Max	0.09462	0.88391	0.14966	0.82489	0.79832	1.41012

Six Variables With Marginals of $p = 0.6$.						
$\mathbf{L}^\infty$	$\mathbf{L}^1$	$\mathbf{L}^2$	ΔH	KL	χ^2	
0.06693	0.69707	0.12522	0.54271	0.54271	0.83689	
0.02309	0.06840	0.01803	0.09435	0.09435	0.19012	
0.02048	0.15115	0.03414	0.03094	0.03094	0.04639	
0.14172	0.92423	0.18072	0.86145	0.86145	1.48379	
0.05632	0.67235	0.11758	0.51658	0.51002	0.77374	
0.01517	0.06239	0.01545	0.09435	0.08556	0.16897	
0.00740	0.10273	0.01657	0.00481	0.01121	0.01549	
0.10825	0.87593	0.18182	0.83532	0.88124	1.55349	
0.12387	0.77780	0.17259	0.17035	0.67547	1.22151	
0.04305	0.09898	0.04042	0.09435	0.16422	0.38154	
0.03395	0.42251	0.08567	-0.34142	0.22115	0.33244	
0.21250	1.05012	0.27717	0.48909	1.30197	2.75889	
0.05778	0.67575	0.11862	0.52468	0.51293	0.77582	
0.01608	0.06295	0.01523	0.09435	0.08499	0.16597	
0.00428	0.09266	0.01427	0.01291	0.01031	0.01425	
0.11488	0.86609	0.17752	0.84342	0.86304	1.51869	
0.05532	0.66825	0.11661	0.50178	0.50178	0.75118	
0.01492	0.06066	0.01563	0.09435	0.08217	0.15638	
0.01368	0.14252	0.02624	-0.00999	0.02360	0.03290	
0.10499	0.86382	0.18197	0.82052	0.85196	1.41162	

Six Variables With Marginals of $p = 0.7$.						
ME	$\mathbf{L}^\infty$	$\mathbf{L}^1$	$\mathbf{L}^2$	ΔH	KL	χ^2
Mean	0.13396	0.70590	0.17014	0.57215	0.57215	1.00699
S.D.	0.04427	0.10019	0.03943	0.12892	0.12892	0.28350
Min	0.03528	0.46667	0.09199	0.28110	0.28110	0.42166
Max	0.23209	0.98617	0.25935	0.99871	0.99871	2.18777
AC						
Mean	0.06046	0.55104	0.10641	0.30221	0.39355	0.60515
S.D.	0.02446	0.06930	0.02436	0.12892	0.06985	0.13456
Min	0.01580	0.22599	0.03931	0.01116	0.07852	0.10103
Max	0.16509	0.79719	0.20786	0.72877	0.63988	1.08699
ChSC						
Mean	0.15813	0.72277	0.19467	-0.20909	0.65235	1.44350
S.D.	0.04501	0.10364	0.04523	0.12892	0.15518	0.46676
Min	0.05964	0.39619	0.08806	-0.50014	0.18956	0.31094
Max	0.28852	1.05776	0.32965	0.21746	1.20192	2.99290
MVIE						
Mean	0.07045	0.56737	0.11485	0.24349	0.41155	0.65145
S.D.	0.02999	0.07966	0.02997	0.12892	0.07721	0.15436
Min	0.01012	0.21047	0.03210	-0.04756	0.07551	0.09649
Max	0.18427	0.83844	0.22663	0.67005	0.68557	1.17962
DAC						
Mean	0.04914	0.52217	0.09689	0.36140	0.36140	0.53010
S.D.	0.01701	0.05697	0.01634	0.12892	0.06033	0.10141
Min	0.01423	0.32305	0.05190	0.07035	0.12955	0.16761
Max	0.13041	0.71499	0.16606	0.78795	0.60765	0.91809

Six Variables With Marginals of $p = 0.8$.						
$\mathbf{L}^\infty$	$\mathbf{L}^1$	$\mathbf{L}^2$	ΔH	KL	χ^2	
0.26820	0.88013	0.30045	0.83350	0.83350	2.34267	
0.02789	0.07664	0.02954	0.13912	0.13912	0.88765	
0.21474	0.67943	0.24045	0.51544	0.51544	0.89400	
0.34526	1.10852	0.38220	1.28131	1.28131	11.90230	
0.03205	0.34262	0.06168	0.28470	0.24246	0.35886	
0.01441	0.03779	0.01116	0.13912	0.03869	0.06861	
0.01037	0.08459	0.01972	-0.03336	0.01042	0.01439	
0.08691	0.48689	0.10639	0.73251	0.38456	0.59871	
0.07638	0.41541	0.09915	-0.17734	0.32363	0.63663	
0.02690	0.05763	0.02489	0.13912	0.06100	0.17681	
0.01442	0.22201	0.03962	-0.49540	0.07655	0.13258	
0.12936	0.54808	0.14759	0.27047	0.50609	1.28914	
0.03134	0.34249	0.06152	0.21248	0.24197	0.36555	
0.01023	0.03334	0.00886	0.13912	0.03597	0.06793	
0.00220	0.05183	0.00808	-0.10557	0.00749	0.01029	
0.07066	0.45298	0.09082	0.66030	0.36212	0.62365	
0.03047	0.33792	0.06043	0.23611	0.23611	0.34950	
0.01149	0.03474	0.00937	0.13912	0.03604	0.06452	
0.00518	0.08948	0.01457	-0.08195	0.01443	0.01995	
0.07706	0.46084	0.09642	0.68392	0.38121	0.65347	

Six Variables With Marginals of $p = 0.9$.						
ME	$\mathbf{L}^\infty$	$\mathbf{L}^1$	$\mathbf{L}^2$	ΔH	KL	χ^2
Mean	0.23114	0.68981	0.26353	0.76366	0.76366	12.71220
S.D.	0.01694	0.04519	0.01815	0.10347	0.10347	12.66190
Min	0.18707	0.58192	0.21877	0.50138	0.50138	1.46620
Max	0.26269	0.79719	0.29936	0.97538	0.97538	172.77814
AC						
Mean	0.01747	0.17579	0.03240	0.14023	0.12240	0.18357
S.D.	0.00713	0.01979	0.00645	0.10347	0.02177	0.04161
Min	0.00605	0.03781	0.01016	-0.12205	0.00388	0.00522
Max	0.04105	0.23261	0.05465	0.35196	0.19367	0.32780
ChSC						
Mean	0.04055	0.21418	0.05209	-0.15790	0.16668	0.33972
S.D.	0.01693	0.03629	0.01650	0.10347	0.04097	0.13072
Min	0.01067	0.10933	0.02141	-0.42018	0.03519	0.06220
Max	0.08461	0.31799	0.09584	0.05382	0.29850	0.82176
MVIE						
Mean	0.01761	0.17419	0.03238	0.08770	0.12313	0.18914
S.D.	0.00937	0.02274	0.00870	0.10347	0.02199	0.04508
Min	0.00102	0.02016	0.00327	-0.17458	0.00231	0.00312
Max	0.04987	0.24706	0.06242	0.29942	0.19928	0.36704
DAC						
Mean	0.01699	0.17325	0.03186	0.11988	0.11988	0.17823
S.D.	0.00765	0.02049	0.00708	0.10347	0.02023	0.03769
Min	0.00456	0.03983	0.00840	-0.14240	0.00572	0.00779
Max	0.04407	0.23889	0.05709	0.33160	0.19406	0.32009

Raw Stat. For Symmetric Sets With Marginal Constraints Part Five

Table C.9: Accuracy measure statistics for 7 binary variables marginally constrained

Seven Variables With Marginals of $p = 0.5$.						
ME	$\mathbf{L}^\infty$	$\mathbf{L}^1$	$\mathbf{L}^2$	ΔH	KL	χ^2
Mean	0.02884	0.70191	0.08137	0.55125	0.55125	0.85358
S.D.	0.00595	0.04470	0.00690	0.06748	0.06748	0.14537
Min	0.00477	0.17046	0.01943	0.03576	0.03576	0.04833
Max	0.04634	0.85980	0.10186	0.79736	0.79736	1.32808
AC						
Mean	0.02884	0.70191	0.08137	0.55125	0.55125	0.85358
S.D.	0.00595	0.04470	0.00690	0.06748	0.06748	0.14537
Min	0.00477	0.17046	0.01943	0.03576	0.03576	0.04833
Max	0.04634	0.85980	0.10186	0.79736	0.79736	1.32808
ChSC						
Mean	0.02884	0.70191	0.08137	0.55125	0.55125	0.85358
S.D.	0.00595	0.04470	0.00690	0.06748	0.06748	0.14537
Min	0.00477	0.17046	0.01943	0.03576	0.03576	0.04833
Max	0.04634	0.85980	0.10186	0.79736	0.79736	1.32808
MVIE						
Mean	-	-	-	-	-	-
S.D.	-	-	-	-	-	-
Min	-	-	-	-	-	-
Max	-	-	-	-	-	-
DAC						
Mean	0.02677	0.68778	0.07926	0.52047	0.52047	0.76865
S.D.	0.00554	0.04127	0.00600	0.06748	0.05510	0.10298
Min	0.00794	0.22950	0.02575	0.00497	0.05989	0.08278
Max	0.04396	0.83553	0.09685	0.76658	0.71510	1.06711

Seven Variables With Marginals of $p = 0.6$.						
$\mathbf{L}^\infty$	$\mathbf{L}^1$	$\mathbf{L}^2$	ΔH	KL	χ^2
0.10436	0.75909	0.13144	0.68065	0.68065	1.24306
0.03803	0.06260	0.02990	0.11600	0.11600	0.32442
0.02907	0.57139	0.07443	0.37263	0.37263	0.57255
0.17855	0.90374	0.19159	0.93252	0.93252	2.06727
0.06607	0.68886	0.10107	0.63267	0.52752	0.80150
0.03263	0.05570	0.02222	0.11600	0.06357	0.11269
0.01355	0.42755	0.05833	0.32465	0.23660	0.39687
0.13625	0.80753	0.15080	0.88455	0.68767	1.09872
0.07466	0.68378	0.10679	0.16552	0.53831	0.90817
0.03691	0.08307	0.03119	0.11600	0.09932	0.22368
0.00199	0.06448	0.00721	-0.14250	0.00608	0.00830
0.14997	0.89815	0.17759	0.41739	0.85039	1.57445
-	-	-	-	-	-
-	-	-	-	-	-
-	-	-	-	-	-
-	-	-	-	-	-
0.03710	0.62100	0.07824	0.44789	0.44789	0.65547
0.01488	0.03884	0.00964	0.11600	0.04428	0.08481
0.01416	0.29349	0.05773	0.13987	0.09290	0.12902
0.07606	0.75749	0.11333	0.69977	0.61224	1.03324

Seven Variables With Marginals of $p = 0.7$.						
ME	$\mathbf{L}^\infty$	$\mathbf{L}^1$	$\mathbf{L}^2$	ΔH	KL	χ^2
Mean	0.25710	0.97591	0.27539	1.03916	1.03916	2.16212
S.D.	0.02790	0.07475	0.02789	0.14241	0.14241	0.46032
Min	0.22025	0.84829	0.23728	0.80271	0.80271	1.43226
Max	0.32519	1.18000	0.34240	1.41301	1.41301	3.93052
AC						
Mean	0.05361	0.54866	0.08270	0.60587	0.40258	0.59908
S.D.	0.02762	0.04477	0.02003	0.14241	0.04560	0.08114
Min	0.01772	0.42840	0.05710	0.36941	0.21138	0.26965
Max	0.12140	0.69524	0.13512	0.97972	0.54866	0.88104
ChSC						
Mean	0.06651	0.53827	0.09040	0.00420	0.42377	0.77956
S.D.	0.02530	0.05601	0.02139	0.14241	0.05694	0.16203
Min	0.00599	0.19360	0.02220	-0.23225	0.08056	0.10508
Max	0.10208	0.65307	0.12083	0.37805	0.57451	1.18127
MVIE						
Mean	-	-	-	-	-	-
S.D.	-	-	-	-	-	-
Min	-	-	-	-	-	-
Max	-	-	-	-	-	-
DAC						
Mean	0.02816	0.48123	0.06142	0.34794	0.34794	0.51042
S.D.	0.01199	0.03058	0.00770	0.14241	0.03446	0.05728
Min	0.01193	0.32626	0.04533	0.11148	0.14491	0.18804
Max	0.06809	0.58132	0.08716	0.72179	0.46036	0.72335

Seven Variables With Marginals of $p = 0.8$.						
$\mathbf{L}^\infty$	$\mathbf{L}^1$	$\mathbf{L}^2$	ΔH	KL	χ^2
0.37009	1.13990	0.39482	1.38460	1.38460	6.04322
0.01117	0.02786	0.01153	0.06762	0.06762	1.83122
0.34327	1.02198	0.36705	1.19326	1.19326	3.37788
0.39706	1.22090	0.42299	1.53707	1.53707	15.24914
0.05747	0.39063	0.07010	0.58656	0.27749	0.41092
0.01117	0.02288	0.00890	0.06762	0.03079	0.06267
0.03065	0.24665	0.04736	0.39523	0.08053	0.09462
0.08445	0.46241	0.09300	0.73903	0.36637	0.60441
0.02394	0.32371	0.04377	0.07383	0.25091	0.42495
0.01043	0.03172	0.00880	0.06762	0.03960	0.10178
0.00059	0.01942	0.00221	-0.11751	0.00111	0.00155
0.05014	0.41908	0.06591	0.22630	0.37662	0.75875
-	-	-	-	-	-
-	-	-	-	-	-
-	-	-	-	-	-
-	-	-	-	-	-
0.01290	0.29935	0.03562	0.21815	0.21815	0.31759
0.00344	0.02267	0.00365	0.06762	0.02559	0.04594
0.00658	0.12600	0.02691	0.02681	0.03014	0.03865
0.02698	0.38135	0.04823	0.37061	0.30603	0.46909

Seven Variables With Marginals of $p = 0.9$.						
ME	$\mathbf{L}^\infty$	$\mathbf{L}^1$	$\mathbf{L}^2$	ΔH	KL	χ^2
Mean	0.28588	0.82324	0.31385	1.01351	1.01351	40.40720
S.D.	0.01609	0.04252	0.01688	0.10881	0.10881	32.29872
Min	0.26624	0.75888	0.29286	0.86241	0.86241	7.70305
Max	0.32363	0.92438	0.35240	1.27309	1.27309	253.61681
AC						
Mean	0.01456	0.18087	0.02604	0.15437	0.13034	0.19665
S.D.	0.00880	0.01547	0.00621	0.10881	0.01541	0.03008
Min	0.00521	0.12968	0.01809	0.00326	0.04381	0.05012
Max	0.04110	0.22276	0.04371	0.41395	0.17813	0.29940
ChSC						
Mean	0.03746	0.21181	0.04480	-0.16385	0.17274	0.37196
S.D.	0.01594	0.03470	0.01509	0.10881	0.04077	0.14362
Min	0.00098	0.03313	0.00365	-0.31495	0.00640	0.00854
Max	0.05703	0.26895	0.06574	0.09573	0.25917	0.71067
MVIE						
Mean	-	-	-	-	-	-
S.D.	-	-	-	-	-	-
Min	-	-	-	-	-	-
Max	-	-	-	-	-	-
DAC						
Mean	0.01431	0.17299	0.02484	0.11716	0.11716	0.16830
S.D.	0.00774	0.01682	0.00582	0.10881	0.01519	0.02431
Min	0.00497	0.13004	0.01704	-0.03395	0.04894	0.05580
Max	0.03775	0.21385	0.04097	0.37674	0.16437	0.25561

C.5 Standard Dev. Marginal and Correlation Symm. Sets.

Symmetric Sets Marginal and Correlation Standard Deviation Part One.

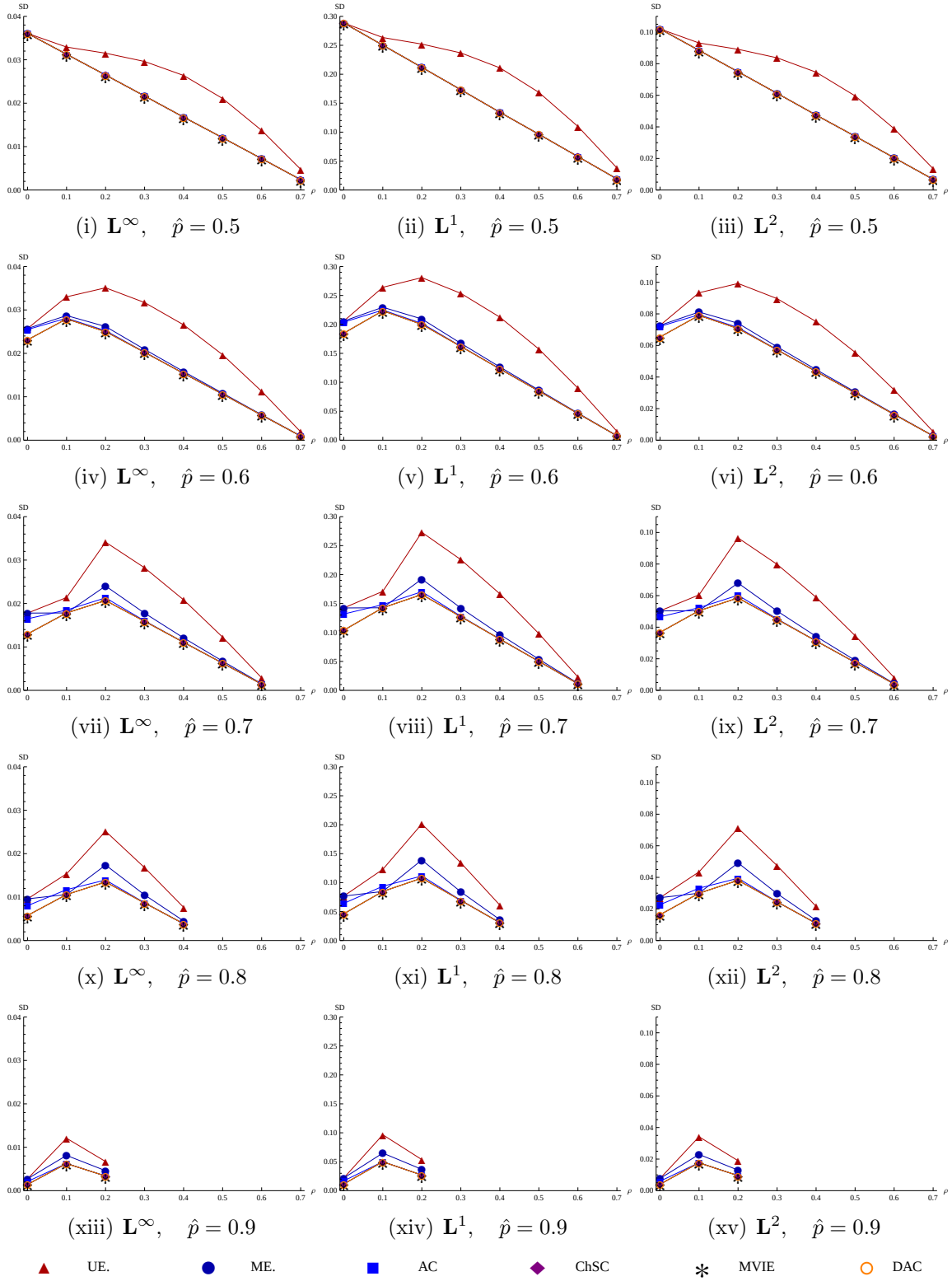

Figure C.13: Standard Dev. for $\mathbb{T}$ with 3 binary random variables (part one).

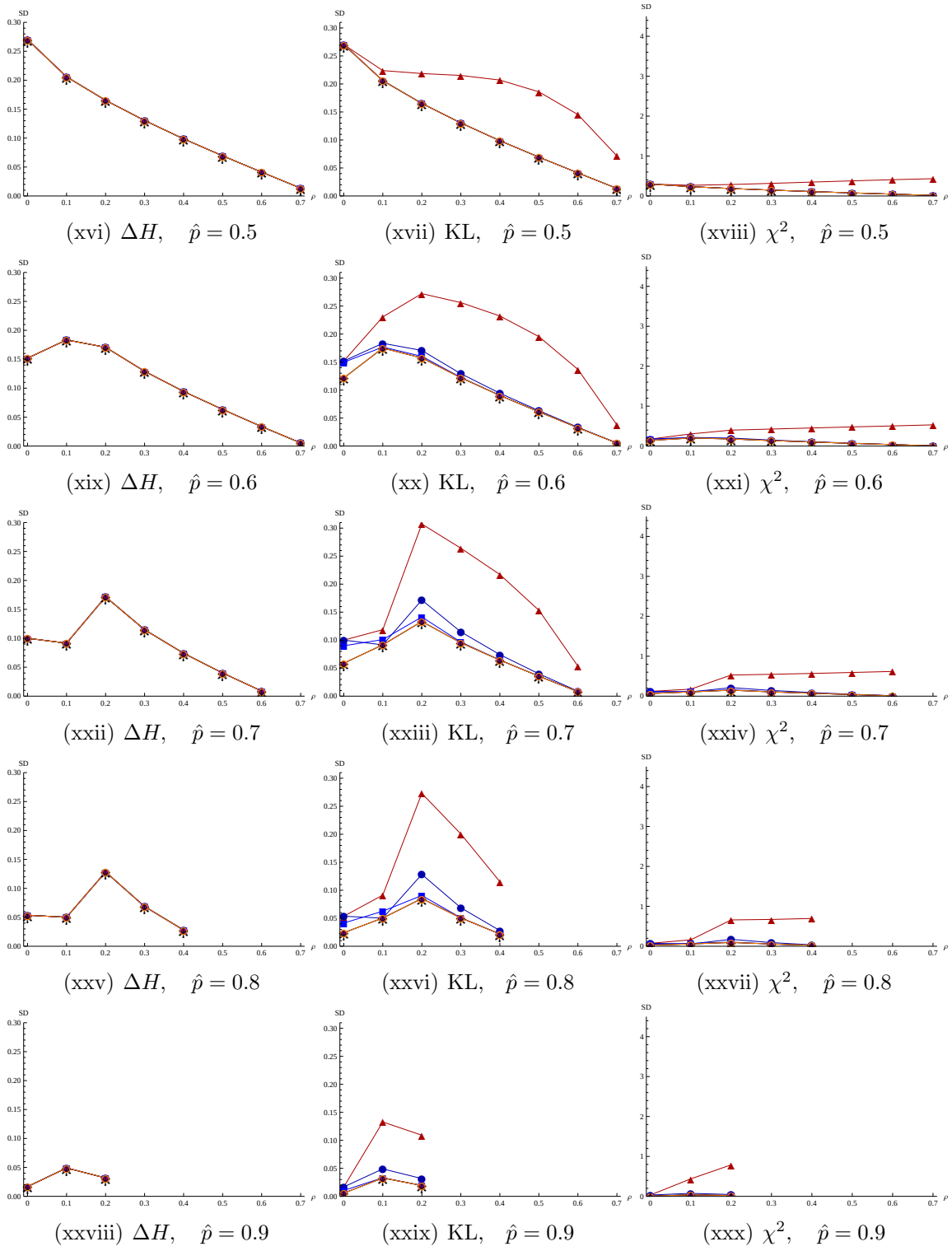

(xvi) ΔH, $\hat{p} = 0.5$ (xvii) KL, $\hat{p} = 0.5$ (xviii) χ^2, $\hat{p} = 0.5$

(xix) ΔH, $\hat{p} = 0.6$ (xx) KL, $\hat{p} = 0.6$ (xxi) χ^2, $\hat{p} = 0.6$

(xxii) ΔH, $\hat{p} = 0.7$ (xxiii) KL, $\hat{p} = 0.7$ (xxiv) χ^2, $\hat{p} = 0.7$

(xxv) ΔH, $\hat{p} = 0.8$ (xxvi) KL, $\hat{p} = 0.8$ (xxvii) χ^2, $\hat{p} = 0.8$

(xxviii) ΔH, $\hat{p} = 0.9$ (xxix) KL, $\hat{p} = 0.9$ (xxx) χ^2, $\hat{p} = 0.9$

Figure C.13: Standard Deviation estimates for accuracy measures (Columns) for truth sets with 3 binary random variables (part two). The truth set shows rank correlation constrains changes (x-axes) and marginal constrains changes $\hat{p}$ (rows).

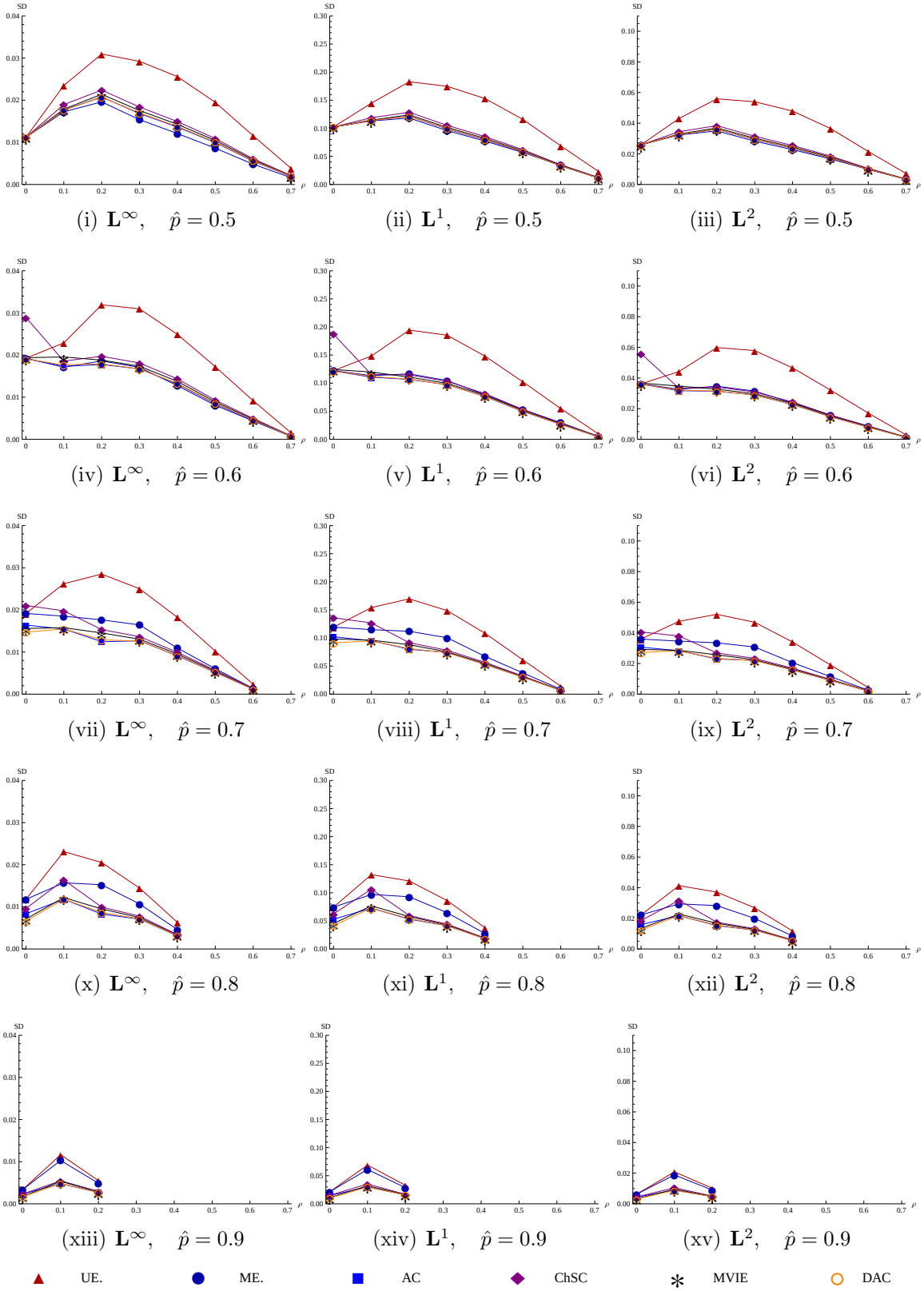

(i) $\mathbf{L}^{\infty}$, $\hat{p} = 0.5$ (ii) $\mathbf{L}^{1}$, $\hat{p} = 0.5$ (iii) $\mathbf{L}^{2}$, $\hat{p} = 0.5$

(iv) $\mathbf{L}^{\infty}$, $\hat{p} = 0.6$ (v) $\mathbf{L}^{1}$, $\hat{p} = 0.6$ (vi) $\mathbf{L}^{2}$, $\hat{p} = 0.6$

(vii) $\mathbf{L}^{\infty}$, $\hat{p} = 0.7$ (viii) $\mathbf{L}^{1}$, $\hat{p} = 0.7$ (ix) $\mathbf{L}^{2}$, $\hat{p} = 0.7$

(x) $\mathbf{L}^{\infty}$, $\hat{p} = 0.8$ (xi) $\mathbf{L}^{1}$, $\hat{p} = 0.8$ (xii) $\mathbf{L}^{2}$, $\hat{p} = 0.8$

(xiii) $\mathbf{L}^{\infty}$, $\hat{p} = 0.9$ (xiv) $\mathbf{L}^{1}$, $\hat{p} = 0.9$ (xv) $\mathbf{L}^{2}$, $\hat{p} = 0.9$

Figure C.14: Standard Dev. for $\mathbb{T}$ with 4 binary random variables (part one).

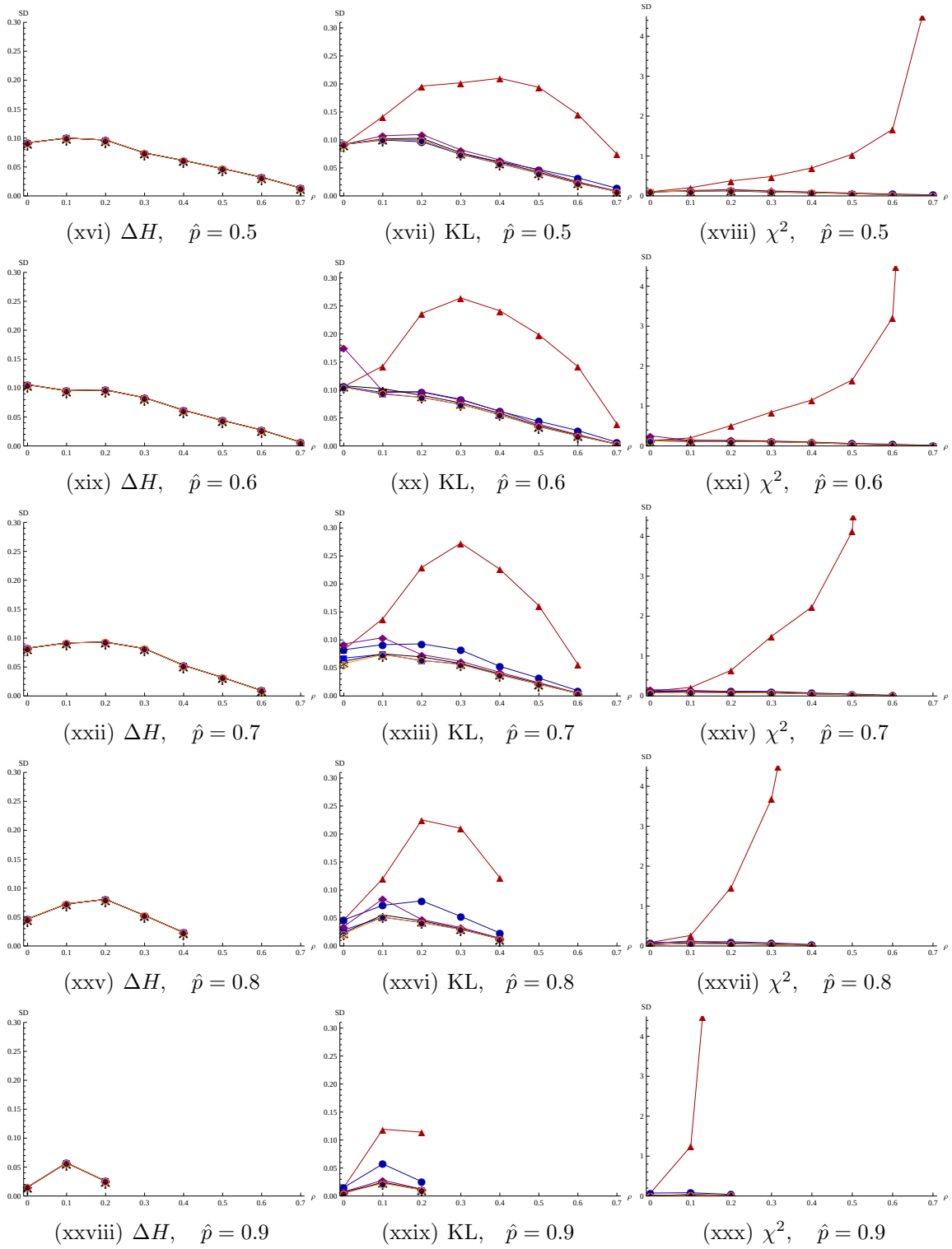

(xvi) ΔH, $\hat{p} = 0.5$ (xvii) KL, $\hat{p} = 0.5$ (xviii) χ^2, $\hat{p} = 0.5$

(xix) ΔH, $\hat{p} = 0.6$ (xx) KL, $\hat{p} = 0.6$ (xxi) χ^2, $\hat{p} = 0.6$

(xxii) ΔH, $\hat{p} = 0.7$ (xxiii) KL, $\hat{p} = 0.7$ (xxiv) χ^2, $\hat{p} = 0.7$

(xxv) ΔH, $\hat{p} = 0.8$ (xxvi) KL, $\hat{p} = 0.8$ (xxvii) χ^2, $\hat{p} = 0.8$

(xxviii) ΔH, $\hat{p} = 0.9$ (xxix) KL, $\hat{p} = 0.9$ (xxx) χ^2, $\hat{p} = 0.9$

Figure C.14: Standard Deviation estimates for accuracy measures (Columns) for truth sets with 4 binary random variables (part two). The truth set shows rank correlation constrains changes (x-axes) and marginal constrains changes $\hat{p}$ (rows).

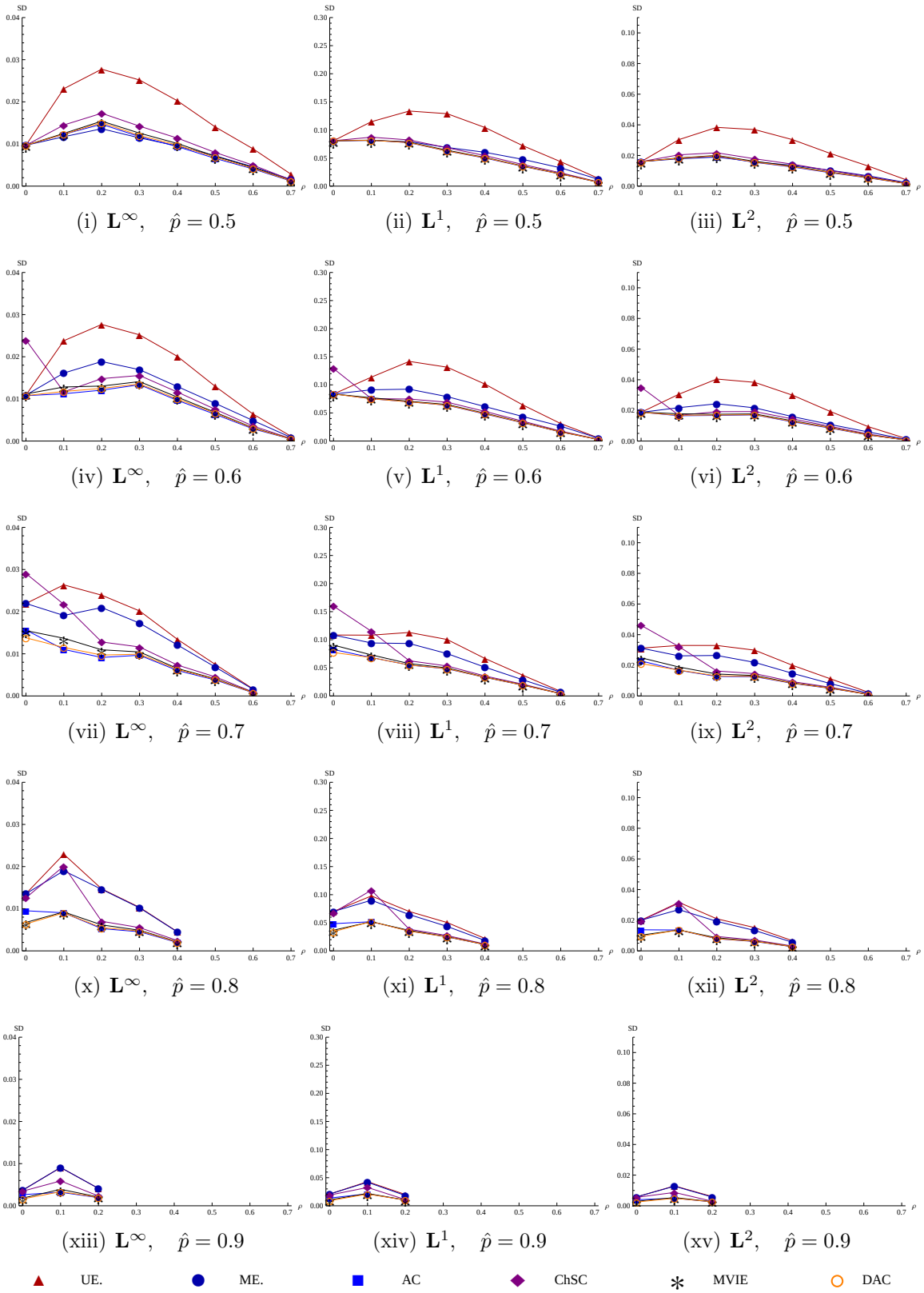

Figure C.15: Standard Dev. for $\mathbb{T}$ with 5 binary random variables (part one).

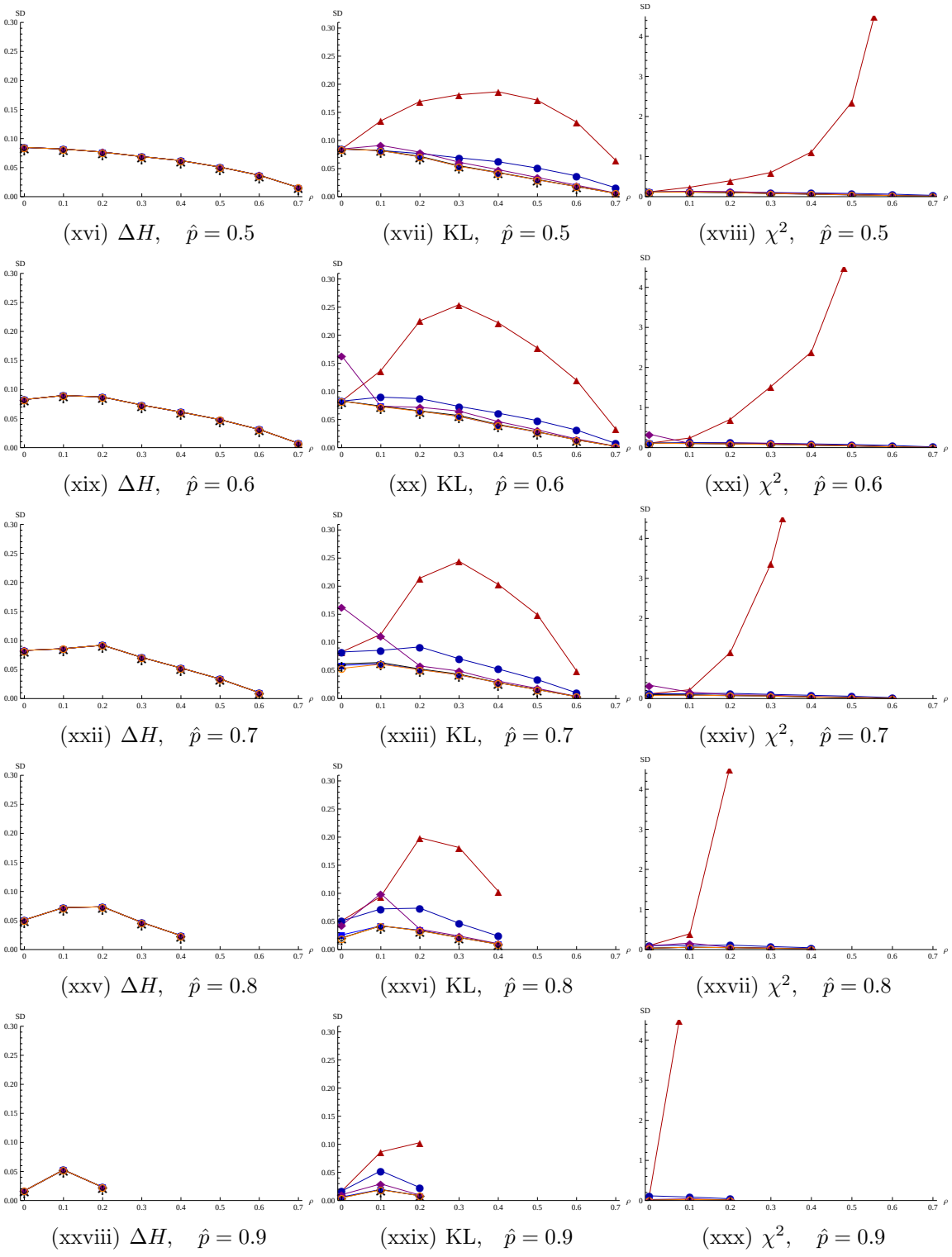

(xvi) ΔH, $\hat{p} = 0.5$ (xvii) KL, $\hat{p} = 0.5$ (xviii) χ^2, $\hat{p} = 0.5$

(xix) ΔH, $\hat{p} = 0.6$ (xx) KL, $\hat{p} = 0.6$ (xxi) χ^2, $\hat{p} = 0.6$

(xxii) ΔH, $\hat{p} = 0.7$ (xxiii) KL, $\hat{p} = 0.7$ (xxiv) χ^2, $\hat{p} = 0.7$

(xxv) ΔH, $\hat{p} = 0.8$ (xxvi) KL, $\hat{p} = 0.8$ (xxvii) χ^2, $\hat{p} = 0.8$

(xxviii) ΔH, $\hat{p} = 0.9$ (xxix) KL, $\hat{p} = 0.9$ (xxx) χ^2, $\hat{p} = 0.9$

Figure C.15: Standard Deviation estimates for accuracy measures (Columns) for truth sets with 5 binary random variables (part two). The truth set shows rank correlation constrains changes (x-axes) and marginal constrains changes $\hat{p}$ (rows).

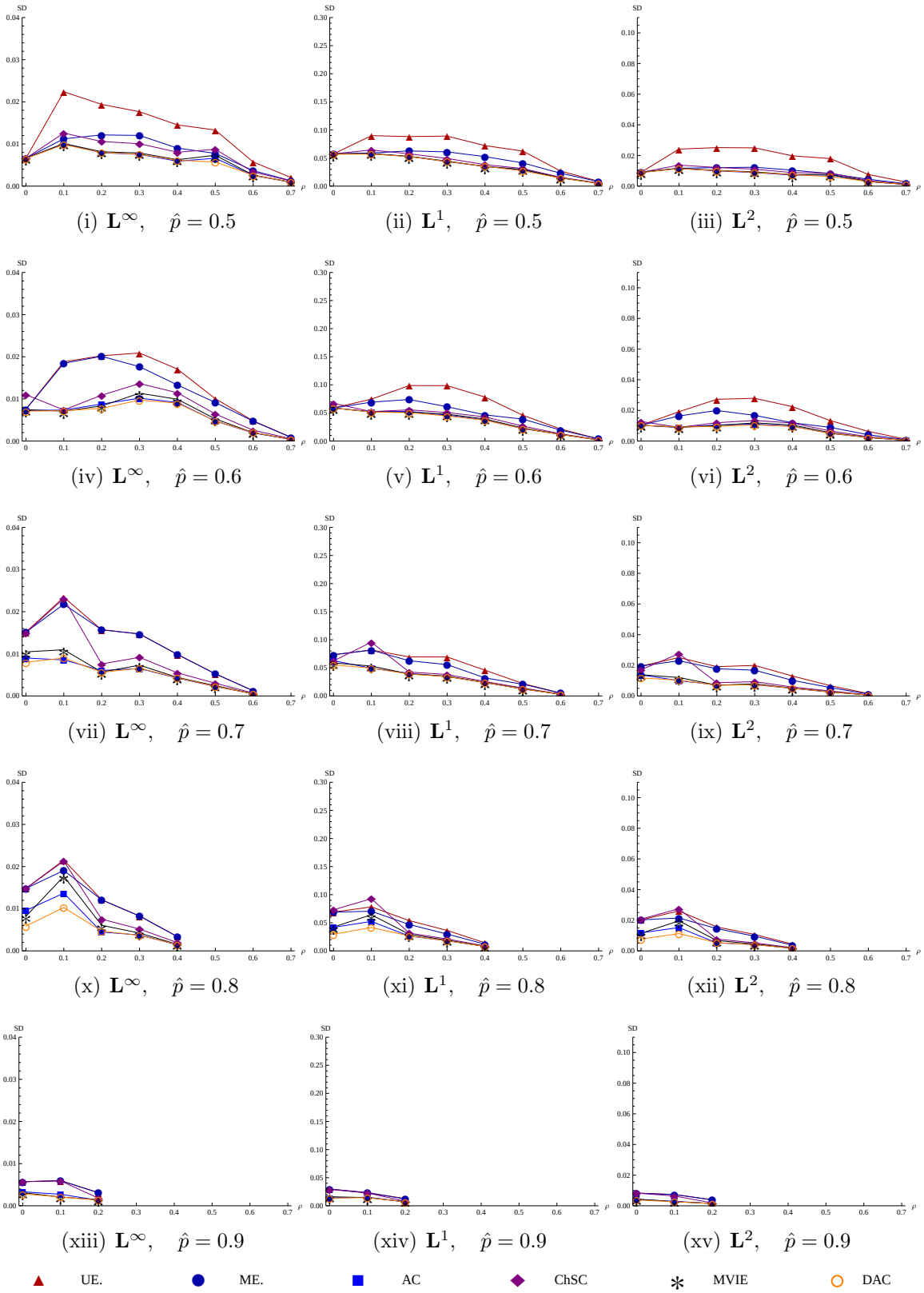

Figure C.16: Standard Dev. for $\mathbb{T}$ with 6 binary random variables (part one).

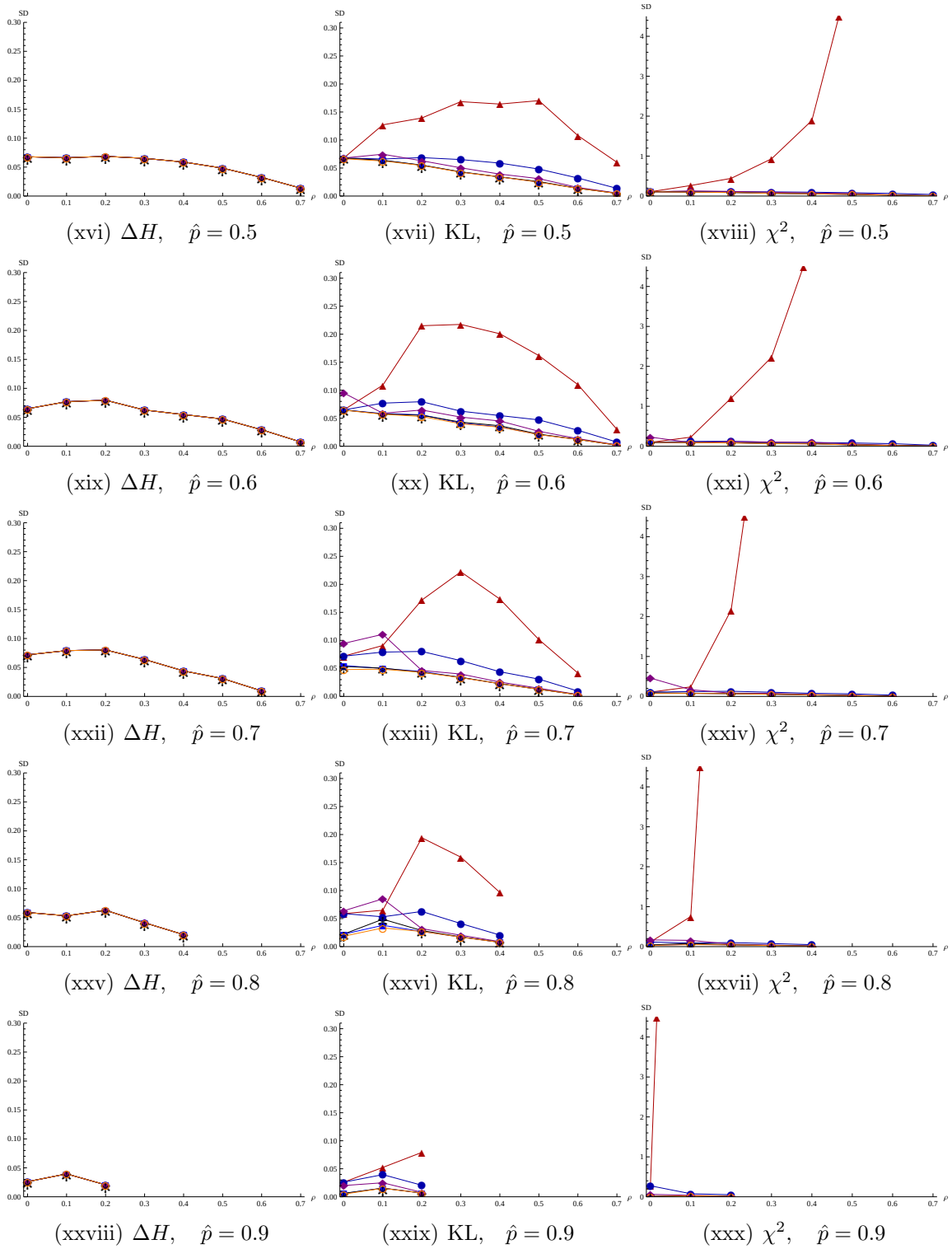

(xvi) ΔH, $\hat{p} = 0.5$ (xvii) KL, $\hat{p} = 0.5$ (xviii) χ^2, $\hat{p} = 0.5$

(xix) ΔH, $\hat{p} = 0.6$ (xx) KL, $\hat{p} = 0.6$ (xxi) χ^2, $\hat{p} = 0.6$

(xxii) ΔH, $\hat{p} = 0.7$ (xxiii) KL, $\hat{p} = 0.7$ (xxiv) χ^2, $\hat{p} = 0.7$

(xxv) ΔH, $\hat{p} = 0.8$ (xxvi) KL, $\hat{p} = 0.8$ (xxvii) χ^2, $\hat{p} = 0.8$

(xxviii) ΔH, $\hat{p} = 0.9$ (xxix) KL, $\hat{p} = 0.9$ (xxx) χ^2, $\hat{p} = 0.9$

Figure C.16: Standard Deviation estimates for accuracy measures (Columns) for truth sets with 6 binary random variables (part two). The truth set shows rank correlation constrains changes (x-axes) and marginal constrains changes $\hat{p}$ (rows).

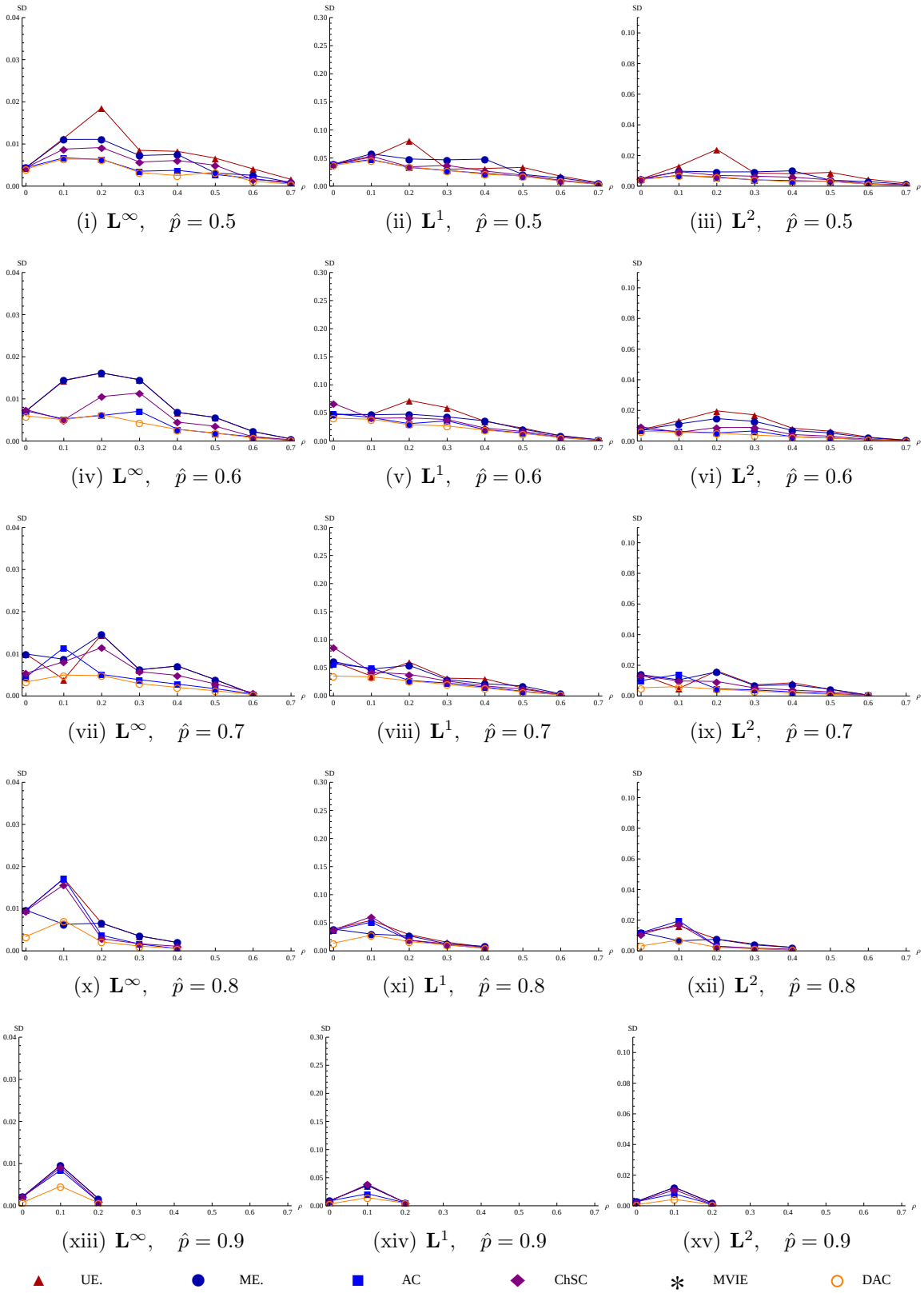

Figure C.17: Standard Dev. for $\mathbb{T}$ with 7 binary random variables (part one).

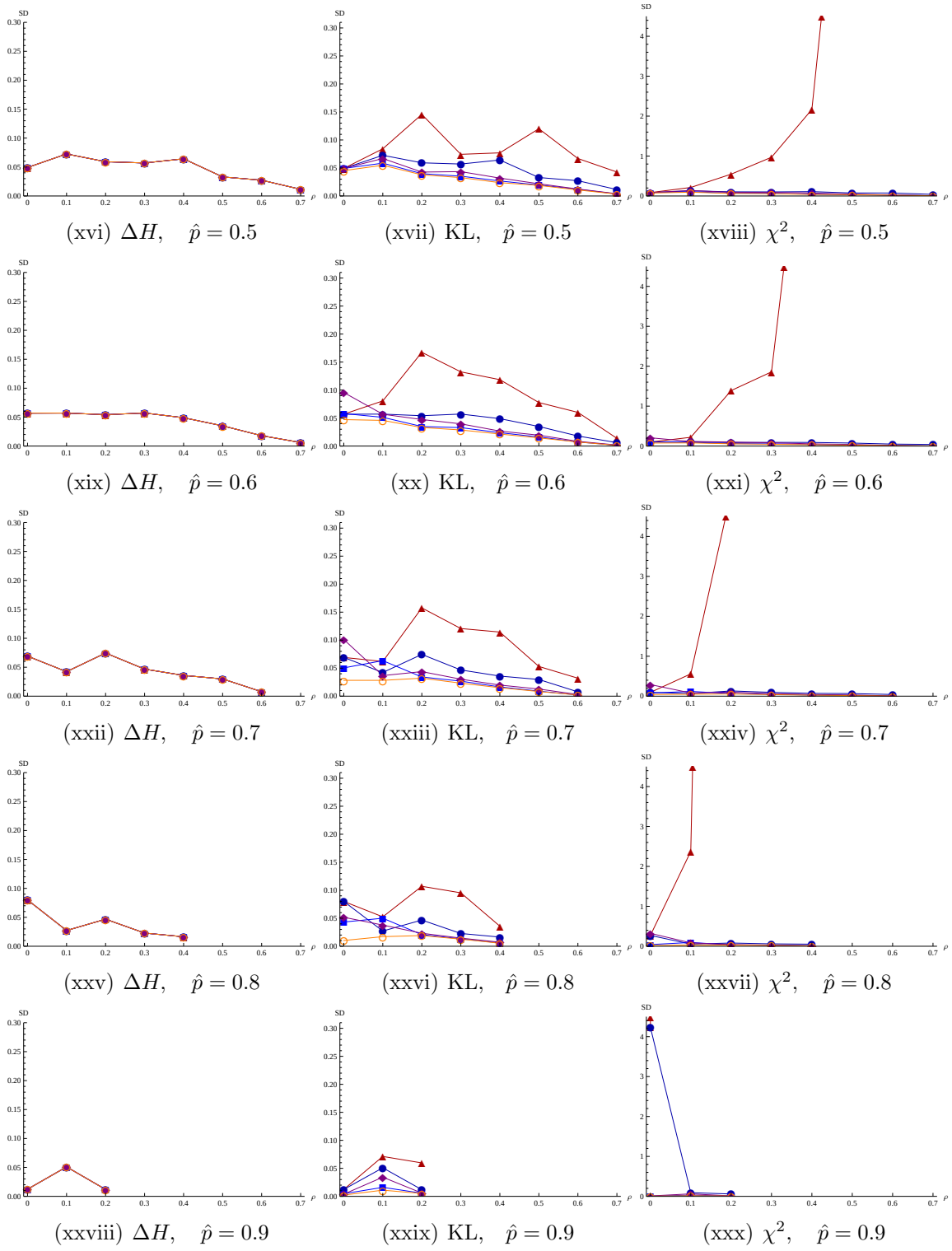

(xvi) ΔH, $\hat{p} = 0.5$ (xvii) KL, $\hat{p} = 0.5$ (xviii) χ^2, $\hat{p} = 0.5$

(xix) ΔH, $\hat{p} = 0.6$ (xx) KL, $\hat{p} = 0.6$ (xxi) χ^2, $\hat{p} = 0.6$

(xxii) ΔH, $\hat{p} = 0.7$ (xxiii) KL, $\hat{p} = 0.7$ (xxiv) χ^2, $\hat{p} = 0.7$

(xxv) ΔH, $\hat{p} = 0.8$ (xxvi) KL, $\hat{p} = 0.8$ (xxvii) χ^2, $\hat{p} = 0.8$

(xxviii) ΔH, $\hat{p} = 0.9$ (xxix) KL, $\hat{p} = 0.9$ (xxx) χ^2, $\hat{p} = 0.9$

Figure C.17: Standard Deviation estimates for accuracy measures (Columns) for truth sets with 7 binary random variables (part two). The truth set shows rank correlation constrains changes (x-axes) and marginal constrains changes $\hat{p}$ (rows).

C.6 Percentage Of Accuracy Marginal, and Correlation Information.

Percentage Of Accuracy. Sets With Three Random Variables, Marginal, and Correlation Information

Table C.10: Percentage of accuracy for sets with marginal and rank correlation information. We present results for symmetric constraints using 3 binary random variables, for all distribution approximations and accuracy measures, while changing the values of $\hat{p} = 0.5$ and respective $\rho^r_{1,2}$.

% Of times		DAC	DAC	DAC	DAC	DAC	DAC	MVIE	MVIE	MVIE	MVIE	MVIE	AC	AC	AC	AC	ChSC	ChSC	ChSC	ME	ME	UE
is better than		MVIE	AC	ChSC	ME	UE	IA	AC	ChSC	ME	UE	IA	ChSC	ME	UE	IA	ME	UE	IA	UE	IA	IA
$\hat{p}$	$\mathbf{L}^\infty$	50%	50%	50%	50%	50%	50%	50%	50%	50%	50%	50%	50%	50%	50%	50%	0%	0%	0%	48%	52%	54%
0.5	$\mathbf{L}^1$	50%	50%	50%	50%	50%	50%	50%	50%	50%	50%	50%	50%	50%	50%	50%	50%	50%	50%	50%	50%	50%
ρ	$\mathbf{L}^2$	50%	50%	50%	50%	50%	50%	50%	50%	50%	50%	50%	50%	50%	50%	50%	50%	50%	50%	50%	50%	50%
0	KL	50%	50%	50%	50%	50%	50%	50%	41%	50%	50%	50%	50%	50%	50%	50%	100%	100%	100%	64%	31%	26%
	χ^2	50%	50%	50%	50%	50%	50%	50%	50%	50%	50%	50%	50%	50%	50%	50%	90%	90%	90%	50%	50%	50%
$\hat{p}$	$\mathbf{L}^\infty$	50%	50%	50%	50%	53%	100%	50%	50%	50%	53%	100%	50%	50%	53%	100%	0%	53%	100%	53%	100%	100%
0.5	$\mathbf{L}^1$	50%	50%	50%	50%	53%	73%	50%	50%	50%	53%	73%	50%	50%	53%	73%	50%	53%	73%	53%	73%	55%
ρ	$\mathbf{L}^2$	50%	50%	50%	50%	53%	100%	50%	50%	50%	53%	100%	50%	50%	53%	100%	50%	53%	100%	53%	100%	60%
0.1	KL	50%	50%	50%	50%	53%	100%	50%	50%	50%	53%	100%	50%	50%	53%	100%	67%	53%	100%	53%	100%	58%
	χ^2	50%	50%	50%	50%	53%	100%	50%	50%	50%	53%	100%	50%	50%	53%	100%	82%	53%	100%	53%	100%	59%
$\hat{p}$	$\mathbf{L}^\infty$	50%	50%	50%	50%	57%	100%	50%	50%	50%	57%	100%	50%	50%	57%	100%	0%	57%	100%	57%	100%	100%
0.5	$\mathbf{L}^1$	50%	50%	50%	50%	57%	100%	50%	50%	50%	57%	100%	50%	50%	57%	100%	50%	57%	100%	57%	100%	64%
ρ	$\mathbf{L}^2$	50%	50%	50%	50%	57%	100%	50%	50%	50%	57%	100%	50%	50%	57%	100%	50%	57%	100%	57%	100%	80%
0.2	KL	50%	50%	50%	50%	57%	100%	50%	50%	50%	57%	100%	50%	50%	57%	100%	83%	57%	100%	57%	100%	71%
	χ^2	50%	50%	50%	50%	57%	100%	50%	50%	50%	57%	100%	50%	50%	57%	100%	90%	57%	100%	57%	100%	70%
$\hat{p}$	$\mathbf{L}^\infty$	50%	50%	50%	50%	60%	100%	50%	50%	50%	60%	100%	50%	50%	60%	100%	0%	60%	100%	60%	100%	100%
0.5	$\mathbf{L}^1$	50%	50%	50%	50%	60%	100%	50%	50%	50%	60%	100%	50%	50%	60%	100%	50%	60%	100%	60%	100%	80%
ρ	$\mathbf{L}^2$	50%	50%	50%	50%	60%	100%	50%	50%	50%	60%	100%	50%	50%	60%	100%	50%	60%	100%	60%	100%	100%
0.3	KL	50%	50%	50%	50%	60%	100%	50%	50%	50%	60%	100%	50%	50%	60%	100%	100%	60%	100%	60%	100%	89%
	χ^2	50%	50%	50%	50%	60%	100%	50%	50%	50%	60%	100%	50%	50%	60%	100%	94%	60%	100%	60%	100%	82%
$\hat{p}$	$\mathbf{L}^\infty$	50%	50%	50%	50%	63%	100%	50%	50%	50%	63%	100%	50%	50%	63%	100%	0%	63%	100%	63%	100%	100%
0.5	$\mathbf{L}^1$	50%	50%	50%	50%	63%	100%	50%	50%	50%	63%	100%	50%	50%	63%	100%	50%	63%	100%	63%	100%	100%
ρ	$\mathbf{L}^2$	50%	50%	50%	50%	63%	100%	50%	50%	50%	63%	100%	50%	50%	63%	100%	50%	63%	100%	63%	100%	100%
0.4	KL	50%	50%	50%	50%	64%	100%	50%	50%	50%	64%	100%	50%	50%	64%	100%	100%	64%	100%	64%	100%	100%
	χ^2	50%	50%	50%	50%	64%	100%	50%	50%	50%	64%	100%	50%	50%	64%	100%	96%	64%	100%	64%	100%	94%
$\hat{p}$	$\mathbf{L}^\infty$	50%	50%	50%	50%	66%	100%	50%	50%	50%	66%	100%	50%	50%	66%	100%	0%	66%	100%	66%	100%	100%
0.5	$\mathbf{L}^1$	50%	50%	50%	50%	66%	100%	50%	50%	50%	66%	100%	50%	50%	66%	100%	50%	66%	100%	66%	100%	100%
ρ	$\mathbf{L}^2$	50%	50%	50%	50%	66%	100%	50%	50%	50%	66%	100%	50%	50%	66%	100%	50%	66%	100%	66%	100%	100%
0.5	KL	50%	50%	50%	50%	68%	100%	50%	50%	50%	68%	100%	50%	50%	68%	100%	100%	68%	100%	68%	100%	100%
	χ^2	50%	50%	50%	50%	69%	100%	50%	50%	50%	69%	100%	50%	50%	69%	100%	98%	69%	100%	69%	100%	100%
$\hat{p}$	$\mathbf{L}^\infty$	50%	50%	50%	50%	70%	100%	50%	50%	50%	70%	100%	50%	50%	70%	100%	0%	70%	100%	70%	100%	100%
0.5	$\mathbf{L}^1$	50%	50%	50%	50%	70%	100%	50%	50%	50%	70%	100%	50%	50%	70%	100%	50%	70%	100%	70%	100%	100%
ρ	$\mathbf{L}^2$	50%	50%	50%	50%	70%	100%	50%	50%	50%	70%	100%	50%	50%	70%	100%	50%	70%	100%	70%	100%	100%
0.6	KL	50%	50%	50%	50%	73%	100%	50%	50%	50%	73%	100%	50%	50%	73%	100%	100%	73%	100%	73%	100%	100%
	χ^2	50%	50%	50%	50%	75%	100%	50%	50%	50%	75%	100%	50%	50%	75%	100%	99%	75%	100%	75%	100%	100%
$\hat{p}$	$\mathbf{L}^\infty$	50%	50%	50%	50%	73%	100%	50%	50%	50%	73%	100%	50%	50%	73%	100%	100%	73%	100%	73%	100%	100%
0.5	$\mathbf{L}^1$	50%	50%	50%	50%	73%	100%	50%	50%	50%	73%	100%	50%	50%	73%	100%	50%	73%	100%	73%	100%	100%
ρ	$\mathbf{L}^2$	50%	50%	50%	50%	73%	100%	50%	50%	50%	73%	100%	50%	50%	73%	100%	50%	73%	100%	73%	100%	100%
0.7	KL	50%	50%	50%	50%	80%	100%	50%	50%	52%	80%	100%	50%	52%	80%	100%	100%	80%	100%	80%	100%	100%
	χ^2	50%	50%	50%	50%	84%	100%	50%	50%	50%	84%	100%	50%	50%	84%	100%	100%	84%	100%	84%	100%	100%

Table C.11: Percentage of accuracy for sets with marginal and rank correlation information. We present results for symmetric constraints using 3 binary random variables, for all distribution approximations and accuracy measures, while changing the values of $\hat{p} = 0.6$ and respective $\rho^r_{1,2}$.

% Of times		DAC	DAC	DAC	DAC	DAC	DAC	MVIE	MVIE	MVIE	MVIE	MVIE	AC	AC	AC	AC	ChSC	ChSC	ChSC	ME	ME	UE
is better than		MVIE	AC	ChSC	ME	UE	IA	AC	ChSC	ME	UE	IA	ChSC	ME	UE	IA	ME	UE	IA	UE	IA	IA
$\hat{p}$	$\mathbf{L}^\infty$	50%	55%	50%	55%	55%	55%	55%	50%	55%	55%	55%	45%	60%	60%	60%	55%	55%	55%	50%	50%	50%
0.6	$\mathbf{L}^1$	50%	55%	50%	55%	55%	55%	55%	50%	55%	55%	55%	45%	60%	60%	60%	55%	55%	55%	50%	50%	50%
ρ	$\mathbf{L}^2$	50%	55%	50%	55%	55%	55%	55%	50%	55%	55%	55%	45%	60%	60%	60%	55%	55%	55%	50%	50%	50%
0	KL	50%	55%	50%	55%	55%	55%	55%	50%	55%	55%	55%	45%	60%	60%	60%	55%	55%	55%	40%	64%	68%
	χ^2	50%	55%	50%	55%	55%	55%	55%	50%	55%	55%	55%	45%	60%	60%	60%	55%	55%	55%	50%	50%	50%
$\hat{p}$	$\mathbf{L}^\infty$	50%	51%	50%	53%	57%	100%	51%	50%	53%	57%	100%	49%	54%	58%	100%	53%	57%	100%	59%	100%	100%
0.6	$\mathbf{L}^1$	50%	51%	50%	53%	57%	63%	51%	50%	53%	57%	63%	49%	54%	58%	65%	53%	57%	63%	59%	69%	50%
ρ	$\mathbf{L}^2$	50%	51%	50%	53%	57%	67%	51%	50%	53%	57%	67%	49%	54%	58%	73%	53%	57%	67%	59%	85%	66%
0.1	KL	50%	51%	50%	53%	57%	72%	51%	50%	53%	57%	73%	49%	54%	58%	91%	53%	57%	73%	59%	100%	52%
	χ^2	50%	51%	50%	53%	57%	80%	51%	50%	53%	57%	81%	49%	54%	58%	100%	53%	57%	81%	59%	100%	52%
$\hat{p}$	$\mathbf{L}^\infty$	50%	52%	50%	53%	61%	100%	52%	50%	53%	61%	100%	48%	55%	62%	100%	53%	61%	100%	64%	100%	100%
0.6	$\mathbf{L}^1$	50%	52%	50%	53%	61%	79%	52%	50%	53%	61%	79%	48%	55%	62%	82%	53%	61%	79%	64%	92%	65%
ρ	$\mathbf{L}^2$	50%	52%	50%	53%	61%	97%	52%	50%	53%	61%	97%	48%	55%	62%	100%	53%	61%	97%	64%	100%	100%
0.2	KL	50%	52%	50%	53%	61%	100%	52%	50%	53%	61%	100%	48%	55%	62%	100%	53%	61%	100%	64%	100%	63%
	χ^2	50%	52%	50%	53%	61%	100%	52%	50%	53%	61%	100%	48%	55%	62%	100%	53%	61%	100%	64%	100%	59%
$\hat{p}$	$\mathbf{L}^\infty$	50%	51%	50%	53%	63%	100%	51%	50%	53%	63%	100%	49%	54%	64%	100%	53%	63%	100%	66%	100%	100%
0.6	$\mathbf{L}^1$	50%	51%	50%	53%	63%	100%	51%	50%	53%	63%	100%	49%	54%	64%	100%	53%	63%	100%	66%	100%	100%
ρ	$\mathbf{L}^2$	50%	51%	50%	53%	63%	100%	51%	50%	53%	63%	100%	49%	54%	64%	100%	53%	63%	100%	66%	100%	100%
0.3	KL	50%	51%	50%	53%	64%	100%	51%	50%	53%	64%	100%	49%	54%	65%	100%	53%	64%	100%	67%	100%	83%
	χ^2	50%	51%	50%	53%	64%	100%	51%	50%	53%	64%	100%	49%	54%	65%	100%	53%	64%	100%	67%	100%	71%
$\hat{p}$	$\mathbf{L}^\infty$	50%	50%	50%	52%	66%	100%	50%	50%	52%	66%	100%	50%	53%	66%	100%	52%	66%	100%	68%	100%	100%
0.6	$\mathbf{L}^1$	50%	50%	50%	52%	66%	100%	50%	50%	52%	66%	100%	50%	53%	66%	100%	52%	66%	100%	68%	100%	100%
ρ	$\mathbf{L}^2$	50%	50%	50%	52%	66%	100%	50%	50%	52%	66%	100%	50%	53%	66%	100%	52%	66%	100%	68%	100%	100%
0.4	KL	50%	50%	50%	52%	67%	100%	50%	50%	52%	67%	100%	50%	53%	68%	100%	52%	67%	100%	70%	100%	100%
	χ^2	50%	50%	50%	52%	68%	100%	50%	50%	52%	68%	100%	50%	53%	69%	100%	52%	68%	100%	70%	100%	83%
$\hat{p}$	$\mathbf{L}^\infty$	50%	50%	50%	52%	69%	100%	50%	50%	52%	69%	100%	50%	52%	69%	100%	52%	69%	100%	71%	100%	100%
0.6	$\mathbf{L}^1$	50%	50%	50%	52%	69%	100%	50%	50%	52%	69%	100%	50%	52%	69%	100%	52%	69%	100%	71%	100%	100%
ρ	$\mathbf{L}^2$	50%	50%	50%	52%	69%	100%	50%	50%	52%	69%	100%	50%	52%	69%	100%	52%	69%	100%	71%	100%	100%
0.5	KL	50%	50%	50%	52%	71%	100%	50%	50%	52%	71%	100%	50%	52%	71%	100%	52%	71%	100%	73%	100%	100%
	χ^2	50%	50%	50%	52%	73%	100%	50%	50%	52%	73%	100%	50%	52%	73%	100%	52%	73%	100%	74%	100%	96%
$\hat{p}$	$\mathbf{L}^\infty$	50%	50%	50%	52%	72%	100%	50%	50%	52%	72%	100%	50%	52%	72%	100%	52%	72%	100%	74%	100%	100%
0.6	$\mathbf{L}^1$	50%	50%	50%	52%	72%	100%	50%	50%	52%	72%	100%	50%	52%	72%	100%	52%	72%	100%	74%	100%	100%
ρ	$\mathbf{L}^2$	50%	50%	50%	52%	72%	100%	50%	50%	52%	72%	100%	50%	52%	72%	100%	52%	72%	100%	74%	100%	100%
0.6	KL	50%	50%	50%	52%	76%	100%	50%	50%	52%	76%	100%	50%	52%	76%	100%	52%	76%	100%	78%	100%	100%
	χ^2	50%	50%	50%	52%	79%	100%	50%	50%	52%	79%	100%	50%	52%	79%	100%	52%	79%	100%	80%	100%	100%
$\hat{p}$	$\mathbf{L}^\infty$	50%	50%	50%	52%	75%	100%	50%	50%	52%	75%	100%	50%	52%	75%	100%	52%	75%	100%	76%	100%	100%
0.6	$\mathbf{L}^1$	50%	50%	50%	52%	75%	100%	50%	50%	52%	75%	100%	50%	52%	75%	100%	52%	75%	100%	76%	100%	100%
ρ	$\mathbf{L}^2$	50%	50%	50%	52%	75%	100%	50%	50%	52%	75%	100%	50%	52%	75%	100%	52%	75%	100%	76%	100%	100%
0.7	KL	50%	50%	50%	52%	85%	100%	50%	50%	52%	85%	100%	50%	52%	85%	100%	52%	85%	100%	86%	100%	100%
	χ^2	50%	50%	50%	52%	90%	100%	50%	50%	52%	90%	100%	50%	52%	90%	100%	52%	90%	100%	91%	100%	100%

Table C.12: Percentage of accuracy for sets with marginal and rank correlation information. We present results for symmetric constraints using 3 binary random variables, for all distribution approximations and accuracy measures, while changing the values of $\hat{p} = 0.7$ and respective $\rho^r_{1,2}$.

% Of times		DAC	DAC	DAC	DAC	DAC	DAC	MVIE	MVIE	MVIE	MVIE	MVIE	AC	AC	AC	AC	ChSC	ChSC	ChSC	ME	ME	UE
is better than		MVIE	AC	ChSC	ME	UE	IA	AC	ChSC	ME	UE	IA	ChSC	ME	UE	IA	ME	UE	IA	UE	IA	IA
$\hat{p}$	$\mathbf{L}^\infty$	50%	58%	50%	60%	60%	60%	58%	50%	60%	60%	60%	42%	68%	68%	68%	60%	60%	60%	51%	52%	51%
0.7	$\mathbf{L}^1$	50%	58%	50%	60%	60%	60%	58%	50%	60%	60%	60%	42%	68%	68%	68%	60%	60%	60%	50%	50%	50%
ρ	$\mathbf{L}^2$	50%	58%	50%	60%	60%	60%	58%	50%	60%	60%	60%	42%	68%	68%	68%	60%	60%	60%	50%	50%	50%
0	KL	50%	58%	50%	60%	60%	60%	58%	50%	60%	60%	60%	42%	68%	68%	68%	60%	60%	60%	68%	24%	19%
	χ^2	50%	58%	50%	60%	60%	60%	58%	50%	60%	60%	60%	42%	68%	68%	68%	60%	60%	60%	50%	50%	50%
$\hat{p}$	$\mathbf{L}^\infty$	50%	53%	50%	50%	57%	100%	53%	50%	50%	57%	100%	47%	47%	54%	100%	50%	57%	100%	57%	100%	100%
0.7	$\mathbf{L}^1$	50%	53%	50%	50%	57%	70%	53%	50%	50%	57%	70%	47%	47%	54%	65%	50%	57%	70%	57%	70%	72%
ρ	$\mathbf{L}^2$	50%	53%	50%	50%	57%	78%	53%	50%	50%	57%	78%	47%	47%	54%	69%	50%	57%	78%	57%	78%	100%
0.1	KL	50%	53%	50%	50%	57%	100%	53%	50%	50%	57%	100%	47%	47%	54%	88%	50%	57%	100%	57%	100%	59%
	χ^2	50%	53%	50%	50%	57%	100%	53%	50%	50%	57%	100%	47%	47%	54%	100%	50%	57%	100%	57%	100%	58%
$\hat{p}$	$\mathbf{L}^\infty$	50%	53%	50%	56%	65%	100%	52%	50%	56%	65%	100%	48%	59%	67%	100%	56%	65%	100%	71%	100%	100%
0.7	$\mathbf{L}^1$	50%	53%	50%	56%	65%	85%	52%	50%	56%	65%	85%	48%	59%	67%	90%	56%	65%	85%	71%	97%	90%
ρ	$\mathbf{L}^2$	50%	53%	50%	56%	65%	92%	52%	50%	56%	65%	92%	48%	59%	67%	100%	56%	65%	92%	71%	100%	100%
0.2	KL	50%	53%	50%	56%	65%	100%	52%	50%	56%	65%	100%	48%	59%	68%	100%	56%	65%	100%	71%	100%	59%
	χ^2	50%	53%	50%	56%	66%	100%	52%	50%	56%	66%	100%	48%	59%	68%	100%	56%	66%	100%	71%	100%	53%
$\hat{p}$	$\mathbf{L}^\infty$	50%	51%	50%	55%	67%	100%	51%	50%	55%	67%	100%	49%	57%	68%	100%	55%	67%	100%	72%	100%	100%
0.7	$\mathbf{L}^1$	50%	51%	50%	55%	67%	100%	51%	50%	55%	67%	100%	49%	57%	68%	100%	55%	67%	100%	72%	100%	100%
ρ	$\mathbf{L}^2$	50%	51%	50%	55%	67%	100%	51%	50%	55%	67%	100%	49%	57%	68%	100%	55%	67%	100%	72%	100%	100%
0.3	KL	50%	51%	50%	55%	69%	100%	51%	50%	55%	69%	100%	49%	57%	70%	100%	55%	69%	100%	73%	100%	86%
	χ^2	50%	51%	50%	55%	70%	100%	51%	50%	55%	70%	100%	49%	57%	71%	100%	55%	70%	100%	74%	100%	67%
$\hat{p}$	$\mathbf{L}^\infty$	50%	51%	50%	54%	69%	100%	51%	50%	54%	69%	100%	49%	55%	70%	100%	54%	69%	100%	74%	100%	100%
0.7	$\mathbf{L}^1$	50%	51%	50%	54%	69%	100%	51%	50%	54%	69%	100%	49%	55%	70%	100%	54%	69%	100%	74%	100%	100%
ρ	$\mathbf{L}^2$	50%	51%	50%	54%	69%	100%	51%	50%	54%	69%	100%	49%	55%	70%	100%	54%	69%	100%	74%	100%	100%
0.4	KL	50%	51%	50%	55%	72%	100%	51%	50%	54%	72%	100%	49%	55%	73%	100%	54%	72%	100%	76%	100%	100%
	χ^2	50%	51%	50%	55%	74%	100%	51%	50%	54%	74%	100%	49%	55%	74%	100%	54%	74%	100%	77%	100%	82%
$\hat{p}$	$\mathbf{L}^\infty$	50%	50%	50%	54%	72%	100%	50%	50%	54%	72%	100%	50%	54%	72%	100%	54%	72%	100%	76%	100%	100%
0.7	$\mathbf{L}^1$	50%	50%	50%	54%	72%	100%	50%	50%	54%	72%	100%	50%	54%	72%	100%	54%	72%	100%	76%	100%	100%
ρ	$\mathbf{L}^2$	50%	50%	50%	54%	72%	100%	50%	50%	54%	72%	100%	50%	54%	72%	100%	54%	72%	100%	76%	100%	100%
0.5	KL	50%	50%	50%	54%	0%	100%	50%	50%	54%	0%	100%	50%	54%	0%	100%	54%	0%	100%	0%	100%	100%
	χ^2	50%	50%	50%	54%	80%	100%	50%	50%	54%	80%	100%	50%	54%	80%	100%	54%	80%	100%	82%	100%	100%
$\hat{p}$	$\mathbf{L}^\infty$	50%	50%	50%	54%	74%	100%	50%	50%	54%	74%	100%	50%	54%	74%	100%	54%	74%	100%	78%	100%	100%
0.7	$\mathbf{L}^1$	50%	50%	50%	54%	74%	100%	50%	50%	54%	74%	100%	50%	54%	74%	100%	54%	74%	100%	78%	100%	100%
ρ	$\mathbf{L}^2$	50%	50%	50%	54%	74%	100%	50%	50%	54%	74%	100%	50%	54%	74%	100%	54%	74%	100%	78%	100%	100%
0.6	KL	50%	50%	50%	54%	84%	100%	50%	50%	54%	84%	100%	50%	54%	84%	100%	54%	84%	100%	86%	100%	100%
	χ^2	50%	50%	50%	54%	89%	100%	50%	50%	54%	89%	100%	50%	54%	89%	100%	54%	89%	100%	91%	100%	100%

Table C.13: Percentage of accuracy for sets with marginal and rank correlation information. We present results for symmetric constraints using 3 binary random variables, for all distribution approximations and accuracy measures, while changing the values of $\hat{p} = 0.8, 0.9$ and respective $\rho^r_{1,2}$.

% Of times		DAC	DAC	DAC	DAC	DAC	DAC	MVIE	MVIE	MVIE	MVIE	MVIE	AC	AC	AC	AC	ChSC	ChSC	ChSC	ME	ME	UE
is better than		MVIE	AC	ChSC	ME	UE	IA	AC	ChSC	ME	UE	IA	ChSC	ME	UE	IA	ME	UE	IA	UE	IA	IA
$\hat{p}$	$\mathbf{L}^\infty$	50%	60%	50%	65%	65%	65%	60%	50%	65%	65%	65%	40%	75%	75%	75%	65%	65%	65%	44%	55%	56%
0.8	$\mathbf{L}^1$	50%	60%	50%	65%	65%	65%	60%	50%	65%	65%	65%	40%	75%	75%	75%	65%	65%	65%	50%	50%	50%
ρ	$\mathbf{L}^2$	50%	60%	50%	65%	65%	65%	60%	50%	65%	65%	65%	40%	75%	75%	75%	65%	65%	65%	50%	50%	50%
0	KL	50%	60%	50%	65%	65%	65%	60%	50%	65%	65%	65%	40%	75%	75%	75%	65%	65%	65%	5%	87%	100%
	χ^2	50%	60%	50%	65%	65%	65%	60%	50%	65%	65%	65%	40%	75%	75%	75%	65%	65%	65%	20%	49%	80%
$\hat{p}$	$\mathbf{L}^\infty$	50%	55%	50%	51%	62%	100%	55%	50%	51%	62%	100%	45%	46%	57%	100%	51%	62%	100%	62%	100%	100%
0.8	$\mathbf{L}^1$	50%	55%	50%	51%	62%	84%	55%	50%	51%	62%	84%	45%	46%	57%	74%	51%	62%	84%	62%	85%	100%
ρ	$\mathbf{L}^2$	50%	55%	50%	51%	62%	91%	55%	50%	51%	62%	91%	45%	46%	57%	80%	51%	62%	91%	62%	92%	100%
0.1	KL	50%	55%	50%	51%	62%	100%	55%	50%	51%	62%	100%	45%	46%	58%	100%	51%	62%	100%	63%	100%	64%
	χ^2	50%	55%	50%	51%	63%	100%	55%	50%	51%	63%	100%	45%	46%	58%	100%	51%	63%	100%	63%	100%	62%
$\hat{p}$	$\mathbf{L}^\infty$	50%	53%	50%	59%	69%	100%	53%	50%	59%	69%	100%	47%	61%	72%	100%	59%	69%	100%	78%	100%	100%
0.8	$\mathbf{L}^1$	50%	53%	50%	59%	69%	100%	53%	50%	59%	69%	100%	47%	61%	72%	100%	59%	69%	100%	78%	100%	100%
ρ	$\mathbf{L}^2$	50%	53%	50%	59%	69%	100%	53%	50%	59%	69%	100%	47%	61%	72%	100%	59%	69%	100%	78%	100%	100%
0.2	KL	50%	53%	50%	59%	72%	100%	53%	50%	59%	72%	100%	47%	61%	74%	100%	59%	72%	100%	79%	100%	67%
	χ^2	50%	53%	50%	59%	73%	100%	53%	50%	59%	73%	100%	47%	61%	75%	100%	59%	73%	100%	80%	100%	55%
$\hat{p}$	$\mathbf{L}^\infty$	50%	51%	50%	57%	71%	100%	51%	50%	57%	71%	100%	49%	58%	72%	100%	57%	71%	100%	79%	100%	100%
0.8	$\mathbf{L}^1$	50%	51%	50%	57%	71%	100%	51%	50%	57%	71%	100%	49%	58%	72%	100%	57%	71%	100%	79%	100%	100%
ρ	$\mathbf{L}^2$	50%	51%	50%	57%	71%	100%	51%	50%	57%	71%	100%	49%	58%	72%	100%	57%	71%	100%	79%	100%	100%
0.3	KL	50%	51%	50%	57%	76%	100%	51%	50%	57%	75%	100%	49%	58%	76%	100%	57%	75%	100%	81%	100%	100%
	χ^2	50%	51%	50%	57%	78%	100%	51%	50%	57%	78%	100%	49%	58%	78%	100%	57%	78%	100%	82%	100%	79%
$\hat{p}$	$\mathbf{L}^\infty$	50%	50%	50%	56%	74%	100%	50%	50%	56%	74%	100%	50%	56%	74%	100%	56%	74%	100%	80%	100%	100%
0.8	$\mathbf{L}^1$	50%	50%	50%	56%	74%	100%	50%	50%	56%	74%	100%	50%	56%	74%	100%	56%	74%	100%	80%	100%	100%
ρ	$\mathbf{L}^2$	50%	50%	50%	56%	74%	100%	50%	50%	56%	74%	100%	50%	56%	74%	100%	56%	74%	100%	80%	100%	100%
0.4	KL	50%	50%	50%	56%	80%	100%	50%	50%	56%	80%	100%	50%	57%	81%	100%	56%	80%	100%	85%	100%	100%
	χ^2	50%	50%	50%	56%	84%	100%	50%	50%	56%	84%	100%	50%	57%	85%	100%	56%	84%	100%	87%	100%	100%
$\hat{p}$	$\mathbf{L}^\infty$	50%	62%	50%	70%	70%	70%	62%	50%	70%	70%	70%	38%	82%	82%	82%	70%	70%	70%	82%	84%	51%
0.9	$\mathbf{L}^1$	50%	62%	50%	70%	70%	70%	62%	50%	70%	70%	70%	38%	82%	82%	82%	70%	70%	70%	90%	66%	28%
ρ	$\mathbf{L}^2$	50%	62%	50%	70%	70%	70%	62%	50%	70%	70%	70%	38%	82%	82%	82%	70%	70%	70%	90%	66%	28%
0	KL	50%	62%	50%	71%	71%	71%	62%	50%	71%	71%	71%	38%	82%	82%	82%	71%	71%	71%	85%	0%	0%
	χ^2	50%	62%	50%	73%	73%	73%	62%	50%	73%	73%	73%	38%	83%	83%	83%	73%	73%	73%	50%	50%	50%
$\hat{p}$	$\mathbf{L}^\infty$	50%	51%	50%	59%	71%	100%	51%	50%	59%	71%	100%	49%	58%	70%	100%	59%	71%	100%	80%	100%	100%
0.9	$\mathbf{L}^1$	50%	51%	50%	59%	71%	100%	51%	50%	59%	71%	100%	49%	58%	70%	100%	59%	71%	100%	80%	100%	100%
ρ	$\mathbf{L}^2$	50%	51%	50%	59%	71%	100%	51%	50%	59%	71%	100%	49%	58%	70%	100%	59%	71%	100%	80%	100%	100%
0.1	KL	50%	51%	50%	59%	75%	100%	51%	50%	59%	75%	100%	49%	58%	74%	100%	59%	75%	100%	82%	100%	68%
	χ^2	50%	51%	50%	59%	77%	100%	51%	50%	59%	77%	100%	49%	58%	77%	100%	59%	77%	100%	83%	100%	60%
$\hat{p}$	$\mathbf{L}^\infty$	50%	51%	50%	60%	74%	100%	51%	50%	60%	74%	100%	49%	60%	74%	100%	60%	74%	100%	84%	100%	100%
0.9	$\mathbf{L}^1$	50%	51%	50%	60%	74%	100%	51%	50%	60%	74%	100%	49%	60%	74%	100%	60%	74%	100%	84%	100%	100%
ρ	$\mathbf{L}^2$	50%	51%	50%	60%	74%	100%	51%	50%	60%	74%	100%	49%	60%	74%	100%	60%	74%	100%	84%	100%	100%
0.2	KL	50%	51%	50%	60%	81%	100%	51%	50%	60%	81%	100%	49%	61%	82%	100%	60%	81%	100%	88%	100%	100%
	χ^2	50%	51%	50%	60%	86%	100%	51%	50%	60%	86%	100%	49%	61%	86%	100%	60%	86%	100%	90%	100%	100%

Percentage Of Accuracy. Sets With Four Random Variables, Marginal, and Correlation Information

Table C.14: Percentage of accuracy for sets with marginal and rank correlation information. We present results for symmetric constraints using 4 binary random variables, for all distribution approximations and accuracy measures, while changing the values of $\hat{p} = 0.5$ and respective $\rho^r_{1,2}$.

% Of times		DAC	DAC	DAC	DAC	DAC	DAC	MVIE	MVIE	MVIE	MVIE	MVIE	AC	AC	AC	AC	ChSC	ChSC	ChSC	ME	ME	UE
is better than		MVIE	AC	ChSC	ME	UE	IA	AC	ChSC	ME	UE	IA	ChSC	ME	UE	IA	ME	UE	IA	UE	IA	IA
$\hat{p}$	$\mathbf{L}^\infty$	54%	54%	54%	54%	54%	54%	48%	50%	50%	50%	50%	55%	55%	55%	55%	54%	54%	54%	50%	50%	50%
0.5	$\mathbf{L}^1$	51%	51%	51%	51%	51%	51%	49%	50%	50%	50%	50%	51%	51%	51%	51%	52%	52%	52%	50%	50%	50%
ρ	$\mathbf{L}^2$	51%	51%	51%	51%	51%	51%	50%	50%	50%	50%	50%	51%	51%	51%	51%	50%	50%	50%	50%	50%	50%
0	KL	51%	51%	51%	51%	51%	51%	50%	50%	50%	50%	50%	51%	51%	51%	51%	100%	100%	100%	50%	44%	39%
	χ^2	51%	51%	51%	51%	51%	51%	50%	50%	50%	50%	50%	51%	51%	51%	51%	95%	95%	95%	50%	50%	50%
$\hat{p}$	$\mathbf{L}^\infty$	45%	46%	57%	52%	60%	97%	48%	58%	51%	60%	97%	57%	52%	60%	97%	46%	65%	95%	58%	98%	86%
0.5	$\mathbf{L}^1$	48%	48%	56%	54%	61%	97%	48%	57%	50%	61%	98%	57%	51%	60%	98%	46%	62%	94%	59%	98%	62%
ρ	$\mathbf{L}^2$	47%	48%	56%	55%	62%	100%	48%	58%	51%	62%	100%	57%	52%	61%	100%	46%	63%	96%	60%	100%	67%
0.1	KL	48%	48%	56%	54%	61%	100%	48%	58%	51%	61%	100%	57%	52%	61%	100%	46%	63%	98%	59%	100%	66%
	χ^2	48%	47%	58%	53%	62%	100%	47%	60%	50%	62%	100%	59%	51%	61%	100%	44%	65%	96%	59%	100%	64%
$\hat{p}$	$\mathbf{L}^\infty$	53%	50%	58%	56%	75%	100%	47%	61%	53%	76%	100%	58%	56%	75%	100%	48%	76%	100%	73%	100%	100%
0.5	$\mathbf{L}^1$	53%	46%	58%	55%	73%	100%	46%	61%	52%	74%	100%	58%	54%	73%	100%	47%	73%	100%	71%	100%	72%
ρ	$\mathbf{L}^2$	53%	45%	58%	56%	74%	100%	47%	61%	53%	74%	100%	58%	56%	74%	100%	48%	74%	100%	73%	100%	86%
0.2	KL	53%	47%	58%	56%	74%	100%	47%	61%	53%	75%	100%	58%	56%	74%	100%	48%	75%	100%	71%	100%	80%
	χ^2	54%	47%	60%	56%	77%	100%	45%	63%	52%	78%	100%	60%	55%	77%	100%	47%	78%	100%	73%	100%	79%
$\hat{p}$	$\mathbf{L}^\infty$	53%	56%	58%	61%	83%	100%	48%	61%	58%	83%	100%	57%	62%	83%	100%	53%	82%	100%	82%	100%	100%
0.5	$\mathbf{L}^1$	52%	55%	57%	59%	82%	100%	47%	61%	56%	81%	100%	57%	60%	81%	100%	52%	81%	100%	81%	100%	96%
ρ	$\mathbf{L}^2$	52%	57%	57%	61%	82%	100%	48%	61%	58%	82%	100%	57%	62%	82%	100%	53%	82%	100%	81%	100%	100%
0.3	KL	53%	54%	58%	61%	84%	100%	48%	61%	58%	83%	100%	57%	62%	83%	100%	53%	83%	100%	81%	100%	94%
	χ^2	54%	54%	60%	61%	87%	100%	47%	63%	58%	87%	100%	59%	62%	87%	100%	53%	86%	100%	85%	100%	89%
$\hat{p}$	$\mathbf{L}^\infty$	53%	52%	57%	65%	89%	100%	49%	61%	62%	89%	100%	56%	66%	89%	100%	58%	88%	100%	89%	100%	100%
0.5	$\mathbf{L}^1$	53%	54%	58%	63%	88%	100%	48%	61%	61%	88%	100%	57%	65%	88%	100%	57%	88%	100%	88%	100%	100%
ρ	$\mathbf{L}^2$	52%	56%	57%	65%	88%	100%	49%	61%	62%	88%	100%	56%	66%	89%	100%	58%	88%	100%	88%	100%	100%
0.4	KL	53%	53%	57%	65%	90%	100%	49%	61%	62%	90%	100%	56%	66%	91%	100%	58%	90%	100%	90%	100%	99%
	χ^2	54%	52%	60%	65%	94%	100%	47%	64%	62%	93%	100%	58%	66%	94%	100%	58%	93%	100%	94%	100%	92%
$\hat{p}$	$\mathbf{L}^\infty$	53%	52%	58%	69%	93%	100%	48%	62%	66%	92%	100%	57%	70%	93%	100%	62%	92%	100%	93%	100%	100%
0.5	$\mathbf{L}^1$	54%	52%	58%	68%	92%	100%	47%	62%	64%	92%	100%	57%	68%	93%	100%	60%	92%	100%	93%	100%	100%
ρ	$\mathbf{L}^2$	53%	53%	58%	69%	93%	100%	48%	62%	66%	92%	100%	57%	70%	93%	100%	62%	92%	100%	93%	100%	100%
0.5	KL	53%	52%	58%	69%	95%	100%	48%	62%	66%	95%	100%	57%	70%	95%	100%	62%	94%	100%	95%	100%	100%
	χ^2	55%	51%	60%	70%	97%	100%	47%	65%	66%	97%	100%	59%	70%	98%	100%	62%	97%	100%	98%	100%	93%
$\hat{p}$	$\mathbf{L}^\infty$	53%	52%	58%	75%	96%	100%	49%	61%	72%	96%	100%	56%	77%	96%	100%	68%	96%	100%	96%	100%	100%
0.5	$\mathbf{L}^1$	52%	54%	57%	74%	96%	100%	48%	61%	71%	96%	100%	56%	75%	96%	100%	67%	95%	100%	96%	100%	100%
ρ	$\mathbf{L}^2$	51%	58%	57%	75%	96%	100%	49%	61%	72%	96%	100%	56%	77%	96%	100%	68%	96%	100%	96%	100%	100%
0.6	KL	53%	54%	58%	76%	98%	100%	49%	61%	73%	98%	100%	56%	77%	98%	100%	69%	98%	100%	98%	100%	100%
	χ^2	54%	53%	60%	76%	100%	100%	48%	64%	73%	99%	100%	58%	77%	100%	100%	69%	99%	100%	100%	100%	91%
$\hat{p}$	$\mathbf{L}^\infty$	53%	53%	57%	82%	98%	100%	49%	61%	79%	98%	100%	55%	83%	98%	100%	76%	98%	100%	99%	100%	100%
0.5	$\mathbf{L}^1$	53%	53%	57%	81%	98%	100%	48%	61%	79%	98%	100%	56%	82%	98%	100%	75%	98%	100%	98%	100%	100%
ρ	$\mathbf{L}^2$	52%	54%	57%	82%	98%	100%	49%	61%	79%	98%	100%	55%	83%	98%	100%	76%	98%	100%	98%	100%	100%
0.7	KL	53%	53%	57%	83%	100%	100%	49%	61%	81%	100%	100%	55%	84%	100%	100%	78%	100%	100%	100%	100%	100%
	χ^2	54%	52%	59%	84%	100%	100%	48%	64%	82%	100%	100%	57%	85%	100%	100%	79%	100%	100%	100%	100%	62%

Table C.15: Percentage of accuracy for sets with marginal and rank correlation information. We present results for symmetric constraints using 4 binary random variables, for all distribution approximations and accuracy measures, while changing the values of $\hat{p} = 0.6$ and respective $\rho^r_{1,2}$.

% Of times		DAC	DAC	DAC	DAC	DAC	DAC	MVIE	MVIE	MVIE	MVIE	MVIE	AC	AC	AC	AC	ChSC	ChSC	ChSC	ME	ME	UE
is better than		MVIE	AC	ChSC	ME	UE	IA	AC	ChSC	ME	UE	IA	ChSC	ME	UE	IA	ME	UE	IA	UE	IA	IA
$\hat{p}$	$\mathbf{L}^\infty$	53%	46%	69%	47%	47%	47%	48%	71%	49%	49%	49%	68%	48%	48%	48%	32%	32%	32%	50%	50%	50%
0.6	$\mathbf{L}^1$	53%	50%	68%	51%	51%	51%	48%	70%	49%	49%	49%	67%	51%	51%	51%	34%	34%	34%	50%	50%	50%
ρ	$\mathbf{L}^2$	53%	49%	69%	49%	49%	49%	48%	71%	48%	48%	48%	68%	51%	51%	51%	33%	33%	33%	50%	50%	50%
0	KL	52%	48%	69%	49%	49%	49%	48%	71%	48%	48%	48%	68%	49%	49%	49%	33%	33%	33%	50%	47%	45%
	χ^2	53%	46%	71%	46%	46%	46%	47%	73%	47%	47%	47%	70%	47%	47%	47%	30%	30%	30%	50%	50%	50%
$\hat{p}$	$\mathbf{L}^\infty$	45%	61%	47%	66%	78%	90%	56%	48%	63%	75%	86%	41%	67%	79%	92%	65%	76%	88%	82%	97%	96%
0.6	$\mathbf{L}^1$	48%	57%	48%	62%	75%	83%	53%	48%	58%	71%	77%	46%	63%	76%	84%	60%	73%	80%	80%	93%	46%
ρ	$\mathbf{L}^2$	48%	57%	46%	64%	76%	86%	53%	49%	60%	73%	81%	45%	65%	77%	87%	62%	74%	83%	81%	95%	71%
0.1	KL	48%	57%	48%	64%	77%	94%	53%	48%	60%	74%	86%	45%	65%	78%	96%	62%	75%	90%	82%	100%	44%
	χ^2	46%	59%	47%	67%	81%	99%	55%	49%	62%	78%	90%	43%	68%	81%	99%	64%	79%	95%	85%	100%	38%
$\hat{p}$	$\mathbf{L}^\infty$	43%	56%	58%	69%	84%	100%	58%	61%	67%	83%	100%	47%	70%	85%	100%	66%	82%	100%	89%	100%	100%
0.6	$\mathbf{L}^1$	47%	55%	52%	65%	82%	96%	55%	60%	63%	81%	94%	48%	67%	83%	97%	62%	80%	93%	87%	100%	70%
ρ	$\mathbf{L}^2$	45%	54%	52%	67%	83%	98%	55%	61%	65%	82%	97%	47%	68%	84%	99%	63%	81%	97%	88%	100%	98%
0.2	KL	46%	53%	55%	67%	84%	100%	56%	61%	65%	83%	100%	49%	69%	85%	100%	63%	83%	100%	89%	100%	64%
	χ^2	44%	54%	58%	70%	88%	100%	58%	63%	68%	87%	100%	49%	72%	89%	100%	65%	86%	100%	92%	100%	56%
$\hat{p}$	$\mathbf{L}^\infty$	53%	54%	58%	69%	88%	100%	56%	62%	68%	88%	100%	58%	70%	89%	100%	66%	87%	100%	92%	100%	100%
0.6	$\mathbf{L}^1$	52%	53%	58%	66%	87%	100%	53%	61%	65%	87%	100%	54%	67%	88%	100%	63%	86%	100%	91%	100%	100%
ρ	$\mathbf{L}^2$	51%	52%	58%	68%	88%	100%	55%	62%	67%	87%	100%	54%	69%	88%	100%	65%	87%	100%	92%	100%	100%
0.3	KL	53%	53%	58%	69%	90%	100%	52%	62%	66%	89%	100%	57%	70%	90%	100%	62%	89%	100%	93%	100%	87%
	χ^2	54%	54%	60%	73%	93%	100%	52%	65%	70%	93%	100%	59%	73%	93%	100%	63%	92%	100%	96%	100%	73%
$\hat{p}$	$\mathbf{L}^\infty$	53%	59%	58%	72%	92%	100%	48%	62%	71%	91%	100%	57%	73%	92%	100%	68%	91%	100%	94%	100%	100%
0.6	$\mathbf{L}^1$	54%	56%	58%	69%	92%	100%	50%	62%	68%	91%	100%	56%	70%	92%	100%	66%	91%	100%	94%	100%	100%
ρ	$\mathbf{L}^2$	53%	58%	58%	71%	92%	100%	51%	62%	70%	91%	100%	56%	72%	92%	100%	67%	91%	100%	94%	100%	100%
0.4	KL	53%	58%	58%	72%	94%	100%	49%	62%	69%	94%	100%	57%	73%	94%	100%	64%	93%	100%	96%	100%	99%
	χ^2	55%	61%	60%	75%	97%	100%	47%	65%	69%	96%	100%	59%	75%	97%	100%	63%	96%	100%	98%	100%	81%
$\hat{p}$	$\mathbf{L}^\infty$	53%	52%	58%	74%	95%	100%	48%	62%	72%	94%	100%	57%	75%	95%	100%	66%	94%	100%	97%	100%	100%
0.6	$\mathbf{L}^1$	51%	54%	57%	71%	95%	100%	47%	61%	69%	94%	100%	57%	71%	95%	100%	66%	94%	100%	96%	100%	100%
ρ	$\mathbf{L}^2$	50%	57%	57%	74%	95%	100%	48%	62%	71%	94%	100%	57%	74%	95%	100%	69%	94%	100%	97%	100%	100%
0.5	KL	52%	54%	58%	73%	97%	100%	48%	62%	70%	97%	100%	57%	75%	97%	100%	66%	97%	100%	98%	100%	100%
	χ^2	54%	53%	60%	74%	99%	100%	47%	64%	71%	99%	100%	59%	76%	99%	100%	66%	99%	100%	100%	100%	85%
$\hat{p}$	$\mathbf{L}^\infty$	53%	60%	58%	77%	98%	100%	49%	62%	75%	97%	100%	56%	79%	98%	100%	72%	97%	100%	99%	100%	100%
0.6	$\mathbf{L}^1$	52%	56%	57%	76%	98%	100%	48%	61%	74%	97%	100%	56%	77%	98%	100%	71%	97%	100%	99%	100%	100%
ρ	$\mathbf{L}^2$	52%	58%	58%	78%	98%	100%	49%	62%	77%	97%	100%	56%	80%	98%	100%	74%	97%	100%	99%	100%	100%
0.6	KL	53%	54%	58%	79%	99%	100%	49%	62%	76%	99%	100%	56%	80%	99%	100%	72%	99%	100%	100%	100%	100%
	χ^2	54%	53%	60%	79%	100%	100%	48%	64%	76%	100%	100%	58%	80%	100%	100%	73%	100%	100%	100%	100%	78%
$\hat{p}$	$\mathbf{L}^\infty$	53%	53%	58%	85%	99%	100%	49%	62%	83%	99%	100%	56%	86%	99%	100%	81%	99%	100%	99%	100%	100%
0.6	$\mathbf{L}^1$	54%	52%	58%	84%	99%	100%	48%	61%	82%	99%	100%	56%	84%	99%	100%	80%	98%	100%	99%	100%	100%
ρ	$\mathbf{L}^2$	53%	53%	58%	86%	99%	100%	49%	62%	84%	99%	100%	56%	86%	99%	100%	82%	99%	100%	99%	100%	100%
0.7	KL	53%	52%	58%	88%	100%	100%	49%	62%	87%	100%	100%	56%	89%	100%	100%	84%	100%	100%	100%	100%	100%
	χ^2	55%	51%	60%	89%	100%	100%	48%	64%	88%	100%	100%	58%	90%	100%	100%	85%	100%	100%	100%	100%	18%

Table C.16: Percentage of accuracy for sets with marginal and rank correlation information. We present results for symmetric constraints using 4 binary random variables, for all distribution approximations and accuracy measures, while changing the values of $\hat{p} = 0.7$ and respective $\rho^r_{1,2}$.

% Of times		DAC	DAC	DAC	DAC	DAC	DAC	MVIE	MVIE	MVIE	MVIE	MVIE	AC	AC	AC	AC	ChSC	ChSC	ChSC	ME	ME	UE
is better than		MVIE	AC	ChSC	ME	UE	IA	AC	ChSC	ME	UE	IA	ChSC	ME	UE	IA	ME	UE	IA	UE	IA	IA
$\hat{p}$	$\mathbf{L}^\infty$	54%	61%	69%	66%	66%	66%	56%	73%	61%	61%	61%	59%	78%	78%	78%	47%	47%	47%	50%	50%	50%
0.7	$\mathbf{L}^1$	54%	63%	68%	69%	69%	69%	58%	72%	65%	65%	65%	57%	79%	79%	79%	50%	50%	50%	50%	50%	50%
ρ	$\mathbf{L}^2$	54%	62%	68%	68%	68%	68%	57%	73%	64%	64%	64%	57%	78%	78%	78%	50%	50%	50%	50%	50%	50%
0	KL	54%	62%	68%	68%	68%	68%	57%	73%	64%	64%	64%	58%	78%	78%	78%	49%	49%	49%	41%	65%	82%
	χ^2	56%	60%	72%	66%	66%	66%	55%	77%	61%	61%	61%	62%	76%	76%	76%	45%	45%	45%	41%	50%	59%
$\hat{p}$	$\mathbf{L}^\infty$	45%	53%	66%	66%	82%	92%	56%	65%	65%	81%	92%	67%	68%	83%	93%	27%	90%	98%	89%	97%	100%
0.7	$\mathbf{L}^1$	49%	54%	66%	64%	80%	86%	52%	64%	63%	79%	85%	67%	66%	81%	87%	30%	89%	96%	88%	95%	60%
ρ	$\mathbf{L}^2$	47%	54%	66%	65%	81%	89%	53%	65%	64%	80%	88%	68%	66%	82%	90%	28%	90%	97%	89%	96%	100%
0.1	KL	45%	53%	66%	66%	86%	96%	54%	65%	64%	84%	93%	67%	67%	87%	97%	31%	90%	100%	92%	100%	30%
	χ^2	41%	54%	69%	69%	90%	100%	58%	68%	68%	88%	100%	70%	71%	90%	100%	29%	93%	97%	94%	100%	24%
$\hat{p}$	$\mathbf{L}^\infty$	46%	62%	47%	76%	90%	100%	57%	58%	72%	89%	100%	44%	77%	91%	100%	71%	88%	99%	96%	100%	100%
0.7	$\mathbf{L}^1$	50%	58%	51%	73%	90%	98%	53%	58%	69%	88%	97%	49%	74%	91%	98%	67%	87%	97%	95%	100%	95%
ρ	$\mathbf{L}^2$	49%	59%	50%	74%	90%	99%	53%	58%	70%	88%	99%	48%	76%	91%	99%	69%	88%	98%	96%	100%	100%
0.2	KL	50%	59%	51%	74%	92%	100%	53%	58%	69%	90%	100%	48%	75%	93%	100%	68%	90%	100%	97%	100%	53%
	χ^2	48%	61%	49%	77%	95%	100%	55%	60%	72%	94%	100%	46%	79%	96%	100%	71%	93%	100%	98%	100%	39%
$\hat{p}$	$\mathbf{L}^\infty$	53%	59%	58%	76%	94%	100%	59%	62%	76%	93%	100%	46%	78%	94%	100%	75%	93%	100%	98%	100%	100%
0.7	$\mathbf{L}^1$	54%	55%	58%	73%	94%	100%	55%	61%	73%	93%	100%	48%	75%	94%	100%	72%	93%	100%	98%	100%	100%
ρ	$\mathbf{L}^2$	53%	54%	58%	75%	94%	100%	57%	62%	74%	93%	100%	49%	77%	94%	100%	73%	93%	100%	98%	100%	100%
0.3	KL	53%	55%	58%	75%	96%	100%	56%	61%	74%	96%	100%	54%	77%	96%	100%	72%	95%	100%	99%	100%	87%
	χ^2	54%	57%	60%	79%	98%	100%	59%	64%	77%	98%	100%	56%	81%	98%	100%	75%	98%	100%	99%	100%	61%
$\hat{p}$	$\mathbf{L}^\infty$	53%	59%	58%	76%	95%	100%	48%	62%	76%	95%	100%	57%	77%	95%	100%	74%	95%	100%	98%	100%	100%
0.7	$\mathbf{L}^1$	52%	56%	58%	74%	95%	100%	51%	61%	73%	95%	100%	56%	75%	95%	100%	72%	95%	100%	98%	100%	100%
ρ	$\mathbf{L}^2$	51%	58%	57%	76%	95%	100%	52%	62%	75%	95%	100%	55%	76%	95%	100%	73%	95%	100%	98%	100%	100%
0.4	KL	53%	58%	58%	77%	97%	100%	49%	62%	75%	97%	100%	56%	78%	98%	100%	72%	97%	100%	99%	100%	100%
	χ^2	54%	61%	60%	81%	99%	100%	48%	64%	78%	99%	100%	58%	81%	99%	100%	75%	99%	100%	100%	100%	75%
$\hat{p}$	$\mathbf{L}^\infty$	53%	52%	58%	79%	97%	100%	49%	62%	78%	97%	100%	56%	79%	97%	100%	77%	97%	100%	99%	100%	100%
0.7	$\mathbf{L}^1$	54%	52%	58%	77%	97%	100%	48%	62%	76%	97%	100%	57%	78%	97%	100%	75%	97%	100%	99%	100%	100%
ρ	$\mathbf{L}^2$	53%	53%	58%	79%	97%	100%	49%	62%	78%	97%	100%	56%	79%	97%	100%	76%	97%	100%	99%	100%	100%
0.5	KL	53%	52%	58%	81%	99%	100%	49%	62%	79%	99%	100%	56%	81%	99%	100%	75%	99%	100%	100%	100%	100%
	χ^2	55%	51%	60%	84%	100%	100%	47%	64%	81%	100%	100%	58%	84%	100%	100%	76%	100%	100%	100%	100%	77%
$\hat{p}$	$\mathbf{L}^\infty$	53%	53%	58%	83%	98%	100%	49%	61%	82%	98%	100%	56%	83%	98%	100%	81%	98%	100%	100%	100%	100%
0.7	$\mathbf{L}^1$	53%	54%	58%	83%	98%	100%	48%	61%	82%	98%	100%	56%	83%	98%	100%	81%	98%	100%	99%	100%	100%
ρ	$\mathbf{L}^2$	52%	56%	58%	84%	98%	100%	49%	61%	83%	98%	100%	56%	84%	98%	100%	82%	98%	100%	99%	100%	100%
0.6	KL	53%	53%	58%	87%	100%	100%	49%	61%	86%	100%	100%	56%	88%	100%	100%	83%	100%	100%	100%	100%	100%
	χ^2	55%	52%	60%	89%	100%	100%	48%	64%	87%	100%	100%	58%	90%	100%	100%	84%	100%	100%	100%	100%	34%

Table C.17: Percentage of accuracy for sets with marginal and rank correlation information. We present results for symmetric constraints using 4 binary random variables, for all distribution approximations and accuracy measures, while changing the values of $\hat{p} = 0.8, 0.9$ and respective $\rho^r_{1,2}$.

% Of times		DAC	DAC	DAC	DAC	DAC	DAC	MVIE	MVIE	MVIE	MVIE	MVIE	AC	AC	AC	AC	ChSC	ChSC	ChSC	ME	ME	UE
is better than		MVIE	AC	ChSC	ME	UE	IA	AC	ChSC	ME	UE	IA	ChSC	ME	UE	IA	ME	UE	IA	UE	IA	IA
$\hat{p}$	$\mathbf{L}^\infty$	54%	67%	69%	81%	81%	81%	62%	73%	78%	78%	78%	53%	92%	92%	92%	66%	66%	66%	61%	59%	48%
0.8	$\mathbf{L}^1$	54%	70%	68%	85%	85%	85%	65%	72%	81%	81%	81%	50%	93%	93%	93%	69%	69%	69%	50%	50%	50%
ρ	$\mathbf{L}^2$	54%	69%	68%	85%	85%	85%	64%	73%	81%	81%	81%	50%	93%	93%	93%	70%	70%	70%	50%	50%	50%
0	KL	54%	69%	68%	84%	84%	84%	64%	73%	81%	81%	81%	51%	93%	93%	93%	68%	68%	68%	59%	3%	1%
	χ^2	57%	67%	73%	85%	85%	85%	62%	78%	80%	80%	80%	56%	94%	94%	94%	65%	65%	65%	50%	50%	50%
$\hat{p}$	$\mathbf{L}^\infty$	53%	46%	68%	67%	87%	99%	48%	71%	72%	89%	99%	67%	66%	87%	99%	24%	94%	100%	94%	100%	100%
0.8	$\mathbf{L}^1$	53%	51%	67%	66%	86%	95%	47%	70%	70%	88%	96%	66%	65%	86%	95%	29%	94%	99%	93%	99%	100%
ρ	$\mathbf{L}^2$	53%	49%	68%	67%	87%	97%	47%	71%	70%	88%	97%	67%	66%	86%	96%	26%	94%	99%	93%	99%	100%
0.1	KL	53%	48%	67%	68%	92%	100%	48%	71%	72%	93%	100%	66%	67%	92%	100%	32%	96%	100%	97%	100%	29%
	χ^2	54%	43%	70%	72%	96%	100%	46%	74%	77%	96%	100%	70%	71%	95%	100%	29%	98%	99%	98%	100%	25%
$\hat{p}$	$\mathbf{L}^\infty$	45%	63%	49%	82%	95%	100%	59%	58%	80%	94%	100%	42%	84%	96%	100%	79%	94%	100%	99%	100%	100%
0.8	$\mathbf{L}^1$	49%	59%	50%	80%	95%	100%	55%	57%	78%	94%	100%	46%	82%	96%	100%	77%	94%	100%	99%	100%	100%
ρ	$\mathbf{L}^2$	49%	60%	49%	81%	95%	100%	56%	58%	79%	94%	100%	45%	83%	96%	100%	78%	94%	100%	99%	100%	100%
0.2	KL	49%	60%	50%	81%	97%	100%	55%	57%	78%	96%	100%	45%	83%	98%	100%	77%	96%	100%	99%	100%	62%
	χ^2	47%	63%	49%	83%	99%	100%	58%	60%	81%	99%	100%	43%	85%	99%	100%	80%	99%	100%	100%	100%	39%
$\hat{p}$	$\mathbf{L}^\infty$	45%	59%	58%	81%	96%	100%	56%	62%	80%	96%	100%	57%	82%	96%	100%	79%	96%	100%	99%	100%	100%
0.8	$\mathbf{L}^1$	47%	56%	56%	79%	96%	100%	54%	61%	78%	96%	100%	53%	80%	96%	100%	77%	96%	100%	99%	100%	100%
ρ	$\mathbf{L}^2$	47%	58%	56%	80%	96%	100%	55%	62%	79%	96%	100%	53%	81%	96%	100%	78%	96%	100%	99%	100%	100%
0.3	KL	51%	58%	58%	81%	98%	100%	52%	62%	79%	98%	100%	56%	81%	98%	100%	77%	98%	100%	100%	100%	99%
	χ^2	53%	61%	60%	84%	100%	100%	51%	64%	82%	100%	100%	58%	84%	100%	100%	80%	100%	100%	100%	100%	72%
$\hat{p}$	$\mathbf{L}^\infty$	53%	60%	58%	83%	98%	100%	49%	61%	83%	98%	100%	56%	83%	98%	100%	82%	98%	100%	100%	100%	100%
0.8	$\mathbf{L}^1$	54%	57%	58%	82%	98%	100%	49%	61%	82%	98%	100%	56%	82%	98%	100%	81%	98%	100%	100%	100%	100%
ρ	$\mathbf{L}^2$	53%	58%	58%	83%	98%	100%	50%	61%	82%	98%	100%	56%	83%	98%	100%	82%	98%	100%	100%	100%	100%
0.4	KL	53%	54%	58%	85%	100%	100%	49%	61%	84%	99%	100%	56%	86%	100%	100%	82%	99%	100%	100%	100%	100%
	χ^2	55%	53%	60%	88%	100%	100%	47%	64%	87%	100%	100%	58%	89%	100%	100%	85%	100%	100%	100%	100%	78%
$\hat{p}$	$\mathbf{L}^\infty$	54%	71%	69%	92%	92%	92%	66%	73%	91%	91%	91%	49%	98%	98%	98%	83%	83%	83%	57%	13%	12%
0.9	$\mathbf{L}^1$	54%	74%	68%	94%	94%	94%	69%	72%	92%	92%	92%	46%	98%	98%	98%	87%	87%	87%	52%	50%	48%
ρ	$\mathbf{L}^2$	55%	73%	69%	94%	94%	94%	68%	73%	93%	93%	93%	46%	98%	98%	98%	87%	87%	87%	51%	46%	24%
0	KL	54%	73%	68%	94%	94%	94%	68%	73%	93%	93%	93%	47%	99%	99%	99%	86%	86%	86%	0%	100%	100%
	χ^2	58%	72%	74%	96%	96%	96%	66%	78%	95%	95%	95%	54%	99%	99%	99%	89%	89%	89%	3%	24%	96%
$\hat{p}$	$\mathbf{L}^\infty$	48%	59%	64%	87%	97%	100%	56%	62%	84%	96%	100%	67%	88%	98%	100%	91%	98%	100%	100%	100%	100%
0.9	$\mathbf{L}^1$	51%	58%	64%	85%	97%	100%	53%	60%	83%	96%	100%	67%	87%	97%	100%	90%	98%	100%	100%	100%	100%
ρ	$\mathbf{L}^2$	50%	58%	65%	86%	97%	100%	54%	61%	83%	96%	100%	68%	88%	98%	100%	91%	98%	100%	100%	100%	100%
0.1	KL	49%	58%	64%	85%	99%	100%	54%	60%	82%	98%	100%	68%	87%	99%	100%	90%	99%	100%	100%	100%	39%
	χ^2	47%	60%	67%	88%	100%	100%	56%	63%	85%	100%	100%	70%	90%	100%	100%	92%	100%	100%	100%	100%	28%
$\hat{p}$	$\mathbf{L}^\infty$	53%	59%	58%	88%	98%	100%	48%	62%	88%	98%	100%	57%	89%	98%	100%	87%	98%	100%	100%	100%	100%
0.9	$\mathbf{L}^1$	54%	56%	58%	87%	98%	100%	52%	61%	87%	98%	100%	55%	88%	98%	100%	86%	98%	100%	100%	100%	100%
ρ	$\mathbf{L}^2$	53%	58%	58%	88%	98%	100%	53%	62%	87%	98%	100%	55%	88%	98%	100%	87%	98%	100%	100%	100%	100%
0.2	KL	53%	58%	58%	88%	100%	100%	50%	62%	87%	100%	100%	56%	89%	100%	100%	86%	100%	100%	100%	100%	100%
	χ^2	55%	62%	60%	91%	100%	100%	48%	65%	90%	100%	100%	58%	91%	100%	100%	89%	100%	100%	100%	100%	88%

Percentage Of Accuracy. Sets With Six Random Variables, Marginal, and Correlation Information

Table C.18: Percentage of accuracy for sets with marginal and rank correlation information. We present results for symmetric constraints using 6 binary random variables, for all distribution approximations and accuracy measures, while changing the values of $\hat{p} = 0.5$ and respective $\rho^r_{1,2}$.

% Of times		DAC	DAC	DAC	DAC	DAC	DAC	MVIE	MVIE	MVIE	MVIE	MVIE	AC	AC	AC	AC	ChSC	ChSC	ChSC	ME	ME	UE
is better than		MVIE	AC	ChSC	ME	UE	IA	AC	ChSC	ME	UE	IA	ChSC	ME	UE	IA	ME	UE	IA	UE	IA	IA
$\hat{p}$	$\mathbf{L}^\infty$	57%	57%	57%	57%	57%	57%	55%	57%	57%	57%	57%	43%	43%	43%	43%	80%	80%	80%	49%	50%	51%
0.5	$\mathbf{L}^1$	58%	58%	58%	58%	58%	58%	53%	53%	53%	53%	53%	50%	50%	50%	50%	45%	45%	45%	50%	50%	50%
ρ	$\mathbf{L}^2$	58%	58%	58%	58%	58%	58%	54%	54%	54%	54%	54%	52%	52%	52%	52%	50%	50%	50%	50%	50%	50%
0	KL	59%	59%	59%	59%	59%	59%	54%	54%	54%	54%	54%	52%	52%	52%	52%	100%	100%	100%	50%	50%	56%
	χ^2	58%	58%	58%	58%	58%	58%	55%	55%	55%	55%	55%	55%	55%	55%	55%	64%	64%	64%	48%	50%	53%
$\hat{p}$	$\mathbf{L}^\infty$	55%	57%	68%	58%	89%	99%	57%	65%	64%	91%	99%	64%	66%	91%	99%	45%	89%	92%	90%	100%	52%
0.5	$\mathbf{L}^1$	59%	58%	70%	66%	89%	100%	50%	70%	62%	91%	100%	69%	64%	91%	100%	45%	88%	98%	88%	100%	41%
ρ	$\mathbf{L}^2$	58%	57%	72%	67%	90%	100%	48%	75%	63%	91%	100%	73%	65%	91%	100%	43%	89%	94%	90%	100%	38%
0.1	KL	59%	59%	73%	68%	91%	100%	48%	76%	62%	92%	100%	74%	64%	92%	100%	41%	90%	99%	90%	100%	51%
	χ^2	60%	59%	78%	67%	92%	100%	45%	81%	61%	94%	100%	79%	64%	94%	100%	37%	92%	97%	92%	100%	52%
$\hat{p}$	$\mathbf{L}^\infty$	57%	57%	71%	84%	99%	100%	61%	62%	84%	99%	100%	59%	87%	99%	100%	70%	98%	100%	96%	100%	98%
0.5	$\mathbf{L}^1$	56%	60%	68%	86%	98%	100%	54%	70%	84%	98%	100%	64%	88%	98%	100%	71%	98%	100%	96%	100%	70%
ρ	$\mathbf{L}^2$	56%	60%	73%	89%	99%	100%	53%	74%	87%	99%	100%	68%	90%	99%	100%	72%	99%	100%	98%	100%	90%
0.2	KL	58%	61%	74%	88%	99%	100%	53%	75%	85%	99%	100%	69%	90%	99%	100%	67%	99%	100%	97%	100%	93%
	χ^2	61%	59%	80%	86%	99%	100%	48%	81%	83%	99%	100%	75%	89%	99%	100%	61%	99%	100%	99%	100%	92%
$\hat{p}$	$\mathbf{L}^\infty$	59%	55%	70%	94%	100%	100%	57%	68%	92%	100%	100%	64%	95%	100%	100%	85%	100%	100%	100%	100%	100%
0.5	$\mathbf{L}^1$	56%	62%	69%	93%	100%	100%	55%	71%	91%	100%	100%	64%	94%	100%	100%	84%	100%	100%	99%	100%	95%
ρ	$\mathbf{L}^2$	54%	61%	73%	95%	100%	100%	54%	78%	93%	100%	100%	69%	96%	100%	100%	86%	100%	100%	100%	100%	100%
0.3	KL	58%	60%	74%	94%	100%	100%	54%	78%	92%	100%	100%	71%	95%	100%	100%	82%	100%	100%	100%	100%	100%
	χ^2	61%	56%	80%	93%	100%	100%	48%	83%	91%	100%	100%	77%	95%	100%	100%	77%	100%	100%	100%	100%	97%
$\hat{p}$	$\mathbf{L}^\infty$	60%	56%	71%	99%	100%	100%	58%	66%	99%	100%	100%	62%	99%	100%	100%	97%	100%	100%	100%	100%	100%
0.5	$\mathbf{L}^1$	53%	61%	65%	99%	100%	100%	58%	67%	99%	100%	100%	60%	99%	100%	100%	96%	100%	100%	100%	100%	100%
ρ	$\mathbf{L}^2$	54%	61%	70%	99%	100%	100%	54%	74%	99%	100%	100%	65%	99%	100%	100%	98%	100%	100%	100%	100%	100%
0.4	KL	57%	61%	71%	99%	100%	100%	54%	75%	99%	100%	100%	66%	99%	100%	100%	94%	100%	100%	100%	100%	100%
	χ^2	61%	58%	77%	99%	100%	100%	49%	80%	98%	100%	100%	73%	99%	100%	100%	91%	100%	100%	100%	100%	96%
$\hat{p}$	$\mathbf{L}^\infty$	64%	62%	76%	99%	100%	100%	42%	78%	100%	100%	100%	75%	100%	100%	100%	98%	100%	100%	100%	100%	100%
0.5	$\mathbf{L}^1$	61%	59%	73%	99%	100%	100%	41%	80%	99%	100%	100%	73%	99%	100%	100%	97%	100%	100%	100%	100%	100%
ρ	$\mathbf{L}^2$	61%	59%	74%	99%	100%	100%	38%	86%	100%	100%	100%	79%	100%	100%	100%	98%	100%	100%	100%	100%	100%
0.5	KL	66%	61%	79%	99%	100%	100%	38%	86%	99%	100%	100%	80%	100%	100%	100%	94%	100%	100%	100%	100%	100%
	χ^2	67%	61%	83%	99%	100%	100%	32%	90%	99%	100%	100%	86%	100%	100%	100%	91%	100%	100%	100%	100%	83%
$\hat{p}$	$\mathbf{L}^\infty$	50%	56%	66%	100%	100%	100%	66%	59%	100%	100%	100%	54%	100%	100%	100%	100%	100%	100%	100%	100%	100%
0.5	$\mathbf{L}^1$	57%	66%	65%	100%	100%	100%	65%	63%	100%	100%	100%	54%	100%	100%	100%	100%	100%	100%	100%	100%	100%
ρ	$\mathbf{L}^2$	54%	66%	70%	100%	100%	100%	64%	68%	100%	100%	100%	57%	100%	100%	100%	100%	100%	100%	100%	100%	100%
0.6	KL	57%	65%	71%	100%	100%	100%	64%	69%	100%	100%	100%	59%	100%	100%	100%	100%	100%	100%	100%	100%	100%
	χ^2	54%	59%	78%	100%	100%	100%	58%	77%	100%	100%	100%	67%	100%	100%	100%	100%	100%	100%	100%	100%	14%
$\hat{p}$	$\mathbf{L}^\infty$	54%	58%	68%	100%	100%	100%	68%	59%	100%	100%	100%	53%	100%	100%	100%	100%	100%	100%	100%	100%	100%
0.5	$\mathbf{L}^1$	59%	67%	67%	100%	100%	100%	66%	63%	100%	100%	100%	53%	100%	100%	100%	100%	100%	100%	100%	100%	100%
ρ	$\mathbf{L}^2$	57%	67%	71%	100%	100%	100%	65%	70%	100%	100%	100%	58%	100%	100%	100%	100%	100%	100%	100%	100%	100%
0.7	KL	60%	67%	71%	100%	100%	100%	65%	71%	100%	100%	100%	60%	100%	100%	100%	100%	100%	100%	100%	100%	100%
	χ^2	59%	62%	78%	100%	100%	100%	58%	78%	100%	100%	100%	69%	100%	100%	100%	100%	100%	100%	100%	100%	0%

Table C.19: Percentage of accuracy for sets with marginal and rank correlation information. We present results for symmetric constraints using 6 binary random variables, for all distribution approximations and accuracy measures, while changing the values of $\hat{p} = 0.6$ and respective $\rho^r_{1,2}$.

% Of times		DAC	DAC	DAC	DAC	DAC	DAC	MVIE	MVIE	MVIE	MVIE	MVIE	AC	AC	AC	AC	ChSC	ChSC	ChSC	ME	ME	UE
is better than		MVIE	AC	ChSC	ME	UE	IA	AC	ChSC	ME	UE	IA	ChSC	ME	UE	IA	ME	UE	IA	UE	IA	IA
$\hat{p}$	$\mathbf{L}^\infty$	59%	53%	63%	60%	60%	60%	31%	58%	71%	71%	71%	61%	70%	70%	70%	43%	43%	43%	27%	46%	63%
0.6	$\mathbf{L}^1$	61%	60%	82%	62%	62%	62%	38%	74%	68%	68%	68%	77%	63%	63%	63%	27%	27%	27%	54%	32%	46%
ρ	$\mathbf{L}^2$	59%	59%	86%	60%	60%	60%	40%	75%	69%	69%	69%	79%	63%	63%	63%	26%	26%	26%	35%	29%	43%
0	KL	62%	61%	90%	63%	63%	63%	38%	85%	67%	67%	67%	87%	65%	65%	65%	16%	16%	16%	43%	100%	100%
	χ^2	61%	60%	94%	62%	62%	62%	36%	90%	64%	64%	64%	92%	66%	66%	66%	11%	11%	11%	62%	99%	47%
$\hat{p}$	$\mathbf{L}^\infty$	54%	60%	68%	88%	100%	100%	54%	68%	88%	100%	100%	63%	91%	100%	100%	91%	100%	100%	100%	100%	99%
0.6	$\mathbf{L}^1$	60%	68%	72%	89%	100%	100%	67%	71%	89%	100%	100%	64%	93%	100%	100%	93%	100%	100%	100%	100%	2%
ρ	$\mathbf{L}^2$	60%	68%	73%	90%	100%	100%	67%	73%	90%	100%	100%	74%	94%	100%	100%	94%	100%	100%	100%	100%	21%
0.1	KL	59%	68%	74%	90%	100%	100%	67%	72%	90%	100%	100%	67%	94%	100%	100%	91%	100%	100%	100%	100%	5%
	χ^2	56%	64%	74%	89%	100%	100%	63%	72%	89%	100%	100%	67%	94%	100%	100%	89%	100%	100%	100%	100%	7%
$\hat{p}$	$\mathbf{L}^\infty$	60%	59%	73%	94%	100%	100%	56%	74%	94%	100%	100%	69%	96%	100%	100%	90%	100%	100%	100%	100%	100%
0.6	$\mathbf{L}^1$	60%	62%	72%	93%	100%	100%	59%	77%	93%	100%	100%	62%	96%	100%	100%	88%	100%	100%	100%	100%	13%
ρ	$\mathbf{L}^2$	59%	62%	75%	94%	100%	100%	61%	82%	95%	100%	100%	67%	97%	100%	100%	90%	100%	100%	100%	100%	90%
0.2	KL	60%	61%	76%	94%	100%	100%	57%	83%	93%	100%	100%	77%	96%	100%	100%	80%	100%	100%	100%	100%	28%
	χ^2	62%	61%	80%	93%	100%	100%	55%	87%	92%	100%	100%	82%	96%	100%	100%	74%	100%	100%	100%	100%	21%
$\hat{p}$	$\mathbf{L}^\infty$	60%	51%	74%	90%	100%	100%	46%	75%	85%	100%	100%	73%	88%	100%	100%	82%	100%	100%	100%	100%	100%
0.6	$\mathbf{L}^1$	54%	52%	72%	92%	100%	100%	42%	81%	88%	100%	100%	76%	90%	100%	100%	84%	100%	100%	100%	100%	98%
ρ	$\mathbf{L}^2$	54%	51%	74%	92%	100%	100%	40%	86%	88%	100%	100%	79%	90%	100%	100%	85%	100%	100%	100%	100%	100%
0.3	KL	59%	57%	80%	95%	100%	100%	39%	86%	91%	100%	100%	81%	94%	100%	100%	81%	100%	100%	100%	100%	95%
	χ^2	62%	56%	84%	96%	100%	100%	36%	89%	91%	100%	100%	85%	94%	100%	100%	77%	100%	100%	100%	100%	62%
$\hat{p}$	$\mathbf{L}^\infty$	60%	56%	73%	95%	100%	100%	54%	72%	94%	100%	100%	67%	95%	100%	100%	91%	100%	100%	100%	100%	100%
0.6	$\mathbf{L}^1$	54%	58%	67%	96%	100%	100%	51%	73%	96%	100%	100%	66%	96%	100%	100%	94%	100%	100%	100%	100%	100%
ρ	$\mathbf{L}^2$	54%	57%	71%	96%	100%	100%	50%	80%	96%	100%	100%	71%	96%	100%	100%	95%	100%	100%	100%	100%	100%
0.4	KL	60%	62%	76%	96%	100%	100%	51%	81%	95%	100%	100%	72%	96%	100%	100%	92%	100%	100%	100%	100%	100%
	χ^2	64%	60%	84%	96%	100%	100%	44%	87%	95%	100%	100%	80%	96%	100%	100%	90%	100%	100%	100%	100%	66%
$\hat{p}$	$\mathbf{L}^\infty$	62%	55%	72%	98%	100%	100%	46%	73%	97%	100%	100%	70%	98%	100%	100%	96%	100%	100%	100%	100%	100%
0.6	$\mathbf{L}^1$	55%	58%	69%	99%	100%	100%	48%	75%	99%	100%	100%	69%	99%	100%	100%	98%	100%	100%	100%	100%	100%
ρ	$\mathbf{L}^2$	56%	58%	73%	99%	100%	100%	44%	79%	99%	100%	100%	72%	99%	100%	100%	98%	100%	100%	100%	100%	100%
0.5	KL	58%	60%	74%	99%	100%	100%	44%	80%	99%	100%	100%	73%	99%	100%	100%	96%	100%	100%	100%	100%	100%
	χ^2	61%	59%	79%	99%	100%	100%	39%	85%	99%	100%	100%	79%	99%	100%	100%	95%	100%	100%	100%	100%	30%
$\hat{p}$	$\mathbf{L}^\infty$	58%	56%	70%	100%	100%	100%	60%	65%	100%	100%	100%	60%	100%	100%	100%	100%	100%	100%	100%	100%	100%
0.6	$\mathbf{L}^1$	58%	61%	69%	100%	100%	100%	56%	68%	100%	100%	100%	60%	100%	100%	100%	100%	100%	100%	100%	100%	100%
ρ	$\mathbf{L}^2$	59%	62%	72%	100%	100%	100%	56%	74%	100%	100%	100%	64%	100%	100%	100%	100%	100%	100%	100%	100%	100%
0.6	KL	63%	64%	75%	100%	100%	100%	56%	75%	100%	100%	100%	66%	100%	100%	100%	100%	100%	100%	100%	100%	100%
	χ^2	65%	60%	81%	100%	100%	100%	51%	81%	100%	100%	100%	74%	100%	100%	100%	100%	100%	100%	100%	100%	3%
$\hat{p}$	$\mathbf{L}^\infty$	53%	56%	69%	100%	100%	100%	48%	62%	100%	100%	100%	61%	100%	100%	100%	100%	100%	100%	100%	100%	100%
0.6	$\mathbf{L}^1$	62%	62%	65%	100%	100%	100%	48%	62%	100%	100%	100%	60%	100%	100%	100%	100%	100%	100%	100%	100%	100%
ρ	$\mathbf{L}^2$	58%	62%	69%	100%	100%	100%	52%	67%	100%	100%	100%	64%	100%	100%	100%	100%	100%	100%	100%	100%	100%
0.7	KL	50%	64%	70%	100%	100%	100%	59%	75%	100%	100%	100%	66%	100%	100%	100%	100%	100%	100%	100%	100%	100%
	χ^2	45%	62%	76%	100%	100%	100%	59%	83%	100%	100%	100%	73%	100%	100%	100%	100%	100%	100%	100%	100%	0%

Table C.20: Percentage of accuracy for sets with marginal and rank correlation information. We present results for symmetric constraints using 6 binary random variables, for all distribution approximations and accuracy measures, while changing the values of $\hat{p} = 0.7$ and respective $\rho^r_{1,2}$.

% Of times		DAC	DAC	DAC	DAC	DAC	DAC	MVIE	MVIE	MVIE	MVIE	MVIE	AC	AC	AC	AC	ChSC	ChSC	ChSC	ME	ME	UE
is better than		MVIE	AC	ChSC	ME	UE	IA	AC	ChSC	ME	UE	IA	ChSC	ME	UE	IA	ME	UE	IA	UE	IA	IA
$\hat{p}$	$\mathbf{L}^\infty$	81%	61%	97%	93%	93%	93%	30%	98%	77%	77%	77%	92%	95%	95%	95%	38%	38%	38%	50%	50%	50%
0.7	$\mathbf{L}^1$	82%	72%	95%	96%	96%	96%	37%	98%	80%	80%	80%	90%	97%	97%	97%	49%	49%	49%	50%	50%	50%
ρ	$\mathbf{L}^2$	84%	72%	96%	95%	95%	95%	33%	99%	78%	78%	78%	92%	97%	97%	97%	45%	45%	45%	50%	50%	50%
0	KL	85%	70%	99%	95%	95%	95%	30%	99%	74%	74%	74%	97%	97%	97%	97%	12%	12%	12%	50%	24%	10%
	χ^2	89%	63%	100%	92%	92%	92%	18%	99%	65%	65%	65%	99%	96%	96%	96%	3%	3%	3%	50%	50%	50%
$\hat{p}$	$\mathbf{L}^\infty$	56%	60%	96%	90%	100%	100%	58%	94%	88%	99%	100%	97%	91%	100%	100%	0%	100%	100%	100%	100%	100%
0.7	$\mathbf{L}^1$	56%	59%	96%	88%	100%	100%	51%	93%	86%	99%	100%	97%	89%	100%	100%	0%	95%	78%	100%	100%	4%
ρ	$\mathbf{L}^2$	56%	61%	96%	89%	100%	100%	52%	94%	87%	100%	100%	98%	90%	100%	100%	0%	100%	100%	100%	100%	100%
0.1	KL	60%	62%	96%	89%	100%	100%	52%	93%	86%	100%	100%	97%	91%	100%	100%	1%	99%	91%	100%	100%	1%
	χ^2	64%	61%	98%	91%	100%	100%	51%	95%	87%	100%	100%	99%	93%	100%	100%	0%	100%	98%	100%	100%	2%
$\hat{p}$	$\mathbf{L}^\infty$	60%	63%	66%	100%	100%	100%	61%	66%	100%	100%	100%	56%	100%	100%	100%	99%	100%	100%	100%	100%	100%
0.7	$\mathbf{L}^1$	56%	63%	63%	100%	100%	100%	62%	62%	100%	100%	100%	51%	100%	100%	100%	99%	100%	100%	100%	100%	77%
ρ	$\mathbf{L}^2$	56%	63%	67%	100%	100%	100%	62%	66%	100%	100%	100%	52%	100%	100%	100%	99%	100%	100%	100%	100%	100%
0.2	KL	57%	65%	71%	99%	100%	100%	62%	71%	99%	100%	100%	57%	100%	100%	100%	98%	100%	100%	100%	100%	8%
	χ^2	57%	62%	77%	100%	100%	100%	59%	76%	100%	100%	100%	65%	100%	100%	100%	96%	100%	100%	100%	100%	4%
$\hat{p}$	$\mathbf{L}^\infty$	59%	55%	72%	100%	100%	100%	49%	70%	99%	100%	100%	68%	100%	100%	100%	99%	100%	100%	100%	100%	100%
0.7	$\mathbf{L}^1$	54%	59%	71%	99%	100%	100%	47%	75%	99%	100%	100%	70%	99%	100%	100%	98%	100%	100%	100%	100%	100%
ρ	$\mathbf{L}^2$	53%	58%	74%	100%	100%	100%	46%	81%	99%	100%	100%	74%	100%	100%	100%	99%	100%	100%	100%	100%	100%
0.3	KL	59%	59%	76%	100%	100%	100%	44%	82%	98%	100%	100%	76%	99%	100%	100%	94%	100%	100%	100%	100%	92%
	χ^2	62%	58%	82%	100%	100%	100%	39%	87%	99%	100%	100%	81%	100%	100%	100%	92%	100%	100%	100%	100%	39%
$\hat{p}$	$\mathbf{L}^\infty$	58%	58%	72%	100%	100%	100%	62%	64%	100%	100%	100%	59%	100%	100%	100%	100%	100%	100%	100%	100%	100%
0.7	$\mathbf{L}^1$	56%	64%	67%	100%	100%	100%	62%	68%	100%	100%	100%	58%	100%	100%	100%	100%	100%	100%	100%	100%	100%
ρ	$\mathbf{L}^2$	55%	65%	72%	100%	100%	100%	61%	74%	100%	100%	100%	62%	100%	100%	100%	100%	100%	100%	100%	100%	100%
0.4	KL	58%	65%	74%	100%	100%	100%	59%	75%	100%	100%	100%	65%	100%	100%	100%	100%	100%	100%	100%	100%	100%
	χ^2	58%	61%	81%	100%	100%	100%	53%	82%	100%	100%	100%	73%	100%	100%	100%	100%	100%	100%	100%	100%	33%
$\hat{p}$	$\mathbf{L}^\infty$	59%	55%	70%	100%	100%	100%	59%	64%	100%	100%	100%	60%	100%	100%	100%	99%	100%	100%	100%	100%	100%
0.7	$\mathbf{L}^1$	56%	62%	70%	100%	100%	100%	53%	72%	100%	100%	100%	64%	100%	100%	100%	100%	100%	100%	100%	100%	100%
ρ	$\mathbf{L}^2$	55%	61%	73%	100%	100%	100%	54%	77%	100%	100%	100%	67%	100%	100%	100%	100%	100%	100%	100%	100%	100%
0.5	KL	62%	61%	76%	100%	100%	100%	54%	77%	100%	100%	100%	69%	100%	100%	100%	100%	100%	100%	100%	100%	100%
	χ^2	64%	58%	81%	100%	100%	100%	49%	83%	100%	100%	100%	76%	100%	100%	100%	100%	100%	100%	100%	100%	4%
$\hat{p}$	$\mathbf{L}^\infty$	57%	54%	73%	100%	100%	100%	62%	63%	100%	100%	100%	59%	100%	100%	100%	100%	100%	100%	100%	100%	100%
0.7	$\mathbf{L}^1$	60%	63%	66%	100%	100%	100%	58%	63%	100%	100%	100%	57%	100%	100%	100%	100%	100%	100%	100%	100%	100%
ρ	$\mathbf{L}^2$	57%	61%	71%	100%	100%	100%	60%	69%	100%	100%	100%	62%	100%	100%	100%	100%	100%	100%	100%	100%	100%
0.6	KL	57%	64%	73%	100%	100%	100%	60%	72%	100%	100%	100%	63%	100%	100%	100%	100%	100%	100%	100%	100%	100%
	χ^2	55%	59%	79%	100%	100%	100%	58%	79%	100%	100%	100%	71%	100%	100%	100%	100%	100%	100%	100%	100%	0%

Table C.21: Percentage of accuracy for sets with marginal and rank correlation information. We present results for symmetric constraints using 6 binary random variables, for all distribution approximations and accuracy measures, while changing the values of $\hat{p} = 0.8, 0.9$ and respective $\rho^r_{1,2}$.

% Of times		DAC	DAC	DAC	DAC	DAC	DAC	MVIE	MVIE	MVIE	MVIE	MVIE	AC	AC	AC	AC	ChSC	ChSC	ChSC	ME	ME	UE
is better than		MVIE	AC	ChSC	ME	UE	IA	AC	ChSC	ME	UE	IA	ChSC	ME	UE	IA	ME	UE	IA	UE	IA	IA
$\hat{p}$	$\mathbf{L}^\infty$	70%	57%	98%	100%	100%	100%	41%	100%	100%	100%	100%	94%	100%	100%	100%	59%	59%	59%	50%	50%	50%
0.8	$\mathbf{L}^1$	69%	64%	98%	100%	100%	100%	46%	100%	100%	100%	100%	92%	100%	100%	100%	65%	65%	65%	50%	50%	50%
ρ	$\mathbf{L}^2$	69%	62%	98%	100%	100%	100%	44%	100%	100%	100%	100%	94%	100%	100%	100%	61%	61%	61%	50%	50%	50%
0	KL	69%	73%	99%	100%	100%	100%	42%	100%	100%	100%	100%	97%	100%	100%	100%	46%	46%	46%	50%	50%	50%
	χ^2	77%	65%	100%	100%	100%	100%	35%	100%	99%	99%	99%	100%	100%	100%	100%	32%	32%	32%	50%	50%	50%
$\hat{p}$	$\mathbf{L}^\infty$	58%	43%	88%	87%	100%	100%	32%	86%	81%	96%	100%	87%	85%	99%	100%	1%	100%	100%	100%	100%	100%
0.8	$\mathbf{L}^1$	70%	50%	88%	86%	100%	100%	16%	86%	76%	94%	100%	88%	83%	98%	100%	2%	100%	100%	100%	100%	100%
ρ	$\mathbf{L}^2$	64%	47%	89%	87%	100%	100%	18%	87%	79%	95%	100%	88%	84%	98%	100%	1%	100%	100%	100%	100%	100%
0.1	KL	70%	57%	89%	87%	100%	100%	17%	86%	77%	100%	100%	88%	84%	100%	100%	7%	100%	100%	100%	100%	0%
	χ^2	65%	51%	93%	89%	100%	100%	23%	88%	81%	100%	100%	90%	86%	100%	100%	5%	100%	100%	100%	100%	1%
$\hat{p}$	$\mathbf{L}^\infty$	62%	55%	74%	100%	100%	100%	48%	71%	100%	100%	100%	72%	100%	100%	100%	100%	100%	100%	100%	100%	100%
0.8	$\mathbf{L}^1$	57%	59%	69%	100%	100%	100%	48%	75%	100%	100%	100%	66%	100%	100%	100%	100%	100%	100%	100%	100%	100%
ρ	$\mathbf{L}^2$	56%	60%	71%	100%	100%	100%	49%	81%	100%	100%	100%	68%	100%	100%	100%	100%	100%	100%	100%	100%	100%
0.2	KL	61%	61%	78%	100%	100%	100%	49%	79%	100%	100%	100%	75%	100%	100%	100%	99%	100%	100%	100%	100%	22%
	χ^2	64%	59%	82%	100%	100%	100%	46%	83%	100%	100%	100%	80%	100%	100%	100%	98%	100%	100%	100%	100%	11%
$\hat{p}$	$\mathbf{L}^\infty$	58%	59%	69%	100%	100%	100%	57%	66%	100%	100%	100%	62%	100%	100%	100%	99%	100%	100%	100%	100%	100%
0.8	$\mathbf{L}^1$	57%	61%	68%	100%	100%	100%	47%	72%	100%	100%	100%	65%	100%	100%	100%	100%	100%	100%	100%	100%	100%
ρ	$\mathbf{L}^2$	57%	60%	69%	100%	100%	100%	49%	76%	100%	100%	100%	68%	100%	100%	100%	100%	100%	100%	100%	100%	100%
0.3	KL	58%	64%	74%	100%	100%	100%	52%	76%	100%	100%	100%	68%	100%	100%	100%	100%	100%	100%	100%	100%	100%
	χ^2	59%	61%	80%	100%	100%	100%	47%	83%	100%	100%	100%	75%	100%	100%	100%	100%	100%	100%	100%	100%	48%
$\hat{p}$	$\mathbf{L}^\infty$	59%	59%	72%	100%	100%	100%	61%	67%	100%	100%	100%	61%	100%	100%	100%	100%	100%	100%	100%	100%	100%
0.8	$\mathbf{L}^1$	55%	63%	66%	100%	100%	100%	59%	68%	100%	100%	100%	59%	100%	100%	100%	100%	100%	100%	100%	100%	100%
ρ	$\mathbf{L}^2$	56%	62%	71%	100%	100%	100%	57%	73%	100%	100%	100%	63%	100%	100%	100%	100%	100%	100%	100%	100%	100%
0.4	KL	59%	64%	73%	100%	100%	100%	57%	74%	100%	100%	100%	65%	100%	100%	100%	100%	100%	100%	100%	100%	100%
	χ^2	62%	59%	81%	100%	100%	100%	52%	82%	100%	100%	100%	73%	100%	100%	100%	100%	100%	100%	100%	100%	4%
$\hat{p}$	$\mathbf{L}^\infty$	49%	78%	94%	100%	100%	100%	76%	96%	100%	100%	100%	69%	100%	100%	100%	96%	96%	96%	100%	100%	50%
0.9	$\mathbf{L}^1$	48%	80%	91%	100%	100%	100%	77%	95%	100%	100%	100%	63%	100%	100%	100%	100%	100%	100%	72%	50%	48%
ρ	$\mathbf{L}^2$	48%	79%	93%	100%	100%	100%	77%	96%	100%	100%	100%	66%	100%	100%	100%	100%	100%	100%	100%	100%	0%
0	KL	54%	79%	95%	100%	100%	100%	75%	98%	100%	100%	100%	74%	100%	100%	100%	85%	85%	85%	99%	0%	0%
	χ^2	61%	74%	100%	100%	100%	100%	67%	100%	100%	100%	100%	95%	100%	100%	100%	88%	88%	88%	100%	99%	0%
$\hat{p}$	$\mathbf{L}^\infty$	57%	70%	99%	100%	100%	100%	76%	99%	100%	100%	100%	100%	100%	100%	100%	100%	100%	100%	100%	100%	100%
0.9	$\mathbf{L}^1$	57%	66%	98%	100%	100%	100%	66%	98%	100%	100%	100%	99%	100%	100%	100%	100%	100%	100%	100%	100%	100%
ρ	$\mathbf{L}^2$	58%	67%	99%	100%	100%	100%	67%	99%	100%	100%	100%	100%	100%	100%	100%	100%	100%	100%	100%	100%	100%
0.1	KL	58%	68%	99%	100%	100%	100%	66%	99%	100%	100%	100%	100%	100%	100%	100%	100%	100%	100%	100%	100%	0%
	χ^2	56%	67%	99%	100%	100%	100%	66%	99%	100%	100%	100%	100%	100%	100%	100%	100%	100%	100%	100%	100%	1%
$\hat{p}$	$\mathbf{L}^\infty$	61%	53%	69%	100%	100%	100%	59%	66%	100%	100%	100%	61%	100%	100%	100%	100%	100%	100%	100%	100%	100%
0.9	$\mathbf{L}^1$	51%	61%	66%	100%	100%	100%	56%	68%	100%	100%	100%	60%	100%	100%	100%	100%	100%	100%	100%	100%	100%
ρ	$\mathbf{L}^2$	50%	61%	70%	100%	100%	100%	55%	75%	100%	100%	100%	65%	100%	100%	100%	100%	100%	100%	100%	100%	100%
0.2	KL	57%	62%	73%	100%	100%	100%	55%	75%	100%	100%	100%	66%	100%	100%	100%	100%	100%	100%	100%	100%	100%
	χ^2	61%	57%	79%	100%	100%	100%	49%	81%	100%	100%	100%	74%	100%	100%	100%	100%	100%	100%	100%	100%	45%

Percentage Of Accuracy. Sets With Seven Random Variables, Marginal, and Correlation Information

Table C.22: Percentage of accuracy for sets with marginal and rank correlation information. We present results for symmetric constraints using 7 binary random variables, for all distribution approximations and accuracy measures, while changing the values of $\hat{p} = 0.5$ and respective $\rho^r_{1,2}$.

% Of times		DAC	DAC	DAC	DAC	DAC	DAC	MVIE	MVIE	MVIE	MVIE	MVIE	AC	AC	AC	AC	ChSC	ChSC	ChSC	ME	ME	UE
is better than		MVIE	AC	ChSC	ME	UE	IA	AC	ChSC	ME	UE	IA	ChSC	ME	UE	IA	ME	UE	IA	UE	IA	IA
$\hat{p}$	$\mathbf{L}^\infty$	-	74%	74%	74%	74%	74%	-	-	-	-	-	44%	68%	54%	44%	71%	58%	0%	44%	21%	27%
0.5	$\mathbf{L}^1$	-	79%	79%	79%	79%	79%	-	-	-	-	-	51%	54%	60%	64%	60%	63%	100%	63%	90%	37%
ρ	$\mathbf{L}^2$	-	81%	81%	81%	81%	81%	-	-	-	-	-	52%	52%	61%	52%	88%	63%	52%	63%	0%	37%
0	KL	-	82%	82%	82%	82%	82%	-	-	-	-	-	52%	39%	61%	1%	0%	63%	0%	72%	0%	3%
	χ^2	-	83%	83%	83%	83%	83%	-	-	-	-	-	51%	49%	62%	32%	30%	71%	0%	72%	0%	18%
$\hat{p}$	$\mathbf{L}^\infty$	-	75%	78%	71%	100%	100%	-	-	-	-	-	74%	64%	100%	100%	44%	98%	95%	100%	100%	40%
0.5	$\mathbf{L}^1$	-	79%	79%	81%	100%	100%	-	-	-	-	-	72%	78%	100%	100%	47%	98%	99%	96%	98%	39%
ρ	$\mathbf{L}^2$	-	75%	78%	80%	100%	100%	-	-	-	-	-	76%	79%	100%	100%	45%	98%	95%	100%	100%	31%
0.1	KL	-	85%	84%	87%	100%	100%	-	-	-	-	-	76%	79%	100%	100%	42%	98%	100%	100%	100%	71%
	χ^2	-	84%	90%	84%	100%	100%	-	-	-	-	-	78%	77%	100%	100%	35%	99%	100%	100%	100%	82%
$\hat{p}$	$\mathbf{L}^\infty$	-	62%	86%	100%	100%	100%	-	-	-	-	-	80%	100%	100%	100%	98%	100%	100%	97%	100%	100%
0.5	$\mathbf{L}^1$	-	68%	71%	100%	100%	100%	-	-	-	-	-	67%	100%	100%	100%	95%	100%	100%	96%	100%	74%
ρ	$\mathbf{L}^2$	-	62%	73%	100%	100%	100%	-	-	-	-	-	79%	100%	100%	100%	98%	100%	100%	100%	100%	97%
0.2	KL	-	75%	89%	100%	100%	100%	-	-	-	-	-	82%	100%	100%	100%	87%	100%	100%	100%	100%	100%
	χ^2	-	73%	94%	100%	100%	100%	-	-	-	-	-	89%	100%	100%	100%	76%	100%	100%	100%	100%	100%
$\hat{p}$	$\mathbf{L}^\infty$	-	71%	81%	100%	100%	100%	-	-	-	-	-	70%	100%	100%	100%	100%	100%	100%	100%	100%	100%
0.5	$\mathbf{L}^1$	-	82%	80%	100%	100%	100%	-	-	-	-	-	56%	100%	100%	100%	100%	100%	100%	100%	100%	99%
ρ	$\mathbf{L}^2$	-	79%	82%	100%	100%	100%	-	-	-	-	-	63%	100%	100%	100%	100%	100%	100%	100%	100%	100%
0.3	KL	-	85%	86%	100%	100%	100%	-	-	-	-	-	66%	100%	100%	100%	99%	100%	100%	100%	100%	100%
	χ^2	-	81%	89%	100%	100%	100%	-	-	-	-	-	81%	100%	100%	100%	96%	100%	100%	100%	100%	100%
$\hat{p}$	$\mathbf{L}^\infty$	-	78%	81%	100%	100%	100%	-	-	-	-	-	73%	100%	100%	100%	100%	100%	100%	100%	100%	100%
0.5	$\mathbf{L}^1$	-	86%	82%	100%	100%	100%	-	-	-	-	-	64%	100%	100%	100%	100%	100%	100%	100%	100%	100%
ρ	$\mathbf{L}^2$	-	84%	83%	100%	100%	100%	-	-	-	-	-	73%	100%	100%	100%	100%	100%	100%	100%	100%	100%
0.4	KL	-	85%	83%	100%	100%	100%	-	-	-	-	-	75%	100%	100%	100%	100%	100%	100%	100%	100%	100%
	χ^2	-	84%	89%	100%	100%	100%	-	-	-	-	-	84%	100%	100%	100%	95%	100%	100%	100%	100%	100%
$\hat{p}$	$\mathbf{L}^\infty$	-	64%	86%	100%	100%	100%	-	-	-	-	-	73%	100%	100%	100%	100%	100%	100%	100%	100%	100%
0.5	$\mathbf{L}^1$	-	84%	86%	100%	100%	100%	-	-	-	-	-	68%	100%	100%	100%	100%	100%	100%	100%	100%	100%
ρ	$\mathbf{L}^2$	-	84%	89%	100%	100%	100%	-	-	-	-	-	73%	100%	100%	100%	100%	100%	100%	100%	100%	100%
0.5	KL	-	85%	91%	100%	100%	100%	-	-	-	-	-	78%	100%	100%	100%	100%	100%	100%	100%	100%	100%
	χ^2	-	81%	95%	100%	100%	100%	-	-	-	-	-	88%	100%	100%	100%	100%	100%	100%	100%	100%	78%
$\hat{p}$	$\mathbf{L}^\infty$	-	67%	80%	100%	100%	100%	-	-	-	-	-	59%	100%	100%	100%	100%	100%	100%	100%	100%	100%
0.5	$\mathbf{L}^1$	-	78%	80%	100%	100%	100%	-	-	-	-	-	53%	100%	100%	100%	100%	100%	100%	100%	100%	100%
ρ	$\mathbf{L}^2$	-	72%	86%	100%	100%	100%	-	-	-	-	-	56%	100%	100%	100%	100%	100%	100%	100%	100%	100%
0.6	KL	-	86%	86%	100%	100%	100%	-	-	-	-	-	60%	100%	100%	100%	100%	100%	100%	100%	100%	100%
	χ^2	-	83%	92%	100%	100%	100%	-	-	-	-	-	72%	100%	100%	100%	100%	100%	100%	100%	100%	0%
$\hat{p}$	$\mathbf{L}^\infty$	-	64%	79%	100%	100%	100%	-	-	-	-	-	77%	100%	100%	100%	100%	100%	100%	100%	100%	100%
0.5	$\mathbf{L}^1$	-	74%	71%	100%	100%	100%	-	-	-	-	-	61%	100%	100%	100%	100%	100%	100%	100%	100%	100%
ρ	$\mathbf{L}^2$	-	72%	72%	100%	100%	100%	-	-	-	-	-	74%	100%	100%	100%	100%	100%	100%	100%	100%	100%
0.7	KL	-	81%	85%	100%	100%	100%	-	-	-	-	-	75%	100%	100%	100%	100%	100%	100%	100%	100%	100%
	χ^2	-	79%	90%	100%	100%	100%	-	-	-	-	-	85%	100%	100%	100%	100%	100%	100%	100%	100%	0%

Table C.23: Percentage of accuracy for sets with marginal and rank correlation information. We present results for symmetric constraints using 7 binary random variables, for all distribution approximations and accuracy measures, while changing the values of $\hat{p} = 0.6$ and respective $\rho^r_{1,2}$.

% Of times		DAC	DAC	DAC	DAC	DAC	DAC	MVIE	MVIE	MVIE	MVIE	MVIE	AC	AC	AC	AC	ChSC	ChSC	ChSC	ME	ME	UE
is better than		MVIE	AC	ChSC	ME	UE	IA	AC	ChSC	ME	UE	IA	ChSC	ME	UE	IA	ME	UE	IA	UE	IA	IA
$\hat{p}$	$\mathbf{L}^\infty$	-	91%	90%	93%	93%	93%	-	-	-	-	-	87%	71%	71%	71%	15%	15%	15%	47%	54%	88%
0.6	$\mathbf{L}^1$	-	83%	98%	86%	86%	86%	-	-	-	-	-	99%	69%	69%	69%	2%	2%	2%	56%	21%	44%
ρ	$\mathbf{L}^2$	-	86%	99%	89%	89%	89%	-	-	-	-	-	99%	68%	68%	68%	1%	1%	1%	28%	25%	38%
0	KL	-	88%	99%	91%	91%	91%	-	-	-	-	-	99%	68%	68%	68%	1%	1%	1%	47%	100%	100%
	χ^2	-	89%	99%	90%	90%	90%	-	-	-	-	-	99%	69%	69%	69%	1%	1%	1%	66%	100%	46%
$\hat{p}$	$\mathbf{L}^\infty$	-	68%	80%	97%	100%	100%	-	-	-	-	-	70%	97%	100%	100%	99%	100%	100%	100%	100%	100%
0.6	$\mathbf{L}^1$	-	75%	92%	97%	100%	100%	-	-	-	-	-	85%	97%	100%	100%	97%	100%	100%	100%	100%	1%
ρ	$\mathbf{L}^2$	-	76%	92%	97%	100%	100%	-	-	-	-	-	86%	97%	100%	100%	99%	100%	100%	100%	100%	5%
0.1	KL	-	78%	94%	99%	100%	100%	-	-	-	-	-	92%	97%	100%	100%	85%	100%	100%	100%	100%	5%
	χ^2	-	77%	92%	100%	100%	100%	-	-	-	-	-	94%	95%	100%	100%	81%	100%	100%	100%	100%	7%
$\hat{p}$	$\mathbf{L}^\infty$	-	61%	84%	99%	100%	100%	-	-	-	-	-	81%	99%	100%	100%	97%	100%	100%	100%	100%	100%
0.6	$\mathbf{L}^1$	-	73%	79%	100%	100%	100%	-	-	-	-	-	72%	100%	100%	100%	96%	100%	100%	100%	100%	2%
ρ	$\mathbf{L}^2$	-	75%	80%	100%	100%	100%	-	-	-	-	-	77%	100%	100%	100%	97%	100%	100%	100%	100%	91%
0.2	KL	-	79%	86%	100%	100%	100%	-	-	-	-	-	79%	100%	100%	100%	93%	100%	100%	100%	100%	45%
	χ^2	-	78%	91%	100%	100%	100%	-	-	-	-	-	89%	98%	100%	100%	86%	100%	100%	100%	100%	44%
$\hat{p}$	$\mathbf{L}^\infty$	-	63%	78%	100%	100%	100%	-	-	-	-	-	86%	100%	100%	100%	98%	100%	100%	100%	100%	100%
0.6	$\mathbf{L}^1$	-	67%	79%	100%	100%	100%	-	-	-	-	-	81%	100%	100%	100%	100%	100%	100%	100%	100%	98%
ρ	$\mathbf{L}^2$	-	60%	77%	100%	100%	100%	-	-	-	-	-	82%	100%	100%	100%	100%	100%	100%	100%	100%	100%
0.3	KL	-	85%	90%	100%	100%	100%	-	-	-	-	-	83%	100%	100%	100%	98%	100%	100%	100%	100%	100%
	χ^2	-	83%	95%	100%	100%	100%	-	-	-	-	-	88%	100%	100%	100%	93%	100%	100%	100%	100%	96%
$\hat{p}$	$\mathbf{L}^\infty$	-	68%	85%	100%	100%	100%	-	-	-	-	-	76%	100%	100%	100%	100%	100%	100%	100%	100%	100%
0.6	$\mathbf{L}^1$	-	82%	83%	100%	100%	100%	-	-	-	-	-	69%	100%	100%	100%	100%	100%	100%	100%	100%	100%
ρ	$\mathbf{L}^2$	-	81%	82%	100%	100%	100%	-	-	-	-	-	74%	100%	100%	100%	100%	100%	100%	100%	100%	100%
0.4	KL	-	85%	92%	100%	100%	100%	-	-	-	-	-	76%	100%	100%	100%	100%	100%	100%	100%	100%	100%
	χ^2	-	80%	95%	100%	100%	100%	-	-	-	-	-	83%	100%	100%	100%	100%	100%	100%	100%	100%	55%
$\hat{p}$	$\mathbf{L}^\infty$	-	62%	79%	100%	100%	100%	-	-	-	-	-	65%	100%	100%	100%	100%	100%	100%	100%	100%	100%
0.6	$\mathbf{L}^1$	-	82%	81%	100%	100%	100%	-	-	-	-	-	60%	100%	100%	100%	100%	100%	100%	100%	100%	100%
ρ	$\mathbf{L}^2$	-	81%	81%	100%	100%	100%	-	-	-	-	-	65%	100%	100%	100%	100%	100%	100%	100%	100%	100%
0.5	KL	-	86%	88%	100%	100%	100%	-	-	-	-	-	69%	100%	100%	100%	100%	100%	100%	100%	100%	100%
	χ^2	-	85%	92%	100%	100%	100%	-	-	-	-	-	81%	100%	100%	100%	100%	100%	100%	100%	100%	14%
$\hat{p}$	$\mathbf{L}^\infty$	-	72%	83%	100%	100%	100%	-	-	-	-	-	68%	100%	100%	100%	100%	100%	100%	100%	100%	100%
0.6	$\mathbf{L}^1$	-	77%	81%	100%	100%	100%	-	-	-	-	-	61%	100%	100%	100%	100%	100%	100%	100%	100%	100%
ρ	$\mathbf{L}^2$	-	77%	85%	100%	100%	100%	-	-	-	-	-	68%	100%	100%	100%	100%	100%	100%	100%	100%	100%
0.6	KL	-	82%	88%	100%	100%	100%	-	-	-	-	-	72%	100%	100%	100%	100%	100%	100%	100%	100%	100%
	χ^2	-	82%	92%	100%	100%	100%	-	-	-	-	-	82%	100%	100%	100%	100%	100%	100%	100%	100%	0%
$\hat{p}$	$\mathbf{L}^\infty$	-	61%	76%	100%	100%	100%	-	-	-	-	-	71%	100%	100%	100%	100%	100%	100%	100%	100%	100%
0.6	$\mathbf{L}^1$	-	73%	78%	100%	100%	100%	-	-	-	-	-	66%	100%	100%	100%	100%	100%	100%	100%	100%	100%
ρ	$\mathbf{L}^2$	-	71%	79%	100%	100%	100%	-	-	-	-	-	67%	100%	100%	100%	100%	100%	100%	100%	100%	100%
0.7	KL	-	75%	83%	100%	100%	100%	-	-	-	-	-	70%	100%	100%	100%	100%	100%	100%	100%	100%	100%
	χ^2	-	72%	89%	100%	100%	100%	-	-	-	-	-	82%	100%	100%	100%	100%	100%	100%	100%	100%	0%

Table C.24: Percentage of accuracy for sets with marginal and rank correlation information. We present results for symmetric constraints using 7 binary random variables, for all distribution approximations and accuracy measures, while changing the values of $\hat{p} = 0.7$ and respective $\rho^r_{1,2}$.

% Of times		DAC	DAC	DAC	DAC	DAC	DAC	MVIE	MVIE	MVIE	MVIE	MVIE	AC	AC	AC	AC	ChSC	ChSC	ChSC	ME	ME	UE
is better than		MVIE	AC	ChSC	ME	UE	IA	AC	ChSC	ME	UE	IA	ChSC	ME	UE	IA	ME	UE	IA	UE	IA	IA
$\hat{p}$	$\mathbf{L}^\infty$	-	85%	92%	100%	100%	100%	-	-	-	-	-	80%	100%	100%	100%	100%	100%	100%	100%	100%	0%
0.7	$\mathbf{L}^1$	-	90%	90%	100%	100%	100%	-	-	-	-	-	91%	100%	100%	100%	85%	85%	85%	81%	80%	63%
ρ	$\mathbf{L}^2$	-	89%	90%	100%	100%	100%	-	-	-	-	-	94%	100%	100%	100%	99%	99%	99%	100%	100%	0%
0	KL	-	90%	94%	100%	100%	100%	-	-	-	-	-	97%	100%	100%	100%	24%	24%	24%	0%	100%	100%
	χ^2	-	91%	96%	100%	100%	100%	-	-	-	-	-	97%	100%	100%	100%	8%	8%	8%	0%	0%	100%
$\hat{p}$	$\mathbf{L}^\infty$	-	100%	85%	93%	100%	100%	-	-	-	-	-	0%	0%	0%	7%	85%	100%	100%	98%	94%	86%
0.7	$\mathbf{L}^1$	-	100%	82%	95%	100%	100%	-	-	-	-	-	0%	0%	3%	8%	90%	100%	100%	100%	100%	100%
ρ	$\mathbf{L}^2$	-	100%	89%	93%	100%	100%	-	-	-	-	-	0%	0%	0%	2%	86%	100%	100%	98%	99%	100%
0.1	KL	-	100%	93%	99%	100%	100%	-	-	-	-	-	0%	0%	100%	94%	82%	100%	100%	100%	100%	2%
	χ^2	-	100%	99%	94%	100%	100%	-	-	-	-	-	0%	0%	100%	100%	60%	100%	100%	100%	100%	5%
$\hat{p}$	$\mathbf{L}^\infty$	-	68%	78%	100%	100%	100%	-	-	-	-	-	74%	100%	100%	100%	100%	100%	100%	100%	100%	100%
0.7	$\mathbf{L}^1$	-	81%	74%	100%	100%	100%	-	-	-	-	-	69%	100%	100%	100%	100%	100%	100%	100%	100%	32%
ρ	$\mathbf{L}^2$	-	75%	74%	100%	100%	100%	-	-	-	-	-	71%	100%	100%	100%	100%	100%	100%	100%	100%	100%
0.2	KL	-	87%	80%	100%	100%	100%	-	-	-	-	-	70%	100%	100%	100%	100%	100%	100%	100%	100%	4%
	χ^2	-	85%	87%	100%	100%	100%	-	-	-	-	-	81%	100%	100%	100%	97%	100%	100%	100%	100%	3%
$\hat{p}$	$\mathbf{L}^\infty$	-	74%	87%	100%	100%	100%	-	-	-	-	-	79%	100%	100%	100%	100%	100%	100%	100%	100%	100%
0.7	$\mathbf{L}^1$	-	85%	84%	100%	100%	100%	-	-	-	-	-	64%	100%	100%	100%	100%	100%	100%	100%	100%	100%
ρ	$\mathbf{L}^2$	-	84%	84%	100%	100%	100%	-	-	-	-	-	71%	100%	100%	100%	100%	100%	100%	100%	100%	100%
0.3	KL	-	85%	92%	100%	100%	100%	-	-	-	-	-	76%	100%	100%	100%	100%	100%	100%	100%	100%	96%
	χ^2	-	83%	97%	100%	100%	100%	-	-	-	-	-	86%	100%	100%	100%	100%	100%	100%	100%	100%	20%
$\hat{p}$	$\mathbf{L}^\infty$	-	67%	86%	100%	100%	100%	-	-	-	-	-	87%	100%	100%	100%	100%	100%	100%	100%	100%	100%
0.7	$\mathbf{L}^1$	-	75%	84%	100%	100%	100%	-	-	-	-	-	81%	100%	100%	100%	100%	100%	100%	100%	100%	100%
ρ	$\mathbf{L}^2$	-	71%	86%	100%	100%	100%	-	-	-	-	-	85%	100%	100%	100%	100%	100%	100%	100%	100%	100%
0.4	KL	-	82%	91%	100%	100%	100%	-	-	-	-	-	87%	100%	100%	100%	100%	100%	100%	100%	100%	100%
	χ^2	-	82%	96%	100%	100%	100%	-	-	-	-	-	95%	100%	100%	100%	100%	100%	100%	100%	100%	27%
$\hat{p}$	$\mathbf{L}^\infty$	-	72%	82%	100%	100%	100%	-	-	-	-	-	88%	100%	100%	100%	100%	100%	100%	100%	100%	100%
0.7	$\mathbf{L}^1$	-	74%	83%	100%	100%	100%	-	-	-	-	-	85%	100%	100%	100%	100%	100%	100%	100%	100%	100%
ρ	$\mathbf{L}^2$	-	69%	81%	100%	100%	100%	-	-	-	-	-	89%	100%	100%	100%	100%	100%	100%	100%	100%	100%
0.5	KL	-	82%	88%	100%	100%	100%	-	-	-	-	-	90%	100%	100%	100%	100%	100%	100%	100%	100%	100%
	χ^2	-	82%	94%	100%	100%	100%	-	-	-	-	-	93%	100%	100%	100%	100%	100%	100%	100%	100%	0%
$\hat{p}$	$\mathbf{L}^\infty$	-	74%	82%	100%	100%	100%	-	-	-	-	-	78%	100%	100%	100%	100%	100%	100%	100%	100%	100%
0.7	$\mathbf{L}^1$	-	82%	79%	100%	100%	100%	-	-	-	-	-	70%	100%	100%	100%	100%	100%	100%	100%	100%	100%
ρ	$\mathbf{L}^2$	-	77%	78%	100%	100%	100%	-	-	-	-	-	76%	100%	100%	100%	100%	100%	100%	100%	100%	100%
0.6	KL	-	86%	88%	100%	100%	100%	-	-	-	-	-	79%	100%	100%	100%	100%	100%	100%	100%	100%	100%
	χ^2	-	83%	96%	100%	100%	100%	-	-	-	-	-	88%	100%	100%	100%	100%	100%	100%	100%	100%	0%

Table C.25: Percentage of accuracy for sets with marginal and rank correlation information. We present results for symmetric constraints using 7 binary random variables, for all distribution approximations and accuracy measures, while changing the values of $\hat{p} = 0.8, 0.9$ and respective $\rho^r_{1,2}$.

% Of times		DAC	DAC	DAC	DAC	DAC	DAC	MVIE	MVIE	MVIE	MVIE	MVIE	AC	AC	AC	AC	ChSC	ChSC	ChSC	ME	ME	UE
is better than		MVIE	AC	ChSC	ME	UE	IA	AC	ChSC	ME	UE	IA	ChSC	ME	UE	IA	ME	UE	IA	UE	IA	IA
$\hat{p}$	$\mathbf{L}^\infty$	-	100%	79%	100%	100%	100%	-	-	-	-	-	0%	100%	100%	100%	100%	100%	100%	100%	100%	50%
0.8	$\mathbf{L}^1$	-	100%	79%	100%	100%	100%	-	-	-	-	-	0%	100%	100%	100%	100%	100%	100%	38%	100%	100%
ρ	$\mathbf{L}^2$	-	100%	81%	100%	100%	100%	-	-	-	-	-	0%	100%	100%	100%	100%	100%	100%	100%	100%	0%
0	KL	-	100%	93%	100%	100%	100%	-	-	-	-	-	3%	100%	100%	100%	100%	100%	100%	100%	0%	0%
	χ^2	-	100%	96%	100%	100%	100%	-	-	-	-	-	55%	100%	100%	100%	100%	100%	100%	25%	3%	0%
$\hat{p}$	$\mathbf{L}^\infty$	-	100%	79%	67%	100%	100%	-	-	-	-	-	6%	0%	47%	100%	21%	100%	100%	100%	100%	100%
0.8	$\mathbf{L}^1$	-	100%	82%	96%	100%	100%	-	-	-	-	-	1%	0%	44%	74%	34%	100%	100%	100%	100%	100%
ρ	$\mathbf{L}^2$	-	100%	80%	95%	100%	100%	-	-	-	-	-	3%	0%	42%	89%	22%	100%	100%	100%	100%	100%
0.1	KL	-	100%	88%	100%	100%	100%	-	-	-	-	-	0%	0%	100%	100%	50%	100%	100%	100%	100%	0%
	χ^2	-	100%	95%	99%	100%	100%	-	-	-	-	-	13%	1%	100%	100%	31%	100%	100%	100%	100%	3%
$\hat{p}$	$\mathbf{L}^\infty$	-	82%	89%	100%	100%	100%	-	-	-	-	-	45%	100%	100%	100%	100%	100%	100%	100%	100%	100%
0.8	$\mathbf{L}^1$	-	83%	86%	100%	100%	100%	-	-	-	-	-	40%	100%	100%	100%	100%	100%	100%	100%	100%	100%
ρ	$\mathbf{L}^2$	-	82%	88%	100%	100%	100%	-	-	-	-	-	42%	100%	100%	100%	100%	100%	100%	100%	100%	100%
0.2	KL	-	87%	91%	100%	100%	100%	-	-	-	-	-	70%	100%	100%	100%	100%	100%	100%	100%	100%	0%
	χ^2	-	85%	95%	100%	100%	100%	-	-	-	-	-	80%	100%	100%	100%	100%	100%	100%	100%	100%	0%
$\hat{p}$	$\mathbf{L}^\infty$	-	71%	87%	100%	100%	100%	-	-	-	-	-	58%	100%	100%	100%	100%	100%	100%	100%	100%	100%
0.8	$\mathbf{L}^1$	-	86%	83%	100%	100%	100%	-	-	-	-	-	53%	100%	100%	100%	100%	100%	100%	100%	100%	100%
ρ	$\mathbf{L}^2$	-	87%	86%	100%	100%	100%	-	-	-	-	-	58%	100%	100%	100%	100%	100%	100%	100%	100%	100%
0.3	KL	-	91%	89%	100%	100%	100%	-	-	-	-	-	62%	100%	100%	100%	100%	100%	100%	100%	100%	100%
	χ^2	-	87%	93%	100%	100%	100%	-	-	-	-	-	75%	100%	100%	100%	100%	100%	100%	100%	100%	47%
$\hat{p}$	$\mathbf{L}^\infty$	-	72%	83%	100%	100%	100%	-	-	-	-	-	75%	100%	100%	100%	100%	100%	100%	100%	100%	100%
0.8	$\mathbf{L}^1$	-	76%	81%	100%	100%	100%	-	-	-	-	-	74%	100%	100%	100%	100%	100%	100%	100%	100%	100%
ρ	$\mathbf{L}^2$	-	79%	82%	100%	100%	100%	-	-	-	-	-	76%	100%	100%	100%	100%	100%	100%	100%	100%	100%
0.4	KL	-	80%	88%	100%	100%	100%	-	-	-	-	-	80%	100%	100%	100%	100%	100%	100%	100%	100%	100%
	χ^2	-	81%	95%	100%	100%	100%	-	-	-	-	-	88%	100%	100%	100%	100%	100%	100%	100%	100%	0%
$\hat{p}$	$\mathbf{L}^\infty$	-	100%	72%	100%	100%	100%	-	-	-	-	-	0%	100%	100%	100%	100%	100%	100%	100%	100%	50%
0.9	$\mathbf{L}^1$	-	100%	75%	100%	100%	100%	-	-	-	-	-	0%	100%	100%	100%	100%	100%	100%	100%	100%	0%
ρ	$\mathbf{L}^2$	-	100%	75%	100%	100%	100%	-	-	-	-	-	0%	100%	100%	100%	100%	100%	100%	100%	100%	0%
0	KL	-	100%	87%	100%	100%	100%	-	-	-	-	-	0%	100%	100%	100%	100%	100%	100%	100%	0%	0%
	χ^2	-	100%	98%	100%	100%	100%	-	-	-	-	-	7%	100%	100%	100%	100%	100%	100%	10%	4%	0%
$\hat{p}$	$\mathbf{L}^\infty$	-	67%	81%	100%	100%	100%	-	-	-	-	-	77%	100%	100%	100%	100%	100%	100%	100%	100%	100%
0.9	$\mathbf{L}^1$	-	83%	81%	100%	100%	100%	-	-	-	-	-	77%	100%	100%	100%	100%	100%	100%	100%	100%	100%
ρ	$\mathbf{L}^2$	-	74%	81%	100%	100%	100%	-	-	-	-	-	77%	100%	100%	100%	100%	100%	100%	100%	100%	100%
0.1	KL	-	98%	81%	100%	100%	100%	-	-	-	-	-	77%	100%	100%	100%	100%	100%	100%	100%	100%	0%
	χ^2	-	98%	84%	100%	100%	100%	-	-	-	-	-	79%	100%	100%	100%	100%	100%	100%	100%	100%	3%
$\hat{p}$	$\mathbf{L}^\infty$	-	78%	89%	100%	100%	100%	-	-	-	-	-	60%	100%	100%	100%	100%	100%	100%	100%	100%	100%
0.9	$\mathbf{L}^1$	-	80%	78%	100%	100%	100%	-	-	-	-	-	44%	100%	100%	100%	100%	100%	100%	100%	100%	100%
ρ	$\mathbf{L}^2$	-	80%	82%	100%	100%	100%	-	-	-	-	-	52%	100%	100%	100%	100%	100%	100%	100%	100%	100%
0.2	KL	-	88%	91%	100%	100%	100%	-	-	-	-	-	56%	100%	100%	100%	100%	100%	100%	100%	100%	100%
	χ^2	-	85%	96%	100%	100%	100%	-	-	-	-	-	79%	100%	100%	100%	100%	100%	100%	100%	100%	43%

Appendix D

A New Approach to DA

D.1 Moment Matching Discretization Procedure

CR's procedure uses EPT to discretize their continuous joint distribution. Specifically, CR fixed probabilities and then solved for conditional fractiles. This approach is difficult to compare to the JDSIM procedure, which fixes values and solves for probabilities. To facilitate comparison, we use a different discretization based on moment matching. We start by discretizing the marginal distributions using EPT and fix the values of the 0.05, 0.50, and 0.95 fractiles for all uncertainties. After discretizing the marginals, we proceed to discretize the conditional distributions using moment matching to find the respective probabilities (Smith, 1993; Bickel et al., 2011).

The joint probability distribution can be decomposed using Equation (D.1).

$$P(PL, H, C, O) = P(PL) \cdot P(H|PL) \cdot P(C|PL, H) \cdot P(O|PL, H, C) \qquad \text{(D.1)}$$

We start by discretizing $P(PL)$ using EPT and the values of the 0.05, 0.50, and 0.95 fractiles with outcomes \$93.47, \$100.00, and \$110.05,

respectively. For these values, we define the probabilities p_l^{PL}, p_b^{PL}, and p_h^{PL} as 0.185, 0.63, and 0.185, respectively. Next, we discretize $P(H|PL = \$100.00)$ using the fixed values {432.92, 800, 1053.60} for H and use moment matching to find the correct probabilities $p_{l|b}^H$, $p_{b|b}^H$, and $p_{h|b}^H$. To completely discretize $H|PL$, we solve Equation (D.2) for the three possible discrete outcomes of PL.

$$p_{l|b}^H + p_{b|b}^H + p_{h|b}^H = 1 \tag{D.2a}$$

$$432.92 \cdot p_{l|b}^H + 800.00 \cdot p_{b|b}^H + 1053.60 \cdot p_{h|b}^H = E[H|PL] \tag{D.2b}$$

$$(432.92)^2 \cdot p_{l|b}^H + (800.00)^2 \cdot p_{b|b}^H + (1053.60)^2 \cdot p_{h|b}^H = E[H^2|PL] \tag{D.2c}$$

We discretize $P(C|PL, H)$ using equivalent equations matching $E[C|PL, H]$ and $E[C^2|PL, H]$ and equivalent coefficients based on the fixed values for C to define $p_{l|..}^C, p_{b|..}^C$ and $p_{h|..}^C$. The complete discretization of $P(C|PL, H)$ requires solving a total of nine moment matching problems, one for each joint outcome of $\{PL, H\}$. Finally, a similar procedure is applied to $P(O|PL, H, C)$, solving a total of 27 moment matching problems. After discretizing all 39 conditional distributions we apply Equation (D.3) as follows.

$$P(PL = l, H = b, C = h, O = b) = p_l^{PL} \cdot p_{b|l}^H \cdot p_{h|l,b}^C \cdot p_{b|l,b,h}^O \tag{D.3}$$

This alternative discretization fixes the values of the variables and models the probabilistic dependence using the probabilities of the joint events, which enables comparison our approach with CR. As shown in Figure 6.12, the two discretizations are very close.

D.2 Rank Correlation Range in Discrete Distributions

Typically, the rank correlation $\rho_{X,Y}$ between two random variables X, Y is perceived to be $-1 \leq \rho_{X,Y} \leq 1$, where the correlation between a variable and itself is defined with the maximum degree of association $\rho_{X,X} = 1$. However, the same concept only applies to discrete distributions when the number of discrete points tends to infinity. For most discrete distributions $\rho_{X,Y}$ is bounded by a scalar $|a_{\hat{m}}| < 1$. For example, when X and Y have each $\hat{m}$ equally likely realizations, Mackenzie (1994) proved that $a_{\hat{m}} = 1 - \frac{1}{\hat{m}^2}$. Then, the rank correlation is bounded by $-1 + \frac{1}{\hat{m}^2} \leq \rho_{X,Y} \leq 1 - \frac{1}{\hat{m}^2}$ and as the number of realizations increases the $\lim_{\hat{m} \to \infty} |a_{\hat{m}}| = 1$.

Unfortunately, the bound presented by Mackenzie is only valid for distributions with equally likely realizations. In more general scenarios there is not a simple formula to define the bounds of $\rho_{X,Y}$. However, we know that the maximum association dictates that $P(Y = y_i | X = x_i) = 1$ for every i. For example, in §6.2.4.2 we calculate the maximum $\rho_{PL,H}$ by assigning joint probabilities such that $P(PL = l | H = l) = P(PL = b | H = b) = P(PL = h | H = h) = 1$ which results in $p_{l,l,\cdot,\cdot} = 0.185,\ p_{b,b,\cdot,\cdot} = 0.63,\ p_{h,h,\cdot,\cdot} = 0.185$, with all other probabilities equal to zero. Then, using Equation 3.9 and as shown in §6.2.4.2, we can calculate $\rho_{PL,H} = 0.74$.

Moreover, since we choose the random variable Y arbitrarily, by setting $Y = X$ we can calculate $\rho_{X,X}$ in the same way we calculate $\rho_{X,Y}$. An example of this is provided in §6.2.3 Table 6.11. Finally, given that the rank correlation uses $P(X)$ instead of X. For any variables X, Y, if $P(X = x_i) = P(Y = y_i)$ for each i, then $\rho_{X,X} = \sup \rho_{X,Y}$.

D.3 Absolute Bounds for Risk Profiles

The characterization of the truth set can be described as a system of linear equations $Ap = b \; \forall \; p \geq 0$, where A is the matrix of coefficients of Equations (3.1), (3.2a), and (3.9) and b represents the expert assessments. The decision variable p has 81 elements, one for each joint outcome of the cdf, and each joint outcome has a corresponding profit $v = \{v_1, v_2, \ldots, v_{81}\}$. Then, for an arbitrary profit u, the LB and UB of the cdf at u can be calculated using the indicator function $\mathbf{1}_{\leq u}(v_i) = 1$ if $v_i \leq u$ and zero otherwise.

The objective function $c_u p$, where $c_u = \{\mathbf{1}_{\leq u}(v_1), \mathbf{1}_{\leq u}(v_2), \ldots, \mathbf{1}_{\leq u}(v_{81})\}$ is used to find the cdf with the min (max) cumulative probability of the random profit V being less than a value u, $\min$ (max) $P(V \leq u)$. Then, for any u, the lower (upper) bound can be calculated with Equation D.4:

$$\min \text{ (max) } c_u p \tag{D.4a}$$

$$s.t. \quad Ap = b \tag{D.4b}$$

$$\forall \; p \geq 0 \tag{D.4c}$$

To produce a complete risk profile LB (UB), we need to solve Equation D.4 for $u = v_1$ to $u = v_{81}$. The value of the objective function for each of the 81 LPs produces the min (max) absolute bound. By selecting $c_u = v$, the same LP provide the theoretical lower (upper) bounds for the mean profits.

Bibliography

Abbas, A. E. (2006). Entropy methods for joint distributions in decision analysis. *IEEE Transactions on Engineering Management 53*(1), 146–159.

Apostolakis, G. and S. Kaplan (1981). Pitfalls in risk calculations. *Reliability Engineering 2*, 135–145.

Bárány, I. and Z. Füredi (1987). Computing the volume is difficult. *Discrete and Computational Geometry 2*(1), 319–326.

Ben-Tal, A., L. E. Ghaoui, and A. Nemirovski (2009). *Robust Optimization*. Princeton, NJ: Princeton series in Applied Mathematics.

Bertsekas, D. P. (1999). *Nonlinear Programming* (Second ed.). Athena Scientific.

Bertsimas, D. and J. Tsitsiklis (1997). *Introduction to Linear Optimization*. Belmont Mass: Athena Scientific.

Bickel, J. E., L. W. Lake, and J. Lehman (2011, July). Discretization, simulation, and Swanson's (inaccurate) mean. *SPE Economics and Management 3*(3), 128–140.

Bickel, J. E. and J. Smith (2006). Optimal sequential exploration: A binary learning model. *Decision Analysis 3*(1), 16–32.

Bickel, J. E., J. E. Smith, and J. L. Meyer (2008). Modeling dependence among geologic risk in sequential exploration decisions. *Reservoir Evaluation and Engineering 3*(4), 233–251.

Boyd, S. and L. Vandenberghe (2004). *Convex Optimization*. Cambridge, UK.: Cambridge University Press.

Casella, G. and R. L. Berger (2002). *Statistical Inference* (Second ed.). Duxbury Advanced Series. California: Thomson Learning.

Cherubini, U., E. Luciano, and W. Vecchiato (2004). *Order Statistics*. West Sussex, England: John Wiley & Sons Ltd.

Chessa, G., R. Dekker, et al. (1999). Correlation in uncertainty analysis for medical decision making: An application to heart-valve replacement. *Medical Decision Making: an International. 19*(3), 276–286.

Clemen, R. T. (1996). *Making Hard Decisions. An Introduction To Decision Analysis* (2nd ed.). Duxbury Press.

Clemen, R. T., G. W. Fischer, and R. L. Winkler (2000, August). Assessing dependence: Some experimental results. *Management Sci. 46*(8), 1100–1115.

Clemen, R. T. and T. Reilly (1999, February). Correlations and copulas for decision and risk analysis. *Management Science 45*(2), 208–224.

Cooke, R. M. and R. Waij (1986). Monte Carlo sampling for generalized knowledge dependence with application to human reliability. *Risk Analysis 6*(3), 335–343.

Cover, T. M. and J. A. Thomas (2006). *Elements of Information Theory* (Second ed.). Wiley Interscience.

David, H. A. (1981). *Order Statistics*. New York: Wiley.

Deming, W. E. and F. F. Stephan (1940). On a least squares adjustment of a sampled frequency table when the expected marginal totals are known. *Ann. Math. Statist. 11*(4), 427–444.

Devroye, L. (1986). *Non-Uniform Random Variate Generation*. New York: Springer-Verlag.

Devroye, L. and G. Lugosi (2000). *Combinatorial Methods in Density Estimation*. New York, NY: Springer-Verlag.

Dyer, M., A. Frieze, and R. Kannan (1995). A random polynomial time algorithm for approximating the volume of convex bodies.

Frees, E. W., J. Carriere, and E. Valdez (1996, June). Annuity valuation with dependent mortality. *The Journal of Risk and Insurance 63*(2), 229–261.

Fritz, J. (1948). Extreme problems with inequalities as subsidiary conditions. *Interscience Studies and Essays, presented to R. Courant on his 60th Birthday*, 187–204.

Ghosh, S. and G. Henderson (2001). Chessboard distributions and random vectors with specified marginals and covariance matrix. *Operations Research 50*(5), 820–834.

Ghosh, S. and S. G. Henderson (2003, July). Behavior of the NORTA method for correlated random vector-generation as the dimension increases. *ACM Transactions on Modeling and Computer Simulation 13*(3).

Grant, M. and S. Boyd (2011, April). CVX: Matlab software for disciplined convex programming, version 1.21. http://cvxr.com/cvx.

Helton, J. C. (1993). Uncertainty and sensitivity analysis techniques for use in performance assessment for radioactive waste disposal. *Reliability Engineering and System Safety 42*, 327–367.

Howard, R. A. (1966). Decision analysis: Applied decision theory. In D. Hertz and J. Melese (Eds.), *Proceedings of the fourth international conference on operational research*, Wiley Interscience, New York,NY, pp. 55–71.

Howard, R. A. (1988, June). Decision analysis: Practice and promise. *Management Science 34*(6), 679–695.

Howard, R. A. and J. E. Matheson (2004). *The Principles an Applications of Decision Analysis*, Volume 1 of *Strategic Decisions Group*. SDG.

Howard, R. A. and J. E. Matheson (2005). Influence diagrams. *Decision Analysis 2*(3), 127–143.

Ireland, C. T. and S. Kullback (1968, March). Contingency tables with given marginals. *Biometrika 55*(1), pp. 179–188.

Jaynes, E. T. (1957). Information theory and statistical mechanics. part 1. *Physical Review 106*(4), 620–630.

Jaynes, E. T. (1963). Information theory and statistical mechanics. part 3. In G. Uhlenbeck. (Ed.), *Statistical Physics*, pp. 181–218. New York: W. A. Benjamin.

Jaynes, E. T. (1968). Prior probabilities. *IEEE Transactions On Systems Science And Cybernetics 4*(3), 227–241.

Jaynes, E. T. (1982). On the rationale of maximum-entropy methods. *Proceedings of the IEEE 70*(9), 939–952.

Jimenez, L. and D. Landgrebe (1998, Feb.). Supervised classification in high dimensional space: Geometrical, statistical and asymptotical properties of multivariate data. *IEEE Transactions on Systems, Man, and Cybernetics 28-C*(1), 39–54.

Jouini, M. N. and R. T. Clemen (1996, June). Copula models for aggregating expert opinions. *Operations Research 44*(3), 444–457.

Kannan, R., L. Lovsz, and M. Simonovits (1996). Random walks and an O*(n^5) volume algorithm for convex bodies. *Random Structures and Algorithms Vol 11*(Issue 1).

Keefer, D. L. (2004). Underlying event model for approximating probabilistic dependence among binary events. *IEEE Transactions on Engineering Management 51*(2), 173–182.

Keefer, D. L. and S. E. Bodily (1983, May). Three-point approximations for continuous random variables. *Management Science 29*(5), 595–609.

Korsan, R. J. (1990). Towards better assessments and sensitivity procedures. In R. Oliver and J. Smith (Eds.), *Influence diagrams, beliefe nets and decision analysis*, pp. 427–454. New York,NY: Wiley & Sons.

Kullback, S. (1967, January). A lower bound for discrimination information in terms of variation. *IEEE Transactions on Information Theory 13*(1), 126 – 127.

Kullback, S. (1968). Probability densities with given marginals. *The Annals of Mathematical Statistics 39*(4), 1236–1243.

Kullback, S. and R. A. Leibler (1951). On information sufficiency. *The Annals of Mathematical Statistics 22*(1), 79–86.

Lichtenstein, S., B. Fischhoff, and L. D. Phillips (1982). Calibration of probabilities: The state of the art to 1980. In D. Kahneman and A. Tversky (Eds.), *Judgement under Uncertainty: Heuristics and Biases*. Cambridge University Press.

Lin Yuan Kesavan, H. (1998, Aug). Minimum entropy and information measure. *Systems, Man, and Cybernetics, Part C: Applications and Reviews, IEEE Transactions on 28*(3), 488 – 491.

Lovasz, L. (1998). Hit-and-run mixes fast. *Mathematical programming 86*(3), 443–461.

Lowell, D. G. (1994). *Sensitivity to relevance in decision analysis.* Ph. D. thesis, Engineering and Economic Systems, Stanford University, Stanford, CA.

Lowenstein, R. (2000). *When Genius Failed: The Rise and Fall of Long-Term Capital Management.* New York, NY: Random House.

Mackenzie, G. R. (1994). *Approximately Maximum Entropy Multivariate Distributions With Specified Marginals and Pairwise Correlations.* Disertation, University of Oregon.

McMullen, P. (1970). The maximum number of faces of a convex polytope. *Mathematika XVII*(2), 179–184.

Miller, A. C. (1990). Towards better assessments and sensitivity procedures by R. Korsan: Discussion by Allen C. Miller. In R. Oliver and J. Smith (Eds.), *Influence diagrams, belief nets and decision analysis.*, West Sussex, England. John Wiley & Sons Ltd.

Min, H.-S. J., W. Beyeler, T. Brown, Y. J. Son, and A. T. Jones (2007). Toward modeling and simulation of critical national infrastructure interdependencies. *IEEE Transactions on Operations Engineering 39*, 57–71.

Nelsen, R. B. (2005). *An Introduction to Copulas* (Second ed.). Springer Series in Statistics. Springer.

Ong, H. L., H. C. Huang, and W. Huin (2003). Finding the exact volume of a polyhedron. *Advances in Engineering Software 34*(6), 351–356.

Pearson, E. S. and J. W. Tukey (1965). Approximate means and standard deviations based on distances between percentage points of frequency curves. *Biometrika 52*(3/4), 553–546.

Presidential Commission on the Space Shuttle Challenger Accident (1986). ***Report of the Presidential Commission on the Space Shuttle Challenger Accident.*** **Washington, DC: Hearings of the Presidential Commission on the Space Shuttle.**

Ravinder, H., D. KLeinmuntz, and J. Dyer. (1988). The reliability of subjective probabilities obtained through decomposition. ***Management Science 32*****(2), 186–199.**

Reilly, T. (2000, Summer). Sensitivity analysis for dependent variables. ***Decision Sciences 31*****(3), 551–572.**

Rubin, P. A. (1984). Generating random points in a polytope. ***Comm. in Statist. - Simulation and Comput. 13*****(3), 375–396.**

Schmidt, B. K. and T. H. Mattheiss (1977). The probability that a random polytope is bounded. ***Mathematics of Operations Research 2*****(3), 292–296.**

Shannon, C. E. (1948). A mathematical theory of communications. ***Bell Systems Technical Journal 23*****(3), 379–423,623–656.**

Sklar, A. (1959). Fonctions de répartition à n dimensions et leurs marges. ***Publ. Inst. Statist. Univ. Paris*****(8), 229–231.**

Smith, A. E., P. B. Ryan, and J. S. Evans (1992). The effect of neglecting correlations when propagating uncertainty and estimating the population distribution of risk. ***Risk Analysis 12*****(4), 467–474.**

Smith, J. E. (1993). Moment methods for decision analysis. ***Management Science 39*****(3), 340–358.**

Smith, R. L. (1984, Dec). Efficient Monte Carlo procedures for generating points uniformly distributed over bounded regions. *Operations Research 32*(6), 1296–1308.

Strichartz, R. S. (2000). *The Way of Analysis* (Revised ed.). Jones and Bartlett Mathematics. Toronto Canada: Jones and Bartlett.

Thomas, M. U. (1979). A generalized maximum entropy principle. *Operations Research 27*(6), 1189–1196.

Vandenberghe, L., S. Boyd, and S. Wu. (1998). Determinant maximization with linear matrix inequality constraints. *SIAM J. Matrix Analysis and Applications 19*, 499–533.

Vazirani, V. V. (2003). *Approximation Algorithms*. New York,NY: Springer.

von Newmann, J. (1963). *Various techniques used in connection with random digits*, Volume 5, pp 768-770 of *Collected Works*. Pergamon Press.

Watanabe, S. (1981). Pattern recognition as a quest for minimum entropy. *Pattern Recognition 13*, 381–387.

Waterloo, U. (1994.). On the relationship between variance and minimum entropy. In *Intern. Publ.* Univ. Waterloo, Waterloo, Ont., Canada.

Winkler, R. L. (1982). Research directions in decision making under uncertainty. *Decision Sciences 13*(4), 517–533.

Ye, Y. (1997). ***Interior Point Algorithms, Theory and Analysis.*** **New York,NY: Wiley Interscience.**

Zhang, Y. (1999, September). An interior-point algorithm for the maximum-volume ellipsoid problem. Technical Report TR98-15, Department of Computational and Applied Mathematics at Rice University, Houston, Tx.

Vita

Luis Vicente Montiel Cendejas was born in Mexico City, Mexico, the son of Q.F.B. Maria Rosa Cendejas and Dr. Luis Isidoro Montiel. He received the Bachelor of Science degree in Engineering from the Instituto Tecnológico de Monterrey at the Mexico City Campus (ITESM-CCM). After graduation he work as a strategy consultant before he decided to return to the academic life. In 2003 he moved to Palo Alto, California and join the Master in Management Science and Engineering Program at Stanford University. One year later, he continue his studies at Columbia University in the Financial Engineering department and in 2006 he transfers to the Operations Research Graduate Program at The University of Texas at Austin. His research interests are in mathematical modeling for optimization under uncertainty with special interest in decision analysis and simulation learning for optimization.

Permanent address: Operations Research Graduate Program at
The University of Texas at Austin,
Austin, TX 78712, USA,
lvmontiel@utexas.edu